



**DHANALAKSHMI SRINIVASAN COLLEGE
OF ARTS AND SCIENCE FOR WOMEN(AUTONOMOUS)**
(Affiliated to Bharathidasan University,Tiruchirappalli)
(Nationally Re-Accredited with 'A' Grade NAAC)
Perambalur – 621212.



A Special issue

20 DECEMBER -2021

DOI: : <http://dx.doi.org/10.22376/ijpbs/ijlpr/SP17/Dec.2021.12.6.4-284>

In Conjunction with



EDITORS**Dr.P. GAJALAKSHMI****Professor & Head****Department of Micro Biology****Dhanalakshmi Srinivasan College of Arts and Science for Women(Autonomous)****Perambalur 621212****Mrs.V .S.SANGEETHA****Assistant Professor****Department of Chemistry****Dhanalakshmi Srinivasan College of Arts and Science for Women(Autonomous)****Perambalur 621212****Dr.C. SURYA****Assistant Professor &Head****Department of BioChemistry****Dhanalakshmi Srinivasan College of Arts and Science for Women(Autonomous)****Perambalur 621212****Dr.K. SOWMIYA****Assistant Professor &Head****Department of Physics****Dhanalakshmi Srinivasan College of Arts and Science for Women(Autonomous)****Perambalur 621212****ABOUT THIS SPECIAL ISSUE**

This special Issue is to create collections of Articles on specific topics. The aim is to build a community of authors and readers to discuss the latest research and develop new ideas and research directions. The articles in this issue are led by Editors who are experts in the subject and oversee the editorial process for papers. This provide a great platform to promote the break through research works. The potentially advanced special issue focussing on biomedical application from branches of life science, Chemistry and Physics. This special issue is a join collaboration between Dhanalakshmi Srinivasan College of Arts & Science for women Autonomous & International journal of Life Science & Pharma Research. This Provide a platform for the researchers to publish their innovative research findings. It was discussed Antibacterial, Antifungal, Anticancer, Antioxidant and Anticonventional activities. It also included papers on phytochemical screening and pharmaceutical activity of medicinal plants and also focused on biosynthesis of Nanomaterials and its Biological applications. The papers in this special issue broadly divided into the applications of Microbiology, Biotechnology, Biochemistry, Chemistry and Physics.

Research coordinators**Dhanalakshmi Srinivasan****College of Arts and Science****for Women(Autonomous)****Perambalur 621212**

CONTENT

SNO	TITLE	PAGE NO
SP-01	GREEN BIOSYNTHESIS AND CHARACTERIZATION OF MAGNETIC IRON OXIDE (Fe_3O_4) NANOPARTICLES USING SEAWEED (SARGASSUM MUTICUM) AQUEOUS EXTRACT	4-10
SP-02	ECO BENIGN SYNTHESIS CHARACTERIZATION AND MICROBIAL TOXIC STUDY OF AG NANOPARTICLES	11-17
SP-03	ANTIMICROBIAL ACTIVITY OF MINE SOIL ISOLATE OF ACTINOMYCETES	18-22
SP-04	SCREENING OF ENZYMES INHIBITORS FROM MARINE BACTERIAL DYNAMICS	23-28
SP-05	ROS MEDIATED APOPTOTIC EFFECT OF L-ASPARAGINASE ISOLATED FROM ASPERGILLUSNIGER ON PANCREATIC CANCER CELL LINE RIN-5F	29-35
SP-06	ISOLATION ,16SRDNA SEQUENCING , OF BACTERIAL ISOLATE FROM THE EARTHWORM	36-40
SP-07	ELECTROCHEMICAL REDUCTION OF CO ₂ USING OXIDE BASED CU AND ZN BIMETALLIC CATALYST	41-46
SP-08	ACTIVITY OF Bi ₂ O ₃ NPS HELPS FOR THE DRUG DEVELOPMENT ON CHENOPODIUM ALBUM	47-51
SP-09	APPLICATION OF WOOD-DECAYING FUNGI ON REACTIVE BLUE DEGRADATION	52-56
SP-10	SYNTHESIS, OF COPPER OXIDE NANOMATERIALS USING FRESH LEAVES OF CHENOPODIUM ALBUMAND EVALUATING ITS ANTIBACTERIAL METHODS.	57-61
SP-11	HEAVY METAL CHROMIUM BIOSORPTION BY LEATHER TANNERY ISOLATED LIVE & DEAD FUNGI.	62-65
SP-12	GREEN SYNTHESIS COPPER OXIDE NANOPARTICLE USING FRESH LEAFS OF CHENOPODIUM ALBUMAND EVALUATED USING FT-IR,UV SPECTRAL STUDIES	66-69
SP-13	ECO-FRIENDLY THE BIOREDUCTION OF SILVER NANOPARTICLES IN MEDICINAL PLANTS EXTRACTS AND BACTERICIDAL ACTIVITY	70-75
SP-14	ANTIOXIDANT ANTIBACTERIAL AND ANTI-INFLAMMATORY ACTIVITY OF WITHANIYA SOMNIFERA	76-81
SP-15	ANTIBIOTIC RESISTANCE IN URINARY TRACT INFECTIONS	82-85
SP-16	IN-VITRO ANTIOXIDANT AND ANTIBACTERIAL ACTIVITY OF AERVA LANATA (LINN.)- A TRADITIONALLY USED PLANT	86-92
SP-17	SYNTHESIS OF CHALCONES BY CLAISEN-SCHMIDT REACTION; STUDY OF THE ANTIOXIDANT PROPERTY OF CINNAMALACETOPHENONE	93-98
SP-18	BIOCHEMICAL PARAMETERS IN THE PATIENTS OF ALCOHOLIC LIVER DISEASE AND TYPE 2 DIABETES MELLITUS: A CROSS-SECTIONAL OBSERVATIONAL STUDY	99-104
SP-19	GREEN SYNTHESIS AND CHARACTERIZATION OF ZERO-VALENT IRON NANOPARTICLES FROM THE LEAF EXTRACT OF PSIDIUM GUAVA PLANT AND THEIR ANTIBACTERIAL ACTIVITY	105-109
SP-20	EXTRACTION OF BIOACTIVE COMPOUNDS FROM ACTINOMYCETES ASSOCIATED WITH LICHEN	110-113
SP-21	ANTIDIABETIC ACTIVITY OF TERMINALIA BELLIRICA ON ALLOXAN INDUCED DIABETIC RATS	114-117
SP-22	SSICACEAE-DERIVED ANTICANCER AGENTS: TOWARDS A COLON CANCER	118-120
SP-23	BIOSYNTHESIS AND CHARACTERISATION OF SILVER NANOPARTICLES FROM UVARIANARUM EXTRACT .	121-125
SP-24	SYNTHESIS CHARACTERISATION AND ANTIBACTERIAL ACTIVITY STUDIES OF PICOLIOHYDRAZIDE(2-PYRIDINE CARBOXYLIC ACID AND HYDRAZIDE)	126-130
SP-26	BIOSORPTION OF HEAVY METALS BY USING FUNGI ISOLATED FROM CONTAMINATED SOIL	138-144
SP-27	SYNTHESIS, CHARACTERIZATION OF PYRAZOLE, AND BIOLOGICAL ACTIVITIES	145-148
SP-28	EFFECT OF TREATED TANNERY EFFLUENT ON ACALYPHA INDICA - A PILOT STUDY	149-153
SP-29	PRELIMINARY PHYTOCHEMICAL SCREENING AND ANTIOXIDANT(IN-VITRO) ACTIVITY OF CENTELLA ASIATICA(L) LEAVES	154-158
SP-30	PHYTOCHEMICAL ANALYSIS AND ANTIMICROBIAL ACTIVITY OF CARDIOSPERMUM HALICACABUM AND COCCINICA INDICA	159-162
SP-31	PHYTOREMEDIATION OF DAIRY SLUDGE AND IT'S PLANTS GROWTH PROMOTION EFFICIENCY	163-167
SP-32	ABIOTIC STRESS TOLERANCE SCREENING IN TRADITIONAL RICE VARIETIES OF TAMILNADU	168-171

SP-33	EVALUATION OF THE ANTIOXIDANT PROPERTY OF 4, 6-DIPHENYL PYRIMIDINE-2-THIONE	172-175
SP-34	SCIENCE OF STREET ART: TECHNIQUES AND METHODS OF LIFE SCIENCE IN ART IN PUBLIC SPACES.	176-178
SP-35	LARVICIDAL ACTIVITY AGAINST MOSQUITO OF BIS-(4-BENZYLIDENE-3-METHYL-1H-PYRAZOL-5(4H)-ONE)-COPPER (II) & BIS-(1,3-CYCLOHEXANEDIONE)-COPPER (II) COMPLEXES : A COMPARATIVE STUDY	179-182
SP-36	GREEN SYNTHESIS AND CHARACTERIZATION OF COPPER NANOPARTICLES DERIVED FROM MURRAYA KOENIGII LEAVES EXTRACT	183-186
SP-37	DETECTION OF ANTIOXIDANT POTENTIAL OF AZIMA TETRACANTHA LAM	187-192
SP-38	ANTICANCER ACTIVITY OF POLYHERBAL FORMULATION AGAINST HUMAN BLOOD CANCER CELLS	193-197
SP-39	BIOSYNTHESIS AND CHARACTERIZATION OF GOLD NANOPARTICLES FROM ARALEIAELATA PLANT EXTRACT	198-201
SP-40	A REVIEW ON MODERN NANOTECHNOLOGY AND FIBERS USING DISTILLATION PROCESS.	202-206
SP-41	2-IMINOPYRAZOLE HAVING REMARKABLE ACTIVITY IN BACTERIAL STRAINS <i>E. COLI</i> AND <i>B. SUBTILIS</i>	207-210
SP-42	HELATION STABILISED COMPLEX BASED ON STABILISHING TRI AZA MACRO CYCLIC LIGANDS	211-216
SP-43	SOLANUM TORVUM UNRIPE FRUIT EXTRACT MEDIATED PHOTOSYNTHESIZED NICKEL OXIDE NANOPARTICLES	217-221
SP-44	MOLECULAR CLONING OF AMYLASE ENCODING GENE FROM <i>BACILLUS SUBTILIS</i>	222-225
SP-45	EFFECT OF BACTERIAL FEED ON PROTEIN PROFILE OF <i>BOMBEX MORI</i>	226-230
SP-46	GREEN SYNTHESIS OF SILVER NANOPARTICLES FROM <i>SANSEVIAERIA</i> EXTRACT	231-235
SP-47	SYNTHESIS AND CHARACTERIZATION OF COBALT OXIDE NANOPARTICLES AND EVALUATION OF IT'S ANTIBACTERIAL ACTIVITY	236-240
SP-48	INVESTIGATION AND CHARACTERIZATION OF COPPER OXIDE NANOPARTICLE USING FRESH LEAVES OF <i>CHENOPODIUM ALBUM</i>	241-244
SP-49	DPPH SCAVENGING TECHNIQUES, SOXHLET EXTRACTION STUDIES ON <i>CENTELLA ASIATICA</i>	245-249
SP-50	ASSESSMENT OF LIVER PROFILE IN MULTI DRUGS RESISTANT (MDR) TUBERCULOSIS PATIENTS ON TREATMENT	250-254
SP-51	A REVIEW ON GREEN SYNTHESIS OF CU AND CUO NANOMATERIALS AND ITS APPLICATIONS COMPARING SOME MEDICINAL PLANTS EVALUATING USING SEM & EDX ANALYSIS	255-258
SP-52	SCREENING OF ENZYME INHIBITORS COMPOUND FROM SQUID INK	259-263
SP-53	ANTIOXIDANT AND ANTIDIABETIC POTENTIAL OF ARECA NUT EXTRACT	264-267
SP-54	BIOSYNTHESIS OF SILVER NANOPARTICLES FROM <i>ARTOCARPUS HIRSUTUS</i> LEAF EXTRACTS	268-271
SP-55	CATALYST FREE SYNTHESIS OF BIS-(N AMINOETHYLETHANOLAMINE)-COPPER (II) COMPLEX AND ITS MEDICINAL ACTIVITY STUDIES	272-275
SP-56	SYNTHESIS AND CHARACTERIZATION OF NICKEL COMPLEXES BY USING VARIOUS ORGANIC LIGANDS AND IT'S MOSQUITO LARVICIDAL ACTIVITY EVALUATION	276-280
SP-57	GREEN SYNTHESIS NICKEL OXIDE NANOPARTICLE USING UNRIPE FRUIT EXTRACT OF <i>SOLANUM TORVUM</i> AND EVALUATING ITS IN-VITRO ANTIFUNGAL ACTIVITY	281-284

Green Biosynthesis And Characterization Of Magnetic Iron Oxide (Fe₃O₄) Nanoparticles Using Seaweed (Sargassum Muticum) Aqueous Extract

Dr .K.Sowmiya, A. Raja, R.Jayasri, Dr. Shalini

Dhanalakshmi Srinivasan College of Arts and Science for Women (Autonomous) Perambalur - 621212.

Abstract: The synthesis of nanoparticles has become a matter of great interest in recent times due to their various advantageous properties and applications in a variety of fields. The exploitation of different plant materials for the biosynthesis of nanoparticles is considered a green technology because it does not involve any harmful chemicals. In this study, iron oxide nanoparticles (Fe₃O₄-NPs) were synthesized using a rapid, single-step, and completely green biosynthetic method by reduction of ferric chloride solution with brown seaweed (BS, *Sargassum muticum*) water extract containing sulphated polysaccharides as the main factor which acts as reducing agent and efficient stabilizer. The structural and properties of the Fe₃O₄-NPs were investigated by X-ray diffraction, Fourier transforms infrared spectroscopy, field emission scanning electron microscopy (FESEM), energy dispersive X-ray fluorescence spectrometry (EDXRF), vibrating sample magnetometry (VSM, and transmission electron microscopy. The average particle diameter as determined by TEM was found to be 18 ± 4 nm. X-ray diffraction showed that the nanoparticles are crystalline, with a cubic shape. The nanoparticles synthesized through this biosynthesis method can potentially be useful in various applications.

Keywords: Green synthesis; iron oxide nanoparticles; magnetic; *Sargassum muticum*

I. INTRODUCTION

In recent years, novel size-dependent physicochemical properties have led to metallic iron nanoparticles of great potential in a wide range of applications, including magnetic storage media ¹, ferrofluids ², biosensors ³, catalysts ⁴, separation processes, and environmental remediation ⁵. Specifically, magnetite (Fe₃O₄) is a common magnetic iron oxide having a cubic inverse spinel. The compound exhibits unique electric and magnetic properties based upon the transfer of electrons between Fe ²⁺ and Fe ³⁺ in octahedral sites ⁶. According to their unique physical, chemical, thermal, and mechanical properties, and also by having suitable surface characteristics, superparamagnetic nanoparticles offer great potential in many biomedical applications, such as cellular therapy, tissue repair, drug delivery, magnetic resonance imaging (MRI), hyperthermia, and magnetofection ⁷. As magnetic particles accumulate in tumor tissues, they can play an important role in detection through MRI or electron microscopic imaging to locate and measure binding or as the drug carrier for certain anti-cancer drugs ⁸. Currently, a large number of physical, chemical, biological, and hybrid methods are available to synthesize different types of nanoparticles ⁹. The nanoparticles formed using each method show specific properties. However, the biosynthesis of metal nanoparticles by plants is currently under development. Green nanotechnology has attracted a lot of attention and includes a wide range of processes that reduce or eliminate toxic substances to restore the environment. The synthesis of metal nanoparticles using inactivated plant tissue ¹⁰, plant extracts ¹¹, exudates ¹², and other parts of living plants ¹³ is a modern alternative for their production. Green synthesis of nanoparticles makes use of environmentally friendly, non-toxic, and safe reagents ¹⁴. Historically, seaweed is a readily available food source that has been consumed by coastal communities likely since the dawn of time. Seaweed is consumed habitually in many countries in South-East Asia ¹⁵. Marine algae refer to a wide variety of different species with different medicinal behavior, which are divided into two groups, namely microalgae and macroalgae. Marine macroalgae or seaweed, are plant-like organisms classified according to their pigmentation into green (chlorophytes), red (rhodophytes, and brown (phaeophytes). Seaweeds are well-known as a functional food for their richness in lipids, minerals, and certain vitamins, and also several bioactive substances like polysaccharides, proteins, and polyphenols, with potential medicinal uses against cancer ¹⁶, oxidative stress ¹⁷, inflammation ¹⁸, allergy ¹⁹, diabetes ²⁰, thrombosis ²¹, obesity ²², lipidemia ²³, hypertensive ²⁴ and other degenerative diseases. Thus, their phytochemicals include hydroxyl, carboxyl, and amino functional groups, which can serve both as effective metal-reducing agents and as capping agents to provide a robust coating on the metal nanoparticles in a single step. The current work describes a green and rapid method using brown seaweed (BS, *Sargassum muticum*) plant extract solution for the biosynthesis of iron oxide nanoparticles in ambient conditions, without any additive protecting nanoparticles from aggregating, template shaping nanoparticles, or accelerants. The current simple synthetic green method using rapid precursors of BS plant extract provides high-yield nanosized materials with good optical properties, and the method can be used to prepare nanocrystalline oxides of other interesting materials. In this work, the characterization and formation mechanisms of Fe₃O₄-NPs are discussed. The Fe₃O₄-NPs were prepared using ferric chloride as an iron precursor and BS extract as a reducing agent and stabilizer.

2. EXPERIMENTAL

2.1. Materials

Ferric chloride hexahydrate (FeCl₃ · 6H₂O, 98%) was purchased from Merck (Darmstadt, Germany) and was used without further purification. Specimens of the brown seaweed (BS, *Sargassum muticum*) were obtained from the coastal areas of Persian Gulf waters. All aqueous solutions were made using distilled deionized water (DDW).

2.2. Extraction Preparation

The BS sample is shown in Figure 9. Specimens of BS were washed and stored at -20°C (Figure 9A). For the production of extract, ground, freeze-dried seaweed samples (about 1 g, Figure 9B) were boiled with DDW (100 mL) in an Erlenmeyer flask while being continuously stirred for 15 min. The extract was cooled to room temperature, filtered, and stored at -20°C before use.

2.3. Preparation of Fe_3O_4 Nanoparticles

Iron oxide nanoparticles (Fe_3O_4 -NPs) were prepared by adding 0.1 M FeCl_3 solution to the BS extract in a 1:1 volume ratio. Fe_3O_4 -NPs were immediately obtained with the reduction process. The mixture was stirred for 60 min and then allowed to stand at room temperature for another 30 min. The obtained colloidal suspensions were then centrifuged and washed several times with ethanol and then dried at 40°C under vacuum to obtain the Fe_3O_4 -NPs.



Figure 1. Brown seaweed (*Sargassum muticum*) (A), Brown seaweed (*Sargassum muticum*) powder (B).

2.4. Characterization Methods and Instruments

FT-IR spectra of the Fe_3O_4 -NPs were recorded over the range of 400–4,000 cm^{-1} on a model spectrum 100 series (Perkin Elmer, Waltman,) FTIR spectrophotometer. The crystalline structure and phase purity of the Fe_3O_4 -NPs produced were identified by X-ray diffraction measurement (XRD-6000; Shimadzu,). Field emission scanning electron microscopy (FESEM) was performed using a Philips JSM-6360LA instrument to study the morphology of magnetic NPs. The energy dispersive X-ray fluorescence spectrometry (EDXRF) was carried out on a DX-700HS spectrometer (Shimadzu). The UV-visible spectra were recorded over the 300–700 nm range with a UV 1650 PC-Shimadzu B UV-visible spectrophotometer

3. RESULTS AND DISCUSSION

3.1. Mechanism of the Fe_3O_4 -NPs Formation in BS Extract

The improvement of reliable, non-toxic, and eco-friendly methods for the synthesis of nanoparticles is of utmost importance to expand their biomedical applications ²⁵. The present work focused on the development of a biosynthetic method for the production of Fe_3O_4 -NPs using brown seaweed (*Sargassum muticum*) extract. As shown in Figure 1A, the color of the Fe^{3+} /BS extract solutions at room temperature rapidly changed from yellow to dark brown, indicating the formation of Fe_3O_4 -NPs in the BS extract.

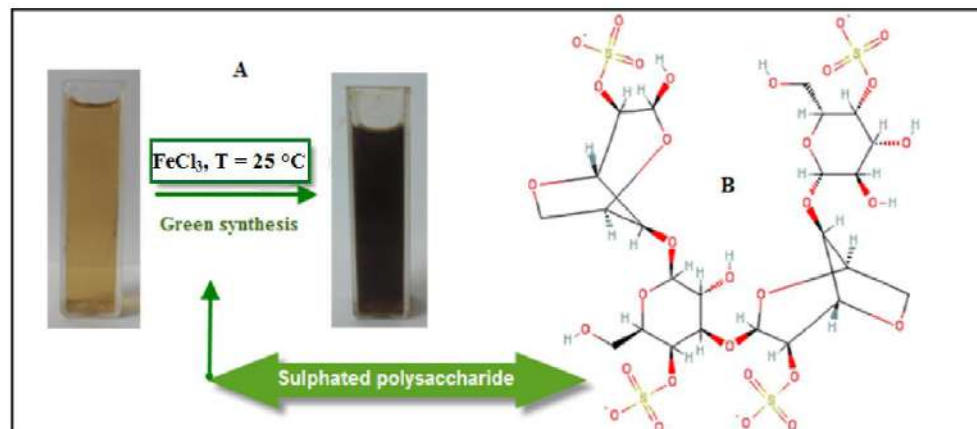


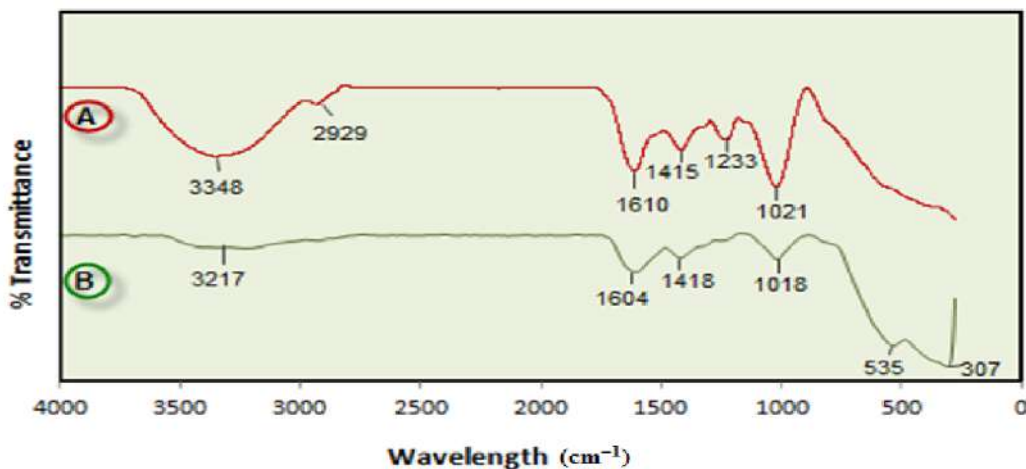
Figure 2. Photograph of synthesized Fe_3O_4 -NPs in BS extract.

The addition of ferric chloride solution as an iron precursor to the BS extract containing sulphated polysaccharides (Figure 1B) as a major component which has sulphate, hydroxyl, and aldehyde group may cause the reduction of Fe^{3+} and stabilization of the nanoparticles. Decreasing pH during the formation of Fe_3O_4 -NPs signifies the involvement of the OH group in the reduction process. Initially, FeCl_3 hydrolyzes to form ferric hydroxide and releases H^+ ions thereafter; ferric hydroxide is partially reduced by the BS extract to form Fe_3O_4 -NPs, while aldehyde groups are oxidized to the corresponding acids. The proposed green synthesis method for Fe_3O_4 -NPs was found to be constructive and extremely reproducible.

3.2. Characterization of Fe_3O_4 Nanoparticles

3.2.1. Infrared Spectroscopy

FTIR spectroscopy was used to identify the functional groups of the active components based on the peak value in the region of infrared radiation. Figure 2 shows FTIR spectra of BS powder and Fe_3O_4 -NPs synthesized in BS extract. After complete bioreduction of iron ions, the BS extract was centrifuged for 2 min to isolate the Fe_3O_4 -NPs from the compounds present in the solution.

**Figure 3.** FT-IR spectrum for the BS powder (A) and Fe_3O_4 -NPs from the biosynthesis reaction (B).

The FTIR spectrum of BS powder has a characteristic stretching vibration band at $1,233\text{ cm}^{-1}$ denoting the asymmetric stretching vibration of the sulfate group, which disappeared after synthesis of Fe_3O_4 -NPs indicated the involvement of the sulfate group in the reduction process and the stabilization of Fe_3O_4 -NPs. This is in agreement with, who reported that sulphated polysaccharides isolated from the marine alga *Porphyra vietnamensis*(Rhodophyta) had a strong ability to synthesize nanoparticles. It is also possible that the sulfate group plays an important role in the reduction of metal ions by oxidation of aldehyde groups in the molecules to carboxylic acids . The band at $1,021\text{ cm}^{-1}$ can be assigned to the symmetric C–O vibration associated with a C–O– SO_3 group . In addition, signals at $3,348\text{ cm}^{-1}$ (OH stretching) and $2,929\text{ cm}^{-1}$ (CH stretching) were also observed. After the reduction of FeCl_3 , the decreases in intensity at $3,217\text{ cm}^{-1}$ imply the involvement of the OH group in the reduction process. The peak at $1,415\text{ cm}^{-1}$ indicates the C–C groups derived from aromatic rings that are present in the BS extract and also the peak at $1,610\text{ cm}^{-1}$ is attributed to the conjugated carbonyl ($-\text{C}=\text{O}$) group stretching vibration. The shift of the band from $1,610\text{ cm}^{-1}$ to $1,604\text{ cm}^{-1}$ was attributed to the binding of a $\text{C}=\text{O}$ group with the nanoparticles. The formation of Fe_3O_4 is characterized by two absorption bands at 535 and 307 cm^{-1} which correspond to the Fe–O bond in magnetite. From the FTIR result, the soluble elements present in BS extract could have acted as capping agents preventing the aggregation of nanoparticles in solution, and thus playing a relevant role in their extracellular synthesis and shaping.

3.2.2. X-ray Diffraction (XRD)

The phase identification and crystalline structures of the nanoparticles were characterized by X-ray powder diffraction. The X-ray diffraction patterns obtained for the Fe_3O_4 -NPs synthesized using BS extract are shown in Figure 3. It is found that there exist strong diffraction peaks with 2θ values of 30.4° , 35.8° , 43.5° , 54.1° , and 57.4° , corresponding to the crystal planes of (200), (311), (511) and (440) of crystalline Fe_3O_4 -NPs, respectively. The results show the spinel phase structure of magnetite and agree with the XRD standard for the magnetite nanoparticles .

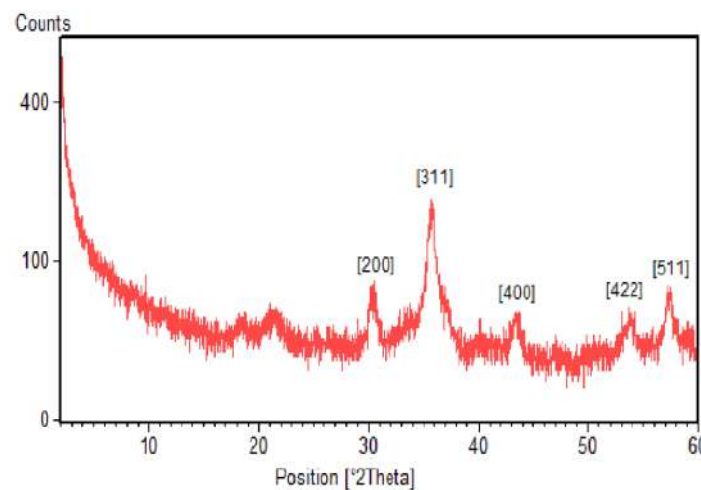


Figure 4. XRD pattern of Fe_3O_4 -NPs synthesized using BS extract.

The average particle sizes of Fe_3O_4 -NPs can be estimated using the Debye-Scherrer equation, which gives a relationship between peak broadening in XRD and particle size that is demonstrated by the following equation:

$$d = k\lambda/(\beta \cos\theta)$$

where d is the particle size of the crystal, k is the Scherrer constant (0.9), λ is the X-ray wavelength (0.15406 nm), β is the width of the XRD peak at half-height, and θ is the Bragg diffraction angle. Using the Scherrer equation the average crystallite sizes of the magnetic Fe_3O_4 -NPs are found to be in the range 17–25 nm.

3.2.3. Morphology and Size Distribution of Nanoparticles

The morphology and structure of the Fe_3O_4 -NPs were further investigated by field emission scanning electron microscopy (FESEM). The FESEM image and EDXRF spectra for the Fe_3O_4 -NPs are shown in Figure 5. The FESEM image (Figure 5A) confirms that the Fe_3O_4 -NPs are cubic. In the EDXRF spectra (Figure 5B), the peaks around 0.8, 6.2, and 6.9 keV are related to the binding energies of Fe. Therefore, the EDXRF spectra for the Fe_3O_4 /seaweed extract confirmed the presence of Fe_3O_4 -NPs in the BS aqueous extract without any impurity peaks.

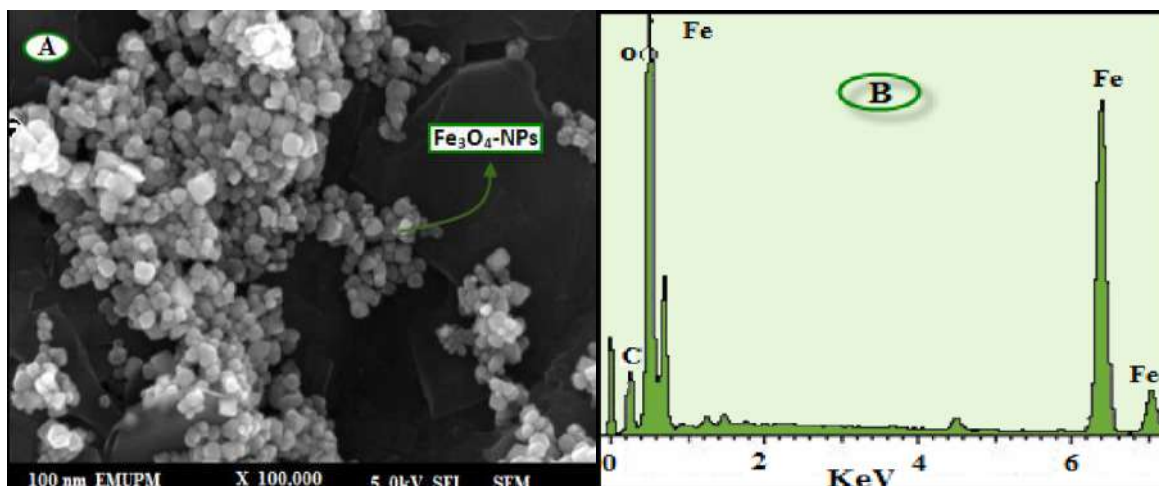


Figure 5. FESEM image (A) and energy-dispersive X-ray fluorescence spectrometry spectra of Fe_3O_4 -NPs synthesized using BS extract (B).

3.2.4. Ultraviolet-Visible Spectroscopy (UV-Vis)

Ultraviolet-visible spectroscopy (UV-Vis) refers to absorption spectroscopy in the UV-Visible spectral region. This means it uses light in the visible and adjacent (near-UV and near-infrared) ranges. The absorption in the visible range directly affects the perceived color of the chemicals involved. In this region of the electromagnetic spectrum, molecules undergo electronic transitions. The UV-Visible spectrum of Fe_3O_4 -NPs in the aqueous BS extract is shown in Figure 6. The two absorption peaks at wavelengths of 402 nm and 415 nm indicate the formation of iron nanoparticles.

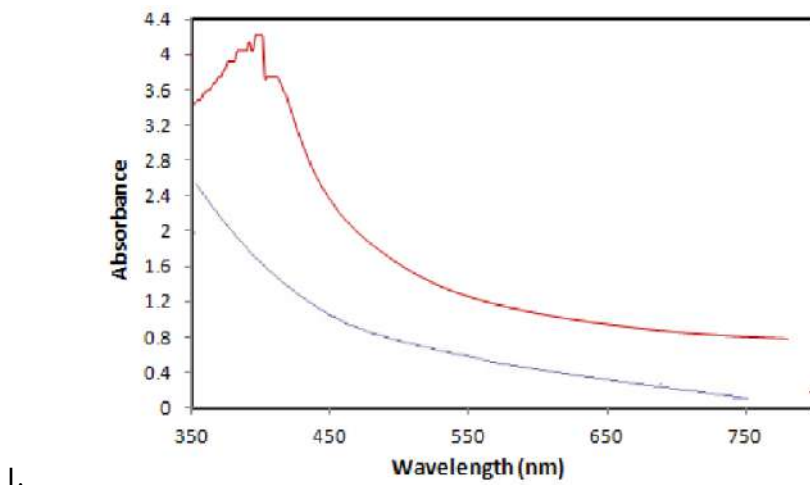


Figure 6. UV-visible absorption spectra of BS (A) and Fe_3O_4 /BS extract (B).

4. CONCLUSIONS

A critical need in the field of nanotechnology is the development of reliable and ecofriendly processes for the synthesis of metal oxide nanoparticles. Fe_3O_4 -NPs with an average size of 18 ± 4 nm and cubic shapes were synthesized by bioreduction of ferric chloride solution with a green method using brown seaweed (*Sargassum muticum*) aqueous extract containssulphated polysaccharides as the reducing agent and efficient stabilizer. The hydroxyl, sulphate, and aldehyde group present in the BS extract are involved in the bioreductionand stabilization of Fe_3O_4 -NPs. The involvement of these groups in biosynthesis is revealed by FTIR analysis. The characteristics of the obtained Fe_3O_4 -NPs were studied using FTIR, XRD, UV-visible, FESEM, EDXRF, TEM, and VSM techniques. Biosynthesis of Fe_3O_4 -NPs using green resources is a simple, environmentally friendly, pollutant-free, and low-cost approach. Functional bioactivity of Fe_3O_4 -NPs (antimicrobial) is comparably higher than particles that were synthesized by the chemical method. This green method of synthesizing Fe_3O_4 -NPs could also be extended to fabricate other, industrially important metal oxides.

5. CONFLICT OF INTEREST

Conflict of interest declared none.

6. REFERENCES

1. Sun, S.H.; Murray, C.B.; Weller, D.; Folks, L.; Moser, A. Monodisperse FePt nanoparticles and ferromagnetic FePt nanocrystal superlattices. *Science* **2000**, *287*, 1989–1992.
2. Jeyadevan, B.; Chinnasamy, C.N.; Shinoda, K.; Tohji, K.; Oka, H. Mn-Zn ferrite with higher magnetization for temperature-sensitive magnetic fluid. *J. Appl. Phys.* **2003**, *93*, 8450–8452.
3. Miller, M.M.; Prinz, G.A.; Cheng, S.F.; Bounnak, S. Detection of a micron-sized magnetic sphere using a ring-shaped anisotropic magnetoresistance-based sensor: A model for a magnetoresistance-based biosensor. *Appl. Phys. Lett.* **2002**, *81*, 2211–2213.
4. Zhang, J.L.; Wang, Y.; Ji, H.; Wei, Y.G.; Wu, N.Z.; Zuo, B.J.; Wang, Q.L. Magnetic nanocomposite catalysts with high activity and selectivity for selective hydrogenation of *ortho*-chloronitrobenzene. *J. Catal.* **2005**, *229*, 114–118.
5. Mahdavi, M.; Ahmad, M.B.; Haron, M.J.; Gharayebi, Y.; Shameli, K.; Nadi, B. Fabrication and characterization of SiO₂/(3-aminopropyl) triethoxysilane-coated magnetite nanoparticles for lead (II) removal from aqueous solution. *J. Inorg. Organomet. Polym. Mater.* **2013**, *23*, 599–607.
6. Abhilash; Revati, K.; Pandey, B.D. Microbial synthesis of iron-based nanomaterials—A review. *Bull. Mater. Sci.* **2011**, *34*, 191–198.
7. JGuoa, J.; Wang, R.; Tjiu, W.W.; Pan, J.; Liu, T. Synthesis of Fe nanoparticles@graphene composites for environmental applications. *J. Hazard. Mater.* **2012**, *225–226*, 63–73.
8. Gupta, A.K.; Gupta, M. Synthesis and surface engineering of iron oxide nanoparticles for biomedical applications. *Biomaterials* **2005**, *26*, 3995–4021.
9. Liu, J.; Qiao, S.Z.; HU, Q.H.; Lu, G.Q. Magnetic nanocomposites with mesoporous structures: synthesis and applications. *Small* **2001**, *7*, 425–443.
10. Padil, V.V.; Cerník, M. Green synthesis of copper oxide nanoparticles using gum karaya as a biotemplate and their antibacterial application. *Int. J. Nanomedicine* **2013**, *8*, 889–898.
11. Shameli, K.; Ahmad, M.B.; Zamanian, A.; Sangpour, P.; Shabanzadeh, P.; Abdollahi, Y.; Zargar, M. Green biosynthesis of silver nanoparticles using *Curcuma longa* tuber powder. *Int. J. Nanomedicine* **2012**, *7*, 5603–5610.
12. Lukman, A.I.; Gong, B.; Marjo, C.E.; Roessner, U.; Harris, A.T. Facile synthesis, stabilization, and anti-bacterial performance of discrete Ag nanoparticles using *Medicago sativa* seed exudates. *J. Colloid Interface Sci.* **2011**, *353*, 433–44.

13. Parsons, J.G.; Peralta-Videa, J.R.; Gardea-Torresdey, J.L. Use of plants in biotechnology: Synthesis of metal nanoparticles by inactivated plant tissues, plant extracts, and living plants. *Dev. Environ. Sci.* **2007**, *5*, 463–485.
14. Salam, H.A.; Rajiv, P.; Kamaraj, M.; Jagadeeswaran, P.; Gunalan, S.; Sivaraj, R. Plants: Green route for nanoparticle synthesis. *Int. J. Biol. Sci.* **2012**, *1*, 85–90. *Molecules* **2013**, *18* 5964
15. Liu, L.; Heinrich, M.; Myers, S.; Dworjanyn, S. Towards a better understanding of medicinal uses of the brown seaweed *Sargassum* in Traditional Chinese Medicine: A phytochemical and pharmacological review. *J. Ethnopharmacol.* **2012**, *142*, 591–619.
16. Namvar, F.; Suhaila, M.; GasemiFard, S.; Behravan, J. Polyphenol-rich seaweed (*Eucheuma cottonii*) extract suppresses breast tumors via hormone modulation and apoptosis induction. *Food Chem.* **2012**, *130*, 376–382.
17. El Gamal, A.A. Biological importance of marine algae. *Saudi Pharm. J.* **2010**, *18*, 1–25.
18. Khan, M.; Choi, J.; Lee, M.; Kim, E.; Nam, T. Anti-inflammatory activities of methanol extracts from various seaweed species. *J. Environ. Biol.* **2008**, *29*, 465–469.
19. Zuercher, A.W.; Fritsché, R.; Corthésy, B.; Mercenier, A. Food products, and allergy development, prevention, and treatment. *Curr. Opin. Biotechnol.* **2006**, *17*, 198–203.
20. Perez, G.R.M.; Zavala, S.M.; Perez, G.S.; Perez, G.C. Antidiabetic effect of compounds isolated from plants. *Phytomedicine* **1998**, *5*, 55–75.
21. Nishino, T.; Fukuda, Nagumo, T.; Fujihara, M.; Kaji, E. Inhibition of the generation of thrombin and factorXa by a fucoidan from the brown seaweed *Eckloniakuroume*. *Thromb. Res.* **1999**, *96*, 37–49.
22. Miyashita, K. The carotenoid fucoxanthin from brown seaweed affects obesity. *Lipid Technol.* **2009**, *21*, 186–190.
23. Mohamed, S.; Hashim, S.N.; Rahman, H.A. Seaweeds: A sustainable functional food for complementary and alternative therapy. *Trends Food Sci. Technol.* **2012**, *23*, 83–96.
24. Wada, K.; Nakamura, K.; Tamai, Y. Seaweed intake and blood pressure levels in healthy pre-school Japanese children. *Nutr. J.* **2011**, *10*, 83–88.
25. Shankar, S.S.; Rai, A.; Ahmad, A.; Sastry, M. Rapid synthesis of Au, Ag and bimetallic Au core-Ag shell nanoparticles using Neem (*Azadirachtaindica*) leaf broth. *J. Colloid Interface Sci.* **2004**, *275*, 496–502.

Eco Benign Synthesis Characterization And Microbial Toxic Study Of Ag Nanoparticles

V.S Sangeetha* ,V.Vanitha ,R.Elayaperumal ,V.Bhakyajothi

DhanalakshmiSrinivasan college of arts and science for women (Autonomous) ,Perambalur-621 212, Tamil Nadu, India

*Corresponding Author: Mail id :sangeethavasanth23@gmail.com

Abstract: In recent years, green synthesis of silver nanoparticles (AgNPs) has gained much interest from chemists and researchers. This study investigates an efficient and sustainable route of AgNP preparation from 1 mm aqueous AgNO₃ using extracts of two plants lablab purpureus and winged bean well adorned for their wide availability and medicinal property. The AgNPs were characterized by UV-visible (vis) spectrophotometer, particle size analyzer (DLS) , scanning electron microscopy (SEM) ,fourier transform infrared spectrometer (FTIR) analysis was carried out to determine the natural the capping agents in each of these extracts. AgNPs obtained showed significantly higher antimicrobial activities against staphylococcus aureus and E.Coli.in comparison to both AgNO₃ and raw plant extracts. activity nearing control levels, through detailed mechanisms of uptake and translocation are yet to be analyzed. The AgNOs prepared are safe to be discharged in the environment and possibly utilized in process of pollution remediation

Keywords: Nanoparticles, Microbial activity, SEM analysis, AgNO₃etc

I. INTRODUCTION

Introduction to Nanoscience and Nanotechnology

The term "nanotechnology" was first used by Norio Taniguchi in 1974, though it was not widely known. Inspired by Feynman's concepts, K. Eric Drexler independently used the term "nanotechnology" in his 1986 book *Engines of Creation: The Coming Era of Nanotechnology*, which proposed the idea of a nanoscale "assembler" which would be able to build a copy of itself and of other items of arbitrary complexity with atomic control¹ . Since then a lot of research on Nanoscience and nanotechnology has carried out throughout the globe . And it has resulted into the discovery of new types of materials which possess physical and chemical properties which are not observed in their bulk counterparts . Harold Kroto and co-workers discovered in 1985, a new allotrope of carbon, fullerene (C₆₀)²⁻⁵ Iijima burst into the scene in 1990s with the discovery of another allotrope of carbon, called carbon nanotubes, and phenomena of superconductivity and ferromagnetism were found in C₆₀ . Nanoscience now deals with the science of materials and technologies having size scales in the range of ~ 1-100 nm. Presently, Nanoscience and technology represents the most active discipline all around the world and is considered as the fastest growing technology revolution, human history had ever seen⁶⁻⁷ This intense interest in the science of the Nanomaterials, which confined within the atomic scales, stems from the fact that these nanomaterials exhibit fundamentally interesting unique properties with great potential of next generation technologies in electronics, computing, optics, biotechnology, medical imaging, medicine, drug delivery, structural materials, aerospace, energy, etc.⁸⁻¹¹

2. MATERIALS AND METHODS

2.1 Preparation Of Flower Extract

The fresh and young flower samples were collected and washed thoroughly with sterile double distilled water (DDW). Twenty gram of sterilized flower samples were taken and cut into small pieces. Finely cut leaves were placed in a 500 ml Erlenmeyer flask containing 100 ml of sterile DDW. After that, the mixture was boiled for 5 minutes and then filtered. The extract was stored in 4 °C

2.2 Synthesis Of Silver Nanoparticles

Silver nitrate was used as precursor in the synthesis of silver nanoparticles. 100 ml flower extract was added to 100 ml of 0.1N AgNO₃ aqueous solution in conical flask of 250 ml content at room temperature. The flask was thereafter put into a shaker (100 rpm) at 500 C and reaction was carried out for a period of 12 hrs. Then the mixture is kept in microwave oven for exposure of heat. The mixture was completely dried after a period of 20 minutes and hence Nanoparticles in form of powders were obtained.

2.3 Uv Visible Spectroscopy Analysis

The colour change in reaction mixture (metal ion solution + flower extract) was recorded through visual observation. The bio reduction of silver ions in aqueous solution was monitored by periodic sampling of solid and subsequently measuring UV visible spectra of the solid sample. UV-visible spectra of sample were monitored as a function of time of reaction on the UV-visible spectroscopy and the investigation was carried out using PERKIN ELMER (Lambda 35 model) spectrometer in the range of 190

nm to 1100 nm.^{11,12}

2.4 Ft-IR Measurement

The Fourier transform infrared (FTIR) investigation is carried out using PERKIN ELMER (Spectrum RXI) spectrometer in the range of 400 cm⁻¹ to 4000 cm⁻¹. The functional groups were identified using the peak Assignments¹³

2.5 XRD Measurement

The sample was drop-coated onto Nickel plate by just dropping a small amount of sample on the plate frequently, allowed to dry and finally thick coat of sample was prepared. The particle size and nature of the silver nanoparticle was determined using X-ray diffraction (XRD)¹⁴. This was carried out using Rigaku miniflex-3 model with 30kv, 30mA with CuK α radians at 2 θ angle.

2.6 SEM Analysis

Sample is dispersed with acetone and exposed in ultrasonics for 5 minutes. Take a drop of a solution from the sample and drop it on the grid, leave until it dries. After drying the sample is inserted into SEM instruments using model is Tecnai T20 Making in FEI, Netherlands operating at 200KeV Tungsten Filament.

2.7 ANTIBACTERIAL ACTIVITY

2.7.1 Micro Organisms And Culture Media

Bacterial cultures such as, *Staphylococcus aureus*, *E.coli*, were obtained from Eumic analytical Lab and Bacterial strains²⁷ were maintained on Nutrient agar slants (Hi media) at 4°C.

2.7.2 Inoculum Preparation

Bacterial cultures were subcultured in liquid medium (Nutrient broth) at 37°C for 8h and further used for the test (105-106CFU/ml). These suspensions were prepared immediately before the test was carried out.

2.8 Preparation of culture media

2.8.1. Nutrient Agar Medium

Nutrient agar medium is one of the most commonly used medium for several routine bacteriological purposes.

Ingredients	:	Grams/Litre
Peptone	:	5gm
Beef extract	:	3gm
Agar	:	15gm
Sodium chloride	:	5gm
Yeast extract	:	1.5gm
pH	:	7.0

After adding all the ingredients into the distilled water it is boiled to dissolve the medium completely and sterilized by autoclaving at 15 lb psi pressure (121°C) for 15 minutes.

2.8.2. Preparation Of Nutrient Broth

The nutrient broth was prepared by the same composition without agar. At the adding all the ingredients into the distilled water it is boiled to dissolve the medium completely and sterilized by autoclaving at 15 lb psi pressure (121°C) for 15 minutes.

2.8.3. Preparation Of Plant Material

Flowers, of the plant materials taken for this study were shade dried individually at room temperature and then powdered by using electric, blender. About 10gm of fresh plant materials (flower). Were extracted with 100ml of distilled water 91:10. They were kept for seven days at room temperature (31°C) for complete extraction. After seven days. The extracts were filtered through what man no.1 filter paper. This extract was collected in both and kept in refrigerator.

2.8.4. Microbial Inoculum Preparation

The nutrient broth were prepared, then identified bacterial colonies were inoculated into the broth culture were used for antimicrobial activity.

2.8.5. Kirby Bauer Agar Well Diffusion Assay

The nutrient agar medium was prepared and sterilized by autoclaving at 121°C 15 lbs pressure for 15 minutes then aseptically poured the medium into the sterile petriplates and allowed to solidify the Bacterial broth culture was swabbed on each petriplates using a sterile buds. Then wells were made by well cutter. The organic solvent extracts of flower were added to each well aseptically. This procedure was repeated for each Petri plates then the petriplates were incubated at 37°C for 24 hrs. After incubation the plates were observed for the zone of inhibition.

3. RESULT AND DISCUSSION

3.1 Uv-Visible Spectroscopy Analysis

UV-Visible spectroscopy analysis showed the absorbance band of silver nanoparticles synthesized using *lablabpurpureus* flower extract at 197.10nm,382.60nm, and 391.30nm which conforms the presence of poly-unsaturated and aromatic compound (Isoquinoline)¹¹⁻¹³.

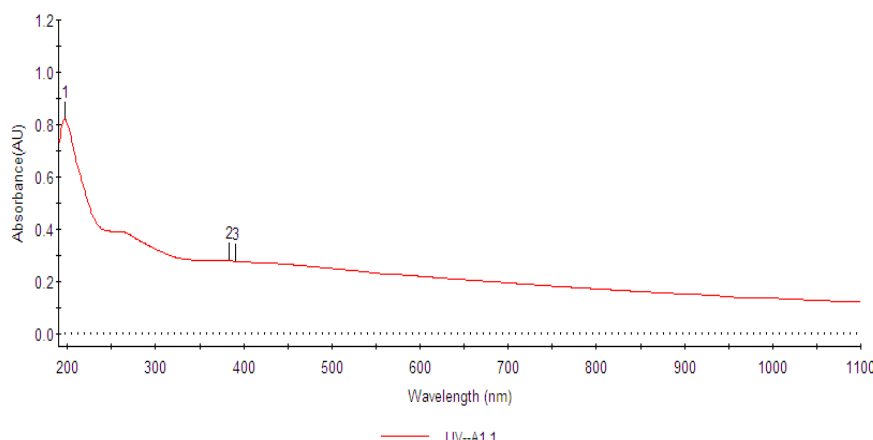


Figure:1 UV-Visible spectrum of synthesized silver nanoparticles using flower extract of *lablab* purpureus

3.2 FT-IR Measurmen

The *lablab* purpureus related functional groups were identified Using the peak assignments. A medium peak at 3734.19cm⁻¹ was assigned to the N-H stretching in amide group, multiple broade peak at 2310.72 cm⁻¹ was assigned to N-H stretching primary ammonium ions group, similar conjugated effects at 1685.79cm⁻¹ was assigned to C=O Stretching anhydride group,a strong peak at 1514.12cm⁻¹ was assigned to N-O stretching¹³⁻¹⁸Nitro compound group, a strong peak at 1141.86cm⁻¹ was assigned to P-O stretching Phosphorus oxide, strong peck at 1091.71cm⁻¹ was assigned to C-O stretching Alkyl aryl ether medium are observed.

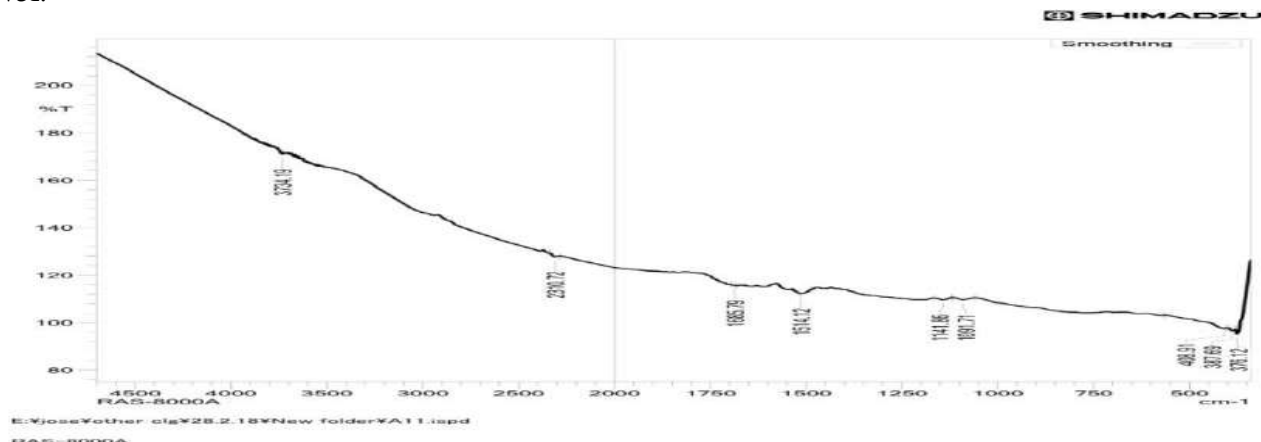


Figure 2: FT-IR Spectrum of synthesized silver nanoparticles using flower extract *lablab* purpureus.

3.3 Sem Analysis

SEM analysis shows uniformly distributed silver nanoparticles on the surfaces of the cells. SEM analysis reveals individual spherical polydisperse AgNPs as well as number of aggregates, which wear irregularly in shape .The size of the silver nanoparticles was found to be 5-50nm, with an average size 14.91nm. The larger silver particles may be due to the aggregation of the smaller ones

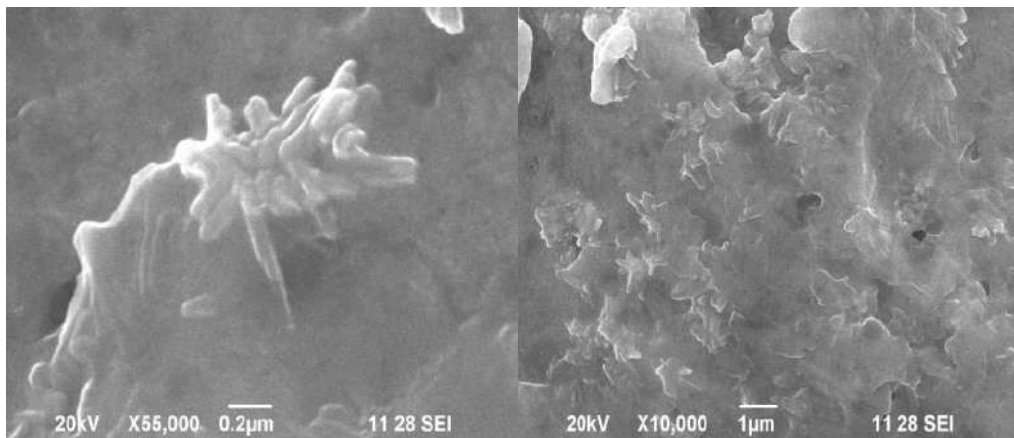


Figure 3 :SEM image of synthesized silver nanoparticles using flower extract of lablab purpureus

3.4 Anti-Microbial Activity

In the present, purpureus maxima flowers exhibited significant anti- microbial activity when compared with standard drug .It is evident from the data presented in table 1 that the sample possesses antibacterial activity. The disc diffusion method result showed the zone of inhibition for 25mg/ml as 12mm, and 10mm, for 50mg/ml showing 14mm and 12mm 75mg/ml showed 16mm and 14mm for 100mg/ml as 23mm, and 20mm,against staphylococcus aureus ,E.coli respectively when compared with standard drug Gentamicin showing 23mm, and 20mm zone of inhibition respectively . then it is evident from the data presented in table 2 that the sample possesses antibacterial activity ²⁷⁻³⁰. The above result shows that the activity of the compound of lablab purpureus maxima flower shows significant antibacterial activities .

SAMPLE		Extract 100 μ l added and Zone of inhibition (mm/ml)				
		25 μ l	50 μ l	75 μ l	100 μ l	Control
AI	<i>Staphylococcus aureus</i>	15	18	20	24	22
	<i>E.coli</i>	15	17	19	22	23

TableI: Anti-bacterial activity of lablabpurpureus maxima flower



Figure 4:Graphical representation of anti- bacterial activity of the compound of lablab purpureus maxima flowers(standard:Gentamicin, concentration 1mg/ml)

Based on the result of the above study on the lablabpurpureus maxima we conclude that the compound of lablab purpureus maxima flowers shows superior anti- bacterial activity against the following microorganisms such as *Staphylococcus aureus*. Also it justifies the claimed uses of flower parts of the lablabpurpureus maxima in the traditional system of medicine to treat various infections and diseases caused by the microbes. Antimicrobial activities are aggravated by increasing the quantity of this compound ,which can be used as an alternative for antibiotics¹⁹⁻²². Therefore, it is necessary to characterization their active compounds and should be investigated for better understanding of its safety, efficacy and prope.

3.5 Uv-Visible Spectroscopy Analysis

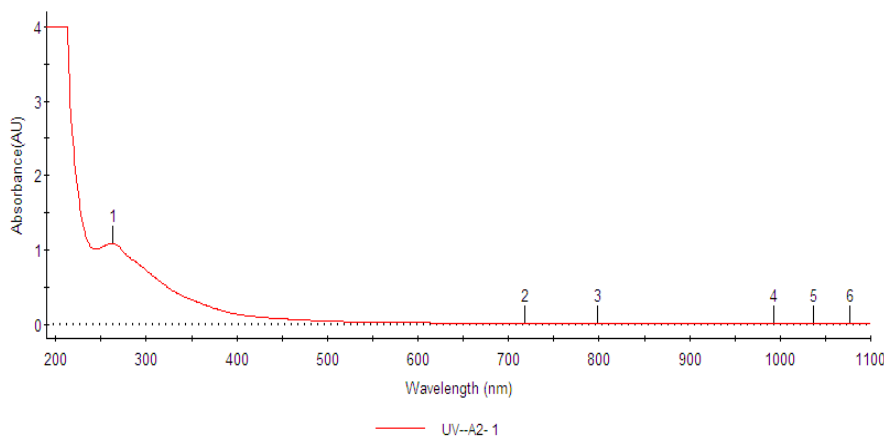


Figure:5 UV-Visible spectrum of synthesized silver nanoparticles using flower extract of winged bean

UV-Visible spectroscopy analysis showed the absorbance band of silver nanoparticles synthesized using winged bean flower extract at 262.50nm ,718.00 nm ,797.80 nm , 993.25 nm ,1036.80 nm , and 1076.60 nm which conforms the presence of poly-unsaturated and aromatic compound (Isoquinoline)

3.6 FT-IR Measurement

The winged bean related functional groups were identified Using the peak assignments. A strong peak at 3736.12 cm^{-1} was assigned to theOH stretching in alcohol group, the strong peak at 2835.36cm^{-1} was assigned to C-H stretching.²²⁻²³Alkane group, strong peak at 2312.65cm^{-1} was assigned to O =C=O Stretching Carbon-dioxide group, a strong peak at 1645.28cm^{-1} was assigned to C=N stretching Imine groups are a strong peak at 1517.98cm^{-1} was assigned to N-O stretching alk Nitro compound groups, a strong peak at 1381.03cm^{-1} was assigned to C-H Stretching Aldehyde group, a strong peak at 1220.94cm^{-1} was assigned to C-O stretching Vinyl ether group, a strong peak at 1051.20cm^{-1} was assigned to C-O stretching Primary alcohol group .

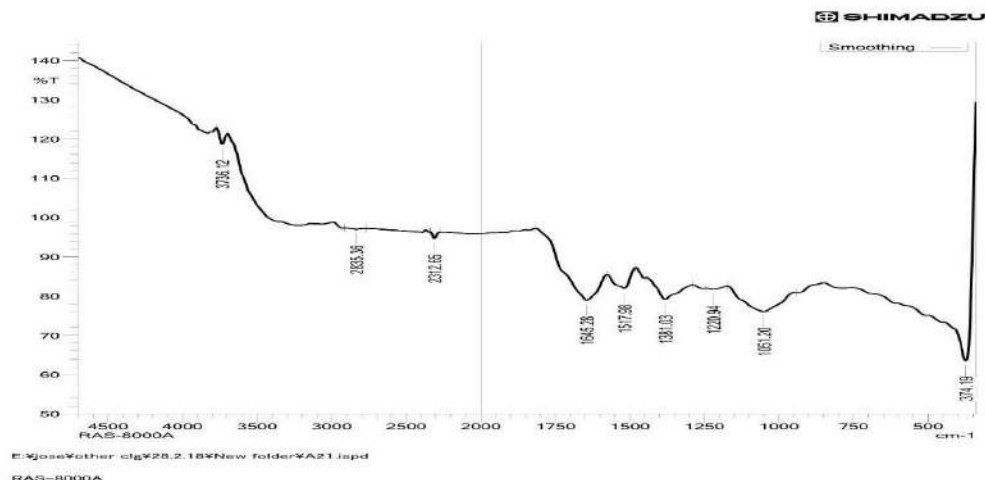


Figure 6: FT-IR Spectrum of synthesized silver nanoparticles using flower extract winged bean

3.7 Sem Analysis

SEM analysis shows uniformly distributed silver nanoparticles on the surfaces of the cells SEM analysis reveals individual spherical polydisperse²⁴⁻²⁵AgNPs as well as number of aggregates, which irregular in shape. The size of the silver nanoparticles was found to be 5-30nm, with an average size 24.25nm. the larger silver particles may be due to the aggregation of the smaller ones. ²⁵⁻²⁷

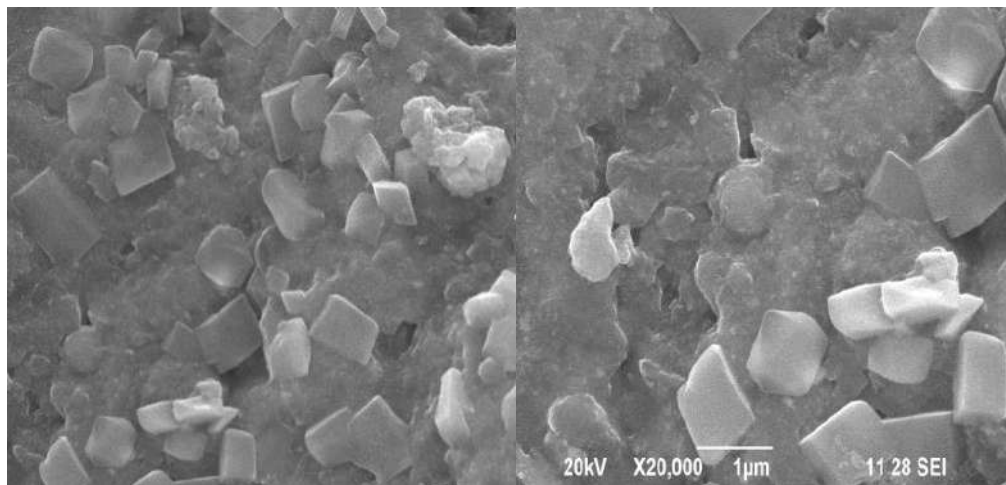


Figure:7 SEM image of synthesized silver nanoparticles using flower extract of winged bean

3.8 Anti-Microbial Activity

In the present isolated ethyl acetate fraction of winged beanflowers exhibited significant anti- microbial activity when compared with standard drug .It is evident from the data presented in table 1 that the sample possesses antibacterial activity. The disc diffusion method result showed the zone of inhibition for 25mg/ml as 12mm, and 10mm, for 50mg/ml showing 14mm and 12mm 75mg/ml showed 16mm and 14mm for 100mg/ml as 23mm, and 20mm,against *staphylococcus aureus* ,*E.coli* respectively when compared with standard drug Gentamicin showing 23mm, and 20mm zone of inhibition respectively ²⁷⁻³⁰ Then it is evident from the data presented in table 2 that the sample possesses antibacterial activity. The above result shows that the activity of the compound of winged bean maxima flower shows significant antibacterial activities

SAMPLE	Extract 100 μ l added and Zone of inhibition (mm/ml)				
	25 μ l	50 μ l	75 μ l	100 μ l	Control
<i>Staphylococcus aureus</i>	16	18	21	23	23
<i>E.coli</i>	15	18	22	26	23

Table2: Anti-bacterial activity of the compound of fabaceae maxima flower

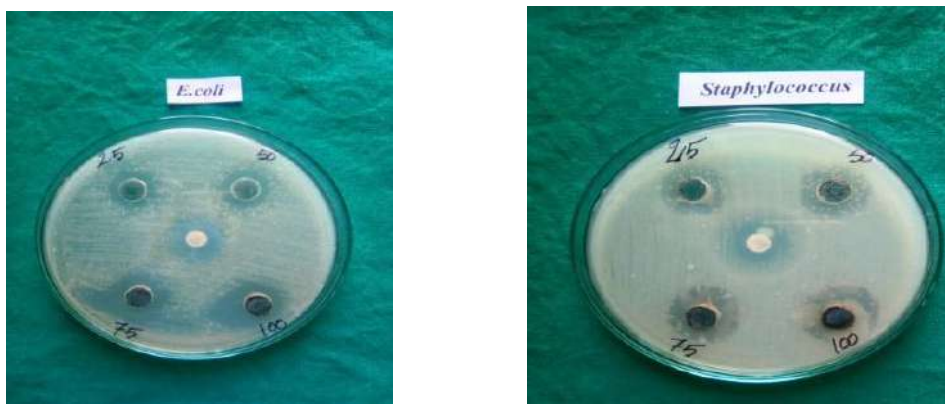


Figure8 :Graphical representation of anti- bacterial activity of the compound of fabaceae maxima flowers(standard:Gentamicin, concentration 1mg/ml)

4. CONCLUSION

Silver nanoparticles (AgNPs) were successfully obtained from bioreduction of silver nitrate solutions using lablab purpureus , and winged bean flower extracts. Owing to varying properties of these two plant species, AgNPs obtained from them also varied in size, the smallest being yield using lablab purpureus and winged bean extracts. AgNPs have been appropriately characterized using UV –vis spectroscopy, SEM, analysis. Results indicated purpureus and winged bean to be a better reducing agent in comparison to neem and lablab purpureus and winged bean flower extracts. FTIR analysis revealed the efficient capping and stabilization properties of these AgNPs . Besides ,they also aided in plants germination and growth by sequestering nutrients for them and could hence be implemented for agricultural purposes. Hence ,due to their benign and stable nature and antimicrobial property, these AgNPs may be well utilized in industrial and remedial purposes. However ,plant uptake and utilization of AgNPs require more detailed research on many issues like uptake potential of various species, process of uptake and translocation and the activities of the AgNPs at the cellular and molecular levels.

5. CONFLICT OF INTEREST

Conflict of interest declared none.

6. REFERENCES

1. C.P. Poole, F.J. Owens, *Introduction to Nanotechnology*, John Wiley & Sons Inc., New Jersey, U.S.A., (2003).
2. W.A. Goddard, *Handbook of Nanoscience, Engineering and Technology*, CRC, Boca Raton; London, (2003).
3. <http://en.wikipedia.org/wiki/Nanotechnology>
4. S. D. Meetei, Ph.D. Thesis, Department of Physics, Manipur University, Manipur, India, (2013).
5. A.K. Geim and K.S. Novoselov, *Nature Mater.*, 6 (2007) 183.
6. H.W. Kroto, J.R. Heath, S.C. O'Brien, R.F. Curl and R.E. Smalley, *Nature*, 318 (1985) 162.
7. S. Iijima, *Nature*, 354 (1991) 56.
8. K.S. Novoselov, A.K. Geim, S.V. Morozov, D. Jiang, Y. Zhang, S.V. Dubonos, I.V. Grigorieva and A.A. Firsov, *Science*, 306 (2004).
9. *Illustrated Oxford Dictionary*, Rev. Ed., Dorling Kindersley, London, (2003)
10. E.L. Wolf, *Nanophysics and Nanotechnology: An Introduction to Modern Concepts in Nanoscience*, Wiley-VCH, Weinheim, Germany, (2004).
11. D. Vogel, P. Krüger and J. Pollmann, *Phys.* 52 (1995) 14316-1431.
12. T. P. Chou, Q. Zhang, G. E. Fryxell and G. Cao, *Adv. Mater.*, 19 (2007) 2588– 2592.
13. S. Rani, P. Suri, P.K. Shishodia and R.M. Mehra, *Sol. Energ. Mat. Sol. Cells*, 92 (2008) 1639–1645.
14. L. M. Sandratskii and P. Bruno, *Phys. Rev. B* 73 (2006) 045203.
15. Y. H. Zheng and J. B. Xia, *Phys. Rev. B* 72 (2005) 195204.
16. J. Kudrnovsk' u, V. Drchal, I. Turek, L. Bergqvist, O. Eriksson, G. Bouzerar, Sandratskii and P. Bruno, *J. Phys. Condens. Matter*, 16 (2004) S5571.
17. S. A. Chambers, T. Droubay, C. M. Wang, A. S. Lea, R. F. C. Farrow, L. Folks, V. Deline, and S. Anders, *Appl. Phys. Lett.*, 82 (2003) 1257.
18. Y. Zou , Z. Qua, J. Fang, and Y. Zhang, *J. Mag. Mag. Mat.*, 321(2009) 3352.
19. J. Iqbal, B. Wang, X. Liu, D. Yu, B. He, and R. Yu, *New J. Phys.*, 11 (2009) 063009.
20. S. Ghoshal and P. S. Anil Kumar, *J. Mag. Mag. Mat.*, 320 (2008) L93.
21. K. Ueda Tabata, H. Tabata, and T. Kawai, *Appl. Phys. Lett.*, 79, 988 (2001).
22. C. Song, F. Zeng, K. W. Geng, X. B. Wang, Y. X. Shen, and F. Pan, *J. Mag. Mag. Mat.*, 309 (2007) 25.
23. .V S Sangeetha , Vanith A, Devi P, BhakyajothiV"Green synthesis of Zinc oxide nanao particle using flower extract of phyla nodiflora" Schoolar National School of leadership vol-9
24. S. Deka, R. Paricha, and P. A. Joy, *Chem. Mater.*, 16 (2004) 1168.
25. O. D. Jayakumar, I. K. Gopalakrishnan, C. Sudakar, R. M. Kadam, and S. K. Kulshreshtha, *J. Alloys Comprd.*, 438 (2007) 258
26. 26.R Elayaperumal , G Vanaja, A Vanith,VSSangeetha "Green synthesis of Glycyrhizagla silver nano particle and conformation of through Microscopy and Spectrophotometric techniques. Eurasian journal of Analytical chemistry ,2017-Feb ,1680-168.
27. 27.C. N. R. Rao and F. L. Deepak, *J. Mater. Chem.*, 15 (2005) 573.
28. 28.R. Podila, W. Queen, A. Nath, J. T. Arantes, A. L. Schoenhalz, A. Fazzio, G. Dalpian, J. He, S. J. Hwu, M. J. Skove, and A. M. Rao, *Nano Lett.*, 10 (2010) 1383.
29. 29.C.W. Bunn, *Proc. Phys. Soc., London*, 47 (1935) 835.
30. 30.A. Gosh, N. Kumari, S. Tiwari and A. Bhattacharjee, *Indian J. Phys.*, 87(11) i.(2013)1099-1104.

Antimicrobial Activity Of Mine Soil Isolate Of Actinomycetes

Dr.Surya.C, Nirmaladevi.P ,Dr.Sathy.A, Sathy.A

Dhanalakshmi Srinivasan College of Arts and Science for Women (Autonomous), Perambalur.

Abstract: Actinomycetes are a potential source of many bioactive compounds which have diverse clinical effects and important applications in medicine for treating various human diseases and disorders. The present study was performed to isolate actinomycete strains with antimicrobial activities using the selective isolation media. Four different actinomycete strains were isolated from 10 soil samples which were collected from different locations of the Salem mine area. These strains were selected based on their morphology. These were characterized and screened for antibacterial activity against 5 bacterial pathogens. The antibiotic stability was observed against *E.coli* (100%), *K.pneumoniae* (80%), *S.aureus* (80%), *S.mutans* (50%), *P.aeruginosa* (80%). 2 isolates (A2, A4) had high antimicrobial activity.

Keywords: Mine Soil Isolate, *K.pneumoniae* , *S.aureus* , *S.mutans* , *P.aeruginosa* . 2 isolates (A2, A4) had high antimicrobial activity.

I. INTRODUCTION

Microbial diversity is a major frontier and future source for the biotechnology sector. Microorganisms produced natural products that are a good source of antibiotics, including actinomycetes¹. Actinomycetes are gram-positive and slow-growing bacteria, distinguished by the development of aerial mycelium. They make mycelium from spores that anchor the substrate. In the vegetative process, the substratum hyphae have a diameter of around 0.5 to 1.0 μm and lack cross-walls. Actinomycetes have acquired prominence in recent years because of their antibiotic capacity²⁻³. Actinomycetes are a group of microbes widely distributed across the world's natural ecosystems and are especially valuable for their organic cycling role. Actinomycetes have unique bioactive metabolites, including antibiotics, enzymes, and plant growth factors. The development of multidrug-resistant pathogens requires unique antimicrobial agents at least 5000 known *Streptomyces* sp. (*Streptomyces avermitilis* and *Streptomyces verticillus*) were produced bioactive compounds⁵⁻⁶.

Antibiotic resistance in bacterial isolates was recorded since the first use of antibacterial agents. Penicillin-resistant *Escherichia coli* were the first to be discovered in 1940 to possess penicillinases that inactivated the drug penicillin, followed by the discovery of penicillin-resistant *Staphylococcus aureus* in 1944⁷. In 2008, the NDM-1 gene, encoding novel beta-lactamase enzyme capable of hydrolyzing penicillins, cephalosporins, and carbapenems was discovered in *Klebsiella pneumonia*. Bacteria possessing the gene were found to be resistant to most of the tested antibacterial agents⁸⁹.

2. MATERIALS AND METHODS

2.1 Collection of soil sample

Soil samples were collected from the different places of the Salem mine area. Samples were collected from a 2-inch depth of the earth's surface.

2.2 Isolation of Actinomycetes

Soil samples were air-dried for 1 week before isolation. This helps in decreasing the population of gram-negative bacteria. The soil suspension method described by Oskay et al. (2004) was used, where 1 g of the soil sample was taken and mixed with 100 ml of sterile distilled water. The soil suspension was shaken vigorously at room temperature (25 ± 2°C) on an orbital shaker at 200 rpm for 1 h. 200 ml of the soil suspension were pipetted and lawn onto Starch Casein Agar (SCA) (Soluble starch, 10.0 g; Casein hydrolysate, 0.3 g; KNO₃, 2.0 g NaCl, 2.0 g; K₂HPO₄, 2.0 g; MgSO₄·7H₂O, 0.05 g; CaCO₃, 0.02 g; FeSO₄·7H₂O, 0.01 g; Agar, 18.0 g; distilled water, 1000 ml; Nystatin, 100 μg/ml; ciprofloxacin, 100 μg/ml) at pH 7. A series of dilutions of the suspension from 10⁻³ to 10⁻⁶ was done with duplicates.

2.3 Morphological characterization

Gross morphology was observed after 2-3 days of growth on (SCA) agar plates by coverslip culture technique. The mycelium structure, arrangement of conidiospore and arthrosppore on the mycelium was observed through the oil immersion (100×). The observed structure was compared with the Manual and the organism was identified.

2.4 Physiological characterization

These tests were performed as described by Gordon (1966, 1967). Physiological tests included biochemical tests (Indole, MR, VP, Citrate, Nitrate reduction, Starch hydrolysis, and Gelatin hydrolysis) and Carbon source utilization (Starch, Dextrose, Fructose, and Maltose).

2.5 Collection of clinical samples

Purulent materials were collected aseptically with the aid of sterile swab sticks from forty patients with different wounds infection at Namakkal Dist in surrounding hospitals. Swab samples were inoculated in peptone water and incubated at 37°C.

2.6 Bacterial Isolation and Identification

Culture plates of Eosin Methylene Blue Agar, MacConkey Agar Nutrient Agar, Blood Agar, and Mannitol Salt Agar were used. The swab sticks used for the collection of the samples were streaked directly on the labeled agar plates and incubated at 37°C for 24 h. After incubation, cultures were examined for significant growth. Subcultures were then made into plates of nutrient agar and incubated for another 24 h. The primary identification of the bacterial isolates was made based on colonial appearance and pigmentation. Biochemical tests were performed to identify microbes. Biochemical tests applied were standard catalase test, citrate utilization, coagulase, oxidase, Methyl red, Voges-Proskauer, Indole production, motility, Glucose, sucrose, maltose, lactose, Characterization, and identification of the isolates was done using the methods of Cowan (1985), Fawole and Oso's (1988) and Cheesbrough .

2.7 Gram staining

Bacterial smears of 16-18 hrs old cultures were made on clean grease-free slides, heat-fixed, and stained as follows. The slide was flooded with crystal violet solution for a minute, drained, and rinsed with water; followed by grams iodine solution for one minute, drained, and rinsed with water. Decolorized with ethyl alcohol for 30 sec and later counterstained with safranin for one minute and observed under an oil immersion microscope.

3. RESULTS

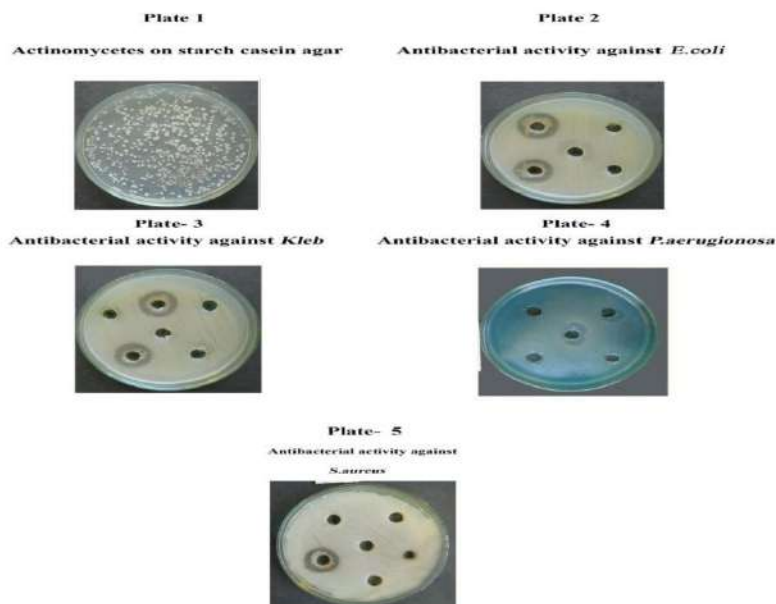
3.1 Isolation of actinomycete

This study was performed to isolate actinomycete strains with antimicrobial activities using the selective isolation media. Four different actinomycete strains were isolated from 10 soil samples collected from different locations of Salem.

Table- I - Screening of antibacterial substance producing Actinomycetes

S.no	Actinomycetes	Bacterial isolates			
		<i>S.aureus</i>	<i>Kleb</i>	<i>P.aeuroginosa</i>	<i>E.coli</i>
1.	A1	-	-	-	-
2.	A2	+	+	+	-
3.	A3	-	-	+	-
4.	A4	+	+	+	+
5.	A5	-	-	-	-

All of these strains were collected by using Starch-casein-nitrate-agar media supplemented with nystatin (100 μ g/ml) to inhibit fungal growth and ciprofloxin (100 μ g/ml) to inhibit the bacterial growth. Several colonies were found from each plate which was shown in plate I. Colonies selected from each plate were 2 to 3 based on colony appearance which is shown in plate I. Colonies having characteristic features such as powdery appearance with convex, concave or flat surface and color ranging from white, gray to pinkish and yellowish were selected. Colonies observed on the 3rd and 4th days were eliminated because actinomycetes are considered slow growers (Currie, 2006). Furthermore, bacterial configurations same as actinomycetes were accepted from gram staining. Thirty-five selected isolates were examined microscopically and identified by their morphological and cultural characteristics. All isolates were inoculated in ISP2 agar media and store at 4°C for further investigation



3.2 Isolation of bacterial isolates from wound samples

Bacterial isolates were obtained from wound samples by selective media and biochemical tests. Totally 20 isolates of 5 different bacterial isolates were obtained such as *E.coli*, *S.aureus*, *S.mutans*, *P.aeruginosa*, and *K.pneumoniae* shown in Figures 2 and 3 and Table I. Among them, the highest occurrence was *S.aureus* and *S.mutans* (30%) second most *K.pneumoniae* (20%) and followed by *Pseudomonas* (15%) and *E.coli* (5%).

3.3 Antibacterial activity of actinomycetes against wound isolates.

All isolates were subjected to antibacterial activity wound isolates such as *K.pneumoniae*, *S.mutans*, *E.coli*, *S.aureus*, and *P.aeruginosa* were shown in figure 1. Among the four isolates of actinomycetes 2 (71.4%) isolates had antimicrobial activity against all bacterial isolates. Out of 2 actinomycetes, 96% was active against *S.mutans* followed by 24% of actinomycetes against *K.pneumoniae*, 20% to *P.aeruginosa*, 16% to *Staphylococcus aureus*, and 8% of isolates active against *E.coli*. This is the lowest percentage of results in our study which means our test pathogen of *E.coli* was high resistance to actinomycetes. In this study, most of the actinomycetes were active against gram-positive bacterial pathogens compared to gram-negative pathogens.



4. DISCUSSION

In the present investigation, actinomycetes were isolated from soil samples collected from different places in mine soil area, Salem, India, which are large and diverse, for the isolation of potent and broad-spectrum antibiotic-producing actinomycetes¹⁰⁻¹¹. Totally 4 isolates of actinomycetes were observed from soil samples by using Starch-casein-nitrate agar media supplemented with nystatin (100 μ g/ml) to inhibit fungal growth and ciprofloxin (100 μ g/ml) to inhibit the bacterial growth. This media is very specific for the isolation of actinomycetes, as only organisms (mostly actinomycetes) that are capable of degrading the polymers in the media can grow¹². Both primary and secondary screening methods were used to screen actinomycetes for antibacterial activity. The first screening was used to select the antibacterial isolates and determine the range of microorganism that was sensitive to the antibiotic. The secondary screening method was crucial to select the isolates for further studies. The result of the screening revealed that four isolates were against bacterial culture. But the best strain was found to be A2 and A4. Nutritional requirements of *Streptomyces* play an important role during the metabolite synthesis process. Amongst various nutritional requirements, carbon sources and nitrogen sources are generally regarded as important factors of metabolism, and several examples of the production of metabolites in media with optimized contents of these components are also described in the literature¹³⁻¹⁴. In this current study, the crude substance was highly active against multidrug resistance *S.aureus*, especially methicillin resistance isolates (MRSA). The previous studies of also observed the anti- MRSA isolates of actinomycetes from soil samples. The present study result was well correlated with previous studies of They reported that actinomycetes species usually show good activity against Gram-positive bacteria, but usually activity against Gramnegative bacteria¹⁵⁻¹⁶. In also reported antagonistic activity of actinomycetes against multidrug drug resistance of gram-positive isolates. Several authors have screened soil samples collected from different parts all over the world for AAPMs as Brazil in the study of ; Morocco India¹⁷. Our isolates were most active against gram-positive bacteria (*Staph. aureus*) than gram-negative bacteria. The reason for different sensitivity between gram-positive and gram-negative bacteria could be ascribed to the morphological differences between these microorganisms, gram-negative bacteria having an outer polysaccharide membrane carrying the structural lipopolysaccharide components¹⁸. The crude extract of *Actinomyces* showed antibacterial activity against several species of human pathogens including both Gram-positive and Gram-negative bacteria. These findings indicated that our produced substance might be the alternative antimicrobial substance as a tool for controlling human diseases. A commercial product containing *Actinomyces* or its effective metabolite (s) is suggested to avoid some of the diseases in humans¹⁹. In the present study, the actinomycetes isolated from soil samples of Salem, Tamil Nadu showed antibiotic activity against Gram-positive and Gram-negative bacteria. These findings indicated that our produced substance might be the alternative antimicrobial substance as a tool for controlling human diseases²⁰⁻²¹.

5. CONFLICT OF INTEREST

Conflict of interest declared none.

6. REFERENCE

1. KasarlaSarika^aGattuSampath^bRasiravathanahalliKaveriyappaGovindarajan^cFuadAmeen^dSuaadAlwakeel^eHussah I.Al Gwaiz^eThampuRaja Komuraiah^aGangallaRavi^a. Antibacterial activities of Actinomycetes isolate collected from soils of Rajshahi, Bangladesh. *Biotechnology Research International*. 8: 1-6
2. Moellering, R.C. (2010). NDM-I- A cause of worldwide concern. *New England Journal of Medicine* 363(25), 2377-2379.
3. Okami, Y. and Hotta, K. (1988). Search and discovery of new antibiotics In Goodfellow, M., Williams, S. T. and Mordarski, M. (eds). *Actinomycetes in Biotechnology*. Academic Press, Inc., San Diego, Calif., pp. 37-67.
4. Janso, J.E. and Carter G.T. (2010) Phylogenetically Unique Endophytic Actinomycetes from Tropical Plants Possess Great Biosynthetic Potential. *Appl. Environ. Microbiol.* 77: 4377-4386
5. Sateesh V. Naikpatil, Rathod J.L. (2011). Antimicrobial and cytotoxic activity of Actinomycetes from Karwar Coast of India. *World Journal of Science and Technology*. 1(1): 07-10.
6. Sree S. Kumar, Rosamma Philip, Achuthankutty C.T. (2006).Anti Demain and J.E. Davies viral property of marine Actinomycetes against White spot syndrome virus in penaeid shrimps. *Current Science*. 91(6): 807-811.
7. Yu, J., Q. Liu, X. Liu, Q. Sun, J. Yan, X. Qi, and S. Fan, (2008).Effect of liquid culture requirements on antifungal antibiotic production by *Streptomyces rimosus* MY02. *Bioresour. Technol.* 99, 2087-2091.
8. Tara Devi Gurung, Chringma Sherpa, Vishwanath Prasad Agrawal, Binod Lekhak (2009). Isolation and characterization of antibacterial Actinomycetes from soil samples of Kalapatthar, Mount Everest region. *Nepal Journal of Science and Technology*. 10: 173-182
9. Dhananjeyan, N. Selvan and K. Dhanapal, (2010). Isolation, Characterization, Screening, and Antibiotic Sensitivity of Actinomycetes from Locally (Near MCAS) Collected Soil Samples. *Journal of Biological Sciences*, 10: 514-519
10. Atta MA, Ahmad MS(2009). Antimycin-A antibiotic biosynthesis produced by *Streptomyces* . AZ-AR-262: taxonomy, fermentation, purification, and biological activities. *Aust J Basic Sci*; 3(1): 126-135.
11. Zu LH, Jiang Y, Li WJ, Wen ML, Li MG, Jiang CL (2005). *Streptomyces roseoalbus* sp. nov., an actinomycetes isolated from soil in Yunnan, China. *Antonie Van Leeuwenhoek* 87:189- 194.
12. M. N. Nadagouda and R. S. Varma, "Green and controlled synthesis of gold and platinum nanomaterials using vitamin B2: density-assisted self-assembly of nanospheres, wires, and rods," *Green Chemistry*, vol. 8, no. 6, pp. 516-518, 2006.
13. T. Hyeon, "Chemical synthesis of magnetic nanoparticles," *Chemical Communications*, vol. 9, no. 8, pp. 927-934, 2003.
14. R. Karmhag, T. Tesfamichael, E. W'ackelg'ard, G. A. Niklasson, and M. Nygren, "Oxidation kinetics of nickel particles: comparison between free particles and particles in an oxide matrix," *Solar Energy*, vol. 68, no. 4, pp. 329-333, 2000.

14. A.Mariam, M. Kashif, S. Arokiyaraj, et al., "Bio-synthesis of NiO and Ni nanoparticles and their characterization," *Digest Journal of Nanomaterials and Biostructures*, vol. 9, no. 3, pp.1007–1019, 2014.
15. Saxena, A. Kumar, and S. Mozumdar, "Ni-nanoparticles: an efficient green catalyst for chemo- selective oxidative coupling of thiols," *Journal of Molecular Catalysis A: Chemical*, vol. 269, no. 1-2, pp. 35–40, 2007.F. Alonso, P. Riente, and M. Yus, "Hydrogen-transfer reduction of carbonyl compounds promoted by nickel nanoparticles," *Tetrahedron*, vol. 64, no. 8, pp. 1847–1852, 2008.
16. Dhakshinamoorthy and K. Pitchumani, "Clay entrapped nickel nanoparticles as efficient and recyclable catalysts for hydrogenation of olefins," *Tetrahedron Letters*, vol. 49, no. 11, pp.1818–1823, 2008.
17. F. Alonso, P. Riente, and M. Yus, "Wittig-type olefination of alcohols promoted by nickel nanoparticles: synthesis of polymethoxylated and polyhydroxylated stilbenes," *European Journal of Organic Chemistry*, vol. 2009, no. 34, pp. 6034–6042, 2009.
18. F. Alonso, P. Riente, and M. Yus, "Alcohols for the α -alkylation of methyl ketones and indirect aza-Wittig reaction promoted by nickel nanoparticles," *European Journal of Organic Chemistry*, vol. 2008, no. 29, pp. 4908–4914, 2008.
19. X.-K. Li, W.-J. Ji, J. Zhao, S.-J. Wang, and C.-T. Au, "Ammonia decomposition over Ru and Ni catalysts supported on fumed SiO₂, MCM-41, and SBA-15," *Journal of Catalysis*, vol. 236, no. 2, pp. 181–189, 2005.
20. Y. Li, B. Zhang, X. Xie, J. Liu, Y. Xu, and W. Shen, "Novel Ni catalysts for methane decomposition to hydrogen and carbon nanofibers," *Journal of Catalysis*, vol. 238, no. 2, pp. 412–424, 2006.

Screening Of Enzymes Inhibitors From Marine Bacterial Dynamics

Dr.Gajalakshmi P*, Nitha V Ravi, Raja A And Helanjenifer I

PG and Research Department of Microbiology, Dhanalakshmi Srinivasan College of Arts and Science For Women (Autonomous), Perambalur-621 212, Tamil Nadu, India

Abstract: Decreasing the reabsorption of glucose in the intestine Acetylcholinesterase [AChE] inhibitors or anticholinesterases that reduce the activity of enzyme acetylcholinesterase that degrades the neurotransmitter acetylcholine in the brain is the therapeutic targets currently introduced in the management of type 2 DM. For neurodegenerative diseases like Alzheimer's and Parkinson's, the inhibitors have a significant pharmacological role. Therefore the present study aimed to screen the effective marine bacterial isolates capable to produce enzyme inhibitors specific for amylase and AchE. The research aims to collect marine water, isolate marine bacteria, to characterize the isolated bacteria, produce secondary metabolite, evaluate AChE inhibition, to quantify the amylase inhibition activity of metabolite.

Keywords: Alzheimer's disease, Acetylcholinesterase, the neurotransmitter acetylcholine

I. INTRODUCTION

1.1 Marine Bacterial Dynamics

The water, sediments, and marine organism in the marine environment provide a unique environment to bacteria. The presence of physical factors such as high salinity, high pressure, acidic pH, the extreme temperature can create a unique environment for microorganisms to produce unique secondary metabolites by the microorganisms. Isolation and identification of natural products with biological properties was the main interest in the marine environment for which numerous organisms and chemical structures were studied¹. Zebrafish requires minimal Labor while rodent models have dominated to date, however, these models are not suitable for large-scale drug screening. The usage of rodents has been more limited due to ethical issues². In the field of Cancer research also the small molecular compounds in marine have contributed. Actinomycetes are gram positive filamentous fungus like bacteria. About 7600 compounds have been produced from Streptomycetes alone. When compared to other microorganisms, marine actinomycetes have the ability to produce secondary metabolites and have a wide nature of pharmacologically properties like antitumour, anti-inflammation³. Apoptosis can be caused in DNA damage or the growth of endothelial cells can be inhibited in cell cycle during mitosis by the action of angiogenesis inhibitors directly on the endothelial cells or other growth factors of angiogenic cascade⁴. Unique molecules such as highly halogenated terpenes were shown to produce from large showy creatures of the sea, such as red algaesponges, and soft corals⁵. The exploration of the extent and diversity of rich terrestrial groups of bacteria in terms of number and diversity of natural product structures; Actinomycetes is going on⁶ natural products of biomedical significance that structurally resemble compounds produced by terrestrial microorganisms have been seen to be harbor in marine microorganisms such as sponges, tunicates⁷.

1.2 Marine Microbial Metabolites

Most of the antibiotics used in agriculture are from the genus Streptomyces which have shown antibacterial effects⁸. Even after treatment with certain chemicals, the spores of rare actinomycete genera including Streptosporangium and Microbispora can remain resistant⁹. Breakdown and recycling of organic compounds. In addition, they play a significant role in the mineralization of organic matter, immobilization of mineral nutrients, fixation of nitrogen is done by actinomycetes, and recycling of organic compounds. In addition, they play a significant role in mineralization of organic matter, immobilization of mineral nutrients, fixation of nitrogen⁸. Large population which constitutes variety organisms such as the complex marine still need to have more studies¹⁰ staurosporinone, salinosporamide A are among the rare and potent bioactivity¹¹. For the metagenomic study of marine microbes, a less cost but effective method is now gaining popularity-Pyrosequencing¹². If study is conducted for the rare marine actinomycetes, it can lead to the discovery of several secondary metabolites¹³.

1.3 Enzymes

To study the activity of plant membrane enzyme chlorophyllase, Nowak et al. discovered the EMMA method which is less cost¹⁴. By targeted therapy, we can treat the tumor, CNS diseases, cardiovascular diseases¹⁵. Using background absorption, a fluorescence signal can be used for the samples in the detection of various diseases¹⁶. An efficient approach for the fabrication of enzymes was given by¹⁷. The in-capillary enzyme assay was developed which is sensitive since the background arises from the enzyme and removal of culture media is also possible¹⁸. Lin et al discovered dual-enzyme co-IMER through which multitargeted enzymes could be demonstrated¹⁹. Streptosporangium and Microbispora spores can resist treatment by various chemicals⁹.

2. MATERIALS AND METHOD

2.1 Isolation of bacteria²²

Marine water is collected from a Nagapattinam beach. To isolate marine bacterial seawater collected aseptically. One mL of water mixed with 9mL distilled water and serially diluted upto 10^7 . 1 mL of 10^7 dilutions was plated on nutrient agar prepared

with 50% seawater. Plates were incubated at 37° C and colony morphology was recorded after 48 h incubation.

2.1.1 Selection of Strain

Microorganisms from agar plates were selected based on colony morphology and subsequently streaked on a modified nutrient agar plate and medium composition was comprised of the following: 0.1 g; Yeast extract 3.0 g; peptone 5 g; NaCl 10.0 g; Glucose 4.0 g; Agar 20.0 g; Distilled water 50 mL; sea water 50mL pH 7.2–7.4.

2.1.2 The physiological and biochemical characteristics

Each isolate was examined based on colony nature, color, diffusible pigment. The bacteria were grown on agar plates for 2 days at 30°C. following biochemical characters were performed

2.2 Biochemical characters²³

2.2.1 Gram's Staining

A preliminary Gram staining was performed to determine the likely organism present. A loopful of organisms was taken from a nutrient agar plate and a smear was made out of it on a glass slide. First, crystal violet (primary stain) was added and left for one minute. After the stipulated time, the slide was washed with distilled water. Secondly, Gram's iodine a mordant stain were added and left for one minute. Again the slide was washed with distilled water and then Decolorization with organic solvents like ethanol or acetone was added in drops to remove the primary stain. Again the slide was washed with distilled water. Finally, secondary stain like safranin was added. After washing and air drying of the slide, it was microscopically observed for the morphology of the organism.

2.2.2. Indole Test

About 2 to 3 ml of peptone water culture was taken in a test tube. Then, 0.5 ml of Kovac's reagent was added into the tube. Then the results were observed for the record.

2.2.3. Methyl Red Test

48 hrs of glucose phosphate culture was taken in a sterile test tube. Then one or two drops of methyl red alcoholic reagent were added. Then the results were observed for the record.

2.2.4. Voges-Proskauer Test

A loopful of culture was inoculated into glucose phosphate broth for 48 hrs. After incubation, Barritt's A and B reagent were added and the results were recorded.

2.2.5. Citrate Utilization

Sterile Simmoncitare agar slant prepared and autoclaved. Slants were prepared by dispensing a 5 ml agar into a test tube. Agar slant tube is inoculated with test culture. Slant kept incubation for 48h.

2.2.6. Catalase Test

Catalase acts as a catalyst in the breakdown of hydrogen peroxide into oxygen and water. The organism was taken in the sterile glass rod and was immersed into the hydrogen peroxide solution. Observed for immediate bubbling and recorded the result.

2.2.7. Oxidase test

The enzyme oxidase when reacts with the reagent N, N- tetramethylparaphenylenediaminedihydrochloride gives colored product indophenol. The bacterial culture was rubbed over a reagent impregnated filter paper disc using a sterile loop. The color change was observed within 10 seconds. The purple color change of the disc indicates oxidase-positive.

2.3 Production and Extraction of metabolite²⁴

Seed cultures were prepared by inoculating bacterial spores into the NB medium (50 mL) and grown at 30°C for 2–3 days with shaking at 200 RPM. The seed cultures were used for mono and co-culture experiments. Monoculture production was carried out on Mineral salt broth, with seawater and trace elements. After 72 h shaking incubation cell-free extract of culture filtrate was mixed with an equal volume of ethyl acetate and compound was extracted after 24 h.

2.4 Amylase inhibition²⁵

Briefly, 0.2ml of 5mg/mL concentration of extracted microbial metabolite made up to 0.2 ml with distilled water, and 400 μ L of starch solution were mixed. The reaction started by the addition of 200 μ L of the enzyme solution (pancreatic extract) and the tubes were incubated at 25°C for 5 min at room temperature. 200 μ L of DNS color reagent (50.68 sodium-potassium tartrate dissolved in 70 mL of 2 M NaOH with 0.026 mM of 3,5-dinitro salicylic acid) and placed in a water bath maintained at 85–90°C for 15 min. The mixture in each tube was diluted with 900 mL of distilled water and the absorbance was measured at 540 nm. For each concentration of the extract used, blank incubation was prepared by replacing the enzyme solution with distilled water (200 μ L) at the start of the reaction, to correct for the absorbance generated by the plant extract. Control incubations, representing 100% enzyme activity,

Inhibition (%) = 100 – % reaction (at min), where % reaction = mean glucose in sample \times 100/mean glucose in control.

2.5 β -Galactosidase Inhibitory Assay²⁶

2- Nitrophenyl β -D-Galactopyranoside as substrate, which is hydrolyzed by β -Galactosidase to release 2-nitrophenyl (colored agent; which can be monitored at 410 nm). Briefly, a mixture of 150 μ L of the samples at different concentrations (0.5–5 mg/mL) and 100 μ L of sodium phosphate buffer 0.1 M (pH=7.6) containing the enzyme β -Galactosidase solution (μ L *E.coli* cell lysate) was incubated at 37°C for 10 min. After pre-incubation, 200 μ L of galactose solution 1 M in sodium phosphate buffer 0.1 M (pH=7.6) was added. The reaction mixtures were incubated at 37°C for 30 min. After incubation, 1 mL of 0.1 M of Na₂CO₃ were added to stop the reaction and the absorbance was recorded at 405 nm using the spectrophotometer. The β -Galactosidase inhibitory activity was expressed as percentage inhibition and calculated using C-T/CX10

2.6 AchE inhibition

To determine the Acetylcholine esterase inhibition from Ellman et al. (1961)²⁰ were modified and applied. An electronic multichannel pipette (Eppendorf, USA) was used to transfer the exact 10 μ L of enzyme solution to 0.5 M Phosphate buffer pH 7 further mixed with 25, 50, and 100 μ L of tested compounds in a solution diluted to final volume 0.2 mL. This was followed by adding 20 μ L of acetylthiocholine iodide (0.4 mM) and DTNB (Sigma-Aldrich, USA) (0.3 mM) to the enzyme solution to observe the reaction. Yellowish or colorless solution was observed during reaction for 30 minutes at room temperature. Changes in absorbance were recorded at 412 nm. Enzyme concentrations used were within the linear range of their toxicity activity. Amantadine is used as a standard drug. Tube without test/standard used control.

Abs of control(C) – Test / C \times 100

3. RESULTS AND DISCUSSION

Bacterial colonies on Agar plates showed 32×10^7 CFU (colony forming unit)/mL of marine water. Most of the colonies were recorded after 24 h. based on colony morphology (Table 1) colonies were designated as marine bacteria 1-5 (MB1-5). Totally five different colonies were selected (plate 1) and sorted out gram staining. MB1-3 were Grams negative rod and only oxidase-positive strains among 5 tested bacterial colonies. MB4 is a Gram-positive rod whereas MB5 is Gram-positive cocci. The biochemical character (table 2; plate 2) reveals except MB1-2 all are indole positive and these two were VP positive. All 5 were MR and catalyze. except for MB1 and MB5, all are utilized citrate positive in nature. During the primary screening, among the five bacterial isolates from marine water the genera were *Pseudoalteromonas* spp, *Halomonas* spp, *Pseudomonas* spp, *Bacillus* sp, and *Enterococci* sp. Members of *Pseudoalteromonas* are characteristically Gram-negative, rod-shaped isolated²¹.

Table 2. Colony nature and biochemical characters

Biochemical test	MB1	MB2	MB3	MB4	MB5
Colony nature	Circular Pale Pink	Irregular yellow tint	Entire Fluorescent green	Rhizoidal white	Punctiform translucent
Gram stain	-rod	-rod	-rod	+rod	+cocci
Indole	-	-	+	+	+
MR	+	+	+	+	+
VP	+	+	-	-	-
Citrate	-	+	+	+	-
Catalase	+	+	+	+	+
Oxidase	+	+	+	-	-
Genera	<i>Pseudoalteromonas</i> sp	<i>Halomonas</i> sp	<i>Pseudomonas</i> sp	<i>Bacillus</i> sp	<i>Enterococci</i> sp

Plate 1. Isolated marine bacteria



Plate 2. Biochemical characteristics Oxides testCatalase test

Indoletest
Enzyme inhibition



Cholinesterases (ChEs) are serine hydrolases that catalyze the hydrolysis of choline esters and are classified according to their substrate specificities. acetylcholine acetylhydrolase or acetylcholinesterase from brain extract activity was retained in control and inhibited on the test(plate 3). The percentage of inhibition was calculated and represented figure 1. Isolate MB3 and MB 4 belongs to *Pseudomoanssp* and *Bacillus* sp have shown 63% inhibition which is equal to standard drug. The galactosidase inhibition was inhibited by isolating MB2 *Halomonassp* metabolite only (table 3). Activity at amylase inhibition among 5 bacterial compounds was found at 100 μ g(Fig 2a-c). enzyme treated with sample and standard showed a decreased level of sugar. The concentration of sugar is estimated from the standard and given in figure 2b. From the number of sugars, the enzyme inhibition was calculated and given in figure 2c. the data reveals isolate MB1, MB2 and MB5 have 71 % inhibition of amylase activity close to standard acarbose inhibition (80%). It would be expected that amylase inhibitors should possess a sugar-like structure e.g. acarbose.

Figure 1. AchE inhibition

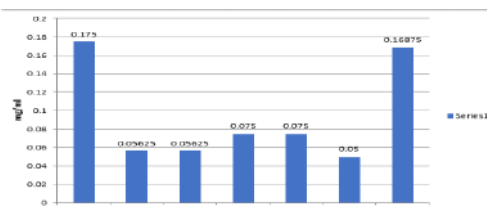


Figure 2 a. standard sugar

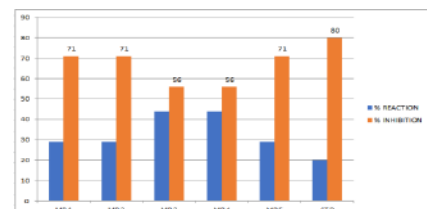


Plate 3.AchE inhibition test



4. SUMMARY AND CONCLUSION

Besides antimicrobial activity, microbial metabolite are important sources of bioactive molecules with acetylcholinesterase and amylase inhibition activity. In this research, five marine associated bacteria were isolated and found to be the genera of *Pseudoalteromonassp*, *Halomonassp*, *Pseudomoanassp*, *Bacillus* sp, and *Enterococci* sp. Out of 5 isolates *Pseudomoanassp* and *Bacillus* sp showed promising acetylcholinesterase enzyme inhibition. Likewise metabolite of *halomonassp* showed galactosidase inhibitory activity. Isolates *Pseudoalteromonassp*, *Halomonassp* and *Enterococci* sp have given maximum 71% amylase inhibition activity. The study concludes marine bacterial isolate as alternate sources for prospective production of such inhibitors. AChE inhibitors are potential therapies for Alzheimer's disease. Overall, the strain *Pseudoalteromonassp* possesses a wide spectrum of enzyme inhibitory, which affords the production of significant bioactive antidiabetic and Alzheimer's drug as potential pharmacological agents.

5. CONFLICT OF INTEREST

Conflict of interest declared none.

6. REFERENCES

- Blunt, J. W., Carroll, A. R., Copp, B. R., Davis, R. A., Keyzers, R. A., and Prinsep, M. R. (2018). Marine natural products. *Nat. Prod. Rep.* 35, 8–53.
- Lidster K, Jefferys J.G, Blumcke I, Crunelli V, Flecknell P, Frenguelli B.G, Gray W.P, Kaminski R, Pitkanen A(2016). Opportunities for improving animal welfare in rodent models of epilepsy and seizures, *J. Neurosci. Methods* 206:2–25.
- Mayer A.M, Rodríguez A.D, Berlinck R.G, Hamann M.T (2007) Marine pharmacology in 2003–4: marine compounds with anthelmintic antibacterial, anticoagulant, antifungal, anti-inflammatory, antimalarial, antiplatelet, antiprotozoal, antituberculosis, and antiviral activities; affecting the cardiovascular, immune and nervous systems, and other miscellaneous mechanisms of action, *Comp. Biochem. Physiol* 145:553–581
- Jeltsch M, Saharinen P, Alitalo K(2013). Receptor tyrosine kinases mediated angiogenesis, *Cold Spring Harb.Perspect.Biol* 5a009183.
- Suzuki M, Vairappan C.S(2005). Halogenated secondary metabolites from Japanese species of the red algal genus Laurencia (Rhodomelaceae, Ceramiales). *Curr.Top. Phytochem* 7:1–34.
- Piel, J. (2004). Metabolites from symbiotic bacteria. *Nat. Prod. Rep.* 21:519–538.
- Fenical W, Jensen P.R.(2006).Developing a new resource for drug discovery: marine actinomycete bacteria. *Nat Chem Biol*2:666–73
- Ramesh S, Rajesh M, Mathivanan N(2009). Characterization of a thermostable alkaline protease produced by marine *Streptomyces fungicidicus* MML1614. *Bioprocess Biosyst Eng*32:791–800.
- Khanna M, Solanki R, Lal R(2011). Selective isolation of rare actinomycetes producing novel antimicrobial compounds. *Int J Adv Biotechnol Res*2:357–75.
- Nowak P, Michalik M, Fiedor L(2013). Capillary electrophoresis as a tool for a cost- effective assessment of the activity of plant membrane enzyme chlorophyllase, *Electrophoresis* 34:3341–3344.
- Rath C.M, Janto B, Earl J, Ahmed A, Hu F.Z, Hiller L(2011). Meta-omic characterization of the marine invertebrate microbial consortium that produces the chemotherapeutic natural product ET-743. *ACS Chem Biol*6:1244–56.
- Jensen P.R, Williams P.G, Oh D.C, Zeigler L, Fenical W(2007). Species-specific secondary metabolite production in marine actinomycetes of the genus *Salinispora*. *Appl Environ Microbiol*73:1146–52.
- Kennedy J, Flemer B, Jackson S.A, Lejon D.P.H, Morrissey J.P (2010). Marine metagenomics: new tools for the study and exploitation of marine microbial metabolism. *Mar Drugs*8:608–28.
- Jensen P.R(2010). Linking species concepts to natural product discovery in the post- genomic era. *J Ind Microbiol Biotechnol*37:219–24.
- Zhang J.M, Yang P.L, Gray N.S(2009). Targeting cancer with small molecule kinase inhibitors, *Nat. Rev. Cancer* 9:28–39.
- Lefkowitz R.B, Schmid Schönbein G.W, Heller M.J(2010). Whole blood assay for elastase, chymotrypsin, matrix metalloproteinase-2, and matrix metalloproteinase-9 activity, *Anal. Chem.* 82:8251–8258.
- Mu X, Qiao J, Qi L(2014). Construction of a D-amino acid oxidase reactor based on magnetic nanoparticles modified by a reactive polymer and its application in screening enzyme inhibitors, *ACS Appl. Mater Interfaces*, 6:12979–12987.
- Harada A, Sasaki K, Kaneta T(2016). Direct determination of lignin peroxidase released from *Phanerochaete chrysosporium* by in-capillary enzyme assay using micellar electrokinetic chromatography, *J. Chromatogr. A* 1440: 145–149.
- Lin P, Zhao S, Lu X(2013). Preparation of a dual-enzyme co-immobilized capillary microreactor and simultaneous screening of multiple enzyme inhibitors by capillary electrophoresis, *J. Sep. Sci.* 36:2538–2543.
- George L, Ellman, K. Diane Courtney, Valentino Andres, Robert M. Featherstone, A new and rapid colorimetric determination of acetylcholinesterase activity, 1961 *Biochemical Pharmacology*, 7(2):88–95 ISSN 0006-2952.
- Sánchez-Porro C, Kaur B, Mann H, Ventosa A. *Halomonas titanicae* sp. nov., a halophilic bacterium isolated from the RMS Titanic. *Int J Syst Evol Microbiol*, 2010, 60:2768–7274. pmid:20061494
- Agung Dhamar Syakti, Priyati Lestari, Satya Simanora, Lilik Kartika Sari, Febrianti Lestari, Fadliyah Idris, Teguh Agustiadi, Syafir Akhlus, Nuning Vita Hidayati, Riyanti. Culturable hydrocarbonoclastic marine bacterial isolates from Indonesian seawater in the Lombok Strait and Indian Ocean. 2019 *Heliyon* 5(5)e01594, ISSN 2405-8440.
- Cowan, Stee's, Manual for the identification of Medical bacteria 3rd Edn, Cambridge University Press, 1993

24. Rajan BM, Kannabiran K. Extraction and Identification of Antibacterial Secondary Metabolites from Marine Streptomyces sp. VITBRK2. *Int J Mol Cell Med.* 2014;3(3):130-137.
25. Unnikrishnan PS, Suthindhiran K, Jayasri MA. Alpha-amylase Inhibition and Antioxidant Activity of Marine Green Algae and its Possible Role in Diabetes Management. *Pharmacogn Mag.* 2015;11(Suppl 4):S511-S515. doi:10.4103/0973-1296.172954
26. Marianna Turkiewicz, Józef Kur, Aneta Białkowska, Hubert Cieśliński, Halina Kalinowska, Stanisław Bielecki. Antarctic marine bacterium *Pseudoalteromonas* sp. 22b as a source of cold-adapted β -galactosidase. *Biomolecular Engineering.* 2003 20(4-6):317-324.

Ros Mediated Apoptotic Effect Of L-Asparaginase Isolated From *Aspergillus niger* on Pancreatic Cancer Cell Line Rin-5f

Sudha N¹, Anandharaj B²

Research Scholar, Department of Microbiology, M.R. Govt. College (Affiliated to Bharathidasan University), Mannargudi-614 001, Thiruvarur Dt, Tamilnadu, India¹
Assistant Professor, Department of Microbiology, M.R. Govt. College (Affiliated to Bharathidasan University), Mannargudi-614 001, Thiruvarur Dt, Tamilnadu, India²

Abstract: Pancreatic cancer is lethal cancer worldwide and ranked to be fourth among cancer-led death. Late prognosis and drug resistance create major clinical challenges, which lead the way for alternative treatment strategies. L-asparaginase catalyzes asparagine to aspartic acid and ammonia and is commonly for treating acute lymphoblastic leukemia (ALL) and other cancers. As L-asparaginase can able to inhibit all cancer cells, the present study was designed to explore the effect of L-asparaginase isolated from *Aspergillus niger* in pancreatic cancer cell line RIN-5F. The effect of L-asparaginase on the proliferation of RIN 5F was assessed by MTT and cell viability. Antioxidant activity and apoptosis induction was performed by spectrophotometric analysis and propidium iodide staining respectively. Further, apoptosis was confirmed by gene expression using reverse transcriptase PCR. We observed significant growth inhibition on the RIN-5F cell line with well-appreciated morphological changes and an increase in apoptotic cell numbers. L-asparaginase showed significant antioxidant activity with an increase in CAT and SOD activities and a decrease in reduced glutathione level (GSH) to compensate for oxidative stress. Elevated Bax gene expression with proportionally low expression of PARP genes confirms the intrinsic pathway of apoptosis. Our results suggest a promising treatment strategy for pancreatic cancer through the apoptotic pathway.

Keywords: asparaginase, cancer, scavengers, cytotoxic, gene suppression etc

I. INTRODUCTION

Pancreatic cancer is a highly lethal cancer with a 1-5 year survival rate ^{1,2}. Most of the cases are detected in the metastatic stage where only 15-20% can undergo surgery. Gemcitabine remains to be the first-line therapy of metastatic pancreatic cancer with adverse side effects ³ and drug resistance necessitates the need for alternative treatment. ROS facilitates the progression of cancer leading to uncontrolled cell proliferation and invasion. This fact throws the spotlight on ROS as an important target for chemotherapeutic drugs that selectively inhibit the growth of cancer cells ⁴. To defend against ROS damage, cells utilize an antioxidant system through antioxidant enzymes and redox-regulating proteins and lead to apoptosis ⁵ through mitochondrial dysfunction. Until now, there has been an intense search for therapeutic regimens that specifically kills cancer cell without inducing major side effects. L-asparaginase, the therapeutic enzyme that catalyzes endogenous amino acid asparagine into L-aspartic acid and ammonia. L-asparaginase treatment reduces L-asparagine in the blood through impairment of DNA and RNA synthesis through blast cell apoptosis in leukemia ⁶. This unique mechanism supported L-asparaginase to use as multidrug chemotherapy for critical lymphoblastic leukemia (CLL). The common source of this enzyme is from various bacterial species, animals, and plants ⁷. The bacterial L-asparaginase caused several severe side effects due to toxicity and hypersensitivity ⁸⁻¹¹. L-asparaginase from eukaryotic microorganisms has fewer adverse effects ¹² which triggered us to evaluate the apoptosis-induction potential of L-asparaginase purified from a fungus *A. niger* on RIN-5F cells.

2. MATERIALS AND METHODS

2.1 L-Asparaginase Producing Fungal Strain

Soil samples were collected from five different farming land of Sivagangai District of Tamilnadu, collected soil samples were dried and passed through 2mm pore size sieve. Then L-Asparaginase producing fungal strain isolated from the Farmland soil by serial dilution method. Screening for L-asparaginase production was done by the rapid-plate assay as described by Gulati et al ¹³. Identification of the fungal strain was done by molecular methods adopting 18 S rRNA analysis. Followed by isolation of genomic DNA, 18s rRNA gene sequence of the fungal isolate was carried out by Sanger's method and the sequences were blasted at NCBI. The pure culture was maintained on potato dextrose agar slant for further studies.

2.2 Anti-Cancer Activity

2.1.1 Cell culture collection and maintenance

RIN5F - cell line used in this study was obtained from the ATCC, the USA with other supplements. Cells were grown in Dulbecco's modified Eagle medium (DMEM) containing 10% fetal bovine serum, 1% penicillin and streptomycin under optimum condition (5 % CO₂ atmosphere at 37°C).

2.2.1 Cell viability assay

Effect of asparaginase on the cell viability of RIN5F was done by MTT assay Mosmann, 1983¹⁴. The cells were exposed to various concentrations of asparaginase (1-10 and 10-100 µg/ml) for 24h in a 96-well plate. At the end of the exposure, the spent medium

was replaced with a fresh medium containing MTT solution (0.5 mg/ml) and incubated at 37°C for 24 hrs. The plates were shaken for 10 minutes at room temperature and analyzed by a multi-well microplate reader at 490 nm and 630 nm. Untreated wells served as control. Differences in the optical density of control and treatment reveal cell viability which can be expressed in percentage.

2.3.1 Trypan Blue Exclusion Assay

The lethality of L-Asparaginase on RIN5F cells was assessed by the trypan blue exclusion test¹⁵. Cells were exposed to L-asparaginase in different concentrations with a seeded density of 10⁶ cells in 6-well plates and incubated at 5% CO₂ for 24 hrs. The cells were trypsinized and stained with trypan blue. The total number of live (stained) and dead (unstained) cells were counted by hemocytometer.

2.4.1 Morphometric changes analysis

L-Asparaginase-induced morphometric changes on the RIN5F were studied by phase contrast and fluorescent microscopy.

2.5.1 Phase Contrast Inverted Microscope

Observation of morphological changes of apoptotic cells was performed according to the method of Moongkarndi et al., 2004¹⁶ with minor modifications. Briefly, 5 × 10⁵ cells were incubated for hours with various concentrations of L-Asparaginase (0, 5, 10, 15, and 50 µg/ml) in a 60 mm diameter tissue culture dishes. The Control group was maintained without L- asparaginase treatment. After incubation for 24 hrs, the medium was removed and cells were washed with PBS. The morphological changes were observed using a phase-contrast inverted microscope (Optika, Singapore) at 200x magnifications.

2.3 Fluorescence Microscopy

2.3.1. Propidium Iodide staining

Apoptotic changes in the L-asparaginase treated cells were analyzed by propidium iodide staining. Cultured cells were treated with different concentrations of L-Asparaginase(5µg, 10µg, and 15µg/ml) for 24 hours. The control and treated cells were washed with PBS twice, fixed with 4 % formaldehyde for 30 minutes. The fixed cells were washed with PBS followed by the addition of propidium iodide stain (1 mg/ml stock; 10 µg/ml, Stained cells were incubated at ambient temperature for 30 minutes)¹⁷. After staining, the excess stain was removed by PBS wash. Apoptotic changes were observed under a fluorescence microscope using selective filters.

2.4 Antioxidative Enzymes Status

2.4.1 Catalase (CAT) assay

CAT activity was estimated by minor modifications of Goth, 1991¹⁸. In this method, a known volume of cell suspension (0.5mL) was added to the reaction mixture, containing 1 mL of 0.01 mol/L phosphate buffers (pH 7.0), 0.5 mL of 0.2 mol/L H₂O₂ or 30% H₂O₂, 0.4 mL H₂O, and incubated for 10 minutes. The enzymatic reaction was stopped by 1 ml of 32.4 mmol/l ammonium molybdate and the chromogenic complex formed was estimated at 405 nm.

2.4.2. Superoxide Dismutase (SOD) Assay

Estimation of SOD activity was done by the method of Luo et al., 2019¹⁹. Cell suspension derived from respective control and treatment group was mixed with 0.2 mL NBT (Nitrobluetetrazolium0.08 mM), 0.4 mL NADH(dihydronecotineamide adenine dinucleotide0.25 mM), and 0.2 mL PMS (phenazine methosulfate0.06 mM) and incubated at dark condition for 10 minutes. Absorbance was read at 560 nm.

2.4.3. Estimation of reduced glutathione (GSH)

Quantification of reduced glutathione was carried out by the method of Jollow et al., 1974²⁰. Homogenate derived from respective treatment group 500 µL (in 0.1 M potassium phosphate buffer (pH 7.4)) was precipitated by the inclusion of 4% sulfosalicylic acid (500µL). The reaction mixture was allowed to incubate at 4°C for 1 hour and centrifuged at 1200g for 20 minutes. The supernatant (33 µL) thus obtained was mixed with 900 µL of 0.1 M potassium phosphate buffer (pH 7.4) and 66 µL of 100 mM dithiobis (2-nitrobenzoic acid) (DTNB). The reaction mixture produces a yellow-colored complex which was measured at an absorbance of 412 nm.

2.4.5. Glutathione S-transferase assay(GST)

A known volume of cell homogenate (500 µl) derived from L- asparaginase dissolved in 3 ml of DMSO solution followed by mixing with 1 ml of CDNB (1 mM/ml). The reaction mixture was read at an absorbance of 340 nm²¹.

2.4.6. Evaluation of changes in marker genes expression

The molecular mechanism of anticancer activity was studied by the determination of marker genes like BAX and PARP expression. Primers for respective genes were designed with the NCBI Primer-BLAST tool. The primer sequences are listed in table 1. β -actin was taken as the control for the housekeeping gene. DNA samples were isolated from the respective treatment group adopting standard isolation protocol after 24 hours of post-treatment. The PCR was performed using thermocycler gradient PCR and amplification reactions were performed in a volume of 25 μ l containing 4.5 μ l of template DNA, 12.5 μ l of 1X PCR Emerald master mixture, each of the specific primers of volume 1 μ l respectively and made up with the remaining volume of distilled water. The amplification includes 1 cycle initial denaturation at 95°C for 2 minutes, 95°C for 1 minute for DNA denaturation, annealing with 54°C for β -Actin, 54.5°C for PARP, and 54.3°C for Bax for 30 seconds followed by 72°C for 1 minute for extension of two strands, 72°C for 5 minutes for final extension and followed for 34 cycles. The PCR products were analyzed on a 1.0% agarose gel containing 1 mg/ml ethidium bromide, 6 μ l of the PCR products with 4 μ l of 6X gel loading dye were loaded into wells and electrophoresis was performed in 1X TAE buffer at 50 V for 2 hours. The gel was visualized under UV and photographed.

Table 2. Primers selection for the analysis of gene expression

Primer sequence	Nucleotide sequences
β -Actin forward	5' TCAAGGTGGGTGTCTTCCTG 3'
β -Actin reverse	5' ATTTGCGGTGGACGATGGAG 3'
Bax forward	5' CGTGTCTGATCAATCCCCGA 3'
Bax reverse	5' GAGGCCAGAAGGCAGGGATTG 3'
PARP forward	5' CCCAGCCTTGTGGAAAACAC 3'
PARP reverse	5' CACCTGCAGAGACAGGCATT 3'

3. STATISTICAL ANALYSIS

Three replicates were taken as mean. The values were expressed as mean (\pm SD) by One-way analysis of variance (ANOVA). The high significance (****) between the samples was performed at $p<0.0001$. Statistical analysis was done using Graphpad Prism version 8.0 statistical software.

4. RESULTS AND DISCUSSION

4.1 Cytotoxic effect

To explore the effect of L-asparaginase on RIN 5F cells, cell viability assay was analyzed by MTT and trypan blue exclusion assay. The LC₅₀ range of the L-asparaginase was found at 10 μ g/ml concentration (Fig. 1). The percentage viability of L- Asparaginase at 1 μ g/ml was 90% and at 10 μ g/ml was 49.73% when compared to untreated cells. The MTT assay also showed inhibited cell proliferation in a dose-dependent manner (1-10 μ g) with 50.18% at 10 μ g/ml (Fig.2).The inhibitory effect of L-Asparaginase was assessed by morphological changes RIN-5F, using phase-contrast microscopy. There was a significant decrease in the number of cells on treatment with L-asparaginase at concentrations 5 μ g,10 μ g, and 15 μ g/ml compared to untreated cells. The morphological changes observed in treated cells include cell shrinkage, cell rounding, and decreased volume (Fig 3. B, C, and D). The normal architecture was observed in untreated cells (Fig. 3A). Morphological changes in cancer cell nuclei were observed by fluorescence microscopy, which differentiates between normal and apoptotic cells. The apoptotic nuclei are represented by concentrated fluorescence indicating condensed or fragmented chromatin on treatment with 15 μ g/ml (Fig. 4D). Cells at low concentrations of 5 μ g and 10 μ g of nanoparticles showed a relatively lesser bright red fluorescence (Fig.4B and C). Untreated cells were completely unstained (Fig 4A). Thus,apoptosis induced by L-asparaginase was observed in a dose-dependent manner. The effect of L-asparaginase on the anti-oxidative enzyme status of the RIN5F cell line was also investigated. L-asparaginase treatment exhibited a significant increase in SOD and CAT activity ($p<0.0001$) compared to control in a dose-dependent manner (Fig.5 and Fig.6). A moderate increase in GST activity (Fig.7) was recorded in L- asparaginase treatment. Comparing the levels of GSH between untreated and treated groups L- asparaginase treatment shows a significant decrease in GSH content ($p<0.0001$) (Fig.8) revealed induction of oxidative stress. The effect of L-Asperginase on expression levels of Bax and PARP was analyzed by reverse transcriptase-polymerase chain reaction (RT-PCR). Results indicated a higher expression level of BAX and a low expression level of PARP with β -actin as control (Fig. 9). Compared to untreated cells, Bax levels increased with a decrease in PARP gene expression upon treatment with L-asparaginase. L-Asparaginase is a therapeutic enzyme produced by microorganisms, used in the treatment of patients suffering from lymphoma and leukemia as a chemotherapeutic agent ^{22,23,24}. It causes the death of tumor cells by acting L-asparagine which is involved in activation and proliferation through amino acid exchange factor ^{25,26}. The incidence of pancreatic cancer is highly predominant with high mortality due to late diagnosis and unsuccessful therapeutic strategies. As L-asparaginase is the first enzyme used as an anticancer agent, we investigated its antiapoptotic and antioxidant activity on pancreatic cell line RIN-5F. The LC₅₀ of L- asparaginase from *A.niger* was 10 μ g/ml concentration, which is less than that of L -Asparaginase activity isolated from bacterial sources in different types of cancer cell lines ^{27,28}. Our experimental results revealed a high cytotoxicity effect with inhibition of cell proliferation in a dose-dependent manner with cell shrinkage and detachment from the surface. Induction of apoptosis is an efficient mechanism to screen anticancer activity. L-asparaginase repressed growth with morphological changes like chromatin condensation and fragmentation, apoptotic bodies resulting in disruption of cell membrane integrity and release of cell organelles, and cell

shrinkage^{29,30}. The fluorescent micrograph depicted in figure 4 demonstrates more number of apoptotic cells in L-asparaginase treatment which depicts the potential induction of cell death via apoptosis. Oxidative stress plays an important role in programmed cell death by activating signaling pathways in several pathophysiological situations. Under oxidative stress, reactive oxygen species (ROS) like superoxide (O_2^-), hydroxyl radical (HO), and hydrogen peroxide (H_2O_2) are generated at high levels leading to cellular damage and cell death³¹. As the first line of defense, antioxidant enzymes like SOD and CAT acts on free radicals to scavenge resulting in an imbalance of free radicals and antioxidant enzymes³². In our study, a significant depletion of SOD and CAT and increased GSH levels was observed in the untreated group of RIN5F cells in a dose-dependent increase. However, no effect on GST activity was observed in all the concentrations. GSH depletion in combination with L-asparaginase also depicts the ability of radical scavenging, growth inhibition, and enhanced apoptosis³¹. Further, apoptosis induction was also confirmed in RIN-5F cells by the increase in the level of the Bax gene and decrease in the PARP gene. Bax is an apoptosis regulatory protein present in the outer membrane of mitochondria and facilitates the discharge of cytochrome c and stimulates Caspase- 9 which in turn activates Caspase 3 resulting in concomitant PARP cleavage. We conclude that L-asparaginase selectively induced apoptosis in pancreatic cancer cell lines through Bax which triggers PARP cleavage^{33,34}.

5. CONCLUSION

L-asparaginase induces a significant anticancer effect in the RIN-5F cell line by the reduction of ROS production through antioxidant defense mechanism of SOD, CAT, and reduced glutathione inducing apoptosis resulting in modulation in the molecular mechanism through BAX –PARP gene. The antioxidant activity with the pro-apoptotic property of L-asparaginase could be a new alternative treatment for pancreatic cancer.

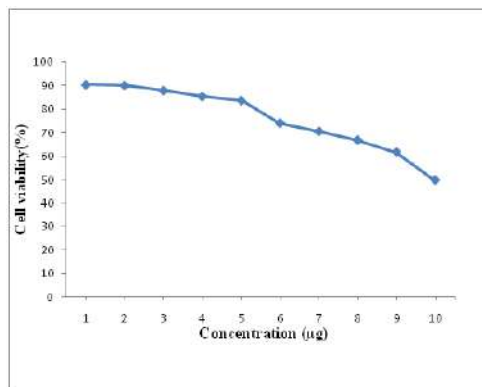


Fig.1 Effect of L- Asparaginase on cell viability of RIN5F cell line

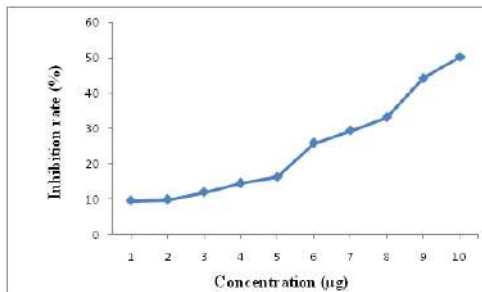


Fig. 2 Cytotoxicity of L-Asparaginase.

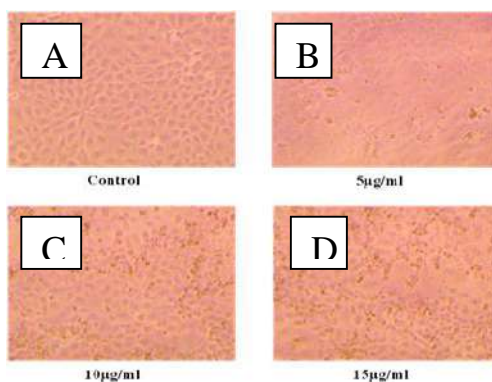


Fig 3. Effect of L- Asparaginase on RIN-5F cells by morphometric analysis using a phase-contrast microscop

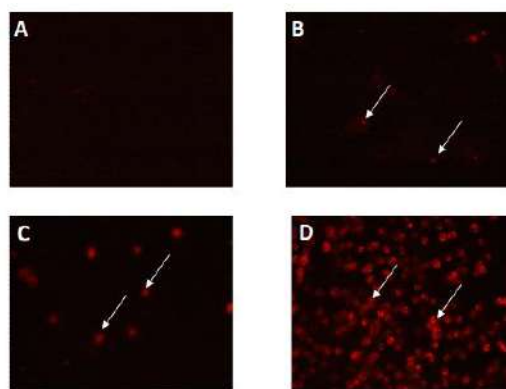


Fig 4. Apoptotic effect of L- Asparaginase on RIN-5F cells

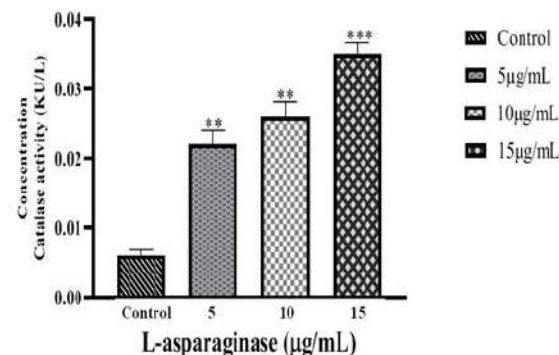


Fig 5. Effect of L- Asparaginase on Catalase (CAT) activity in RIN-5F cells

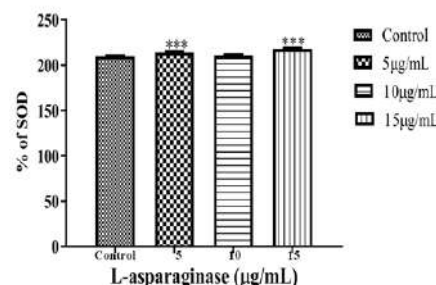


Fig 6:Effect of L- Asparaginase on Superoxide dismutase (SOD) activity in RIN-5F cells

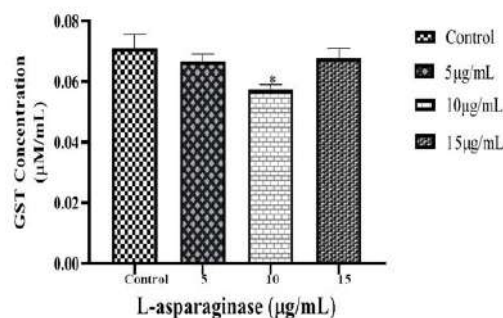


Fig 7:Effect of L- Asparaginase on Glutathione-S-transferase activity in RIN-5F cells

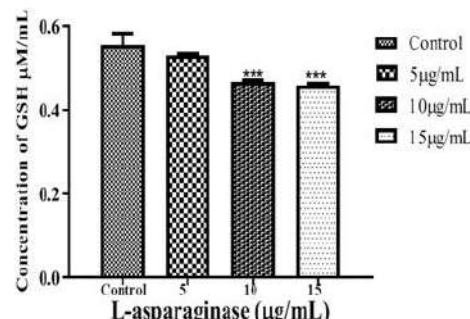
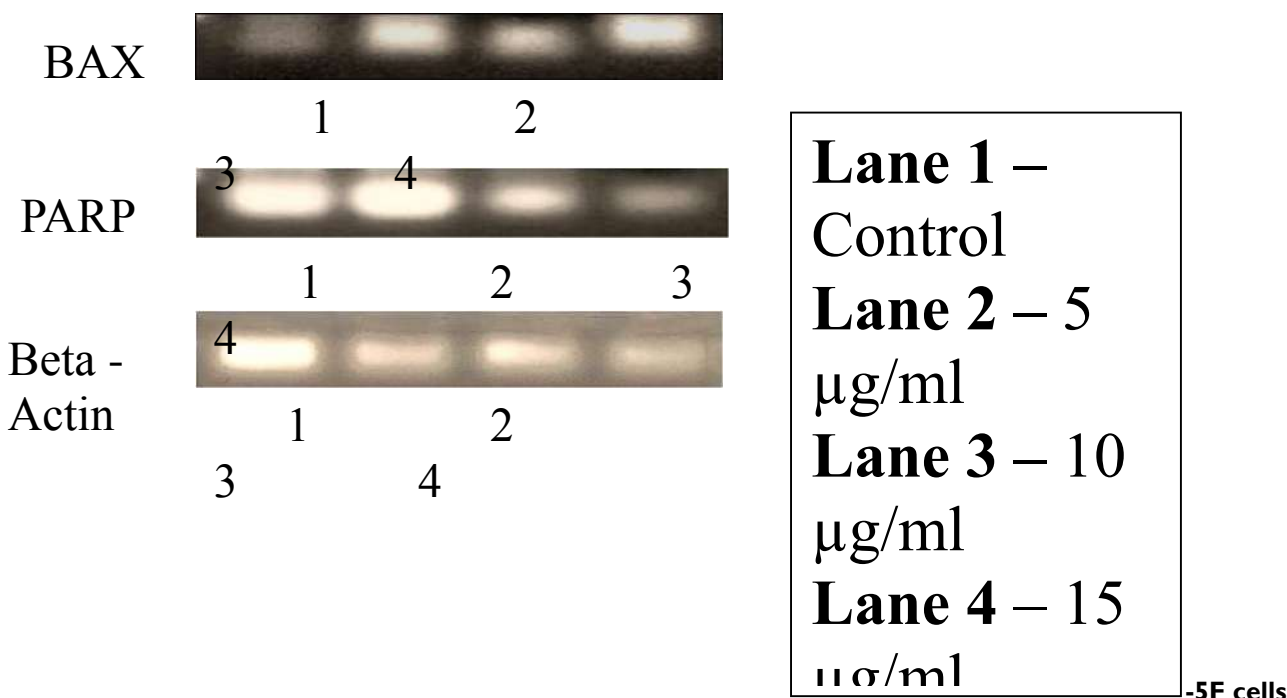


Fig 8:Effect of L- Asparaginase on reduced glutathione content of RIN**Fig 9: Effect of L-asparaginase on BAX and PARP gene expression**

6. CONFLICT OF INTEREST

Conflict of interest declared none.

7. REFERENCE

1. Jernal A, Siegel R, Ward E, Hao Y, Xu J, Thun MJ. Cancer statistics, 2002. CA cancer J clin. 2002;52(1):23-47.
2. Wang S-J, Gao Y, Chen H, et al. Dihydroartemisinin inactivates NF- κ B and potentiates the anti-tumor effect of gemcitabine on pancreatic cancer both in vitro and in vivo. Cancer Lett. 2010;293(1):99-108.
3. Mouhid L, de Cerdón MG, Vargas T, et al. Identification of antitumoral agents against human pancreatic cancer cells from Asteraceae and Lamiaceae plant extracts. BMC Complement Altern Med. 2018;18(1):1-11.
4. Wang J, Yi J. Cancer cell killing via ROS: to increase or decrease, that is the question. Cancer Biol Ther. 2008;7(12):1875-1884.
5. Schieber M, Chandel NS. ROS function in redox signaling and oxidative stress. Curr Biol. 2014;24(10):R453-R462.
6. Leventhal BG, Henderson ES. Therapy of acute leukemia with drug combinations which include asparaginase. Cancer. 1971;28(4):825-829.
7. Pronk MMEJ, Verger P, Olempska-Bier Z, Walker R. Asparaginase from *Aspergillusoryzae* expressed in *Aspergillusoryzae*. SafEval Certain food AdditContam. 2008;55.
8. Moola ZB, Scawen MD, Atkinson T, Nicholls DJ. *Erwiniachrysanthemi* L-asparaginase: epitope mapping and production of antigenically modified enzymes. Biochem J. 1994;302(3):921-927.
9. Rossi F, Incorvaia C, Mauro M. Hypersensitivity reactions to chemotherapeutic antineoplastic agents. RecentiProg Med. 2004;95(10):476-481.
10. Pieters R, Hunger SP, Boos J, et al. L-asparaginase treatment in acute lymphoblastic leukemia: a focus on *Erwiniiasparaginase*. Cancer. 2011;117(2):238-249.
11. Ramya LN, Doble M, Rekha VPB, Pulicherla KK. L-Asparaginase as potent anti-leukemic agent and its significance of having reduced glutaminase side activity for better treatment of acute lymphoblastic leukaemia. ApplBiochemBiotechnol. 2012;167(8):2144-2159.
12. Sarquis MI de M, Oliveira EMM, Santos AS, Costa GL da. Production of L-asparaginase by filamentous fungi. Mem Inst Oswaldo Cruz. 2004;99(5):489-492.
13. Gulati R, Saxena RK, Gupta R. A rapid plate assay for screening L-asparaginase producing micro-organisms. Lett ApplMicrobiol. 1997;24(1):23-26.
14. Mosmann T. Rapid colorimetric assay for cellular growth and survival: application to proliferation and cytotoxicity assays. J Immunol Methods. 1983;65(1-2):55-63.
15. Li W, Yuan X, Nordgren G, et al. Induction of cell death by the lysosomotropic detergent MSDH. FEBS Lett. 2000;470(1):35-39.

16. Moongkarndi P, Kosem N, Kaslungka S, Luanratana O, Pongpan N, Neungton N. Antiproliferation, antioxidation and induction of apoptosis by *Garcinia mangostana* (mangosteen) on SKBR3 human breast cancer cell line. *J Ethnopharmacol.* 2004;90(1):161-166.
17. Hezel M, Ebrahimi F, Koch M, Dehghani F. Propidium iodide staining: a new application in fluorescence microscopy for analysis of cytoarchitecture in adult and developing rodent brain. *Micron.* 2012;43(10):1031-1038.
18. Goth L. A simple method for determination of serum catalase activity and revision of reference range. *ClinChimacta.* 1991;196(2-3):143-151.
19. Luo S, Jiang X, Jia L, et al. In vivo and in vitro antioxidant activities of methanol extracts from olive leaves on *Caenorhabditis elegans*. *Molecules.* 2019;24(4):704.
20. Jollow DJ, Mitchell JR, Zampaglione N, Gillette JR. Bromobenzene-induced liver necrosis. Protective role of glutathione and evidence for 3, 4-bromobenzene oxide as the hepatotoxic metabolite. *Pharmacology.* 1974;11(3):151-169.
21. Pippenger CE, Browne RW, Armstrong D. Regulatory antioxidant enzymes. In: *Free Radical and Antioxidant Protocols*. Springer; 1998:299-313.
22. Emadi A, Zokae H, Sausville EA. Asparaginase in the treatment of non-ALL hematologic malignancies. *Cancer ChemotherPharmacol.* 2014;73(5):875-883.
23. Avramis VI. Asparaginases: biochemical pharmacology and modes of drug resistance. *Anticancer Res.* 2012;32(7):2423-2437.
24. Covini D, Tardito S, Bussolati O, et al. Expanding targets for a metabolic therapy of cancer: L-asparaginase. *Recent Pat Anticancer Drug Discov.* 2012;7(1):4-13.
25. Krall AS, Xu S, Graeber TG, Braas D, Christofk HR. Asparagine promotes cancer cell proliferation through use as an amino acid exchange factor. *Nat Commun.* 2016;7(1):1-13.
26. Baskar G, George GB, Chamundeeswari M. Synthesis and characterization of asparaginase bound silver nanocomposite against ovarian cancer cell line A2780 and lung cancer cell line A549. *J InorgOrganometPolym Mater.* 2017;27(1):87-94.
27. Abakumova OY, Podobed O V, Borisova AA. Anti-tumor activity of *Yersinia pseudotuberculosis* L-asparaginase. *Biomed khim.* 2008;54(6):712-719.
28. Pritsa AA, Papazisis KT, Kortsaris AH, Geromichalos GD, Kyriakidis DA. Antitumor activity of L-asparaginase from *Thermusthermophilus*. *Anticancer Drugs.* 2001;12(2):137-142.
29. Mathi P, Nikhil K, Das S, Roy P, Bokka VR, Botlagunta M. Evaluation of in vitroanticancer activity and GC-MS analysis from leaf *Sophorainterrupta*Bedd. *Int J Pharm Pharm Sci.* 2015;7:303-308.
30. O'Brien MA, Kirby R. Apoptosis: A review of pro-apoptotic and anti-apoptotic pathways and dysregulation in disease. *J Vet EmergCrit care.* 2008;18(6):572-585.
31. Pelicano H, Carney D, Huang P. ROS stress in cancer cells and therapeutic implications. *Drug Resist Updat.* 2004;7(2):97-110.
32. Ighodaro OM, Akinloye OA. First line defence antioxidants-superoxide dismutase (SOD), catalase (CAT) and glutathione peroxidase (GPX): Their fundamental role in the entire antioxidant defence grid. *Alexandria J Med.* 2018;54(4):287-293.
33. Tayarani-Najaran Z, Makki F-S, Alamolhodaei N-S, Mojarrab M, Emami SA. Cytotoxic and apoptotic effects of different extracts of *Artemisia biennis*Willd. on K562 and HL-60 cell lines. *Iran J Basic Med Sci.* 2017;20(2):166.
34. Zhang Q, Bao J, Yang J. Genistein-triggered anticancer activity against liver cancer cell line HepG2 involves ROS generation, mitochondrial apoptosis, G2/M cell cycle arrest and inhibition of cell migration. *Arch Med Sci AMS.* 2019;15(4):1001.

Isolation, 16srdna Sequencing, Of Bacterial Isolate From The Earthworm

Sujithra.,NirmalaDevi.P. Dr.Sathyaa.R, Thusmithaa.S

Dhanalakshmisrinivasan College of Arts and Science for Women (Autonomous), Perambalur

Abstract: An earthworm is a tubular, segmented worm of the phylum Annelida. They occur worldwide and are commonly found in soil, eating live and dead organic matter. The present study was to isolate a bacteria from earthworm and its molecular identification by 16s rDNA sequencing. In the present study, the bacterial colonies were isolated from the earthworm. The DNA was isolated from the bacterial culture and subjected to 16s rRNA sequencing. The sequencing results were further analysed using BLAST and phylogenetic tree analysis. The results showed that the bacterial isolate was *Acinetobacter junii*. The bacterial sequence was further submitted to GenBank in NCBI.

Keyword: *Acinetobacter junii*, earthworm ,RNA, DNA,thrombosis

I. INTRODUCTION

Earthworms are harmless creatures that live in the soil. They are eco-friendly, playing the significant role in decomposing organic wastes, enhancing soil fertility, and improving soil drainage¹. Earthworms have been used from ancient times in oriental countries as drugs for prevention and treatment of various diseases, and have found applications such as intracystic calculus-contraction and releasing-stimulating agent, anti-choloplania agent, parturifacient, hair growth tonic, antifebrile, spasm-treating agent, hemiplegia-treating agent, urination improving agent, anti-bronchial asthma agent, antihypertensi agent, therapeutic medical for thrombosis and others²⁻³. The 5' region of the mitochondrial DNA gene cytochrome C oxidase subunit I (COI) is the standard marker for DNA barcoding. Our previous study has demonstrated that COI and 16S ribosomal DNA (rDNA) were reliable in species identification of ticks and a DNA barcoding system for ticks based on three DNA markers (COI, 16S rDNA, and 18S rDNA) was developed⁴. However, there are still several problems with this DNA barcoding system⁵. First, the primer pair COI-F/COI-R is not efficient in the recovery of COI from tick specimens; second, our previous study only focused on the tree-based method⁶. The availability and declining cost of DNA sequencing mean that data on the diversity, variation and evolution of organisms is more widely available than ever before. Increasingly, thousands of organisms are being sequenced at the whole-genome scale⁷⁻⁸. This had a particular impact on the study of pathogens, whose evolution occurs rapidly enough to be observed over relatively short periods. Consequently, the occurrence of epibiotic bacteria on marine organisms and the composition, structure, specificity, and stability of the epibiotic bacterial communities known today remain for the most part unexplored⁹⁻¹⁰. Genetic characterization of microbial diversity through amplification and sequence analysis of the 16S rRNA genes (rDNAs) has been successful in a wide range of environments.

2. MATERIALS AND METHODS

2.1 Materials Required

Nutrient Agar medium, Nutrient broth, Whatman filter paper No. 1, Gentamicin antibiotic solution, test samples, test tubes, beakers conical flask, spirit lamp, double distilled water and petri-plates.

2.2 Sample Collection

The sample from Earthworm was collected from in our garden Arasalur Perambalur district (11.2342° N, 78.8807° E)

2.3 Enumeration Of Earthworm Microbes

0.1g of earthworm was taken in the Eppendorf tube and 1 ml sterile distilled water was added. To finally mashed the earthworm. Filtrate jelly was used for enumerate bacteria by serial dilutions from 10¹ to 10⁸. The 10⁴ and 10⁸th dilution was used for bacterial isolation.

2.4 Nutrient Agar Medium

The medium was prepared by dissolving Peptone- 0.25gm, NaCl- 0.25gm, Yeast Extract- 0.1gm, Beef extract- 0.05gm and Agar powder- 0.875gm commercially available Nutrient Agar Medium in 50ml of distilled water. The dissolved medium was autoclaved at 15 lbs pressure at 121°C for 15 minutes. The autoclaved medium was mixed well and poured onto 100mm petriplates (25-30ml/plate) while still molten¹³.

2.5 Identification Of Micro- Organism

The isolated sample was streaked on the nutrient agar medium.

2.6 Characterization Of Microorganism

2.6.1. Gram staining

A loop full of samples was spread in the slide, which was taken from the plate¹⁴. The slide was smeared in the flame. The Crystal Violet dye was added, kept it for 1 min and washed the slide in the water. Gram Iodine was added and kept for 1 minute then it washed out. The decolourising agent was added, kept it 1 min and then it was out finally the strain was added after a minute it was washed in the water. It was observed under microscope the purple colours indicate Gram Positive and the pink colour was indicated as Gram Negative.

2.6.2. Motility

The motility test was performed by a hanging drop method. The cover was taken its edge was coated with Vaseline. The loop full of samples was transferred into the coverslip and placed it over the cavity slide. The slide was viewed under a microscope and observed the organism, whether it was motile or non-motile.

2.7 IMVIC TEST (Physical Chemical Characterization)

2.7.1. Indole test

Inoculate the bacteri to be tested in tryptone broth. To allow incubation at 37 degree celcius for 24hrs. After Incubation add a few drops of the Kovacs reagent.¹⁵ The formation of a red colour ring top is positive reaction (or) pink colour ring at the top positive reaction and yellow colour ring at the top negative reaction.

2.7.2. Methyl red test

Inoculate the bacterium to be tested in MRVP broth. To allow test tube incubate at 37 degree celcius for 24hrs. After incubation, 5 drops of the methyl red reagent was added. Formation of red colour ring top of the positive reaction, formation of yellow colour ring at top negative reaction.

2.8 DNA Isolation

DNA was isolated from the samples modified from the standardized salting-out procedure. Small bacterial culture samples were placed in 1.5 mL tubes separately and then added 500 μ L of Solution 1 and 10% of 10 μ L SDS. Homogenize the sample with sterile homogenizer. And 5 μ L of Proteinase K was added (20 mg/mL). The mixture was incubated at 55 °C for 2 hrs in a water bath (with occasional mixing/quick vortex) for easy digestion¹⁶. After complete digestion, the sample was kept on ice for 10 min. To this, 250 μ L of Solution 2 was added (saturated NaCl) and inverted several times to mix. Subsequently, the samples were chilled on ice for 5 min. Then the samples were centrifuged at 8000 rpm for 15 min. After that, about 500 μ L of clear supernatant were collected into a newly-labeled 1.5 mL tube. Then twice the volume of 100% molecular biology grade ethanol was added to precipitate the DNA¹⁷⁻¹⁸. Then the samples were centrifuged at 11,000 rpm for 15 min. After that, the supernatant was removed and 500 μ L of ice-cold 70% ethanol was added to the precipitate for washing. Sample was spun at 11000 rpm, for 5 min. Carefully, removed the supernatant, then pipetted out excess liquid and allowed it to partially dry with lid-off at room temperature. Partially dried DNA was re-suspended in 100 μ L of 1X TE buffer.

2.9 Quantification of DNA

Quantity of the extracted DNA was checked in a UV spectrophotometer (SHIMADZU, JAPAN) by taking the optical density (OD) at 260 nm and 280 nm. The quality was checked by measuring the ratio of absorbance at 260 nm and 280 nm (260/280). The value between 1.7 - 1.8 indicates good quality DNA without protein/RNA contamination. DNA quantification was done according to the following calculation: a sample showing 1 OD at 260 nm is equivalent to 50 μ g of DNA/mL. The OD of each DNA sample at 260 nm was measured and quantified accordingly²⁰. 0.24g of agarose powder was soaked in 30 mL of 1X TAE buffer and boiled until it formed into a clear solution. Then it was allowed to cooldown to approximately 50 °C. Then added 1.5 μ L of ethidium bromide and mixed well. It was poured in a gel casting plate with an already adjusted gel comb and kept at room temperature for 1/2 hrs for solidification. The gel was soaked in a 1X TAE buffer in the electrophoresis tank. 3 μ L of DNA with 3 μ L of gel loading dye was loaded in the wells using micropipettes. It was run at 70 V for 15 to 20 min. The orange color (DNA) bands were observed in UV illuminators.

2.10 Pcr Amplification

PCR amplification is done using the standard protocol.

3. RESULT

3.1 Gram staining of bacterial isolates

Differentiation of gram-positive and gram-negative bacteria and different morphology of bacterial culture identified using

atrinocular microscope. The results showed that, totally 13 different bacterial species were isolated. They belong to bacillus and cocci.

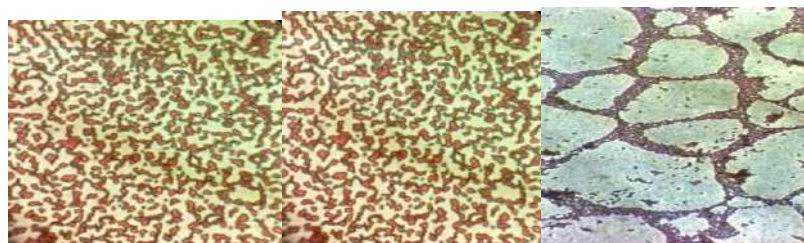


Figure 2. Gram staining images of bacterial isolates

3.2 Motility table

The hanging drop technique is a well-established method for examining living, unstained, very small organisms. The unique colonies from the gram staining results were subjected to motility assay. The results showed that the bacterial isolates were motile in nature.

S.NO	Sample	Motility
1.	10^4	Motile
2.	10^8	Motile

Table 2. Motility of bacterial isolates from the earth worm

3.3 Biochemical characterization of bacterial isolate by IMViC test

The biochemical identification of bacterial colonies by IMViC test was performed for the bacterial isolates of earthworm species. The bacterial isolates showed negative results except methyl red in 10^8 isolate.

Figure 3. Biochemical characterization of bacterial isolates by IMViC test



3.4 Molecular identification of bacterial isolate by 16s rRNA sequencing

The 16s rDNA region is universally accepted as a DNA barcode for bacterial species. PCR amplification of the 16s rDNA region for the bacterial isolate resulted in a predicted~700 amplicon, using BigDye Terminator v3.1 following the manufacturer's protocol. Each 16s rDNA genome sequence was subjected to BLAST to verify their identity. Consensus was obtained for the bacterial species. The BLAST analysis for the consensus 16s rDNA sequences exhibited 100% similarity with *Acinetobacter junii*. The 16s rDNA sequences of bacterial isolates were deposited in GenBank.

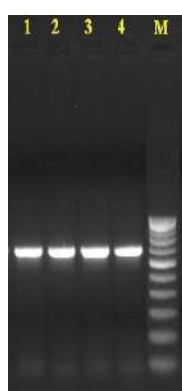


Figure 4. Shows the PCR amplification of 16S rRNA gene

4. DISCUSSION

The sequence analysis of 16S rDNA is the most common molecular method for the identification of bacteria, but most studies have mainly focused on method development and anecdotal case reports¹¹. On the basis of key reports and previous clinical work, we selected a set of universal reference primers to amplify 16S rDNA and identify previously “difficult-to-identify” bacteria in clinical setting¹². In addition, the ITS region (especially ITS2) is heavily used for the identification of fungi. The identification of standard strains and common clinical isolates by PCR and sequencing in this study demonstrates that this method is consistent with conventional laboratory methods¹³⁻¹⁴. This molecular identification method offers numerous desirable features: (1) convenience, as common molecular biology methods and techniques are used in the procedure (including efficient one-step DNA extraction, PCR, electrophoresis, commercial sequencing, and sequence analysis); (2) Availability, as it is based on well established theories and methods (including amplicon preparation by PCR, commercial sequencing, and GeneBank verification); and (3) cost-effectiveness, as the cost of the procedure can be lower than ever for the development of information and technology¹⁵⁻¹⁶. The aim of the present study was to isolate a bacteria from the earthworm and their molecular identification by 16S rRNA sequencing and phylogenetic tree analysis. Furthermore, we isolated a bacterial DNA and quantified it using a UV-spectrophotometer by taking the optical density (OD) at 260 nm and 280 nm¹⁷. The quality was checked by measuring the ratio of absorbance at 260 nm and 280 nm (260/280). The value between 1.7 - 1.8 indicated the quality of DNA was good without protein/RNA contamination¹⁸. Lysis of microbial cells from the environmental habitats marks a critical step in a PCR-mediated approach. Insufficient or preferential disruption of cells will most likely bias the view of the composition of microbial diversity as DNA or RNA, which is not released from the cells, will not contribute to the final analysis of diversity¹⁹⁻²¹. Leonardo et al., 2015, identified microbes related to N₂O fluxes in soil with sugarcane crops.

5. CONCLUSION

Soil contains one of the most diverse microbiomes of the terrestrial biosphere, with a gram (dry weight) of soil having 10⁹ or more microbial cells. *L. terrestris* is a model anecic earthworm, feeding on both soil and litter. Ingested material therefore delivers an enormous number of microorganisms to the oxygen-deficient digestive system of the earthworm. Sequencing long dual indexed rDNA amplicons on ONT's MinION is a simple, cost-effective, accurate, and universal approach for eukaryote DNA barcoding. Long rDNA amplicons offer high phylogenetic and taxonomic resolution across broad taxonomic scales from kingdom down to species. They also prove to be an excellent complement to mitochondrial COI-based barcoding in annelid. The observed taxonomic bias is possibly a result of taxon-specific length variation of the rDNA cluster and preferential amplification of species with shorter rDNA. Further research into the sources of the observed bias is required before long rDNA amplicon sequencing can be utilized as a reliable resource for the analysis of bulk samples.

6. CONFLICT OF INTEREST

Conflict of interest declared none.

7. REFERENCE

- Ishii Y, Sumi H, Yoshida E (2009) Method of producing a dry earthworm powder. Patent US 20090238891 A1.
- Edwards & Bohlen (1996) Edwards CA, Bohlen PJ. *Biology and ecology of earthworms*. London: Chapman & Hall; 1996.
- Lee (1985) Lee KE. *Earthworms: their ecology and relationships with soils and land use*. Sydney: Academic Press; 1985.
- Stephenson (1930) Stephenson J. *The Oligochaeta*. Oxford: Clarendon Press; 1930.
- Pan R, Zhang Z-J, He R-Q (2010) Earthworm protease. *Applied and Environmental Soil Science*, Vol. 2010, Article ID 294258, 13 pages.
- Darwin C. On the formation of mould. *Proc. Geol. Soc. Lond.* 1838;2:574–576.
- Darwin C. John Murray; London, UK: 1859. *On the origin of species by means of natural selection, or the preservation of favoured races in the struggle for life*.
- Darwin C. John Murray; London, UK: 1881. *The formation of vegetable mould through the action of worms, with some observations on their habits*.
- Bohlen P. J., Scheu S., Hale C. M., McLean S. M., Groffman P. M., Parkinson D. Non-native invasive earthworms as agents of change in northern temperate forests. *Frontiers in Ecology and the Environment*. 2004;2:427–435
- Brussaard L, Aanen DK, Briones MJI, Decaëns T, Deyn GBD, Fayle TM, et al. Biogeography and Phylogenetic Community Structure of Soil Invertebrate Ecosystem Engineers: Global to Local Patterns, Implications for Ecosystem Functioning and Services and Global Environmental Change Impacts In: *Soil Ecology and Ecosystem Services*.
- Wall DH, Bardgett RD, Behan-Pelletier V, Henrick J, Jones H, Ritz K, et al. editors. *Oxford: University Press*; 2013. pp. 201–232.
- Venables BJ, Fitzpatrick LC, and Goven AJ 1992 Earthworms as indicators of ecotoxicity. In: *Ecotoxicology of Earthworms*, ed Greig-Smith PW, Becker H, Edwards PJ, Heimbach F. Intercept, Ltd, Andover, Hants, UK, 197–206.
- Jones, Lawton & Shachak (1994) Jones CG, Lawton JH, Shachak M. Organisms as ecosystem engineers. *Oikos*. 1994;69:373–386.
- Turbé et al. (2010) Turbé A, De Toni A, Benito P, Lavelle P, Lavelle P, Ruiz N, Van der Putten WH, Labouze E, Mudgal S. Soil biodiversity: functions, threats and tools for policy
- Logan CY, Nusse R (2004) The Wnt signaling pathway in development and disease. *Annu Rev Cell Dev Biol* 20: 781–810. [PubMed] [Google Scholar]

16. Kaler P, Godasi BN, Augenlicht L, Klampfer L (2009) The NF-kappaB/AKT-dependent Induction of Wnt Signaling in Colon Cancer Cells by Macrophages and IL-1beta. *Cancer Microenviron.* [PMC free article] [PubMed]
17. Klopocki E, Kristiansen G, Wild PJ, Klaman I, Castanos-Velez E, et al. (2004) Loss of SFRP1 is associated with breast cancer progression and poor prognosis in early stage tumors. *Int J Oncol* 25: 641–649. [PubMed] [Google Scholar]
18. Rask K, Nilsson A, Brannstrom M, Carlsson P, Hellberg P, et al. (2003) Wnt-signalling pathway in ovarian epithelial tumours: increased expression of beta-catenin and GSK3beta. *Br J Cancer* 89: 1298–1304. [PMC free article] [PubMed] [Google Scholar]
19. Su HY, Lai HC, Lin YW, Liu CY, Chen CK, et al. (2010) Epigenetic silencing of SFRP5 is related to malignant phenotype and chemoresistance of ovarian cancer through Wnt signaling pathway. *Int J Cancer* 127: 555–567. [PubMed] [Google Scholar]
20. Boon HS, Olatunde F, Zick SM. Trends in complementary/alternative medicine use by breast cancer survivors: comparing survey data from 1998 and 2005. *BMC Womens Health.* 2007;7:4. [PMC free article] [PubMed] [Google Scholar]
21. Greenlee H, Kwan ML, Ergas IJ, et al. Changes in vitamin and mineral supplement use after breast cancer diagnosis in the pathways study: a prospective cohort study. *BMC Cancer.* 2014;14:382–397. [PMC free article] [PubMed] [Google Scholar]

Electrochemical Reduction Of Co2 Using Oxide Based Cu And Zn Bimetallic Catalyst

Ramasamy Shanmugapriya*, Dr.P. Visvamithran, Dr Gurumoorthi, G vanaja

Dhanalakshmi Srinivasan College of Arts & Science for Women (Autonomous) Perambalur, Tamil Nadu-621212

ABSTRACT: Electrochemical decrease of carbon dioxide (ERCO2) driven by non-traditional wellsprings of energy is a positive way to deal with creating a shut circle CO2 cycle. It will lessen CO2 discharges by bringing down CO2 levels in the air and changing over it into high-energy-thickness carbon-based powers like alcohols and hydrocarbons. Monometallic copper based impetuses are generally detailed for ERCO2 to an assortment of mechanically significant carbon items. In any case, difficulties like high over potential, wild item selectivity, and impetus deactivation repress their advancement. Oxide-determined bimetallic CuZn_x electrocatalysts have been proposed as choices for accomplishing high selectivity for various important items. In this review, the co-precipitation approach has been utilized to plan CuO with different amounts of ZnO dopants. HRTEM, FESEM, XRD, and XPS were utilized to direct definite morphological and basic examinations on the electrode. The electrochemical presentation was estimated utilizing an H-type electrochemical cell in a watery 0.1 M KHCO3 electrolyte. The assessment of various CuO-ZnO_x (where x=5, 10, 15 and 20 wt.%) impetuses for ethanol usefulness and Faradaic effectiveness are of specific significance. Among contemplated electrocatalysts, the most elevated Faradaic proficiency of 22.27 % was acquired for ethanol utilizing CuO-ZnO10 at - 0.80 V (versus RHE) with the creation pace of around 121 μ mol h⁻¹ L⁻¹. The streamlined terminal (CuO-ZnO10) shows long haul dependability for somewhere around 12 h. Post portrayal of the impetus was additionally directed to get an understanding into the dynamic destinations, which demonstrated that CO2 decrease occurred on diminished oxide locales (for example metallic destinations) as opposed to metal oxides.

Keywords: Copper(II) nitrate trihydrate (Cu(NO₃)₂•3H₂O), zinc nitrate hexahydrate (Zn(NO₃)₂•6H₂O), and sodium carbonate (Na₂CO₃)

I. INTRODUCTION

The worldwide transportation industry is defied with three major issues, in particular unrefined petroleum value flimsiness, non-renewable energy source consumption, and severe natural arrangements. Among different choices biofuels are as a rule forcefully investigated as a choice since they have less intricacies as far as handling, stockpiling, transportation, and use in inner ignition motors. Ethanol is viewed as one of the best inexhaustible fuel in light of its tantamount higher warming worth (23.4 MJ/L), serious ness, predominant eco-friendliness, and numerous natural benefits. Numerous nations presented ethanol mixing program in re penny years. Hence, change of waste electrochemical decrease might be useful to satisfy world increasing ethanol interest and simultaneously it will likewise diminish the CO2 discharges from the environment. Electrochemical decrease of CO2 (ERCO2) to ethanol is 12e⁻ exchange measure. The coupling of the principle response intermediate *CO on the electrocatalysts surface for the C-C bond arrangement, is considered as significant and complex advance in the creation of ethanol. Likewise, CO2 is profoundly steady particle and requires high energy for transformation, which makes ERCO2 measure more troublesome. To gauge these issues and the imbalances that has been building in the system more carefully, the chapter examines the changing dynamics of oil markets.¹ Then again, Cu with Zn shows concealment of HERs and advances multi carbon items with higher selectivity. Additionally, Zn is more environmentally harmless and reasonable when contrasted with various co impetuses like Ag, Pd, and Au. Li et. al. detailed the impact of creation and mathematical design of CuO-ZnO impetuses for the particular creation of C₂H₄ and C₂H₅OH. Utilizing 8CuO/2ZnO/C electrocatalyst, 24.0 % Faradaic effectiveness (FE) was accomplished at - 0.75 V versus reversible hydrogen terminal (RHE). As per their report, the diminished ZnO nanoparticles supply additional CO to decreased CuO nanoparticles which increment the *CO surface inclusion for C coupling. The uniform dissemination of Cu and Zn molecules in the electrocatalysts was found to improve CO overflow impacts.² detailed progressively mesoporous-macroporous (HMMP) Cu/Zn combination impetuses for fluid C₂ items. In the previous work, metallic Cu nanoparticles (Cu NPs), Cu NPs on N-doped graphene (Cu_x/NGN)¹⁶ and oxide-inferred Cu-Zn nanoparticles upheld on N-doped graphene were utilized for the ERCO2 with a plan to create ethanol. Among these electrocatalysts, the metallic Cu NPs blended by substance reduction technique showed just 5.8 % FE for ethanol at - 0.8 V (versus RHE), in any case, it created formate with 45.4 % FE at a similar applied potential. Further, the electrocatalysts with high degree of surface heterogeneity and accessibility of numerous adja penny dynamic destinations to work with the adjustment of various adsorbed response intermediates, the copper upheld on nitrogen doped graphene (Cu_x/NGN) Cu NPs were utilized for ethanol creation³. The twenty wt.% copper on NGN showed uniform scattering of Cu on NGN and delivered ethanol with 25.72 % FE at - 1.0 V (versus RHE). From the writing, it has been inferred that ZnO is utilized as a co-impetus to works with nearby *CO fixation and coupling of *CO transitional prompting further developed ethanol selectivity.⁴ In light of this thought, oxide determined Cu-Zn bimetallic oxides supported on N-doped graphene has been likewise announced in our earlier work.⁵ The cathode having 20 wt.% Zn with copper on NGN (CuZn20/NGN) showed the most elevated selectivity for ethanol production (FE = 34.25%). The enzymatic oxidation of ethanol occurs primarily in the liver, first to acetaldehyde by the enzyme alcohol dehydrogenase and then conversion to acetic acid by the enzyme aldehyde dehydrogenase. Acetic acid is available for the formation of acetyl coenzyme A, which enters the Krebs cycle and is eventually metabolized to carbon dioxide and water⁶. The improved presentation of CuZn20/NGN is because of synergistic impact of N-doped dynamic locales and Cu-Zn bury face in the electrocatalyst. Electrochemical CO₂ Reduction to Hydrocarbons on a Heterogeneous Molecular Cu Catalyst in Aqueous

Solution⁷ In the current work, oxide inferred Cu-Zn bimetallic oxides (CuO-ZnO_x) (without N-doped graphene support) were synthesized through a simple co-precipitation method followed by calcination in air atmosphere, using cupric nitrate and zinc nitrate as Cu and Zn precursor, respectively. The potential of such alternative feed stocks and ethanol conversion technologies need to be exploited to increase ethanol availability for blending. The review indicates that ethanol is most suitable fuel for spark ignition engines due to its higher octane number⁸. The loading percentage of Cu to Zn in the electrocatalysts can be easily adjusted by changing the precursor concentrations. The activity and selectivity of synthesized CuO-ZnO_x were studied by various electrochemical characterization method. The hikes in fuel prices affect the automobile, power generation, and agriculture sectors. Due to hikes in fuel prices and depletion of fossil fuel reservoirs, the world's moving towards renewable sources like alternative fuels⁹.

2. EXPERIMENTAL

2.1 Materials

Copper(II) nitrate trihydrate (Cu(NO₃)₂•3H₂O), zinc nitrate hexahydrate (Zn(NO₃)₂•6H₂O), and sodium carbonate (Na₂CO₃) were obtained from S. D. Fine Chemicals Ltd. (India). The catalytic performance of these materials for ethanol production in aqueous conditions is discussed in terms of current density, overpotential, and faradaic efficiency¹⁰. Nafion solution (5 wt.%), Nafion-117 membrane, potassium bicarbonate (KHCO₃), and HPLC grade chemicals required for HPLC analysis were obtained from Sigma-Aldrich (India).¹¹ Carbon papers (NOS1005) were pro cured from Ce-Tech (Japan). Carbon dioxide (99.999%) and nitro gen (99.999%) were procured from Sigma Gases and Services, India. All chemicals were used as received without further purification and the solutions required for electrochemical experiments were freshly prepared using ultrapure water. Converting atmospheric CO₂ into low-carbon fuels or small-molecule organic compounds not only benefits CO₂ emission reduction, but also can be used as a carrier of energy storage, which exhibits great significance to alleviate energy shortage and global environmental pollution¹².

2.2 Synthesis Of The Catalysts

Straightforward co-precipitation technique was utilized to blend CuO-ZnO_x (x= 5, 10, 15 and 20 wt.%) utilizing Cu(NO₃)₂•3H₂O, Zn(NO₃)₂•6H₂O, and NaOH as beginning materials. At first, 4 mM of Cu(NO₃)₂•3H₂O was broken up in 200 mL ultrapure water, and a particular measure of Zn(NO₃)₂•6H₂O was added to the arrangement according to required conditions. This arrangement is held under consistent mix ring and temperature was expanded to 80 °C. Afterward, the NaOH solution was added drop-wise under consistent blending until the pH arrived at 14, bringing about the encouraged item¹³. From that point onward, the as accelerated response item was washed more than once with deionized water and ethanol until supernatant pH came to 7. At last, the item was kept for the time being in a stove at 80°C¹⁴. The dried goad uct was then calcined in cylindrical heater at 350 °C in air atmo circle for 2 h and afterward temperature was bit by bit expanded to 700 °C to improve the crystallinity of CuO-ZnO_x¹⁵. The schematic flowchart for the combination of CuO-ZnO_x¹⁶.

2.3 Physico-Chemical Characterization

Precious stone constructions were concentrated on utilizing X-beam diffraction (XRD) procedure and performed on X-beam powder Crystal structures were concentrated on utilizing X-beam diffraction¹⁷ (XRD) strategy and performed on X-beam powder diffractometer (X'Pert³ MRD, Malvern Panalytical Technologies, UK). Morphology of the materials was assessed utilizing field discharge checking electron microscopy (FESEM) and transmission electron microscopy (TEM) on JSM 6100 and JEM 2100 magnifying lens separately (both from JEOL Ltd., Japan) the major side reaction in aqueous solutions, the hydrogen evolution reaction can be inhibited by increasing the energy barrier for H₂ formation and tuning the electrolyte diffusion toward the electrocatalyst surface, thus enhancing the Faradaic efficiencies of CO₂RR products¹⁸. The oxidation state was assessed utilizing X-beam photoelectron spectroscopy (XPS) and surface synthesis by energy dispersive X-beam spectroscopy (EDX) identifiers furnished with HRTEM. XPS spectra were recorded utilizing X-beam photoelectron spectroscopy (Thermo Fischer Scientific Inc. USA). CasaXPS Version 2.3.23 programming was utilized for the deconvolution of acquired crude XPS spectra. The BET surface region and absolute pore volume of materials were assessed by N₂ sorption isotherms recorded at -196°C utilizing AutosorbiQ (Quantachrome Instruments, Germany) instrument¹⁹. These portrayal reads were performed for CuO and best performing CuO-ZnO₁₀ nanoparticles. er diffractometer (X'Pert³ MRD, Malvern Panalytical Technologies, UK). Morphology of the materials was assessed utilizing field outflow examining electron microscopy (FESEM) and transmission electron microscopy (TEM) on JSM 6100 and JEM 2100 magnifying lens separately (both from JEOL Ltd., Japan)²⁰. The oxidation state was assessed utilizing X-beam photoelectron spectroscopy (XPS) and surface creation by energy dispersive X-beam spectroscopy (EDX) finders outfitted with HRTEM. XPS spectra were recorded utilizing X-beam photoelectron spectroscope (Thermo Fischer Scientific Inc. USA). CasaXPS Version 2.3.23 programming was utilized for the deconvolution of crude XPS spectra. The BET surface region and complete pore volume of materials were assessed by N₂ sorption isotherms recorded at -196°C utilizing AutosorbiQ (Quantachrome Instruments, Germany) instrument. These portrayal reads were performed for CuO and best performing CuO-ZnO₁₀ nanoparticles. Where, Z is the number of electrons (Z = 2, 6, 12 and 18 for formic acid, methanol, ethanol, and n-propanol); N is the number of moles of a product (mol L⁻¹) obtained from HPLC or 1H NMR; Q is the total charge passed through the system recorded during electrolysis (Coulombs, C); F is the Faraday constant (96485 C mol⁻¹); V is catholyte volume (L). The production rate of ethanol (μmol h⁻¹ L⁻¹) was calculated using Eq. 2 Productivity = N t (2) Where, t is a total electrolysis time (2 h)

3. RESULTS AND DISCUSSION

3.1 Physico-Chemical Characterization

The oxide inferred bimetallic CuO-ZnO_x impetuses with various wt.% of ZnO were orchestrated by the co-precipitation strategy followed by high temperature calcination. For controlled analysis study, CuO nanoparticles without ZnO content were likewise ready. The crystallinity of the impetuous is significant for ERCO₂ to different helpful synthetics²¹ In this manner, the translucent designs of selected impetuses were assessed by XRD estimations. As displayed in Fig. 2a, the diffraction pinnacles of CuO overwhelm different pinnacles of ZnO since CuO has a higher weight rate than that of ZnO. Tops at 2 θ of 35.37, 38.56, 48.54, 58.02, and 61.24° compare to monoclinic CuO (- 111), (111), (- 202), (202), and (- 113) aspects, respectively (JCPDS #01-078-0428). The tops at 2 θ of 31.78, 47.55, 56.61, and 67.87° are recorded to hexagonal ZnO (100), (102), (110), and (112) aspects, separately (JCPDS #01-089-0510). Wide diffraction tops with bigger full-width at the half greatest (FWHM) affirm that the CuO and ZnO are in nanoscale size. The crystallite size (D) of CuO and CuO-ZnO₁₀ is determined from notable Debye Scherrer condition (D=0.9λ/β cos θ)²² where, D, λ, and β is the normal crystallite size, frequency of incident x-beam bar, and FWHM separately. The extraordinary diffraction pinnacle of CuO at 2 θ of 31.77° was utilized for estimation. The normal crystallite sizes were observed to be around 19-22 nm. Electrochemical execution is enormously influenced by the chemical nature of the electrocatalyst. Subsequently, XPS was utilized to concentrate on a superficial level creation and oxidation condition of chosen CuO and CuO-ZnO₁₀ impetuses. Fig. 2b and Fig. 2c shows the high-goal Cu 2p XPS spectra deconvoluted into two pinnacles. Tops at 933.89 and 954.41 eV compared to the Cu 2p_{3/2} and Cu 2p_{1/2}, respectively. The distinction in restricting energies of Cu 2p_{3/2} and Cu 2p_{1/2} is observed to be 20.52 eV, which is exceptionally near standard worth of Cu 2p in CuO, affirming the CuO stage. What's more, satellite tops at 943.0 and 962.6 eV, affirm the valence province of Cu²⁺. In Fig. 2d, the Zn 2p_{1/2} and Zn 2p_{3/2} pinnacles can be found at 1045.39 and 1022.20 eV, individually²³. The limiting energy contrast between Zn 2p_{1/2} and Zn 2p_{3/2} pinnacles is 23.2 eV, which agreed with the writing of an incentive for ZnO. Morphology and design of CuO and ZnO were researched by FESEM and HR-TEM investigation. Fig. 3 shows the FESEM pictures for CuO and CuO-ZnO₁₀ nanoparticles. The examples show a spherical morphology and the normal molecule size is revolved around 40 nm. Since every one of the particles are in nanosize, the anodes ought to have a superior synergist reaction because of the great surface to volume proportion, however different factors like nature, shape, and source/mass arrangement can fundamentally affect cathode effectiveness. Essential examination shows that main Cu, Zn, and O is noticed, proposing an arranged example is liberated from pollutants. Tests display circle like morphology with extensive agglomeration (Fig. 4). The molecule sizes are in nanoscale for both CuO and CuO-ZnO₁₀ tests. SAED design shows little spots with rings in the two examples, affirming the polycrystalline nature. All the comparing gem planes of ZnO and CuO, listed in the SAED design, are in acceptable concurrence with XRD examines. The EDS elemental planning of chosen CuO-ZnO₁₀ test (Fig. S5) unmistakably shows the uniform conveyances of CuO and ZnO nanoparticles²⁴. These results are in accordance with XRD and FESEM.

3.2 Electrochemical Measurements

The electrocatalytic execution of the various anodes was contemplated by recording LSVs in CO₂ and N₂ soaked 0.1 M KHCO₃ fluid arrangements. The anodes were pre-diminished by performing various outputs at a sweep pace of 50 mV s⁻¹ before each LSV tests. Fig. 5a presentations the LSVs on all CuO/ZnO_x electrodes in CO₂ soaked arrangement. Fig. 5a likewise shows LSV of representative CuO/ZnO₁₀ cathode in N₂ immersed electrolyte. The CD saw in CO₂ immersed electrolyte is higher than that of N₂ soaked electrolyte at the possibilities more prominent than - 0.6 V (versus RHE), proposing CuO-ZnO_x is dynamic for CO₂ decrease with respect to the HER¹¹. Little decrease around - 0.4 V (versus RHE) shows incomplete decrease of ZnO stage. Likewise, when the LSVs of various CuO-ZnO_x cathodes in CO₂ immersed solution are thought about, the CuO anode shows higher mathematical CD than the ZnO stacked terminals. Moreover, the CD reduce as the level of ZnO in the CuO-ZnO_x increase. The higher ZnO stacked cathodes ought to have more uncovered Zn surface than Cu surface, subsequently, the mathematical action of the Cu-Zn terminal reduce with expanding ZnO content. This is because of the way that Cu facially favors HER than Zn I. To concentrate on the impact of applied potential on ERCO₂ item distribution, CA estimations were completed in two compartment H type electrochemical cells at various possibilities going from - 0.4 V to - 1.0 V (versus RHE) for 2 h. Crisp working anode was utilized in each analysis. Fig. S7 shows ordinary current-likely bends for all CuO-ZnO_x cathodes at various applied possibilities. The unexpected decline in current thickness was seen at the starting phase of the experiments because of the decrease of electrocatalyst itself. The CD value came to a consistent value where genuine ERCO₂ is normal. The outline of charge used at various applied possibilities using every one of the five anodes is displayed in Fig. 5b. The higher anode movement was shown by CuO terminal where absolute 30.29 C charge was devoured trailed by CuO-ZnO₅, CuO-ZnO₁₀, CuO-ZnO₁₅, and CuO-ZnO₂₀ where 27.87, 25.16, 23.26, and 20.48 C charge was utilized on the use of - 0.8 V (versus RHE) for 2 h. The outcomes obtained in the CA tests are in concurrence with the LSV butt-centric uses. After the CA tests for 2 h, the fluid item is put away at 4 °C to limit the misfortunes of unstable items. Further, it was examined by HPLC and ¹H NMR, where four unique items, including methanol (CH₃OH), ethanol (CH₃CH₂OH), n-propanol (CH₃CH₂CH₂OH), and formate (HCOO⁻) were distinguished in the vast majority of the examples. The efficiency bends for every one of the terminals are displayed in Fig. 6a and Fig. S8. The formate requires just 2e⁻ for age of one atom in this manner; the arrangement pace of HCOO⁻ is higher over alcohols at the every concentrated on potential. Likewise, the efficiency of formate expanded with expansion in applied potential beginning from almost 100 μmol L⁻¹h⁻¹ at - 0.4 V (versus RHE) to 1000 μmol L⁻¹h⁻¹ at - 1.0 V (versus RHE). The comparative pattern was seen if there should be an occurrence of methanol, ethanol, and n-propanol. The highest usefulness for ethanol was seen to be 160 μmol L⁻¹h⁻¹ at - 1.0 V (versus RHE) utilizing CuO-ZnO₁₀ anode through with CuO, CuO-ZnO₅, CuO-ZnO₁₅, and CuO-ZnO₂₀ cathodes it was 68, 109, 112, and 116 μmol L⁻¹h⁻¹ separately at similar conditions. N propanol is likewise recognized past - 0.8 V (versus RHE) over completely concentrated on cathodes. It

is additionally revealed that thermodynamically methanol is the most un-supported item than that of ethanol and n-propanol. Creation rates are significant for modern sending of ERCO2 measure. Also, computation of Faradaic productivity gives thought regarding selectivity and financial plausibility of the cycle. Curiously, the CuO-ZnOx terminals showed diverse FE for methanol, ethanol, n-propanol, and formic corrosive relying upon the CuO to ZnO proportion (Fig. 6b and Fig. S9). Joining ZnO into CuO upgrades the C2+ items selectivity, For this, the cyclic voltammograms (CV) were recorded in non-Faradaic locale at various output rates (10-100 mV sec⁻¹) using 0.1 M KHCO₃ electrolyte arrangement. As displayed in Fig. S10, there was no dynamic redox top in the filtering likely scope of 0.21 to 0.41 V (versus RHE). The incline of anodic current thickness versus filter rate plot gives Cdl esteem. The most extreme Cdl of 2.6 mF cm⁻² was found for CuO-ZnO10 anode followed by CuO-ZnO5 (1.8 mF cm⁻²), CuO (1.3 mF cm⁻²), CuO-ZnO15 (1.1 mF cm⁻²), and CuO-ZnO20 (0.9 mF cm⁻²). ECSA was then determined by partitioning the Cdl by the capacitance of exposed CuO²³. The ECSA (standardized by CuO) was observed to be 1, 1.38, 2, 0.84, and 0.69 for CuO, CuO-ZnO5, CuO-ZnO10, CuO ZnO15, and CuO-ZnO20 individually. To reveal insight into the dynamic instrument of the ERCO2 over the CuO-ZnOx cathodes, a plot of the log of the general current lair sity versus the potential (Tafel plot) was acquired by LSV information. As displayed in Fig. 7, CuO cathode shows a Tafel incline of 144 mV dec⁻¹ which is closer to hypothetical Tafel slant (118 mV dec⁻¹) for beginning e-move to CO₂ atom for the generation of *CO₂. Interestingly, ZnO stacked cathodes show higher Tafel slant than CuO alone, and with expansion in ZnO stacking, the Tafel slant is likewise expanding. The most noteworthy Tafel slop of 208 mV dec⁻¹ was noticed for CuO-ZnO20, demonstrating that its response kinetics is altogether more vulnerable than that of CuO-ZnO5, CuO-ZnO10, and CuO-ZnO15 having Tafel slant of 151, 171, and 189 mV dec⁻¹ individually. Tafel inclines of the relative multitude of cathodes are in concur ment with LSV bents. As a general rule, the multi-carbon item selectivity of ERCO2 is administered by the limiting strength of adsorbed *CO and *H on the terminal surface. Many creators reported that the Cu has a moderate restricting energy for adsorbed *CO, subsequently *CO species can additionally take e-and *H, and com bine with one more *CO for multi-carbon creation. On the opposite side, Zn terminals has a moderately feeble restricting strength for promotion sorbed*CO hence, *CO desorbs from anode surface without responding further and delivers CO with high selectivity. Numerous analysts proposed Cu-Zn composite electrocatalyst for multi-carbon creation^{7, 23-24}. The created CO and Zn dynamic destinations might have moved to Cu dynamic site having high restricting energy *CO. Two *CO consolidate by taking required e-and *H for the multi-carbon item age. Curiously, in these tests, with improved CuO-ZnO10 terminal, ethanol production was observed to be higher when contrasted with that with CuO electrode. That implies, CuO-ZnO10 anode gives adjusted CO stock for higher CO dimerization. The ZnO in the electrocatalyst gives advantageous CO to expand the nearby CO focus on the Cu surface and thusly, *CO surface inclusion, prompting the acceleration of CO-to-ethanol items change. An ideal ZnO mass stacking, at a particular potential, supplies CO at a rate that accomplishes an immersion of *CO surface inclusion. Also, expanding Zn content past 10% in the CuO-ZnOx cathode, brings about an overabundance supply of CO, and in this manner brings down the *CO dimerization. Hydrogen absorbs dissociatively on span locales between the Cu and Zn iotas, which is a significant stage in the reactant hydrogenation of CO₂ to deliver ethanol. It is noticed that the harmony between CO stockpile rate and CO dimerization rate with balance hydrogen accessibility can just decide the ideal FE of C2+ items. It is likewise revealed that the development of C-C bonds on Cu-Zn is thermodynamically ideal since it shows lower energy toward the bound intermediates *CO-*CO than that on the unadulterated Cu (111). Additionally, the unadulterated Cu (111) surface shows the biggest C-C distance demonstrating a helpless propensity for the C-C coupling. Be that as it may, Cu with Zn shows diminished C-C distance demonstrating a higher possibility for the C-C coupling²⁴. To test the drawn out toughness and soundness of the CuO-ZnO10 cathode, ERCO2 tests were performed over a lengthy period at the enhanced conditions. The absolute current thickness was kept up with at around - 3.74 mA cm⁻² during the 12 h running (Fig. 8a). In addition, the CuO-ZnO10 additionally kept its unique morphology after the strength test (Fig. S11). Likewise, post portrayal by EDX uncovers that the surface natural synthesis has changed and extra K recognized after 2 h ERCO2 which proposes the surface harming because of adsorption of K⁺ from the electrolyte or arrangement of graphitic carbon. Reusability probes CuO-ZnO10 terminal were additionally performed for 6 back to back runs. During reusability tests, the terminal was washed by water and reused for the next run. As displayed in Fig. 8b, the ethanol selectivity is kept up with for initial 3 reuse runs however later it diminished. The reduction in ethanol selectivity is principally attributed to dynamic surface harming as examined before. The response dynamic locales were examined by performing XRD butt-centric of working anode after 0, 10, and 120 min of ERCO2. The XRD examples of delegate terminals are displayed in Fig. S12. Prior to ERCO2, both the cathodes show CuO and ZnO stages as it were. After 10 min ERCO2, the force of CuO and ZnO tops has de wrinkled and power of metallic stage Cu has expanded because of decrease of CuO and ZnO itself at starting time. Irrelevant CuO and ZnO force tops are seen after 2 h CO₂ decrease. It is inferred that the CO₂ decrease can occur on metallic locales of Cu and Zn.

4. CONCLUSION

The CuO-ZnOx electrocatalysts were effectively ready by a basic co-precipitation strategy and utilized for electrochemical reduction of CO₂. The Cu/Zn nuclear proportions can be changed by just changing the antecedent fixations. The CuO terminal displays low selectivity for ethanol with under 9% Faradaic effectiveness (FE). Conversely, expansion of 10 wt.% ZnO with CuO (for example CuO-ZnO10) gives worked on reactant selectivity for ethanol with FE of ~22.3% at -0.8 V (versus RHE) and an absolute current thickness of - 3.78 mA cm⁻². It is accepted that the science of the decreased Cu-Zn interface assumes a significant part in the ethanol selectivity. Additionally, the CuO ZnO10 impetus shows superb long haul strength with no appreciable change in current thickness for something like 12 h. The momentum re hunt features the meaning of bimetallic applications. Synthetic organization of electrocatalysts can be effortlessly tuned by blending different kinds of metals/metal oxides. This review would open the chances for practical improvement of CO₂ change electrocatalysts that are both proficient and might be financially savvy in enormous scope manufactor.

5. CONFLICT OF INTEREST

Conflict of interest declared none.

6. REFERENCES

1. K.R. Bandyopadhyay, COVID-19 and the big oil price crash: exploring the anatomy, sustainable development insights from India, in: P. Dasgupta, A.R. Saha, R. Singhal (Eds.), *Sustainable Development Insights from India*. India Studies in Business and Economics, Springer, Singapore, 2021, pp. 239–257.
2. M. Murshed, M.M. Tanha, Oil price shocks and renewable energy transition: Empirical evidence from net oil-importing South Asian Economies, *Energ. Ecol. Environ.* (2020) 1–21.
3. S. Dongare, N. Singh, H. Bhunia, Nitrogen-doped graphene supported copper nanoparticles for electrochemical reduction of CO₂, *J. CO₂ Util.* 44 (2021) 101382.
4. J.A. Okolie, A. Mukherjee, S. Nanda, A.K. Dalai, J.A. Kozinski, Next-generation biofuels and platform biochemicals from lignocellulosic biomass, *Int. J. Energ. Res.* (2021) 1–25.
5. Techno-economic and life cycle assessment of an integrated hydrothermal carbonization system for sewage sludge *J. Clean. Prod.*
6. S.T. Coelho, J. Goldemberg, Alternative transportation fuels: contemporary case studies, *Encycl. Energy* 1 (2004) 67–80.
7. Q. Fan, M. Zhang, M. Jia, S. Liu, J. Qiu, Z. Sun, Electrochemical CO₂ reduction to C₂₊ species: heterogeneous electrocatalysts, reaction pathways, and optimization strategies, *Mater. Today Energy* 10 (2018) 280–301.
8. P. Sakthivel, K. Subramanian, R. Mathai, Indian scenario of ethanol fuel and its utilization in automotive transportation sector, *ResourConservRecycl* 132 (2018) 102–120.
9. J. Baffes, M.A. Kose, F. Ohnsorge, M. Stocker, *The Great Plunge in Oil Prices: Causes, Consequences, and Policy Responses, Consequences, and Policy Responses*, Policy Research Note, PRN/15/01, World Bank, Washington, DC, 2015.
10. D. Karapinar, C.E. Creissen, J.G. Rivera de la Cruz, M.W. Schreiber, M. Fontecave, Electrochemical CO₂ reduction to ethanol with copper-based catalysts, *ACS Energy Lett* 6 (2021) 694–706.
11. K.P. Kuhl, E.R. Cave, D.N. Abram, T.F. Jaramillo, New insights into the electrochemical reduction of carbon dioxide on metallic copper surfaces, *Energy Environ. Sci.* 5 (2012) 7050–7059.
12. D. Jesic, D.L. Jurkovic, A. Pohar, L. Suhadolnik, B. Likozar, Engineering photocatalytic and photoelectrocatalytic CO₂ reduction reactions: mechanisms, intrinsic kinetics, mass transfer resistances, reactors and multi-scale modelling simulations, *Chem. Eng. J.* 407 (2020) 126799.
13. M.G. Kibria, J.P. Edwards, C.M. Gabardo, C.T. Dinh, A. Seifitokaldani, D. Sinton, E.H. Sargent, Electrochemical CO₂ reduction into chemical feedstocks: from mechanistic electrocatalysis models to system design, *Adv. Mater.* 31 (2019) 1807166.
14. N. Thonemann, A. Schulte, From laboratory to industrial scale: a prospective LCA for electrochemical reduction of CO₂ to formic acid, *Environ. Sci. Technol.* 53 (2019) 12320–12329.
15. Y. Zheng, A. Vasileff, X. Zhou, Y. Jiao, M. Jaroniec, S.-Z. Qiao, Understanding the roadmap for electrochemical reduction of CO₂ to multi-carbon oxygenates and hydrocarbons on copper-based catalysts, *J. Am. Chem. Soc.* 141 (2019) 7646–7659.
16. S. Dongare, N. Singh, H. Bhunia, Nitrogen-doped graphene supported copper nanoparticles for electrochemical reduction of CO₂, *J. CO₂ Util.* 44 (2021) 101382.
17. P. Liu, H. Liu, S. Zhang, J. Wang, C. Wang, Significant role of reconstructed character on CuO-derived catalyst for enhanced electrocatalytic reduction of CO₂ to multicarbon products, *Electrochim. Acta* 354 (2020) 136753.
18. D. Ren, J. Gao, S.M. Zakeeruddin, M. Grätzel, Bimetallic electrocatalysts for carbon dioxide reduction, *CHIMIA Int. J. Chem.* 73 (2019) 928–935.

19. W. Zhu, L. Zhang, P. Yang, X. Chang, H. Dong, A. Li, C. Hu, Z. Huang, Z.J. Zhao, J. Gong, Morphological and compositional design of Pd–Cu bimetallic nanocatalysts with controllable product selectivity toward CO₂ electroreduction, *Small* 14 (2018) 1703314.
20. R. Geiousthy, M.M. Khaled, K. Alhooshani, A.S. Hakeem, A. Rinaldi, Graphene/ZnO/Cu₂O electrocatalyst for selective conversion of CO₂ into n-propanol, *Electrochim. Acta* 245 (2017) 456–
21. S. Dongare, N. Singh, H. Bhunia, Oxide-derived Cu-Zn nanoparticles supported on N-doped graphene for electrochemical reduction of CO₂ to ethanol, *Appl. Surf. Sci.* 556 (2021) 149790.
22. N. Thaweesaeng, S. Supankit, W. Techidheera, W. Pecharapa, Structure properties of as-synthesized Cu-doped ZnO nanopowder synthesized by co-precipitation method, *Energy Procedia* 34 (2013) 682–688.
23. S. Kusama, T. Saito, H. Hashiba, A. Sakai, S. Yotsuhashi, Crystalline copper (II) phthalocyanine catalysts for electrochemical reduction of carbon dioxide in aqueous media, *ACS Catal* 7 (2017) 8382–8385.
24. B. Cullity, S. Stock, in: *Elements of X-Ray Diffraction*, Prentice Hall, Upper Saddle River, NJ, 2001, p. 38

Activity Of Bi_2O_3 Nps Helps For The Drug Development On *Chenopodium Album*

M.Deepa,R.M.Srinivasan,V.Vijayakumar.Hariharapriya

Dhanalakshmi Srinivasan College of arts and science for women (Autonomous), Perambalur Tamilnadu-621212

Abstract: To synthesize bismuth oxide nanoparticles by using fresh leaf extract of *Chenopodium album*. characterized the synthesized bismuth oxide nanoparticle and evaluated the in vitro antifungal activity using synthesized nanoparticles. Characterization was determined using UV-Visible spectroscopy, FT- IR, analysisNatural surroundings devour consecrated with the plant as an enchanted wonder to crop enormous secondary metabolites as bioactive molecules. The prepared AG NPs showed high catalytic behavior and also magnificent antimicrobial possessions alongside together gram-negative and gram-positive microscopic organisms. To synthesize silver NPs, 1 mM arrangement of AgNO_3 was set up into an Erlenmeyer cup with 1 ml of plant extract to a final volume of 10 ml AgNO_3 of solution. The setup was brooded in a dull compartment at room temperature to limit the photoactivation of AgNO_3 . Decrease of Ag^+ to Ag^0 is affirmed via reduction change of arrangement after drab to dark-colored. The aforementioned development remained additionally affirmed through utilizing UV-Vis spectroscopy. The absorption bands recorded at 442, 470, and 510 cm^{-1} are attributed to Bi_2O_3 . FT-IR analysis confirmed the presence of functional groups in the capping agent and also the formation of Bi_2O_3 NPs. FT-IR spectra of synthesized Bi_2O_3 NPs were represented in Figure 2. Figure 2. FT-IR spectra of Bi_2O_3 nanoparticle. Copper nanoparticles are very little and have remarkable attributes which incorporate catalytic behavior and antifungal/antibacterial activities which aren't found in business copper.

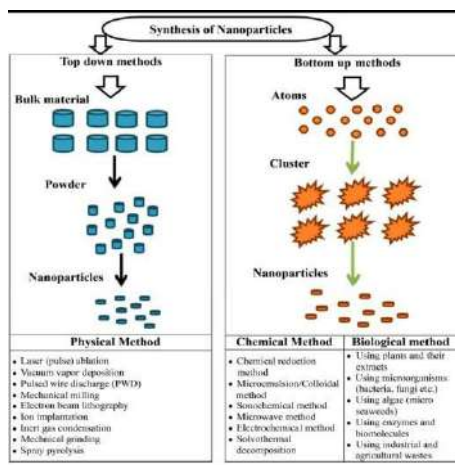
Keywords: UV-Visible spectroscopy, FT- IR, Drug delivery, *C. Albicans*,*Chenopodium album*.

I. INTRODUCTION

Nanotechnology is a developing implement by way of the drug transport system in numerous severe illnesses. It is an advanced method that comprises the production, design, characterization, and application of devices, structures, and systems by regulating the nanometer scale of its size and shape. It has a 1 nm to 100 nm of the size range. The materials which include the size of about 100 nm were termed nanoparticles. It may be categorized as polymeric (natural and synthetic) nanoparticles, metal nanoparticles (Fe_2O_3 , Au nanoparticles, and Ag NPs), and lipoidal (biodegradable) NPs. Metallic nanoparticles synthesized by using plant or plant extract are a method in advance in the direction of greener methodology for drug delivery application. Silver nanoparticles display decent anti-bacterial activity in place of silver has been extensively used as a therapeutic and antibacterial agent over fast decades ¹⁻⁴. Similarly, silver nanoparticles (AgNPs) hold antiviral, antiplatelet, anti-inflammatory, and antifungal activity. Ag NPs may be produced via numerous methods, viz., photochemical reduction (photoreduction, microwave reduction, and X-ray radiolysis), chemical reduction (polyol process, micro-emulsion techniques, thermal reduction,) and physical methods. Medicinal plants demonstrate the key natural basis for drug design and then treat as in the form of ailments for healing purposes. Nanoparticles afford findings to ecological and technical contests in several regions namely medicine, water-treatment, catalysis, and solar energy conversion ⁵. Predominantly CuO nanoparticles devise supposed a prodigious covenant of prominence as they frequently exhibit distinctive and significantly improved chemical, physical and biotic belongings as related to their equivalents of the large scale. CuO nanoparticles, display pronounced attention in recent times due to their distinctive physical and chemical belongings in addition to low-cost preparation. Copper nanoparticles devise various uses as sensors ⁶, as catalysts ⁷, as super-strong materials ⁸, and as heat transfer systems ⁹. Some other applications of nanoparticles such as stability in place of matrix-bound particles, disinfecting property and antimicrobial activity could be promoted for the usage of nanoparticles in plasters to pelt hospital equipment and wall paints ^{10,11}.

I.I GREEN SYNTHESIS

Plant extracts were widely used as reducing agents rather than synthetic chemical compounds. An assembly of scientists effectively steadied as well as produced silver NPs by an entirely green methodology that is an inexpensive, mild, renewable method and the absence of the hazardous toxic reducing agent. These were the underlying methods for the discovery and development of Ag NPs. Around 2.0 ml test substance was pulled back as of response blend at various time intervals, also the greatest absorbance remained estimated utilizing UV-1800 UV-VIS spectrophotometer. Afterward, the response blend sifted over 0.23-mm Steritop Millipore channels, which may be joined with a vacuum siphon. Ag NPs were isolated from the centrifugation of filtrates at 90,609g for 15 mins. Devise chipped away at the green combination of silver NPs. The plant removes acts both as a lessening specialist just as a topping operator. New leaves stood washed by floating faucet water, trailed via twofold refined water, and also dried with air. Magnificently amended leaves stayed bubbled with twofold refined water for about 20 mins, then the concentrate stood put away at 4°C before the usage. These additionally anticipated another, the basic, one-step, fast green strategy used to produce silver NPs via plant concentrates of *Crotalaria retusa* just utilizing *Terminalia arjuna* in place of lessening and settling operators. (Ajitha)



1.2 COPPER NANOPARTICLES

A copper nanoparticle is a copper-based molecule with a 1 to 100 nm size assortment. In addition, the same way as other different types of NPs, copper-based particles will be shaped through common procedures or over chemical synthesis. Cu NPs were exceptionally compelling as a consequence of their authentic uses for example coloring reagents and also advanced medicinal properties. Copper nanoparticles have solid synergist movement, and incredible porosity, the nanoparticles can accomplish a greater yield with dumpier reaction time while used as substances in the synthesis of organics and organometallics ¹². The initiation of antimicrobial activity was done by its nearby cooperation of bacteriological layers in addition to discharged metal particles in solutions ¹³. As the NPs oxidize gradually in solutions, Cu⁺ ions were discharged when the lipid film is nearby and that will make dangerous hydroxyl free radicals. At that point, these radicals dismantle lipids of cell films over oxidation in the direction of deteriorating the layers. Therefore, the intracellular substances leak out of cells over the destructed layers; the cells were never again ready to support basic biological procedures ¹⁴. After a while, every one of its adjustments within the cell brought about to lead cell passing via free radicals.

1.3 ZINC NANOPARTICLES

ZnO NPs that have diameters across under 100 nanometers. It has huge superficial territory comparative with its size and great synergist movement ¹⁵. Zinc oxide NPs were accepted as one amongst three supreme delivered nanomaterials, alongside TiO₂ NPs and SiO₂ NPs ¹⁶. The greatest well-known utilization of zinc oxide NPs as of sunscreens. It was utilized because they reflect bright light, however, are sufficiently little to designate straightforward towards noticeable light. In addition, they were examined to execute hurtful microbes in wrapping ¹⁷, and UltraViolet-defensive materials ¹⁸. Predominantly CuO nanoparticles devise supposed a prodigious covenant of prominence as they frequently exhibit distinctive and significantly improved chemical, physical and biotic belongings as related to their equivalents of the large scale ^{19,20}. In both methodologies, synthesis of NPs was depending on using physical and chemical strategies which includes effective cost and probably risky to nature and also utilization of poisonous and hazardous substances may liable for different organic dangers

2. METHODS

2.1 Preparation of plant extract

The extract solution was equipped by using leaves of the *Chenopodium album* plant ²¹⁻²². The leaves of the fresh plant had been rinsed with deionized water and finely cut into small pieces. Then the plant material was boiled with 100 mL of distilled water at 100°C, sifted by using Whatman No. 1 filter paper then kept at 4°C for additional experimentation. Synthesis of Bismuth oxide nanoparticles. In the preparation of Bismuth oxide nanoparticles, samples Bi(NO₃)₃.5H₂O (0.1g) was first dissolved in enough quantity of deionized water and mixed with 10mL of *Chenopodium album* plant extract solution under vigorous stirring with a magnetic stirrer at 1000 rpm at room temperature for three hours ²³⁻²⁵. Then 1ml of 10% NaOH solution was added to the reaction mixture to adjust the pH of the reaction mixture. The collected dried crude product was maintained at 150°C for 12 hrs in the oven. The obtained powder was calcined at 500 °C for 3 hrs and then crushed into fine powder by using pestle mortar.

2.2 Characterization studies

Bismuth oxide nanoparticles synthesized by using green chemistry technique were confirmed with the help of UV-Visible spectrophotometer (Shimadzu) and FT- IR spectrophotometer (Shimadzu) spectrum in the range 4000-400 cm⁻¹, Powder XRD, SEM, and EDX examination.

2.3 Biological screening Antifungal activity

The minimal inhibitory concentration (MIC) was determined by the broth microdilution method

3. RESULT AND DISCUSSION

3.1 Optical Characterization

The reduction of Bi^{3+} ions to Bi^0 NPs by aqueous leaf extract of *Chenopodium album* was visually observed by color variation in the reaction mixture. The gradual color change in solution from pink to brown. This indicates that the metal chlorides were reduced to form their respective nanoparticles.²⁶⁻²⁷

3.2 UV-Visible Analysis Of Bi_2O_3 NPs

The UV-visible absorption peak arising from 200-400 nm denotes the development of Bi_2O_3 NPs. In our work, the extreme absorption peak seemed at 234 nm directs the individual SPR band for Bi_2O_3 NPs with lesser particle size.

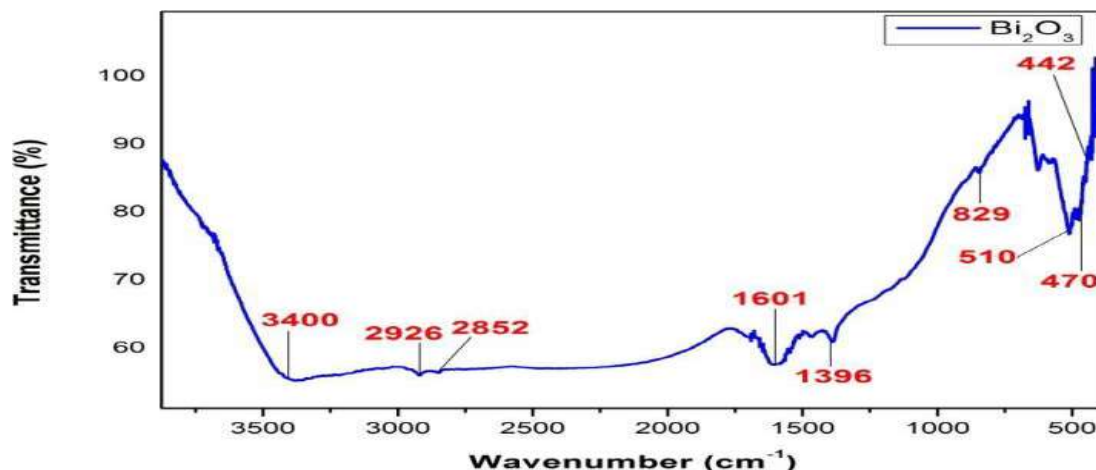


Figure 2 FT-IR Analysis of Bi_2O_3 NPs

The FT-IR spectrum was noted in the ranges from 400-4000 cm^{-1} . The NH group may have appeared as a result of the manifestation of alcohol at 3400 cm^{-1} . The bands at $2800 - 3000 \text{ cm}^{-1}$ signify the existence of a C-H functional group of alkanes. The peaks at 1601 and 1396 cm^{-1} showed the incidence of C-O and C=O from the PVP moiety. The absorption band at 829 cm^{-1} is a consequence of Bi–O–Bi bonds. The strong absorption band at 442 cm^{-1} is due to the stretching mode of Bi–O. This is in agreement with the data reported in reference. The absorption bands recorded at 442 , 470 , and 510 cm^{-1} are attributed to Bi_2O_3 . FT-IR analysis confirmed the presence of functional groups in the capping agent and also the formation of Bi_2O_3 NPs. FT-IR spectra of synthesized Bi_2O_3 NPs were represented in Figure 2. Figure 2. FT-IR spectra of Bi_2O_3 nanoparticle.

Element	Atomic Number	Weight %	Atom %	Weight % Error
O	8	7.42	51.14	1.70
Bi	83	92.58	48.86	5.10
Total	-	100.00	100.00	-

Table 1. Elemental composition of Bi_2O_3 nanoparticle

3.3 Antifungal Activity

The synthesized nanoparticle 2 and *Chenopodium album* fresh leaf extract 1 were evaluated for antifungal activity against four different fungal species. Compound 2 shows remarkable antifungal activity than compound 1. Compound 2 shows high antifungal activity in two fungal species namely *C. Albicans* and *M. audouinii*. Compound 2 with the MIC value of $01 \mu\text{g}/\text{mL}$ was highly active than control clotrimazole with the MIC value of $02 \mu\text{g}/\text{mL}$ in *C. Albicans*. Compound 2 with the MIC value of $02 \mu\text{g}/\text{mL}$ shows high antifungal activity than clotrimazole with the MIC value of $04 \mu\text{g}/\text{mL}$ in *M. audouinii*. The results were summarized in Table 1.

4. CONCLUSION

Bismuth oxide nanoparticle was synthesized using fresh leaf extract of *Chenopodium album*. The synthesized nanoparticle was characterized and confirmed using UV, FT-IR, XRD, and SEM analysis, the results showed that Bi_2O_3 NPs were synthesized properly. The *in-vitro* antifungal activity depicts the effective antifungal activity of Bi_2O_3 NPs. This concludes that further studies on Bi_2O_3 NPs help for drug development.

5. CONFLICT OF INTEREST

Conflict of interest declared none.

6. REFERENCE

1. Ajitha, Y.A.K. Reddy, P.S. Reddy, Green synthesis and characterization of silver nanoparticles using Lantana camara leaf extract, *Mater. Sci. Eng. C* 49 (2015) 373–381.
2. K. Sironmani Daniel, Silver nanoparticles—universal multifunctional nanoparticles for bio-sensing, imaging for diagnostics and targeted drug delivery for therapeutic applications, in: Dr. IzetKapetanovic (Ed.), *Drug Discovery and Development-Present and Future*, InTech. (2011) 477–478.
3. T.N.V.K.V. Prasad, E.K. Elumalai, S. Khateeja, Evaluation of the antimicrobial efficacy of phytogenic silver nanoparticles, *Asian Pac. J. Trop. Biomed.* (2011) 82-85.
4. C. Dipankar, S. Murugan, The green synthesis, characterization and evaluation of the biological activities of silver nanoparticles synthesized from Iresine herbstii leaf aqueous extracts, *Colloids Surf. B: Biointerfaces* 98 (2012) 112-119.
5. C.T. Hsieh, J.M. Chen, H.H. Lin, H.C. Shih, “Synthesis of well-ordered CuO nano fibers by a self-catalytic growth mechanism”, *Appl Phys Lett.*, 82 (2003) 3316-3318.
6. S. Ashokkumar, S. Ravi, V. Kathiravan, S. Velmurugan, Synthesis of silver nanoparticles using A.indium leaf extract and their antibacterial activity, *Spectrochimica Acta Part A: Molecular and Biomolecular Spectroscopy*, 134 (2015) 34-39.
7. H. Bar, D.K. Bhui, G.P. Sahoo, P. Sarkar, S.P. De, A. Misra, Green synthesis of silver nanoparticles using latex of *Jatropha curcas*, *Colloid Surf. A*, 339 (2009) 134-139.
8. T. Tuutijarvi, J. Lu, M. Sillanpaa, G. Chen, As (V) adsorption on maghemite nanoparticles, *J.Hazard. Mater.* 166 (2009) 1415-1420.
9. T. Tuutijarvi, J. Lu, M. Sillanpaa, G. Chen, GA adsorption mechanism of arsenate on crystal gamma- Fe 2 O 3 nanoparticles, *J. Environ. Eng.* 136 (2010) 897-905.
10. T. Premkumar, K.E. Geckeler, Nanosized CuO particles via a supramolecular”, strategy. *Small.* 2(2006) 616-620.
11. H. Raja Naika, K. Lingaraju, K. Manjunath, D. Kumar, G. Nagaraju, D. Suresh, H. Nagabhushana, Green synthesis of CuO nanoparticles, using Gloriosa superba L. extract and their antibacterial activity”,, *Journal of Taibah University for Science.* 9 (2015) 7- 12.
12. N.A. Dhas, C.P. Raj, A. Gedanken, “Synthesis, Characterization, and Properties of Metallic Copper Nanoparticles”, *Chem. Mater.* 10 (1998) 1446-1452
13. J. Ramyadevi, K. Jeyasubramanian, A. Marikani, G. Rajakumar, A.A. Rahuman, Synthesis and antimicrobial activity of copper nanoparticles. *Mater. Lett.* 71 (2012) 114-116.
14. Y. Wei, S. Chen, B. Kowalczyk, S. Huda, T.P. Gray, B.A. Grzybowski, Synthesis of Stable, Low-Dispersity Copper Nanoparticles and Nanorods and Their Antifungal and Catalytic Properties. *J. Phys.Chem. C.* 114 (2010) 15612-15616.
15. Y. Zhang, Y.R. Leu, R.J. Aitken, M. Riediker, Inventory of Engineered Nanoparticle-Containing Consumer Products Available in the Singapore Retail Marketand Likelihood of Release into the Aquatic Environment”; *International Journal of Environmental Research and Public Health.* 12 (2015)8717-8743.
16. R.Kessler, Engineered Nanoparticles in Consumer Products: Understanding a New Ingredient”; *Environmental Health Perspectives.* 119 (2011) 120-125
17. C.S. Iosub, E. Olăreț, A.M. Grumezescu, A.M. Holban, E. Andronescu, Toxicity of nanostructures a general approach”, *Nanostructures for Novel Therapy*, Elsevier, (2017) 793-809.
18. L. Wang, A.J. Ryan, Introduction to electrospinning, *Electrospinning for Tissue Regeneration*, Elsevier, pp. (2011) 3-33. C.T. Hsieh, J.M. Chen, H.H. Lin, H.C. Shih, “Synthesis of well-ordered CuO nanofibers by a self-catalytic growth mechanism”,, *Appl Phys Lett.*, 82 (2003) 3316-3318.,
19. X. Zhang, G. Wang, X. Liu, J. Wu, M. Li, J. Gu, H. Liu, B. Fang, “Different CuO nanostructures: synthesis, characterization, and applications for glucose sensors”, *J Phys Chem C Nanomater Interfaces*, 112 (2008) 16845-16849.
20. Y. Suresh, S. Annapurna, A.K. Singh, G. Bhikshamaiah, Green Synthesis and Characterization of Tea Decoction Stabilized Copper Nanoparticles, *International Journal of Innovative Research in Science Engineering and Technology*, 3 (2014) 11265-11270.

21. A.K. Mittal, Y. Chisti, U.C. Banerjee, Synthesis of metallic nanoparticles using plant extracts. *Biotechnol Adv.* 31 (2013) 346-356.
22. Hodaei, A. Ataie, E. Mostafavi, Intermediate milling energy optimization to enhance the characteristics of barium hexaferrite magnetic nanoparticles. *J Alloys Comp.* 640 (2015) 162-168.
23. E. Mostafavi, A. Babaei, A. Ataie, Synthesis of nano-structured $\text{La}_{0.6}\text{Sr}_{0.4}\text{Co}_{0.2}\text{Fe}_{0.8}\text{O}_3$ perovskite by co-precipitation method. *J Ultrafine Grained Nanostructured Mater.* 48 (2015) 45-52.
24. P. Lesani, A. Babaei, A. Ataie, et al. Nanostructured MnCo_2O_4 synthesized via co- precipitation method for SOFC interconnect application. *Int J Hydrogen Ener.* 41 (2016) 20640-20649.
25. A.K. Mittal, Y. Chisti, U.C. Banerjee, Synthesis of metallic nanoparticles using plant extracts. *Biotechnol Adv.* 31 (2013) 346-356.
26. P. Raveendran, J. Fu, S.L. Wallen, Completely “green” synthesis and stabilization of metal nanoparticles. *J Am Chem Soc.* 125 (2003) 13940-13941.
27. S. Aryal, C.M.J. Hu, L. Zhang, Polymeric nanoparticles with precise ratiometric control over drug loading for combination therapy. *Mol Pharm.* 8 (2011) 1401-1407.

Application Of Wood-Decaying Fungi On Reactive Blue Degradation

Sangavai C, SenthilManikkam J, Haseena M, KaleeswariSudha M

DhanalakshmiSrinivasan College Of Arts And Science For Women (Autonomous),Perambalur-621212.

Abstract: Laccase is a copper-containing polyphenol oxidase found in many plant species and is widely distributed in fungi including wood-rotting fungi. As laccase act on various types of substrates, several different compounds have been used as indicators for laccase production. Some indicators used are Guaiacol, Tannic acid 2, 2-and-bis (3- zethylbenzthiazoline-6-sulphonic acid) (ABTS), Syringaldazine, and polymeric dyes like remazolbrilliant blue-R (RBB-R). Therefore, the present study was undertaken on, screening of laccase-producing fungi from various environmental samples using different indicator compounds in agar plates and methods. Qualitative assay analysis on fungi possesses the good ability for the synthesis of laccase enzyme at pH 5.5 was studied. Laccases are multicopper enzymes that catalyze the oxidation of a wide range of phenolic and non-phenolic aromatic compounds and participate in several applications such as bioremediation, bio pulping, textile, and food industries. Dye degrading wood-decaying fungi *Schizophyllum commune* were isolated from wood and laccase production detected by growth on PDA supplemented with 0.02% guaiacol showing laccase activity. The present study emphasizes the isolation of efficient laccase from mushroom fungi spent and their use for azo dye degradation. The primary isolates were isolated by enrichment culture technique using guaiacol as substrate and laccase production cycle for the isolates was studied and found that peak production was by 72 hours. Degradation efficiency enhanced by the addition of metal ion CuSO₄ and found to be 73% on reactive blue and 74 % on Turquoise Blue. The fungi *Schizophyllumcommune* produce extracellular laccase on culture filtrate found to be an effective dye degrading source.

Keywords: Laccase, Dye degradation, Wood-rotting fungi, zethylbenzthiazoline, guaiacol

I. INTRODUCTION

I.1 Fungal Laccase

Ascomycetous fungi showing potential to degrade lignin include *Aspergillus* sp., *Geotrichum* sp., *Oxyporuslatemarginatus*, *Trichodermaatroviride*, *Trichodermaharzianum*, *Trichodermalongibrachiatum*. Among the Basidiomycetes species, *TrametesVersicolor* and *Phanerchaetechrysosporiumarenaceum* now the most worked organism for laccase synthesis because of their exceptional lignin-degrading capacity. Examples of other laccase producers include *Pleurotusostreatus*¹, *Marasmiusquerophilus*, *Pleurotuspulmonarius*, *Ganodermaadspersum*², *Pycnoporuscinnabarinus* and *Pycnoporusanguineus*, *Chaetomiumthermophilum* and *Phelbiaradiata*, and *P. floridensis*³. Enzyme production is an expanding field of biotechnology. Laccase (E.C. 1.10.3.2, p-benzenedial: oxygen oxidoreductase) can catalyze the oxidation of various aromatic compounds (particularly phenol) with the concomitant reduction of oxygen to water. The role of laccase in lignin and phenolic compound degradations has been evaluated in a large number of biotechnological applications such as dye degradation, bioremediation of some toxic chemical wastes, wastewater, and soil treatments, and also biosensor developments. In particular, the ability to biodegrade various types of dyes by white-rot fungi has proven to be effective.

I.2 Reactive Dyes

Reactive dyes form a new chemical compound when they come into contact with a fiber molecule. Reactive dyes are applied either from a solution with high pH or from neutral solutions that are later alkalinized through a separate process. Due to rapid industrialization and urbanization, a lot of chemicals including dyes, pigments, and aromatic molecular structural compounds were widely used in several industrial applications such as textiles, printing, pharmaceuticals, food, toys, paper. Effluent that is released from the production process of textiles is not properly disposed of, can cause grave environmental pollution, sometimes to levels that can threaten human health, livestock, wildlife, aquatic lives and collapse the entire ecosystem. The presence of dyes in the effluent causes an unpleasant appearance by imparting the color and its breakdown products are toxic, carcinogenic, and mutagenic^{4,18}.

I.3 Impacts Of Reactive Dye

Effluents from the textile industries contain reactive dye in a concentration range of 5-1500mg/L. The processing of dye-contaminated effluents is currently a primary environmental problem^{5,19}. The biological activities also differ greatly between the dyes and, despite the similarities of the structures; the toxicological properties cannot be generalized according to the reference of only one chemical group⁶. Toxicity of *Bacillus velezensis* can degrade and detoxify completely the toxicity presented by the metabolites of the azo dye Direct Red⁷.

I.4 Bioremediation Of Azo Dyes By Enzymes

Textile dyes are decolorized by microorganisms in two major ways, either adsorption on microbial biomass or biodegradation of dyes by the cells or enzymes. The use of biomass is particularly useful if the effluent is highly toxic and does not support the

growth and maintenance of microbial cells¹⁵.

1.5 Bacterial Degradation

Work on bacterial degradation of dyes was started in the 1970s with a report on *Bacillus subtilis*. Azoreductase results in the production of colorless aromatic amines which may be toxic, mutagenic, and carcinogenic to animals^{8,20}

1.6 Algal Biodegradation

Algal culture also can degrade azo dyes through azoreductase. *Chlorella* and *Oscillatoria* were capable of degrading azo dyes to aromatic amines and further to simple organic compounds. *Synechocystis* and *Phormidium* can remove reactive dyes such as Reactive Red, Remazol Blue, and Reactive Black B⁹

1.7 Biodegradation Of Fungi

A group of fungal organisms can decolorize a wide range of dyes. The degradation of some xenobiotics by other white-rot fungi is known to occur under non-ligninolytic conditions and would mainly be through the laccase enzyme activity¹⁰. The enzyme system of basidiomycetes fungi is non-specific in the degradation of pollutants and even acts on mixtures of pollutants¹¹. Laccase has been widely used for various types of dye decolorization studies¹². The major advantage of laccase is that it degrades the dye by a non-specific free radical mechanism to form phenolic products thereby avoiding the formation of aromatic amines¹⁶. The aerobic degradation by laccase yielded products that are less toxic than the original dye¹⁷.

Table 1. Enzymes produced by microorganisms degrade azo dye

MICROORGANISMS	ENZYME	DYE
<i>Pycnoporus cinnabarinus</i>	Laccase	Bromophenol Blue, Orange G, Amaranth, and Malachite Green
Not available	Manganese peroxidase	Reactive Orange 16, remazol Brilliant Blue R
<i>Streptomyces kranskii</i>	Lignin Peroxidase	Reactive Blue 59
<i>Pleurotus ostreatus</i>	Peroxidase and Laccase	Remazol Brilliant Blue R

2. MATERIALS AND METHOD

2.1 Collection Of Wood Adopted Fungi

The study was initiated at the time of the rainy season during February 2021. Wood growing mushrooms with soil debris were collected from a local tea shop and bought to the lab for further studies.

2.2 Isolation Of Fungi

1 gram of the collected sample was added to 10 ml of sterile water and mixed. The suspension was serially diluted from 10^{-1} to 10^{-5} dilution factors. Later, 1.0 ml of each dilution was spread on the surface of the Potato Dextrose Agar (PDA) medium plate which is containing 0.01% Chloramphenicol and incubated at 30 °C for 7 days. Fruiting bodies of mushrooms were used for the isolation. Mycelium was isolated by aseptically moving the upper unexposed part of the basidiocarp on PDA. The plates were incubated at 37 °C for 7 days. Distinct fungal colonies were isolated and repeatedly subcultured until pure cultures were obtained. The cultures were maintained on PDA slants and spore morphology was identified using Lactophenol cotton blue staining.

2.3 Laccase Screening

Laccase production was carried out by inoculation of mycelium from each strain onto PDA plates containing 0.02% Guaiacol and CuSO₄ as indicator compound and it was incubated at 30 °C for 7 days. The formation of reddish-brown halo in Guaiacol supplemented plates indicated a positive laccase secretion. Fungal mat collected and lysed in phosphate buffer under sonication and tested on Turquoise Blue decolorization.

2.4 Qualitative Screening

Screening for laccase-positive cultures was carried out in 250 mL Erlenmeyer flasks containing 100 mL of yeast extract peptone dextrose-copper sulphate (YPD-Cu) medium with 50 ppm of reactive blue. Selected mycelia from PDA plates were used to inoculate the production. Flasks were sterilized at 121 °C for 15 min and incubated with shaking at 120 rpm at room temperature. The percentage of azodye degradation was recorded as follows

$$\% = \frac{T-C}{T} \times 100$$

2.5 Extracellular Enzyme Activity

The Laccase activity was assayed at room temperature by using 10mM Guaiacol in 100 mM sodium acetate buffer (pH 5.0). The reaction mixture contained 3ml acetate buffer, 1ml Guaiacol, and 1ml enzyme source. The change in the absorbance of the reaction mixture containing guaiacol was monitored at 470 nm for 10 mins of incubation using a UV Spectrophotometer. Enzyme activity is measured in U/ml which is defined as the amount of enzyme catalyzing the production of one micromole of colored product per min per ml.

2.6 Calculation

$$\text{Volume activity (U/ml)} = \Delta A_{470\text{nm}}/\text{min} \times 4 \times V_t \times \text{dilution factor}/\epsilon \times V_s$$

Where,

V_t = final volume of reaction mixture (ml) = 5.0

V_s = sample volume (ml) = 1

ϵ = extinction co-efficient of guaiacol = 6,740/M/cm

4 = derived from unit definition & principle

Sampling was done 72 h for laccase activity

3. RESULTS AND DISCUSSION

The grayish-white split gill mushroom (plate 1a) was collected and the fruiting bodies were scattered or clustered on hardwood logs and branches. The fruiting body was 1-4 cm wide and laterally attached to the substratum, stipeless or irregular to shell-shaped (plate 1b) related to *the Schizophyllum commune*. The Medulla region of pileus was made up of loosely arranged hyphae and was heteromerous. the colony was white, the mycelial mat was purely white spreading throughout the surface of the medium, the reverse of the plate was darkened, clamps present, hyphae thin-walled, septate, hyaline and 2 x 3.125 mm thick. *S. commune* is a ubiquitous fungus growing on a variety of trees and decaying wood reported by ¹⁴The low-cost and eco-friendly nature of biological methods using Fungal strains like *Rhizopusarrhizus*, *Aspergillusniger*, *Rhizopusoryzae**PleurotusFlorida*, and *Rhizoctoniasolani* has already been reported in dye degradation. Among the various fungal strains, white-rot fungi (WRF) have been reported as the most effective fungi in the dye decolorization process. The potent fungal strain for laccase production was screened on 0.06% guaiacol containing PDA medium (plate 2). the fungal isolates were screened for laccase production on PDA medium supplemented with 0.02% guaiacol as substrates developed reddish brown zones in the medium due to oxidative polymerization of guaiacol, which marked the presence of laccase. A control run without any fungal inoculation showed no decolorization. The white-rot fungus is the most common laccase producer among all fungi¹³. The crude laccase extracted from fungal cell lysate to decolorize Turquoise Blue showed 33-74% decolorization (plate 3) between 250-1000 μ L by 36h (table1).

Table 1. The activity of crude fungal cell lysate on

The volume of cell lysate μ L	% of decolorization
250	33
500	48
750	62
1000	74

Table 2. Reactive blue degradation

S.NO	Medium	% 48 h	% 72h	Assay
1	Fungi + guaiacol + CUSO_4	40	73	63.42 U/mL
2	Fungi	25	51	52.88 U/mL

Fig 1. isolation of wood-decaying fungi

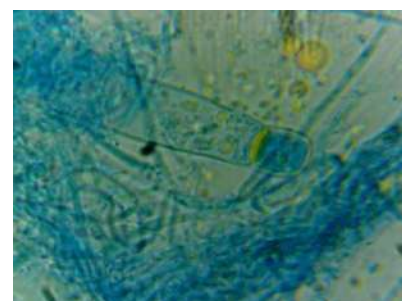
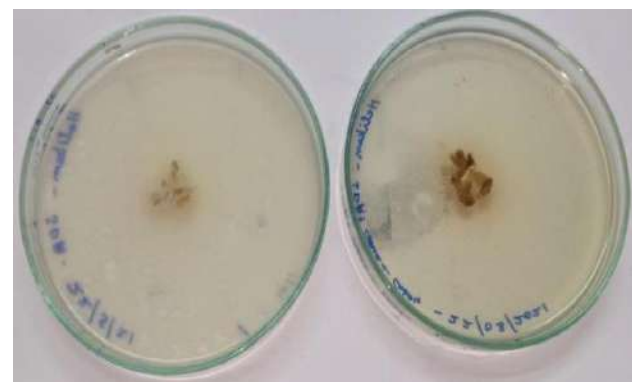


Fig 2. Preliminary lactase screening**Plate 3.preliminary Turquoise Bluedegradation ability of fungal lysate**

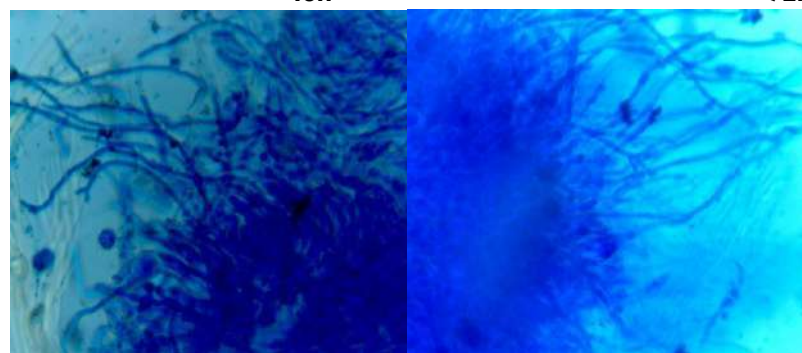
(100-2250-750-1000µL)

Plate 4.Reactive blue degradation

24 h

48h

72h

Without CuSO₄With CuSO₄**Plate 5.Laccase assay of culture filtrate of fungi**

The laccase enzyme production both for mushroom spent samples and was tested using guaiacol and cuso4 as substrate and its degradation on reactive blue was noted (table 2). It was found that these samples didn't show any effective degradation of reactive blue when used alone at 48 and 72 h(51%). but the addition of copper sulfate and guaiacol the percentage of decolorization was 73%(plate 4).The medium with copper sulphate and guaiacol showed complete degradation of all the azo dyes with variation in time (Figure). The result was found to be significant when guaiacolwaslaccase substrate, where reactive blue was completely degraded by fungi.Laccase activity in the medium reached a maximum on the 3rd day. The enzyme assay (plate 5) reveals activity was 63.42 U/mL at pH 5.8 with inducer (guaiacol) and was 52.88 U/mL at pH 6.5 without inducer at room temperature.

4. CONFLICT OF INTEREST

Conflict of interest declared none.

5. REFERENCES

1. Hou, H.M., Zhou, J.T., Wang, J., Du, C.H., Yan, B., 2004: Enhancement of laccase production by *Pleurotusostreatus* and its use for the decolorization of anthraquinone dye. *Process Biochemistry* 39(11): 1415–1419.
2. Songulashvili, G., Elisashvili, V., Wasser, S.P., Nevo, E., Hadar, Y., 2007: Basidiomycetes laccase and manganese peroxidase activity in submerged fermentation of food industry wastes. *Enzyme and Microbial Technology* 41(1-2): 57–61
3. Arora, D.S., Gill, P.K., 2012: Production of ligninolytic enzymes by *Phlebia*
4. Xu M, Guo J, Cen Y, Zhong X, Cao W and Sun G 2005. *Shewanella* decolorization is sp. Nov., a dye decolorizing bacterium isolated from activated sludge of a waste-water treatment plant. *Int. J. Syst. Evol. Microbiol.*, 55: 363-368.
5. Lata H, GargV.K and GuptaR.K 2007. Removal of a basic dye from aqueous solution by adsorption using *Partheniumhysterophorus*: An agricultural waste. *Dyes and Pigments*, 74: 653 -658.
6. Moawad H, Abdel-Rahim W.M and KhalafallahM 2003. Evaluation of bio-toxicity of textile dyes using two bioassays. *Journal of Basic Microbiology*, 43: 218-229
7. Oliveira G.A.R, Ferraz E.R.A, Chequer F.M.D, Grando M.D, Angeli J.P.F, Tsuboy M.S, Marcarini J.C, Mantovani M.S, Osugi M.E, LizierT.M, Zanoni M.V.B and Oliveira D.P 2010. Chlorination treatment of aqueous samples reduces but does not eliminate, the mutagenic effect of the azo dyes Disperse Red 1, Disperse Red 13, and Disperse Orange 1. "Mutation. Research/Genetic Toxicology and Environmental Mutagenesis, 703: 200-208.
8. McMullan G, MeehanC, Conneely A, Kirby N, Robinson T, NigamP, Banat I.M., Marchant R and Smyth W.F 2001. Microbial decolorization and degradation of the textile dyes. *Appl/MicrobiolBiotechnol*, 56(1 -2): 81 -87.
9. Karacakaya P, KilicN.K, DuyguE and DonmezG2009 Stimulation of reactive dye removal by Cyanobacteria in media containing triacontanolhormone. *J.Hazard. Mater.*, 172: 1635- 1639.
10. Fu Y and ViraraghavanT 2001. Removal of acid blue 29 from an aqueous solution by *Aspergillusniger*. *Am. Assoc. Text. Chem. Color. Rev*, 1(1): 36-40.
11. MachadoK.M.G, Matheus D.R and Bononi V.L.R 2005. Ligninolytic enzymes production and remazol brilliant blue R decolorization by tropical brazilian basidiomycetous fungi. *Braz J. Microbiol*, 36: 246 252.
12. Iark D, Buzzo A.J, Garcia J.A, Córrea A, HelmV. G and Corrêa R.C.G 2019. Enzymatic degradation and detoxification of azo dye Congo red by a new laccase from *Oudemansiellacanarii*. *Bioresour.Technol*, 289:121655.
13. FuY and Viraraghavan T 2001. Fungal decolorization of dye wastewater, a review. *Bioresource Technology*, 79(8): 251 - 262.
14. Durand F, Jebrak G, Pessaire D, Fournier M, Bernuau J (2016). Hepatotoxicity of antitubercular treatments: rationale for monitoring liver status. *Drug Safety*; 16: 394–405.
15. Abbara A, Chitty S, Roe JK, Ghani R, Collin S, Ritchie A. (2017). Drug-induced liver injury from antituberculous treatment: a retrospective study from a large TB center in the UK. *BMC Infectious Diseases*; 17: 231- 240.
16. Tostmann A, Boeree MJ, Aarnoutse RE, de Lange WC, van der Ven AJ, Dekhuijzen R (2008). Anti-tuberculosis drug-induced hepatotoxicity: a concise up-to-date review. *J GastroenterolHepatol.*; 23:192–202
17. India TB report, 2019. Revised National TB Control Programme Annual Report, Central TB Division, Min. of Health Govt. of India; 1 – 244.
18. Ramaswamy S, Musser JM. Molecular genetic basis of antimicrobial agent resistance in *Mycobacterium tuberculosis*: 1998 update. *Tuber Lung Dis*. 1998;79(1):3-29
19. Devarbhavi H. Antituberculous drug-induced liver injury: current perspective. *Trop Gastroenterol*. 2011 Jul-Sep;32(3):167-74
20. Keshavjee S, Gelmanova I. Y, Shin S. S, Mishustin Y S, Andreev P. G, Atwood S, Furin J. J, Miller A. (2012). Hepatotoxicity during treatment for multidrug-resistant Tuberculosis: occurrence, management, and outcome. *Int j tube lung dis* 16(5): 596–603.

Synthesis, Of Copper Oxide Nanomaterials Using Fresh Leaves Of Evaluating Its Antibacterial Methods.

V.Bhakyajothi , Senthil Kumaran , S.Suguna, M.Srinivasan

Dhanalakshmi Srinivasan college arts and science for women (Autonomous), perambalur Tamilnadu-621212

Abstract: In the present work, synthesize copper oxide nanoparticles by using the fresh leaf of *Chenopodium album* have been investigated. The synthesized nanoparticles characterized using various characterization technique, and effectively utilized for the *in-vitro* antibacterial activity. CuO nanoparticles are of considerable technical importance. Non-toxicity, thermal consistency, high functional surface area, and the simplicity of processing allowed this commodity for greater usage. There are also special properties, for example, CuO nanostructures have amazing photoconductive and photochemical properties with can to the nanoscale range. CuO NPs (2) were checked against two gram-negative bacteria (*Escherichia coli*, *Pseudomonas aeruginosa* along with two gram-positive bacteria *Staphylococcus aureus* and *Bacillus cereus*). The elemental composition of the synthesized CuO NPs was confirmed by EDX analysis. The weight percentage of Copper and Oxygen atoms were 71.10 and 28.90 respectively. All the diffraction peaks are in good agreement with the standard pattern for the pure monoclinic phase of copper-oxide nanoparticles. There is no impurity peaks were observed. The intense peaks indicate the highly crystalline nature of the formed nanoparticles.

Keywords: *Chenopodium album*, copper oxide nanoparticles, EDX, SEM mapping, XRD analysis, Anti bacterial activity.

I. INTRODUCTION

The main reason NPs have deemed an option to antibiotics is that in certain situations NPs can effectively avoid microbial drug resistance. The rampant use of antibiotics has led to numerous public health hazards, such as superbugs that do not respond to any existing drug and epidemics against which medicine does not have any defense¹. Significant in combating drug resistance is the search for new, effective bactericidal materials and NPs have been established as a promising approach to solving this problem. In certain situations, however, NPs may also facilitate the evolution of bacterial resistance. We address the positive and negative aspects of the interactions between NPs and drug-resistant bacteria in this portion.¹⁻⁵ The effects of NPs on microbial resistance As a new line of defense against microbial resistance and MDR, increasing numbers of NP variants and NP-based materials have been utilized. Various types of NPs have different mechanisms to counter microbial resistance. The section "Antibacterial Mechanisms of NPs" presents various antibacterial mechanisms of NPs according to the metabolic process involved. One of the agreed associations between nanomaterials and antibacterial activity is as follows: "Nanomaterials are highly promising as antibacterial complements to antibiotics and are gaining considerable interest as they could fill the gaps where antibiotics frequently struggle.^{5,6} "However, nanomaterials as a strong carrier will supplement and endorse conventional antibiotics.⁷ This section focuses on the distinct features and complementary advantages of using NPs/nanotechnologies as antibacterial agents compared to traditional antibiotics, which can be summarized as follows: 1) overcoming existing antibiotic resistance mechanisms listed in the section 'Antibacterial activity of NPs' including disruption of bacterial membranes and hindrance of Supervising the current processes of antibiotic resistance⁸, 2) combatting microbes using multiple mechanisms simultaneously⁹⁻¹⁰, and 3) acting as good carriers of antibiotics. Overcoming the existing antibiotic resistance mechanisms. Most types of NPs can overcome at least one of the common mechanisms of resistance mentioned in the section "Antibacterial activity of NPs" (including disruption of bacterial membranes and impedance to biofilm formation). These effects are the result of the NPs bactericidal mode, which is based on their particular physicochemical properties. Unlike typical antibiotics, the measurements of NPs are common, 100 nm. Their unusually small scale contributes to novel properties, such as improved cell activity due to a higher area-to-mass ratio and flexible and controllable application¹¹⁻¹⁴. The processes by which NPs disrupt bacterial membranes are defined in detail in the section on "Antibacterial cycle of NPs;" alternatively, this section considers the interaction of NPs with cell barriers (including cell walls and membranes) and the synthesis of bacterial proteins. Because of its strongly conserved existence, the bacterial cell membrane is hard to modify with only a few genetic changes, which also decreases the probability of bacterial drug resistance. Biofilm formation hindrance is an important mechanism in addition to disrupting bacterial membranes, as biofilms play an important role in the development of bacterial resistance. The unique composition and structure of bacterial biofilms provide the embedded microorganisms with shelter or protection, helping them escape most antibiotics. Furthermore, bacterial biofilms are "a breeding place" for regular mutations of tolerance and the communication and modification between specific bacterial cells with such mutations¹⁵. Studies have shown that many NPs, including Au-based NPs , Ag-based NPs, Mg-based NPs¹⁶, NO NPs^{17,18}, ZnO NPs⁷, CuO NPs¹⁹, Fe₃O₄ NPs, and YF NPs, can prevent or overcome the formation of biofilms. Greater biofilm prevention is achieved through a smaller size and a higher surface area-to-mass ratio, and the particle shape of NPs also has a remarkable effect on biofilm destruction (e.g., NPs with a rod-like shape are more effective than NPs with a spherical shape). Cupric Oxide (CuO) CuO is one of copper's primary oxide and higher oxide. It is an antiferroelectric p-type semiconductor with a gap of about 1.4 eV in the narrow band. CuO has a unit cell and is monoclinic. It is highly insoluble and thermally stable oxide, and very suitable for applications in glass, optics, and ceramic. CuO is used as a flux for CA metallurgy, as an optical polishing agent for glass, as a dye, and in galvanic electrodes. Since the starting material is low cost and easy accessibility, the preparation methods are inexpensive¹⁰, CuO has gained interest.

1.1 Properties Of Cupric Oxide

Table 1. Some basic properties of Cupric oxide at room temperature

Chemical Name	Copper (II) Oxide
Other names	Cupric oxide
Chemical Formula	CuO
Molecular Weight	79.545 g/mol
Appearance	black to brown powder
Density	6.31 g/cm ³
Melting point	1,326 °C
Boiling point	2000°C
Solubility	Insoluble in water, soluble in ammonium chloride, potassium cyanide
Refractive Index	2.63

1.2 Cupric Oxide Nps

Because of their broad variety of possible applications such as high-temperature superconductors, gas sensors giant magnetic resistance materials, solar energy transformation and preparation of organic-inorganic nanostructure composites, glucose sensors, field emission sensors, heterogeneous catalysts, and lithium-based nanoparticles, CuO nanoparticles are of considerable technical importance. Non-toxicity, thermal consistency, high functional surface area, and the simplicity of processing allowed this commodity for greater usage. There are also special properties, for example, CuO nanostructures have amazing photoconductive and photochemical properties with can to the nanoscale range. A variety of morphologies such as nanowires, nanoneedles, nano leaves, nanorods, nanoribbons, CuO nanostructures nanotube arrays have been designed utilizing various techniques. There are many routes required to produce CuO NPs, including chemical bath process, sol-gel method, gas-phase oxidation, micro-emulsion, sonochemical, microwave irradiation, alkoxide-based path, solid-state room temperature reaction system, electrochemical methods, precipitation-pyrolysis ¹².

2. MATERIAL AND METHOD

2.1 Chemicals

All materials were purchased from Nice and Loba chemicals. Solvents that were used during the reactions were of high purity and were used without further purification.

2.2 Collection Of Plant Materials

The plant material *Chenopodium album* was collected from the local places of the Ariyalur area. The freshly collected whole plant was used for the synthesis of copper oxide nanoparticles.

2.3 Preparation Of Plant Extract

The extract solution was equipped by using leaves of the *Chenopodium album* plant. The leaves of the fresh plant had been rinsed with deionized water and finely cut into small pieces. Then the plant material was boiled with 100 mL of distilled water at 100°C, filtered by using Whatman No. 1 filter paper, and stored at 4°C for further experimentation^{20,21}.

2.4 Synthesis Of Copper Oxide Nanoparticles

In the preparation of Copper Oxide nanoparticles, samples Cu(NO₃)₂.3H₂O (0.1g) was first dissolved in enough quantity of deionized water and mixed with 10mL of *Chenopodium album* plant extract solution under vigorous stirring with a magnetic stirrer at 1000 rpm at room temperature for 3hr. Then 1ml of 10% NaOH solution was added to the reaction mixture to adjust the pH of the reaction mixture. The precipitated solid was filtered and dried. The crude product was maintained at 150°C for 12 hrs in the oven. The obtained powder was calcined at 500 °C for 3 hrs and then crushed into fine powder by using pestle mortar.²²

2.5 Characterization Studies

Copper oxide nanoparticles synthesized by using green chemistry technique were confirmed with the help of UV-Visible spectrophotometer (Shimadzu) and FTIR spectrophotometer (Shimadzu) spectrum in the range 4000-400 cm⁻¹, Powder XRD, SEM, and EDX examination.

2.6 Antibacterial Activity

Antibacterial behavior of the aqueous leaf extract of *Chenopodium album* (1)

CuO NPs (2) were checked against two gram-negative bacteria (*Escherichia coli*, *Pseudomonas aeruginosa* along with two gram-positive bacteria *Staphylococcus aureus* and *Bacillus cereus*) that were preserved on the agar slants of the nutrient. The antimicrobial behavior was performed as defined by the Institute of Clinical and Laboratory Standards. Bacterial immunity to CuO NPs was tested using an assay to disperse the disks. Triplicates of the CuO NPs were used in sterile deionized water dilutions of (200, 100, 50, 25, and 12.5). Initially, the isolates were incubated at 4°C for 15min, and then overnight at 37°C. Good test outcomes were graded when an inhibition zone was found across the well after the incubation time then a digital vernier caliper was used to calculate the inhibition zone diameter ¹³⁻¹⁵.

2.7 Minimum Inhibitory Concentration (MIC) Determination

The bacterial isolates, which were used to prepare 0.5 McFarland, were incubated at 37°C overnight. A minimum of 10ml tube nutrient broth medium was prepared and each sample was inoculated aseptically with 1ml of the respective bacterial suspension (approximately 108 CFU / mL). Five dilutions of aqueous leaf extract of *Chenopodium album* (1) CuO NPs (2) (200, 100, 50, 25, and 12.5) were prepared in sterile deionized water and negative control (without CuO NPs) was used. Tests for each isolate were performed in triplicates. The inoculated sets were overnight incubated to 37°C. The apparent turbidity in each tube was examined during the incubation time. Of the measured strain, the lowest concentration without turbidity is defined as the MIC. Tubes showed no turbidity on nutrient agar plates cultivated and incubated overnight at 37°C.

3. RESULTS AND DISCUSSION

The *Chenopodium album* plant was collected around Ariyalur and was identified using the *Flora of the presidency of Madras* and the fresh plant extract plays a key role in copper oxide nanoparticle synthesis.

EDX Analysis of CuO nanoparticle ¹⁶⁻¹⁸

The elemental composition of the synthesized CuO NPs was confirmed by EDX analysis. The manifestation of copper and oxygen peaks in the EDX spectra confirmed that the synthesized material was CuO NPs (Figure 5). The weight percentage of Copper and Oxygen atoms were 71.10 and 28.90 respectively. The further peaks extant in the spectra may be as a result of the existence of bioorganic or impurities in the solution. The elemental composition of CuO nanoparticles was represented in Table 2.

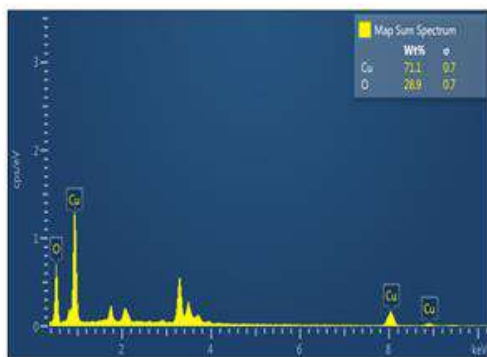


Figure 5. EDX spectra of CuO nanoparticle.

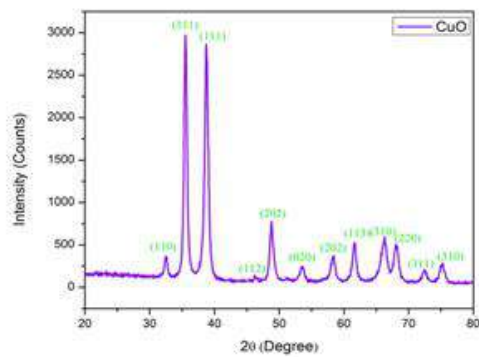


Figure 6. XRD spectra of CuO nanoparticle

Table 2. Elemental composition of CuO nanoparticle

Element	Atomic Number	Weight %	σ
O	8	28.90	0.7
Cu	30	71.10	0.7
Total	-	100	-

3.1 Xrd Analysis

The XRD pattern of aqueous leaf extract of *Chenopodium album* derived CuO NPs were represented in Figure 6. The diffraction peaks at $2\theta = 32.4^\circ, 35.5^\circ, 38.7^\circ, 46.1^\circ, 48.8^\circ, 53.6^\circ, 58.4^\circ, 61.6^\circ, 66.2^\circ, 68.0^\circ, 72.4^\circ$ and 75.2° were respectively indexed to (110), (111), (111), (112), (202), (020), (113), (310), (220), (311) and (310) planes of monoclinic structure of CuO NPs. The obtained diffraction peaks were matched with standard CuO NPs. All the diffraction peaks are in good agreement with the standard pattern for the pure monoclinic phase of copper-oxide nanoparticles (JCPDS No. 80-0076). There is no impurity peaks were observed. The intense peaks indicate the highly crystalline nature of the formed nanoparticles. From the observed main diffracted peak, the average crystalline size can be calculated using the Scherer equation,

$$k\lambda = \frac{D(hkl)}{\beta \cos\theta}$$

Where $D_{(hkl)}$ is the average crystalline size, k is shaped constant (0.89), λ is the wavelength of the incident x-ray (CuK α source, $\lambda = 0.15405$ nm), β is the full width half maximum (FWHM), θ is the incident angle of x-ray. The average crystallite size of the synthesized CuO nanoparticles was 12.45 nm.

3.2 In Vitro Antibacterial Activity

The in vitro antibacterial activity was screened against two Gram-negative bacteria namely, *E. coli*, *P. aeruginosa*, and two Gram-positive bacteria namely, *S. aureus*, *B. cereus* using ciprofloxacin as a standard drug. Minimum inhibitory concentration (MIC) values were determined using the standard agar method. MIC values of the aqueous leaf extract of *Chenopodium album* (1) and synthesized CuO nanoparticle (2) were presented in Table 3. The synthesized CuO nanoparticle shows remarkable antibacterial activity than aqueous leaf extract of *Chenopodium album* (1). CuO nanoparticle 2 shows high antibacterial activity with the MIC value of 23.10 $\mu\text{g/mL}$ than control ciprofloxacin with the MIC value of 25.00 $\mu\text{g/mL}$ in *E. coli*. CuO nanoparticle 2 shows high antibacterial activity with the MIC value of 28.63 $\mu\text{g/mL}$ than control ciprofloxacin with the MIC value of 50.00 $\mu\text{g/mL}$ in *B. cereus*. CuO nanoparticle 2 displayed moderate activity in bacterial cultures *P. aeruginosa* and *S. aureus* with the MIC value of 36 and 28 $\mu\text{g/mL}$ than standard ciprofloxacin. Interestingly, The synthesized CuO nanoparticle (2) shows remarkable antibacterial activity than control Ciprofloxacin in both pathogens *E. coli* and *B. cereus* respectively.¹⁹⁻²²

Table 2. Antibacterial activity of aqueous leaf extract of *Chenopodium album* (1) and synthesized CuO nanoparticle (2)

Comp.No.	MIC $\mu\text{g/mL}$			
	<i>E. coli</i>	<i>P. aeruginosa</i>	<i>S. aureus</i>	<i>B. cereus</i>
1	30.56 \pm 1.18	42 \pm 0.64	34 \pm 1.46	38.23 \pm 2.68
2	23.10 \pm 0.56	36 \pm 1.28	28 \pm 0.32	28.63 \pm 1.34
Ciprofloxacin	25.00 \pm 0.95	30 \pm 0.0	20 \pm 0.0	50.00 \pm 1.75

^aValue were the means of three replicates \pm SD.

4. CONCLUSION

In conclusion, the copper oxide nanoparticle was synthesized using fresh leaf extract of *Chenopodium album*. The synthesized nanoparticle was characterized and confirmed using UV-Visible, FT-IR, XRD, FE-SEM, EDX, and SEM mapping analysis, the results showed that CuO Nps were synthesized properly. The *in-vitro* antibacterial assay depicts the effective antibacterial activity of CuO Nps. This concludes that further studies on CuO Nps help for drug development.

5. CONFLICT OF INTEREST

Conflict of interest declared none.

6. REFERENCES

1. Hsueh PR. New Delhi Metallo- β -lactamase-1 (NDM-1): an emerging threat among Enterobacteriaceae. *J Formos Med Assoc.* 2010;109(10):685–687.
2. Poole K. Mechanisms of bacterial biocide and antibiotic resistance. *J Appl Microbiol.* 2002;92(suppl):55–64.
3. Jayaraman R. Antibiotic resistance: an overview of mechanisms and a paradigm shift. *Curr Sci India.* 2009;96(11):1475–1484.
4. Knetsch MLW, Koole LH. New strategies in the development of antimicrobial coatings: the example of increasing usage of silver and silver nanoparticles. *Polymers Basel.* 2011;3:340–366.
5. Romero D, Aguilar C, Losick R, Kolter R. Amyloid fibers provide structural integrity to *Bacillus subtilis* biofilms. *Proc Natl Acad Sci U S A.* 2010;107(5):2230–2234.
6. Huh AJ, Kwon YJ. “Nanoantibiotics”: a new paradigm for treating infectious diseases using nanomaterials in the antibiotics resistant era. *J Control Release.* 2011;156(2):128–145.
7. Hajipour MJ, Fromm KM, Ashkarran AA, et al. Antibacterial properties of nanoparticles. *Trends Biotechnol.* 2012;30(10):499–511.
8. Reyes VC, Opot SO, Mahendra S. Planktonic and biofilm-grown nitrogen-cycling bacteria exhibit different susceptibilities to copper nanoparticles. *Environ Toxicol Chem.* 2015;34(4):887–897.
9. Edmundson M, Thanh NT, Song B. Nanoparticles based stem cell tracking in regenerative medicine. *Theranostics.* 2013;3(8):573–582.
10. Ramalingam B, Parandhaman T, Das SK. Antibacterial effects of biosynthesized silver nanoparticles on surface ultrastructure and nanomechanical properties of gram-negative bacteria viz. *Escherichia coli* and *Pseudomonas aeruginosa*. *ACS Appl Mater Interfaces.* 2016;8(7):4963–4976.

11. Gurunathan S, Han JW, Dayem AA, Eppakayala V, Kim JH. Oxidative stress-mediated antibacterial activity of graphene oxide and reduced graphene oxide in *Pseudomonas aeruginosa*. *Int J Nanomedicine*. 2012;7:5901–5914.
12. Nagy A, Harrison A, Sabbani S, Munson RS Jr, Dutta PK, Waldman WJ. Silver nanoparticles embedded in zeolite membranes: release of silver ions and mechanism of antibacterial action. *Int J Nanomedicine*. 2011;6:1833–1852.
13. Leung YH, Ng AM, Xu X, et al. Mechanisms of antibacterial activity of MgO: non-ROS mediated toxicity of MgO nanoparticles towards *Escherichia coli*. *Small*. 2014;10(6):1171–1183.
14. Chaudhuri AD. Recent changes in guidelines on programmatic management of drug-resistant tuberculosis in India 2019: a paradigm shift in tuberculosis control The Journal of Association of Chest Physicians. 2020;8 (2); 53 – 63.
16. Durand F, Jebrak G, Pessaire D, Fournier M, Bernauau J (2016). Hepatotoxicity of antitubercular treatments: rationale for monitoring liver status. *Drug Safety*; 16: 394–405.
17. Abbara A, Chitty S, Roe JK, Ghani R, Collin S, Ritchie A. (2017). Drug-induced liver injury from antituberculous treatment: a retrospective study from a large TB center in the UK. *BMC Infectious Diseases*; 17: 231- 240.
18. Tostmann A, Boeree MJ, Aarnoutse RE, de Lange WC, van der Ven AJ, Dekhuijzen R (2008). Anti-tuberculosis drug-induced hepatotoxicity: a concise up-to-date review. *J Gastroenterol Hepatol*; 23:192–202
19. India TB report, 2019. Revised National TB Control Programme Annual Report, Central TB Division, Min. of Health Govt. of India; I – 244.
20. Ramaswamy S, Musser JM. Molecular genetic basis of antimicrobial agent resistance in *Mycobacterium tuberculosis*: 1998 update. *Tuber Lung Dis*. 1998;79(1):3-29
21. Devarbhavi H. Antituberculous drug-induced liver injury: current perspective. *Trop Gastroenterol*. 2011 Jul-Sep;32(3):167-74
22. Keshavjee S, Gelmanova I. Y, Shin S. S, Mishustin Y S, Andreev P. G, Atwood S, Furin J. J, Miller A. (2012). Hepatotoxicity during treatment for multidrug-resistant Tuberculosis: occurrence, management, and outcome. *Int j tube lung dis* 16(5): 596–603.
23. Singh, U. N. (2021) "After The Deluge: An Action Notebook for a Responsible Sociolinguist", IARS' International Research Journal. Vic. Australia, 11(1), pp. 44–50. DOI: 10.51611/gars.irj.v11i1.2021.155.

Heavy Metal Chromium Biosorption By Leather Tannery Isolated Live & Dead Fungi

Haseena M, Dr.P.Viswanathan, Sangavai C, Kaleeswari Sudha, Nandhini S

Dhanalakshmi Srinivasan College Of Arts And Science For Women (Autonomous),Perambalur-621212

Abstract: The microorganisms are used to convert toxic heavy metals into less harmful ones. Microbes play a significant role in the bioremediation of heavy metal contaminated soil and wastewater. Bio-absorption, a passive cation bonding process by dead or living organisms, represents the least costly way to remove toxic heavy metals from industrial wastewater. The ability of microorganisms to remove metal ions in solution has been extensively studied; In particular, live and dead fungi have been recognized as a promising class of low-cost adsorbents for the removal of heavy metal ions. In this study, isolates were used to classify Cr (VI) and Ni (II) biocommunications to evaluate their application for the removal of heavy metals from industrial wastewater. This article aims to review and compare dead and living fungal biosynthesis methods for extracting heavy metal from polluted environments and examine the factors affecting heavy metal removal and biosorption methods for removing metal by various fungal organisms.

Keywords: Heavy metal ion, Chromium, Dead fungi, Ni(II).

I. INTRODUCTION

Global population growth and industrial growth have led to the pollution of the marine environment by metals over the past three decades¹. Disposal of sewage and industrial effluents causes a serious pollution problem to water bodies and agriculture lands. The industrial activities of the last century resulted in a large increase in the human release of heavy metals². Chromium, Mercury, cadmium, lead and arsenic are the most popular heavy metals that cause human poisoning¹. Water bodies and agricultural lands are polluted by disposal of sewage and industrial effluents³. The increasing requirement of leather and its products led to the establishment of a large Commercial tanning industry due to the growth of the population. Chromium is considered to be toxic to living organisms amongst heavy metals⁴. Biologically non-essential systems such as higher levels of heavy metals, highly acidic pH, and low levels of nutrients can cause toxicity in the soil for the growth of vegetation⁵. Environmental pollution due to chromium and its compounds is widespread because of wide applications in industries⁶. The higher level of metal (iron, nickel, chromium, zinc, cadmium, manganese, and copper) that are present in the treated tannery wastewater will contaminate the agricultural soil. It causes serious health hazards when the coops and vegetables are consumed by the consumer⁷. With these wastes, especially in the case of clay, the properties of the soil are altered⁸. Wastes from raw tanneries contain components of chromium and sulfide. Effluents from raw hide processing tanneries contain components of chromium and sulphides in most cases with a major proportion of dyes. Majority of tanneries worldwide use chromium (Cr III and Cr IV), which are highly toxic and poses a serious threat to the environment upon improper disposal of their waste water. Even at low concentrations, these salts have a toxic effect on the food chain of fish and inhibits photosynthesis of aquatic plants⁷. Most tanneries around the world use chromium (Cr III and Cr IV), which are highly toxic and pose a serious threat to the environment due to improper disposal of their wastewater. Even at low concentrations, these salts have a toxic effect on the food chain of fish and aquatic plants photosynthesis inhibit⁸⁻⁹. These metal ions are environmentally sustainable and non-degradable. Accumulation of heavy metals is the result of the removal of concentrated metal waste by industries¹⁰. As a result of the these problems, there is a growing interest in metal-microbial interactions by various scholars and scientists to find suitable methods for dealing with and stabilizing heavy metals in water, soil and waste¹¹. These contaminants have been used for a variety of purposes, including chemical precipitation, filtration, ion exchange, reverse osmosis, evaporation, membrane technology, carbon sequestration, precipitation, sewage freezing, selation, redox and electrochemical treatment¹²⁻¹³. To overcome those limitations, biologic methods are highly recommended because they are environmentally friendly, fast and inexpensive¹⁴. The large amounts of wastewater can treat with low biomass concentration and short time. This is the other advantages of a biological system¹⁵. The chromium concentration of plants that are grown in the area of treated tannery effluent was determined and it was found to be a high concentration of chromium¹⁶. Chromium in this form is hard, stable and resistant to chemical changes such as oxidation or rust. Steel mixed with chromium is harder and brittle than steel and more stainless. Metals in other environmental pollutants may also occur naturally and be present in the environment. Therefore, human exposure to metals is ineluctable, and some studies reported common differences in the toxicity of metals¹⁷⁻¹⁸. Carcinogenic metals are arsenic, cadmium and chromium disrupt DNA synthesis and repair¹⁹. The toxicity of heavy metal is dose dependent. Overweening exposure leads to severe effects in animals and humans, leading to enhanced DNA damage and neuropsychiatric disorders²⁰. Biosorption is the process of cation binding from industrial waste water by dead, living microbial biomass, stands for potentially cost- effective method of removing toxic heavy metals from industrial waste waters. Inactive microbial biomass frequently possess a higher relationship for metal ions compared with living biomass probably due to the absence of competitive protons synthesized during metabolism²¹. Dead fungal cells sequester metals through chemical functional groups of the material respect the cell and especially the cell wall which constitutes a huge level of the cellular dry weight. Fungal cell surfaces can be considered as a mosaic of various functional groups where arrangement edifices with metals can be form. Among these group are carboxyle (- COOH), amide (- NH²), thiol (- SH), phosphate (PO⁴ 3-), and hydroxide (- OH)²². Heavy metal accumulations in vital human organs via the consumption of crops after the discharge of tannery effluents for irrigation

purpose. This results into various degrees of illnesses on acute and chronic exposure, such as cancer, kidney failure, skin problems and cholera²³. The most hazardous environmental pollutants are toxic heavy metals like Cr, Zn, Pb, Cu and Cd are mostly absorbed and get accumulated in various plant part as free metals, which may adversely affect the plant growth and metabolism. Chromium cause major diseases in cattle and human. Nickel cause cancer in human and cattle²⁴.

1.1 Dead And Live Fungi

Biosorption of heavy metals These pollutants are introduced into the aquatic systems significantly as a result of various industrial operations²⁵. Fungal cell walls and their components play an important role in cell absorption and also take up suspended metal particles and colloids. Dead fungal cells sequester metals through chemical functional groups of the material comprising the cell and particularly the cell wall which constitutes a large percentage of the cellular dry weight²². Fungal cell surfaces can be regarded as a mosaic of different functional groups where coordinations complexes with metals can be formed. Among these group are carboxyl (-COOH), amide (-NH₂), thiol (-SH), phosphate (PO₄³⁻), and hydroxide (-OH). One of the main benefits of biosorption is considered to be the inhibition of metal accumulation by growth, or nutrient or excreted metabolism, disrupting the growth of biology from its function into a metal-absorbing substance²⁶. Interaction of heavy metal with white-rot fungi require trace amounts of essential heavy metals such as Cd, Mn or Zn for their growth, but these metals are toxic when present in excess. Fungi are a large and diverse group of eukaryotic microorganisms, of which three groups are of major practical importance, including mold, yeast, and fungi²⁷. Their cell membrane is made up of thin, double-layered lipids, mainly phospholipids and sterols (about 40% of the membrane content) and protein molecules (approximately 60%)²¹.

1.2 Metal Uptake By Dead Biomass

Different authors define biosorption in different terms. The passive extraction of metal ions from a liquid solution by a dead / inactive organism. Studies show that biosynthesis is the activity of living and dead organisms to extract metal ions from aqueous solution. The main dry weight of the fungal cell wall is 80% to 90% of a mixture of polysaccharides, proteins and lipids such as glucans, citrulline, mannans and phosphomannan²⁸. First, the metal ions in solution are bonded to the cell wall of the biosorbents because the cell wall is the primary component that interacts with the metal ions. The site from which the metal is removed from the detected solution is classified as extra-cell accumulation / precipitation, intracellular accumulation and cell surface absorption / precipitation. A method used to kill stem cells) has been shown to increase the metal uptake of dead cell fungi rather than dry cells. Method of Heavy metal cell surface absorption by Dead organism physical absorption, Ion exchange, electrical reactions and metal ion Complex. Fungi have the ability to secrete extensive extracellular enzymes into their growth environment or growth medium. It lead to the potential to grow on a wider carbon source⁹. Fungi have a high ion transfer ability within their cell walls. Microorganisms are play a key role in biodegradable of heavy metals from polluted soil and sewage, but when exposed to high concentrations of heavy metals, it can be detrimental to their growth and function²⁶.

1.3 Live Biomass Metal Uptake

The living cell cell wall is negatively charged due to myths formed from functional groups that are easily attached to the metal ions available in solution²⁹. In the case of the second step process, the metabolic effect leads to the transport of metal ions across the cell membrane after cell surface interaction. Contaminants can travel through the cell membrane to the cell and accumulate endogenous and cell metabolic cycles³⁰.

2. CONCLUSION

The use of fungal biomaterials to remove heavy metals and / or to recover economically valuable metals from waste water is attractive in industrial waste water treatment. The heavy metal removal process has many attractive features including relatively wide temperature and removal of metal ion above pH. This is mainly due to the characteristic of the fungal cell wall with polysaccharides, proteins and large functional groups that can interact with heavy metals by large chemical forces. Furthermore, fungi have a number of mechanisms (body absorption, absorption, precipitation, complex formation, bioammonization, biomimicry and biotransformation) and anonymous functional molecules for the removal of heavy metal ions, and are therefore considered reliable biosynthesizers. The use of genetically modified strains for specific industrial applications will become one of the major subjects of biosorption engineering in the future to produce economically attractive similar sorbent products.

3. CONFLICT OF INTEREST

Conflict of interest declared none.

4. REFERENCES

1. Franca, S, Vinagre, C, Cacador, I and Cabral, HN. 2005. Heavy metal concentrations in sediment, invertebrates and fish in three salt marsh areas subjected to different pollution loads in the Tagus Estuary (Portugal). *Marine Pollution Bulletin*, 50: 993–1018.
2. Mahdi Balali-Mood¹,Kobra Naseri¹,Zoya Tahergorabi¹,Mohammad Reza Khazdair² and Mahmood Sadeghi(2021), oxic Mechanisms of Five Heavy Metals: Mercury, Lead, Chromium, Cadmium, and Arsenic Front. Pharmacol., 13 April 2021.
3. Singh, S., Eapen, S. and D Zouza, S.F., 2006 Cadmium accumulation and its influence on lipid peroxidation and antioxidative system in an aquatic plant, *Bacopamonnieri L. Chemosphere* 62,233-246.
4. Rout, G.R., S. Samantary and P. Das. Differential chromium tolerance among eight mungbean cultivars grown in nutrient culture. 1998, *J. Plant Nutr.*, 20: 473-483.
5. M Brar; SS Malhi; AP Singh: CL Arora; KS Gill, *Can. J. Soil Sci.*, 2000, 80, 465-471.
6. Sharma S., Malavika P.(2014) Bioremediation of tannery wastewater by chromium resistant fungal isolate *Fusarium chlamydosporium* SPFS2-g. *Current World Environment*. 9:721-727.
7. Noorjahan, C. Physicochemical characteristics, identification of fungi and biodegradation of industrial effluent. *Journal of Environment and Earth Science*, v. 4, No. 4, p. 32-39, 2014.
8. Bosnic, M.; Buljan, J.; Daniels, R. P. Pollutants in tannery effluents. Vienna: United Nations Industrial Development Organization, 2000.
9. Bello, O. A.; Abubakar, B. Y.; Abdullahi, I. O. Efficiency of *Aspergillus niger*, *Aspergillus flavus* and *Microsporum nanum* to remove heavy metals from refinery effluent. *Journal of Advances in Biology and Biotechnology*, v. 6, No. 3, p. 1-6, 2016.
10. E. L. Andersson, “Analysis of various bioreactor configurations for heavy metal removal using the fungus *Penicillium ochro-chloron*,” *Worcester Polytechnic Institute*, Worcester, MAS, USA, 1999.
11. S. Siddiquee, K. Rovina, S. A. Azad, L. Naher, S. Suryani, and P. Chaikaw, “Heavy metal contaminants removal from wastewater using the potential filamentous fungi biomass: a review,” *Journal of Microbial & Biochemical Technology*, vol. 7, no. 6, pp. 384–395, 2015.
12. Y. Jin, Y. Luan, Y. Ning, and L. Wang, “Effects and mechanisms of microbial remediation of heavy metals in soil: a critical review,” *Applied Sciences*, vol. 8, no. 8, p. 1336, 2018.
13. Khan, M. Aftab, S. Shakir et al., “Mycoremediation of heavy metal (Cd and Cr)-polluted soil through indigenous metallotolerant fungal isolates,” *Environmental Monitoring and Assessment*, vol. 191, no. 9, p. 585, 2019.
14. N. C. Joshi, “Biosorption: a green approach for heavy metals removal from water and waste waters,” *RJLBPCS*, vol. 4, no. 1, pp. 1–59, 2018.
15. Ayangbenro and O. Babalola, “A new strategy for heavy metal polluted environments: a review of microbial biosorbents,” *International Journal of Environmental Research and Public Health*, vol. 14, no. 1, p. 94, 2017.
16. Zouboulis, P. Samaras, A. Ntolia, K. Goudoulas Division of Chemical Technology, Department of Chemistry, Aristotle University of Thessaloniki, Thessaloniki 54124, Greece Department of Pollution Control Technologies, Technological Educational Institute of West Macedonia, Kozani 50100, Greece 2000.
17. Vahter, M., Åkesson, A., Lidén, C., Ceccatelli, S., and Berglund, M. (2007). Gender differences in the disposition and toxicity of metals. *Environ. Res.* 104 (1), 85–95.
18. Tchounwou, P. B., Yedjou, C. G., Patlolla, A. K., and Sutton, D. J. (2012). Heavy metal toxicity and the environment. *Mol. Clin. Environ. Toxicol.* 101, 133–164.
19. Clancy, H. A., Sun, H., Passantino, L., Kluz, T., Muñoz, A., Zavadil, J., et al. (2012). Gene expression changes in human lung cells exposed to arsenic, chromium, nickel or vanadium indicate the first steps in cancer. *Metallomics* 4 (8), 784–793.
20. Choi, J., Bae, S., Lim, H., Lim, J.-A., Lee, Y.-H., Ha, M., et al. (2017). Mercury exposure in association with decrease of liver function in adults: a longitudinal study. *J. Prev. Med. Public Health* 50 (6), 377.

21. S. Ghaed, E. K. Shirazi, and R. Marandi, "Biosorption of copper ions by *Bacillus* and *Aspergillus* Species," *Adsorption Science & Technology*, vol. 31, no. 10, pp. 869–890, 2013.
22. Haseena M, Raja A, Sangavai C, Roja B, Kiruba Ranjani A(2019), BIOSORPTION OF HEAVY METAL CHROMIUM BY LIVE AND DEAD FUNGI ISOLATED FROM LEATHER TANNERY , Scholar: National School of Leadership: Vol. 8 No. 2.2 (2019).
23. M. U. Mustapha and N. Halimoon, "Microorganisms and biosorption of heavy metals in the environment: a review paper," *Journal of Microbial & Biochemical Technology*, vol. 07, no. 05, pp. 253–256, 2015.
24. Thippeswamy B, Shivakumar CK, Krishnappa M. Bioaccumulation potential of *Aspergillus niger* and *Aspergillus flavus* for removal of heavy metals from paper mill effluent. *J Environ Biol.* 2012 Nov;33(6):1063-8. PMID: 23741802.
25. Ahalya N., Ramachandra T V., Kanamadi R D.(2003). Biosorption of heavy metals. *Research journal of chemistry and environment.* 7(4):71-79.
26. Y. Sağ, "Biosorption of heavy metals by fungal biomass and modeling of fungal biosorption: a review," *Separation and Purification Technology*, vol. 30, no. 1, pp. 1–48, 2001.
27. Petr Baldrian (2003). Interaction of heavy metals with white rot fungi. *Enzyme and microbial technology.* 32:78-91.
28. Abdi and M. Kazemi, "A review study of biosorption of heavy metals and comparison between different biosorbents," *Journal of Materials and Environmental Science*, vol. 6, no. 5, pp. 1386–1399, 2015.
29. Khan, M. Aftab, S. Shakir et al., "Mycoremediation of heavy metal (Cd and Cr)-polluted soil through indigenous metallotolerant fungal isolates," *Environmental Monitoring and Assessment*, vol. 191, no. 9, p. 585, 2019.
30. R. Dhankhar and A. Hooda, "Fungal biosorption - an alternative to meet the challenges of heavy metal pollution in aqueous solutions," *Environmental Technology*, vol. 32, no. 5, pp. 467–491, 2011.

Green Synthesis Copper Oxide Nanoparticle Using Fresh Leafs Of *Chenopodium album* and Evaluated Using FT-IR, UV Spectral Studies

S.Suguna¹, DrJijimon thomas², S.Sathyakumar¹, V.Vijayakumar¹, C.Usharani¹

¹DhanalakshmiSrinivasan College of Arts and Science for Womens (autonomous) perambalur.621212

²Marivanios College ,Thiruvandpuram,Kerala.

Abstract: Recent development in nanoscience and nanotechnology has contributed to the wide applications of metal and metal oxides nanoparticles in several field of sciences, research institutes and industries. Among all metal oxides, copper oxide nanoparticles (CuONPs) regained more attention due to their distinctive properties and applications. The high cost of reagents, equipment and environmental hazards associated with the physical and chemical methods of synthesizing CuONPs has been a major setback. In order to puffer solution to the aforementioned challenges by reducing environmental pollution and production of cheaper nanoparticles with good properties and efficiency, this review focus on collection of comprehensive information from recent developments in the synthesis, characterization and applications from previous scientific findings on biological method of synthesizing CuONPs due to the acclaimed advantages of been cheap, environmentally friendly, convenient and possibility of been scale up in into large scale production reported by numerous researchers. Our finding also support the synthesis of CuONPs from plant sources due to relative abundance of plants for the production of reducing and stabilizing agents required for CuONPs synthesis, potential efficiency of plant biomolecules in enhancing the toxicity effect of CuONPs against microbes, prevention of environmental pollution due of nontoxic chemicals and degradation effectiveness of CuONPs synthesized from plant sources. Furthermore, this study provides useful information on the rapid synthesis of CuONPs with desired properties from plant extracts. To synthesize copperoxide nanoparticle by using fresh leaf of *Chenopodium album*. To characterize the synthesized copperoxide nanoparticle. To evaluate the *in-vitro* antibacterial activity using synthesized nanoparticles.

Keywords: copper oxide nanoparticle, FT-IR, UV spectra, *Chenopodium album*, *in-vitro* antibacterial

I. INTRODUCTION

Bacterial infections constitute a significant cause of recurrent infections and death. Because of its cost-effectiveness and successful efficacy, antibiotics have become the favored therapeutic tool for bacterial infections.¹⁻² However, several studies have provided direct evidence that widespread antibiotic use has resulted in multidrug-resistant bacterial strains emerging. In reality, super bacteria, which are immune to almost all antibiotics, have evolved recently due to antibiotic misuse.³⁻⁴ Studies have shown that these bacteria carry a gene called NDM-1 which is superresistance. The major antibiotic groups currently in use have three bacterial targets: synthesis of the cell wall, translation machinery, and machinery for DNA replication. Unfortunately, against each of those modes of action, bacterial resistance may develop⁵⁻⁶. Resistance mechanisms include expression of enzymes that modify or degrade antibiotics such as β -lactamases and aminoglycosides modification of cell compounds such as vancomycin resistance cell wall and tetracycline resistance ribosomes and expression of efflux pumps that provide simultaneous antibiotic resistance.⁷⁻⁸ Most antibiotic resistance pathways are inaccessible to nanoparticles (NPs) because the mode of action of NPs is direct contact with the bacterial cell wall, without the need to enter the cell; this increases the possibility that NPs would be less vulnerable to fostering bacterial resistance than antibiotics. Hence the focus was on new and exciting NP-based materials with antibacterial activity.⁹⁻¹⁰ Most bacteria exist as a biofilm, which often contains various species interacting with each other and their environment. Biofilms are basically microbial aggregates which depend on a solid surface and extracellular items, such as extracellular polymeric substances (EPSs). Bacteria move onto the surface reversibly but the expression of EPSs makes the attachment irreversible. Once the bacteria are settled, the bacterial flagellum synthesis is inhibited, and the bacteria rapidly multiply, resulting in a mature biofilm being developed¹¹⁻¹². The bacteria are stuck together at this point, creating a barrier that can withstand antibiotics and provide a source for chronic systemic infections. Biofilms thus represent a serious threat to health. In addition, Biofilm bacteria can produce superantigens to evade the immune system.¹³⁻¹⁴ Bacterial infections therefore remain a major issue despite the abundance of antimicrobial drugs and other modern antibacterial agents. Due to their inherent resistance to both antimicrobial agents and host defenses, chronic infections linked to planktonic bacteria and biofilms are always hard to cure. Biofilms in particular are less restrained by antibacterial agents than those of the respective planktonic bacteria.

2. MATERIAL AND METHODS

2.1 Chemicals

All materials were purchased from Nice and Loba chemicals. Solvents that were used during the reactions were of high purity and used without further purification.

2.2 Collection Of Plant Materials

The plant material *Chenopodium album* was collected from the local places of Ariyalur area. Freshly collected whole plants were used for the synthesis of copper oxide nanoparticles.

2.3 Preparation Of Plant Extract

The extract solution was equipped by using leaves of *Chenopodium album* plant. The leaves of fresh plant that had been rinsed with deionized water and finely cut into small pieces. Then the plant material was boiled with 100 mL of distilled water at 100°C, filtered by using whatman No. 1 filter paper and stored at 4°C for further experimentation.

2.4 Synthesis Of Copper Oxide Nanoparticles

In the preparation of Copper Oxide nanoparticles, samples $\text{Cu}(\text{NO}_3)_2 \cdot 3\text{H}_2\text{O}$

(0.1g) was first dissolved in enough quantity of deionized water and mixed with 10mL of *Chenopodium album* plant extract solution under vigorous stirring with a magnetic stirrer at 1000 rpm at room temperature for 3hr. Then 1ml of 10% NaOH solution was added to the reaction mixture to adjust the pH of the reaction mixture.

The precipitated solid was filtered and dried. The crude product was maintained at 150°C for 12 hrs in the oven. The obtained powder was calcined at 500 °C for 3 hrs and then crushed into fine powder by using pestle mortar.

2.5 Characterization Studies

Copper oxide nanoparticles synthesized by using green chemistry techniques were confirmed with the help of UV-Visible spectrophotometer (Shimadzu) and FTIR spectrophotometer (Shimadzu) spectrum in the range 4000-400 cm^{-1} .

2.6 Antibacterial Activity

Antibacterial behavior of the aqueous leaf extract of *Chenopodium album* (1)

CuO NPs (2) was checked against two gram negative bacteria (*Escherichia coli*, *Pseudomonas aeruginosa* along with two gram positive bacteria *Staphylococcus aureus* and *Bacillus cereus*) that were preserved on the agar slants of the nutrient. The antimicrobial behaviour was performed as defined by Institute of Clinical and Laboratory Standards. Bacterial immunity to CuO NPs was tested using an assay to disperse the disks. Triplicates of the CuO NPs were used in sterile deionized water dilutions of (200, 100, 50, 25, and 12.5). Initially, the isolates were incubated at 4°C for 15min, and then overnight at 37°C. Good test outcomes were graded when an inhibition zone was found across the well after the incubation time then a digital vernier caliper was used to calculate the inhibition zone diameter.

2.7 Minimum Inhibitory Concentration (MIC) Determination

The bacterial isolates, which were used to prepare 0.5 McFarland, were incubated at 37°C overnight. A minimum of 10ml tube nutrient broth medium was prepared and each sample was inoculated aseptically with 1ml of the respective bacterial suspension (approximately 108 CFU / mL). Five dilutions of aqueous leaf extract of *Chenopodium album* (1) CuO NPs (2) (200, 100, 50, 25 and 12.5) were prepared in sterile deionized water and a negative control (without CuO NPs) was used. Tests for each isolate were performed in triplicates. The inoculated sets were overnight incubated to 37°C. The apparent turbidity in each tube was examined during the incubation time. Of the measured strain the lowest concentration without turbidity is defined as the MIC. Tubes showed no turbidity on nutrient agar plates cultivated and incubated overnight at 37°C.

3. RESULTS AND DISCUSSION

The *Chenopodium album* plant was collected around Ariyalur and was identified using the *Flora of presidency of Madras* and the fresh plant extract plays a key role in copper oxide nanoparticle synthesis.¹⁵⁻¹⁶.

3.1 Optical Characterization

The reduction of Cu^{2+} ions to Cu^0 NPs by aqueous leaf extract of *Chenopodium album* was visually observed by color variation in the reaction mixture. The gradual color change in solution from light green to sky blue. This indicates that the metal nitrates were reduced to form its respective nanoparticles.¹⁷⁻¹⁸.

3.2 Uv-Visible Spectroscopy

The UV-visible absorption peak arises from 300-380 nm denote the development of CuO NPs. In our study, the extreme absorption peak seemed at 365 nm to direct the individual SPR band for CuO NPs with lesser particle size. **Figure 1** displays UV-vis spectra of CuO NPs synthesized by greener protocol.¹⁹⁻²⁰

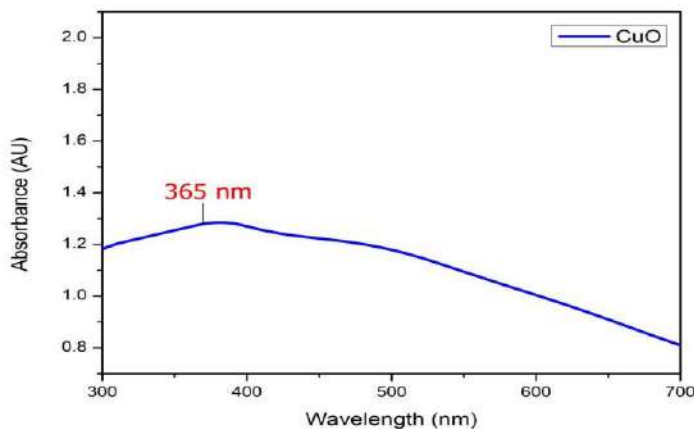


Figure 1 UV – Visible spectra of CuO nanoparticle.

3.3 FT-IR Analysis Of Metal Oxide Nanoparticles Synthesized By Using Aqueous Leaf Extract Of *Chenopodium Album*.

The FT-IR spectrum noted in the ranges from 400-4000 cm^{-1} . A wide peak at 3428.71 cm^{-1} agrees to the O-H group which appeared as a result of the manifestation of Hydroxyl moiety 131 . The bands at 2800 - 3000 cm^{-1} signify the existence of C-H functional group of alkanes 130 . The peaks (1626.66 cm^{-1}) showed the incidence of carbonyl moiety (C=O) which confirms the leaf extract having enzymes or proteins 129.. The band at 516.34 cm^{-1} approves the existence of Cu-O vibrations 131 . FT-IR analysis confirmed the presence of functional groups in the capping agent and also the formation of CuO NPs. FT-IR spectra of green synthesized CuO NPs was represented in Figure 2.

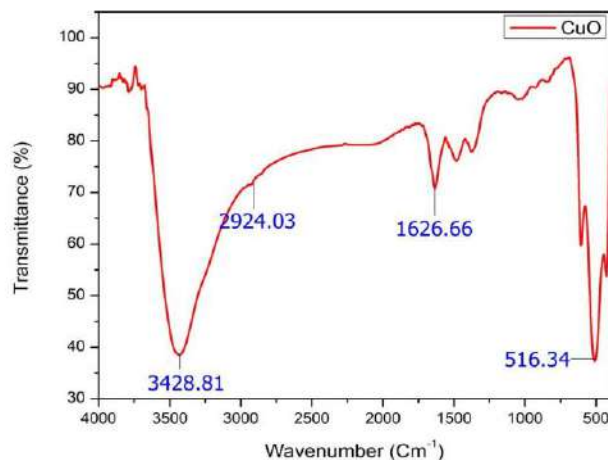


Figure 2. FT-IR spectra of CuO nanoparticle.

4. CONCLUSION

The copper oxide nanoparticle was synthesized using fresh leaf extract of *Chenopodium album*. The synthesized nanoparticle was characterized and confirmed using UV-Visible FT-IR, mapping is, the results showed that CuONps were synthesized properly. This concludes that the further studies on CuONps helps for drug development.

5. CONFLICT OF INTEREST

Conflict of interest declared none.

6. REFERENCES

1. Hsueh PR. New Delhi metallo- β -lactamase-I (NDM-I): an emerging threat among Enterobacteriaceae. *J Formos Med Assoc.* 2010;109(10):685–687.
2. Poole K. Mechanisms of bacterial biocide and antibiotic resistance. *J Appl Microbiol.* 2002;92(suppl):55–64.
3. Jayaraman R. Antibiotic resistance: an overview of mechanisms and a paradigm shift. *CurrSci India.* 2009;96(11):1475–1484.

4. Knetsch MLW, Koole LH. New strategies in the development of antimicrobial coatings: the example of increasing usage of silver and silver nanoparticles. *Polymers Basel*. 2011;3:340–366.
5. Romero D, Aguilar C, Losick R, Kolter R. Amyloid fibers provide structural integrity to *Bacillus subtilis* biofilms. *Proc Natl Acad Sci U S A*. 2010;107(5):2230–2234.
6. Huh AJ, Kwon YJ. “Nanoantibiotics”: a new paradigm for treating infectious diseases using nanomaterials in the antibiotics resistant era. *J Control Release*. 2011;156(2):128–145.
7. Hajipour MJ, Fromm KM, Ashkarran AA, et al. Antibacterial properties of nanoparticles. *Trends Biotechnol*. 2012;30(10):499–511.
8. Reyes VC, Opot SO, Mahendra S. Planktonic and biofilm-grown nitrogen-cycling bacteria exhibit different susceptibilities to copper nanoparticles. *Environ Toxicol Chem*. 2015;34(4):887–897.
9. Edmundson M, Thanh NT, Song B. Nanoparticles based stem cell tracking in regenerative medicine. *Theranostics*. 2013;3(8):573–582.
10. Ramalingam B, Parandhaman T, Das SK. Antibacterial effects of biosynthesized silver nanoparticles on surface ultrastructure and nanomechanical properties of gram-negative bacteria viz. *Escherichia coli* and *Pseudomonas aeruginosa*. *ACS Appl Mater Interfaces*. 2016;8(7):4963–4976.
11. Gurunathan S, Han JW, Dayem AA, Eppakayala V, Kim JH. Oxidative stressmediated antibacterial activity of graphemeoxide and reduced graphene oxide in *Pseudomonas aeruginosa*. *Int J Nanomedicine*. 2012;7:5901–5914.
12. Nagy A, Harrison A, Sabbani S, Munson RS Jr, Dutta PK, Waldman WJ. Silver nanoparticles embedded in zeolite membranes: release of silver ions and mechanism of antibacterial action. *Int J Nanomedicine*. 2011;6:1833–1852.
13. Leung YH, Ng AM, Xu X, et al. Mechanisms of antibacterial activity of MgO: non-ROS mediated toxicity of MgO nanoparticles towards *Escherichia coli*. *Small*. 2014;10(6):1171–1183.
15. Jung WK, Koo HC, Kim KW, Shin S, Kim SH, Park YH. Antibacterial activity and mechanism of action of the silver ion in *Staphylococcus aureus* and *Escherichia coli*. *Appl Environ Microbiol*. 2008;74(7):2171–2178.
16. Khameneh B, Diab R, Ghazvini K, FazlyBazzaz BS. Breakthroughs in bacterial resistance mechanisms and the potential ways to combat them. *Microb Pathog*. 2016;95:32–42.
17. Beyth N, Houria-Haddad Y, Domb A, Khan W, Hazan R. Alternative antimicrobial approach: nano-antimicrobial materials. *Evid Based Complement Alternat Med*. 2015;2015:246012.
18. Pelgrift RY, Friedman AJ. Nanotechnology as a therapeutic tool to combat microbial resistance. *Adv Drug Deliv Rev*. 2013;65(13–14):1803–1815.
19. Mühling M, Bradford A, Readman JW, Somerfield PJ, Handy RD. An I. N. Michiraa, D.N. Katithib, P. Gutoc, G. N. Kamaud, P. Bakere, E. Iwuohaf, International Journal of Sciences: Basic and Applied Research, 2014, 13(2), 63-76.
20. R. Kiruba, G. Alagumuthu, International journal of Pharmacy, 2014, 4(4), 195-200.

Eco-Friendly The Bioreduction Of Silver Nanoparticles In Medicinal Plants Extracts And Bactericidal Activity

Mrs.G.Vanaja ,Dr.A.Priya,Dr.TAdinaveen, R. Saranya

DhanalakshmiSrinivasan College of arts and science for women (Autonomous), Perambalur-621212

Abstract: An eco-friendly green mediated synthesis of inorganic nanoparticles is a fast growing research in the limb of nanotechnology. This study reports the synthesis of silver Nanoparticles by using *Glycyrrhizaglabra* leaf extract. Visually, the formation of silver nanoparticles was confirmed by observing the colour changes from pale yellow to dark brown colour and an intense peak was observed in the UV- spectrophotometer at 460 nm. The possible functional groups in the plant extracts were identified by FT-IR analysis. This novel green approach is a rapid, facile and used for large scale production of metallic nanoparticles.

Keywords: Nanoparticle, UV, IR, NMR, *Glycyrrhizaglabra*

I. INTRODUCTION

Nanotechnology is a powerful new technology for taking apart and reconstructing nature at the atomic and molecular level. Nanotechnology embodies the dream that scientists can remake the world from the atom up, using atomic level manipulation to transform and construct a wide range of new materials, devices, living organisms and technological systems. Nanotechnology and nanoscience involve the study of phenomena and materials, and the manipulation of structures, devices and systems that exist at the nanoscale, <100 nanometers (nm) in size. To put 100nm in context: a strand of DNA is 2.5nm wide, a protein molecule is 5nm, a red blood cell 7,000 nm and a human hair is 80, 000 nm wide. The properties of nanoparticles are not governed by the same physical laws as larger particles, but by quantum mechanics¹⁻³. "Nanotechnology is the creation of functional materials, devices and systems through control of matter on the nanometer length scale (1-100 nanometers), and exploitation of novel phenomena and properties like physical, chemical, biological, mechanical, electrical. at that length scale." ⁴⁻⁵. Nanoparticles are small clusters of atoms about 1 to 100 nanometers long. 'Nano' derives from the Greek word "nanos", which means dwarf or extremely small. It can be used as a prefix for any unit like a second or a liter to mean a billionth of that unit. A nanosecond is a billionth of a second. A nanoliter is a billionth of a liter. And therefore a nanometer is a billionth of a meter or 10^{-9} m. A nanoparticle (or nanopowder or nanocluster or nanocrystal) is a microscopic particle with at least one dimension less than 100nm, due to a wide variety of potential applications in biomedical, optical, and electric fields. Nanoparticles are of great scientific interest as they are effectively a bridge between bulk materials and atomic or molecular structures⁶⁻⁸.

2. MATERIALS AND METHODS

Homogenate was prepared by weighing 20grams of fresh leaves of *Glycyrrhizaglabra* collected from Pattukkottai. Washed thoroughly (thrice) in distilled water and homogenized using a mortar and pestle. The homogenate was then filtered using a sterile gauze cloth. This homogenate extract prepared was then transferred to a sterile container. Simultaneously, the extract was evaporated to obtain dry powder. Both the extract and powder were used for the study of qualitative phytochemical analysis⁹⁻¹⁰.

2.1 Preparation Of Silver Nitrate Solution

Commercially purchased silver nitrate (molecular weight-169.87) was used to prepare 1mM concentrations. Appropriate amount of silver nitrate was weighed and dissolved in distilled water.

2.2 Preparation Of Silver Nanoparticles

To 750 ml of each millimolar concentration of silver nitrate, 7.5 ml of the leaves of *Glycyrrhizaglabra* extract homogenate was added, respectively into a clean conical flask. The conical flasks were then exposed to the sunlight (while being continuously shaken) for the synthesis of the nanoparticles to begin. The colors of the mixture turns from green to brown when exposed to sunlight and once it turns colorless the particles settle at the bottom of the flasks. The particles were then centrifuged (high speed centrifuge) and the supernatant was removed. To the particles now settled at the bottom of the centrifuge tubes, about 1ml acetone was added for the removal of the moisture content from the nanoparticles. The nanoparticle suspensions were transferred to a watch glass, air dried, collected, weighed and stored in a sterile container¹¹⁻¹³.

2.3 UV-VIS Spectra Analysis

The bioreduction of Ag⁺ ions in solutions was monitored by measuring the UV-VIS spectrum of the reaction medium. The UV-VIS spectral analysis of the sample was done by using U-3200 Hitachi spectrophotometer at room temperature operated at a resolution of 1 nm between 200 and 800 nm ranges

2.4 FT-IR Analysis

For FT-IR measurements, the Ag nanoparticles solution was centrifuged at 10,000 rpm for 30 min. The pellet was washed three times with 20 ml of deionized water to get rid of the free proteins/ enzymes that are not capping the silver nanoparticles. The samples were dried and grinded with KBr pellets and analyzed on a Shimadzu FT-IR Affinity 1 model in the diffuse reflectance mode operating at a resolution of 4 cm⁻¹

2.5 Fourier-Transform Spectrometers

The Michelson interferometer Radiation leaves the source and is split. Half is reflected to a stationary mirror and then back to the splitter. This radiation has travelled a fixed distance. The other half of the radiation from the source passes through the splitter and is reflected back by a movable mirror. Therefore, the path length of this beam is variable. The two reflected beams recombine at the splitter, and they interfere (e.g. for any one wavelength, interference will be constructive if the difference in path lengths is an exact multiple of the wavelength. If the difference in path lengths is half the wavelength then destructive interference will result). If the movable mirror moves away from the beam splitter at a constant speed, radiation reaching the detector goes through a steady sequence of maxima and minima as the interference alternates between constructive and destructive phases¹⁴⁻¹⁶. If monochromatic IR radiation of frequency, $f(ir)$ enters the interferometer, then the output frequency, f_m can be found by;

$$f_m = \frac{v}{1.5 \times 10^{11}} \times f(ir)$$

Where v is the speed of mirror travel in mm/s. Because all wavelengths emitted by the source are present, the interferogram is extremely complicated. The moving mirror must travel smoothly; a frictionless bearing is used with electromagnetic drive. The position of the mirror is measured by a laser shining on a corner of the mirror. A simple sine wave interference pattern is produced. Each peak indicates mirror travel of one half the wavelength of the laser. The accuracy of this measurement system means that the IR frequency scale is accurate and precise¹⁸. In the FT-IR instrument, the sample is placed between the output of the interferometer and the detector. The sample absorbs radiation of particular wavelengths. Therefore, the interferogram contains the spectrum of the source minus the spectrum of the sample. An interferogram of a reference (sample cell and solvent) is needed to obtain the spectrum of the sample. After an interferogram has been collected, a computer performs a Fast Fourier Transform, which results in a frequency domain trace (i.e. intensity vs. wavenumber). The detector used in an FT-IR instrument must respond quickly because intensity changes are rapid (the moving mirror moves quickly). Pyroelectric detectors or liquid nitrogen cooled photon detectors must be used. Thermal detectors are too slow. To achieve a good signal to noise ratio, many interferograms are obtained and then averaged. This can be done in less time than it would take a dispersive instrument to record one scan

2.6 Scanning Electron Microscopy (Sem)

The supernatant from the maximum time-point of production (of silver nanoparticles) was air-dried. The synthesized silver nanoparticles fabricated on glass substrates were done for the determination of the formation of silver nanoparticles. The morphology and size of silver nanoparticles were investigated using Scanning Electron Microscope (VEGA 3 TESCAN). The micrographs were recorded by focusing on clusters of particles¹⁹.

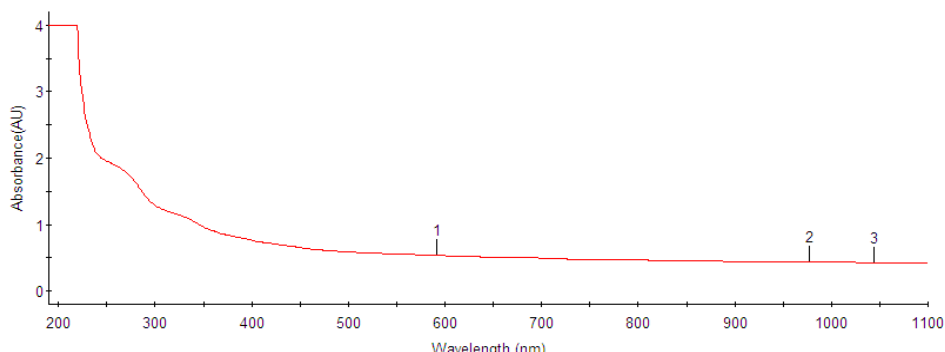
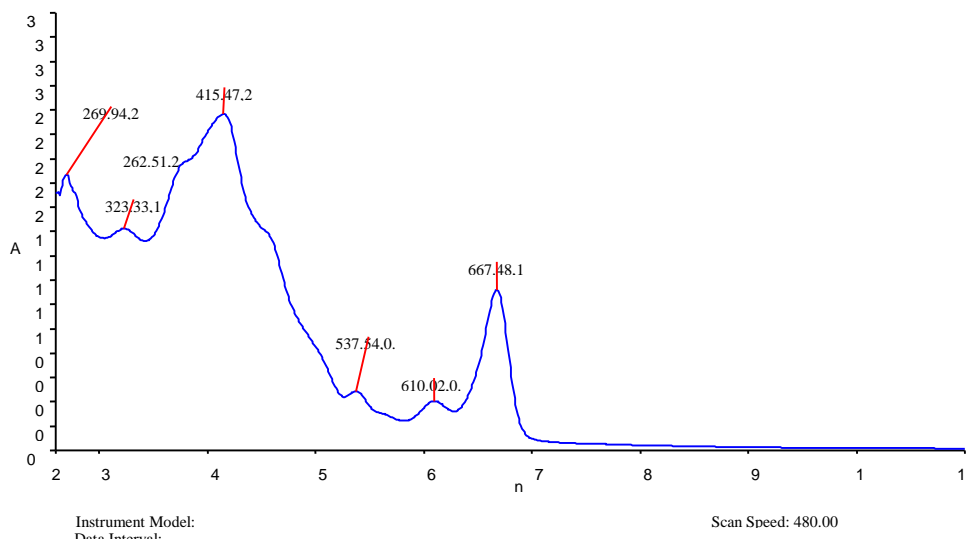
3. RESULTS AND DISCUSSION

Table 1: Preliminary phytochemical investigation of Glycyrrhiza glabra leaf Extract

S.No	Phytochemical compound	Results of qualitative tests
1	Sugars	-
2	Terpenoids	+
3	Alkaloids	+
4	Phenolic compounds	+
5	Tannins	+
6	Flavonoids	+
7	Glycosides	+
8	Quinones	+
9	Steroids	+
10	Coumarins	+

Table -2: Synthesis of silver nanoparticles in plant extract.

S.No	Plant extract+AgNO ₃ leaf	Color change		pH change		Color intensity	Time	Result
		Scientific name	Before	After	Before			
I	<i>Glycyrrhizaglabra</i>	Light yellow	Brown	4.0	4.60	+++	20 min	Positive

Note: +++: Dark brown**Fig: 1 UV-VIS analysis of *Glycyrrhizaglabra* leaf extract****Fig: 2 FT -IR analysis of *Glycyrrhizaglabra* leaf extract****Spectrum Name:Glycyrrhizaglabra**

3.1 Phytochemical Analysis

The phytochemical analysis of *Glycyrrhizaglabra* leaf extract showed the presence of alkaloids, tannins, flavonoid, quinines, steroids, coumarins and phenolic compounds. Sugar alone was absent in the leaf extract (Table I). Various herbs and spices have been reported to exhibit antioxidant activity and antimicrobial properties. A majority of the antioxidant antimicrobial properties is attributed to the flavones, isoflavones, flavonoids, anthocyanin, coumarin, lignans, catechins and isocatechins. Antioxidant based drug formulations are used for the prevention and treatment of complex diseases like atherosclerosis, stroke, diabetes, Alzheimer's disease and cancer ¹³. Cancer chemoprevention by phytochemicals may be one of the most feasible approaches for cancer control. Phytochemicals obtained from vegetables, fruits, spices, teas, herbs and medicinal plants, such as alkaloids, terpenoids and other phenolic compounds, have been proven to suppress experimental carcinogenesis in various organs in pre-clinical models. Recent studies have indicated that mechanisms underlying chemopreventive potential may be a combination of antioxidant, anti-inflammatory, immune-enhancing and hormone modulation effects, with modification of drug metabolizing

enzymes, influence on cell cycle and cell differentiation, induction of apoptosis, suppression of proliferation and angiogenesis, playing roles in the initiation and secondary modification stages of neoplastic development (Rabi and Gupta, 2008). Our plant also contains alkaloids, terpenoids and other phenolic compounds.

3.2 Snps Synthesis

In the current study, Silver Nano Particles (SNPs) was synthesized. Synthesis of SNPs were indicated by the Color Change from yellow to brown and the pH was changed from 4.0 to 4.60. Table -2 shows the colour change during the synthesis of silver nanoparticles. The synthesis and application of nanomaterial is in the limelight in modern nanotechnology. Plants including herbs, lower plants, higher plants, weeds etc. contain an array of secondary metabolites such as phenolic compound, terpenoids, essential oils, and flavonoids, which helps in the reduction of metal ion and formation of nanoparticles. The present investigation demonstrated the formation of silver nanoparticles by the reduction of aqueous silver metal ions by plant extracts prepared using *Glycyrrhizaglabra*. In the present study SNPs were synthesized by using flower extract of *Glycyrrhizaglabra* rapidly within 20 min of incubation period and yellowish brown colour was developed by addition of Silver Nitrate. The time duration of change in colour and thickness of the colour varies from plant to plant. The reason could be the quantitative variation in the formation of SNPs (or) availability of H⁺ ions to reduce the silver. It is well known that SNPs exhibit yellowish brown colour in aqueous solution due to excitation of surface plasmon vibrations in silver nanoparticles. Silver nitrate is used as a reducing agent as silver has distinctive properties such as good conductivity, catalytic and chemical stability. The aqueous silver ions when exposed to herbal extracts were reduced in solution, thereby leading to the formation of silver hydrosol²⁰.

3.3 Detection And Characterization Of Phyto Silver Nanoparticles

Visual Observation: After treatment of flower extract of *Glycyrrhizaglabra* with AgNO₃, the colour change of the reaction mixture was visually observed. The time taken for the reaction mixture to change colour was noted. The reduction of silver ions into silver particles during exposure to the plant extract was followed by colour change from colorless or pale yellow to brown. It is well known that silver nanoparticles exhibit yellowish brown colour in aqueous solution due to excitation of surface plasmon vibrations in silver nanoparticles.

3.4 Uv- Vis- Spectroscopy

The reduction of silver metal ions to silver nanoparticles was preliminarily analysed using UV-Vis Spectrophotometer between 300-700nm and depicted in Fig: 1. This analysis showed an absorbance peak at 420 nm which was specific for Ag nanoparticles. UV-visible spectroscopy is an important technique to determine the formation and stability of metal. Nanoparticle in aqueous solution. The reaction mixture changes the colour by adding various concentrations of metal ions. These color changes arise because of the excitation of surface plasmon vibrations in the silver Nanoparticle. It shows yellowish to dark brown in colour. The dark brown colour of silver colloid is accepted to surface plasmon resonance (SPR) arising due to the group of free conduction electrons induced by an interacting electromagnetic field¹⁴⁻¹⁵. The synthesis of silver nanoparticles was confirmed firstly by visual observation: the yellowish colour of petal extracts turned to brown after addition of AgNO₃ 10-3 M solution due to excitation of surface plasmon vibrations indicating the formation of silver nanostructures.

3.5 Ft-Ir Analysis

FT-IR measurement was carried out to identify the possible biomolecules responsible for capping and efficient stabilization of Ag Nanoparticle synthesized using *Glycyrrhizaglabra* leaf extract. This spectrum shows a lot of absorption bands indicating the presence of active functional groups in the synthesized silver Nanoparticles. The intensity peaks are slightly increased for the period of silver nanoparticle synthesis like 3470, 2832, 2719, 1630 cm⁻¹. Fig: 2 shows the band at 3470 corresponds to O-H and H Stretching vibrations of alkaline phenol. The peak at 2832 indicates OH stretching vibrations to carboxylic acid. The peak at 2719 represents a C (trible bond) in plane bend to alkenes. The peak at 1630 corresponds to N-H, C-Br stretch in vibrations to primary amines. The weak band at 1362 indicates C-H stretching vibrations and it corresponds to the presence of aromatic acids in the flower extract of silver nanoparticles. The presence of active functional groups in seed extract results in the swift reduction of silver ions to silver Nanoparticles. To obtain a good signal to noise ratio of silver nanoparticles were taken in the range 669-3400 cm⁻¹. (Fig: 2). FT-IR spectra showing the presence of IR peaks assigned to polyphenols and also the existence of IR bands characteristic of amide I and amide II groups specific for proteins/enzymes suggest that flavonoids and proteins present in aqueous petal extracts of ornamental plants could be responsible for the reduction of silver ions and for the stabilization of the photosynthesized noble metal nanoparticles.

3.6 Sem Analysis

The SEM image showing the high intensity of silver nanoparticles synthesized by *Glycyrrhizaglabra* extract further confirmed the development of silver nanostructures. SEM provided further insight into the morphology and size details of the silver nanoparticles. SEM analysis showed the particle size of about 100 nm as well the crystal structure of the nanoparticles. The silver nanoparticles synthesized via green route are highly toxic to MultiDrug Resistant (MDR) bacteria hence have a great potential in Biomedical applications. The present study showed a simple, rapid, economical route to synthesize silver nanoparticles. Application of such eco-friendly nanoparticles in bactericidal, wound healing and other medical and electronic applications makes this method potentially exciting for the large-scale synthesis of other inorganic materials (nano-materials)¹⁸⁻²⁰.

4. SUMMARY AND CONCLUSION

In the preset investigation silver nanoparticles were synthesized from *Glycyrrhizaglabraleaf* extract and the synthesis of nanoparticles were confirmed both visually and by spectrophotometrically. In visual observation the colour change of the solution, confirms the synthesis of AgNPs. UV-VIS, FT-IR and SEM analysis confirmed the presence of AgNPs by their respective peaks and images. The present study represents a clean, non-toxic as well as eco-friendly procedure for synthesizing AgNPs of *Glycyrrhizaglabraleaf* extract. The capping around each particle provides a regular chemical environment formed by the bio-organic compound present in *Glycyrrhizaglabraleaf* extract, which may be chiefly responsible for the particles to become stabilized. This technique gives us a simple and efficient way for the synthesis of nanoparticles with tunable optical properties governed by particle size. The synthesis of silver nanoparticles was demonstrated by visual inspection and by performing some spectral techniques (UV-VIS absorption, FT-IR spectroscopy and SEM analysis). FT-IR results proved that bioactive compounds responsible for silver bioreduction could be proteins and flavonoids present in the aqueous extracts of *Glycyrrhizaglabrapresumed* to act as reducing and capping agents for the silver nanoparticles preventing the agglomeration of the particles and thereby stabilizing the nanoparticles. From the nanotechnology point of view, this is a noteworthy development for synthesizing AgNPs economically. In conclusion, this green chemistry approach toward the synthesis of AgNPs possesses several advantages viz, easy process by which this may be scaled up, economic viability, etc. Applications of such eco-friendly nanoparticles in bactericidal, wound healing and other medical and electronic applications, makes this method potentially stimulating for the large-scale synthesis of other inorganic materials, like nanomaterials. The present study included the bio-reduction of silver ions through medicinal plant extracts.

5. CONFLICT OF INTEREST

Conflict of interest declared none.

6. REFERENCE

1. Abha vermal, prakashjoshi&arvindarya synthesis of plant-mediated silver nanoparticles using plant Extract of *sonchusasper*International Journal of Nanotechnology and Application (IJNA)Vol. 3, Issue 4, Oct 2013, 11-18.
2. Abou El-Nour MM, Eftaiha A, Al-Warthan A, Ammar RAA. Arab J. Chem. 2010, 3: 182, 135.DOI: 10.1016/j.arabjc.2010.04.008
3. Acker C I, Brandão R, Rosário A R, Nogueir C W. Antioxidant effect of alkynylselenoalcohol compounds on liver and brain of rats in vitro Environmental Toxicology and Pharmacology 2009; 28: 280–28
4. Acker C I, Brandão R, Rosário A R, Nogueir C W. Antioxidant effect of alkynylselenoalcohol compounds on liver and brain of rats in vitro Environmental Toxicology and Pharmacology 2009; 28: 280–287
5. Ahmad, A. and Sastry, M.A. Biological synthesis of triangular gold nanoprisms. *Nat. Mater.*, 3, 2004, 482-488.
6. Akindele AJ, Adeyemi OO. Antiinflammatory activity of the aqueous leaf extracts of *Byrsocarpuscoccineus*. *Fitoterapia* 2007; 78: 25-28.
7. Anandan1, R. Eswaran1, A.Doss2, G. Sangeetha3 and S. P. Anand. Chemical Compounds Investigation of AervalanataLeaves – A Potential Folklore Medicinal Plant., *Bulletin of Environment, Pharmacology & Life Sciences* Volume 1, Issue 1, December 2011: 20-23
8. Bhattacharya, D, Gupta, R. K,Crit. Rev. Biotechnol. 2005, 25, 199.
9. Biswas, A. Aktas, O.C.Schumann, U.Saeed, U. Zaporjtchenko and Faupel F. (2004). Tunable multipleplasmon resonance wavelengths response from multicomponent polymer-metal nanocomposite systems. *Applied Physical Letter*, 84: 2655-2657.
10. Chandran, S.P,Chaudhary, M, Pasricha, R. Ahmad, A.Sastry, M. *Biotechnol. Prog.*2006, 22, 577. DOI: 10.1021/bp0501423.
11. C. Song, F. Zeng, K. W. Geng, X. B. Wang, Y. X. Shen, and F. Pan, *J. Mag. Mag. Mat.*, 309 (2007) 25.
12. V S Sangeetha , Vanith A, Devi P, BhakyajothiV"Green synthesis of Zinc oxide nanao particle using flower extract of phyla nodiflora" Schoolar National School of leadership vol-9
13. S. Deka, R. Paricha, and P. A. Joy, *Chem. Mater.*, 16 (2004) 1168.
14. O. D. Jayakumar, I. K. Gopalakrishnan, C. Sudakar, R. M. Kadam, and S. K. Kulshreshtha, *J. Alloys Comrnd.*, 438 (2007) 258
15. R Elayaperumal , G Vanaja, A Vanith,VSSangeetha "Green synthesis of Glycyrrhizagla silver nano particle and conformation of through Microscopy and Spectrophotometric techniques. "Eurasian journal of Analytical chemistry ,2017-Feb ,1680-168.

16. C. N. R. Rao and F. L. Deepak, *J. Mater. Chem.*, 15 (2005) 573.
17. R. Podila, W. Queen, A. Nath, J. T. Arantes, A. L. Schoenhalz, A. Fazzio, G. Dalpian, J. He, S.
18. K.S. Novoselov, A.K. Geim, S.V. Morozov, D. Jiang, Y. Zhang, S.V. Dubonos, I.V. Grigorieva and A.A. Firsov, *Science*, 306 (2004).
19. Illustrated Oxford Dictionary, Rev. Ed., Dorling Kindersley, London, (2003)
20. S. Rani, P. Suri, P.K. Shishodia and R.M. Mehra, *Sol. Energ. Mat. Sol. Cells*, 92 (2008) 1639–1645.

ANTIOXIDANT ANTIBACTERIAL AND ANTI-INFLAMMATORY ACTIVITY OF WITHANIYA SOMNIFERA

RojaB ,Gajalakshmi P, Dr.K.Rajesh, Nitha.V.Ravi, Gayathri R

PG and Research Department of Microbiology, DhanalakshmiSrinivasan College of Arts and Science For Women (Autonomous), Perambalur-621 212, Tamil Nadu, India

Abstract: Medicinal plants are a source of natural active compounds widely used by tribes around the world for many ailments. Different types of rheumatic diseases is one of the major concern in the present world. Developing safer and anti-inflammatory Drug is one of the major focus among researcher. One of the problem is the reappearance of the symptoms if the medication is stopped. *Withania somnifera*, a traditional Indian medicinal plant, has anti-stress, antioxidant, analgesic, anti-inflammatory, cardioprotective, tonic, antispasmodic, immune modulating and immune stimulating effects. Other actions include anti-inflammatory, immunomodulatory, anti-tumor, anti-angiogenic, anti-invasive and chemopreventive effects. The aim of the study is to produce anti-inflammatory and antioxidant drug from the root of *W.somnifera*. The objectives of the study are to extract *W.somnifera* root compounds with ethanol, analyze Phytochemical of *W.somnifera* root, testing of antibacterial activity, testing of antioxidant activity and to screen anti inflammatory property WS extract.

Keywords: *W.somnifera*, Analyze phytochemical, Anti Inflammatory, Rheumatic Diseases

I. INTRODUCTION

Over 3000 years, Ashwagandha or *Withania somnifera* (WS) is considered as an important herb in Ayurveda¹. Indian ginseng and winter cherry is the other. In treatment of various infections, the root of the plant can be used². Due to the presence of steroid lactones in the root, it plays an important role in antifungal, antibacterial, antitumor³. It is as important 'Rasayana' as "SattvicKaphaRasayana" in Indian Ayurveda⁴. AsgandNagori and AsgandDakani are the 2 varieties of Ashwagandha⁵. Due to the role in medical science, AsgandNagori is important.

Taxonomical Classification

Kingdom: Plantae, Plants;
 Sub kingdom :Tracheobionta, Vascular plants;
 Super division :Spermatophyta, Seeds plants;
 Division :Angiosperma
 Class :Dicotyledons
 Order :Tubiflorae
 Family :Solanaceae
 Genus :Withania
 Species :somniferaDunal

Due to the anti sedative, anticonvulsant properties *W.somnifera* is Dunal (Solanaceae), also known as ashwagandha is considered in medical science for the treatment stress, neurological problems, stress⁷. As dietary supplements, the use of herbal medicine is higher. Side effect is lesser when compared to others and also economically at less price⁸. In India and Iran *Withania somnifera* is considered as a folk medicine. When taken alone or in combination of other drugs, the plant can lead to higher sex appeal and also for the treatment of infertility⁹. In males reversible spermicidal can be seen due to the usage of WS plant says the various studies³. These plants were considered for treatment by Chinese. In India, Rig-veda says about the importance of this plant and afterwards it was entered in Ayurveda¹⁰. In different parts of the country, all the parts of this plant such as root, flower, stem, flower is considered as an ancient therapy of various diseases¹¹. Various pharmacological and biological characters possessing phytochemical have been discovered¹². Ashwagandha have been shown to increase energy, increasing the level of hemoglobin in blood, elevating the memory by activating the brain and nerves and also seen to increase the cell mediated immunity³. Both specific as well as non specific immunity can be increased by the usage of this plant¹⁴. To understand the antimicrobial effect in various parts such as seed, leaves, root several research have been taken place¹⁵. Solanaceae is the family to which Ashwagandha belongs¹⁶. For the solution of anti aging and in the treatment of various infections, researches are going on by the antioxidant properties of food plants¹⁷. *Withania somnifera* have anti stress and anti tumoractivity¹⁸. Ashwaganda in spite of various benefit, it also have antibacterial effect¹⁹. The secondary metabolites from the root of Ashwaganda is also been studied²⁰.

2. MATERIALS AND METHOD

2.1 Plantmaterial And Preparation Of The Extracts

The rhizome of the ashwagandha was shade dried and a coarse powder was prepared (particle size~0.25mm) and was subjected to successive extraction using solvents with increasing polarity ethanol, by continuous cold and heat extraction. The aqueous extract was prepared by maceration with water.

2.2 Preparation Of The Plant Extracts

The air dried roots were finely powdered using an electric grinder. For conventional extraction (refluxing), 5 g of powdered plant material was mixed with 50 ml of acetone in a round bottom flask and refluxed for about 5 h at 60 °C. Liquid extracts obtained were separated from the solid residue by vacuum filtration, concentrated using a rotary evaporator. Boiling method A total of 5 gm of powdered sample was taken and mixed with 50 ml distilled water in a round bottom flask and boiled for ½ hour separately. The residue was removed by filtration through Whatmann No:1 filter paper and the aqueous extract was concentrated

2.3 Phytochemical Analysis

Revealing of vital phytochemical constituents was carried out for all the extracts using the standard procedures²¹⁻²⁴.

Test for Flavonoids

2ml of 2.0%NaOH Mixture was mixed with aqueous plant crude extract; concentrated yellow colour was produced, which became colourless when we added 2 drops of diluted acid to the mixture. This result showed the presence of flavonoids.

Keller Kiliani Test:

A solution of glacial acetic acid (4.0ml) with 1drop of 2.0%FeCl3 mixture was mixed with the 10 ml aqueous plant extract and 1 ml H₂SO₄ concentrated. A brown ring formed between the layers which showed the entity of cardiac steroid glycosides.

Test for terpenoids:

2.0 ml of chloroform was added with the 5ml aqueous plant extract and evaporated o the water bath and then boiled with 3 ml of H₂SO₄ concentrated. A grey colour formed which showed the presence of terpenoids.

Detection of tannins:

A small quantity of extract was mixed with water and heated in a water bath. The mixture was filtered and ferric chloride was added to the filtrate. A dark green colour was formed. It indicates the presence of tannins.

Test for Steroids:

2 ml of chloroform and concentrated H₂SO₄ were added with the 5 ml aqueous plant crude extract. In the lower chloroform layer red colour appeared that indicated the presence of steroids.

Test for phenols:

To 2 ml of each extract, 2 ml of 5% aqueous ferric chloride were added; formation of blue colour indicated the presence of phenols in the sample extract

Test for saponins:

5.0 ml of distilled water was mixed with aqueous crude plant extract in a test tube and it was mixed vigorously. The frothing was mixed with a few drops of olive oil and mixed vigorously and the foam appearance showed the presence of saponins.

Detection of Alkaloids:

Extracts were dissolved individually in dilute hydrochloric acid and filtered. The filtrates were used to test the presence of alkaloids.

Mayer's test:

Filtrates were treated with Mayer's reagent. Formation of a yellow cream precipitate indicates the presence of alkaloids.

Antioxidant activity of WS extract²⁵

Assay for ferric reducing antioxidant power (FRAP) FRAP assay is based on the ability of antioxidants to reduce Fe³⁺ to Fe²⁺ in the presence of 2,4,6-tri(2-pyridyl)-s-triazine (TPTZ), forming an intense blue Fe²⁺TPTZ complex with an absorption maximum at 593nm. This reaction is pH-dependent (optimum pH 3.6). The decrease in absorbance is proportional to the antioxidant content. The FRAP assay was performed according to the method of Benzie and Strain. (1996). The FRAP reagent contained 2.5ml of a 10mM TPTZ solution in 40mM HCl, 2.5ml of 20mM FeCl₃.6H₂O and 25ml of 300mM acetate buffer (pH 3.6). It was freshly prepared and warmed at 37°C. The reaction mixture contained 900µl FRAP reagent, 90µl water and 30µl of one of the different concentrations (0.1, 0.2 and 0.3mg/ml) of each W. somnifera root extract and control was prepared without plant extract. The reaction mixture was incubated at 37°C for 30 minutes and the absorbance was measured at 593nm. The standard curve was prepared by using different concentrations of FeSO₄ (10-100µM) and concentrations of the different samples were estimated using the standard curve.

2.4 Antibacterial Activity Assay²⁶⁻²⁷

Antibacterial activity was determined against E.coli and Pseudomonas aeruginosa on Muller Hinton agar. Two Agar plates were prepared and spreaded with test pathogen. One plate is used for agar well diffusion method and another plate used for disc diffusion assay. 100µL of culture filtrate and solvent extract were used for agar well diffusion. For disc diffusion a known volume of test sample is loaded on sterile disc and placed over the surface of agar. All the plates were kept under incubation for 24 h. The zone of inhibition was recorded.

2.5 Albumin Denaturation Assay²⁸

Reaction mixture consisted of 0.2 ml of egg albumin (from fresh hen's egg), 2.8 ml of phosphate buffered saline (pH 6.4) and 2 ml of varying concentrations of the test extract, by which the concentrations (µg/ml) became 100-1000. Similar volume of double-distilled water served as control. Then the mixtures were incubated at 37°C ± 2°C in a biological oxygen demand incubator for 15 min and then heated at 70°C for 5 min. After cooling, their absorbance was measured at 660 nm (Systronix

Spectrophotometer 150) by using the vehicle as blank. Diclofenac sodium and rumalaya forte at the final concentrations ($\mu\text{g/ml}$) of 1000 were used as reference. Test extracts were chosen such that they remained the nearest possible to the standard therapeutic mode.

The percentage inhibition of protein denaturation was calculated by using the following formula:

$$\% \text{ inhibition} = 100 \times ([V_t/V_c] - 1)$$

Where, V_t = absorbance of test sample, V_c = absorbance of control.

3. RESULT AND DISCUSSION

Withania somnifera sample was collected (Plate 1) phytochemical present in root were extracted by solvent and water. The presence of phytochemical was qualitatively (plate 2) determined and result are given in (Table 1). Solvent based test shows absence of tannins, phenols and saponins and presence of flavonoids, Glucosides, Terpenoids, steroids and alkaloids. The aqueous test based on presence of flavonoids, salkowskis and terpenoids and absence of tannins, steriods, phenols, saponins and alkalooids. Presence of alkloid was observed only in acetone extraction. Similar reports were obtained⁶. The crude and solvent extract antibacterial activity of *Withania somnifera* done by agar well and disc diffusion method. Agar well diffusion of tested extract showed good antibacterial activity against *E.coli* (Plate 3) maximum zone 18 mm WS extract and 16 mm respective for *E.coli* and *P.aeruginosa* at 100 μg and 14 mm at 50 μg . The antibacterial activity of extract against pathogen revealed presence of antibacterial compounds potent and superior than third generation of floxacin. *P.aeruginosa* was found to be resistant on standard and inhibited by WS extract.

TABLE I : QUALITATIVE ANALYSIS OF W.SOMNIFERA

SERIAL NO	TEST	Ethanol Extract
1.	Flavonoids Test	Positive
2.	Keller killiani- Glucosides	Positive
3.	Salkowski:s - Steroids	Positive
4.	Terpenoids Test	Positive
5.	Tannins Test	Negative
7.	Phenols Test	Negative
8.	Saponins Test	Negative
9.	Meyer Test-alkaloid	Positive
10.	Wagner Test -alkaloid	Positive

Plate 1. Phytochemical Extraction W.somnifera



a)W.somnifera b)Sample Extraction



Plate 2 : Phytochemical Test

Table 2: Antibacterial Activity Of W.Somnifera

ORGANISM	100 μg	50 μg	Standard ofloxacin 50 μg
<i>E.coli</i>	18	14	16
<i>P.aeruginosa</i>	16	14	--

Plate 3. Antibacterial study**3.1 Antioxidant And Anti Inflammatory**

Several herbal products are good sources of antioxidants, which can supplement the actions of endogenous antioxidants. To prevent oxidative damage caused by imbalance in the exogenous oxidant-antioxidant systems these herbal extracts can be used. In the present investigation, the extracts of the ashwagandha root were prepared in ethanol solvents of have had antioxidant activities of all the extracts were evaluated in several assay systems. FRAP assay measures the reducing ability of antioxidants against oxidative effects of reactive oxygen species. The antioxidant potential is estimated by ability of compound to reduce TPRZ-Fe (III) complex to TPTZ-Fe (II). In the current study chloroform and alcoholic extracts of *W. somnifera* exhibited greater total antioxidant power in FRAP assay compared to other extracts (plate 4). The percentage of antioxidant was 430mM at 100 μ g which is maximum and 200 mM at 25 μ g/mL. The activity of WS at 100 μ g was equal to the activity of ascorbic at 250 μ g which gave 450mM (figure 1)

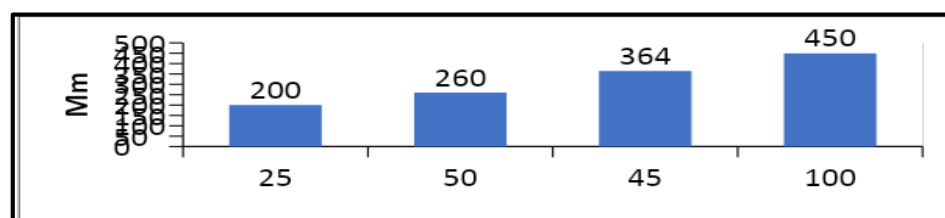


Figure 1. FRAP antioxidant percentage

Inhibition of protein denaturation of phytoconstituent of WS was compared with standard (plate 5). Root extracts of *W. somnifera* at the dose of 1000 μ g/ml exhibited an anti-inflammatory activity that became significant ($P < 0.01$) with a 72% more inhibitory effect than the control presented (1000 μ g/ml) induced significant 48% anti-inflammatory effect. The anti-inflammatory effect of positive control (diclofenac) at concentration of 1000 μ g/ml was lesser than that of the WS extract noted on albumin denaturation assay (plate 4). WS showed 21, 48, 54, 60 and 72% of denaturation inhibition and standard diclofenac gave 12, 1835, 38, 48% among 100, 250, 500, 750 and 1000 μ g (fig 2).

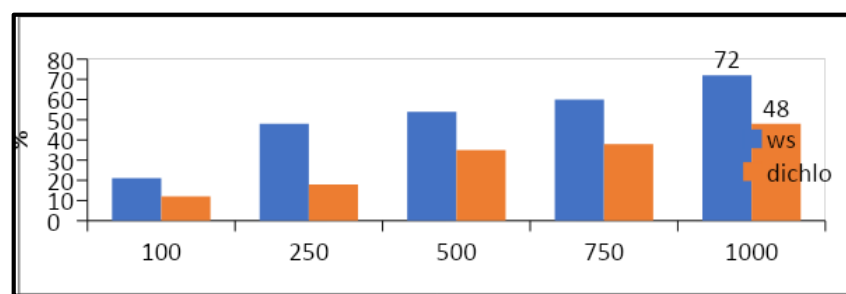


Figure 2. percentage of albumin denaturation inhibition

Plate 4. FRAP ASSAY**Plate 5 Anti Inflammatory**

4. SUMMARY AND CONCLUSION

Withania somnifera (WS), also known as ashwagandha, is an important herb in ayurvedic and indigenous medical systems. The present study was designed to evaluate the antioxidant and antibacterial activities of root extract of WS. The extracts of *W. somnifera* showed the presence of following phytochemicals, i.e., alkaloids, flavonoids, tannins and steroidare major detected compound. Antibacterial activities were measured using the agar well diffusion method and five pathogenic Gram-negative bacteria: *Escherichia coli*, and *Pseudomonas aeruginosa*. The WS root extracts displayed the highest activity against 18 mm and 16 mm zone of inhibition among *E.coli* and *P.aeruginosa*. The values for FRAP, ferrous chelation and inhibition on ws extracts ranged 200- 470 mM The present findings exhibited a concentration dependent inhibition of protein (albumin) denaturation by the test extract throughout the concentration range of 100-1000 from 20-72%. *W. somnifera* exhibited significant antibacterial activities against Gram-negative bacteria, %. In addition it have good antioxidant and anti inflammatory properties In this study, it was found that phytochemical biological potential of *W. somnifera* confirm the ethnomedical uses of this medicinal plant as well as to identify the plant part that gives the highest antioxidant, antibacterial and anti inflammatory activities.

5. CONFLICT OF INTEREST

Conflict of interest declared none.

6. REFERENCE

1. Vinotha S, Thabrewl, Ranjani S, 2015 Phytochemical Screening of Various Extracts of Root of *Withania Somnifera* (L) Dunal. Archives Business of Research. 3, 179-187
2. Rathi Vaibhav, Dhingra Ashwani, Chopra Bhawna. *Withania somnifera* Book: Naturally Occurring Chemicals Against Alzheimer's Disease 2021 401-407 DOI: 10.1016/B978-0-12-819212-2.00034-7
3. Singh N, Bhalla M, de Jager P, Gilca M. An overview on ashwagandha: a Rasayana (rejuvenator) of Ayurveda. Afr J Tradit Complement Altern Med. 2011;8(5 Suppl):208-213. doi:10.4314/ajtcam.v8i5S.9
4. Mirjalili MH, Moyano E, Bonfill M, Cusido RM, Palazón J. Steroidal lactones from *Withania somnifera*, an ancient plant for novel medicine. Molecules. 2009;14(7):2373-2393. Published 2009 Jul 3. doi:10.3390/molecules14072373
5. Nawab John Dar, Muzamil Ahmad, Neurodegenerative diseases and *Withania somnifera* (L): An update, Journal of Ethnopharmacology. 256, 2020, 112769, ISSN 378-8741.
6. Singh, G., Sharma, P. K., Dudhe, R., & Singh, S. "Biological activities of *Withania somnifera*." Ann Biol Res 1.3 (2010): 56-63.
7. Sangwan RS, Chaurasiya ND, Misra LN, Lal P, Uniyal GC, Sharma R, Sangwan NS, Suri KA, Qazi GN, Tuli R. Phytochemical variability in commercial herbal products and preparations of *Withania somnifera* (ashwagandha) Curr Sci. 2004;86:461-465.
8. Martins Ekor The growing use of herbal medicines: issues relating to adverse reactions and challenges in monitoring safety. Front Pharmacol. 2013; 4: 177. Published online 2014 Jan 10. doi: 10.3389/fphar.2013.00177.
9. Nasimi Doost Azgomi R, Zomorodi A, Nazemyieh H, et al. Effects of *Withania somnifera* on Reproductive System: A Systematic Review of the Available Evidence [published correction appears in Biomed Res Int. 2019 Nov 21;2019:7591541]. Biomed Res Int. 2018;2018:4076430. Published 2018 Jan 24. doi:10.1155/2018/4076430
10. Gupta Ashish, Mahdi Abbas Ali, Shukla Kamla Kant, Ahmad Mohammad, Bansal Navneeta, Sankhwar Pushplata, Sankhwar Satya. Efficacy of *Withania somnifera* on seminal plasma metabolites of infertile males: A proton NMR study at 800 MHz. Journal of ethnopharmacology 2013;149
11. Petrovska BB. Historical review of medicinal plants' usage. Pharmacogn Rev. 2012;6(11):1-5. doi:10.4103/0973-7847.95849
12. Dar N. J., A. Hamid, and M. Ahmad (2015), "Pharmacologic overview of *Withania somnifera*, the Indian Ginseng," Cellular and Molecular Life Sciences, vol. 72, no. 23, pp. 4445-4460.
13. Pandey MM, Rastogi S, Rawat A.K. Indian herbal drug for health care and overview. Int J Alt Med. 2008;6(1):1-
14. Subbu Lakshmi S, Chelladurai G, Suresh B. In vitro studies on medicinal plants used against bacterial diabetic foot ulcer (BDFU) and urinary tract infected (UTI) causing pathogens. J Parasit Dis. 2016;40(3):667-673. doi:10.1007/s12639-014-0555-y
15. Shanab B, Adwan D, Abu-Safiya D, Jarrar N, Adwan K. Antibacterial activities of some plant extracts utilized in popular medicine in Palestine. Turk J Biol. 2005;28(2-4):99-102. Pandey, A.K. and Chowdhry, P.K. (2006) Propagation techniques and harvesting time on productivity and root quality of *Withania somnifera*. Journal of Tropical Medicinal Plants Vol.7:79-81.
16. Bhatnagar M, Sisodia SS, Bhatnagar R. 2005. Antiulcer and antioxidant activity of *Asparagus racemosus* willd and *Withania somnifera* Dunal in rats. Ann N Y Acad Sci 1056:261-278.

17. Saiyed, N. Jahan, S. F. Majeedi, and M. Roqaiya (2016). "Medicinal properties, phytochemistry and pharmacology of *Withaniasomnifera*: an important drug of Unani Medicine," *Journal of Scientific & Innovative Research*, vol. 5, no. 4, pp. 156-60.
18. Pham-Huy LA, He H, Pham-Huy C. Free radicals, antioxidants in disease and health. *Int J Biomed Sci.* 2008;4(2):89-96.
19. Narendra Singh, Mohit Bhalla, Prashanti de Jager, Marilena Gilca 2011 An Overview on Ashwagandha: A Rasayana (Rejuvenator) of Ayurveda. *Afr J Tradit Complement Altern Med. Aquaculture.* 8, 208-213.
20. Owais M., K.S.Sharad, A.Shehzad, M.Saleemuddin (2005). Antibacterial efficacy of *Withaniasomnifera* (ashwagandha) an indigenous medicinal plant against experimental murine salmonellosis. *Phytomedicine.* 12, 229-235.
21. Kokate CK. A textbook of practical pharmacognosy. Vallabh Prakashan, Edition 5, 2005:105-111.
22. Rahman Gul, Syed Umer Jan, Syed Faridullah, Samiullah Sherani, Nusrat Jahan, "Preliminary Phytochemical Screening, Quantitative Analysis of Alkaloids, and Antioxidant Activity of Crude Plant Extracts from *Ephedra intermedia* Indigenous to Balochistan", *The Scientific World Journal*, vol. 2017, Article ID 5873648, 7 pages, 2017. <https://doi.org/10.1155/2017/5873648>
23. O. O. Debiyi and F. A. Sofowora, "Pytochemical screening of medical plants," *Iloydia*, vol. 3, pp. 234-246, 1978.
24. G. E. Trease and W. C. Evans, "Phenols and phenolic glycosides," in *Textbook of Pharmacognosy*, vol. 12, pp. 343-383, Balliere, Tindall and Co Publishers, London, UK, 1989.
25. Benzie IF, Strain JJ. The ferric reducing ability of plasma (FRAP) as a measure of "antioxidant power": the FRAP assay. *Anal Biochem.* 1996 Jul 15;239(1):70-6. doi: 10.1006/abio.1996.0292. PMID: 8660627.
26. A Shirodkar; A Gahlaut; AK Chhillar; R Dabur. *Journal of Pharmaceutical Analysis* 2012, 3(6), 421-428.
27. F Zheng; S Wang; S Wen; M Shen; M Zhu; X Shi. *Biomaterials.*, 2013, 34(4), 1402-1412.
28. N Shah; H Kataria; SC Kaul; T Ishii; et al. *Cancer Science.*, 2009, 100(9), 1740-1747.

A Review On Antibiotic Resistance In Urinary Tract Infections

Nitha V Ravi, Dr. K. Rajesh, Roja B

PG and Research Department of Microbiology, Dhanalakshmi Srinivasan College of Arts and Science For Women (Autonomous), Perambalur-621 212, Tamil Nadu, India

Abstract: Resistance of antibiotics has become a global concern worldwide. Urinary Tract Infections have become a common clinical case especially in females. The aim of the study is to identify antibiotics showing highest resistance in Urinary Tract Infections and thereby create an awareness on the increasing resistance rate which points out for the discovery of new antibiotics. In this article we review various articles and check which antibiotic shows the highest resistance in Urinary Tract Infections (UTI). Ampicillin (53%) which belongs to Aminoglycosides Group whose resistance is through Altering penicillin binding protein. The other members of Beta lactam drugs are Penicillin was found to have highest resistance in Urinary Tract Infections followed by Trimethoprim/Sulfamethoxazole (46%), Amoxicillin clavulanate (40%) and Ciprofloxacin (40%). *E. coli* was the common organism isolated followed by *Klebsiella* species. Studies show that there is an increasing rate of antibiotic resistance in UTI. Judicious use of antibiotics and following the correct prescription method can limit the cases of antibiotic resistance in the community.

Keywords: Ampicillin, Urinary Tract Infections, Aminoglycosides Group

INTRODUCTION

Sir Alexander Fleming discovered Penicillin and thereafter the discovery of antibiotics. Antibiotics protected people from various infections. But all the antibiotics have developed resistance. Due to the increasing drug resistance, the development of new antibiotics have become an important aspect in Medical Science¹. Scientists worldwide have worked on the crisis that is facing the medical science but the resistance is being attained by various antibiotics². Urinary tract infection (UTI) is the multiplication of bacteria in urine with a presence of 100,000 or more organisms per ml of urine. The most bacterial cause of UTI is *E. coli* (80%) followed by *Proteus mirabilis*, *Klebsiella* species. The fungal causes can be *Candida albicans*, *Cryptococcus neoformans*. Viral causes can be Adenovirus, Cytomegalovirus, Measlesvirus. Adhesion of organisms is an important factor in the pathogenesis of UTI. UTI can be asymptomatic or symptomatic as in Urethritis, Cystitis, Pyelonephritis. Complications include Septicaemia, Chronic renal failure. Midstream urine is the most suitable sample collected. Screening methods include Microscopical examination, Chemical method such as TTC and enzymatic methods such as Glucose Oxidase Test, Catalase Test. Culture methods include Pour plate method, calibrated loop method. Susceptibility testing is carried out by Kirby-Bauer disc diffusion method. Treatment is based on antibiotic sensitivity test. Resistance of 88.3% for Ampicillin, 72.7% for piperacillin, 66.7% for clindamycin, amoxicillin/clavulanic acid 66.2% finally 50% was shown for trimethoprim/sulfamethoxazole³. High resistance for nitrofurantoin and least for Fosfomycin⁴. 89.9% resistance to ampicillin, 75.6% to Oxacillin, 85.4% to piperacillin, 56.1% to clindamycin, 74.5% to amoxicillin/clavulanic acid and 50% to trimethoprim/sulfamethoxazole⁵. 65.1% resistance to trimethoprim-sulfamethoxazole, 38.3% to cephalothin, 27.3% to cefuroxime, 16.9% to ciprofloxacin finally least 17.1% to amoxicillin-clavulanic acid. 9.1% to ceftriaxone and 7.7% resistance to nitrofurantoin⁶. 75.0% resistance to amoxicillin plus clavulanic acid, 76.2% to piperacillin plus tazobactam, 76.2% to cefotaxime, 81.0% to cefuroxime, 81.0% to ciprofloxacin and lastly 81.0% trimethoprim plus sulphamethoxazole⁷. Resistance of 85.0% to ampicillin, 73.8% to amoxicillin-clavulanate, 42.9% to trimethoprim-sulfamethoxazole, 37.3% to cefazolin. Resistance of Ampicillin - 100%, Ceftriaxone - 33.3%, Ciprofloxacin - 17.4%⁹. Resistance to ampicillin of 45.9%, nitrofurantoin of 14.3%, Ciprofloxacin of 9.7% and least in levofloxacin of 8.1%. Most frequent organism was *E. coli* with 69.5% resistance to ampicillin, 27.5% to amoxicillin/clavulanic acid, lastly 0.4% to nitrofurantoin¹¹. The most frequently isolated organism was *E. coli* followed by *Klebsiella*. Ampicillin had the highest resistant rate followed by amoxicillin/clavulanic acid then by trimethoprim/sulfamethoxazole and lastly by ciprofloxacin¹². The most common organism isolated was *E. coli* followed by *Enterococcus faecalis*. Cotrimoxazole and fluoroquinolones were seen to be resistant¹³. *E. coli* being the commonly isolated organism followed by *Klebsiella*. Ampicillin, Amoxicillin and Cephalosporins belonging to 2nd generation are resistant¹⁴. *E. coli* being the common organism isolated. 30% resistance to trimethoprim/sulfamethoxazole followed by 22% to cephalothin¹⁵. *E. coli* resistance of 82% to amoxicillin, 64% resistance to trimethoprim-sulphamethoxazole, 58% to cephalothin, 30% to ciprofloxacin, 21% to amoxicillin/clavulanate and finally 12% to gentamicin¹⁶. *E. coli* being the common organism isolated followed by *Klebsiella pneumonia*. Resistance of Gram negative organism to amoxicillin followed by trimethoprim/sulfamethoxazole of 65.7% followed by ciprofloxacin and finally ceftriaxone¹⁷. Most commonly isolated was *E. coli* which was 42% followed by *Klebsiella* 12.2%. Amoxicillin resistance to 97.9%, 90% to doxycycline followed by 78.3% resistance to piperacillin, 63.9% resistance to sulphonamides/trimethoprim and finally 42.2% to cefaclor¹⁸. *E. coli* being the most common organism isolated was found to be 94.9% resistant to ampicillin whereas *K. pneumoniae* 100% resistant to penicillin¹⁹. Most common antibiotics are resistant to Gram negative organisms found in urinary tract infections²⁰. Cotrimoxazole had a high resistant rate to most of the pathogens isolated²¹. Imipenem showed high resistance to *P. aeruginosa*²². Common symptoms such as dysuria and micturition are commonly seen in patients while in some cases they will be no symptoms. On consulting usage of antibiotic is considered as a result of which the increase in antibiotic resistance is seen²³. Only after knowing the risk factors involved, treatment and control measures can be effective²⁴. The practice of antimicrobial peptides and probiotics are used for urinary tract infections. There are only few studies done on what can be replaced instead of antibiotics in the case of antibiotic resistance²⁵. One of the problems that pediatrics are facing is the Recurrent urinary tract infection (rUTI). In small children, the treatment becomes difficult. Oral medicines are not considerable due to the increase in drug resistance. To outcome this

problem, prophylactic antibiotics are preferred²⁶. High rise in the resistance of Enterobacterales which are community-acquired are seen²⁷. In elder people the treatment with medicines is common. This is same even in the case of urinary tract infections specially in Clindamycin. All antibiotics had showed resistance pattern in Capital Region than as compared to SkåneRegion²⁸. Community acquired E. faecalis strains have involvement of pathogenesis which are virulence determinant as it is commonly seen²⁹. Urine cultures related to pediatric cases are resistant to most of the antibiotics. Doing treatment with Cephalexin or Trimethoprim-Sulfamethoxazole (TMP-SMX) is not efficient in treatment. Cases of Urinary tract infections can be treated with Nalidixic acid, Nitrofurantoin and even in recurrent cases of urinary tract infections, these drugs are effective. Cases of Urinary tract infections which are complicated can be treated with Ciprofloxacin and Meropenam³⁰. Nitrofurantoin can be given for the patients who are having community-acquired UTI which are uncomplicated³¹. Usage of empirical antibiotics is the best method which is cost effective. Only if the antibiotic resistance is low, empirical antibiotic is preferred but if the antibiotic resistance is high, then the effective method is systematic treatment³². Elder people suffering from bladder infections shows asymptomatic bacteruria³³. Based on the resistance of antibiotics only the selection of antibiotic can be determined³⁴. Urinary tract infection cases are mostly seen in aged women. A chance of not diagnosis can also be seen. Due to the increase in resistance to various antibiotics, the treatment becomes difficult. Specially in cases of elderly people diagnosis and treatment becomes a problem³⁵. Treatment with antibiotics should be done in an efficient way³⁶. Due to the high rise of antibiotic resistance, treatment without antibiotics is effective. More studies are required in this area³⁷. In cases of catheter associated gram negative bacilluria norfloxacin is effective³⁸. E.coli strains showed a very less decrease susceptibility to amoxycillin antibiotic. This is due to the presence of R-TEM enzymes. It is very important to know the microorganisms causing Urinary tract infections and the resistance of various antibiotics is essential while giving medication to patients³⁹.

RESISTANCE OF ANTIBIOTICS IN URINARY TRACT INFECTIONS

Antibiotics	Percentage
Ampicillin	53%
Trimethoprim/Sulfamethoxazole	46%
Amoxicillin Clavulanic Acid	40%
Ciprofloxacin	46%

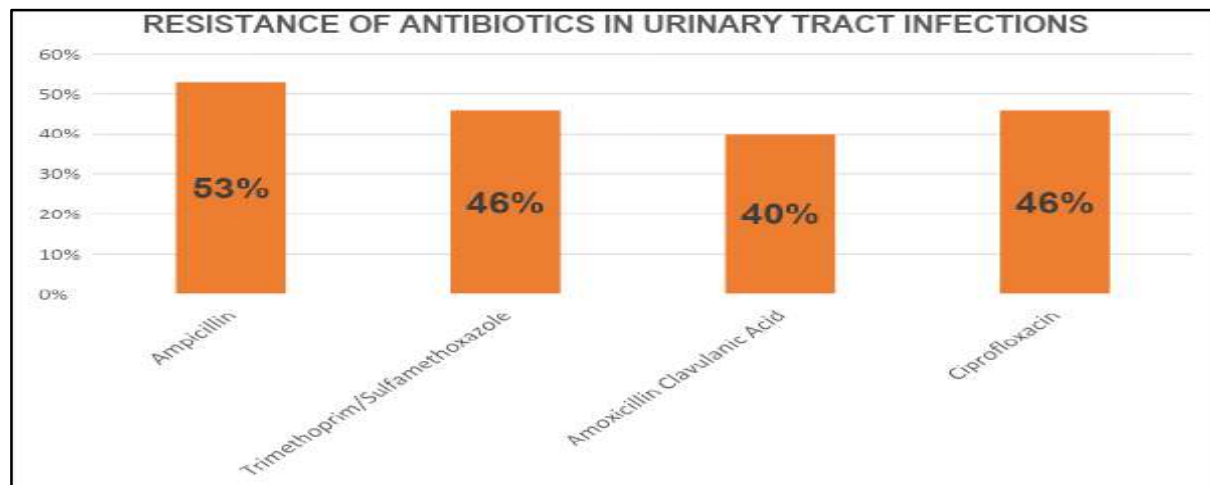


TABLE SHOWING RESISTANCE OF VARIOUS ANTIBIOTICS AND THE CLASS OF ANTIBIOTIC THEY BELONG

ANTIBIOTICS	NUMBER OF RESISTANCE	PERCENTAGE OF RESISTANCE	Antibiotic group
Ampicillin	8	53%	Penicillin
Amoxicillin clavulanic acid	6	40%	Penicillin
Trimethoprim/Sulfamethoxazole	7	46%	Sulfonamides
Piperacillin	4	26%	Penicillin
Ciprofloxacin	6	40%	Fluoroquinolones
Doxycycline	1	65%	Tetracycline
Nitrofurantoin	3	20%	Nitrofuran
Levofloxacin	1	6%	Fluoroquinolones
Gentamycin	1	6%	Aminoglycosides
Clindamycin	1	6%	Macrolides
Ciprofloxacin	1	6%	Fluoroquinolones
Cefotaxime	1	6%	Cephalosporins
Cefuroxime	2	13%	Cephalosporins
Cefazolin	2	13%	Cephalosporins
Ceftriaxone	1	6%	Cephalosporins
Cephalothin	4	26%	Cephalosporins

Highest frequency of resistance was found in Ampicillin (53%), Trimethoprim/Sulfamethoxazole(46%), followed by Amoxicillin clavulanic acid(40%) and finally SCiprofloxacin(40%). *E.coli* was the most common organism isolated followed by *Klebsiella* species. Ampicillin and Amoxicillin clavulanic acid belong to Beta lactam group in which resistance is through Altering penicillin binding protein. The other members of Beta lactam drugs are Penicillin, Methicillin. Trimethoprim/Sulfamethoxazolebelong to sulfonamides class of antibiotic. They inhibit the metabolic pathway. Resistance is due to mutation in dhps gene which allowPABA to bind but has greatly reduced binding of Sulfamethoxazole. Resistance to Trimethoprim is by mutation in the dhfrgene with reduced binding of trimethoprim. Ciprofloxacin belong to fluoroquinolones class of antibiotics. They act by inhibiting gyrase. Resistance is due to mutation in either the Gyr A subunit of gyrase which reduce the ability of the drugs to bind to their targets.

HIGHEST RESISTANCE RATE ANTIBIOTICS AND THE CLASS THEY BELONG

Ampicillin	Betalactams
Trimethoprim/Sulfamethoxazole	Sulfonamides
Amoxicillin clavulanic acid	Betalactams
Ciprofloxacin	Fluoroquinolones

CONCLUSION

From the review of various articles, it was found that Ampicillin has the greatest resistance of 53% followed by Trimethoprim/Sulfamethoxazole(46%)Which belongPenicillin class of antibiotics. The use of antibiotics without consulting Doctor may lead to resistance of that antibiotic. Such antibiotic abuse in society occurs even due to the incompletion of the antibiotic dosage.UTI is a very common infection in females and the resistance of antibiotics is a serious concern. The judicious method of antibiotic usage and antibiotics if used only when needed can help to control antibiotic resistance.

REFERENCES

1. C. Lee Ventola. The Antibiotic Resistance Crisis. *Pharmaceutics and diagnostics*. 2015; 40(4): 277–283
2. Bilal Aslam, Wei Wang, Muhammad Imran Arshad, Mohsin Khurshid, Saima Muzammi, Muhammad Hidayat Rasool, Muhammad Atif Nisar, Ruman Farooq Alvi, Muhammad Aamir Aslam, 3 Muhammad Usman Qamar, Muhammad Khalid Farooq Salamat, Zulqarnain Baloch. Antibiotic resistance: a rundown of a global crisis. *Antibiotic resistance: a rundown of a global crisis*. 2018; 11: 1645–1658
3. Syed Suhail Ahmed, Ali Shariq, Abdulaziz Ajlan Alsalloom, Ibrahim H. Babikir, and Badr N. Alhomoud, Uropathogens and their antimicrobial resistance patterns: Relationship with urinary tract infections. *International journal health science*. 2019; 13(2): 48–55
4. Erdem.Rising. Antimicrobial Resistance of Pathogens in Urinary Tract Infection. *Journal Global International disease*. 2019; 10(3): 117–118
5. Osama Al Wutayd 1, Abdullah Al Nafeesah 2, Ishag Adam 3, Ibrahim Babikir. The antibiotic susceptibility patterns of uropathogens isolated in Qassim. *The journal of infection in developing countries*. 2018; 12(11): 946–95
6. P Bhola 1, N R Mvelase, Y Balakrishna, K P Mlisana, K SweSwe-Han. Antimicrobial susceptibility patterns of uropathogens isolated from pregnant women in KwaZulu-Natal Province. *South African Medical Journal*. 2020; 110(9): 872–876
7. Barbara Kot 1, Agata Grużewska 2, Piotr Szweda 3, Jolanta Wicha 4, Urszula Parulska. Antibiotic Resistance of Uropathogens Isolated from Patients Hospitalized in District Hospital in Central Poland. 2021; 10(4): 447.
8. İlke Ozahilpek , Abdulkadir Bozaykut, Didem Caktir Arman, Rabia Gonul Sezer. Antimicrobial resistance patterns of uropathogens among children in Istanbul, Turkey. *The Southern Asian journal of tropical medicine and public health*. 42(2): 355–62
9. Abubaker A Abujnah , Abdulaziz Zorgani , Mohamed A M Sabri , Hanan El-Mohammady , Rania A Khalek , Khalifa S Ghenghesh. Multidrug resistance and extended-spectrum β -lactamases genes among *Escherichia coli* from patients with urinary tract infections in Northwestern Libya; 2015, 2; 10: 26412.
10. George G Zhanel 1, Tamiko L Hisanaga, Nancy M Laing, Melanie R DeCorby, Kim A Nichol, Lorraine P Palatnik, Jack Johnson, Ayman Noreddin, Godfrey K M Harding, Lindsay E Nicolle, Daryl J Hoban, NAUTICA Group. Antibiotic resistance in outpatient urinary isolates: final results from the North American Urinary Tract Infection Collaborative Alliance (NAUTICA). *International journal antimicrobial agents*. 2005; 26(5): 380–8.
11. Tanjalić, Sanda Gračan, Adela Arapović, Vesna Capkun, Mirna Subat-Dežulović, Marijan Saraga. Changes in bacterial resistance patterns in children with urinary tract infections on antimicrobial prophylaxis at University Hospital in Split. *Medical Science monitor*. 2011; 17(7): CR355–61.
12. L Soubra 1, S Kabbani 2, M F Anwar 3, R Dbouk 4. Spectrum and patterns of antimicrobial resistance of uropathogens isolated from a sample of hospitalised Lebanese patients with urinary tract infections. *Journal global antimicrobial resistance*. 2014; 2(3): 173–178.
13. Maria Antonia De Francesco 1, Giuseppe Ravizzola, Laura Peroni, Riccardo Negrini, Nino Manca. Bacterial Uropathogens Causing Urinary Tract Infection and Their Resistance Patterns Among Children in Turkey. *Medical Science Monitor*. 2016; 18(6): e26610
14. Ralucalsac 1 2, Diana-Georgiana Basaca 2, Ioana-Cristina Olariu 1 2, Ramona F Stroescu 2 3, Andrada-Mara Ardelean 1 2, Ruxandra M Steflea 1 2, Mihai Gafencu 1 2, Adela Chirita-Emandi 2 4, Iulia Cristina Bagiu 5, Florin George Horhat 5, Dan-

DumitruVulcanescu 2, Dan Ionescu 6, Gabriela Doros 1 2. Antibiotic Resistance Patterns of Uropathogens Causing Urinary Tract Infections in Children with Congenital Anomalies of Kidney and Urinary Tract. Children 2021;2021;8(7):585.

15. Kara N Saperston 1, Daniel J Shapiro 1, Adam L Hersh 1, Hillary L Coppl. A comparison of inpatient versus outpatient resistance patterns of pediatric urinary tract infection.Comparative study.2014;191(5 Suppl):1608-13.

16. A J Matute , E Hak, C A M Schurink, A McArthur, E Alonso, M Paniagua, E Van Asbeck, A M Roskott, F Froeling, M Rozenberg-Arska, I M Hoepelman. Resistance of uropathogens in symptomatic urinary tract infections in León, Nicaragua. International journal antimicrobial agent.2004;23(5):506-9.

17. Frédérique Randrianirina 1, Jean-Louis Soares, Jean-François Carod, Elisoa Ratsima, Vincent Thonnier, Patrice Combe, Pierre Grosjean, Antoine Talarmin. Antimicrobial resistance among uropathogens that cause community-acquired urinary tract infections in Antananarivo, Madagascar. Antimicrobial chemotherapy.2007;59(2):309-12

18. A Elmanama , N M Elaiwa, A E Y El-Ottol, F H Abu-Elamreen. Antibiotic resistance of uropathogens isolated from Al-Shifa hospital in Gaza Strip in 2002. Chemotherapy.2006;18(3):298-302.

19. Kald Beshir Tuem 1, Rahel Desta 1, Helen Bitew 2, Seid Ibrahim 3, Hailemichael Zeru Hishe 4. Antimicrobial resistance patterns of uropathogens isolated between 2012 and 2017 from a tertiary hospital in Northern Ethiopia. Journal of global antimicrobial resistance. 2019;18:109-114

20. Jan Hrbacek 1, Pavel Cermak 2, Roman Zachoval. Current Antibiotic Resistance Trends of Uropathogens in Central Europe: Survey from a Tertiary Hospital Urology Department 2011-2019. Antibiotics. 2020;9(9):630.

21. B A Tantry 1, S Rahiman. Antibacterial resistance and trend of urinary tract pathogens to commonly used antibiotics in Kashmir Valley. West Indian Medical Journal.2012;61(7):703-7.

22. Li Qian 1, Tracy Camara, J Kyle Taylor, Kathy W Jones. vv Microbial uropathogens and their antibiotic resistance profile from hospitalized patients in Central Alabama. Microbial laboratory Science.2012;25(4):206-11

23. Thomas A Waller, Sally Ann L Pantin, Ashley L Yenior, George G A Pujalte . Urinary Tract Infection Antibiotic Resistance in the United States. Prim Care.2018;45(3):455-466

24. B Ternes 1, F M E Wagenlehner2. Guideline-based treatment of urinary tract infections. Urologe A.2020;59(5):550-558.

25. Mohammad Reza Asadi Karam, Mehri Habibi, Saeid Bouzari. Urinary tract infection: Pathogenicity, antibiotic resistance and development of effective vaccines against Uropathogenic Escherichia coli. Mol Immunol.2019;108:56-67.

26. Anum Khan, Ravi Jhaveri , Patrick C Seed , Mehreen Arshad . Update on Associated Risk Factors, Diagnosis, and Management of Recurrent Urinary Tract Infections in Children. Pediatric Infect Dis Soc.2019;11;8(2):152-159.

27. S Palagin, M V Sukhorukova, A V Dekhnich, M V Edelstein, T S Perepanova , R S Kozlov. Current state of antibiotic resistance of pathogens causing community-acquired urinary tract infections in Russia, Belarus and Kazakhstan: results of the international multicenter study Darmis-2018]. Urologia.2020;(1):19-31.

28. Frédérique Randrianirina 1, Jean-Louis Soares, Jean-François Carod, Elisoa Ratsima, Vincent Thonnier, Patrice Combe, Pierre Grosjean, Antoine Talarmin. Antimicrobial resistance among uropathogens that cause community-acquired urinary tract infections in Antananarivo, Madagascar. Antimicrobial chemotherapy.2007;59(2):309-12

29. Abdullah Karimi, Zohreh Ghalavand, Fatemeh Fallah, Parisa Eslami, Mahmoud Parvin, Masoud Alebouyeh, Marjan Rashidian. Prevalence of virulence determinants and antibiotic resistance patterns of Enterococcus faecalis strains in patients with community-acquired urinary tract infections in Iran. Int J Environ Health Res.2018;28(6):599-608.

30. N Younis 1, K Quol, T Al-Momani, F Al-Awaishah, D Al-Kayed. Antibiotic resistance in children with recurrent or complicated urinary tract infection. NMA J Nepal Med Assoc.2009;48(173):14-9.

31. Michael McQuilkin, Alexander Lund, Wyatt Palmer. Antimicrobial resistance of uncomplicated urinary tract infections in northern Utah. Clin Lab Sci.2008;21(2):99-101

32. Rui Wang, Christine LaSala. Role of antibiotic resistance in urinary tract infection management: a cost-effectiveness analysis. Am J Obstet Gynecol.2021;225(5):550.e1-550

33. J D McCue. Urinary tract infections in the elderly. Pharmacotherapy.1993;13(2 Pt 2):51S-53S

34. V VRafalskiy, E V Dovgan. Resistance of urinary tract pathogens and the choice of antimicrobial therapy: deceptive simplicity]. Urologia.2017 Jul;(3):104-110.

35. Linda Nazarko. Recurrent urinary tract infection in older women: an evidence-based approach. Br J Community Nurs.2013;18(8):407-8, 410-2

36. Chris C Butler , Frank Dunstan, Margaret Heginbothom, Brendan Mason, Zoë Roberts, Sharon Hillier, Robin Howe, Stephen Palmer, Anthony Howard. Containing antibiotic resistance: decreased antibiotic-resistant coliform urinary tract infections with reduction in antibiotic prescribing by general practices. Br J Gen Pract.2007;57(543):785-92.

37. Jennifer Kranz , Stefanie Schmidt , Laila Schneidewind . Current Evidence on Nonantibiotic Prevention of Recurrent Urinary Tract Infections. Eur Urol Focus.2019;5(1):17-19.

38. E J Goldstein. Prevention of bacterial resistance in urinary tract infections. Eur Urol.1991;19 Suppl 1:28-32.

39. M Chomarat. Resistance of bacteria in urinary tract infections. Int J Antimicrob Agents.2000;16(4):483-7

In-Vitro Antioxidant And Antibacterial Activity Of Aerva Lanata (Linn.)-A Traditionally Used Plant

***Susan Kurian, ¹Ananthakrishnan R, and ¹Blessy Joy**

¹ Department of Zoology, Mar Ivanios College (Autonomous) Thiruvananthapuram, Kerala. India.

Abstract: *Aerva lanata* (Linn.) belonging to the Amaranthaceae family have several medicinal properties. The present study aimed to determine the phytochemical components, *in-vitro* antioxidant activity, and antibacterial activity of the ethyl acetate and methanol extract of *Aerva lanata*. Phytochemical analysis of *Aerva lanata* extracts revealed the presence of alkaloids, carbohydrates, glycosides, steroids, terpenoids, tannins, sugar, saponins, flavonoids, phenols, and proteins. The results showed the presence of many bioactive compounds in both ethyl acetate and methanol extract of the plant thus responsible for the antioxidant activities. The methanol extract shows a high IC₅₀ value of 537. 63 μ g/ml when compared to ethyl acetate extract which is 438.49 μ g/ml for DPPH scavenging activity. The antibacterial activity and the minimal inhibitory concentration (MIC) of the plant extracts were examined against five bacterial strains. The highest zone of inhibition was shown by the ethyl acetate extract against *Staphylococcus aureus* and *Clostridium perfringens* strains.

Keywords: *Aerva lanata*, antioxidant, phytochemical, antimicrobial, minimum inhibitory concentration.

I. INTRODUCTION

Aerva lanata, belonging to the family Amaranthaceae is a succulent perennial herb with many medicinal properties. The whole plant especially the leaf is edible. It is an integral part of traditional Ayurvedic and Siddha treatments because of its antibacterial, antidiabetic, hepatoprotective, and diuretic activities¹⁻⁴. Traditionally, a decoction of the entire plant is used in the cure of diarrhea, cholera, diuretics, kidney, malaria, and liver disorders^{2, 5}. The dried roots of the plant are used as a sedative and also used for nasal bleeding in summer, bronchitis, ear complaints, asthma, jaundice, removal of kidney stones, gonorrhea, antirheumatic, and as an antivenin^{6,7}. The methanolic and ethyl acetate extracts of *Aerva lanata* have some interesting antimicrobial activity¹. The phytochemical investigation done by Anita et al., 2013⁸, by using the hydro-alcoholic extract of *Aerva lanata* flowers showed the presence of flavonoids, glycosides, carbohydrates, alkaloids, and phytosterols. Alkaloids, Phenolic compounds, Phytosterols, Carbohydrates, Proteins, Amino acids, Flavonoids, and Quinones were observed in different solvent extract⁹. The phytochemical investigation of *Aerva lanata* reveals that it is a valuable source of different classes of biologically active compounds like steroids, alkaloids, flavonoids, terpenoids, and various phenolics¹⁰. Many medicinal properties of *Aerva lanata* were reported. In the present study, a systematic investigation was done to evaluate the phytochemical analysis, antioxidant, and antibacterial activity of the ethyl acetate and methanol extracts of *Aerva lanata*. Phytochemical analysis along with an antimicrobial screening of the plant is suggested to assess its potential as a medicinal herb.

2. MATERIALS AND METHODS

2.1 Collection of plant materials

The whole plant of *Aerva lanata* was collected from different parts of the Kottayam district.

2.2 Preparation of the plant extracts

The entire fresh plant materials were collected washed and shade dried. The dried plant materials were ground to a fine powder using an electric grinder. The dried and powdered plant material was successively extracted with ethyl acetate (ALE) and methanol (ALM) in the soxhlet apparatus until it became colorless according to the standard methods^{11,12}. Each extract was concentrated by using a rotary vacuum evaporator and stored in the refrigerator for further analysis.

2.3 Percentage Yield

The extract obtained with each solvent was weighed and the percentage yield was calculated in terms of dried weight of the plant material using the formula:

$$\% \text{Yield} = (\text{Dry weight of the extract} / \text{Dry weight of leaf sample}) \times 100.$$

2.4 Phytochemical screening

The plant extract was subjected to various phytochemical tests to determine the active constituents present. Each of the extracts was analyzed for the presence of alkaloids, saponin, steroid, carbohydrates, flavonoids, alkaloid, terpenoid, phenol, quinone, cardiac glycoside, and tannin using the standard methods with slight modification as described by Sofowara (1993)¹²,

Trease and Evans (1989)¹³ and Harborne (1973)¹⁰.

Saponin test

1 ml extract is mixed with 1ml distilled water and shaken well. The formation of froth indicated the presence of saponins.

Steroid test

1ml extract is mixed with 1ml glacial acetic acid and 1ml sulphuric acid. The presence of green color indicates the presence of steroids. Carbohydrate test: 1ml extract was treated with 1ml molisch reagent and 2/3 drops of sulphuric acid. The deep violet color indicates the presence of carbohydrates.

Flavonoid test

To 1ml of the plant extract 3/4 drops of concentrated sulphuric acid and magnesium turnings are added. A pink color indicates the presence of flavonoids.

Alkaloid test

1ml extract was treated with 1ml of dragendorff's reagent. The formation of orange-red color indicates the presence of alkaloids.

Terpenoid test

To 1ml of the extract 4/5 drops of concentrated sulphuric acid and 1ml chloroform were added. The dark red color indicates the presence of terpenoids.

Test for phenols

1ml extract was treated with 1ml 10% ferric chloride and 2ml distilled water. The formation of deep blue color indicated the presence of phenol.

Quinone test

To 1ml of the extract, a few drops of concentrated sulphuric acid were added. The yellow color indicates the presence of quinone.

Cardiac glycoside test

1ml extract was treated with 1ml glacial acetic acid, 0.5 ml ferric chloride solution, and four drops of concentrated sulphuric acid. The formation of dark green color indicated the presence of cardiac glycoside.

Tannin test

To 1ml of the extract 1ml 10% ferric chloride solution was added. The formation of red color indicated the presence of tannin.

2.5 Estimation of Total Phenolic Content (TPC)

The total phenolic content of the extracts was estimated using Folin- Ciocalteau spectrometric method proposed by Singleton et al., (1999)¹⁴. Test samples were dissolved in 1 % DMSO and were mixed with 1 ml 95 % ethanol. 0.25 ml of Folin- ciocalteau was added to each test tube. After 2 min, 0.75 ml of 20 % sodium carbonate was added and the volume was made up to 5 ml with distilled water. The mixture was vortexed, left for 2h and the absorbance was measured at 700 nm. Total phenolic content was expressed as mg of gallic acid equivalent (GAE)/g of plant extract.

2.6 Antioxidant activity

2.6.1 DPPH radical scavenging activity

Free radical scavenging activity of the extracts of *A. lanata* was measured by the methodology proposed by Brand Williams et al., (1995)¹⁵. 3mg of DPPH in 100ml of 70% methanol was used as a working solution of DPPH. Each extract (0.5 ml) was added to 2.5ml freshly prepared DPPH solution and mixed vigorously. The reduction of the DPPH radical was measured by continuous monitoring the decrease in absorbance at 517 nm until a stable value was obtained. All the experiments were carried out in triplicates. A blank reading was obtained using methanol instead of samples and ascorbic acid was used as the positive control. Percent inhibition was determined according to the equation:

$$\% \text{ inhibition} = [(\text{Absorbance of blank} - \text{Absorbance of the sample}) / \text{Absorbance of blank}] \times 100.$$

IC_{50} value (mg extract/ml) was the inhibitory concentration at which DPPH radicals were scavenged by 50% which was calculated from percentage inhibition.

2.7 Antibacterial activity

2.7.1 Microbial strains

The bacterial strains were collected from the Cashew Export Promotion Council of India (CEPCI), Kollam, Kerala, India. Two gram-positive bacteria: *Staphylococcus aureus* and *Clostridium perfringens*; three gram-negative bacteria: *Escherichia coli*, *Vibrio cholera*, and *Salmonella typhi* were used in the study.

2.7.2 Agar Well Diffusion Method

50 μ g/ml of the extracts were taken for the antimicrobial assay. The five test bacteria namely, *Staphylococcus aureus*, *Clostridium perfringens*, *Salmonella typhi*, *Vibrio cholera*, and *Escherichia coli* were inoculated in 10mL of Nutrient Broth and kept for overnight incubation. 11.7g of Mueller-Hinton Agar (MHA) was dissolved in 300 mL of distilled water. The sterilized MHA was poured into Petri plates in the Laminar Air Flow Chamber. The test bacteria were swabbed onto the MHA plates using sterile cotton swabs. Wells were punched in the culture plates using Sterile Well Borer. Kanamycin (positive control) and the respective solvent (negative control) were added to the rest of the wells and incubated. The diameter of the zone of inhibitions was measured in millimeters after 24 h.

2.7.3 Minimum Inhibitory Concentration

The extracts exhibited high antimicrobial activity at a concentration of 50 μ g/ml against *Staphylococcus aureus* and *Clostridium perfringens*. Therefore, this concentration was manipulated to determine their minimum inhibitory concentrations (MIC) using the agar well diffusion method. Different concentrations of 10, 20, 30, and 50 μ g/ml were used and the plates were incubated at 37°C for 24 h. The MIC was considered as the lowest concentration which inhibited the growth of the respective microorganisms.

2.8 Statistical Analyses

The experiments were carried out in triplicates and their mean values were taken. Microsoft Excel was used for working out the statistical part.

3. RESULTS

The present investigation shows the phytochemical analysis, *in-vitro*-antioxidant activity, and antimicrobial activity of ethyl acetate and methanol extracts of the plant *Aerva lanata*. The percentage yield of the ethyl acetate and methanol extracts were 3.6 % and 8.0 % respectively.

3.1 Phytochemical Analysis

Phytochemical analysis of *Aerva lanata* extracts revealed the presence of alkaloids, carbohydrates, glycosides, steroids, tannins, sugar, flavonoids, and phenols in the ethyl acetate extract while the presence of saponin, alkaloids, and terpenoids in the methanol extracts (Table.I).

Table I: Phytochemical screening of the ethyl acetate and methanol extract of *Aerva lanata*

Sl.No	Phytochemicals	ALE	ALM
1.	Saponin	--	++
2.	Steroid	++	+
3.	Carbohydrate	+	--
4.	flavonoid	++	+
5.	Alkaloid	++	++
6.	Terpenoid	--	++
7.	Phenol	++	+
8.	Quinone	--	+

9.	Cardiac glycoside	+	+	
10.	Tannin	++		--
	ALE- Ethyl acetate extract of <i>A.lanata</i> ; ; +++ ALM- Methanol extract of <i>A.lanata</i> ;			

'+' -(slightly present), '++' - (strongly present) , '-' - (absent)

The total phenolic content of ethyl acetate and methanol extract of *Aerva lanata* was estimated as 52.12 ± 0.15 mg of GAE/g of dry plant extract and 15.1 ± 0.81 mg of GAE/g of dry plant extract respectively as obtained from a standard curve of gallic acid ($y = 0.017x - 0.015$, $R^2 = 0.952$).

3.2 In-vitro Antioxidant Activity

The free radical scavenging activity was found to be dose-dependent and the results were compared with ascorbic acid, which was used as the standard. The percentage of DPPH scavenging capacity of the crude extracts of *A.lanata* is depicted in fig. 2. The IC_{50} value of ethyl acetate and methanol extracts of *A.lanata* were found to be 438.59 ± 0.08 μ g/ml and 537.63 ± 0.08 μ g/ml respectively for DPPH scavenging activity.

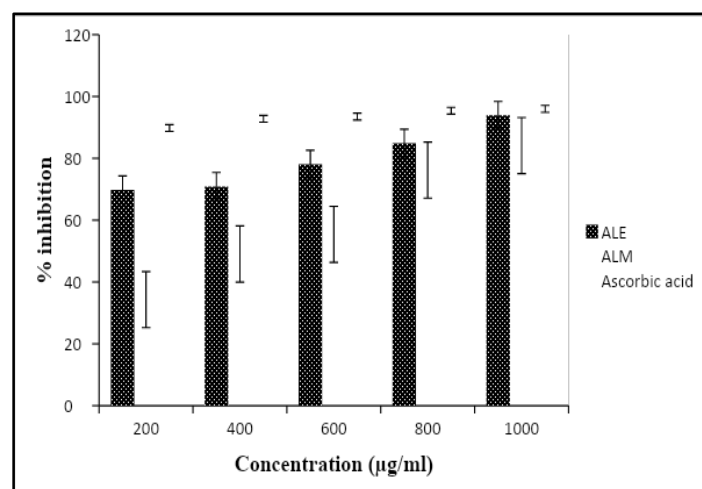


Fig. 1: DPPH radical scavenging activity of ethyl acetate (ALE) and methanol (ALM) extracts of *Aerva lanata*

3.3 Antibacterial Activity

The *in vitro* antimicrobial activity of ethyl acetate and methanol extracts of *Aerva lanata* against different bacterial strains are shown in Figure 2 and Table 2. Both the extracts of the plant showed antimicrobial activity against most of the test organisms. The highest zone of inhibition was shown by the ethyl acetate extract. Maximum antibacterial activity was exhibited against *Staphylococcus aureus* and *Clostridium perfringens* strains. Minimum Inhibitory Concentration (MIC) of ethyl acetate (ALE) and methanol extracts (ALM) of *A.lanata* against *Staphylococcus aureus* (Table.3) and *Clostridium perfringens* (Table. 4) shows the maximum activity for ethyl acetate extract.

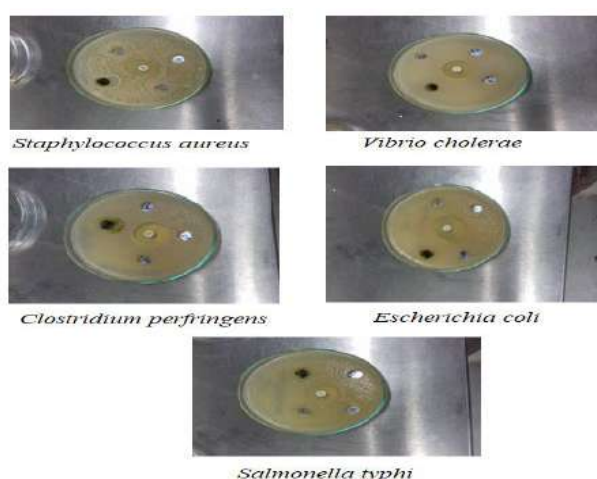


Fig 2: Antimicrobial activity of selected bacterial strains showing zone of inhibition

Each disc received 50mg/ml of ethyl acetate and methanol extract of *A.lanata*. 10 mg/ml of standard (Kanamycin) and solvent (negative control)

Table 2. Table showing the zone of inhibition of ethyl acetate (ALE) and methanol (ALM) extract of *A.lanata*.

Microbial Strains	Zone of Inhibition (in mm)		
	Kanamycin (standard)	ALE (50 µg/ml)	ALM (50 µg/ml)
<i>Staphylococcus aureus</i>	21	19	11
<i>Clostridium perfringens</i>	23	21	11
<i>Salmonella typhi</i>	26	15	13
<i>Escherichia coli</i>	26	14	12
<i>Vibrio cholera</i>	22	10	0

Table 3: Minimum Inhibitory Concentration (MIC) of ethyl acetate (ALE) and methanol extracts (ALM) of *A.lanata* on *Staphylococcus aureus*

Bacterial strain	Concentration (µg/ml)	Zone of Inhibition (in mm)	
		ALE	ALM
<i>Staphylococcus aureus</i>	10	15	10
	20	18	13
	30	20	14
	50	21	15

Table 4: Minimum Inhibitory Concentration (MIC) of ethyl acetate (ALE) and methanol (ALM) extracts of *A.lanata* on *Clostridium perfringens*

Bacterial strain	Concentration (µg/ml)	Zone of Inhibition (in mm)	
		ALE	ALM
<i>Clostridium perfringens</i>	10	14	10
	20	15	14
	30	16	17
	50	18	17

DISCUSSION

Preliminary analysis helps to identify the phytochemical constituents which are known to exhibit medicinal as well as physiological activities. The phytochemical analysis of the present study revealed the presence of steroids, flavonoids, alkaloids, phenol, cardiac glycoside, tannins in the ethyl acetate extract and saponins, steroid, flavonoid, alkaloid, terpenoid, phenol, quinone, cardiac glycoside in the methanol extract of *A.lanata* respectively which is shown in the table1. The medicinal value of plants lies in these bioactive phytochemical constituents that produce definite physiological effects on the human body¹⁶⁻¹⁷. The antioxidant activity of many compounds of botanical origin is proportional to the phenolic content. The present study shows that both ethyl acetate and methanolic extract of *A.lanata* had considerable scavenging effects on the DPPH radical which was increasing with the increase in the concentration of the sample from 200 – 1000 µg/ml. DPPH assay is based on the principle that DPPH radical on accepting a hydrogen atom from the scavenger molecule i.e. antioxidant, results in a reduction of unpaired valence electron at one atom of nitrogen bridge in DPPH leading to the change of purple color to yellow with a concomitant decrease in absorbance at 515 nm¹⁵. The color changes from deep purple to yellow or the reduction in intensity reveals the antioxidant potential of the test compound. Different Concentrations (200, 400, 600, 800, 1000µg/ml) of ethyl acetate and methanol extracts of *A.lanata* were tested for their DPPH scavenging activity. The IC₅₀values of ALE and ALM were 438.59 and

537.63 μ g/ml respectively. In the present analysis antibacterial activity of ethyl acetate and methanol extract of *Aerva lanata* was examined against five bacterial species which includes two gram-positive and three gram-negative strains namely, *Staphylococcus aureus*, *Clostridium perfringens*, *Escherichia coli*, *Vibrio cholera*, and *Salmonella typhi* using agar well diffusion method. The agar disc diffusion method was used to evaluate the antimicrobial activity by measuring the inhibition zone against the test microorganisms. The methanol extract showed little zone of inhibition against tested bacterial strains compared to ethyl acetate extract except for *vibrio cholera*. The methanol extract does not affect *V.cholera* compared to ethyl acetate extract. A similar result was reported in which ethyl extract of *Aerva lanata* showed antibacterial activity against *B. cereus*, *S. aureus*, and *Klebsiella* species¹⁸. The effectiveness of an antibacterial agent is measured by its ability to inhibit and kill bacteria.

CONCLUSION

The present study aimed at the primary phytochemical analysis, antioxidant property screening, antifungal activity, and antimicrobial activity of the ethyl acetate and methanol extract of *Aerva lanata* belonging to the family Amaranthaceae. Phytochemical analysis of *Aerva lanata* extracts revealed the presence of alkaloids, carbohydrates, glycosides, steroids, terpenoids, tannins, sugar, saponins, flavonoids, phenols, and proteins. The results showed the presence of many bioactive compounds in both ethyl acetate and methanol extract of the plant thus responsible for the antioxidant activities. The quantitative analysis estimated the number of phenols and was expressed in terms of gallic acid equivalent. The methanol extract shows a high IC₅₀ value of 537.63 μ g/ml when compared to ethyl acetate extract which is 438.49 μ g/ml. The antibacterial activity and the minimal inhibitory concentration (MIC) of the plant extracts were examined against five bacterial strains. The highest zone of inhibition was shown by the ethyl acetate extract against *Staphylococcus aureus* and *Clostridium perfringens* strains. It can be concluded that the preliminary phytochemical analysis supports the presence of bioactive compounds responsible for the antioxidant activities¹⁹. Therefore it could be a potential source of natural antioxidants that could have great importance as a therapeutic agent²⁰.

ACKNOWLEDGEMENT

The authors are thankful to the Principal and the Department of Zoology, Mar Ivanios College for timely help and valuable suggestions.

AUTHORS CONTRIBUTION STATEMENT

Ananthakrishnan R. has done the phytochemical work, antioxidant activity and antimicrobial activity, and manuscript writing. Susan Kurian coordinated the work and helped to draft the manuscript.

CONFLICT OF INTEREST

No conflict of interest was declared by the authors.

REFERENCES

- Chowdhury D, Sayeed A, Islam A, et al. (2002). Antimicrobial activity and cytotoxicity of *Aerva lanata*. *Fitoterapia* 73:92–4
- Majmudar FI, Shah MB, Patel KN, Shah BK. (1999). *Aerva lanata* – it's diuretic and hepatoprotective activity. *Indian J Nat Prod* 15:9–12.
- Vetrichelvan T, Jagadeesan M, Senthil PM, et al. (2000). Diuretic and anti-inflammatory activities of *Aerva lanata* in rats. *Indian J Pharm Sci* 62:300–2.
- Nevin KG, Vijayammal PL. (2005b). Pharmacological and immunomodulatory effects of *Aerva lanata* in Dalton's lymphoma ascites-bearing mice. *Pharm Biol* 43:640–6.
- Nagaraju N, Rao KN. (1990). A survey of plant crude drugs of Rayalaseema, Andhra Pradesh, India. *J Ethnopharmacol* 29:137–58.
- Kakrani HKN, Saluja AK. (1994). Traditional treatment through herbs in Kutch district, Gujarat state, India. Part II. Analgesic, anti-inflammatory, antirheumatic, antiarthritic plants. *Fitoterapia* 65:427–30.
- Selvanayagam ZE, Gnanavandan SG, Balakrishnan K, Rao RB. (1994). Antisnake venom botanicals from ethnomedicine. *J Herbs Spices Med Plants* 2:45–100.
- Anita A, Retna A.M (2013) Review on the medicinal plant-Aerva Lanata. Asians journal of biochemical and pharmaceutical research 3.
- Nagaratna A, Prakash LH, Harini A (2014) Pharmacological review on gokhra ganja. Journal of pharmacognosy and phytochemistry 2.
- Sara Musaddiq, Kiran Mustafaa, Sajjad Ahmadb, Samina Aslama, Basharat Alic, Samia Khakwania, Naheed Riazb, Muhammad Saleemb, and Abdul Jabbarb (2018) Pharmaceutical, Ethnopharmacological, Phytochemical and Synthetic Importance of Genus *Aerva*: A Review. *Natural Product Communications*, 13(2) 375-385.
- Harborne J.B. (1973). *Phytochemical Methods; A guide to modern techniques of plant analysis*. 2nd Edition, London New York.
- Sofowora A (1993). Screening plants for bioactive agents. *Medicinal plants and traditional medicinal in Africa*. 2nd Ed. Spectrum Books Ltd, Sunshine House, Ibadan, Nigeria; p. 134-56.

13. Trease GE, Evans WC (1983) *Pharmacognosy* Bailliere Tindall London, p. I.
14. Behera, B. C., Verma, N., Sonone, A., &Makhija, U. (2008).RETRACTED: Antioxidant and antibacterial properties of some cultured lichens.
15. Brand-Williams, W., Cuvelier, M. E., &Berset, C. L. W. T. (1995).Use of a free radical method to evaluate antioxidant activity. *LWT-Food Science and Technology*, 28(1), 25-30.
16. Gajalakshmi S, Vjayalakshmi S, Rajeshwari DV (2013) Pharmacological activities of *A. lanata*: a prospective review, International Research journal of pharmacy 3
17. M, H. (2019). ANTIDIABETIC AND ANTIOXIDANT ACTIVITY OF LEAVES OF ALPINIA PURPURATA BY ALPHA-AMYLASE AND ALPHA-GLUCOSIDASE ASSAY METHOD. Scholar: National School of Leadership, 8(2.2). Retrieved from <https://jconsortium.com/index.php/scholar/article/view/26>
18. Paramasivam Raghavendran, Dominic Sophia, Chinthamony Arul Raj, Thangarajan Starlin, and Velliur Kanniappan Gopalakrishnan (2012).Phytochemical Screening, Antioxidant Activity of Aerve lanata(L)- An Invitro Study. *Asian Journal of Pharmaceutical and Clinical Research*, 5(2); 77-81.
19. Singleton VL, Singleton R Orthofer,(1999) Lamuela-Raventos RM. Analysis of total phenols and other oxidation substrates and antioxidants employing folin-ciocalteu reagent. *Methods Enzymol*;299:152–78.
20. Perez, G.R.M.; Zavala, S.M.; Perez, G.S.; Perez, G.C. Antidiabetic effect of compounds isolated from plants. *Phytomedicine* 1998, 5, 55–75.

Synthesis Of Chalcones By Claisen-Schmidt Reaction; Study Of The Antioxidant Property Of Cinnamalacetophenone

Suju C. Joseph* and Ratheesh S. Nair

PG & Research Department of Chemistry
Mar Ivanios College (Autonomous)
Thiruvananthapuram-695015, Kerala, India

Abstract: Chalcones are the important constituent of many natural sources and exhibit a wide range of biological properties. The basic structure of chalcones consists of two phenyl rings (A & B) and an α,β -unsaturated double bond. Two chalcones namely, benzalacetophenone and cinnamalacetophenone were synthesized by Claisen-Schmidt reaction by condensing acetophenone with benzaldehyde and cinnamaldehyde respectively in the presence of an aqueous alkali. The first step in this reaction involves the nucleophilic addition of the carbanion derived from aryl ketones to the carbonyl carbon of aromatic aldehydes. The second step involves the dehydration of the hydroxyl ketones to form the conjugated α,β -unsaturated ketones, or chalcones. The structures of these synthesized chalcones were confirmed by NMR (^1H , ^{13}C), FTIR & MASS spectral data. The antioxidant property of cinnamal acetophenone was then evaluated by Halliwell's method using Fenton's reagent and deoxyribose. Chalcone was found to scavenge the hydroxyl radicals generated by Fenton's reagent preventing the degradation of deoxyribose into malondialdehyde as indicated by the Thiobarbituric acid test, illustrating the antioxidant property of cinnamalacetophenone.

KEYWORDS: Chalcones, Claisen-Schmidt reaction, cinnamalacetophenone, Halliwell's method, antioxidant property,

INTRODUCTION

Chalcones or benzylideneacetophenones is an important class of natural products and belongs to the Flavonoid family which has been reported a wide spectrum of biological activities including anti-inflammatory, anti-mutagenic, anti-bacterial, and anti-fungal.^{1, 2, 3} It was first isolated from Chinese liquorice (*Glycyrrhiza inflata*).⁴ It has 1, 3-diaryl-1-ones skeletal system which was recognized as the main pharmacophore for chalcones. From plants, stable chalcone moiety cannot be isolated because of the presence of enzyme chalcone synthetase (CSH) which immediately converts chalcone into flavanone (Fig. I). The name "Chalcones" was given by Kostanecki and Tambor.⁵ In chalcones, two aromatic rings are linked by an aliphatic three-carbon chain. Chalcone bears a very good synthon so a variety of novel heterocycles with a good pharmaceutical profile can be designed. These are colored compounds because of the presence of the chromophore (-CO-CH=CH-).⁶

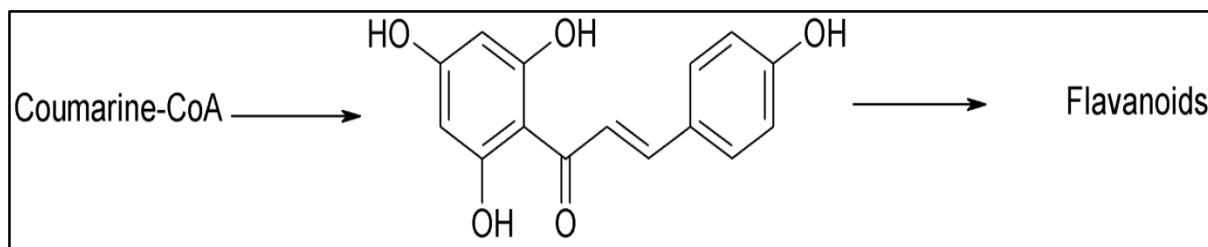


Figure I

Yuh-Hee in 2002 synthesized a different series of chalcone derivatives, which are having 90% inhibitory activity against *Mycobacterium tuberculosis*. They also performed pharmacophore mapping analysis on chalcone derivatives and concluded that ring A containing hydrophobic group and ring B containing hydrogen bonding substituents are better for antitubercular activity. Sylvie synthesized a series of chalcone derivatives and screened for cytotoxic activity against the K562 human leukemia cell line using the MTT assay method. But only one compound (*E*)-3-(3-hydroxy-4-methoxyphenyl)-prop-2-en-1-one showed maximum activity, among that five compounds showed distinct and potent inhibitory effects on the growth of *Trypanosoma cruzi* and only two compounds showed strong inhibitory activity on the growth of *L. braziliensis* *in vitro*. They also concluded that the position of the substituent on the chalcone derivatives plays an important role in their antiprotozoal activity. Fabio *et al* synthesized a new series of chalcone derivatives and tested them *in vitro* to inhibit aldose reductase enzyme (ALR2) and their specificity towards the target enzyme.⁷ All the compounds displayed an affinity for ALR2. With the help of X-ray crystallography studies, they also proved that for efficient inhibition of ALR2, the presence of hydroxyl group in the ring A or in case of their absence, the carboxylic moiety in the molecule is important for the interaction ALR2.⁸

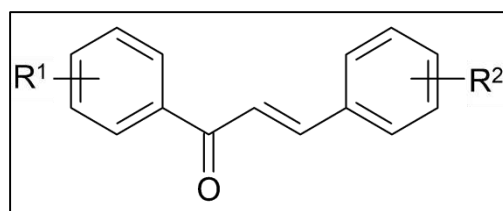
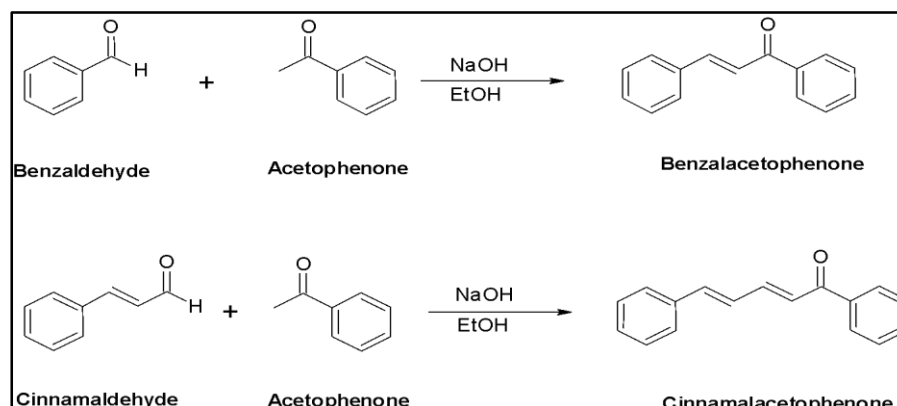


Figure 2

In a biological system, an antioxidant can be defined as "any substance that when present at low concentrations compared to that of an oxidizable substrate would significantly delay or prevent oxidation of that substrate".¹ The oxidizable substrate may be any Molecule that is found in foods or biological materials, including carbohydrates, DNA, lipids, and proteins⁹. Food is a multi-component system composed of a variety of biomolecules, and therefore, this definition describes well an antioxidant. However, regulatory bodies that overlook the food supply categorize antioxidants under food additives and define them as "substances used to preserve food by retarding deterioration, rancidity, or discoloration due to oxidation"¹⁰ (Code of Federal Regulations, Food and Drug Administration). In foods, much of the work on antioxidants have emphasized retardation of lipid oxidation, which eventually triggers and transforms to the oxidation of other macromolecules such as proteins. The objective of this chapter is to summarize the available information on the chemistry of compounds that act as anti-oxidants and to study the antioxidant property of cinnamalacetophenone.

MATERIALS AND METHODS

Chalcones were prepared by base catalyzed condensation of acetophenone with benzaldehyde and cinnamaldehyde in alcohol¹¹. 10% solution of sodium hydroxide (NaOH) was added dropwise with stirring for 4-5 hrs. The reaction mixture was kept at room temperature. The progress of the reaction & purity of the synthesized compounds was monitored by TLC using silica gel-G as stationary phase, hexane: chloroform¹² (3:1) as mobile phase, and iodine vapor was used as detecting agent. The entire compounds gave satisfactory R_f value (Scheme-1).



Scheme-I

All melting points (m.p) were determined in open capillaries on the Jindal melting point apparatus & were uncorrected. The purity of the compounds was routinely checked by thin layer Chromatography (TLC) using silica gel (Merck). The instruments used for spectroscopic data are IR: Jasco FTIR-470 spectrometer (KBr) with diffuse reflectance method; MS-JEOL SX102 Mass spectrometry by using Argon/Xenon¹³ (6Kv, 10 Ma) as the FAB gas and *m*-nitro benzyl alcohol (NBA) as the matrix. ¹H NMR was recorded on a Brucker WM-400 (400 MHz FT NMR) spectrometer using TMS as an internal standard.

EXPERIMENTAL PROCEDURES

I) SYNTHESIS OF BENZALACETOPHENONE

PART I – CONDENSATION OF ACETOPHENONE WITH BENZALDEHYDE

40 mL ethanol and 5mL of 10 % aq. NaOH solutions were added to a 250 mL RB flask. The RB flask was placed in an ice-water bath and cooled to approximately 20 °C. Then the flask was removed from the ice bath¹. A mixture of benzaldehyde¹⁴ (4.8g, 0.0472mol) and acetophenone (5.6 g, 0.0472mol) was added to the RB flask in approximately 5 min and stirred for 1 h. The reaction mixture was filtered, washed with water, and dried to afford 9.6 g of the crude product.

PART 2 – RECRYSTALLIZATION

A hot water bath was prepared by placing approximately 50 mL of water into a 100 mL beaker. Water was heated to boiling. 15 mL ethanol was added to the 250 mL RB flask containing solid benzalacetophenone. The RB flask was placed in the hot water

bath and stirred continuously for 5 min. Another 10 mL of ethanol was added to the RB flask and stirred continuously till all the solid had dissolved. Then the RB flask was removed from the hot water bath and allowed to cool at room temperature. If necessary, scratch inside the RB flask with a glass rod to induce crystallization¹⁵ Once the RB flask was cooled to room temperature it was further cooled in an ice water bath for 5-10 min allowing the crystallization to complete. The yellow crystals obtained were collected and dried to make ethanol-free.

PART 3 – CHARACTERIZATION OF THE PRODUCT

The product was then analyzed by NMR (¹H, ¹³C), FTIR, and mass spectroscopic techniques.

DATA AND CALCULATIONS

Mass product crystals: 8.54 g (0.041 mol)

Theoretical Yield: 9.82 g

Percent Yield: 87 %

Observed melting point: 102 °C¹²

Literature value: 103°C

¹H NMR (400 MHz, CDCl₃): δ 7.38 (3 H, m), 7.47 (2 H, m), 7.54 (2 H, m), 7.80 (1 H, d, J=15.7 Hz)

¹³C NMR (100 MHz, CDCl₃): δ 190.4, 144.7, 138.1, 134.8, 132.7, 130.4, 128.8, 128.5, 128.4, 128.3, 121.9

MS (m/z) : 209.10 (M⁺+1)

IR (neat): 1654.3, 1599.7 cm⁻¹

i) SYNTHESIS OF CINNAMALACETOPHENONE

PART I–CONDENSATION OF ACETOPHENONE WITH CINNAMALDEHYDE

50 mL ethanol and 8 mL of 10 % aq. NaOH solutions were added to a 250 mL RB flask. The RB flask was placed in an ice-water bath and cooled to approximately 20 °C. Then the flask was removed from the ice bath. A mixture of cinnamaldehyde (11.5g, 0.0871 mol) and acetophenone (10.5g, 0.0871 mol) was added to the RB flask in approximately 5 min and stirred for 1 h. The reaction mixture was filtered¹⁶, washed with water, and dried to afford 18.6 g of the crude product.

PART 2 – RECRYSTALLIZATION

A hot water bath was prepared by placing approximately 50 mL of water into a 100 mL beaker. Water was heated to boiling. 25 mL ethanol was added to the 250 mL RB flask containing solid cinnamalacetophenone. The RB flask was placed in the hot water bath and stirred continuously for 5 min. Another 15 mL of ethanol was added to the RB flask and stirred continuously till all the solid had dissolved. Then the RB flask was removed from the hot water bath and allowed to cool at room temperature. If necessary, scratch inside the RB with a glass rod to induce crystallization. Once the RB was cooled to room temperature it was further cooled in an ice water bath for 5-10 min allowing the crystallization¹⁷ to complete. The yellow crystals were collected and dried to make ethanol-free.

PART 3 – CHARACTERIZATION OF THE PRODUCT

The product was then analyzed by NMR (¹H, ¹³C), FTIR, and mass spectroscopic techniques.

DATA AND CALCULATIONS:

Mass product crystals: 16.7 g (0.071 mol)

Theoretical Yield: 20 g

Percent Yield: 82 %

Observed melting point: 132 °C

Literature value: 133 °C¹²

¹H NMR (400 MHz, CDCl₃): δ 7.02 (2 H, d, J = 3.9 Hz), 7.08 (1 H, d, J = 14.7 Hz), 7.39 (3 H, m), 7.46 (4 H, m), 7.51 (2 H, m), 7.98 (2 H, m)

¹³C NMR (100 MHz, CDCl₃): δ 190.5, 144.8, 141.8, 138.2, 136.1, 132.6, 129.2, 128.8, 128.5, 128.3, 127.3, 126.9, 125.4

MS (m/z) : 235.20 (M⁺+1)

IR (neat): 1661.7, 1506.2 cm⁻¹

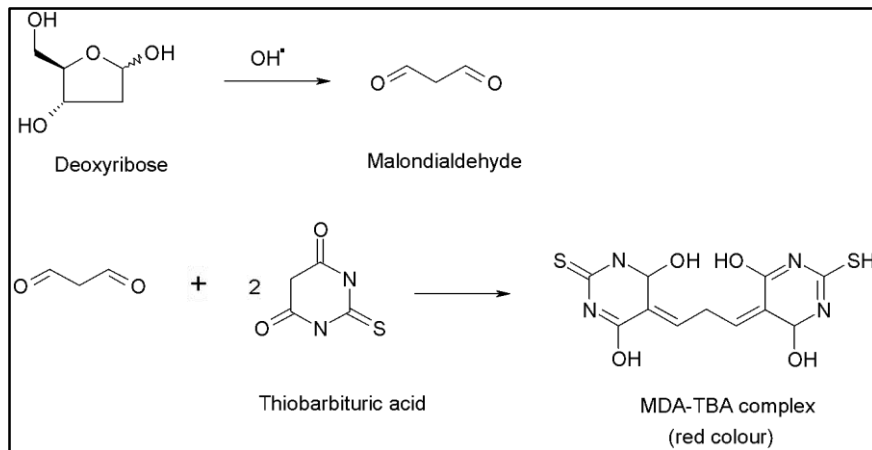
EVALUATION OF THE ANTIOXIDANT PROPERTY OF CINNAMALACETOPHENONE

The deoxyribose assay method as described by Halliwell¹⁸ has been followed to determine the antioxidant property of cinnamalacetophenone. This method uses the hydroxyl radicals generated from Fenton's reagent to degrade 2-deoxy-D-ribose resulting in the formation of malondialdehyde (MDA), which could be identified by a redcolor formed on treatment with thiobarbituric acid (TBA). The red color is due to the formation of the MDA-TBA complex. Fenton's reagent is prepared by the addition of ferrous sulphate to hydrogen peroxide in equimolar proportion Ferrous Iron (II) is oxidized by hydrogen peroxide ferric iron (III), a hydroxyl radical, and a hydroxylanion. The hydroxyl free radical generated by Fenton's reagent is a powerful,

non-selective oxidant. Oxidation of an organic compound by Fenton's reagent is rapid and exothermic (heat-producing) and results in the reduction of contaminants to primarily carbon dioxide and oxygen.



The hydroxyl free radical then reacts with deoxyribose degrading it to form malondialdehyde. The extent of the degradation depends on the available hydroxyl free radicals. The malondialdehyde is identified by the red complex formed on reaction with thiobarbituric acid that absorbs strongly at 532 nm (Scheme 2). The decomposed products of deoxyribose are 2-thiobarbituric acid-reactive substances (TBARS). If an antioxidant is present in the system, it scavenges the hydroxyl radicals generated and protects the deoxyribose from degradation producing a lesser amount of TBARS; accordingly, the intensity of red color produced will be less.



Scheme 2

Cinnamalacetophenone has a conjugated system and is expected to be easily oxidized. The capability of cinnamalacetophenone to scavenge hydroxyl radicals has been studied by preparing various concentrations of it in ethanol and measuring the intensity of the red color formed in each case by UV absorbance at 532 nm.

EXPERIMENTAL PROCEDURE

Deoxyribose Assay

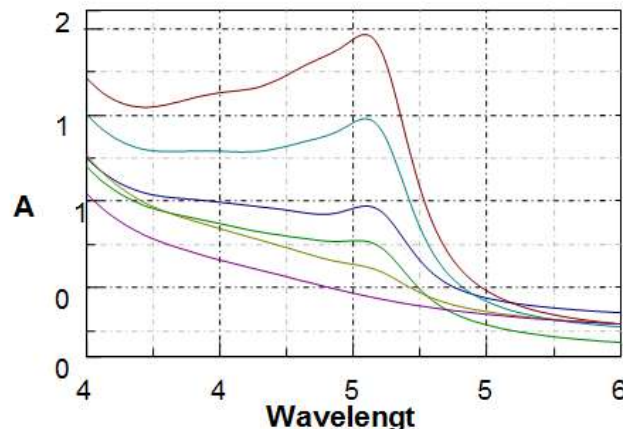
The assay was performed as described by Halliwell ¹⁹. All solutions were freshly prepared. Into a solution of 2-deoxyribose (1mL, 0.00037M) was added buffer phosphate (1mL) (pH 7.4), H₂O₂ (1mL, 0.004 M), 1 mL of various concentrations of chalcone (0.0096 M, 0.0192 M, 0.0384 M, 0.0769 M, 0.1538 M), and ferrous sulphate (1mL, 0.004 M). After an incubation period of 30 min at 310 K, the extent of deoxyribose degradation was measured by the TBA reaction. 3 ml of TBA (prepared by dissolving 100 mg in 10 mL ethanol) was added to the reaction mixture and heated for 15 min at 353 K. After the mixture was cooled, the absorbance at λ 532 nm is noted against a blank ¹⁹(the same solution but without sample).

RESULTS AND DISCUSSION

The activity test as a hydroxyl radical scavenger was conducted *in vitro* by using the Halliwell method. The reaction was started by adding ferrous sulphate and H₂O₂ to produce a radical that will react with deoxyribose. The reaction was stopped by adding a TBA reagent that would give a red color if the malondialdehyde was formed as the result of the reaction between the radical and deoxyribose. The absorbance of the red color was measured by using a UV spectrophotometer at the optimum wave number. The percentage (%) activity as an antioxidant was calculated as the percentage of the absorbance decrease of the product of the synthesis that could prevent the degradation of the 2-deoxyribose compared to the blank. When the sample of the synthesis works well as the hydroxyl radical scavenger, then it will decrease the deoxyribose degradation ²⁰ so that the malondialdehyde-TBA complex will only give the low intensity of red color. Thus, the more intense the red color, the less active the sample is. The graph showing the absorbance sample at different concentrations against wavelength is then obtained as shown in figure 3. The percentage inhibition (I %) was calculated by the formula for the concentrations of the sample.

$$\% = \frac{A_{\text{blank}} - A_{\text{sample}}}{A_{\text{sample}}} \times 100 \%$$

The IC₅₀ value represented the concentration of the compounds that caused 50% inhibition. 50% inhibition was determined to be 0.0192 M for chalcone.



Colour code	Concentration	Absorbance	I %
	Blank (without sample)	1.893	
	0.0096 M	1.473	27.43
	0.0192 M	0.996	50.9
	0.0384 M	0.752	62.9
	0.0769 M	Nil	
	0.1538 M	Nil	

Figure 3

CONCLUSION

Benzalacetophenone and cinnamalacetophenone were synthesized by Claisen-Schmidt reaction in good yield. The progress of the reaction & purity of the synthesized compounds was monitored by TLC using silica gel-G as stationary phase, chloroform: hexane (1:3) as mobile phase and iodine vapor was used as detecting agent. The entire compounds gave a satisfactory R_f value. The structures of benzalacetophenone and cinnamalacetophenone were confirmed by NMR (1H , ^{13}C), FTIR, and MASS spectra. Cinnamalacetophenone was found to be an effective active hydroxyl radical scavenger as determined by Halliwell's method. 50% inhibition was determined to be 0.0192 M for cinnamalacetophenone.

ACKNOWLEDGEMENT

UGC, New Delhi is gratefully acknowledged for the financial support.

CONFLICT OF INTEREST

Conflict of interest declared none.

REFERENCES

1. Katritzky AR, Pozharskii AF. Handbook of heterocyclic chemistry. 2nd ed. New York: Pergamon Press; 2000.
2. Noga EJ, Barthalmus GT, Mitchell MK. Cyclic amines are selective cytotoxic agents for pigmented cells. *Cell Biol Int Rep*. 1986;10(4):239-47. doi: [10.1016/0309-1651\(86\)90070-6](https://doi.org/10.1016/0309-1651(86)90070-6).
3. Nagaraj A, Sanjeeva Reddy C. Synthesis and biological study of novel bis-chalcones, bis-thiazines and bis-pyrimidines. *J Iran Chem Soc*. 2008;5(2):262-7. doi: [10.1007/BF03246116](https://doi.org/10.1007/BF03246116).
4. Mahadevan KM, Prakash GK, Anunakumar DB, Kumaraswamy B, Sherigara BS. *Indian J Chem*. 2006;45B:1699.
5. Kostanecki M, Tambor SA. *Acta Pharm*. 1989;58:467.
6. Atwal KS, Rovnyak GC, Kimball SD, Floyd DM, Moreland S, Swanson BN, Gougoutas JZ, Schwartz J, Smillie KM, Malley MF. Dihydropyrimidine calcium channel blockers. 2. 3-substituted-4-aryl-1,4-dihydro-6-methyl-5-pyrimidinecarboxylic acid esters as potent mimics of dihydropyridines. *J Med Chem*. 1990;33(9):2629-35. doi: [10.1021/jm00171a044](https://doi.org/10.1021/jm00171a044), PMID 2391701.
7. Fabio KH, Popat KH, Vasoya SL. *Indian J Heterocycl Chem*. 1992;12:217.
8. Vashi K, Naik KB. *Asian J Chem*. 2005;17:240.
9. Bhatt DJ, Kamdar GC, Parikh AR. *J Inst Chem (India)*. 1984;56:233.
10. Lakhani R, Parikh. *J Inst Chem (India)*. 1987;59:230.

11. Joshi HS, Parikh ARJ, Inst Chemists (India), 1990.
12. Desai CM, Patel D, Joshi HD. *J Inst Chem (India)*. 2004;76:94.
13. Halliwell BM, Murcia MA, Chirico S, Aruoma OI. Free radicals and antioxidants in food and in vivo: what they do and how they work. *Crit Rev Food Sci Nutr.* 1995;35(1-2):7-20. doi: [10.1080/10408399509527682](https://doi.org/10.1080/10408399509527682), PMID 7748482.
14. Tsujimoto M, Coll J. *Engl imp. University Tokyo*; 1908. p. 4181.
15. C. Moureu; C. Dufraisse, *compt. rend.* 1922;174:258.
16. C. Moureu; C. Dufraisse, *compt. rend.* 1922;175:127.
17. C. Moureu; C. Dufraisse. *J Chem Soc.* 1925;127.
18. Moureu C, Dufraisse C. The negative catalysis of auto-oxidation. Anti-oxygenic activity. *J Chem Technol Biotechnol.* 1928;47(32):819-28. doi: [10.1002/jctb.5000473202](https://doi.org/10.1002/jctb.5000473202).
19. Lowry CD, Egloff G, Morrell JC, Dryer CG. Inhibitors in Cracked Gasoline. *Ind Eng Chem.* 1933;25(7):804-8. doi: [10.1021/ie50283a021](https://doi.org/10.1021/ie50283a021).
20. Bolland JL, P. *Discuss. Farad. Società*. 1947;2:252.

Biochemical Parameters In The Patients Of Alcoholic Liver Disease And Type 2 Diabetes Mellitus: A Cross-Sectional Observational Study

Juhi Aggarwal¹, Sojit Tomo¹, Pradhumn Katara¹, Jyoti Batra¹, Aarushi Batra²

¹Santosh Deemed to be University, Ghaziabad, Uttar Pradesh -201009.

²LLRM Medical College, Meerut, U.P., INDIA

Corresponding Author: Dr.JyotiBatra

E-Mail: dean.research@santosh.ac.in

Abstract: Alcohol is a hepatotoxin that is commonly consumed worldwide and is associated with a spectrum of liver injury including simple steatosis/fatty liver, alcoholic hepatitis, fibrosis, and cirrhosis. Chronic liver diseases (CLD) cause significant morbidity and mortality worldwide. Diabetes and alcohol consumption are two of the most prevalent public health problems in the Indian population. The biochemical markers for chronic alcohol consumption that have been most commonly studied are serum GGT, AST, ALT, ALP, mean corpuscular volume (MCV), and carbohydrate-deficient transferrin (CDT). The present study was aimed to analyze the various liver function enzymes in chronic alcoholics with type 2 diabetes mellitus.

Keywords: Biochemical parameters, type 2 diabetes, Chronic liver diseases, haemoglobin, liver disease

INTRODUCTION

Alcohol is a hepatotoxin that is commonly consumed worldwide and is associated with a spectrum of liver injury including simple steatosis/fatty liver, alcoholic hepatitis, fibrosis, and cirrhosis. Chronic liver diseases (CLD) cause significant morbidity and mortality worldwide. Alcohol causes significant hepatocyte injury by the generation of free radicals, cytokine release, hypoxic injury, and adduct formation ¹. Diabetes and alcohol consumption are two of the most prevalent public health problems in the Indian population. Due to improved curative services and vaccination coverage, infectious diseases had been controlled to a great extent. As an effect, there is a shift from communicable to non-communicable diseases. Among non-communicable diseases, diabetes stands first which causes both health and economic burden to the patients as well as the country. There were around 463 million of the world's population were living with diabetes in 2019. In 2020, according to the International Diabetes Federation (IDF), 88 million people are suffering from Diabetes mellitus in the Southeast Asia region. Of these 88 million people, 77 million belong to India. Alcohol influences glucose metabolism in several ways in diabetic patients as well as in non-diabetic patients. If consumed with food, alcohol is the preferred fuel and causes higher blood glucose levels leading to insulin response. Further, as alcohol inhibits both gluconeogenesis and glycogenolysis, its acute intake without food may provoke hypoglycemia, especially in cases of depleted glycogen stores and in combination with a sulphonylurea. Thus alcohol consumption potentiates ill health effects of diabetes ². Approximately 60%-90% of individuals who drink more than 60 ml of alcohol per day have been shown to have hepatic steatosis ^{3,4}. However, less than half of individuals with alcoholic steatosis, who continue to drink alcohol, will progress to fibrosis and only 10%-20% will eventually progress to cirrhosis ⁵⁻⁶. Nonetheless, once steatohepatitis has developed, the risk of the development of cirrhosis is increases compared with simple steatosis ⁷. In addition, individuals who have demonstrated steatohepatitis who continue to drink alcohol or who develop symptomatic alcoholic hepatitis have higher rates of progression to cirrhosis compared with those who subsequently abstain from alcohol consumption or who have never had an episode of symptomatic alcoholic hepatitis. Alcoholic cirrhotics who abstain from alcohol consumption for at least 1.5 years have improved survival rates compared to those that continue to drink ⁸. The biochemical markers for chronic alcohol consumption that have been most commonly studied are serum GGT, AST, ALT, ALP, mean corpuscular volume (MCV), and carbohydrate-deficient transferrin (CDT). An AST to ALT ratio over 2 is highly suggestive of Alcoholic Liver Disease. Most patients with non-Alcoholic Liver Disease have AST to ALT ratios below one. Specific IgA antibodies directed towards acetaldehyde-derived protein modifications are frequently seen in alcoholics and thus, IgA levels are increased in chronic Alcoholic liver disease. An increased ratio of IgA to IgG is highly suggestive of ALD. While there are no ideal non-invasive biomarkers currently available to differentiate between simple steatosis and alcoholic steatohepatitis, newly discovered biomarkers for non-alcoholic steatohepatitis (NASH) may be potentially applied to ALD in the future. The present study was aimed to analyze the various liver function enzymes in chronic alcoholics with type 2 diabetes mellitus ⁹.

MATERIALS AND METHODS

This was a descriptive cross-sectional study conducted at the Department of Biochemistry, Santosh Medical College and Hospital, Ghaziabad, India from January 2020 to September 2020. The present study was approved by the Institutional ethical committee and review board. The study was conducted on 255 individuals out of the thesis 99 were adult Males aged 45-60 years patients with a positive history of prolonged alcohol intake for \geq five years with Alcoholic Liver Disease considered as case and 156 age and sex-matched individuals with Alcoholic Liver Disease with no history of diabetes Mellitus were considered as control ¹⁰⁻¹¹. Exclusion Criteria: Patients with autoimmune disease, hemolytic anemia, or infections of the liver, renal problem, and history of any substance abuse were excluded from the study. Patients who tested positive for Hepatitis B surface antigen and indicated the presence antibody of Hepatitis C virus were excluded from the study. Also, subjects were recruited in the present study only after obtaining written informed consent ¹²⁻¹⁴. Sample collection and record-keeping: A total of 5ml of blood was drawn by venipuncture under aseptic precaution in the fasting condition in a plain tube. Serum was separated and biochemical

parameters include Fasting and Postprandial blood glucose, total protein, albumin, globulin aspartate transaminase (SGOT), alanine transaminase (SGPT), alkaline phosphatase (ALP) and γ -glutamyltranspeptidase (GGT) were assayed by using Roche fully automated clinical chemistry analyzer- Cobas c111. Demographic, biochemical, and clinical parameters of study subject were recorded using pre-printed and pre-structured Performa with provision to record name, age, sex, duration of diabetes type 2, dietary habit, drinking habit, smoking habit, family history of the disease, socio-economic status, community, occupation and present, and past clinical history ¹⁵.

RESULTS

The study includes a total of 255 individuals with the age group 40-60 years among them, 99 were the case and 156 were the control. The median age (IQR) of the study participants and controls was 53.4 (46.9-57.1) years and 54.6(74.4-57.8) years, respectively. Table 1 shows the mean and standard deviation for both study groups height (cm), Weight(kg), BMI(kg/m^2). A significantly increased level was observed in mean FBS and mean PBBS in the cases compared to control. However, GL and Ferritin were insignificantly increased, and mean SGOT, mean SGPT, mean BILT, mean BILD, mean APL, mean TPR were insignificantly decreased in case comparison to controls (Table 2). Among the cases, fever was most prevalent 41.41% whereas ascetics were less prevalent 8% (Table 3). There was a positive and significant correlation of Age with FBS and a negative significant correlation of Age with SGPT, TPR in study participants. There was a positive and significant correlation of FBS with PPBS and a negative significant correlation of FBS with BILD and SGPT in study participants (Table 4).

Table 1: Demographic parameters in control and diabetic population

S.No	Characteristics	Non-Diabetic control (n=156)	Diabetic population (n=99)
1	Age (years)		
	Median	54.6	53.4
	IQR	(47.4 - 57.8)	(46.9 - 57.1)
2	Height(cm)		
	Mean	155.0	154.4
	SD	5.86	5.31
3	Weight(kg)		
	Mean	74.3	78.6
	SD	9.41	8.20
4	BMI(kg/m^2)		
	Mean	35.5	39.6
	SD	5.52	5.27
5	Waist circumference(cm)		
	Mean	94.2	99.4
	SD	11.81	10.53
	P (Value)	0.001	
6	Systolic blood pressure(mm/Hg)		
	Mean	123	162
	SD	17	9.2
	P (Value)	0.001	
7	Diastolic blood pressure(mm/Hg)		
	Mean	108	122
	SD	6.45	6.25
	P (Value)	0.001	

A significantly increased level was observed in mean FBS and mean PBBS in the cases compared to control. However, GL and Ferritin were insignificantly increased, and mean SGOT, mean SGPT, mean BILT, mean BILD, mean APL, mean TPR were insignificantly decreased in case comparison to controls (Table 2). Among the cases, fever was most prevalent 41.41% whereas ascetics were less prevalent 8% (Table 3). There was a positive and significant correlation of Age with FBS and a negative significant correlation of Age with SGPT, TPR in study participants. There was a positive and significant correlation of FBS with PPBS and a negative significant correlation of FBS with BILD and SGPT in study participants (Table 4).

Table 2: Mean compression table of the Biochemical parameters among both study groups.

S.No	Biochemical Parameters	Non-Diabetic control (n=156)	Diabetic population (n=99)	P-Value (at the 0.05 level)
1	FBS(mg/dl)			
	Mean	101.33	194.16	0.001*
	SD	14.88	64.06	

		PPBS (mg/dl)			
2	Mean	213.19		252.35	0.001*
	SD	89.77		94.54	
3	BIL T				
	Mean	0.99		0.85	0.201
4	SD	1.03		0.65	
	BIL D				
5	Mean	0.48		0.33	0.105
	SD	0.83		0.37	
6	SGOT (U/L)				
	Mean	97.17		44.11	0.089
7	SD	305.20		57.11	
	SGPT (U/L)				
8	Mean	118.12		42.70	0.063
	SD	398.15		58.60	
9	ALP (g/dl)				
	Mean	344.31		322.06	0.576
10	SD	367.41		182.37	
11	GL				
	Mean	3.07		5.95	0.214
	SD	0.24		28.74	
	GGTP				
	Mean	74.72		51.31	0.130
	SD	140.20		77.73	
	FERRITIN (NG/ML)				
	Mean	363.90		376.89	0.141
	SD	66.67		71.25	

*Correlation is significant at the 0.05 level (2-tailed)

Table 3: Distribution of cases according to the clinical presentation in diabetic subjects (N=99)

Clinical features		Number of cases (N=99)			% prop (CI at 95%)	
Fever		41			41.41% (31.71 – 51.12)	
Vomiting		28			28.28% (19.69 – 38.22)	
Jaundice		12			12.12% (6.06 – 20.02)	
Abdominal pain		35			35.35% (26.01 – 45.60)	
Hepatomegaly		26			26.26% (17.93 – 36.07)	
Ascitis		8			8.08% (3.55 – 15.30)	
Pruritis		14			14.14% (17.95 – 22.59)	

Table 4: Correlation among the Biochemical parameters in all study participants (N=255)

		AGE	FBS	PPB S	BIL T	BIL D	SG OT	SGP T	ALP	TPR	GL	GG TP	
FBS	Pearson Correlation	.140*											
	Sig. (2-tailed)	.026											
PPBS	Pearson Correlation	.073	.371*										
	Sig. (2-tailed)	.246	.000										
BIL T	Pearson Correlation	-.061	-.112	-.015									
	Sig. (2-tailed)	.332	.074	.811									
BIL D	Pearson Correlation	-.056	-.126*	-.048	.880*								
	Sig. (2-tailed)	.376	.045	.450	.000								

	tailed)											
SGOT	Pearson Correlation	-.118	-.112	.025	.630*	.627*						
	Sig. (2-tailed)	.060	.073	.691	.000	.000						
SGPT	Pearson Correlation	-.144*	-.124*	-.001	.620*	.711*	.963*					
	Sig. (2-tailed)	.022	.048	.990	.000	.000	.000					
ALP	Pearson Correlation	-.120	-.026	-.014	.410*	.492*	.239*	.329*				
	Sig. (2-tailed)	.055	.683	.821	.000	.000	.000	.000				
TPR	Pearson Correlation	-.295*	-.064	-.016	-.166*	-.139*	-.031	-.031	-.188*			
	Sig. (2-tailed)	.000	.310	.803	.008	.027	.625	.619	.003			
GL	Pearson Correlation	-.046	.003	.087	-.020	-.018	-.015	-.015	-.028	.004		
	Sig. (2-tailed)	.469	.956	.166	.749	.777	.813	.810	.659	.947		
GGTP	Pearson Correlation	.002	-.020	.032	.394*	.616*	.415*	.498*	.430*	-.118	-.013	
	Sig. (2-tailed)	.973	.751	.617	.000	.000	.000	.000	.000	.061	.835	
FERRI TIN	Pearson Correlation	.045	.049	.024	.080	.099	.036	.053	.077	-.088	-.021	.073
	Sig. (2-tailed)	.470	.432	.706	.203	.113	.563	.401	.220	.163	.735	.246

*Correlation is significant at the 0.05 level (2- tailed)

**Correlation is significant at the 0.01 level (2- tailed)

DISCUSSION

Sorbi et al in 1994 suggested that an elevated serum AST to ALT ratio has been proposed as an indicator of alcohol-induced organ damage¹⁰. Hyperbilirubinemia, Hypoalbuminemia, and high ALT levels thus reflect the diminished hepatic activity of the liver enzymes, which made them leak into the serum from damaged hepatocytes due to the location of ALT in the cytosol. ALT provides reliable evidence for the liver injury caused by acute alcohol intoxication¹¹. The increase in AST may be due to increased cell membrane permeability, cell necrosis and mitochondrial leakage into the blood, caused by excessive alcohol consumption. Since AST is located in both the cytosol and mitochondria, serum levels depend markedly on the degree of liver damage. Cohen et al also observed that an SGOT/SGPT ratio greater than 2 is highly suggestive of alcoholic hepatitis and cirrhosis¹². It was reported that most patients with high alcohol consumption but without severe liver disease do not have an AST/ALT ratio above one. A high AST/ALT ratio suggests advanced ALD. Serum AST values should be taken into account for liver biopsy and treatment protocol for hepatitis C infection¹³. Some interrelated reasons have been reported for the high AST/ALT ratio in ALD due to decreased hepatic ALT activity, pyridoxal-5'-phosphate depletion in the liver of alcoholics, and mitochondrial damage leading to an increase in the serum activity of mitochondrial aspartate in patients with high alcohol consumption. GGT is located in several tissues of the kidney, pancreas, and liver and plays a role in the metabolism of glutathione, facilitating amino acid transport. The activity of serum GGT is induced by ALD and cholestasis, not by renal disease. Several researchers have reported significant elevation in GGT in patients with ALD, and even in light and moderate drinkers. A study by Cushman et al showed that elevated serum GGT levels in drinkers were related more closely to the biological effects of alcohol consumption rather than to the amount of alcohol consumed. 45% of alcoholics showed increased levels of gamma-glutamyltranspeptidase¹⁴. Irie et al found that GGT synthesis and protein expression were increased in ALD, leading to elevated serum levels of GGT that were commonly noted in patients with the disease. We found in our study also that levels of GGT were elevated significantly due to regular intake of alcohol¹⁵. Many authors have shown that the determination of liver function enzymes, lactate dehydrogenase, prothrombin time, and blood urea nitrogen are useful for the diagnosis and clinical evaluation of patients with different pathologies related to alcoholic patients¹⁶. Studies by Yamada et al in a 5-year follow-up study¹⁷ showed that elevated serum GGT levels are directly proportional to alcoholism-related hypertension. In a study conducted in 2005, it was concluded that low socio-economic, hypertension and physical inactivity are significant predictors of diabetes mellitus¹⁸. In many studies, they state that the proportion of abnormal liver functions tests varied in a gender wise manner. In a multivariate study by Stringhini et al BMI, deranged levels of lipid profile and unhealthy dietary habits go hand in hand with the incidence of type 2 diabetes mellitus¹⁹. In a recent study conducted by Deshpande N et al, it was depicted that liver function tests along with serum ferritin, blood urea, creatinine, blood glucose, and hemoglobin are directly related to the pathogenesis

and progression of alcoholic liver cirrhosis ²⁰⁻²⁴

Furthermore, the proportion of normal and abnormal values for the enzymes AST and ALT varied significantly between males and females. It is increasingly believed that abnormal hepatocellular functions are strongly related to type 2 DM[21]. Analytical studies have linked elevated liver enzymes with hyperglycemia and/or insulin resistance. Abnormal LFTs in type 2 DM have also been attributed to factors like non-alcoholic fatty liver disease and underlying hepatitis C infection. In a study conducted in 2014, it was established that there was a significant positive correlation between alcoholism, liver injury, and liver function parameters.

CONCLUSION

The result of this study established that alcohol drinking is associated with several alterations in cell functions, the disintegration of the plasma membrane, inhibition of key cellular metabolism, and a change ineffective mechanism for detoxification of harmful components. Hyperbilirubinemia and Hypoalbuminemia are common features of alcoholics. Monitoring GGT, ALP, AST, and ALT in combination is a sensitive means of detecting the severity of alcohol-induced liver damage. Internationally, the AST/ALT ratio is accepted as a dependable marker for the diagnosis of ALD. ALD has a prime economic burden on society as well. This provides reliable evidence for the liver injury caused by acute alcohol intoxication. We recommended screening for alcohol abuse in all adult patients presenting to the hospital as an early modality for detection of ALD so that it can reduce the morbidity and mortality due to ALD.

CONFLICT OF INTEREST

Conflict of interest declared none.

REFERENCE

1. Sherlock S, Dooley J; Alcohol and the liver. Chapter 22, Diseases of the liver and biliary system, Blackwell Science Publications 11 the edition, 2002; 381-396.
2. Siobhan C Maty, Susan A Everson-Rose, Mary N Haan, Trivellore E Raghunathan, and George A Kaplan. Education, income, occupation, and the 34-year incidence (1965–99) of Type 2 diabetes in the Alameda County Study. *Int J Epidemiol.* 2005 December; 34(6): 1274–1281.
3. Crabb DW. Pathogenesis of alcoholic liver disease: newer mechanisms of injury. *Keio J Med* 1999; 48: 184-188 [PMID: 10638142]
4. Becker U, Deis A, Sørensen TI, Grønbaek M, Borch-Johnsen K, Müller CF, Schnohr P, Jensen G. Prediction of risk of liver disease by alcohol intake, sex, and age: a prospective population study. *Hepatology* 1996; 23: 1025-1029 [PMID: 8621128]
5. Altamirano J, Bataller R. Alcoholic liver disease: pathogenesis and new targets for therapy. *Nat Rev Gastroenterol Hepatol* 2011; 8: 491-501 [PMID: 21826088 DOI: 10.1038/nrgastro.2011.134]
6. Teli MR, Day CP, Burt AD, Bennett MK, James OF. Determinants of progression to cirrhosis or fibrosis in pure alcoholic fatty liver. *Lancet* 1995; 346: 987-990 [PMID: 7475591]
7. Deleuran T, Grønbaek H, Vilstrup H, Jepsen P. Cirrhosis and mortality risks of biopsy-verified alcoholic pure steatosis and steatohepatitis: a nationwide registry-based study. *Aliment Pharmacol Ther* 2012; 35: 1336-1342 [PMID: 22490057 DOI: 10.1111/j.1365-2036.2012.05091.x]
8. Xie YD, Feng B, Gao Y, Wei L. Effect of abstinence from alcohol on survival of patients with alcoholic cirrhosis: A systematic review and meta-analysis. *Hepatol Res* 2013; Epubahead of print [PMID: 23607793 DOI: 10.1111/hepr.12131].
9. Cara Torruellas, Samuel W French, and Valentina Medici, Diagnosis of alcoholic liver disease: *World J Gastroenterol.* 2014 Sep 7; 20(33): 11684-11699.
10. Sorbi D, Boynton J, Lindor KD. The ratio of aspartate aminotransferase to alanine aminotransferase: potential value in differentiating nonalcoholicsteatohepatitis from alcoholic liver disease, *Am J Gastroenterol* 1999; 94: 1018-1022.
- 11.. M Adak , AN Thakur , K Adhikari. Study of Biochemical Markers in Alcoholic Liver Disease: Hospital-Based Case-Control Study. July – September 2012 RJPBCS Volume 3 Issue 3, 987- 995.
- 12.. Cohen JA, Kaplan MM. The SGOT/SGPT ratio--an indicator of alcoholic liver disease. *Dig Dis Sci* 1979; 24: 835-838.
13. Assy N, Minuk GY. Serum Aspartate But Not Alanine Aminotransferase Levels Help To Predict The Histological Features of Chronic Hepatitis C Viral Infections in Adults. *Am J Gastroenterol* 2000; 95(6): 1545-1550.
- 14.. Cushman P, Jacob G, Barboriak JJ, Anderson AJ. Biochemical markers for alcoholism: sensitivity problems. *Alcoh Clin Exp Res* 1984; 8(3): 253-257.
15. Irie M, Suzuki N, Sohda T, Anan A, Iwata K, Takeyama Y, Watanabe H, Fischer P, Scherberich JE, Sakisaka S. Hepatic expression of gamma-glutamyltranspeptidase in the human liver of patients with alcoholic liver disease. *Hepatol Res* 2007; 37(11): 966-973.
- 16 . G. J. MagarianL. M. Lucas, andK. L. Kumar. Clinical significance in alcoholic patients of commonly encountered laboratory test results. *West J Med.* 1992 Mar; 156(3): 287–294.

17. Yamada Y¹,Ishizaki M,Kido T,Honda R,Tsuritani I,Ikai E,Yamaya H. Hypertension Alcohol, high blood pressure, and serum gamma-glutamyltranspeptidase level. (Dallas, Tex. : 1979),01 Dec 1991, 18(6):819-826.
18. Siobhan C Maty, Susan A Everson-Rose, Mary N Haan, Trivellore E Raghunathan, and George A Kaplan. Education, income, occupation, and the 34-year incidence (1965-99) of Type 2 diabetes in the Alameda County Study Int J Epidemiol. 2005 December; 34(6): 1274-1281.
19. Stringhini S, Tabak A, Akbaraly T, Sabia S, Shipley M, Marmot M et al. Contribution of modifiable risk factors to social inequalities in type 2 diabetes: prospective Whitehall II cohort study. BMJ 2012;345.
20. NeeleshDeshpande, SabithaKandi, ManoharMuddeshwar, Rajkumar Das, K V Ramana. A Study of Biochemical and Hematological Markers in Alcoholic Liver Cirrhosis. *World Journal of Nutrition and Health*. 2014; 2(2):24-27.
21. Dr. Walter A, Dr. Mohammed Ashraf. A study correlating the quantity and duration of alcohol consumption with liver function tests. IOSR Journal of Dental and Medical Sciences, Volume 13, Issue 3 Ver. III. (Mar. 2014), PP 70-75.
22. Kavuru, N. S. and Krishnan, S. (2021) "Delayed Inhalational Injury due to Accidental Muriatic Acid Poisoning", IARS' International Research Journal. Vic. Australia, 11(2), pp. 15-17. DOI: 10.51611/iars.irj.v11i2.2021.161.
23. ManishaArora, Roshan Kumar Mahat, Sudeep Kumar, Anita Sharma, JyotiBatra. Evaluation of AST/ALT Ratio in patients of alcoholic Liver Disease. 2015; Bulletin of pharmaceuticals and medical sciences (BOPAMS)vol.3 issue1,3027-3030.
24. V.S. Chopra, Mani Goel, JyotiBatra, KavitaDhar, Jyotsna Sharma. Liver Toxicity in HIV – Infected Patients Receiving Antiretroviral Therapy that includes HIV – I Protease Inhibitors; Journal of Pharmacy and Biological Sciences. 11 (04); 99 – 103,2016 (2016-17), July-Aug

Green Synthesis And Characterization Of Zero-Valent Iron Nanoparticles From The Leaf Extract Of Psidium Guajava Plant And Their Antibacterial Activity

Dr .K.Sowmiya, Dr. Revathi, Dr. P. Moorthi, P. Dhivya

Dhanalakshmi Srinivasan College of Arts and Science for Women (Autonomous) Perambalur - 621212.

Abstract: Green synthesis of metallic nanoparticles has accumulated an ultimate interest over the last decade due to their distinctive properties that make them applicable in various fields of science and technology. Metal nanoparticles that are synthesized by using plants have emerged as nontoxic and ecofriendly. In this study, a very cheap and simple conventional heating method was used to obtain the iron nanoparticles (FeNPs) using the extract obtained from the leaves of the *Psidiumguajava* plant. The obtained iron nanoparticles were characterized by UV-Vis spectroscopy, FTIR spectroscopy, XRD, Cyclic Voltammetry, SEM, EDAX, and the antibacterial activity was studied against *Bacillus cereus*, *Escherichia coli*, *Klebsiella pneumonia*, and *Staphylococcus aureus* by the standard disc diffusion method. The synthesized FeNPs were found to be 27nm which was confirmed by XRD.

Keywords: FeNPs, *Psidiumguajava*, UV-Vis, FTIR, XRD, Cyclic Voltammetry, SEM-EDAX

INTRODUCTION

Matter can be broadly divided into two categories based on size: Macroscopic and Mesoscopic. A Macroscopic matter is visible to the naked eye whereas mesoscopic particles such as bacteria and cells that have dimensions on the order of micron(s), can be observed with optical microscopes. Falling into the gap between the microscopic and the mesoscopic is another class of matter, the nanoscopic particles.¹ Nanotechnology is a very broad area comprising of nanomaterials, nanotools, and nanodevices.² Nanoscale iron particles are recently in great interest in environmental remediation circles in the removal of organic and inorganic pollutants from aqueous solutions.³ The attention into zero-valent iron nanoparticles has been increasing considerably since the growth of a green production technique in which extracts from leaves are used.^{4,5} Nowadays iron nanoparticles (Fe NPs) are synthesized by plant extracts and are used to remove nitrate in water. These Iron nanoparticles are considered as cleaner productions that can be used for the efficient removal of nitrate.⁶ In this method of green synthesis, there is no requirement for high pressure, energy, temperature, or toxic chemicals. Hence nowadays many researchers are diverting themselves from using synthetic methods.⁷ Zero-valent iron nanoparticles (nZVI) have already proven their efficacy in the reductive disposal of a wide array of environmental contaminants in numerous laboratory and field trials.⁸ The synthesis of nZVI by the recently developed green bottom-up method is extremely promising.⁹ Biosynthesis of metal nanoparticles extracted from different parts (mostly leaves) of the plant is the most effective process of synthesis at a very affordable cost. During the synthesis bioreduction of metal ions takes place. According to the researchers, the polyol components present in the plant extract are responsible for the reduction of iron ions whereas water-soluble heterocyclic components stabilize the nanoparticles formed. Appropriate precursors such as ferric chloride can be used for the reduction of plant extracts.¹⁰⁻¹⁷

MATERIALS AND METHODS

Reagents and chemicals

Ferric Chloride (FeCl₃) and all analytical grade chemicals were purchased from TCI Chemicals, Chennai. Freshly prepared triple distilled water was used throughout the experiment.

Preparation of leaf extract by boiling method

Psidiumguajava leaves were selected from the Nagamalai area, Madurai, Tamilnadu, India based on cost-effectiveness and ease of availability (**Figure 1**). Fresh and healthy leaves were collected locally and rinsed thoroughly first with tap water followed by distilled water to remove all the dust and unwanted visible particles, cut into small pieces. About 10 g of these finely incised leaves were weighed and transferred into 250 mL beakers containing 100 mL distilled water and boiled for about 20 min. The extracts were then filtered thrice through Whatman No. 1 filter paper to remove particulate matter and to get clear solutions which were then refrigerated (4 °C) in 250 mL Erlenmeyer flasks for further experiments. In every step of the experiment, sterility conditions were maintained for effectiveness and accuracy in results without contamination.



Figure 1 Image of *Psidiumguajava*

UV-Vis spectra Analysis

Samples (1 mL) of the suspension were collected periodically to monitor the completion of bioreduction of Fe^{3+} in aqueous solution, followed by dilution of the samples with 2 ml of deionized water and subsequent scan in UV-visible (vis) spectra ¹⁸, between wavelengths of 200 to 700 nm in a spectrophotometer (Beckman - Model No. DU - 50, Fullerton), having a resolution of 1 nm ¹⁹.

FTIR analysis

FTIR analysis of the dried FeNPs was carried out through the potassium bromide (KBr) pellet (FTIR grade) method in 1:100 ratio and the spectrum was recorded using Jasco FT/IR-6300. Fourier transform infrared spectrometer ²⁰ equipped with JASCO IRT-7000. Intron Infrared Microscope using transmittance mode operating at a resolution of 4 cm⁻¹.

X-ray Diffraction (XRD)

The crystal structure of the produced FeNPs was determined and confirmed by using an X-ray diffractometer ²¹ (Model PW 1710 control unit Philips Anode material Cu, 40 KV, 30 M.A, optics: Automatic divergence slit) with Cu K α radiation $\lambda=1.540\text{5}\text{ \AA}$ over a wide range of Bragg angles ($30^\circ \leq 2\theta \leq 80^\circ$). Elemental analysis of the sample was examined by energy dispersive analyses of X-rays with the JED-2300 instrument. The crystallite domain size was calculated from the width of the XRD peaks, assuring that they are free from non-uniform strains. The particle size of the prepared sample was determined by using Scherrer's equation as follows $D \approx 0.94\lambda/\beta\cos\Theta$, where D is the average crystallite domain size perpendicular to the reflecting planes, λ is the X-ray wavelength, β is the full width at half maximum (FWHM) and Θ is the diffraction angle.

Scanning Electron Microscopy – Energy Dispersive X-ray Spectrometry (SEM-EDX) Analysis

The microstructure and composite homogeneity of the obtained samples were investigated using an SEM/EDX scanning microscope JEOL-JSM 64000 LV. Energy-dispersive X-ray analysis measurements were performed under standard conditions. The Iron nanoparticles were centrifuged at 10,000 rpm for 30 min and the pellet was redispersed in 10 mL ethanol and washed 3 times with sterile distilled water to obtain the pellet. The pellet was dried in an oven and thin films of dried samples (10 mg/mL) were used for compositional analysis.

RESULTS AND DISCUSSION

Synthesis of Iron nanoparticles

The fresh leaves of *Psidiumguajava* broth solution were prepared by taking 100g of thoroughly washed and finely cut plants in a 500ml Erlenmeyer flask along with 200ml of sterilized double distilled water and then boiling the mixture for 15min before finally decanting it. The extract was filtered through Whatman filter paper no 1 and stored at -4°C. The filtrate was treated with an aqueous 1mM FeCl_3 solution in an Erlenmeyer flask and the mixture was heated at 60°-70°C for 10-15 minutes. As a result, a black-colored solution was formed; indicating the formation of iron nanoparticles. The Iron nanoparticle solution thus obtained was purified by repeated centrifugation at 10,000 rpm for 10 min. As a black color solution was further confirmed by UV-Visible spectrum analysis. It showed that aqueous Iron ions could be reduced by aqueous extract of plant parts to generate extremely stable Iron nanoparticles in water(**Figure 2**).



Figure 2 Formation of Iron nanoparticles and it is identified by the color change. (A) FeCl_3 solution, (B) plant extract (C) plant extract with FeCl_3 solution.

UV – Visible spectral analysis

Synthesized FeNPs using UV-visible spectroscopy were studied and the recorded spectra are shown in **Figure 3**. The absorption behavior shown in Figure 3 arises due to surface Plasmon resonance (SPR)¹⁸. As the Psidiumguajava leaf extract was added to the aqueous FeCl_3 solution, the color of the solution changed from yellow to a black color indicating FeNPs formation. Figure 3 shows the UV-Vis spectra of the synthesized FeNPs which gives a broad absorption band at around 254.12nm. Such observation is characteristic of transition metal elements where the observed broad peaks are due to transitions within the filled and unfilled d-orbital compounded by influence from other external factors¹⁹. This peak at 254.12 nm due to the presence of the Iron nanoparticles in the Fe^0 state. Synthesized FeNPs using UV-visible spectroscopy were studied and the recorded spectra are shown in **Figure 3**.

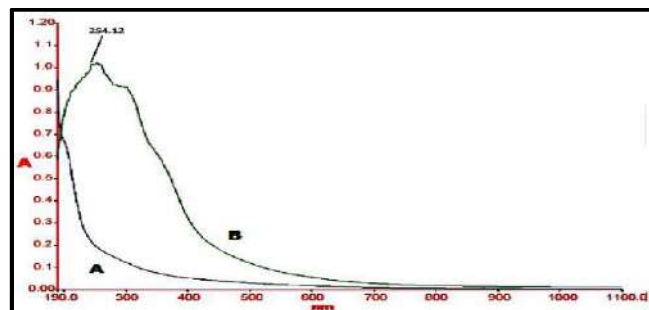


Figure 3 (A) UV-Visible absorption spectra of Psidiumguajava leave extract. (B) UV-visible absorption spectra of synthesized Iron nanoparticles, showing the surfaceplasmon resonance peak at 254.12 nm

FTIR analysis

FTIR analysis was carried out to identify the possible interaction between the biomolecules and Fe^{3+} during the biogeneric reduction reactions. The FTIR data for FeNPs containing Psidiumguajava leaf extract is shown in **Figure 4**. The band at 3466 cm^{-1} is assigned for O-H stretching vibration of alcohol and phenol compounds and bands observed at 2075 cm^{-1} , 1637 cm^{-1} , 670 cm^{-1} are due to the C-O stretching, C=O stretching mode of the carbonyl functional groups in alcohol, ethers, acids, and esters. The carbonyl band at 1637 cm^{-1} was shifted to 1690 cm^{-1} during the formation of FeNPs. The shift in bands at 1690 cm^{-1} was indicating the coordination of carboxylic acid with FeNPs and 688 cm^{-1} is attributed to zero-valent iron, Fe^0 as reported in the literature.

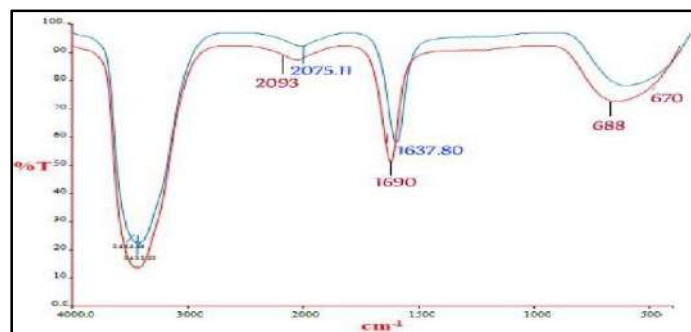


Figure 4 FTIR spectra of a) Psidiumguajavaleaf extract and b) Iron nanoparticles synthesized using the leaf extract of Psidiumguajava

From the analysis of the FTIR study, we revealed that the carbonyl group from the amino acid residue, carbohydrates, and phytochemical constituents has the stronger ability to bind metal NPs(capping of FeNPs) to prevent the agglomeration and thereby stabilize the medium. This suggests that biological molecules could perform the dual function of formation and stabilization of FeNPs in the aqueous medium. Water soluble heterocyclic compounds such as flavonoids, alkaloids were mainly

responsible for the reduction and stabilization of NPs. These results implied that tannins, Spain, flavonoids, steroids, carbohydrates, polyphenol, glycosides present in *Psidiumguajava* leaf extract play a major role in the reduction of Fe^{3+} ²⁰.

X-ray Diffraction (XRD)

The sample of FeNPs could be also characterized by X-ray diffraction analysis of dry powders. The diffraction intensities were recorded from 10° to 80° at 2 theta angles (**Figure 5**). The results for FeNPs revealed four diffraction peaks²¹ [42(100), 44(002), 48(101), 77(110)] are indexed as cubic (JCPDS file no-655099). The mean size of nanoparticles is calculated using Debye Scherrer's equation by determining the width of the (101) peak²².

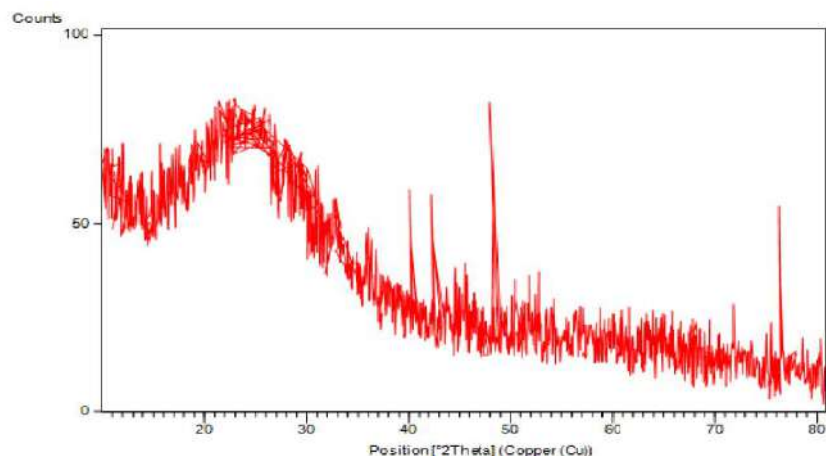


Figure 5 X-ray diffractograms of Iron nanoparticles

All the peaks in the XRD pattern can be readily indexed to a hexagonal structure of Iron as per available literature. The size of the sample was calculated from Scherrer's formula

The size of Iron nanoparticles synthesized by green synthesis was estimated to be 27×10^{-9} nm

Scanning Electron Microscopy- Energy Dispersive X-ray Spectrometry (SEM-EDX) Analysis

The presence of elemental Iron can be seen in the graph presented by EDX, Which indicates the reduction of Iron ions to elemental Iron. The result of EDAX gives a clear idea about the elements present in the biosynthesized nanoparticles. The EDAX profile of Phyto-capped FeNPs shows the strong signal of the Fe atom indicates the crystalline property as shown in **Figure 6** the vertical axis displays the number of X-ray counts whilst the horizontal axis displays energy in Kev. The optical absorption peak is at 7Kev which is typical for the absorption of metallic Iron nanocrystallites. Other than these signals for C, O is observed which may originate from the biomolecules capped to the surface of the FeNPs, Mn, and Cl due to plant constituents.

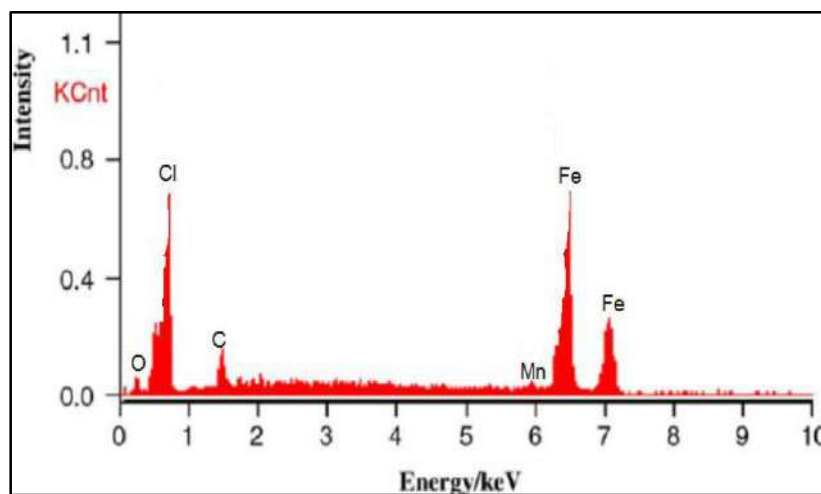


Figure 6 SEM-EDX profile of the synthesized iron nanoparticles

To determine the morphology of the synthesized FeNPs the sample was analyzed with a Scanning electron microscope (SEM). FeNPs synthesized using the extract of leaves of *Psidiumguajava* are studied under SEM and shown in **Figure 7**. It indicates that FeNPs formed are agglomerated because of the adhesive nature having the morphology of irregular appearance.

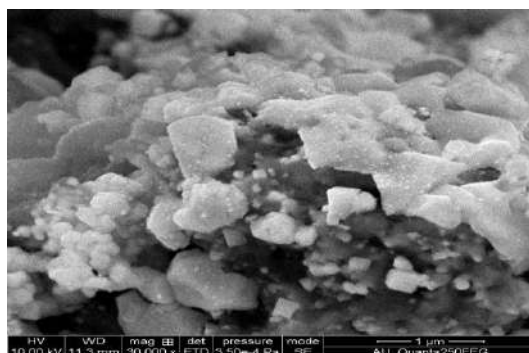


Figure 7 SEM image of the synthesized iron nanoparticles

CONCLUSION

The extract of the Psidiumguajava plant may be capable of producing Iron nanoparticles. Under the UV-Visible wavelength, nanoparticles showed a surface Plasmon resonance behavior. The color change was also remarkable when Ferric Chloride was mixed with the reducing agent of plant extract. The biosynthesized FeNPs were characterized by UV-Vis spectroscopy, FTIR spectroscopy, XRD, SEM-EDAX. From the XRD analysis, the average crystal of Iron nanoparticles was found to be 27nm. Overall, this approach is highly promising for the green-sustainable production of FeNPs.

References

1. Pattanayak, Monalisa, P. L. Nayak, International Journal of Plant, Animal and Environmental Sciences, 2013, 3(1), 68-78.
2. M. Herlekar, S. Barve, R. Kumar, Journal of Nanoparticles, 2014, 2014, 1-9.
3. T. Shahwana, S. Abu Sirriaha, M. Nairat, E. Boyaci, A.E. Eroglu, T.B. Scott, K.R Hallam, Chemical Engineering Journal, 2011, 172, 258–266.
4. S. Machado, S.L. Pinto, J. P. Grosso, H. P. A. Nouws, J. T. Albergaria, C. Delerue-Matos, Science of the total environment, 2013, 445 - 446, 1-8.
5. MonalisaPattanayak, P. L. Nayak, World Journal of Nano Science & Technology, 2013, 2(1), 06-09.
6. T. Wang, J. Lin, Z. Chen, M. Megharaj, R. Naidu, Journal of Cleaner Production. 2014, 83, 413-419.
7. Y. Liu, S.A. Majetich, R. D. Tilton, D. S. Sholl, G. V. Lowry, Environmental Science & Technology. 2005, 39 (5), 1338–1345.
8. Gabor Kozma, Andrea Ronavari, Zoltan Konya, AkosKukovecz, ACS Sustainable Chemistry & Engineering. 2016, 4 (1), 291–297.
9. S. Machado, JG. Pacheco, HP. Nouws, JT. Albergaria, C. Delerue-Matos, Science of the total environment. 2015, 15(533), 76-81.
10. W. C. W .Chan, D. J. Maxwell, X. Gao, R. E. Bailey, M. Han, S. Nie, Current Opinion in Biotechnology, 2002, 13(1), 40-46.
11. A. Thess, R. Lee, P. Nikolaev, H. Dai, P. Petit, J. Robert, C. Xu, Y. H. Lee, S. G. Kim, A. G. Rinzler, Science, 1996, 273(5274), 483-487.
12. B. Z. Zhan, M. A. White, T. K. Sham, J. A. Pincock, R. J. Doucet, K. V. R. Rao, K. N. Robertson, T.S. Cameron, Journal of the American Chemical Society, 2003, 125(8), 2195-2199.
13. A. L. Linsebigler, G. Lu, J. T. Yates, Chemical reviews. 1995, 95 (3), 735–758.
14. H. Zhang, R. L. Penn, R. J. Hamers, J. F. Banfield, J. Phys. Chem., B., 1999, 103 (22), 4656–4662.
15. R. F. Service, Science, 1998, 281(5379), 940-942.
16. N. L. Rosi, D. A. Giljohann, C.S. Thaxton, A. K. R. Lytton-Jean, M. S. Han, C.A. Mirkin, Science, 2006, 312(5776), 1027-1030.
17. D. G. Shchukin, J. H. Schattka, M. Antonietti, R. A. Caruso, J. Phys. Chem. B., 2003, 107(4), 952-957.
18. R. Veerasamy, TZ. Xin, S. Gunasagaran, TFW. Xiang, EFC. Yang, N. Jeyakumar, Journal of Saudi Chemical Society, 2011, 15(2), 113-120.
19. I. N. Michiraa, D.N. Katithib, P. Gutoc, G. N. Kamaud, P. Bakere, E. Iwuohaf, International Journal of Sciences: Basic and Applied Research, 2014, 13(2), 63-76.
20. R. Kiruba, G. Alagumuthu, International journal of Pharmacy, 2014, 4(4), 195-200.
21. E. Laviron, Journal of Electroanalytical Chemistry and Interfacial Electrochemistry 1979, 101(1), 19-28.
22. K. Shamel, MB. Ahmad, M. Zargar, WM. Yunus, A. Rustaiyan, NA. Ibrahim, International Journal of Nanomedicine, 2011, 2011(6), 581-590.

Extraction Of Bioactive Compounds From Actinomycetes Associated With Lichen

V.S.Sangeetha^{1*} ,M.Durga² V.Vanitha¹ ,R.Elayaperumal¹

¹Dhanalakshmi Srinivasan college of arts and science for women Autonomous Perambalur Tamilnadu-621212

¹*Corresponding Author
Mail id :sangeethavasanth23@gmail.com

Abstract: In the present scenario, entire globe urgently require two important reforms, one with economic reform and another one with antibiotic reform. Among them antibiotic reform is urgently needed one to control the emergence of new pathogenic forms and blooming of multiple antibiotic resistant human pathogens leading to limited or no treatment options. In order to treat such infection and avoid an epidemic to occur new treatment method must be made available by discovery of new structural chemotypes that can inhibit the growth of pathogenic organisms by new modes of actions. The screening and characterization of promising strains of actinomycetes producing potential antibiotics and other therapeutics are focusing on the response of antioxidant systems of bacterium which is important in various oxidative stress conditions. Actinomycetes are gram positive bacterium of the order actinomycetes they are characterized by filamentous morphology DNA with a high in G+C content presence of LL diaminopimelic acid (LL-DAP) and the presence or absence of characteristic sugars in the cell wall. Actinomycetes taxa from diverse habitat with unique metabolic activity often led to the of novel antimicrobial agent various antimicrobial agent .In Present study bioactive compound are extracted from actinomycetes and characterised.

Key words:Actinomycetes, Lichens, screening, antibiotics

INTRODUCTION

Lichens are complex symbiotic associations between a fungus (mycobiont) and an alga (photobiont) with unique characteristics in plant kingdom. Many species extremely slow-growing rates ranging from ≤ 0.9 mm/year ¹⁻³. In general, crustose lichens have substantially lower growth rates as compared to foliose lichens ⁴⁻⁶. Water is absorbed when the lichen's water potential is below the atmospheric water potential, which generally happens at relatively low temperatures ($<20^{\circ}\text{C}$) and high relative humidity ($>75\text{-}95\%$) (Palmqvist et al., 2008). About 40-50% of lichen's dry mass is composed of carbon, which they mainly gain from the photobiont's photosynthesis ⁷⁻⁹.

MATERIAL AND METHODS

Sample collection

Lichen samples were collected from Karaikal region of northern coastal region located in Tamil Nadu. Intact well dried lichen samples were chosen and segregated based on the thallus morphology and general ¹⁰⁻¹¹. The morphological features of thallus and fruiting bodies were observed under Stereozoom microscopes. Spot test was carried out by 10% aqueous solution of potassium hydroxide (K), Steiner's stable Para-Phenylenediamine solution (PD) and calcium hypochlorite solution. Anatomical investigation of fruiting bodies was observed under light microscope and compound microscope. Identified specimens were reconfirmed at National Botanical Research Institute (NBRI)-Lucknow ¹²⁻¹⁴.

Sample pretreatment and selective isolation of Actinomycetes

The lichen samples were washed with sterile water for a few minutes. Followed by washing in 3.15% calcium hypochlorite solution for 10 min. Consecutively, washed with 10% sodium hydrogen carbonate solution for 15 min and 1% sodium azide for 2 min. Lichen samples were rinsed with sterile distilled water followed by washed with disinfectant and homogenized finally with sterile water. Approximately 2 mg of lichen thallus was randomly picked and homogenized. 1mL of homogenate was serially diluted, plated on starch casein agar amended with Cycloheximide (50 mg/L) and Nalidixic acid (20 mg/L) and incubated the samples at 30°C for 7-15 days.

Morphological characterization – Coverslip Method

The Actinomycetes colonies were streaked the plate containing starch casein agar and the sterile cover slip was taken and the coverslip are inserted into the medium at 40° angle without disturb the agar surface of the medium, then the plate are incubated at 37°C for 4 to 7 days after incubation the cover slip are taken and placed the microscopic slide and observed under the microscope in different objective. ¹⁵⁻¹⁷

Biochemical Characterization

Actinomycetes is different method identified the physiological characteristics such as urease test, catalase test, cellulose test and nitrate reduction test urease Urease amidohydrolase) was discovered around 150 years ago. The first ureolytic microorganism, *Micrococcus ureae*, was isolated from urine in 1864 by van Tieghem. However, Musculus obtained the first ureolytic enzyme in 1874 from putrid urine, and as proposed by Miquel in 1890, it was named urease.

Christensen's Urea agar

The urease medium was prepared in 1000ml and the medium was sterilized in 1210c. This medium was poured into the petri plate, in each plate 20 ml is transferred. After solidification the medium to be streaked on the isolated colony and then incubated at 30°C for 48 hrs. Change in colour of the medium from orange to deep pink indicated the production of urease.

RESULT AND DISCUSSION

Collected lichen sample was washed in tap water for 2 min. 70% ethanol and 3% sodium hypochlorite is used for surface sterilization. Finally, sterile water was added and homogenized. 1 mL of Extract was serially diluted, plated in starch casein agar (SCA) and incubated at 37°C ¹⁸. Eight different isolated colonies have been found on SCA agar plate with varied colony shape and color. The isolated colonies are further streaked using quadra streak technique in order to obtain a pure strain of Actinomycetes .

Strain no	Strain name	Colony morphology
1	7	Powdery colony
2	RRI	Light white colony
3	2(1)	Dirty white powdery colony
4	1(2)	White powdery with dirty white layer
5	L2MD8 1	Creamy white colony
6	2(2)	Powdery creamy colony
7	6(3)	Light white colony

Fresh SCA medium was prepared, autoclaved at 121°C for 15 mins and poured in a plate under laminar air flow chamber for maintaining a sterile environment to avoid other contaminations from the surrounding. After streaking the strain in sterile SCA medium, sterilized coverslip are placed at an angle of 40°C in a slanting position. *Actinomycetes* is thread-like filaments in morphology which tends to grow above the surface of the coverslip. This coverslip technique is to determine the morphological of the *Actinomycetes*

Microscopic characterization

Certain biochemical characterization has been performed that helps in ease identification of *Actinomycetes*. All the eight strains of *Actinomycetes* isolated from the Lichen sample showed no colour change from orange to pink that indicates the presence of urease. Similarly, all the seven strains of *Actinomycetes* are negative in Oxidase test showing no formation of effervescence when treated with 2% H2O2. DNA isolation is performed to all the isolated *Actinomycetes* such that to determine the Genus and Species name of them using Molecular techniques. Before DNA isolation, all the strains were inoculated into a sterile SCA broth medium and allowed to grow for about 7 to 8 days for their growth of cells. After incubation at room temperature 1.5ml sample was taken and centrifuged in which supernatant consists of medium is removed from the pellet and steps regarding DNA extraction are started. The cells were preliminarily broken, made all the internal cell materials to come out and remove or separate all the cell materials from our main product DNA and purified ²⁰. They are performed using certain chemicals that play a role in breaking, bringing out, separating and purifying our target template DNA. ²¹

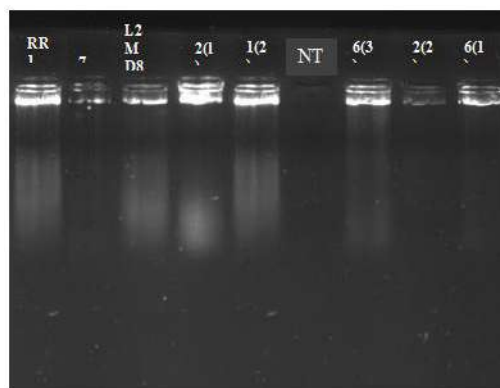


Figure :I DNA isolation

Antimicrobial activity

Extraction of secondary product from Actinomycetes is performed. Culture are centrifuged at 10,000rpm for about 10 mins to separate the supernatant and pellet and transferred into a fresh tube. The cell pellet are washed with distilled water completely to avoid any cellular contaminants. With the help of separating funnel, methanol is added to the supernatant to extract the compounds from them ²³⁻²⁵. Under sterile condition, using mortar and pestle, the pellet was completely grinded with methanol and the extract were transferred to a fresh tube. Both the supernatant and pellet extract are stored in fridge. To the extracts, Antimicrobial activity is determined by inoculating a known volume of extract onto four different pathogens plated in bacterial medium ²⁶. LB medium is prepared, sterilized in autoclave at 121°C for 15mins. They were poured into sterilized plates under the laminar air flow chamber to maintain the aseptic condition. Four different pathogens like *Staphylococcus*, *E.coli*, *Pseudomonas*, and *Enterococci* were taken and sub- cultured. The sub cultured pathogens were incubated at 37°C for 24 hours. After incubation the pathogens were swabbed by using the sterile cotton bud on the solidified Luria Britani plates. Wells were created on the pathogenic plates and 30µl of the methanol extracts were injected into the well with the help of micropipette

Strain	E.coli	Pseudomo nasaerugin osa	Staphylo coccus	Bacillus subtilis	Enterobac ter	Salmonel la	Aeromon as	Klebs iella
RRI	19mm±1	-	-	9mm±1	-	-	-	-
7	6mm±1	-	-	-	-	-	-	-
L2MD 8	-	13 mm±1	-	-	-	-	-	-
6(3)	-	-	-	-	-	-	-	-
1(2)	-	-	-	-	2 mm±1	-	-	-
2(2)	-	-	-	2mm±1	-	-	-	-
6(1)	-	-	-	-	-	-	-	-
2(1)	-	3 mm±1	-	-	-	-	-	-

Thus from the antibacterial activity test, it has been found that strain RRI has activity towards *E.coli* and *Bacillus subtilis* with 19mm. Strain 7 shows activity towards *E.coli* with 6mm. Maximum zone of inhibition was found in RRI with 19mm in *E.coli* and 13mm in *P.aeruginosa* by L2MD8

CONCLUSION

Actinomycetes associated with lichens from Ramanathapuram are collected and isolated using streak method. 7 strains of actinomycetes were found and were purified using a spread plate technique to get a pure colony. Their morphological and biochemical characters were studied along with molecular characterization. From the broth strain, bioactive compounds were extracted using ethylacetate and water extract separately. To both the extracts antibacterial activity was studied in which solvent extract show no zone of inhibition whereas water extract of 2 strains showed maximum inhibiting activity on *E.coli* and *Pseudomonas aeruginosa*. In future, the Extracted DNA has to be sent for sequencing to identify the culture which shows activity. The water extract which shows activity should be sent out for GC-MS, HPLC And NMR for purification and identification of compound and its structure that shows activity towards pathogens.

REFERENCES

1. Mandrioli, P., Caneva, G. & Sabbioni, C. Cultural Heritage and Aerobiology: Methods and Measurement Techniques for Biodeterioration Monitoring (Springer, Verlag Berlin Heidelberg, 2003).
2. Berdy J (2012) Thoughts and facts about antibiotics: where we are now and where we are heading. *J Antibiot* 65:385–395
3. Davies J, Wang H, Taylor T, Warabi K, Huang XH, Andersen RJ (2005) Uncalamycin, a new enediyne antibiotic. *Org Lett* 7:5233– 5236
4. Motohashi K, Takagi M, Yamamura H, Hayakawa M, Shin-ya K (2010) A new angucycline and a new butenolide isolated from lichen-derived *Streptomyces* spp. *J Antibiot* 63:545–548
5. Dülger, B., Güçin, F., Aslan, A., 1998. Cetrariaislandica (L.) Ach. Likenin AntimikrobiyalAktivitesi. *Tr. J. Biol.* 22, 111-118.13
6. Aslan, A., Güllüce, M., Atalan, E., 2001. A Study of Antimicrobial Activity of Some Lichens. *Bull. Pure Appl. Sci.* 20, 23-26.
7. Williams, S.T., Lanning, S. And Wellington, E.M.H. (1983) Ecology of actinomycetes In: The Biology of Actinomycetes (Goodfellow, M., Mordarski, M. And Williams, S.T., Eds.), pp. 481–528. Academic Press, London, UK.
8. Jensen, P.R., Dwight, R. And Fenical, W. (1991) Distribution of actinomycetes in nearshore tropical marine sediments. *Appl. Environ. Microbiol.* 57, 1102–1108.
9. Arifuzzaman.M, Khatun.M.R and Rahman.H,(2010), Isolation and screening of actinomycetes from Sundarbans soil for antibacterial activity , African Journal of Biotechnology Vol. 9(29), pp. 46154619.

10. Arunachalam.R, Wesely.E.G, George.J and Annadurai, (2010). Novel Approaches for Identification of *Streptomyces noboritoensis* TBG-V20 with Cellulase Production, Current Research in Bacteriology 3 (1): 15-26.
11. Baskaran, R, Vijayakumar, R and Mohan, P. M,(2011) Enrichment method for the isolation of bioactive actinomycetes from mangrove sediments of Andaman Islands, India Malaysian Journal of Microbiology, Vol 7(1), 1-7.
12. Dhanasekaran, D, Selvamani,S , Panneerselvam.A and Thajuddin.N, (2009), Isolation and characterization of actinomycetes in Vellar Estuary, Annagkoil, Tamil Nadu African Journal of Biotechnology Vol. 8 (17), 4159-4162.
13. Goodfellow, M and Haynes, (1984), Actinomycetes in marine sediments in Biological, biochemical and biomedical aspects of actinomycetes (eds.) Ortiz-ortiz, I.,L.F. Bjalil and V.Yakoleff, Academic Press, London.453-472
14. Don L. Crawford,t,James M. Lynch, John,M. Whippes, And Margaret, A. OUSLEY(1993), Isolation and Characterization of Actinomycete Antagonists of a Fungal Root Pathogen Applied and environmental Microbiology, 3899-3905.
15. Hong.K, Gao.A.H, Xie.Q,Y, Gao.H, Zhuang.L, Lin.H.P, Yu.H.P, Li.J, Yao.X.S, (2009), Actinomycetes for Marine Drug Discovery Isolated from Mangrove Soils and Plants in China, licensee Molecular Diversity Preservation International, Basel, Switzerland, 7(1): 24-44
16. Jeffrey, L. S. H,(2008), Isolation, characterization and identification of actinomycetes from agriculture soils at Semongok, Sarawak African Journal of Biotechnology Vol. 7 (20), pp. 3697-3702.
17. Kumar,S.V, Sahu, M.K and Kathiresan .K (2005), Isolation and characterization of streptomycetes producing antibiotics from a mangrove environment, Asian Jr. Of Microbial.Biotech Env.Sc.Vol. 7 No. (3); 457-464.
18. Lechevalier. M.P., Prauser.H, Labeda.D.P, Ruan.J.S and Lechevalier.H.A. (1986). Two new genera of nocardioformactinomycetes: Amyco/ata gen. Nov. And Amyco/atopsis gen. Nov. Int. J. Syst. Bacteriol. 36:29-37.
19. Mincer TJ, Jensen PR, Kauffman CA, Fenical W, (2002), Widespread and persistent populations of a major new marine actinomycete taxon in ocean sediments. Appl Environ Microbiol , 68: 50055011.
20. Oskay M, same A, Azeri C (2004). Antibacterial activity of some actinomycetes isolated from farming soils of Turkey. Afr. J. Biotechol 3: 441-6.
- 21.. SatheejaSanthi.S, Jose.A, and Solomon.J, R.D (2010), Isolation and Characterization of antagonistic actinomycetes from Mangrove sediments, International Journal of Current Research , 3: 020-023.
22. Thenmozhi.M, and Kannabiran.K,(2010), Studies on Isolation, Classification and Phylogenetic Characterization of Novel Antifungal *Streptomyces* sp. VITSTK7 in India Current Research Journal of Biological Sciences 2(5): 306-312.
23. Waksman SA. (1961). Theactinomycetes Classification identification and description of genera and species, 2. Baltimore, USA:Williams and Wilkins Company 327.
24. Williams, S.T and Davies. F.L., (1964), Use of Antibiotics for Selective Isolation and Enumeration of Actinomycetes in Soil J .Mierobiol., 38, 251-261.
25. Walker JD, Colwell RR,(1975), Factors affecting enumeration and isolation of actinomycetes from Chesapeake Bay and Southeastern Atlantic Ocean sediments. Mar Biol , 30: 193-201.
26. Hopwood, D.A., Buttner, M.J., Bibb, M.J., Kieser, T. And Charter, K.F. 2000. Antibiotic production by *Streptomyces*.Practical *Streptomyces* Genetics, 1: 1- 42.

Antidiabetic Activity Of *Terminalia Bellirica* On Alloxan Induced Diabetic Rats

Dr.Surya.C, Sathish.S, Dr.Sathyia.R, Nirmala Devi. P, Arulmozhi

Dhanalakshmi College of Arts and Science for Women (Autonomous), Perambalur.

Abstract: Diabetes mellitus is one of the common metabolic disorders and 10% of the population. Suffer from this disease throughout the world. Insulin and oral hypoglycemic agents are still the major players in the management of the disease but many adverse effects were, observed and they did not reduce diabetic associated complications. Currently, available treatment is far from satisfactory and is expensive. Many indigenous Indian medicinal plants are successfully used to manage diabetes. Plant drugs are frequently considered to be less toxic and free from side effects than synthetic ones. However, the search for new anti-diabetic drugs continues. Keeping this view, the present study aimed to evaluate the anti-diabetic *Terminalia bellirica*. Administration of *Terminalia belliricato* AXN rats restored the level of glucose profile. This confirms the antidiabetic activity of *Terminalia bellirica*. The potential antidiabetic activity of *Terminalia belliricais* due to the presence of phytochemical constitution present in the plant. Some of these phytochemicals such as Carbohydrates, Free amino acids, Alkaloids, Flavonoids, Tannins, Saponin, Quinones, Glycosides, Cardiac glycosides, Terpenoids, and polyphenolic compounds have possessed antidiabetic activity.

Keywords: *Terminalia bellirica*, Phytochemicals, Diabetes mellitus, Lipid profile.

INTRODUCTION

Diabetes is a metabolic disorder of carbohydrates, fat, and protein, affecting a large number of the population in the world¹. Diabetes mellitus is not a single disorder but is a group of metabolic disorders characterized by chronic hyperglycemia, resulting from defects in insulin secretion, insulin action, or both². Increased thirst, increased urinary output, ketonemia, and ketonuria are the common symptoms³. Diabetes mellitus has caused significant morbidity and mortality due to microvascular (retinopathy, neuropathy, and nephropathy) and macrovascular (heart attack, stroke, and peripheral vascular disease) complications reductase as a key enzyme, catalyze the reduction of glucose to sorbitol and is associated in the chronic complications of diabetes such as peripheral neuropathy and retinopathy⁴. The use of aldose reductase inhibitors and -glucosidase inhibitors has been reported for the treatment of diabetic complications . Based upon the etiology, diabetes mellitus can be divided into two main types, Type 1, "Juvenile Diabetes Mellitus" (Insulin Dependent Diabetes Mellitus), and Type 2, "Adult type" (Non-Insulin Dependent Diabetes Mellitus)⁵. Type 1 occurs in childhood, mainly due to the destruction of pancreatic -cell islets through autoimmune-mediated, resulting in absolute insulin deficiency⁶. Type 2 is more associated with adult hood and elderly people, which are mainly due to insulin resistance or abnormal insulin secretion . Herbal medications have been used for the treatment of a variety of ailments, a huge number of the population in the world is entirely dependent on traditional medicines. From the ethnobotanical information, about 800 plants which may possess anti-diabetic potential have been found⁷⁻⁸ .In folk / tribal medical practice, many plants are used to treat diabetes mellitus in south.¹⁰⁻¹¹

Terminalia bellirica.

Kingdom: Plantae
(unranked) : Eudicots
Order: Myrales
Genus: Terminal
Kingdom: Plantae
(unranked) : Eudicots
Order: Myrales
Species; belliricia

MATERIALS AND METHODS

Collection of Plant materials:

The fully mature *Terminalia bellirica* leaves were collected from Tamil University in January 2015 at Thanjavur, Tamil Nadu, and South India.

Preparation of ethanolic leaf extract

The collected *Terminalia bellirica* leaves were cut into small pieces and shade dried at room temperature. The *Terminalia bellirica* leaves were soaked with methanol (50%) for 48 hours. A semi-solid extract was obtained after the complete elimination of alcohol under reduced pressure.

Preliminary phytochemical tests

The phytochemical test was carried out in the leaf extract of *Terminalia bellirica* using standard procedures to identify phytochemical constituents

Antidiabetic activity

Male albino rats of Wistar strain approximately weighing 180-190g were used in this study. They were healthy animals purchased from the Indian Institute of Science, Bangalore. The animals were housed in spacious polypropylene cages bedded with rice husk. The animal room was well ventilated and maintained under standard experimental conditions (Temperature $27 \pm 2^\circ\text{C}$ and 12 hours light/dark cycle) throughout the experimental period. All the animals were fed with a standard pellet diet and water was provided *ad libitum*. They were acclimatized to the environment for one week before experimental use. The experiment was carried out according to the guidelines of the Committee for Control and Supervision of Experiments on Animals (CPCSEA), New Delhi, India.

Alloxan induced, Diabetic rats

NIDDM was induced in overnight fasted adult male Wistar albino rats weighing 150–200 g by a single intraperitoneal injection of 120 mg/kg alloxan monohydrate (Loba Chemie) . This model has been used in earlier studies to induce type II diabetes in rats . Glibenclamide (2.5 mg/kg) was used as the standard drug. After 72 h of alloxan injection, stable hyperglycemia was confirmed by estimating the glucose level in the urine of rats by Benedict's qualitative test . Plant extracts at a dose of 500mg/kg were orally given once a day for 15 days after hyperglycemia was confirmed by the elevated glucose levels in urine determined at 72 h. The animals were divided into six groups of six animals each as follows. Each animal was marked for identification and regular monitoring.

Group I	-	Vehicle control were injected with buffer alone (Non-diabetic)
Group II	-	Diabetic control
Group III	-	<i>Terminalia bellirica</i> leaves extracts at a dose of 500mg/kg was orally given once a day for 20 days.
Group IV	-	Diabetic standard as 2.5mg/kg of Glibenclamide, p.o was orally given once a day for 20 days.

Collection of blood and preparation of serum sample

At the end of the experimental period, the animals were killed by cervical dislocation after overnight fasting. The blood sample was collected. The blood was allowed to clot by standing at room temperature for 30 minutes and then refrigerated for another 30 minutes. The resultant clear part was centrifuged at 3000 rpm for 10minutes and then the serum (supernatant) was isolated and stored refrigerated until required for biochemical analysis.

BIOCHEMICAL ESTIMATION

Estimation of Glucose

Glucose was estimated by GOD/POD method 0.01ml of serum was mixed with 1.0ml of buffered enzyme reagent and incubated at 37°C for 15 minutes. The absorbance of the working standard and test was measured at 505nm against blank in a spectrophotometer.Values were expressed as mg/dl serum

Estimation of hemoglobin

Haemoglobin was estimated by the Cyanmethaemoglobin method

Reagents

20 μ l of blood was added to 5ml of Drabkin's solution. Mixed well and allowed to stand for 10minutes. Read the absorbance at 540nm with Drabkin's solution as blank. Read the absorbance of the standard in the same way. Values were expressed as g/dl.

RESULTS

The present study was carried out on the plant sample revealed the presence of medicinally active constituents. The phytochemical characters of the *Terminalia bellirica* investigated a summarized in Table I. The present study was carried out to evaluate the Antidiabetic activity of *Terminalia bellirica* on alloxan-induced diabetic rats. The observations made on different groups of experimental animals were compared as follows

Table I. Phytochemical screening of *Terminalia bellirica*

TEST	RESULT
Tannin	+
Phlobatannins	+
Saponin	+
Flavonoids	+
Steroids	++
Terpenoids	+
Triterpenoids	++
Alkaloids	+
Carbohydrate	+
Amino acid	++
Anthroquinone	+
Polyphenol	++
Glycoside	++

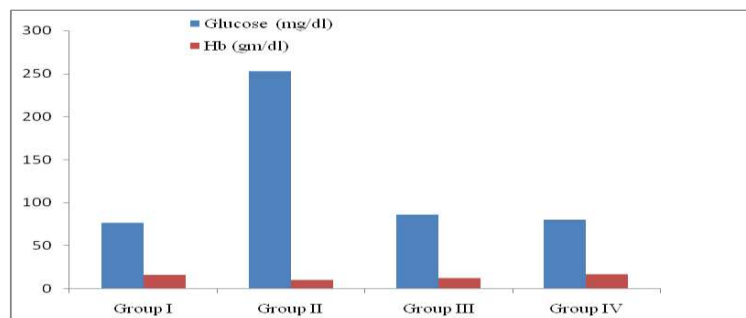


Fig. I. Effect of *Terminalia bellirica* on Glucose and Hb in normal and experimental rats.

Fig. I Represents the levels of Glucose and Hb in normal and experimental rats. Group II Diabetic rats showed a significant increase in the level of Glucose when compared to Group I rats. Group III and IV Diabetic rats treated with *Terminalia bellirica* and standard as glibenclamide significantly decreased in the level of Glucose when compared to group II. Group II Diabetic rats showed a significant decrease in the content of Hb when compared to Group I rats. Group III and IV Diabetic rats treated with *Terminalia bellirica* and standard as glibenclamide significantly increased in the level of Hb when compared to group II.

DISCUSSION

Diabetes mellitus is one of the most common chronic diseases associated with carbohydrate metabolism⁸⁻¹⁰. Alloxan (AXN) is commonly used for experimental induction of type-I diabetes mellitus, which causes selective pancreatic islet beta-cell cytotoxicity mediated through the release of nitric oxide (NO)¹². This results in a rapid reduction in pancreatic islet pyridine nucleotide concentration and subsequent beta-cell necrosis. This damages a large number of β cells, resulting in a decrease in endogenous insulin release, which paves the way for the decreased use of glucose by the tissues¹⁰. The action of AXN on mitochondria generates SOD anions, which leads to diabetic complications¹³⁻¹⁵. Based on the above perspectives, in the present study, oxidative stress has been assessed in rats made diabetic by AXN (Szkudelki 2001). Sulfonylureas such as glibenclamide are often used as a standard antidiabetic drug in AXN-induced diabetes to compare the efficacy of a variety of antihyperglycemic compounds¹⁶⁻¹⁷. The ethanolic extract of *Terminalia bellirica* (Group III) was treated on Alloxan-induced diabetic rats (Group II). The results were compared with control (Group I) and the positive control glibenclamide (Group IV) after 15 days of treatment based on biochemical parameters¹⁸. After the Alloxan induction, glucose, lipid profiles, protein, and Hb were restored to control

level with the administration of the known drug glibenclamide and plant extracts of *Terminalia bellirica*¹⁹⁻²⁰

CONFLICT OF INTEREST

Conflict of interest declared none.

REFERENCE

1. Ahmad A., Balakrishnan B.R., Akhtar R and Pimprikar R.2009. Antidiabetic activity of leaves of *Tephrosia villosa* Pers. in alloxan-induced diabetic rats. *Pharm Res* . 2: 528-531
2. Allain C.C., and Poon L.S. et al.1974. Enzymatic determination of total serum cholesterol. *Clinical Chemistry* .20: 470-5
3. Allain C.C. Poon L.S. Chan C.S.G. Richmond W and Fu P.C (1974). Enzymatic determination of total serum cholesterol. *Clinical Chemistry* 20: 470-5
4. Arjun P. Shivesh J. Sahu A.N(2009). Antidiabetic activity of aqueous extract of *Eucalyptus citriodora* Hook. in alloxan-induced diabetic rats. *Pharmacogn Mag* . 5: 51-54
5. Aderibigbe AO, Lawal BA, Oluwa gbemi JO. The antihyperglycemic effect of *Telfaria occidentalis* mice. *Afr J Med Med Sci* 1999, 28, 171-175.
6. Balaraman A.K. Singh J. Dash S and Maity T.K (2010). Antihyperglycemic and hypolipidemic effects of *Melothria maderaspatana* and *Coccinia indica* in Alloxan induced diabetes in rats. *Saudi Pharm J* .18: 173-178.
7. Beuge J.A and Aust S.D (1978). The thiobarbituric acid assay. *Methods in Enzymology* 52: pp 306-307.
8. Bihari C.G. Manaswini B. Keshari P.S. Kumar T.S(2011).phytochemical investigation & evaluation for the antidiabetic activity of leafy extracts of various *Ocimum* (Tulsi) species by alloxan-induced diabetic model. *J Pharm Res* .4: 28-
9. Biradar S.M. Rangani A.T. Kulkarni V.H. Joshi H. Habbu P.V and Smita D.M (2010). Prevention of onset of hyperglycemia by extracts of *Argyrea cuneata* on alloxan-induced diabetic rats. *J Pharm Res* . 3: 2186-2187.
10. Bnouham M. Ziyyat A. Mekhfi H. Tahri A and Legssyer A (2006). Medicinal plants with potential antidiabetic activity -A review of ten years of herbal medicine research (1990-2000). *Int J Diabetes Metab* .14: 1-25.
11. Chaturvedi N. Sharma S (2010). Antidiabetic and antihyperlipidemic activity of water-soluble solid extract of *Ficus bengalensis* Linn. bark in rats. *Biochem Cell Arch* .10: 65-69.
12. Craig M.E. Hattersley A. Donaghue K.C (2009). Definition, epidemiology, and classification of diabetes in children and adolescents. *Pediatr Diabetes*.10: 3-.
13. Dacie J.V and Lewis S.M (1968). *Practical Hematology*, 4th edition J and A, Churchill, UK. p37.
14. Dewanjee S. Das A.K. Sahu R. Gangopadhyay M (2009). Antidiabetic activity of *Diospyros peregrina* fruit: effect on hyperglycemia,hyperlipidemia and augmented oxidative stress in experimental type 2 diabetes. *Food Chem Toxicol*. 47: 2679-2685.
15. Dheer R. Bhatnagar P(2010). A study of the antidiabetic activity of *Barleria prionitis* Linn. *Indian J Pharmacol*.42: 70-73
16. Wani V.K. Dubey R.D. Verma S. Sengottuvelu S and Sivakumar T (2011). Antidiabetic activity of methanolic root extract of *Mukia maderaspatana* in Alloxan induced diabetic rats. *Int J Pharm Technol Res* . 3: 214-220.
17. Warjeet Singh L (2011). Traditional medicinal plants of Manipur as anti-diabetics. *J Med Plants Res* . 677-687.
18. Warjeet Singh L(2011). Traditional medicinal plants of Manipur as anti-diabetics. *J Med Plants Res* . 5: 677-687.
19. Werner M. Gabrielson D.G and Eastman G (1981). Ultramicro determination of serum triglycerides by bioluminescent assay. *Clinical Chemistry*. 27: pp268-271.
20. Yoshino K, Miyauchi Y, Kanetaka T, Takagi Y, Koga K. Antidiabetic activity of a leaf extract prepared from *Salacia reticulata* in mice, *BiosciBiotechnol Biochem* 2009, 73, 1096-1104

Brasicaceae-Derived Anticancer Agents: Towards A Colon Cancer

Shalin S, Dr. K.Sowmiya, Dr. C. Surya, NithaV.Ravi

DhanalakshmiSrinivasan College of Arts and Science For Women (Autonomous), Perambalur.

Abstract: Brassica Oleracea Var. Italica is typically known as broccoli. Is an edible green plant in the cabbage circle of relatives. Broccoli has an anti-cancer pastime. Broccoli additionally consists of a compound glucoraphanin which may be processed into an anti-most cancers compound sulphoraphane. This sulphoraphane is mentioned to have anti-cancer activity. Several experimental studies also verify the preventive impact of sulphoraphane in the chemically induced lung, breast, renal, prostate, and colon cancers. Broccoli is an underutilized food in India. Moreovebroccoli can be applied for its anti-most cancers ability for preventing most cancers. The primary intention of this take a look is to save you and treat colon cancer with the aid of the use of broccoli.

Keyword: Brassica Oleracea, Anti cancer Activity, Colon Cancer, Bioactive phytochemical

INTRODUCTION

Cancer is one of the causes of mortality globally. In 2008, 8 million deaths were recorded due to malignant diseases, and miles are estimated to attain 11 million by using 2030. Various factors contributed to the prevalence of cancer. This disorder takes place all around the world it incidence, mortality, and survival quotes vary drastically among one of a kind elements of the arena, which will be because of factors like population structure lifestyle, genetic element, and surroundings¹. Even as a few lifestyle factors, along with cigarette smoking, are properly stated as affecting most cancers, the position of food plan is less well known. But, food plans may be connected to as many as 70% - eighty% of cases of colorectal most cancer² Ordinary intake of culmination and veggies appreciably contributes to reducing the chance of developing belly, colorectal, rectal, and breast most cancers. Europe-extensive research by way of the ECU prospective investigation into cancer and vitamins (EPIC) has proven that eating a very big amount of vegetables and fruits four hundred-800g every day, can lessen the threat of growing cancer of the mouth, throat, larynx, and esophagus by using to a 3rd, and stomach and lung cancer- by a quarter³ (global most cancers Fund/American institute for most cancers studies 2018) A take look confirmed that a plant-based eating regimen resulted in a forty six% reduced chance of colon cancer and seventy three% decreased danger of rectal most cancers (wang p et al ., 2015) Broccoli is the maximum prized member of the Cruciferous⁴(Brassicaceae) circle of relatives that consists of several veggies. It's miles widely cultivated inside the Mediterranean regions, Asia and North America, mainly in California. Nutrient and fitness advantages of broccoli include diabetes, obesity, gastrointestinal disturbances and is considered to be an anti-inflammatory and anti-cancer agent⁵Several research has said the chemopreventive and anti-most cancers houses of dietary retailers. It has been found that vegetable consumption is associated with a decreased hazard of growing most cancers. In theBrassicaceae own family, such as broccoli and cauliflower, as these greens are a source of glucosinolates ⁷.Broccoli incorporates a big quantity of glucosinolates. The chemopreventive houses of sulforaphane towards cancer through both blockading and suppressing

Clinical category of Brassica oleracea var. Italica

State	: Plantae
Department	: Flowering plant Dicotyledons
Order	: Capparales Family: Brassicaceae
Genus	: Brassica L
Species	: Brassica oleracea

Bioactive phytochemicals

The useful consequences are commonly attributed to bioactive phytochemicals gift that includes hydroxycinnamic acids, flavonoids (e.G., quercetin, kaempferol, myricetin), carotenoids (lutein), and glucosinolates (e.G., glucoraphanin) ⁸⁻¹⁰The biologically energetic sorts of the glucosinolates are isothiocyanates which might be generated utilizing the motion of the enzyme myrosinase that is launched whilst the plant tissue is chopped or chewedFitness selling phytonutrients in cruciferous greens had been gaining interest for their powerful results in fighting cancer. Sulforaphane turns on gene expression, supporting clear carcinogenic from the body extra quick¹¹. It triggers the liver to produce a detoxification enzyme called phase II enzyme, which assists neutralize cancer-inflicting substances.

Sulforaphane

Sulforaphane (SFN) is an isothiocyanate this is found in cruciferous vegetables, with excessive attention in broccoli. The effects of the maximum recent studies suggest that multi-targeted sulforaphane moves may additionally make contributions to the prevention and treatment of cancer. Protective houses of sulforaphane had been determined in each degree of carcinogenesis

Nutrients present in broccoli

Broccoli is scientifically known as BRASSICA OLERACEA VAR.ITALICA a cruciferous inexperienced vegetable is one promising underexploited plant. It is a supply of precious vitamins diet A, C, and riboflavin¹²⁻¹⁴. It's also excellent in iron and calcium and is nonfattening meals and possesses various medicinal houses . Broccoli includes multiple nutrients with anti-most cancers houses along with di indolmethene and selenium broccoli is a modulator of the immune reaction machine with anti-viral, anti-bacterial, and anti-cancer activity cardio protective, anti-obesity, anti-diabetic, anti-inflammatory, and immune modulatory sports. Broccoli additionally contains a compound "glucoraphanin", which may be processed into an anti-most cancers compoundsulphoraphane¹⁵⁻¹⁶. Broccoli has fiber (2.60%) and carbohydrates (6.Sixty-four%). It is a rich supply of minerals together with potassium, phosphorus, and sodium. Moreover, broccoli gives folic acid (US branch of Agriculture 2008)¹⁷. Broccoli has gained interest because of the struggles on patenting genotypes with high concentrations of glucosinolates displaying nice effects in cancer remedies

Advantages of broccoli

plant life had been the number one source of drugs for early drug discovery. In developing international locations, because of economic factors, almost eighty% of the population nonetheless relies upon plant extracts as a supply of medication. Due to the increasing chance of continual illness international, global fitness company (WHO) is encouraging developing international locations to apply conventional natural drug treatments for the remedy of diverse persistent ailments. Broccoli has many health-promoting compounds ¹⁸. Inflammation increases the cell proliferation will increase apoptosis and will increase the risk of developing most cancers. Bioactive substances present in broccoli can lessen infection by way of activating detoxification enzymes, clearing the unfastened radicals and inducing immune capabilities. Isothiocyanates sluggish down the pastime of a great deal irritation mechanism. Among pronounced antimost cancers capabilities, sulforaphane changed into also determined to lessen irritation Helicobacter pylori are pretty associated with numerous gastrointestinal sicknesses which include gastric contamination, gastric ulcer, and so forth. The reproductive potential in gastric acid of H. Pylori depends on the production of the urease enzyme. Sulphoraphane and other isothiocyanates gift are broccoli inhibit urease produced by H. Pylori The nutrients present in broccoli help us in many methods consisting of diet ok for the functioning of many proteins concerned in blood clotting, vitamin C builds collagen, which forms body tissue and bone, and facilitates cuts and wounds heal¹⁹⁻²⁰. Diet C is an effective antioxidant and protects the body from destructive unfastened radicals, diets excessive in fiber sell digestive health. A high fiber intake can also help decrease LDL cholesterol, Potassium – a mineral and electrolyte this is vital for the feature of nerves and heart contraction, Folate – is vital for the manufacturing and preservation of the latest cells inside the frame .

The function of broccoli in combating cancer

Different chemo preventative procedures had been sought to interfere with initiation and manipulate malignant progression. The Brassica's own family of cruciferous greens which includes broccoli is a wealthy source of glucosinolates, which can be metabolized to isothiocyanate compounds. Amongst some related versions of isothiocyanates, sulforaphane (SFN) has surfaced as a specifically amazing chemopreventive agent-based totally on its ability to target more than one mechanisms inside the cellular to govern carcinogenesis. .

CONCLUSION

Broccoli is an underutilized food in India. Moreover, broccoli can be utilized for its anti-cancer capability for stopping cancer. Broccoli integrated recipes will assist in stopping various varieties of cancers as they have got anti-most cancers pastime and presence of sulphoraphane which helps towards cancer and lots of other conditions.

CONFLICT OF INTEREST

Conflict of interest declared none.

REFERENCES

1. Abbaoui B, Lucas CR, Riedl KM, Clinton SK, Mortazavi A (2018) Cruciferous vegetables, isothiocyanates, and bladder cancer prevention. *Mol Nutr Food Res* 62(18):e1800079
2. Ghoncheh M, Pakzad R, Hasanzadeh H, Salehiniya H. Incidence and mortality of uterine cancer and relationship with Human Development Index in the world. *Cukurova Medical Journal*. 2017;42(2):233–240.
3. Chen Z, Wang P, Woodrow J, Zhu Y, Roebothan B, et al. (2015) Dietary patterns and colorectal cancer: results from a Canadian population-based study. *Nutr J* 14: 18.
4. World Cancer Research Fund / American Institute for Cancer Research (2007) *Food, Nutrition, Physical Activity, and the Prevention of Cancer: a Global Perspective*. AICR, Washington DC, USA.s 9.
5. Vasanthi, H. R., ShriShriMal, N., Das, K. D., *Curr. Med. Chem.* 2012, 19, 2242 - 51.
6. M.A.Albrecht, C.W. Evans, and C.L.Raston, "Green chemistry and the health implications of nanoparticles," *Green Chemistry*, vol. 8, no. 5, pp. 417–432, 2006.
7. J. M. DeSimone, "Practical approaches to green solvents," *Science*, vol. 297, no. 5582, pp. 799–803, 2002.
8. H. Rui, R. Xing, Z. Xu, Y. Hou, S. Goo, and S. Sun, "Synthesis, functionalization, and biomedical applications of multifunctional magnetic nanoparticles," *Advanced Materials*, vol. 22, no. 25, pp. 2729–2742, 2010.
- 9.l. Brigger, C. Dubernet, and P. Couvreur, "Nanoparticles in cancer therapy and diagnosis, " *AdvancedDrugDelivery Reviews*,

vol. 54, no. 5, pp. 631–651, 2002.

10. A. K. Gupta and M. Gupta, "Cytotoxicity suppression and cellular uptake enhancement of surface modified magnetic nanoparticles," *Biomaterials*, vol. 26, no. 13, pp. 1565–1573, 2005.

11. K. Petcharoen and A. Sirivat, "Synthesis and characterization of magnetite nanoparticles via the chemical co-precipitation method," *Materials Science and Engineering B: Solid-State Materials for Advanced Technology*, vol. 177, no. 5, pp. 421–427, 2012.

12. F. Jia, L. Zhang, X. Shang, and Y. Yang, "Non-aqueous sol-gel approach towards the controllable synthesis of nickel nanospheres, nanowires, and nanoflowers," *Advanced Materials*, vol. 20, no. 5, pp. 1050–1054, 2008.

13. D.-H. Chen and S.-H. Wu, "Synthesis of nickel nanoparticles in water-in-oil microemulsions," *Chemistry of Materials*, vol. 12, no. 5, pp. 1354–1360, 2000.

14. D. Chen and R. Xu, "Hydrothermal synthesis and characterization of nanocrystalline γ -Fe₂O₃ particles," *Journal of Solid State Chemistry*, vol. 137, no. 2, pp. 185–190, 1998.

15. S. Basak, D.-R. Chen, and P. Biswas, "Electrospray of ionic precursor solutions to synthesize iron oxide nanoparticles: modified scaling law," *Chemical Engineering Science*, vol. 62, no. 4, pp. 1263–1268, 2007.

16. G. W. Yang, "Laser ablation in liquids: applications in the synthesis of nanocrystals," *Progress in Materials Science*, vol. 52, no. 4, pp. 648–698, 2007.

17. B. Nagaraj, N. B. Krishnamurthy, P. Liny, T. K. Divya, and R. Dinesh, "Biosynthesis of gold nanoparticles of *Ixoracoccinea* flower extract & their antimicrobial activities," *International Journal of Pharma and Bio Sciences*, vol. 2, no. 4, pp. 557–565, 2011.

18. M. Kowshik, S. Ashtaputre, S. Kharrazi, et al., "Extracellular synthesis of silver nanoparticles by a silver-tolerant yeast strain MKY3," *Nanotechnology*, vol. 14, no. 1, pp. 95–100, 2003.

19. M. N. Nadagouda and R. S. Varma, "Green and controlled synthesis of gold and platinum nanomaterials using vitamin B2: density-assisted self-assembly of nanospheres, wires, and rods," *Green Chemistry*, vol. 8, no. 6, pp. 516–518, 2006.

20. I. Brigger, C. Dubernet, and P. Couvreur, "Nanoparticles in cancer therapy and diagnosis," *Advanced Drug Delivery Reviews*, vol. 54, no. 5, pp. 631–651, 2002.

Biosynthesis And Characterisation Of Silver Nanoparticles From *Uvarianarum* Extract .

Sujithra.M,Sathya.RNirmalaDevi.P, Prema.P

Dhanalakshmisrinivasan College of Arts and Science for Women (Autonomous), Perambalur.

Abstract: *Uvarianarum* has anticancer, anti-inflammatory, antifungal and anti-HIV properties which are effective in action. The aim of the study was to biosynthesize silver nanoparticles using *Uvarianarum* leaves extract and determine their anticancer activity against MCF-7 breast cancer cell line. Silver nanoparticles has become an important prioritized nanomaterial among the others as they are non-toxic to the cells exhibiting as a defensive inorganic antimicrobial agent. Presence of AgNPs confirmed with yellowish-brown colour at 8:2 ratio. The synthesized nanoparticles were characterized through SEM analysis along with Fluorescence microscope analysis. The EtBr/Ao staining results suggest that AgNPs may exert its antiproliferative effect on MCF-7 cell line by suppressing its growth and inducing apoptosis. The cytotoxic activity studied by MTT assay in MCF-7 cell lines revealed that the *U. narum* AgNPs were non-toxic exhibiting 50% growth inhibition as 22.19 μ g/ml. The outcomes revealed that the *U. narum* AgNPs as the most active, in terms of IC50, with a more pronounced efficacy against breast cancer cell lines.

Keywords: *Uvarianarum*, breast cancer cells, silver nanoparticles, anticancer activit.

I. INTRODUCTION

Breast cancer, a heterogeneous disease, is the commonly diagnosed malignant cancer among women in various countries and the incidence rate of breast cancer has been rising rapidly over the past few decades worldwide¹. Most of the well-established breast cancer risk factors include family history, age at menarche, age at menopause, and reproductive history²⁻³. Breast cancer cells are able to spread to distant sites, specifically lung, liver, bone, and brain where they proliferate into macroscopic masses that lead to death of most patients. Much progress has been made in early detection and better treatment of breast cancer, leading to improved survival³. A substantial number of epidemiological studies examined the associations between individual foods and the risk of breast cancer⁴⁻⁵. High intakes of red meat, animal fats, and refined carbohydrates associated with an increased risk, whereas intake of fruits, vegetables, whole grains, and dietary fiber had been linked with a reduced risk of breast cancer⁶. The studies suggested that potentially modifiable lifestyle factors, particularly diet, plays an important role in breast cancer prevention^{7,8}. Globally, breast cancer is the most frequently diagnosed cancer in women, with an estimated 1.38 million new cases per year⁹. For those with BRCA1/2 mutations, the risks are higher than for the average woman. HIF-1 is a major driver of breast cancer development and metastasis, and there is great interest in the potential to mitigate tumour hypoxia in this disease increasing cellular vitamin C content can moderate the hypoxic response^{10,11}. Nanoparticle size, shape and core composition are strong determinants of cellular uptake. DOX-loaded polymeric nanoparticles showed a similar trend, with a higher cellular uptake for rod-like and worm-like nanoparticles than spherical nanoparticles in MCF-7 cells^{12,13}. Biological synthesis of Ag NPs from herbal extract and/or microorganisms has appeared as an alternative approach as these routes have several advantages over the chemical and physical methods of synthesis¹⁴. It is also a well-established fact that these routes are simple, cost-effective, eco-friendly and easily scaled up for high yields and or production. Biosynthesis of metal and metal oxide nanoparticles using biological agents such as bacteria, fungi, yeast, plant and algal extracts has gained popularity in the area of nanotechnology¹⁵. Plants and their parts contain carbohydrates, fats, proteins, nucleic acids, pigments and several types of secondary metabolites which act as reducing agents to produce nanoparticles from metal salts without producing any toxic by-product^{16,17}.

MATERIALS AND METHODS

2.1 Authentication of plant materials

The plant material *uvarianarum* was collected from Tiruchirappalli, Tamil Nadu, India.

2.2 Reagents

DMEM medium, Fetal Bovine Serum (FBS) and antibiotic solution were from Gibco (USA), DMSO (Dimethyl sulfoxide) and MTT (3-4,5 dimethylthiazol-2-yl-2,5-diphenyl tetrazolium bromide) (5 mg/ml) were from Sigma, (USA), IX PBS was from Himedia, (India). 96 well tissue culture plates and wash beakers were from Tarson (India). Silver nitrate was purchased from Fisher Scientific (Pittsburgh).

2.3 Preparation of *uvarianarum* plant extract

The *uvarianarum* plant were washed thoroughly and cut into fine pieces and heated at 60° C with 100 ml of distilled water for 60 min. Then the extract was primarily filtered with tissue paper and then secondary filtration with the Whatman filter paper. The filtered plant extract was used for the synthesis of silver nanoparticles^{15, 17}.

2.4 Bio-synthesis of U. AgNPs

The plantextract was used for the synthesis ofAgNPs. To synthesize AgNPs from *uvarianarum* plant extract a different ratio of 0.01N AgNO₃ and plant extract was used(5:5,6:4,7:3,6:4,8:2,9:1)¹⁸.

2.5 Characterization of U. AgNPs

The plantextract and synthesized silver nanoparticles along with AgNO₃ solution was analysed through the SEM analysis.

2.6 SEM analysis of biosynthesized AgNPs

The biosynthesized silver nanoparticles were characterized using high resolution SEM analysis. The samples were prepared by simple drop coating of the suspension of silver solutions onto an electric clean glass and allowing the solvent (water) to evaporate. The samples were left to dry completely at room temperature

2.7 Cell culture

MCF-7 (Human breast cancer cells)cell line were cultured in liquid medium (DMEM) supplemented 10% Fetal Bovine Serum (FBS), 100 ug/ml penicillin and 100 µg/ml streptomycin, and maintained under an atmosphere of 5% CO₂ at 37°C.

2.8 MTT Assay

The U. AgNPs sample was tested for *in vitro* cytotoxicity, usingMCF-7 cells by 3-(4,5-dimethylthiazol-2-yl)-2,5-diphenyltetrazolium bromide (MTT) assay. Briefly, the cultured MCF-7 cells were harvested by trypsinization, pooled in a 15 ml tube. Then, the cells were plated at a density of 1×10⁵ cells/ml cells/well (200 µL) into 96-well tissue culture plate in DMEM medium containing 10 % FBS and 1% antibiotic solution for 24-48 hour at 37°C. The wells were washed with sterile PBS and treated with various concentrations of the U. AgNPs sample in a serum free DMEM medium. Each sample was replicated three times and the cells were incubated at 37°C in a humidified 5% CO₂ incubator for 24 h. After the incubation period, MTT (20 µL of 5 mg/ml) was added into each well and the cells incubated for another 2-4 h until purple precipitates were clearly visible under an inverted microscope. Finally, the medium together with MTT (220 µL) were aspirated off the wells and washed with 1X PBS (200 µl)^{19, 20}.

2.9. ETBr/AO staining

Briefly, 5 × 10⁵ cells/ml of MCF-7 cells were plated in a 24 well tissue culture plate and treated with U. AgNPs sample in a serum free DMEM medium. The plate was incubated at 37°C at 5% Co2 incubator for 24 hours. After incubation, 50 µl of 1 mg/ml acridine orange and ethidium bromide were added to the wells and mixed gently. Finally, the plate was centrifuged at 800 rpm for 2 minutes and evaluated immediately within an hour and examined at least 100 cells by fluorescence microscope using a fluorescent filter.

SEM analysis of biosynthesized AgNPs

The biosynthesized silver nanoparticles were characterized using high resolution SEM analysis. The samples were prepared by simple drop coating of the suspension of silver solutions onto an electric clean glass and allowing the solvent (water) to evaporate. The samples were left to dry completely at room temperature.

RESULTS

3.1 Synthesis of silver nanoparticles

Silver nanoparticles was synthesized and optimized by various parameters using *U. narum* plant extracts in different ratio (9:1,6:4,7:3,5:5,8:2).The presence of AgNPs in *U. narum* was confirmed with the yellowish-brown colour formation.The synthesis rate of silver nanoparticles increased in 8:2 ratio.

3.2 SEM analysis of biosynthesized AgNPs

The biosynthesized AgNPs were subjected to SEM analysis. The results showed that the silver nanoparticles were spherical in shape and their nano in their size as shown in Fig 3 and 4.

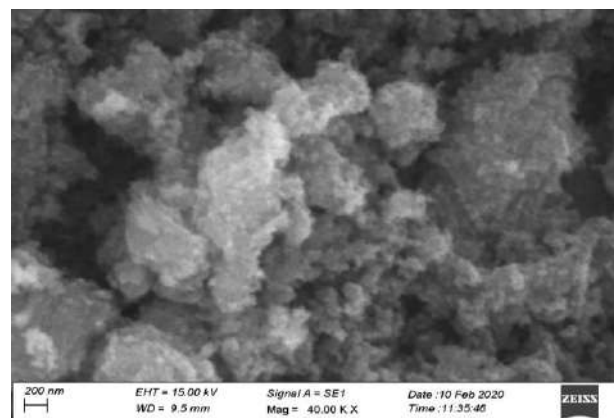


Fig I: SEM image of biosynthesised U. AgNPs at 200nm

The anti-cancer activity of MCF-7 cell line was increased with increase in concentration of U-AgNPs. There was a change in the percentage of cell viability in control and U. AgNPs treated MCF-7 cells. The inhibitory concentration at 50% (IC50) was observed at 22.19 $\mu\text{g}/\text{ml}$ of AgNPs for MCF-7 cells.

3.3 MTT assay

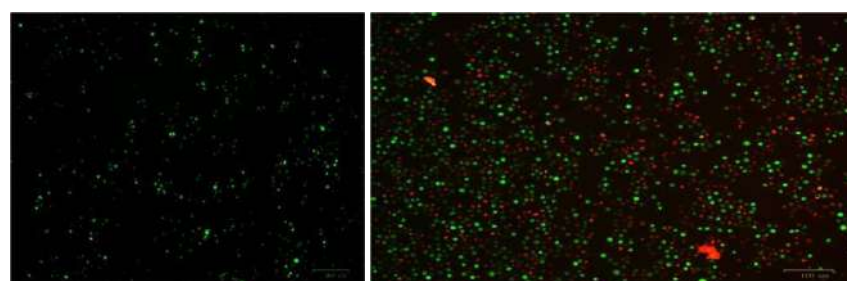
The anti-cancer activity of MCF-7 cell line was increased with increase in concentration of U-AgNPs. There was a change in the percentage of cell viability in control and U. AgNPs treated MCF-7 cells. The inhibitory concentration at 50% (IC50) was observed at 22.19 $\mu\text{g}/\text{ml}$ of AgNPs for MCF-7 cells.

**A. OD Value at 570 nm
Control Mean OD value: 0.250**

S. No	Tested sample concentration ($\mu\text{g}/\text{ml}$)	OD Value at 570 nm (in duplicates)
1.	Control	0.250 0.250
2.	100 $\mu\text{g}/\text{ml}$	0.142 0.165
3.	90 $\mu\text{g}/\text{ml}$	0.153 0.141
4.	80 $\mu\text{g}/\text{ml}$	0.117 0.153
5.	70 $\mu\text{g}/\text{ml}$	0.123 0.156
6.	60 $\mu\text{g}/\text{ml}$	0.136 0.141
7.	50 $\mu\text{g}/\text{ml}$	0.119 0.143
8.	40 $\mu\text{g}/\text{ml}$	0.120 0.127
9.	30 $\mu\text{g}/\text{ml}$	0.125 0.115
10.	20 $\mu\text{g}/\text{ml}$	0.108 0.093
11.	10 $\mu\text{g}/\text{ml}$	0.153 0.143

1.4 ETBr/AO staining

The U. AgNPstreated MCF-7 cells were subjected to AO/EB staining. AO entering the nucleus, stains live cells in green fluorescent colour whereas EB penetrating the dead cells are stained in red due to loss of membrane integrity. The antiproliferative effect of AgNPs biosynthesized from plant extract upon staining showed apoptotic changes. A progressiveincrease in the number of apoptotic cells was noted in AgNPs treated cells compared to the control cells.(Fig. A and b).



Fig(A)

Fig(B)

DISCUSSION

Uvarianarum is a source of an essential oil with a large, woody, climbing shrub. The plant is harvested from the wild for local use as a medicine where essential oil obtained from the roots is used in the treatment of various diseases¹⁸. A scant shrub with globose-cylindrical, red, aggregate fruit and aromatic odour of the roots are the distinguishing character of the plant. Macroscopically the root shows the cortex, interrupted by some secretory cells containing granular reddish brown or essential oil and resin, patches of secondary phloem and thick-walled lignified cells. Starch grains and calcium oxalate crystals are found in the cortex. However, further studies like experimental and clinical studies can be conducted to explore its utility¹⁹. In the present study the silver nanoparticles were synthesized using the aqueous extract of *U. narium*. Silver nanoparticles was synthesized and optimized by various parameters using *U. narium* plant extracts in different ratio (9:1, 6:4, 7:3, 5:5, 8:2). The presence of AgNPs in *U. narium* was confirmed with the yellowish-brown colour formation. The synthesis rate of silver nanoparticles increased in 8:2 ratio. The biosynthesized AgNPs were subjected to SEM analysis²⁰. The results showed that the silver nanoparticles were spherical in shape and their nano in their size as shown in Fig. MTT assay is metabolized by all cells; the assay can be used with all cell types where the entire assay is performed in a single microplate. The anti-cancer activity of MCF-7 cell line was increased with increase in concentration of U-AgNPs. There was a change in the percentage of cell viability in control and U. AgNPs treated MCF-7 cells. The inhibitory concentration at 50% (IC50) was observed at 22.19 µg/ml of AgNPs for MCF-7 cells. The U. AgNP treated MCF-7 cells were subjected to AO/EB staining. AO entering the nucleus, stains live cells in green fluorescent colour whereas EB penetrating the dead cells are stained in red due to loss of membrane integrity^{21,22}. The antiproliferative effect of AgNPs biosynthesized from plant extract upon staining showed apoptotic changes. A progressive increase in the number of apoptotic cells was noted in AgNPs treated cells compared to the control cells. (Fig. 6). The present study deals with early cellular response induced by the AgNPs treatment in an attempt to define events involved in cytotoxicity, involved in inducing apoptosis and to design chemotherapeutic agents^{23,24}.

CONCLUSION

This study demonstrated the biosynthesis of AgNPs using extract from leaves of *U. narium* by an eco-friendly, simple and efficient method. These synthesized nanoparticles having potential anticancer activity against MCF-7 cells may be suitable for application in pharmaceutical industries and for many uses.

REFERENCE

1. Colditz GA, Bohlke K. Priorities for the primary prevention of breast cancer. CA Cancer J Clin. 2014;64:186–194. doi: 10.3322/caac.21225. [PubMed] [CrossRef] [Google Scholar]
2. Interagency Breast Cancer and Environment Research Coordinating Committee. Breast Cancer and the Environment: Prioritizing Prevention. 2013. https://www.niehs.nih.gov/about/assets/docs/breast_cancer_and_the_environment_prioritizing_prevention_508.pdf. Accessed 25 Oct 2016.
3. Kruk J, Aboul-Enein HY. Environmental exposure, and other behavioral risk factors in breast cancer. Curr Cancer Ther Rev. 2006;2:3–21. doi: 10.2174/157339406775471795. [CrossRef] [Google Scholar]
4. President's Cancer Panel; National Cancer Institute. Reducing Environmental Cancer Risk: What We Can Do Now. 2010. https://deainfo.nci.nih.gov/advisory/pcp/annualreports/pcp08-09rpt/pcp_report_08-09_508.pdf. Accessed 25 Oct 2016.
5. Fenton SE. A special issue dedicated to a complex tissue. Reprod Toxicol. 2015;54:1–5. doi: 10.1016/j.reprotox.2015.05.004. [PubMed] [CrossRef] [Google Scholar]
6. Jemal A, Siegel R, Xu J, Ward E. Cancer statistics, 2010. CA Cancer J Clin. 2010;60(5):277–300. doi: 10.3322/caac.20073. [PubMed] [CrossRef] [Google Scholar]
7. Thomson CA. Diet and breast cancer: understanding risks and benefits. Nutrit Clin Pract. 2012;27(5):636–650. doi: 10.1177/0884533612454302. [PubMed] [CrossRef] [Google Scholar]
8. Ziegler RG, Hoover RN, Pike MC, Hildesheim A, Nomura AM, West DW, Wu-Williams AH, Kolonel LN, Horn-Ross PL, Rosenthal JF, et al. Migration patterns and breast cancer risk in Asian-American women. J Natl Cancer Inst. 1993;85(22):1819–1827. doi: 10.1093/jnci/85.22.1819. [PubMed] [CrossRef] [Google Scholar]
9. Levi F, La Vecchia C, Gulei C, Negri E. Dietary factors and breast cancer risk in Vaud, Switzerland. Nutr Cancer. 1993;19(3):327–335. doi: 10.1080/01635589309514263. [PubMed] [CrossRef] [Google Scholar]
10. La Vecchia C, Decarli A, Franceschi S, Gentile A, Negri E, Parazzini F. Dietary factors and the risk of breast cancer. Nutr Cancer. 1987;10(4):205–214. doi: 10.1080/01635588709513958. [PubMed] [CrossRef] [Google Scholar]
11. Logan CY, Nusse R (2004) The Wnt signaling pathway in development and disease. Annu Rev Cell Dev Biol 20: 781–810. [PubMed] [Google Scholar]
12. Kaler P, Godasi BN, Augenlicht L, Klampfer L (2009) The NF-kappaB/AKT-dependent Induction of WntSignaling in Colon Cancer Cells by Macrophages and IL-1beta. Cancer Microenviron. [PMC free article] [PubMed]
13. Klopocki E, Kristiansen G, Wild PJ, Klaman I, Castanos-Velez E, et al. (2004) Loss of SFRP1 is associated with breast cancer progression and poor prognosis in early stage tumors. Int J Oncol 25: 641–649. [PubMed] [Google Scholar]
14. Rask K, Nilsson A, Brannstrom M, Carlsson P, Hellberg P, et al. (2003) Wnt-signalling pathway in ovarian epithelial tumours: increased expression of beta-catenin and GSK3beta. Br J Cancer 89: 1298–1304. [PubMed]
15. Su HY, Lai HC, Lin YW, Liu CY, Chen CK, et al. (2010) Epigenetic silencing of SFRP5 is related to malignant phenotype and chemoresistance of ovarian cancer through Wntsignaling pathway. Int J Cancer 127: 555–567. [PubMed] [Google Scholar]

16. Boon HS, Olatunde F, Zick SM. Trends in complementary/alternative medicine use by breast cancer survivors: comparing survey data from 1998 and 2005. *BMC Womens Health.* 2007;7:4. [PMC free article] [PubMed] [Google Scholar]
17. Greenlee H, Kwan ML, Ergas IJ, et al. Changes in vitamin and mineral supplement use after breast cancer diagnosis in the pathways study: a prospective cohort study. *BMC Cancer.* 2014;14:382–397. [PMC free article] [PubMed] [Google Scholar]
18. Link AR, Gammon MD, Jacobson JS, et al. Use of self-care and practitioner-based forms of complementary and alternative medicine before and after a diagnosis of breast cancer. *Evid Based Complement Alternat Med.* 2013;2013:1–16. [PMC free article] [PubMed] [Google Scholar]
19. Greenlee H, Kwan ML, Ergas IJ, et al. Changes in vita min and mineral supplement use after breast cancer diagnosis in the pathways study: a prospective cohort study. *BMC Cancer.* 2014;14:382–397. [PMC free article] [PubMed] [Google Scholar]
20. Link AR, Gammon MD, Jacobson JS, et al. Use of self-care and practitioner-based forms of complementary and alternative medicine before and after a diagnosis of breast cancer. *Evid Based Complement Alternat Med.* 2013;2013:1–16. [PMC free article] [PubMed] [Google Scholar]
21. Matsuno RK, Pagano IS, Maskarinec G, Issell BF, Gotay CC. Complementary and alternative medicine use and breast cancer prognosis: a pooled analysis of four population-based studies of breast cancer survivors. *J Womens Health (Larchmt)* 2012;21:1252–1258. [PMC free article] [PubMed] [Google Scholar]
22. Greenlee H, Kwan ML, Ergas IJ, et al. Complementary and alternative therapy use before and after breast cancer diagnosis: the Pathways Study. *Breast Cancer Res Treat.* 2009;117:653–665. [PMC free article] [PubMed] [Google Scholar]
23. Semenza GL. HIF-1: upstream and downstream of cancer metabolism. *CurrOpin Genet Dev.* 2010;20(1):51–56. doi: 10.1016/j.gde.2009.10.009. [PMC free article] [PubMed] [CrossRef] [Google Scholar]
24. Semenza GL. The hypoxic tumor microenvironment: a driving force for breast cancer progression. *BiochimBiophysActa.* 2016;1863(3):382–391. doi: 10.1016/j.bbamcr.2015.05.036. [PMC free article] [PubMed] [CrossRef] [Google Scholar]

Synthesis Characterisation And Antibacterial Activity Studies Of Picoliohydrazide(2-Pyridine Carboxylic Acid And Hydrazide)

RamasamyShanmugapriya* ,DrGurumoorthi, DrP.Visvamithran, ManikanDeepa

DhanalakshmiSrinivasan College of Arts &Science for Women (Autonomous) Perambalur, Tamil nadu-621212

Abstract:Hydrazides subsidiaries are the kind of natural mixtures containing a nitrogen-nitrogen covalent bond with one of the substituents being an acyl bunch. Hydrazides and their subordinates have acquired noticeable quality in light of their antibacterial,anti-incendiary, anticancer, antiplatelet, antimalarial, pain relieving and cancer prevention agent action. Notwithstanding this they are likewise utilized as expected inhibitors for controlling consumption of many metals including gentle steel [1].Hydrazide-hydrazone establish a class of natural mixtures, which draws in the consideration of restorative physicists because of the way that they contain azomethine bunch ($-\text{NH}-\text{N}=\text{CH}-$) associated with carbonyl gathering, which is answerable for their diverse drug applications and makes conceivable the amalgamation of various heterocyclic frameworks.

Keywords:Hydrazides,anti-inflammatory,hydrazone,antiplatelet, antimalarial, analgesicetc

INDRODUCTION

Hydrazides act also to hydrazines, on the grounds that an alkyl or an acyl revolutionary bound to the NH end of $\text{NH}-\text{NH}_2$ doesn't fundamentally impact the reactivity of the NH_2 bunch. Carbonyl mixtures are regularly utilized as derivatization reagents¹. A portion of the hydrazides and practically equivalent to hydrazone are psychopharmacological specialist like monoamine oxidase (MAO) inhibitor and serotonin antagonists. Recently, sulfonylhydrazides have been generally utilized as a harmless to the ecosystem sulfur source since they are steady, promptly open and smell free. The principle course to combine hydrazide-hydrazone subordinates is the warming of proper hydrazides of carboxylic or heterocarboxylic acids with various aldehydes or ketones in different natural solvents like ethanol, methanol or butanol .A great deal of organically significant hydrazide-hydrazone subsidiaries with various utilitarian gatherings have been incorporated from a wide range of carbonyl mixtures. An assortment of strategies have been utilized to plan hydrazides, some of them include the response of acids or their subsidiaries with hydrazine hydrate, anhydrides and corrosive chlorides, albeit the more well known strategy for the readiness of hydrazides accomplished by the hydrazinolysis². Hydrazone compounds as it was referenced above because of their azo methane bunch exercises have attracted the consideration of numerous scientists integrating various mixtures of hydrazone by the notable hydrazinolysis method .Hydrazides are known to incorporate a fundamental class of organically dynamic natural compounds(Tabanca et, al., 2013) These hydrazides and their buildup items were expressed to have a wide scope of natural exercises just as antibacterial movement ,tuberculostatic properties , HIV inhibitors , pesticidal, antifungal ³ . A portion of the hydrazides and practically equivalent to hydrazone are psychopharmacological specialist like monoamine oxidase (MAO) inhibitor and serotonin adversaries .Hydrazide-hydrazone compounds are intermediates as well as they are moreover extremely successful natural mixtures by their own doing. At the point when they are utilized as intermediates, new subsidiaries can be blended by utilizing the dynamic hydrogen part of $-\text{CONHN}=\text{CH}-$ azometine group ⁴.

REVIEW OF LITERATURE

Studies show series of 4-(morpholin-4-yl)-N'-(arylidene)benzohydrazide were synthesized using appropriate synthetic route. Schiff bases mediated different 4-(morpholin-4-yl)-N'-(arylidene) benzohydrazides synthesized and Antimycobacterial activity of the was carried out by luciferase reporter phages (LRP) assay. Percentage reduction in relative light units (RLU) for isoniazid was also calculated ⁵. The test compounds showed significant antitubercular activity against *Mycobacterium tuberculosis* H37Rv. Amongst the compounds tested 4-(morpholin-4-yl)-N'-(arylidene)benzohydrazides found to be the most potent, activity against *M. tuberculosis* H37Rv and to have a greater activity against clinical isolates ¹⁴ Newhydrazide derivatives of imidazo[1,2-a]pyridine were synthesized and evaluated for antituberculosis activity. The reaction of 2-[(2-carboxyimidazo[1,2-a]pyridine-3-yl)sulfanyl] acetic acid hydrazide with various benzaldehydes gave N-(arylidene)-2-[(2-carboxyimidazo[1,2-a]pyridine-3-yl)sulfanyl]acetic acid hydrazide derivatives. The chemical structures of the compounds were elucidated by IR,(1)H-NMR, FAB-MS spectral data and elemental analysis. Antituberculosis activities of the synthesized compounds were determined by broth microdilution assay, the MicroplateAlamar Blue Assay in BACTEC 12B medium. The results of BACTEC 460 Radiometric System against *Mycobacterium tuberculosis* H37Rv was 6.25 microg/mL; the tested compounds showed significant inhibition ⁶New compounds containing 4-hydroxy-N'-(1,3-thiazolidin-2-ylidene)benzohydrazide moiety is basically for superior antimycobacterial activity studied by QSAR and further, the biological activity of the compound can be predicted before synthesis. The 3D-QSAR studies for the set of 4-hydroxy-N'-(1,3-thiazolidin-2-ylidene)benzohydrazide and their derivatives were carried out by using V-life MDS (3.50)⁷. The various statistical methods such as Multiple Linear Regression (MLR), Partial Least Square Regression (PLSR), Principle Component Regression(PCR) and K nearest neighbour (kNN) were used. The kNN showed good results having cross validated r^2 0.9319, r^2 for external test set 0.8561 and standard error of estimate 0.2195. The docking studies were carried out by using Schrodinger GLIDE module which resulted in a good docking score in comparison with the standard isoniazid. The designed compounds were further subjected for synthesis and biological evaluation. Antitubercular evaluation of these compounds showed that (4.a), (4.d) and (4.g) were found as potent inhibitors of H37RV⁸.

novel series of 4-pyrrol-1-yl benzoic acid hydrazide analogs, some derived 5-substituted-2-thiol-1,3,4-oxadiazoles, 5-substituted-4-amino-1,2,4-triazolin-3-thione and 2,5-dimethyl pyrroles have been synthesized in good yields and characterized by IR, NMR, mass spectral and elemental analyses⁹. Compounds were evaluated for their preliminary in vitro antibacterial activity against some Gram-positive and Gram-negative bacteria and compounds were screened for antitubercular activity against *Mycobacterium tuberculosis* H37Rv strain by broth dilution assay method. Some compounds showed very good antibacterial and antitubercular activities.

Synthesis of picoliohydrazide(2-pyridine carboxylic acid hydrazide)¹⁰

0.875g of 2, 3-dichlorobenzaldehyde is taken in a conical flask. Then it is dissolved in 10ml of methanol. 0.685g of 2-pyridiccarboxylic acid hydrazide is dissolved in 20ml water. Then these two mixtures are mixed using a magnetic stirrer. After 10 minutes of stirring the white precipitate crude is yielded (Fig. 1). The crude sample was recrystallized from ethanol. The purity of the compound was checked by Thin Layer Chromatography (TLC).

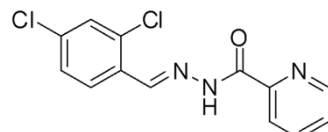


Fig 1: Structure of (E)-N'-(2,4-dichloroethylidene)picolinohydrazide.¹¹

SOLUBILITY TEST

Solubility of the compound was tested using water, methanol, ethanol, hexane, dichloromethane, benzene, ethyl acetate, chloroform and DMSO. 1mg of compound was added to 10ml of solvent and solubility was tested under three different conditions such as cold condition and hot condition corresponding to the boiling point of the solvent¹².

CRYSTALLIZATION

After synthesis the compound is dissolved 0.1g in 10ml ethanol and kept in a conical flask at RT for several days until the formation of crystals.

Characterization

Some physical methods were used to elucidate the bonding and structure of the synthesized ligands and complexes and to confirm the expected properties. While the ligands were characterized by usual methods such as analytical techniques such as TLC, molar conductance, magnetic susceptibility and spectral techniques such as IR and NMR techniques, it differs for complexes depending on the nature of the ligands and the metal ions involved. The presence of paired or unpaired electrons of the metal ions imparts the magnetic behavior of the complexes¹³.

UV analysis

The synthesized compound is subjected to UV-visible analysis. DMSO used as blank. The OD is recorded between 200-700nm.

FTIR

Infrared spectra were obtained on a Bomen FTIR MB-102 spectrometer in KBr pellets.

NMR

¹H NMR (200 MHz) and ¹³C NMR (50 MHz) spectra were recorded on BrukerAvance DRX200 spectrometers at the SASTRA university, thanjavur.

Analytical techniques

Elemental Analysis

Our objective is to detect the presence of nitrogen, sulphur, chlorine, bromine and iodine in synthesized ligands by Lassaigne's test. A small piece of dry sodium was melted in a fusion tube. Then 0.1g of solid substance was added to the molten sodium. It was heated gently at first, then to red hotness. Quickly plunged the red hot end of the tube into 10mL distilled water in a china dish. It is stirred well with broken end of the tube, boiled and filtered¹⁴.

Test for nitrogen

Few crystals of ferrous sulphate was added with 1ml of fusion extract. It was boiled, cooled and then added two-ml of diluted

sulfuric acid. Sodium cyanide is converted to sodium ferrocyanide on treating with ferrous sulphate. The green colour solution developed, it indicates the presence of nitrogen.

BIOLOGICAL ACTIVITY

Antitubercular activity

Disc diffusion method was used for antibacterial activity. The *M.smegmatis* MTCC300 strain is used in this study. Dubose oleic medium with bovine albumin used for assay. A stock solution of extract was prepared by dissolving 1 mg/MI of ethanol. The stock solution was then loaded to sterile disc at concentrations of 25, 50, and 100 μ g. 30 μ g rifampicin used as positive control and ethanol served as negative control. Each of the discs were allowed to air dry and place over the test pathogen swabbed on agar plates and incubated at 37° C under anaerobic condition for 3 days. The zone of inhibition was measured¹⁵.

RESULTS AND DISCUSSION

Efforts are being made here to investigate the coordination properties of 2, 3-dichlorobenzaldehyde and picolinic acid synthesizes as given in Figure 2. The compounds are crystallized(plate 1) and tested for solubility among different solvent (plate 2). The data given in Table 1 reveals that the synthesized compound was insoluble among hexane and water under RT and cold conditions. Solubility is higher in methanol, ethanol, ethylacetate, DMSO and dichloromethane and partial in benzene and chloroform. TLC(plate 3) reveals that the compound is pure and having higher R_f value 0.9 among polar solvent, moderate in benzene (0.6) and no mobility in hexane solvent.

Figure 2. Synthesis of (E)-N'-(2,4-dichlorobenzylidene)picolinohydrazide :

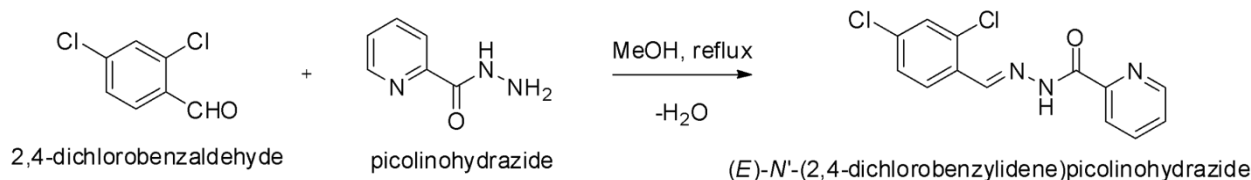


Table 1. Solubility test for MBSPDO

S.no.	Solvents	Room temperature	Hot condition	Rf value
1	Water	Insoluble	Insoluble	-
2	Methanol	Soluble	Soluble	0.95 cm-1
3	Ethanol	Soluble	Soluble	0.97 cm-1
4	Hexane	Insoluble	Insoluble	-
5	Benzene	Soluble	Soluble	0.66 cm-1
6	Ethyl acetate	Soluble	Soluble	0.90 cm-1
7	Chloroform	Soluble	Soluble	0.94cm-1
8	Dimethylsulphoxide	Soluble	Soluble	0.97cm-1
9	Dichloromethane	Soluble	Soluble	0.90 cm-1

Spectral Characterization

FT-IR Spectral studies

In order to study the functional group of the synthesized Schiff base, the IR spectrum was compared with the general functional ranges. The IR spectrum of Schiff base showed characteristic broad band at 3429 cm^{-1} can be attributed to $\nu(\text{N-H})$ and aromatic $\nu(\text{ArC-H})$ stretching vibrations appeared at 3079 cm^{-1} . It is indicated, the Schiff base also having intermolecular O...H hydrogen bonding. The weak interaction depends on the concentration of the solution. In this spectrum was recorded with a very dilute sample. Another distinctive vibration expected for N-N is observed at 1910 cm^{-1} . Generally carbonyl group stretching vibrations appear at 1680-1700 cm^{-1} but in this case appeared at 1605 cm^{-1} ; this is due to an amide group present in the compound which decreases the carbonyl functional group¹⁶. The newly generated C=N stretching vibration appeared at 1451 cm^{-1} along with other fingerprint region signals and all other peaks are in good agreement with the proposed structure. The FT-IR spectral data are given in Table 2.

Table 2. Important IR bands of Schiff base with their assignments.

Vibrations	$\nu(\text{N-H})$	$\nu(\text{ArC-H})$	$\nu(\text{N-N})$	$\nu(\text{C=O})$	$\nu(\text{C=N})$
Peak (cm^{-1})	3429	3079	1910	1605	1451

NMR spectra analysis

In the ¹H NMR spectrum, the proton attached to C5 & C7 carbon showed as a singlet. It was the unique proton that appeared

as a sharp singlet without multiplicity and used to calibrate other peaks. The characteristic amine N-H appeared as a broad singlet. The three protons attached on the phenyl ring appeared as two doublets at 7.40 and 7.98 ppm and one sharp singlet discussed earlier. On the other hand, the four protons associated with pyridine ring were identified as two doublets at 8.35 and 8.68 ppm and two multiplets at 7.80 and 8.05 ppm. The detailed assignments of protons were given in Table 3 and Figure 3.

Table 3. NMR Spectroscopic Data (δ) of (E)-N'-(2,4-dichlorobenzylidene)picolinohydrazide

S. No	Position Assignment	^1H (δ , ppm)	^{13}C (δ , ppm)
1	1	--	132.8
2	2	--	131.0
3	3	7.70, s	129.1
4	4	--	128.3
5	5	7.40, d	127.0
6	6	7.98, d	129.0
7	7	8.36, s	138.7
8	8	--	--
9	9	8.0, br	--
10	10	--	157.0
11	1'	--	--
12	2'	--	151.8
13	3'	8.35, d	122.4
14	4'	8.05, m	137.5
15	5'	7.80, m	127.3
16	6'	8.68, d	148.0

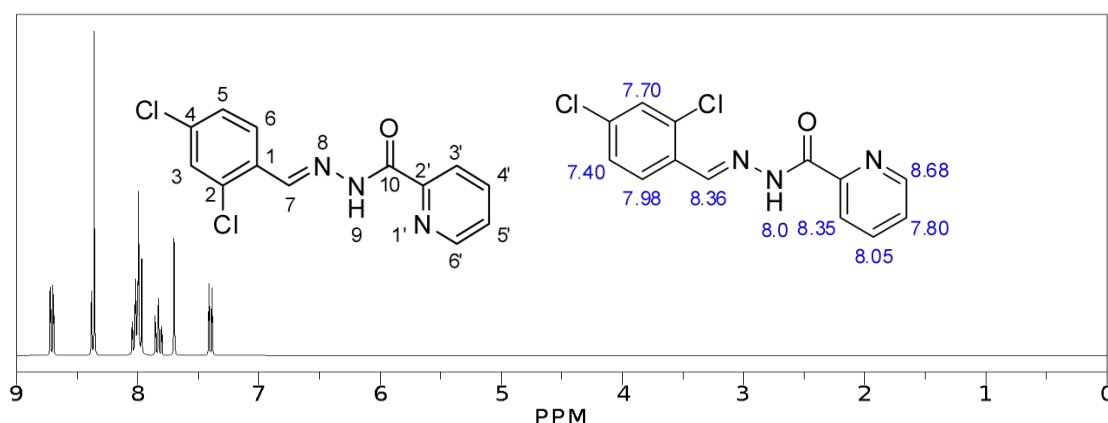
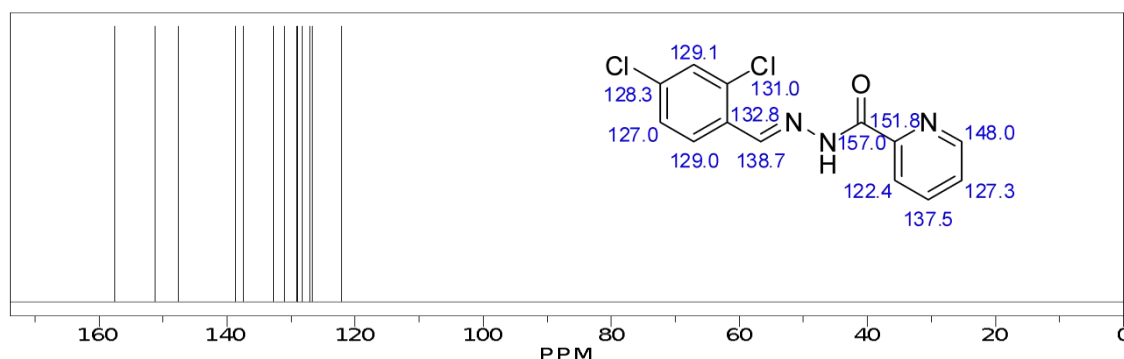


Figure 3. ^1H NMR spectrum of (E)-N'-(2,4-dichlorobenzylidene)picolinohydrazide

In the ^{13}C NMR spectrum, the discernible amide carbonyl appeared at 157.0 ppm and it clearly indicates a molecule having an amide group on its skeleton¹⁷. Next, the carbon attached to the nitrogen atom on the pyridine ring appeared at 151.8 and 148.0 ppm. The newly formed imine carbon peak appeared around 138.7 ppm. The chlorine attached quaternary carbon appeared at 131.0 and 128.3 ppm. The remaining six C-H carbons are show six signals in the range of 122.4 to 137.5 ppm. Peak assigning of other carbons was show in Figure 4.



**Figure 4. ^{13}C NMR spectrum of (E)-N'-(2,4-dichlorobenzylidene)picolinohydrazide
UV-Visible absorption spectra analysis**

UV-visible absorption spectra of (*E*)-N'-(2,4-dichlorobenzylidene)picolinohydrazide in solvent which exhibit absorption bands at 264 nm. Normally, pyridine absorbs at visible region and its linkwith other azo units reduces its absorption. The longer wavelength bands can be attributed to the $\pi-\pi^*$ transitions of the (*E*)-N'-(2,4-dichlorobenzylidene)picolinohydrazide¹⁸. antibacterial activity of compound is shown in Table 4.

Table 4. antibacterial activity of compound

Organism	Zone and inhibition mm in dm				
	NC	Rif pc	25 μ g	50 μ g	100 μ g
<i>M.smegmatis</i>	—	20	12	12	18

IN SILICO DOCKING WITH MYCOLIC ACID SYNTHESIS

These compounds showed great hydrophobic contributions and for each established system 100 ns of molecular dynamics simulations were performed and the binding free energy was calculated¹⁹. The results for the ligand molecules selected are shown in Table 5. Ligand performs hydrophobic interactions of its dihydroxybenzene ring with the TRP 60, GLU84 and GLY 59 with $2.40 \geq 2.05 \geq 2.28$ Å hydrogen bond distance. The free energy is -7.2 and -7.5. Hydrogen interactions with the same residues have already been verified in other studies²⁰

Table 5. scoring of intermolecular interaction between receptor and ligand

Pose	Score	Residues	Distance of hydrogen
Pose 1	-7.5	TRP 60 LIG1N	2.40
Pose 2	-7.2	GLU84 -LIG1O GLY 59-LIG1O	2.053 2.286

CONCLUSION

In the present study, substituted picolinohydrazide was synthesized and evaluated as antibacterial compared with standard drug rifampicin and results interpret that having nitrogen as heteroatom in the heterocyclic nucleus found to be more potent than the standard drug rifampicin. Insilico study reveals that the synthesized compound capable to inhibit mycolic acid synthase and might be a novel antimycobacterial agent.

REFERENCE

1. Srivastava F., Pandeya SN., Yadav MK., Singh BK. Journal name 2013, vol page no
2. Popiolek Ł, Biernasiuk A. *Chem Biol Drug Des*. 2016; 88(6):873-883.
3. Govindasami T. *Int J Org Chem*, 2011, 1 (9):71-77.
4. El-Faham A, and Albericio F., *Chem Rev*, 2011
5. Hanumanagoud H. and Basavaraja, KM., (2013), Synthesis and biological evaluation of some new oxadiazole and pyrazole derivatives incorporating benzofuran moiety. *Der Pharma Chem*, 5
6. Kumar D, Kumar NM, Ghosh S, Shah K. *Bioorg Med Chem Lett* 2012, 22:212–215
7. Özkar Y, Tunah Y, Karaca H, Işıkdağ İ. *Eur J Med Chem* 2010, 45:3293–3298
8. Munoz-Davila MJ. *Antibiotics* 2014, 3:39–48
9. Velezheva V, Brennan P, Ivanov P, Koronienko A, Lyubimov S, Kazarian K, Nikonenko B, Majorov K, Apt A. *Bioorg Med Chem Lett* 2016, 26:978–985
10. Rutkauskas K, Mickevičius V, Kantminienė K, Stasevych M, Komarovska-Porokhnyavets O, Musyanovych R, Novikov V. *Chemija*, 2013, 24(1):74–80
11. Kumar P, Narsimhan B, Ramasamy K, Mani V, Mishra RK, Majeed Abdul AB. *Montash Chem*. 2013, 144:825-849
12. Raparti V, Chitre T, Bothara K, Kumar V, Dangre S, Khachane C. *European Journal of Medicinal Chemistry*. 2009, 44(10):3954-3960
13. Raparti V, Chitre T, Bothara K, Kumar V, Dangre S, Khachane C, Gore S, Deshmane B. *Eur J Med Chem*. 2009, 44(10):3954-60
14. Kaplancikli ZA, Turan-Zitouni G, Ozdemir A, Teulade J C. *Arch Pharm (Weinheim)*. 2008, 341(11):721-4.
15. Ritesh. P., Bhole , Deepak. D., Borkar , Kishore. P., Bhusari , Prashant. A., Patil. *Journal of the Korean Chemical Society*. 2012., 56(2): 236-245
16. Joshi S. D. , Vagdevi H. M. , Vaidya V. P. 2008 *Eur. J. Med. Chem.* 43
17. S. Kusama, T. Saito, H. Hashiba, A. Sakai, S. Yotsuhashi, Crystalline copper (II) phthalocyanine catalysts for electrochemical reduction of carbon dioxide in aqueous media, *ACS Catal* 7 (2017) 8382–8385.
18. AliAkbarKhandar, FarhadAkbariAfkhami, HaraldKrautscheid, Kenneth Kristoffersen, ZelihaAtioglu, MehmetAkkurte and Carl HenrikGoritz, *Acta Cryst.* (2017). 73, 698–701
19. HadiAdibia, SaeedZakerb, HamidMonkaresia (2012) 1(1), 60-66
20. Fatehia. K. Mohamed, *DerChemicaSinica*, (2010), 1 (1): 20-31
21. GadadaNaganagowda, Reinout. Meijboom, and AmornPetsom, Hindawi Publishing Corporation(2014), 9
22. Heng-Yu Qian *Acta Chim. Slov.* (2012), 66, 995–1001

One-Pot Multi-Component Synthesis Of Thiobarbituricacid Involved Ultra Short Actingbarbiturates As Sedative And Hypnotics

M.Deepa*, M Srinivasan, V. Vijayakumar, A.Aarthi

Dhanalakshmi Srinivasan College of arts and science for women (Autonomous), Perambalur Tamilnadu-621212

Abstract: Barbituric acid is a synthesized novel bio-active thiobarbituric acid analogues. The synthesis sequence followed conventional organic synthetic protocol. To screen different metal chlorides for catalyst performance. To be report here a simple but effective procedure for the synthesis of 2- imino thio barbituric acid analogues via Schiff base multi-component condensation reaction. Monitoring the completion of reaction with the help of TLC (Thin- layer chromatography)technique. To be characterize the final product by FT-IR (Fourier-transform infrared spectroscopy), ¹H NMR (Proton nuclear magnetic resonance), and ¹³ C NMR (Carbon-13 nuclear magnetic resonance) spectralanalysis. The further antifungal studies of synthesized compounds is against fungalstrains.

Keywords: Barbit, Anticonvulsants TLC, FT-IR, ¹³C NMR, Thiobarbituric acid

INTRODUCTIION

Barbituricacidalsocalledasmalonylurea, wasdiscoveredbychemistAdolphVon Bayer in the year 1863 . Some Schiffbase and their metal complexes exhibit biologicalactivity as antibiotics, antiviral and antitumor agents¹⁻². IUPAC name of barbituric acid is pyrimidine-2,4,6 (1H,3H,5H)-trione. The structure and numbering of the barbituric acid is as in **Fig. 1.1**

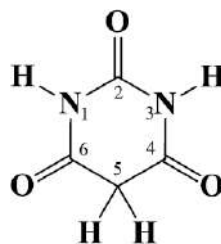


Fig. 1.1: Barbituric acid (A)

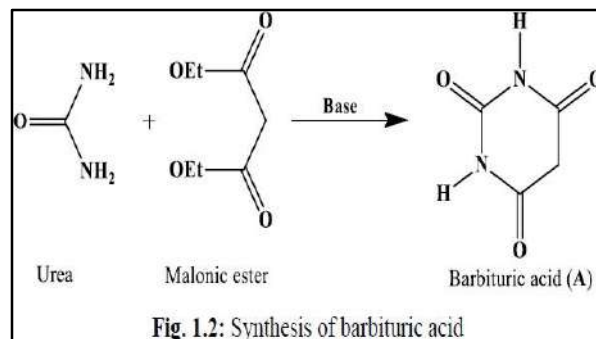


Fig. 1.2: Synthesis of barbituric acid

Barbituric acid was first synthesized by the reaction of urea with diethyl malonate in basic medium. During the reaction urea undergo condensation with the diethyl malonate to afford the product ²(**Fig. 1.2**). From the literature, it is proved that barbituric acid is pharmacologically inactive, but the derivatives of barbituric acid called barbiturates are having pharmacological applications as mentioned in further sections. The green synthesis by microwave irradiation was chosen as route due to its novelty, cleanliness, efficiency, time and solvent saving properties compared with the conventional methods which lack these advantages; such as time consume and wasting environment polluting organic solvents to achieve the same efficiency in synthesis.³ Barbituricaciddiscoveryprovidedthebasefortheintroductionofnumber of barbiturates that would be used in the medical field. As a catalyst, we incorporate gold nanoparticles into polystyrene nanoreactors stabilized by polyethylene glycol. ...⁴The earlier use of barbituric acid derivatives wereas sedatives and hypnotics. These derivatives can induce mild sedation and can also be used for local and to talanaesthesia³⁻⁶. Innumerable barbituric acid derivatives were synthesized from the past few decades but only certain barbiturates have been employed for clinical usage. it demonstrates the reactivity of these arylidene derivatives in heterocyclic synthesis with emphasis on the most recent findings. The others are synthetic substances which are convenient and important intermediates for the synthesis of a variety of useful and novel heterocyclic systems.⁵Catalysis by aniline hydrochloride is ineffective in benzene as solvent because of the insolubility of the salt, but the reaction can be strongly catalyzed by soluble acids,⁶. Barbiturates were the only drugs which clinically employed as anaesthetics, anticonvulsants, anxiolytics, sedatives and hypnotics in the beginning of 19th century.

History of Barbiturates and Their Developments

Barbiturates are the derivatives of barbituric acid which obtained by the structural modification of barbituric acid. The simple barbiturates can be obtained by the substitution at 1,3 and at 5th position of barbituric acid (Fig. 1.1). The various derivatives of barbituric acids can be classified into 1,3 di substituted barbiturates, 1,3,5 tri substituted barbiturates, 5,5'-disubstituted barbiturates etc. The use of solvent retards the rate of the reaction and requires a much longer reaction time than that for neat conditions⁷. Thio barbituric acid is a derivative of barbituric acid and is obtained by the replacement of oxygen atom at C-2 of barbituric acid with sulphur atom. Similar to barbiturates, thio barbiturates have been obtained by the structural modification of thio barbituric acid at 1,3 and 5th positions. The various functionalgroups such as alkyl, aryl, alkenyl etc may be introduced at 1,3 and at 5th position of barbituric acid or thio barbituric acid. The C-5 position of barbituric acid/thio barbituric acid contain highl yacid

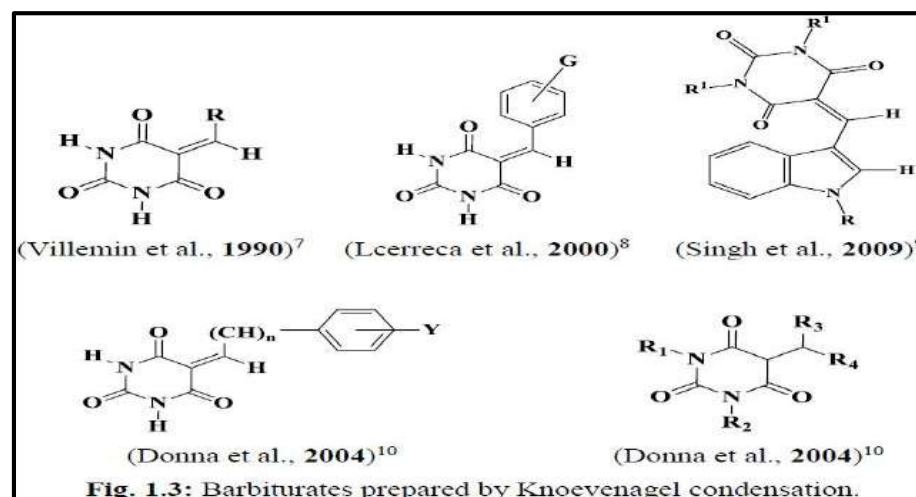


Fig. 1.3: Barbiturates prepared by Knoevenagel condensation.

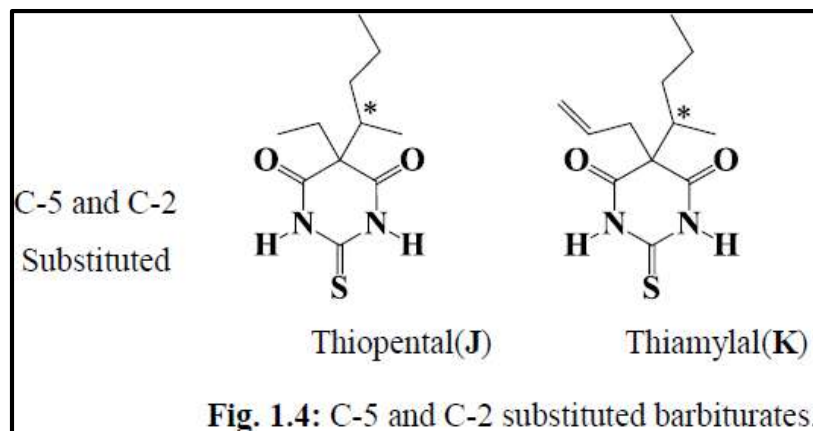


Fig. 1.4: C-5 and C-2 substituted barbiturates.

ic hydrogen atoms and can undergo Knoevenagel condensation to give barbiturates and thiobarbiturates . Organic reactions under solvent-free conditions have gained in popularity in recent years^{7,8}. The various such derivatives found in literature are shown in

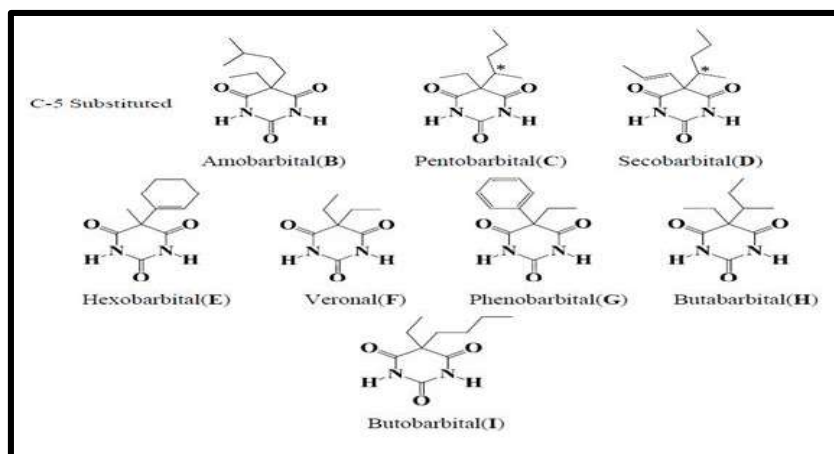


Fig.1.5.

Veronal (**F**), is also called barbital is a derivative of barbituric acid prepared by substitution at C-5 position. The chemical name of veronal is 5,5 diethyl barbituric acid and was synthesized first time by Fisher and Mering in 1902 ⁹. This compound become clinically used true hypnotic drug. These flow reactions also exhibited high performances, thus allowing the scale-up of this reaction system for industrial use.¹⁰ Similarly other analogues of barbituric acid synthesized were the phenobarbital (**G**) also called as luminal, butobarbital (**H**) and butobarbital (**I**) which acts as sedatives and antagonists (**Fig. 1.4**). After many years of introduction of barbiturates in clinical trials, some oxybarbiturates are still using as drugs for treatment of serious forms of insomnia and in the treatment of some epilepsy types. Compound with Schiff base core are widely used for industrial purposes and also exhibit a broad range of biological activities^{10,11}. Diethyl barbituric acid was the first barbiturate entered the market in the name of barbital, malonal or gardenal. Conrad and Guthzeit synthesized the barbital in 1881 by the reaction of barbituric acid with ethyl iodide. This compound was introduced clinically as a hypnotic drug in 1991 by the two companies from the Germany E-Merck and F. Bayer Co. Diethyl acetyl urea was synthesized and analysed by Von Mering and Von Bayer and was found to be more potent hypnotic drug than sulphonal. The same authors analysed the hypnotic properties of Veronal by in-vivo method. The studies demonstrated that hypnotic power of veronal was greater than that of diethyl-acetyl urea. This new hypnotic drug veronal was filed for patent by Fischer in 1903 and further its research data was published in the form of report. Since, veronal is having hypnotic, anticonvulsant and sedative properties it can be used for treating manic patients and melancholic patients. It also been employed as an effective inducer of sleep in insomniacs. Phenobarbital (**G**) a similar analogue of veronal (**F**) was first prepared in 1911 by Horlein by substituting one of the ethyl groups with phenyl group. In 1912 it was employed as a hypnotic drug for the first time by Loewe and his co-workers. Later this drug was also been used for the treatment of epilepsy and soon it became king of barbiturates. These two barbiturates i.e. veronal (barbital) and luminal (phenobarbital) become the first two representatives of barbiturates and were accepted by US pharmacopoeia as well as British pharmacopoeia in 1926 and 1932 respectively. Later, these two drugs were also been included in pharmacopoeia internationalis. The application of this solvent-free MW approach to multicomponent reactions is highlighted that can be adapted for high-speed parallel synthesis of the library of dihydropyrimidine-2(1H)-ones and imidazo[1,2-a]annulated pyridines, pyrazines, and pyrimidines.¹² Subsequently in 1921 butobarbital (**I**) was synthesized by Poulenc brothers. This hypnotic drug was three times stronger than that of barbital and called by other names butobarbitone, soneryl and neonal. The period of action for this drug was much shorter than other analogues (due to its high lipophilicity) and it reduces possible rebound drowsiness after its administration. The reason for its quick and effective action is because of its high lipophilicity. Its high lipophilicity is the reason for its rapid and efficient action.

Later on many barbiturates were synthesized and one such derivatives were mobarbital (**B**) in 1923 and secobarbital (**D**) in 1929. Both these derivatives were known to exhibit similar pharmacological properties as of butobarbital. Other series of drugs added were the phenobarbital (**G**) and thiopental (**J**) which were synthesized by Tabern and Volwiler in 1930. Hexobarbital (**E**) was synthesized by Kropp and Tauby by the addition of methyl group to the alkyl chain of butobarbital.¹⁵

This drug was used as anaesthesia for patients while surgery during the period

1940's. Due to its excellent lipophilicity its duration of action was reduced. Since these drugs cause some muscular movements, the modifications of basic core structure of barbituric acid was made by introducing the sulphur group at C-2 position of pentobarbital (**C**).

Many attempts were made to synthesize the sulphur derivatives of pentobarbital called pentothal and was become only representative of thiobarbiturate. After the clinical trials, this drug was accepted by many pharmacopoeia including British and US.

Thiobarbiturates were successfully employed as intravenous anaesthetic drugs and one such drug was pentothal (**J**). The results of the clinical use of pentothal was published in 1936. The search of potent anaesthetic barbiturates was continued and some of the new barbiturates discovered were the thiobutobarbital in 1952 and methohexitalin 1956. Methohexitalin was more potent than thiopental in terms of quick recovery in patients and was proved from its clinical trials. The subsequent development of many other anaesthetic drugs for intravenous administration lead to the reduction in usage of barbiturates. Condensation reactions of aldehydes and amines occur efficiently in a water suspension medium, and the reaction products are collected easily by filtration.¹³ Schiff bases are aldehyde- or ketone-like compounds in which the carbonyl group is replaced by an imine or azomethine group.¹⁴ Infrared irradiation promoted the formation of a series of Schiff bases in the condensation reaction between benzaldehydes and anilines, in the absence of solvent.¹⁵

Barbiturates and its Classification

Barbiturates are segregated into four different classes. The classification is according to their metabolic degradation and deposition of tissues. The hydrocarbon chain length attached at C-5 position of barbituric acid is the key role in controlling the barbiturates with respect to duration of effect and the protein binding affinity.

I Ultra short acting barbiturates

These barbiturates metabolized rapidly and are lipophilic in nature. These derivatives have been used as intravenous anaesthetics. The barbiturates hexobarbital (**E**), thiopental (**J**), thiamylal (**K**) are classified under this category and all of which have hydrocarbon substitution at C-5 with more than four carbon units.

II Short acting barbiturates

These are also lipid soluble in nature and binds to proteins. These barbiturates are generally employed as hypnotics and which makes the patients fall asleep. The derivatives of this class have very low renal clearance capacity and have a half-life of about three hours. The advantage of using these barbiturates is that there will not be any next day drowsiness after administration.

These compounds have similar structures as of ultra-short acting analogues. There are many examples for short acting barbiturates which includes pentobarbital (**C**) and secobarbital (**D**).

III Intermediate acting barbiturates

These can be used as hypnotics for the patients who getting awake in the midnight. Half-life period of these molecules is about three to six hours. Intermediate acting barbiturates cause next day drowsiness. Butabarbital (**H**) and amobarbital (**B**) are the examples for this category of barbiturates. Long acting barbiturates. The derivatives which cause hypnotic effect of more than six hours, inducing sedation followed by next day drowsiness are the long acting barbiturates. These compounds are having anticonvulsant effects besides hypnotic effects. Examples of long acting barbiturates are phenobarbital (**G**) and veronal (**F**).

Down Fall of Barbiturate Therapy

Since overdose of barbiturates results in the death cases across the world, the use of barbiturates as sedatives is banned in many countries. The over dosage of barbiturates cause acute poisoning in the body of the patient treated. Barbiturates mixture with other compounds could even become common procedure in USA for the execution of prisoners who sentenced to death. There were thousands of death occurred all over the world during nineteenth century due to the over dose of barbiturates. Due to the death reports, prescription of barbiturate drugs was get restricted by medical advisory council in Britain and subsequently in other countries. The awareness among citizens was made through campaign on the use and restrictions of barbiturates (CURB) during 1970's.

Presently Using Barbiturates as Sedative and Hypnotics

Even though barbiturates are restricted in use, number of these analogues are still being used for many pharmacological applications. Phenobarbital (**G**) is used for new born babies suffering from kernicterus and hyper-bilirubinemia, since it is capable of enhancing the bilirubin transport in patients having hemolytic jaundice. Dominant cerebral hemisphere can be identified before the neurosurgery by the intravenous administration of amobarbital (**B**). Severe traumatic brain damage can be cured by the use of barbiturates which reduce the intracranial pressure. The high dosage of barbiturates for the patients suffering with brain damage can increase the intracranial pressure lowering effect twice. The mechanism involved in activity of barbiturate are vascular tone modification and metabolism reduction which results in low oxygen demand from cerebral tissue. Due to their effective action, the barbiturates phenobarbital and amobarbital are even now considered as preferential drugs for the treatment as anticonvulsants and hypnotics.

Action of Barbiturates - Mechanism

Our nervous system consisting of some special cells called neurons. The central and peripheral nervous system to the regular function through communication between the neurons. The neurons present in the central nervous system do not undergo direct communication since they are separated by a space named synaptic cleft which restrict the direct communication between the two next to next neurons. For the communication between the adjacent neurons, neurotransmitters are used and there are two types of neurotransmitters namely excitatory neurotransmitters and inhibitory neurotransmitters. Excitatory neurotransmitters enhances excitation (increases the action potential) of the nerve cells whereas inhibitory neurotransmitters calm down (reduces the action potential) the nerve cells. In our human body system main inhibitory neurotransmitter present is gamma amino butyric acid which is commonly called as GABA. The neurotransmitter GABA is recognized by receptor known as GABAa receptor and which releases the Cl⁻ ions to the intracellular fluid which in turn reduces the action potential of nerve cells. Due to identification of GABA by GABA a receptor and release of chloride ions, our anxiety tension and excitation will be controlled. These GABAa receptors become the target for many anaesthetic agents, tranquilizer, sedatives and which includes barbituric acid derivatives. These barbiturates bind to the GABAa receptor complex which linked to the neurons and thereby induce the release of Cl⁻ which inhibits the fire of action potential of neurons. So this results in the calm down of nerve cells, reducing the anxiety tension, excitation and inducing sedation.

Barbiturates-New Era

Since from the discovery of barbituric acid, many of its derivatives called barbiturates have been synthesized and employed for wide range of applications as sedatives, hypnotics, anticonvulsants and anxiolytic agents. In the recent years, many research groups have been working on the modifications of barbituric acid, which lead to the synthesis of a wide variety of novel barbiturates having broad range of pharmacological applications. The pharmacological applications of this new era barbiturates include antibacterial, antifungal, antiviral, antioxidant, anti-inflammatory, anti-diabetic and anticancer activities. The synthesis and pharmacological activities of this new era barbiturates is discussed in the further section. Some notable biological activity of pyrimidine derivatives include adenosine receptor antagonists ^{16,17}

MATERIAL AND METHODS

General materials and characterization techniques:

All materials were purchased from Nice and Loba chemicals.

The IR spectra (KBr) was recorded in KBr on a shimadzu 8201pc (4000-400 cm⁻¹). The ¹H NMR and ¹³C NMR spectra were recorded on a JEOL-300 MHz. The Elemental analysis (C, H, and N) were recorded using an Elemental analyzer model (Varian EL III). (TLC) with silica gel plate are used due to pure

General method for the synthesis of mannich base analogue of thiobarbituricacid (2) via Mannich base reaction.

The reactants Thiobarbituricacid (1) (0.005mol, 0.72g), Phenylhydrazine (0.005mol, 0.5mL) and 3,4,5-trimethoxybenzaldehyde (0.005mol, 0.98g) were mixed together in a pestle mortar at room temperature. After the completion of reaction indicated by TLC, the reaction mixture was cooled in ice-cold water. It is filtered and dried. The product was recrystallized in ethanol to get pure product.

2-phenyl-6-thioxo-3-(3,4,5-trimethoxyphenyl)-3,3a,6,7-tetrahydro-2H-pyrazolo[3,4-d]pyrimidin-4(5H)-one (2)

Brown solid; mw: 412.46; m.p. 168°C; IR (cm⁻¹): 3301.89 (NH), 3009.53 (Ph-CHstr), 2851.23 (CH), 1587.84 (C=N), 1452.95 (C=S); ¹H-NMR (400 MHz, CDCl₃): δ= 9.20 (1H, NH), 7.82 (1H, s, NH), 6.70 (7H, m, Phenyl ring), 4.10(2H,s,CH), 3.83(9H,s,-OCH₃); ¹³C-

NMR (100 MHz, CDCl₃): δ= 208.30 (1C, C=O), 190.0 (1C, C=S), 175.20 (1C, C=N), 158.70, 137.85, 137.25, 110.10 (12C, Ph), 72.50 (2C, -CH). Elemental analysis: Calcd. for C₂₀H₂₀N₄O₄S:

Elemental Analysis: C, 58.24; H, 4.89; N, 13.58 %; Found: C, 58.22; H, 4.90; N, 13.60 %;

The minimal inhibitory concentration (MIC) was determined by the broth microdilution method according to the Clinical and Laboratory Standards Institute (CLSI) (The National Committee for Clinical Laboratory Standards). *In vitro* antifungal activity of the final compounds **1** and **2** were evaluated against standard strains; *Aspergillus Niger*, *Microsporum audouinii*, *Cryptococcus Neoformans* and *Candida albicans*. 10 mg of product dissolved in DMSO (250 μL) water (750 μL) are utilized. Fifty μL of a bacterial suspension, obtained from a 24h culture (~106cfu/mL) was added to each well with a final DMSO concentration of 1:16. The incubated target involved at thirty five degree celcius for 24 hours. We tested ceftazidime as antimicrobial agents for quality control of the method

RESULTS AND DISCUSSION

The synthesis of compound **2** was illustrated in scheme 1. Compound **2** was synthesized by condensation method via novel catalyst free cyclocondensation reaction ¹⁸⁻¹⁹. The formation of the title compound was confirmed by recording the IR, ¹H NMR, ¹³C NMR spectra, and elemental analyses. The IR spectra of compound **2** showed absorption bands at 3301.89, 2851.23 and 1587.84 cm⁻¹ corresponding to the NH, CH and C=N groups, respectively. The ¹H NMR spectra of compound **2** showed a sharp singlet at □ 9.20 for NH proton and a singlet at □ 3.83 for -OCH₃ proton ²⁰. The ¹³C NMR spectra of compound **2** showed

peaks at □ and □ 72.50 corresponding and CH respectively.

Compds	MIC (μg/mL)			
	<i>Aspergillus Niger</i>	<i>Candida albicans</i>	<i>Microsporum audouinii</i>	<i>Cryptococcus Neoformans</i>
1	32	20	56	12
2	60	04	01	25
Clotrimazole	02	06	02	05

characteristic 208.30, 190.0 ppm to C=O, C=S carbons,

The synthesized compounds **1** and **2** were evaluated for antifungal activity against four different fungal species. The final compound **2** shows remarkable antifungal activity than compound **1**. Compound **2** shows high antifungal activity in two fungal species namely *C. albicans* and *M. audouinii*. Compound **2** with the MIC value of 0.4 μg/mL was highly active than control clotrimazole with the MIC value of 0.6 μg/mL in *C. albicans*. Compound **2** with the MIC value of 0.1 μg/mL shows high antifungal activity than clotrimazole with the MIC value of 0.2 μg/mL in *M. audouinii*. The results were summarized in Table I.

Table I. Antifungal activity of compounds **1** and **2**



Figure 1.9: IR spectrum of compound **2**.

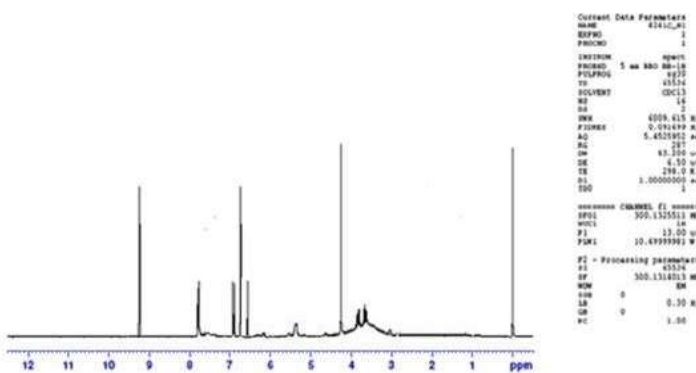


Figure 1.10: ^1H NMR spectrum of compound 2.

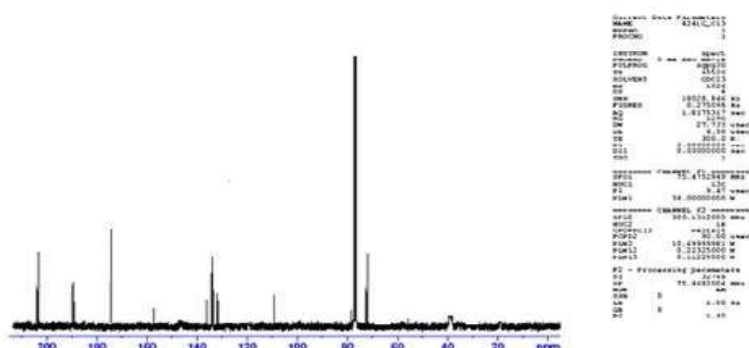


Figure 1.11: ^{13}C NMR spectrum of compound

CONCLUSION

In conclusion, the one-pot multi-component synthesis of thiobarbituric acid analogue (**2**) via condensation reaction by using novel catalyst free grindstone method. Synthesized thiobarbituric acid derivative was confirmed by FT-IR, ¹H NMR, and ¹³C NMR spectral analysis. A series of imines was synthesized by an ultrasound-assisted reaction of aldehydes and primary amines using silica as the promoter. Products were obtained in high yields even in large scale synthesis. Green chemistry is an eco-friendly and rapid emerging field of chemistry which offers a green alternative to conventional chemistry practices. It focuses on the reduction, recycling and removal of the use of toxic and hazardous chemicals through innovative alternative routes making desired products with minimum environment impact. The compounds **1** and **2** were further evaluated for antifungal activity. The results shows that the 2-iminobarbituric acid derivative **2** having remarkable activity in fungal strains. This concludes that compound **2** having an ability to act as a fungicide in future. since this technique has attracted broad range of interest from the scientific and practical viewpoints. The derivatives were subjected to antimicrobial activity using different bacterial strains (*Klebsiella pneumoniae*, gram negative bacteria and *Staphylococcus epidermidis*).

REFERENCES

1. Schiff H., *Ann. Chim.Paris*, 1864;131:118.
2. D.R. Williams, *Chem. Rev.*, 72: 203 (1972).
3. Patai S., *The Chemistry of the carbon-nitrogen double bond*, John Wiley & Sons Ltd.London, 1970.
4. Zheng Y., Ma K., Li H., Li J., He J., Sun X., *Catal Lett*, 2009;128:465–74.
5. Moffett RB., InRabjohn N., *John Wiley & Sons, Inc*, 1963:605–8.
6. Taguchi K., Westheimer F.H., *J Org Chem*, 1971;36:1570–2.
7. Love BE., Ren J., *J Org Chem*, 1993; 58:5556–8.LookG.C.,MurphyM.M.,CampbellD.A.,GallopM.A.,*TetrahedronLett*, 1995; 36:2937–40.
11. Chakraborti A.K., Bhagat S., Rudrawar S., *Tetrahedron Lett*, 2004;45:7641–4. 10.Billman J.H., Tai K.M., *J Org Chem*, 1958;23:535–9.
12. Armstrong III J.D., Wolfe C.N., Keller J.L., Lynch J., Bhupathy M., Volante R.P., *Tetrahedron Lett*, 1997;38:1531–2. (a) J.O. Metzger, *Angew. Chem. Int. Ed.*, 1998, 37, 2975; (b) C.J. Li, T.H. Chan, *Tetrahedron*, 1999, 55, 11149
13. Liu G., Cogan D.A., Owens T.D., Tang T.P., Ellman J.A., *J Org Chem*, 1999; 64:1278–84. Baricordi N., Benetti S., Biondini G., de Risi C., Pollini G.P., *TetrahedronLett* 2004; 45:1373–5.
14. Varma R.S., Dahiya R., Kumar S., *Tetrahedron Lett*, 1997; 38(12):2039–42.
15. SchmeyersJ.,TodaF.,BoyJ.,KauppG.,*JChemSocPerkinTrans*, 1998;2:989– 93.
16. Vass A., Duda's J., Varma R.S., *Tetrahedron Lett*, 1999;40:4951–4.
17. Tanaka K., Shiraishi R., *Green Chem*, 2000;2:272–3.
18. Andrade C.K.Z., Takada S.C.S., Alves L.M., Rodrigues J.P, Suarez P.A.Z., Branda R.F., *Synlett*, 2004;12:2135–8.
19. Vazquez M.A., Landa M, Reyes L., Miranda R., Tamariz J., Delgado F., *Synth Commun*, 2004;34(15):2705–18.
20. Gopalakrishnan M., Sureshkumar P., Kanagarajan V., Thanusu J., Govindaraju R., *J Chem Res*, 2005;5:299–303.
21. Gopalakrishnan M., Sureshkumar P., Kanagarajan V., Thanusu J., *Res Chem Intermed*. 2007; 33:541–8.

22. 20. Guzen K.P., Guaresemini A.S., Orfao A.T.G., Cella R., Pereira C.M.P., Stefani H.A., Tetrahedron Lett, 2007;48:1845–8. Gedye R., Smith F., Westaway K., Ali H., Baldisera L., Laberge L., *Tetrahedron Lett*, 1986;27:279–82. Giguere R.J., Bray T.L., Duncan S.M., Majetich G., *Tetrahedron Lett*, 1986; 27:4945–8.

23. Kumar S., Nirajan M.S., Chaluvvaraju K.C., Jamakhandi C.M., Kadadevar D. *Journal of Current Pharmaceutical Research*, 2010; 01:39–42.

Biosorption Of Heavy Metals By Using Fungi Isolated From Contaminated Soil

Sangavai C, Senthil Manikkam J, Shameena

Dhanalakshmi Srinivasan College Of Arts And Science For Women (Autonomous),Perambalur-621212.

Abstract: Microorganisms have been reported to extract heavy metals from wastewater Contaminated soil through bioaccumulation and biosorption. An attempt was, therefore, made to isolate fungi from sites contaminated with heavy metals for higher tolerance and removal from soil. Four different fungal isolated viz:*A. niger*, *A. flavus* and *A. fumigatus* and *T. viride* were isolated from the soil sample using the plate culture technique. All the isolates were shown to exhibit heavy metals tolerance by growing in heavy metals such as molybdate, silver nitrate, manganese chloride, and Mercury chloride amended medium separately. The biosorption of heavy metals potential by the fungi was determined by measuring the growth biomass and optical density (OD). In soon of concentration, the maximum Uptake of 86.21 mg/g of molybdate was observed in *T. viride*. Maximum uptake of molybdate (12.5mg/g) was found in *A. fumigatus* minimum uptake of molybdate (12.5mg/g) found in *A. niger*. The maximum Uptake in 5ppm concentration (43.85mg/g) of silver nitrate was observed in *T. viride*. Minimum uptake of silver nitrate (14.2mg/g) was observed in *A. niger*. In 10ppm concentration the maximum Uptake (57.14mg/g) and minimum uptake (25mg/g) were observed in *T. viride* and *A. niger* respectively *A. fumigatus* was unable to uptake the silver nitrate higher concentration.

Keywords: Heavy metals, Cadmium, Lead, Nickel, Manganese, *A. niger*

INTRODUCTION

Heavy metals contamination has been recognized as a major environmental concern due to its pervasiveness and persistence. As they are not biodegradable, there is a crucial need to develop techniques, which should be efficient, economical, and rapidly deployable in a wide range of physical settings like chemosensors in general, and sensorsbased conducting polymers in particular. Heavy metals are a group of metals and metalloids that have relatively high density and are toxic even at ppb levels ¹. Heavy metals can also cause kidney damage. After exposure to heavy metals, the excretion of low-molecular-weight proteins increases. In addition, heavy metals also have the potential to increase the formation of kidney stones and the risk of cancer. ² On the other hand, soil pollution is due to contamination from domestic and industrial pollutants. Some common soil pollutants are solvents, hydrocarbons, and heavy metals. Fossil fuels also cause contamination to soil and water. Common sources of fossil fuel pollution include petrochemical plants, power-generating plants, petroleum refineries, the production and distribution of fossil fuels, road transport (i.e., motor vehicles), and aircraft industries. ^{2,15}.

Heavy metals soil contamination and toxicity

Soil pollution can be both deliberate and not. Deliberate pollution includes wastewater irrigation, pesticides, animal manures, fertilizers, leaded paint, mine ore waste (mine tailing), sewage sludge, spillage of petroleum distillates, coal combustion residues, waste dumpings. These metals present in the soil cause risks to all the biosphere and are taken up through direct ingestion, absorbed by plants which can be hazardous both to the plant and also to the food chain that eats the plant, altering the properties of the soil such as the pH, color, porosity, and natural chemistry thus impacting the quality of the soil, and also contaminating the water ^{3,16}.

Heavy metals	Toxicity
Fe,Mo,Mn	Low toxicity
Zn, Ni, Cu, V,Co,W,Cr	Average toxicity
As, Ag, Sb,Cd,Hg,Pb,U	High toxicity

MATERIALS AND METHODS

Collection of soil samples

For the present research work, the soil samples were collected from the various industrial effluent soil sampling sites. Two sampling areas were identified, based on the extent of heavy metals and their bi-products pollutants being discharged. Soil samples were collected in new sterile plastic bags and kept on iceboxes during transportation. The samples were stored at 4°C in the refrigerator for isolation of fungi. The metal tolerant fungi were isolated from industrial effluent soil by using PDA. The suppress the bacterial growth, streptomycin, (30mg/lit) was added in the medium. The medium was allowed to solidify, and then the plates were put in an inverted position for 24 hours at room temperature ^{4,17}. The fungal isolates from the PDA plate were identified based on the microscopically examined.

Screening of fungal Isolates for Tolerance to Heavy Metals (Munees and Mulgeta 2013)

Heavy metal tolerant fungal isolates were further screened for tolerance to Sodium molybdate, Silver nitrate, Maganenes

chloride, and Mercury chloride at 3 ppm of heavy metals individually on PDA. All the fungal isolated were streaked on a PDA medium containing 3 ppm of each of the four heavy metals separately. Streaking of fungal isolates on normal PDA medium served as control (normal growth) for comparison of growth of fungal isolates on PDA medium containing different concentrations of heavy metals. Observations on the growth of fungal isolate were made after 72 h of incubation. The growth of fungal isolates was recorded as growth or absent growth in comparison to control.

Metal biosorption assay

The heavy metal bioadsorption by filamentous fungi was determined using the standard procedure ^{5,18}

Preparation of Adsorbent

100ml of the PD broth 20ml of potato extract and 2 gm of glucose were added in a conical flask and were made up to 100ml with distilled water. Flask was tightly closed with a cotton plug and then aluminum foil and autoclaved at 121°C and 15 psi for 20minutes. Later on, the flask was opened under laminar flow and fungus was inoculated into each flask. The flasks were agitated on a rotatory shaker for 3-4 days at 150 rpm and 30C temperature. After 3-4 days thick beds of fungal biomass were developed and used for further biosorption experiments.

Uptake of Heavy Metals by fungal Isolates from Liquid Media

Potato dextrose broth containing different concentrations of 5, 10, and 15 ppm heavy metals was dispensed in 20 ml into to 100ml conical flask and sterilized at 15 lbs/psi for 15 min. This flask was inoculated with the mycelia plugs of isolated fungus and put on a shaker at 150 rpm at 28±2C for 7 days. For each heavy metal, control was maintained only with Potato dextrose medium with an appropriate fungal culture. Fungal growth was harvested by filtration using Whatman filter paper No.2 after 7 days. The harvested fungal biomass was rinsed with double distilled water 3-4 times and dried in a hot air oven at 80°C for 18h. The heavy metal concentration in the filtrate was estimated ^{6,19}. The uptake of heavy metal by fungal biomass was calculated using the following equation

$$qe(\text{mg/g}) = \frac{C \times V \times 100}{W}$$

qe:concentration of heavy metal accumulated by fungal biomass,(mg/g) C: concentration of heavy metal(ppm)
V:(ml) the volume of the aqueous medium W:(g) is the dry weight of the fungal biomass.

Determination of optical density

The optical density of fermented broth was determined 1st and 7th days of treatment.

The calculation of optical density is as follows as Initial OD- final OD×100

Initial OD

Effect of different pH uptake in heavy metals by fungal isolated from liquid media

Potato dextrose broth containing different concentrations of 5,10 and 15 ppm heavy metals were dispensed in 20ml into 100ml conical flasks, as described earlier and the pH was adjusted to 3, 5, 9, and 11 and sterilized at 15 lbs/psi for 15 min. These flasks were inoculated with the mycelia plugs of isolated fungus and put on the shaker at 150 rpm at 28±2C for 7 days. For each heavy metal, control was maintained only with Potato dextrose medium with an appropriate fungal culture. The harvested fungal biomass was rinsed with double distilled water 3-4 times and dried in the hot air

RESULTS

Isolation of metal tolerant fungi

From the soil sample collected from heavy metal contaminated industries were subjected to plating technique for mycological examination a total number of four fungal colonies were isolated. They were represented by morphologically distinct four micro fungi. All of them were three species such as *A.niger*.*A.flavus*. and *A.fumigatus* followed by one species from the *Trichoderma* genera was *T.viride* (table 1; plate 1)

Screening of heavy metal tolerant fungi

The isolated four fungal cultures *A. Niger*. *A. Flavus*. And *A. fumigatus* and *T.viride* were screened for their heavy metal tolerant by growing in heavy metals such as molybdate, silver nitrate, manganese chloride, and Mercury chloride amended medium Separately, All the fungal isolated were showed growth on the particular heavy metal amended medium and the potential of fungi in heavy metals degradation were determined by measuring the biomass and optical density (Table 2; plate 2) Growth and uptake of heavy metals by the fungi from liquid media Growth and uptake of heavy metals by the fungi were determined by measuring the biomass and optical density (OD) using a spectrophotometer. The result showed various levels of difference

between the fungi and in the concentration (Table 3 -6; plate 3-6).

Uptake of heavy metals by *A.niger* from liquid media

The biosorption capacity of *Aspergillus fumigatus* isolates towards the various heavy metals was investigated. the fungal isolated with 5ppm concentration of heavy metals and the uptake of molybdate. Silver nitrate manganese chloride and Mercury chloride were 12.5, 14.2, 16.67, and 14.29 mg/g and their optical density was recorded as 8.3, 52.38, 0.0, and 22.22 respectively. While in 10ppm concentration molybdate uptake was 33.3 mg/g silver nitrate and manganese chloride uptake was recorded as 25 mg/g, and it was failed to uptake the mercury chloride. The OD measurement was observed as 28.57, 27.28, 23.08, and 40.0% for molybdate silver nitrate, manganese chloride, and Mercury chloride respectively by the fungi

Uptake of heavy metals by *A.flavus* from liquid media

The biosorption by *A. flavus* isolates when grown at 5ppm concentration of molybdate silver nitrate manganese chloride and Mercury chloride the uptake capacity was recorded as 27.7, 25, 41.6, and 25 mg/g and OD was 20, 61.6, 18.1, and 27.78 respectively. In 10ppm concentration molybdate uptake was 50mg/g manganese chloride uptake was recorded as 25 mg/g and Mercury chloride uptake was 55.6 mg/g and it was inefficient for uptake of silver nitrate. the degradation efficiency of molybdate, silver nitrate, manganese chloride, and Mercury chloride by the fungi was observed as 7.1, 6.09, 38.46 and 10%.

Uptake of heavy metals by *A.fumigatus* from liquid media

The uptake of heavy metals such as a molybdate, silver nitrate, and manganese chloride by *A.fumigatus* was found to be 41.6, 37 and 38.rmg/g in 5ppm concentration while in 10ppm concentration of molybdate and manganese chloride fungal uptake was recorded as 55.5 and 54.mg/g *A.fumigatus* was unable to uptake the silver nitrate and Mercury chloride in higher concentration in 5ppm concentration the degradation efficiency of molybdate, silver nitrate manganese chloride, and Mercury chloride by the fungi was observed as 14.9, 28.6, 10.2, and 24% while in 10ppm concentration it was 5.8, 23.3, 25.5 and 3.6%.

Uptake of heavy metals by *T.viride* from liquid media

In the investigation, the biosorption of molybdate, silver nitrate manganese chloride, and Mercury chloride by the fungi *T.viride* was analyzed in 5ppm concentration and it was observed that 86.21, 43.85, 40.32, and 25mg/g and OD was measured as 38.5, 4.7, 3.8 and 23.3%. the culture was grown at 10ppm concentration of the same heavy metals the uptake level by the fungi was recorded as 50, 57.14, 64.51, and 50mg/g, and the optical density was observed as 29.5, 3.7, 1.7, and 22.8%

Table 1 Identification of fungal isolates.

S.NO	Strain No	Fungal name
1	SL1	<i>Aspergillus niger</i>
2	SL2	<i>Aspergillus flavus</i>
3	SL3	<i>Aspergillus funigatus</i>
4	SL4	<i>Trichoderma viride</i>

Table:2 Preliminary screening of heavy metal(5ppm conc) degradation test by plate assay.

Heavy metals	Fungal isolates	Biosorbents of heavy metals
Sodium molybdate	<i>Aspergillus niger</i>	+
	<i>Aspergillus flavus</i>	+
	<i>Aspergillus funigatus</i>	+
	<i>Trichoderma viride</i>	+
Silver nitrate	<i>Aspergillus niger</i>	+
	<i>Aspergillus flavus</i>	+
	<i>Aspergillus funigatus</i>	+
	<i>Trichoderma viride</i>	+
Manganese Chloride	<i>Aspergillus niger</i>	+
	<i>Aspergillus flavus</i>	+
	<i>Aspergillus funigatus</i>	+
	<i>Trichoderma viride</i>	+
Mercury chloride	<i>Aspergillus niger</i>	+
	<i>Aspergillus flavus</i>	+
	<i>Aspergillus funigatus</i>	+
	<i>Trichoderma viride</i>	+

Table 3 Growth(mycelia biomass) of *Aspergillus niger* in different heavy metal concentrations supplemented within PD medium.

Heavy metal	Concentration(ppm)	Mycelial Biomass(g)	Dry biomass(g)	% of growth
Sodium molybdate	5	4.3	0.8	12.5
	10	6.2	0.6	33.3
Silver mitrate	5	8.1	0.7	14.2
	10	5.9	0.8	25
Manganese chloride	5	3.0	0.6	16.67
	10	5.4	0.8	25
Mercury chloride	5	5.9	0.7	14.29
	10	0.2	-	-
Control		6.6	0.8	-

Table 4: Growth(mycelia biomass) of *Aspergillus flavus* in different heavy metal concentrations supplemented within PD medium.

Heavy metal	Concentration(ppm)	Mycelial Biomass(g)	Dry biomass(g)	% of growth
Sodium molybdate	05	9.9	0.9	27.7
	10	7.5	1.0	50
Silver mitrate	0.5	6.6	1.0	25
	10	0.5	-	-
Manganese chloride	0.5	6.0	0.6	41.6
	10	10.1	0.9	55.6
Mercury chloride	0.5	11.9	1.0	25
	10	8.2	0.9	55.6
control		4.7	0.9	-

Table 5 Growth(myceliabiomass) of *aspergillus fumigatus* in different heavy metal concentrations supplemented within PD medium.

Heavy metal	Concentration(ppm)	Mycelial Biomass(g)	Dry biomass(g)	% of growth
Sodium molybdate	5	6.2	2.4	41.6
	10	8.4	3.6	55.5
Silver mitrate	5	3.6	2.7	37.6
	10	-	-	-
Manganese chloride	5	4.8	2.6	38.4
	10	5.8	3.7	54.0
Mercury chloride	5	-	-	-
	10	-	-	-
control		7.8	5.4	-

Table 6 Growth (mycelia biomass) of *Trichoderma viride* in different heavy metal concentrations supplemented within PD medium.

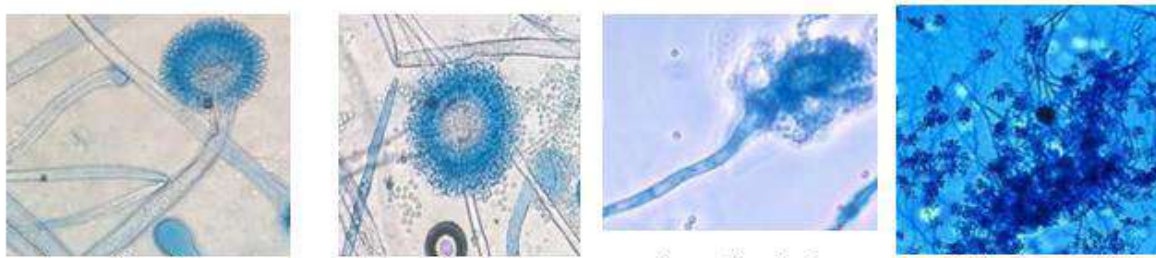
Heavy metal	Concentration(ppm)	Mycelial Biomass(g)	Dry biomass(g)	% of growth
Sodium molybdate	05	3.2	0.29	86.21
	10	3.5	0.4	50
Silver mitrate	05	4.6	0.57	43.85
	10	3.8	0.35	57.14
Manganese chloride	05	05	0.62	40.32
	10	04	0.31	64.51
Mercury chloride	05	4.4	0.4	25
	10	4.2	0.4	50
control		3.8	0.35	-

Table 7: Biosorbents of heavy metal(%) in flask trails.

Name of the fungi	Concentration (ppm)	Molybdate (%)	Silver nitrate (%)	Manganese Chloride (%)	Mercury Chloride(%)
Aspergillus niger	05	8.3	52.38	-	22.22
	10	28.57	27.28	23.08	40.0
Aspergillus flavus	05	20	61.9	18.1	27.78
	10	7.1	6.9	36.46	10

Aspergillus funigatus	05	14.9	28.6	10.2	24
	10	5.8	23.3	25.5	3.6
Trichoderma viride	05	38.5	4.7	3.8	23.3
	10	29.5	3.7	1.7	22.8

Plate 1: Isolated fungal species from microscopy.



Aspergillus niger

Aspergillus flavus

Aspergillus fumigatus

Trichoderma viride

Plate 2: Preliminary screening test for heavy metals tolerance by Plate assay



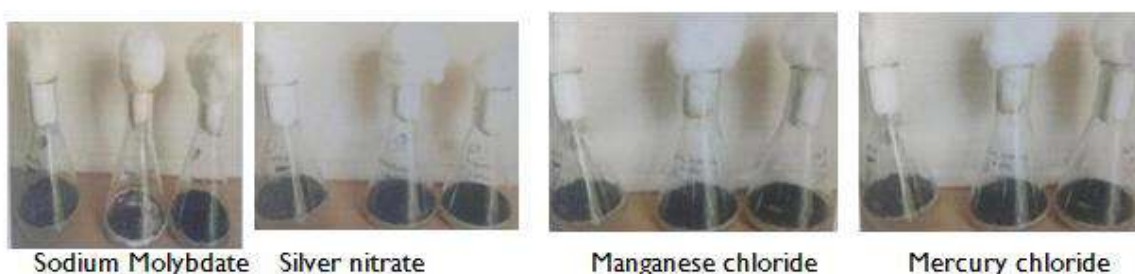
Manganese chloride

Sodium Molybdate

Silver nitrate

Mercury chloride

Plate 3: Aspergillus niger growth in PD broth supplemented with different heavy metals (con. At 5& 10 ppm)



Sodium Molybdate

Silver nitrate

Manganese chloride

Mercury chloride

Plate 4: Aspergillus flavus growth in PD broth supplemented with different heavy metals (con. At 5& 10 ppm)



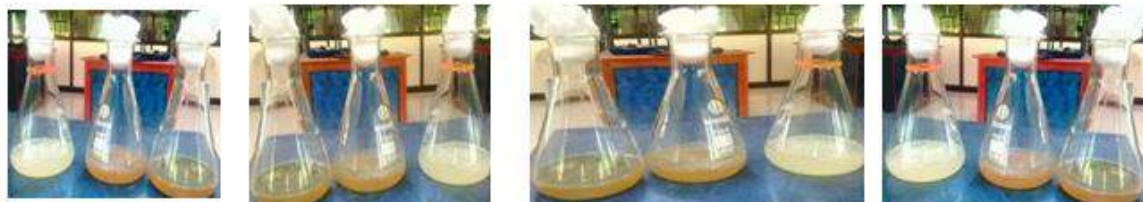
Sodium Molybdate

Silver nitrate

Manganese chloride

Mercury chloride

Plate 5: Aspergillus fumigatus growth in PD broth supplemented with different heavy metals (con. At 5 & 10 ppm)

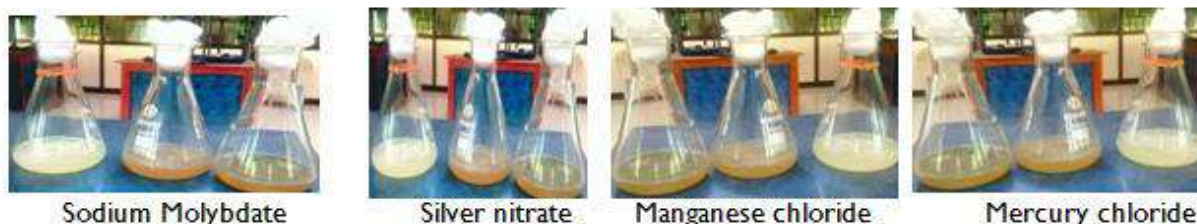


Sodium Molybdate

Silver nitrate

Manganese chloride

Mercury chloride

Plate 6: *Trichoderma viride* growth in PD broth supplemented with different heavy metals (con. At 5 & 10 ppm)

Sodium Molybdate

Silver nitrate

Manganese chloride

Mercury chloride

Increased use of metals and chemicals in process industries has resulted in the generation of large quantities of effluent that contain a high level of toxic heavy metals. Their presence due to lack of proper disposal poses environmental problems due to their non-degradable and persistent nature. These metals enter into human beings and animals through the food chain and cause many metabolic disorders ^{7,8}. Using microorganisms as biosorbents for heavy metals is an attractive alternative to existing methods such as chemical precipitation, chemical oxidation or reduction, electrochemical treatment, filtration, ion exchange, and membrane technologies for toxicity reduction and recovery of valuable metals from industrial effluents, because of good performance and low-cost biosorbent materials ¹⁹. The process may be ineffective or expensive, especially when dissolved heavy metals concentration in the solution ranged. Bioremediation of heavy metals involving microorganisms could be brought about by employing methods such as bioaccumulation, biosorption, bio-precipitation, and uptake by purified biopolymers from microbial cells ^{9,20}

Isolation of metal tolerant fungi

Heavy metal-resistant microbes might be present in heavy metal contaminated sites. The resistance and efficiency of microbes for the removal of heavy metals vary greatly. Therefore, there is a need to isolate and screen heavy metal tolerant fungi and bacteria from heavy metals contaminated sites. Thus, in the present investigation four isolates *Aspergillus niger*, *Aspergillus flavus*, *Aspergillus fumigatus*, and *Trichoderma viride* were identified as heavy metal contaminated soils. Similarly, seventy-six fungal isolates tolerant to heavy metals were isolated from samples of sewage, sludge, and industrial effluent contaminated with heavy metals such as Pb, Cd, Cr, and Ni using standard methods ^{10,21}. This proved that the fungi are capable of growing in heavy metal contaminated soils. Fungi constitute a high proportion of the microbial biomass in soil. Being widespread in the soil the large surface-to-volume ratio and high metabolic activity, fungi can contribute significantly to heavy metal dynamics in soil ^{11,21}

Screening of heavy metal tolerant fungi

The biosorption of heavy metals ions by microorganisms is a promising property with a great potential for industrial applications. The mechanisms of biosorption are beyond the scopes of the research and can be found elsewhere ^{12,22}. Fungal enzymes degrade heavy metals by incorporating them into their metabolic pathways and by utilizing them as their carbon and energy source. All the isolates were streaked and the PDA medium served as control (normal growth) for comparison of growth of fungal isolates on PDA medium containing heavy metals. Observations on the growth of fungal isolates were made after 72 hrs of incubation. The growth of fungal isolates was recorded as normal growth or absent growth in comparison to control. Four isolates tolerant to heavy metals were isolated from soil samples *Aspergillus niger*, *Aspergillus flavus*, *Aspergillus fumigatus* and *Trichoderma viride* was found tolerant to sodium molybdate, silver nitrate, manganese chloride, and mercury chloride.

Growth and uptake of heavy metals by fungal isolates from liquid media

Biosorption commonly refers to the technique of passive radioactive elements or metallic ions by active and denatured biomass. These biological agents possess the property of metal-sequestering and can be utilized to reduce metal ions concentration in the aqueous solution even from ppb level. In the present study highly tolerant filamentous fungal *Aspergillus niger*, *Aspergillus flavus*, *Aspergillus fumigatus*, and *Trichoderma viride* heavy metal polluted soil were checked against heavy metals viz; molybdate, silver nitrate, manganese chloride, and mercury chloride were further evaluated for their growth tolerance to at 5 and 10 ppm of heavy metal concentrations. The biosorption capacity may vary extensively and mainly it is depending upon the metal ions and biosorbent involved in the process, the use of denatured biomass can be of great concern. With these dead biomasses, heavy metal ions were accumulated on cell walls, while no specific molecules were found as particular sites for metal chelating. In the present investigation, the biosorption capacity using different fungal isolates was influenced by the concentration of metal ions.

Similarly, another study reported the investigation of *Aspergillus niger* biosorption that is reflecting a similar pattern of biosorption^{13,23}. Biosorption techniques employing microbial biomass as biosorbent as both alive and heat-killed dead biomass of several filamentous fungi (*Mucor spp.*, *Aspergillus spp.*, *Penicillium spp.*, *Rhizopus spp.*) have been employed^{14,24}.

CONFLICT OF INTEREST

Conflict of interest declared none.

REFERENCE

1. Abdulwahab RH (2015) Fungal biosorption and tolerance of heavy metals Agric Sci Technol 5:77–80
2. Ali H, Khan E, Ilahi I (2019) Environmental chemistry and ecotoxic and heavy metals and the kidney. Critical Care Nephrology (Third Edition), pp 1324–1330.34(2):406–413
3. Masindi V., Muedi K.L. (2018) Environmental contamination by heavy metals ,Heavy Metals, InTech 115.
4. Cheesbrough M (2006) District laboratory practice in tropical countries. Part Cambridge University Press, CambridgeMartin S, Griswold W. Human health effects of heavy metals. *Environmental Science and Technology Briefs for Citizens*. 2009
5. Yan G. and Viraraghavan T. (2000) Effect of Pretreatment on the Biodsorption of Heavy Metals on *Mucor rouxi*. Water South Africa Journal, 26, 119-123.
6. Munees A, Mulgeta K (2013) Recent trends in microbial biosorption of heavy metals: a review. Indian J Exp Biol 1(1):19–26.
7. Malik, A. (2004) Metal Bioremediation through Growing Cells. Chemosphere, 30, 261-278.
8. Abdullah Luqman Chuah , Abdullah Luqman ChuahA. JumasiahAzni Idris, Azni Idris, S.Y. Thomas Choong (2005), Rice Husk as a Potentially Low-Cost Biosorbent for Heavy Metal and Dye Removal: An Overview. Desalination 175(3):305-316.
9. Chaney RL, Angle JS, Broadhurst CL, Peters CA, Tappero RV (2007) Improved understanding of hyper-accumulation yields commercial phytoextraction and phytomining technologies. J Environ Qual 36:1429–1443.
10. Solarask, S., May, T., Roddick, F.A. and Lawrie, A.C. (2009) Isolation and screening of natural organic matterdegrading fungi, Chemosphere 75, 751-758.
11. Sosak-Swiderska, B. (2010). Effect of heavy metals on soil fungi. EGU General Assembly 2010, held 2-7 th. May, 2010 in Vienna, Austria.
12. Chang, J.S., Law, R. and Chang, C.C.(1997):—Biosorption of lead, copper and cadmium bybiomass of *Pseudomonas aeruginosa* PU 21,|| Water Research 31, 1651–1658
13. Ahmed, M. M. M.; Abdalla, H. A., 2005. Use of different nitrogen sources in the fattening of yearling sheep. Small Rumin. Res., 56 (1-3): 39-45
14. Ahmad, S.T., Joyce, M.V., Boggess, B., O'Tousa, J.E. (2006). The role of *Drosophila ninaG* oxidoreductase in visual pigment chromophore biogenesis. J. Biol. Chem. 281(14): 9205–9209.
15. Ahemad A, Malik A (2012) Bioaccumulation of heavy metals by zinc resistant bacteria isolated from agricultural soils irrigated with wastewater. Bacteriol J 2:12–21.
16. Bahobil A, Bayoumi RA, Atta HM, El-Sehrawey MM (2017) Fungal biosorption for cadmium and mercury heavy metal ions isolated.
17. Rosen C.J.(2002) *Lead in the home garden and urban soil environment*, Communication and Educational Technology Services, University of Minnesota Extension.
18. Khodadoust, K. R. Reddy, and K. Maturi,(2004) “Removal of nickel and phenanthrene from kaolin soil using different extractants,” *Environmental Engineering Science*, vol. 21, no. 619.G. W. Yang, “Laser ablation in liquids: applications in the synthesis of nanocrystals,” *Progress in Materials Science*, vol. 52, no. 4, pp. 648–698, 2007.
20. B. Nagaraj, N. B. Krishnamurthy, P. Liny, T. K. Divya, and R. Dinesh, “Biosynthesis of gold nanoparticles of *Ixora coccinea* flower extract & their antimicrobial activities,” *International Journal of Pharma and Bio Sciences*, vol. 2, no. 4, pp. 557–565, 2011.
21. M. Kowshik, S. Ashtaputre, S. Kharrazi, et al., “Extracellular synthesis of silver nanoparticles by a silver-tolerant yeast strain MKY3,” *Nanotechnology*, vol. 14, no. 1, pp. 95–100, 2003.
22. M. N. Nadagouda and R. S. Varma, “Green and controlled synthesis of gold and platinum nanomaterials using vitamin B2: density-assisted self-assembly of nanospheres, wires, and rods,” *Green Chemistry*, vol. 8, no. 6, pp. 516–518, 2006
23. Hsueh PR. New Delhi Metallo-β-lactamase-1 (NDM-1): an emerging threat among Enterobacteriaceae. *J Formos Med Assoc*. 2010;109(10):685–687.
- 24.. Poole K. Mechanisms of bacterial biocide and antibiotic resistance. *J Appl Microbiol*. 2002;92(suppl):55–64.

Synthesis, Characterization Of Pyrazole, And Biological Activities

V.Bhakyajothi¹, R.Elayaperumal¹, Dr T.Adinaveen¹, S.Suguna¹

¹Dhanalakshmi Srinivasan college arts and science for women (Autonomous), Perambalur Tamilnadu-621212

Abstract: To synthesize novel bio-active Pyrazole. The synthesis sequence followed the eco-friendly green chemistry technique (Grindstone method). The synthesis sequences are illustrated by novel eco-friendly and inexpensive catalyst FeCl_3 . synthesis of pyrazole analogs. To be reported here is a simple but effective procedure for the synthesis of pyrazole analogue via multi-component cyclo condensation reaction. Monitoring the completion of reaction with the help of the TLC (Thin-layer chromatography) technique. To characterize the final product by FT-IR (Fourier-transform infrared spectroscopy), ^1H NMR (Proton nuclear magnetic resonance), and ^{13}C NMR (Carbon-13 nuclear magnetic resonance) spectral analysis. The synthesized compound was further evaluated for antifungal activity.

Keywords: Pyrazole, FeCl_3 , FT-IR, ^1H NMR, Heterocyclic compounds and Anti fungal activity

INTRODUCTION

Heterocyclic compounds

A heterocyclic compound is a cyclic compound that has atoms of at least two different elements as members of its ring(s). The counterparts of heterocyclic compounds are homocyclic compounds, the rings of which are made of a single element. Although heterocyclic compounds may be inorganic, most contain at least one carbon. Since in organic chemistry non-carbons usually are considered to replace carbon atoms, they are called heteroatom, meaning different from carbon and hydrogen (rings of heteroatom of the same element are homocyclic). Heterocyclic compounds can be usefully classified based on their electronic structure. The saturated heterocycles behave like the acyclic derivatives. Thus, piperidine and tetrahydropuran are conventional amines and ethers, with modified steric profiles. Therefore, the study of heterocyclic chemistry focuses especially on unsaturated derivatives, and the preponderance of work and applications involves unstrained 5- and 6-membered rings. Included are pyridine, thiophene, pyrrole, and furan. Another large class of heterocycles is fused to benzene rings, which for pyridine, thiophene, pyrrole, and furan are quinoline, benzothiophene, indole, and benzofuran, respectively. The fusion of two benzene rings gives rise to a third large family of compounds, respectively the acridine, dibenzothiophene, carbazole, and dibenzofuran. The unsaturated rings can be classified according to the participation of the heteroatom in the pi-system.¹⁻⁷ Pyrone derivatives are present in natural products. Kojic acid, for example, is an antibiotic derived from the action of certain molds on starches or sugars. The steroid bufotalin and its poisonous ester bufotoxin are obtained from the skin glands of toads. The benzopyrylium cation is the parent of a large number of natural products. Chroman, or 3,4-dihydro-2H-1-benzopyran, is itself not found in nature, but the chroman unit is present in many natural products. Vitamin E (α -tocopherol), a substituted chroman, is found in plant oils and the leaves of green vegetables, whereas coumarin, or 2H-1-benzopyran-2-one, is used in perfumes and flavorings, and its derivative dicoumarin (dicumarol, or discoumarol), a blood anticoagulant, are products of living organisms. The most convenient method is the Claisen-Schmidt condensation of equimolar quantities of aryl-methyl ketone with aryl aldehyde in the presence of alcoholic akali. Chalcones are used to synthesize several derivatives like Flavones, pyrazolines, 3-chlorochromones, 1,5-benzothiazepines, and having different heterocyclic ring systems.

MATERIAL AND METHODS

General materials and characterization techniques

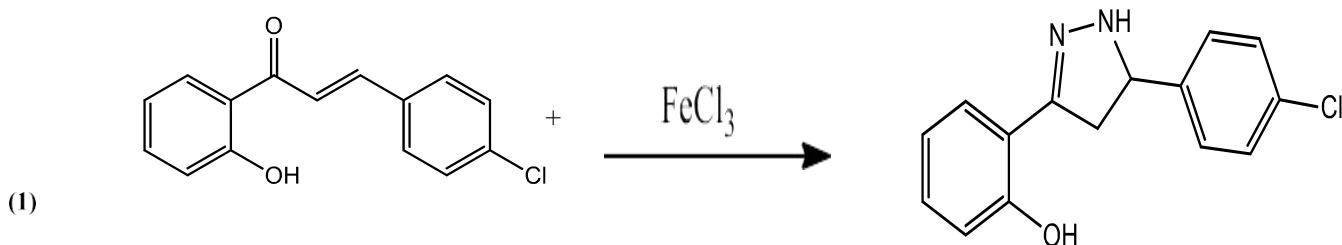
All materials were purchased from Nice and Loba chemicals. Chemistry: Melting points were recorded in open capillary tubes and were uncorrected. The IR spectra (KBr) were recorded in KBr on a shimadzu 8201pc (4000-400 cm^{-1}). The ^1H NMR and ^{13}C NMR spectra were recorded on a JEOL-300 MHz. The Elemental analysis (C, H, and N) were recorded using an Elemental analyzer model (Varian EL III). The purity of the compounds was checked by thin-layer chromatography (TLC) with silica gel plates. A general method for the synthesis of pyrazole (2) via multi-component cyclo condensation reaction. The reactants 3-(4-chlorophenyl)-1-(2-hydroxyphenyl)prop-2-en-1-one (1) (0.002mol, 0.5g), hydrazine hydrate (0.001mol, 0.5mL) and FeCl_3 (0.002mol, 0.3g) were mixed together in a pestle and mortar. The reaction was monitored by TLC. After the completion of the reaction indicated by TLC the reaction mixture was cored into ice-cold water. The brown-colored precipitate was formed it is filtered and dried. The product was recrystallized in ethanol to get pure product 2-(5-(4-chlorophenyl)-4,5-dihydro-1H-pyrazol-3-yl)phenol (2) Brown solid; mw: 272.73; m.p. 240°C; IR (cm^{-1}): 3275.52 (NH), 2922.0 (Ph-CHstr), 2854.76 (CH₂), 1565.31 (C=N); $^1\text{H-NMR}$ (400 MHz, CDCl_3): δ = 10.8 (1H, s, OH), 9.20 (1H, s, NH), 6.9-7.3 (8H, m, Phenyl ring), 4.64 (1H, s, -CH), 3.80 (2H, s, -CH₂); $^{13}\text{C-NMR}$ (100 MHz, CDCl_3): δ = 157.0 (1C, C=N), 152.70, 137.8, 137.2, 102.1 (12C, Ph), 60.8 (1C, -CH), 45.0 (1C, -CH₂). Elemental analysis: Calcd. For $\text{C}_{15}\text{H}_{13}\text{ClN}_2\text{O}$: Elemental Analysis: C, 66.06; H, 4.80, N, 10.27 %; Found: C, 66.03; H, 4.80; N, 10.30 %.

Biological screening Antifungal activity

The minimal inhibitory concentration (MIC) was determined by the broth microdilution method according to the Clinical and Laboratory Standards Institute (CLSI) (The National Committee for Clinical Laboratory Standards). *In vitro* antifungal activity of the final compounds 1 and 2 were evaluated against standard strains; *Aspergillus Niger*, *Microsporum audouinii*, *Cryptococcus Neoformans* and *Candida albicans*. The antibacterial and antifungal assays were performed in Mueller–Hinton broth and Sabouraud dextrose broth, respectively. All the synthesized compounds were weighed (10 mg), dissolved in DMSO (250 μ L), and diluted with water (750 μ L) to prepare the stock solutions of 10 mg/mL. The serial dilution from 2048 to 1 μ g/mL was made in a 96-well plate. Fifty μ L of a bacterial suspension, obtained from a 24 h culture (~106 cfu/mL) was added to each well with a final DMSO concentration of 1:16. The plates were incubated at 35 °C for 24 h. We tested ceftazidime as antimicrobial agents for quality control of the method. Each experiment was carried out in duplicate.⁸⁻¹²

RESULTS AND DISCUSSION

The synthesis of pyrazole was illustrated in scheme 1. The optimization in catalysts were shown in Table 1. Compound 2 was synthesized by the condensation method. The formation of all the compounds was confirmed by recording the IR, ¹H NMR, ¹³C NMR spectra, and elemental analyses. The IR spectra of compound 2 showed absorption bands at 3275.52, 2922.00 and 1565.31 cm^{-1} confirms the presence of NH, Ph-CH, and C=N groups, respectively. The ¹H NMR spectra of compound 2 showed a sharp singlet at δ 9.20 for NH proton and a singlet at δ 4.64 for -CH- proton. The ¹³C NMR spectra of compound 2 showed characteristic peaks at δ 157.0, 60.80 and 45.0 ppm corresponding to C=N, CH, and CH₂ carbons, respectively.



Scheme 1: Synthetic route of proposed compound (2)
Table 1: Optimization of catalyst.

S. No.	Catalysts	Yield (%)		
		0.5 Mole %	1 Mole %	2 Mole %
1	TiCl ₂	-	-	-
2	SnCl ₂	-	-	48
3	ZnCl ₂	13	37	46
4	ZrOCl ₂	-	-	10
5	CuCl ₂	19	38	68
6	FeCl ₃	42	92	-

Antifungal activity

The compounds 1 and 2 were evaluated for antifungal activity against four different fungal species. The final compound 2 shows remarkable antifungal activity than compound 1. Compound 2 shows high antifungal activity in two fungal species namely *C. albicans* and *M. audouinii*. Compound 2 with the MIC value of 03 μ g/mL was highly active than control clotrimazole with the MIC value of 06 μ g/mL in *C. albicans*.²⁰ Compound 2 with the MIC value of 02 μ g/mL shows high antifungal activity than clotrimazole with the MIC value of 03 μ g/mL in *M. audouinii*.¹³⁻¹⁹ The results were summarized in

Table 2. Antifungal activity of compounds 1 and 2

Compds	MIC (μ g/mL)			
	<i>Aspergillus Niger</i>	<i>Candida albicans</i>	<i>Microsporum audouinii</i>	<i>Cryptococcus Neoformans</i>
1	34	28	53	16
2	56	03	02	28
Clotrimazole	01	06	03	05

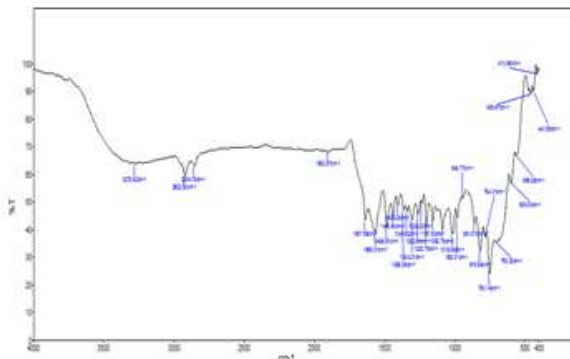


Figure 1: IR spectrum of compound 2.

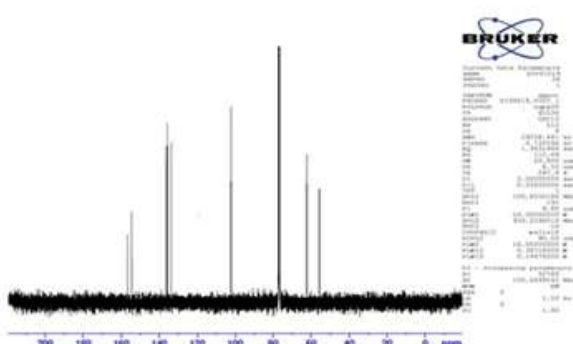


Figure 2: ^1H NMR spectrum of compound 2.

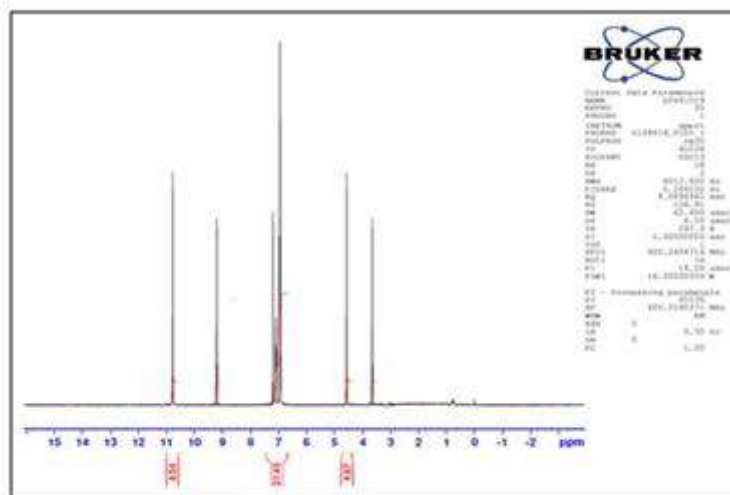


Figure 3: ^{13}C NMR spectrum of compound 2

CONCLUSION

In conclusion, the synthesis of pyrazole (2) via one-pot multi-component cyclo condensation reaction by using novel (Grindstone method). Synthesized pyrazole derivative was confirmed by FT-IR, ¹H NMR, and ¹³C NMR spectral analysis. The compounds 1 and 2 were further evaluated for antifungal activity. The results show that the pyrazole derivative 2 has remarkable activity in fungal strains. This concludes that compound 2 can act as a fungicide in the future.

CONFLICT OF INTEREST

Conflict of interest declared none.

REFERENCES

1. Campagne E; "Adrien Albert and the Rationalization of Heterocyclic Chemistry", *J Chemical Education* 1986, Volume 6, 860. doi:10.1021/ed063p860.
2. Katritzky A R and Boulton J A; "Advances in Heterocyclic Chemistry", Vols. I to 27, (Ed.), Academic Press, New York (1963-1980).
3. Weissberger A; "The Chemistry of Heterocyclic Compounds", Vols. I to 29, (Ed.), Wiley Interscience, New York (1950 to 1975).
4. Katritzky A R; "Physical Methods in Heterocyclic Chemistry", Vols. I to 5, (Ed.), Academic Press, New York (1963 to 1973).
5. Elderfield R C; "Heterocyclic Chemistry", Vols. I to 9, (Ed.), Wiley, New York (1950 to 1967).
6. Joule J A and Smith G F; "Heterocyclic Chemistry", Van Nostrand Reinhold Co., 2nd Ed, London (1978).
7. Weast R C and Astle M J; "C. R. C. Handbook of Chemistry and Physics", (Eds.), C. R. C. Press, Inc., 63rd Ed, Florida U. S. A. (1983).
8. Fletcher J H, Dermer O C, and Fox R B; "Nomenclature of Organic Compounds, Principles, and Practice", American

Chemical Society Washington, D. C., *Adv. Chem. Ser.*

- 9. Katritzky A R; "Handbook of Heterocyclic Chemistry", Pergamon Press, New York (1985).
- 10. Gilchrist T L; "Heterocyclic Chemistry", Pitman London (1985).
- 11. McNaught in A. D; "Advances in Heterocyclic Chemistry", Vol. XX, Katritzky A R, and A J, Boulton (Eds.), Academic Press, New York (1976) 175.
- 12. Newkome G R and W W Pandler; "Contemporary Heterocyclic Chemistry", John Wiley, New York (1982).
- 13. Katritzky A R; "Comprehensive Heterocyclic Chemistry", Vol. 1-8.
- 14. Coffee BS; "Rodd's Chemistry of Carbon Compounds", Vol. IV, Part A, (Ed.), Elsevier, London
- 15.. M. Kowshik, S. Ashtaputre, S. Kharrazi, et al., "Extracellular synthesis of silver nanoparticles by a silver-tolerant yeast strain MKY3," *Nanotechnology*, vol. 14, no. 1, pp. 95–100, 2003.
- 16. M. N. Nadagouda and R. S. Varma, "Green and controlled synthesis of gold and platinum nanomaterials using vitamin B2: density-assisted self-assembly of nanospheres, wires, and rods," *Green Chemistry*, vol. 8, no. 6, pp. 516–518, 2006
- 17. Hsueh PR. New Delhi Metallo- β -lactamase-1 (NDM-1): an emerging threat among Enterobacteriaceae. *J Formos Med Assoc.* 2010;109(10):685–687.
- 18. Poole K. Mechanisms of bacterial biocide and antibiotic resistance. *J Appl Microbiol.* 2002;92(suppl):55–64.
- 19. Jayaraman R. Antibiotic resistance: an overview of mechanisms and a paradigm shift. *Curr Sci India.* 2009;96(11):1475–1484.

Effect Of Treated Tannery Effluent On *Acalypha Indica* - A Pilot Study

Haseena M, Senthil Manikkam J, Sangavai C, Kaleeswari Sudha, Nandhini S

Dhanalakshmi Srinivasan College of Arts And Science For Women (Autonomous), Perambalur-621212.

Abstract: Tannery effluent creates various waste products depending upon the process used. Tannery water creates a lot of nutritional and growth promotion demand for Soil and Plants. The present study deals with the physical and chemical parameters of treated tannery effluent and analyses the morphological, Biochemical, Antibacterial activity, and Phytochemical analysis of *Acalypha Indica* plant samples. The present study deals to compare and analyze the pollution effect on the plant growing in the unpolluted and polluted areas.

Keywords: Tannery effluent, Wastewater analysis, Heavy metals, Antibacterial activity, and Phytochemical analysis.

INTRODUCTION

Disposal of sewage and industrial effluents causes a serious pollution problem to water bodies and agricultural lands¹. The increasing requirement of leather and its products led to the establishment of large Commercial tanning industry due to the growth of the population². In tannery Industry during the process skin to leather, chemicals like chromium, Sodium chloride, sulphate, calcium salt, ammonium salts, sodium sulphide, alkali, acids, fat, liquor and organic dyes and large amount of water is used. Excess amount of dissolved salts, high BOD & COD are contained in the resultant effluents³. Chromium is considered to be toxic to living organisms amongst heavy metals⁴. Biologically non-essential systems such as higher level of heavy metals, highly acidic pH and low levels of nutrients can cause toxicity in the soil for the growth of vegetation⁵. The chromium concentration of plants that are grown in the area of treated tannery effluent was determined and it was found to be a high concentration of chromium⁶. The higher level of metal (iron, nickel, chromium, zinc, cadmium, manganese, and copper) that are present in the treated tannery wastewater will contaminate the agricultural soil. It causes serious health hazards when the coops and vegetables are consumed by the consumer⁷. *Acalypha indica* is a plant for indicating environmental pollution and as a suitable plant for phytoremediation reported⁸. The pollution from the effluents of leather industries is a major environmental and social concern, which results in extremely high values of TSS, TDS, TS, BOD, COD, Cd, Ni, Cr, and Pb⁹. The treated tannery effluent has a higher chromium concentration than the discharge limit. Even at low concentrated chromium effluent discharge continuously can disrupt the food chain by causing a toxic effect on aquatic life¹⁰. Cr > Ni > Zn > Cu was the order of levels of heavy metals in the industrial wastewater. The aquatic system or agricultural fields pose a risk of transfer into the food web when those heavy metals are discharged¹¹. Tannery waste should be treated effectively before release, which may cause a major hazard that affects the drinking water¹². The disposal of sewage and industrial effluents from uncontrolled urbanization causes a serious pollution problem when disposed into the water bodies. Heavy metals are difficult to remove from the environment, unlike many other pollutants¹³. The most prominent sources of chromium were tanneries which can cause pollution to the aquatic environment. Wastewater from tanneries contaminates surface water and sediments to an unacceptable level, if not treated adequately¹⁴.

AIM & OBJECTIVES

Therefore, the present study was carried out with the following objectives Identification, selection, and collection of *Acalypha indica* plants that are widely and luxuriously grown in natural and tannery industrial areas Measure the Total solids, Total dissolved solids, and suspended solids in the Treated Tannery effluent, Determination of chloride, Hardness, Calcium, Magnesium, pH in the effluent and Soil sample. Qualitative phytochemical analysis and Antibacterial activity of *Acalypha indica* grown in natural and tannery industrial areas, Assess the environmental demands of wastewater by COD

MATERIALS AND METHODS

Tannery Water Analysis

Collection of Tannery Water Sample

The treated tannery water was collected from KMM Leather Factory located at Sempat, Tiruchirappalli. It was collected in a plastic container and taken to the laboratory for further analysis.

Analysis of Physico-Chemical Parameters

The Effluent Physical characters of color, pH, total suspended solids (TSS), total dissolved solids (TDS), Total Hardness, and Chemical Oxygen Demand were carried out by simple laboratory method¹⁵. The chemical parameters of Chloride, Magnesium, Calcium(Ca. and Sulphate(SO₄²⁻) were determined by wastewater examination of standard APHA methods¹⁶.

Soil Analysis

The polluted soil sample was collected from the treated tannery effluent area at KMM Tannery, Tiruchirapalli, Tamil Nadu. The normal soil sample was collected from Green House at Dhanalakshmi Srinivasan College of Arts and Science for Women (Autonomous), Perambalur, Tamil Nadu, India. It was taken to the laboratory & stored for further analysis. Physico-Chemical Parameters of color, Texture, pH & Chloride were analyzed in the polluted soil sample¹⁷.

Plant analysis

Collection of Plant Sample

The polluted plant sample was collected from the treated tannery effluent area at KMM tannery industry, Tiruchirapalli, Tamil Nadu, and the normal plant sample was collected from Green House at Dhanalakshmi Srinivasan College of arts and science for women (Autonomous), Perambalur, Tamil Nadu. The plant sample was taken to the laboratory and stored for further analysis.

Morphological Analysis

The stem length and diameter of both polluted and normal plant was measured for each species using a measuring scale. Root length, lamina length, lamina width, number of leaves, and node of both the plant's leaves were further measured using the method suggested¹⁸.

Plant extract preparation

The leaves of both polluted and normal plants were dried and then ground to a fine powder with a blender machine. The extraction was done at room temperature. The powder was soaked in absolute ethanol at a 1:20 ratio for seven days and then filtered by Whatman filter paper number 1. The extracts were stored at 4°C for further use¹⁹.

The pH of Leaf extracts

1g of fresh leaf sample of both plants was homogenized. The extracts were centrifuged at 5000rpm for 10 minutes. The supernatant was collected and the pH was measured by a digital pH meter.

Bacterial Culture

A bacterial culture is a method of bacteria organisms by following them to reproduce in predetermined culture media under controlled laboratory conditions. Both gram-positive and gram-negative bacteria were taken for Antibacterial screening. The bacterial colony were cultured freshly on a nutrient broth and incubated for 24 hours at 37°C. Then the cultures were used for Antibacterial screening²⁰.

Disc Diffusion Method

The disc diffusion method was used for antibacterial activity. The plant extract was then impregnated into sterile, blank discs 6mm in diameter. 5ml of the extract was spotted alternately on both sides of the discs and allowed to dry before the next 5ml was spotted to ensure precise impregnation. All the discs were fully dried before the application on the bacterial lawn. Ethanol was used as a control disc. Antibacterial activity was evaluated by measuring the diameter of the inhibition zone around the discs. Antibacterial activity was expressed as the mean zone of inhibition diameter (mm) produced by the leaf extract²¹.

Phytochemical Analysis

The *Acalypha* leaves were subjected to phytochemical screening such as Carbohydrates, Alkaloids, Flavonoids, Glycosides (Quinones, Phenols, Terpenoids, Tannins, Anthraquinones, Steroids²²). (Harborne, J. B. (1998) and Saponins .

RESULT

Tannery water Analysis

The physical and chemical analysis of wastewater reveals the characteristics of the tannery effluent in table I. The effluent of wastewater was dark brown. The color was found to be 1.54 in the wavelength of 400nm and 760nm. The wastewater pH was measured by using a pH meter. It was slightly neutral 6.96. The chemical oxygen demand was measured to be very low in the wastewater. The chemical oxygen demand was found to be – 1,086.1 mg/l in the contaminated tannery wastewater. The amount of chloride in the wastewater was 6,770 mg/l¹². Calcium, magnesium, and sulphate cause the permanent hardness of the wastewater. Hardness was estimated by using the titration method. The total hardness in the wastewater sample was calculated to be 640 mg/l²³. The total solids were measured by using an unfiltered wastewater sample via the evaporation method. The total solids were found to be 114.84 mg/l. The dissolved solids are a measure of iron dissolved in the tannery wastewater²⁴. Dissolved solids were measured by using the evaporation method. The total dissolved solids were estimated to be 74.54 mg/l. Suspended solids are the total solids suspended in the wastewater²⁵. The suspended solids were measured by using the

evaporation method. The total suspended solids were found to be 40.3 mg/l in the tannery wastewater. Calcium is a chemical parameter of wastewater. The calcium was estimated by using the titration method. The calcium content in the wastewater was found to be 228 mg/l. Magnesium is a chemical parameter of waste water. The value of Mg was calculated by subtracting the value of calcium from the total hardness. The magnesium content in waste water found to be 412 mg/l.

Table 1. The physical and chemical analysis of waste water		
S. No	Parameters	Result
1	Colour	1.55
2	pH	6.95
3	COD	-1058.1 mg/l
4	Chloride	6740.95 mg/l
5	Total Hardness	641 mg/l
6	Total Solids(TS)	114.94 mg/l
7	Total Dissolved Solids(TDS)	73.54 mg/l
8	Total Suspended Solids(TSS)	41.3 mg/l
9	Calcium	229 mg/l
10	Magnesium	411 mg/l

Soil Analysis

The physical and chemical parameters of both polluted and normal soil samples were analyzed. The color of the polluted soil sample was black whereas the normal soil sample was brown. The texture of the polluted soil sample was oily clumsy and the texture of the normal soil sample was crumbled with less moisture. The pH of the polluted soil sample was 6.18 and the normal soil sample pH was found to be 6.56. The amount of chloride present in both polluted and normal soil samples was found to be 8,596.6 mg/l and 70.9 mg/l.

Table 2- Morphological analysis of normal and polluted <i>Acalypha indica</i>			
S. No	Part of the plants	Normal plant	Polluted plant
1	Stem length	25cm	21cm
2	Stem diameter	0.5cm	0.3cm
3	Root length	0.9cm	0.7cm
4	Leaf length	0.6cm	0.5cm
5	Leaf diameter	0.4cm	0.3cm
6	No. of leaves	55	48

Plant Analysis

Morphological analysis of plant sample

The plant root length, stem length, stem diameter, leaf length, leaf diameter, and number of leaf count by using a measuring scale. The plant size was measured. The morphological measurement was measured to both polluted and normal plant samples. The results were evaluated in (Table 2).

Table 3- Antibacterial activity of normal and polluted <i>Acalypha indica</i>			
S. No	Culture Name	Normal plant (cm)	Polluted plant (cm)
1	<i>E. Coli</i>	1.7	2.2
2	<i>Salmonella paratyphi</i>	1.1	1.6
3	<i>Pseudomonas aeruginosa</i>	1	2.1
4	<i>Klebsilla aerogenes</i>	1.5	1.6
5	<i>Streptococcus pneumonia</i>	1.9	2.5
6	<i>Staphylococcus aureus</i>	1.7	2.0
7	<i>Bacillus cereus</i>	1.4	1.7

Leaf extract pH

The pH of the plant leaf extract was measured by using a pH meter. The polluted plant and normal plant pH were measured. The pH of the polluted plant leaf extract was found to be 6.48 whereas that of normal plant pH was found to be 6.76

Antibacterial activity

The antibacterial activity of ethanolic extract of *Acalypha indica* of both polluted and normal plant leaves were shown significant zone of inhibition against both Gram-positive and Gram-negative Bacteria. The result of the zone of inhibition were evaluated in (Table 3).

Phytochemical analysis

The study of phytochemical analysis of *Acalypha indica* was done for the screening of active medicinal chemical constituents in both polluted and normal plant samples²⁶. The result of the phytochemical analysis of *Acalypha indica* of both plant samples were evaluated in (Table 4).

Table 4 – Phytochemical analysis of normal and polluted <i>Acalypha indica</i>			
S. No	Test	Normal plant	Polluted plant
1	Alkaloids	+	-
2	Terpenoids	+	-
3	Tannins	+	+
4	Anthraquinones	-	-
5	Saponins	+	+
6	Carbohydrate	-	-
7	Flavonoids	+	+
8	Glycosids	+	-
9	Quinones	-	-
10	Phenol	-	+
11	Steroids	+	-

DISCUSSION

The waste water and plant growing in the soil contaminated with waste water viz.. *Acalypha indica* were collected with kind permission from KMM tannery Trichy. And their colour, pH, total solids (TS), chemical oxygen demand (COD), chloride, Total hardness, Total dissolved solids(TDS), Total suspended solids(TSS), calcium and magnesium were determined²⁷. The physico chemical characteristics were analyzed. The color of wastewater was dark brown with value of 1.54 thus indicating the presence of various chemicals and organic matter in the effluent²⁸. The pH of the sample was found to be 6.96. It is nearly neutral. The COD was found to be -1068.1(mg/l). Calcium was found to be 228(mg/l) and the chloride content of the sample was found to be 6770(mg/l). The total hardness of the sample was found to be 640(mg/l). And these values indicate that the sample is contaminated with high organic content as evidenced by the works of ²⁸⁻²⁹. The *Acalypha indica* species plant collected from normal soil exhibited a length of 25 cm. The same plant collected from soil polluted with tannery effluent exhibited a length of 21 cm. The normal plant showed a higher length than that of the polluted sample. The normal plant leaf diameter was found to be 0.5cm which was higher than the polluted plant 0.3cm. The normal plant showed a higher number of leaf counting of 55 than that of polluted plants³⁰. Biochemical analyze were performed on both samples. The leaf extracts of *Acalypha indica* from normal and polluted areas showed negligible differences in their pH. Both plant leaf extracts were exhibited near-neutral pH. The Antibacterial activity of both polluted and normal plant extract of *Acalypha indica* shows that the zone of inhibition is higher with normal plant extract than with polluted plant extract. The phytochemical analysis of *Acalypha indica* shows the presence of alkaloids, terpenoids, glycosid and steroids which of these substances were present in normal plant extract but these substances shows absence in the polluted plant extract. Whereas tannins, saponins, and flavonoids are present in both normal and polluted plant extract. And anthraquinones, carbohydrates, glycosides were shown absent in both the plant extract. The results indicate that the tannery effluent pollution affects the normal growth of the plant. The plant sequester chromium at a high level and accumulate Cr in the leaf rather than the other parts of the plant. These results point out the plant taken for the study can be considered as a potential candidate for phytoremediation in further studies.

CONCLUSION

The wastewater and plant sample *Acalypha indica* species were collected from the KMM tannery industry, Semmbat, Tiruchirapalli, TamilNadu. The wastewater physical and chemical, parameters of color, pH, total solids (TS), chemical oxygen demand(COD), Chloride, Total hardness, Total dissolved solids, Total suspended solids, calcium, and magnesium were analyzed. All the results indicated that the wastewater is highly contaminated. The polluted plant was compared to the normal *Acalypha indica* species plant collected from Dhanalakshmi Srinivasan College of Arts and Science for Women (A), Perambalur. The polluted plant morphological, biochemical, Antibacterial activity, and phytochemical analysis sequestration were analyzed. The Antibacterial activity and phytochemical analysis content showed a decreased level than a normal plant. These analyses showed that the plant can play a role in phytoremediation after further potential studies.

CONFLICT OF INTEREST

Conflict of interest declared none.

REFERENCE

1. Singh, S., Eapen, S. and D Zouza, S.F., 2006 Cadmium accumulation and its influence on lipid peroxidation and antioxidative system in an aquatic plant, *Bacopamonnieri L. Chemosphere* 62,233-246.
2. Singh, R. K; Kumar, S. and Kumar, A. 2008, [17 K Ramasamy, S Mahimairaja, R Naidu. OR remediation of soils contaminated with chromium due to tannery waste disposal. Chapter 28. DL Wise et al. Eds. Remediation Engineering of Contaminated Soils, 2000, 583-615, Dekker, Inc, New York.
3. J. Jawahar, M. Chinnadurai, J. K. S. Ponselvan, and G. Annadurai, "Pollution from tanneries for treatment of effluent," *Indian Journal of Environmental Protection*, vol. 18,pp.

4. Rout, G.R., S. Samantary and P. Das(1998), Differential chromium tolerance among eight mungbean cultivars grown in nutrient culture, *J. Plant Nutr.*, 20: 473-483.
5. M Brar; SS Malhi; AP Singh; CL Arora; KS Gill, *Can. J. Soil Sci.*, 2000, 80, 465-471.
6. A.I. Zouboulis, P. Samaras, A. Ntolia, K. Goudoulas(2000), Division of Chemical Technology, Department of Chemistry, Aristotle University of Thessaloniki, Thessaloniki 54124, Greece Department of Pollution Control Technologies, Technological Educational Institute of West Macedonia, Kozani 50100, Greece 2000.
7. Mohanta, M. K., Salam, M. A., Saha, A. K., Hasan, A. and Roy, A. K., 2010. Effects of tannery effluents on survival and histopathological changes in different organs of *Channa punctatus*. *Asian Journal of Experimental Biological Sciences*, 1(2), 294-302.
8. Das, A.K., F.Ahmed, N.N. Biswas, S. Dev, M.M. Masud, 2005. Diuretic Activity of *Acalypha indica*. *Dhaka Univ J Pharm Sci*, 4:1-2 31
9. Manjushree Chowdhury & M. G. Mostafa &Tapan Kumar Biswas &Abul Mandal & Ananda Kumar Saha (2015), Springer International Publishing Switzerland.
10. H. Oliveira(2012, "Chromium as an environmental pollutant: insight on induced plant toxicity: a review," *Journal of Botany*, Article ID 375843, 8 pages, 2012.
11. Kisku.G.C.S.C.Baraman and SK.Bhargava(2000), "contamination of soil and plants with potentially toxic elements irrigated with mired industrial effluent and its impact on the environment" *water Air soil pollution.*, 120,121-137.
12. Alebel Abebe Belay(2010), Impacts of chromium from tannery effluent and evaluation of alternative treatment options. *Environ Protection* 2010:1:53-8.
13. Rengel, Z., "Physiological mechanisms underlying differential nutrient efficiency of crop genotypes", In *Mineral nutrition of crops* (ed Rengel Z), pnp 231-269. Food Products Press, NY (1999). 11.
14. G. Durai and M. Rajasimman, 2011. *Biological Treatment of Tannery Wastewater - A Review*. *Journal of Environmental Science and Technology*, 4: 1-17.
15. Tolulope E. Aniyikaiye, Temilola Oluseyi, John O. Odiyo and Joshua N. Edokpayi(2019), *Physico-Chemical Analysis of Wastewater Discharge from Selected Paint Industries in Lagos, Nigeria*, *International Journal of Environmental research and public health*,16, 1235;
16. APHA (American Public Health Association) Standard Methods for the Examination of Water and Wastewater (20th Ed.), APHA, Washington, DC, USA (1998)
17. Kannan, K., Rajasekaran, G., Raveen, R. 2009. Bacterial analysis of soil samples collected in and around a sugar mill in Tamilnadu. *J. Ecobiol.*, 24: 191 195.
18. Khan, M.H.: Induction of oxidative stress and antioxidant metabolism in *Calamus tenuis* leaves under chromium and zinc toxicity. *Ind. J. Plant Physiol.*, 12, 353-359 (2007).
19. Karthy, E. S., Ranjitha, P., Mohankumar, A. (2009). Antimicrobial potential of plant seed extracts against multidrug resistant methicillin resistant *Staphylococcus aureus* (MDR-MRSA). *International Journal of Biology*, 1, 34-40.
20. Phurpa Wangchuk (2014), *Phytochemical analysis, bioassays, and the identification of drug lead compounds from the Bhutanese medicinal plants*, Research Online .
21. Sr. Prema Kumari Jonnada, Louis Jesudas and Varaprasad Bobbarala(2015), *Phytopharmaceutical Studies of Selected Medicinal Plants Subjected to Abiotic Elicitation (Stress) in Industrial Area*, Open access peer reviewed chapter, DOI: 10.5772/61891.
22. Harborne, J. B. (1998). *Phytochemical Methods*. London: Chapman & Hall.
23. Imran Ahmed, Muddasar Habib, Unsia Habib, Abdul Hai, and Amad Ullah Khan(2016), *Analysis and Treatment of Tannery Waste Water by using Combined Filtration and Coagulation Treatment Process*, *Proceedings of the Pakistan Academy of Sciences: Pakistan Academy of Sciences : B. Life and Environmental Sciences* 53 (3):179–183.
24. Abbas, M. Sarfraz, S. M. Mehdi, G. Hassan, and O. U. Rehman(2007), "Trace elements accumulation in soil and rice plants irrigated with the contaminated water," *Soil and Tillage Research*, vol. 04, no. 2, pp. 503-509.
25. Sharmila S, Jeyanthi Rebecca L and Md Saduzzaman(2013), Biodegradation of Tannery effluent using *Prosopis juliflora*, *International Journal of ChemTech Research CODEN(USA): IJCRGG ISSN : 0974-4290*, Vol.5, No.5, pp 2186-2192.
26. Vasantha, K. (2014). Antibacterial activity and Phytochemical Analysis of *Acalypha indica* L.. *International Journal of Pharmacy and Natural Medicines*. Vol.2. 151-155.
27. Bisschops and H. Spanjers, "Literature review on textile wastewater characterisation" (2003), *Environmental Technology*, Vol. 24. p p 1399-1411.
28. Gautam, S. and S.N. Pandey: Growth and biochemical responses of nickel toxicity on leguminous crop (*Lens esculentum*) grown in alluvial soil. *Res. Environ. Life Sci.*, 1, 25-28 (2008).
29. Radojevic M and Bashkin VN (2007), *Practical environmental analysis*. 2nd Ed. The Royal Society of Chemistry, UK.
30. Arifa zereen, abdul wahid, zaheer-ud-din khan and andleeb anwar sardar Department of Botany, GC University, Lahore, pakistan effect of tannery wastewater on the growth and yield of sunflower (*Helianthus annuus* L.) 2013.

Preliminary Phytochemical Screening And Antioxidant(In-Vitro) Activity Of *Centella Asiatica(L)* Leaves

**S.Suguna¹, V.Vijayakumar¹, S.Satheesh kumar¹, M.Hafila banu¹, V.Bakkiyajothi¹
Bindu Alex²**

¹Dhanalakshmi Srinivasan College of Arts and Science for Womens (autonomous) perambalur.621212

²Mar Ivanious College (Autonomous) Thiruvananthapuram,Kerala,India

Abstract : Numerous physiological and biochemical processes within the physical body may produce oxygen centered free radicals and other reactive oxygen species as byproducts. More production of such free radicals can cause oxidative damage to biomolecules (e.g. lipids, proteins, DNA), eventually leading to many chronic diseases like atherosclerosis, cancer, diabetes, aging, and other degenerative diseases in human. Plants (fruits, vegetables, medicinal herbs, etc.) may contain a good sort of radical scavenging molecules, like phenolic compounds (e.g. phenolic acids, flavonoids, quinones, coumarins, lignans, stilbenes, tannins), nitrogen compounds (alkaloids, amines), vitamins, terpenoids (including carotenoids), and a few of endogenous metabolites, which are rich in antioxidant activity. The intake of natural antioxidants has been related to reduce risks of cancer disorder, cardiovascular disease, diabetes, and other diseases related to aging. The present study is to investigate the in-vitro antioxidant activity of the plant *Centellaasiatica L*

Key words: *Centellaasiatica*, free radicals, oxidants, bio molecules.

INTRODUCTION

Oxidants are generated in aerobic organisms as byproduct of normal cellular metabolism. Oxidants have both beneficial and deleterious effects, like while they are essential for normal life, their excessive production has been linked to disease development¹⁻². In nature oxidants in two forms both molecular and free radical. Free radical is any atom, molecule or ion with one or more unpaired electrons and it is capable of independent existence. Free radicals are produced during oxidation/reduction reactions involving one electron transfer³⁻⁴, or when a covalent bond is broken and one electron from each pair remains with each group. For this presence of unpaired electron(s), free radicals are considerably more reactive and participate in a number of physiological and patho-physiological functions⁵⁻⁶. The most important class of radical species generated in living systems are oxygen derived radicals, which are referred as reactive oxygen species (ROS). In the etiology of several diseases like arthritis, cancer, atherosclerosis etc, free radicals play an important vital role⁷⁻⁸. The oxidative damage to DNA may play a vital role in aging and the presence of intracellular oxygen also can be responsible for initiating a chain of inadvertent reaction at the cellular level and these reactions cause damage to critical cell biomolecules. These radicals are highly toxic and thus generate oxidative stress in plants.⁹⁻¹⁰

MATERIALS AND METHODS

Plant source selected for the present study was *Centellaasiatica (L.)* Leaves of the selected plant was collected from in and around Trichy, identified with the help of Flora of Presidency of Madras and authenticated with the specimen deposited at RAPINAT Herbarium, Department of Botany, St. Joseph's college, Trichy.

IN - VITROANTIOXIDANT ASSAY (DPPH Radical scavenging Assay .

Antioxidant activity can be measured using DPPH radical scavenging assay method. Antioxidants react with DPPH, a stable radical that was reduced to DPPH: H form. The degree of discolouration indicates the scavenging potential of the antioxidant compound or solution.

1. Plant Extract	:	10mg/ 10ml
2. Phosphate buffer	:	pH 6.6
3. DPPH Solution	:	7.88mg/ 100ml
4. Ascorbic acid	:	10mg/ 100ml

The free radical scavenging capacity of the aqueous extract of *Pisoniaalba* Span. was determined by using DPPH. DPPH (200 μ M) solution was prepared in 95% methanol. From the stock plant extract solution (100,250,500,750 and 1000 μ g/ ml) were taken in five test tubes. 0.5ml of freshly prepared DPPH solution was incubated with a test drug and after 10 minutes, absorbance was taken as 517 nm using a spectrophotometer. Standard ascorbic acid was used as reference.

REDUCING POWER ASSAY (ManmohanSinghal et al., 2011)

1. Plant extract	:	50mg/10ml
2. Phosphate buffer	:	pH 6.6

3. Potassium ferricyanide	: 1g/100ml
4. Trichloroacetic acid	: 10mg/100ml
5. Ferric chloride	: 0.1g/100ml
6. Ascorbic acid	: 10mg/100ml

1 ml of varying concentrations (1-5 mg/ml) of extract was mixed with 2.5 ml phosphate buffer and 2.5 ml of potassium ferricyanide. The mixture was incubated at 50°C for 20 min. Aliquots of near 2.5 ml of trichloroacetic acid were added to the mixture, which was then centrifuged at 3000 rpm for 10min. The upper layer of solution (2.5 ml) was mixed with equal volume of distilled water, to this 0.5ml of freshly prepared ferric chloride solution was added and the absorbance was measured at 700 nm. Increased absorbance of the reaction mixture indicates an increase in reducing power.

NITRIC OXIDE SCAVENGING ACTIVITY

Nitric oxide (NO) was generated from sodium nitroprusside (SNP) and was measured by the Griess reagent. SNP in aqueous solution at physiological pH spontaneously generates NO, which interacts with oxygen to produce nitric ions that can be estimated by the use of Griess reagent.

1. Plant extract	: 10mg/10ml
2. Phosphate buffer	: 0.025M, pH 7.4
3. Sodium nitroprusside	: 5mM
4. Ascorbic acid	: 10 mg/100ml
5. Griess reagent	

Solution A: 0.1% naphthylethylenediaminedihydrochloride dissolved in dis. water

Solution B: 1% sulfanilic acid in 5% phosphoric acid A & B mixed in the ratio 1:1

Sodium nitroprusside (5 mM) in standard phosphate buffer solution was incubated with different concentrations (200-1000 μ g/ml) of the ethanol and aqueous plant extract dissolved in phosphate buffer (0.025 M, pH 7.4) and tubes were incubated at 25 °C for 5 hours. Control tube without the plant extract, but with an equivalent amount of buffer was maintained in an identical manner. After 5 hours, 0.5ml of the incubated solution was removed and diluted with 0.5ml of Griess reagent (1% sulfanilic acid, 5 % phosphoric acid, and 0.1 % naphthylethylenediaminedihydrochloride). The absorbance of the chromophore formed during diazotization of nitrite ions with sulfanilic acid and its subsequent coupling with naphthylethylenediamine was read at 546 nm.

ABTS⁺ RADICAL SCAVENGING ACTIVITY

1. Plant extract : 10mg/10ml
2. Phosphate buffer : 0.1M, pH 7.4
3. ABTS Solution
4. ABTS Solution (2Mm): 0.0274g of ABTS was dissolved in 25 ml of distilled water.
5. Potassium persulphate (70Mm): 0.0946g of potassium per sulphate was dissolved in 5ml of distilled water.
6. ABTS Reagent: ABTS reagent solution was mixed with 0.1 of potassium persulphate solution. The solution was stored in dark place for 2 hours.
7. Ascorbic acid: 10mg of ascorbic acid was dissolved in distilled water and made up to 100 ml using standard flask.

Varying concentration (20 - 100 μ g/ml) of plant extract and standard ascorbic acid solutions were taken into series of test tubes. 2ml of ABTS solutions was added and the volume was made up to 1ml with ethanol. To the control 2ml of ABTS solution and 1ml with ethanol was added. The solutions were read immediately at 734 nm.

SUPEROXIDE RADICAL SCAVENGING ACTIVITY

Reagents:

1. Plant extract: 10mg/10ml
2. NADPH: 468 μ m: 33.20mg NADPH was dissolved in 100 ml of distilled water.
3. Nitro blur tetrazolium: 156 μ m 12.75mg of NBT was dissolved in 100ml of distilled water.
4. Phenazinemethosulfate: 6 μ m 1.83mg of PMS was dissolved in 100ml of distilled water.
5. Phosphate buffer: pH7.8

Solution A (0.1M): 1.56g of mono sodium dihydrogen orthophosphate was dissolved in 100ml of distilled water.

Solution B (0.1M): 1.77g of dissolution hydrogen orthophosphate was dissolved in 100ml Of distilled water.

The phosphate buffer was prepared by mixing the solutions A and B adjusting pH7.8.

6. Ascorbic acid: 10mg of ascorbic acid was dissolved in distilled water and the volume made up to 100ml using standard flask.

Phenazinemethosulfate: nictotinamide adenine dinucleotide system was used for the generation of superoxide anion. 0.2-1ml of

ethanol and aqueous extract was mixed with 0.5ml NBT and 0.5ml NADH was mixed. The reaction mixture incubated at 25⁰ C for 5 minutes. After 5 minutes absorbance of the mixture was measured at 560nm against blank. The percentage of inhibition was determined by comparing the results of the control and test sample.

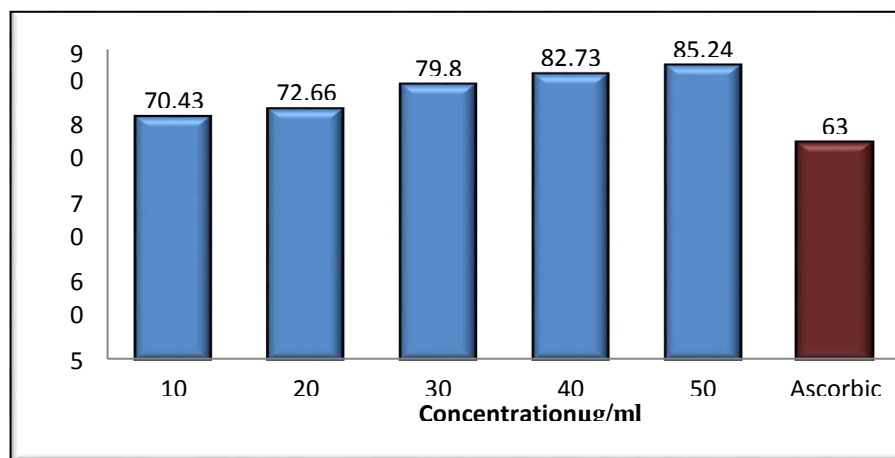
RESULTS AND DISCUSSION

INVITRO ANTIOXIDANT ACTIVITY OF CENTELLA ASIATICA (L.)

Table 1- DPPH Scavenging assay of Centellaasiatica (L.) leaves

S. NO	Concentration (µg/ml)	% Activity
1	10	70.43
2	20	72.66
3	30	79.8
4	40	82.73
5	50	85.24
6	Ascorbic Acid (30µg/ml)	63.00
IC50 Value = 7.0µg/ml		

Figure 1 – DPPH Scavenging potential of aqueous extract of Centellaasiatica (L.)



The result depicts the increased antioxidant effect on DPPH (Diphenyl -2- picrylhydrazyl) with increase in concentration of the test drug (10 – 50 µg/ml). The result was comparable with that of standard ascorbic acid¹¹⁻¹² The maximum percentage inhibition of DPPH radical was 85.24% at a concentration of 50µg/ml. The percentage of inhibition of DPPH is strongly dependent on concentration of plant extract. The mean IC50 Value of the plant was found to be 7.0µg/ml¹³⁻¹⁴.

Table 2 - ABTS⁺ inhibition potential of aqueous extract of Centellaasiatica (L.) leaves

S. NO	Concentration (µg/ml)	% Activity
1	10	26.6
2	20	41.1
3	30	67.7
4	40	88.8
5	50	94.4
6	Ascorbic acid (30 µg/ml)	72.5
IC50 Value =22.1 µg/ml		

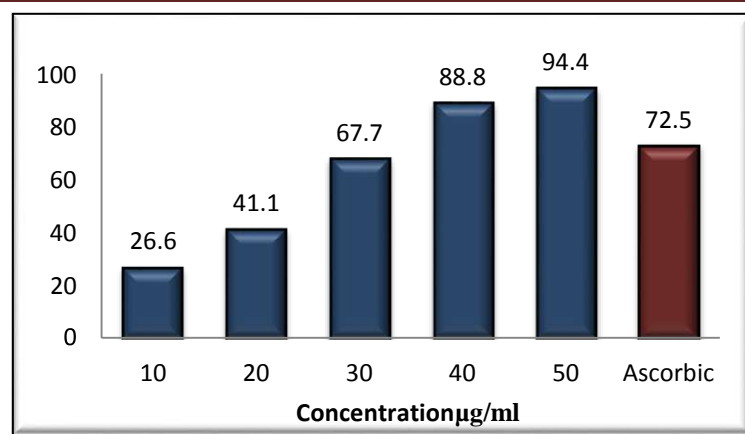


Figure 2 - ABTS⁺ Inhibition potential of aqueous extract of *Centellaasiatica* (L.)leaves.

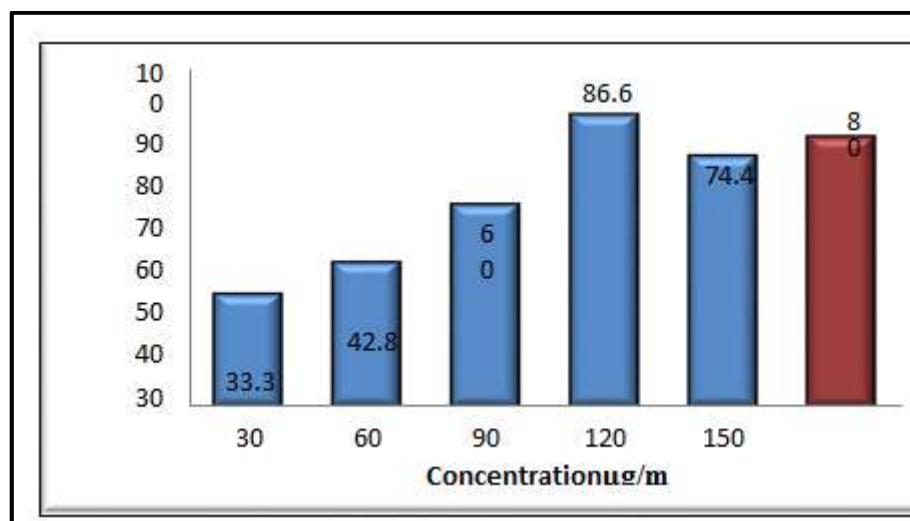
The ABTS cation radical which absorbs at 743 nm (giving a bluish- green colour) is formed by the loss of an electron by the nitrogen atom of ABTS (2,2'-azino-bis(3- ethylbenzthiazoline-6-sulphonic acid)¹⁵⁻¹⁶. This has a characteristic wavelength absorption spectrum. ABTS chemistry involves direct generation of ABTS radical mono cation with no involvement prior to addition of the antioxidant test system, rather than the generation of the radical taking place continuously in the presence of antioxidants¹⁷⁻¹⁸. From the Table - 2, it is found that the low concentration (10 $\mu\text{g/ml}$) showed 26.6 %. ABTS⁺ radical inhibition potentials were found at high concentration (50 $\mu\text{g/ml}$) which showed 94.4% activity. The result was comparable with that of standard ascorbic acid. The IC₅₀ value was found to be 22.1 $\mu\text{g/ml}$. Results are presented as the ability of phenols to scavenge 50% of free radical ABTS IC₅₀. ABTS radical cation was produced in the stable form using potassium persulphate. After getting the stable absorbance, the antioxidant plant extract is added to the reaction medium and the antioxidant power measured by studying decolorization¹⁹⁻²⁰.

Table 3 - Reducing power assay of aqueous extract of *Centellaasiatica* (L.) leaves.

S. No	Concentration ($\mu\text{g/ml}$)	% Activity
1	30	25
2	60	36.7
3	90	56.75
4	120	68.7
5	150	84.6
6	Ascorbic acid (30 $\mu\text{g/ml}$)	80
IC ₅₀ Value = 75 $\mu\text{g/ml}$		

From Table 3 it was known that the higher percentage (74.4%) of reducing power was visualized 150 $\mu\text{g/ml}$. The result was found to be constantly increasing with that of increasing concentration of the plant drug. The result was comparable with that of standard ascorbic acid. The IC₅₀ value was found to be 75 $\mu\text{g/ml}$.

Figure 3 - Reducing power assay of aqueous extract of *Centellaasiatica* (L.) leaves



CONCLUSION

From the literature review the plant was selected for their antioxidant potential. Hence in the present study the *Centellaasiatica* L. belonging to the family Apiaceae was selected and carried out for its free radical scavenging activity. Leaves of the selected plants material was authenticated, shade dried water extract were used to screen the antioxidant potentials, employing various in vitro assay procedures. Standardization is essential for global acceptance herbal medicine, hence phytochemical screening were determined for the plant drug under study as per the Indian Ayurvedic Pharmacopoeia.(IAS). Water extract showed dose dependent DPPH radical scavenging activity with IC₅₀ value of 70 μ g/ml respectively. The tested extract has the capacity to inhibit the NO radical production and scavenge the H₂O₂, superoxide radicals. The test drug also showed potent reducing power. To conclude that the findings of this study supports the view, the aqueous extract of *Centellaasiatica* L exhibited optimum levels of antioxidant activities in all models. It needs further studies that plant extracts endowed with potentially exploitable antioxidant activities.

CONFLICT OF INTEREST

Conflict of interest declared none.

REFERENCES

1. Halliwell, B.; Gutteridge, J. M. C. *Free Radicals in Biology and Medicine*, Clarendon Press, Oxford, 1993.
2. Nelson. D. L.; Cox, M. M. *Lehninger Principles of Biochemistry* (5th ed), Freeman,
3. H. & company, San Francisco, 2008.
4. Cadenas, E.; Davies, K. J. A. *Free Radic. Biol. Med.* 2000, 29, 222–230.
5. Kovacic, P.; Pozos, R. S.; Somanathan, R.; Shangari, N.; O'Brien, P. J. *Curr. Med. Chem.* 2005, 12, 2601–262.
6. Remacle, J.; Raes, M.; Toussaint, O.; Renard, P.; Rao, G. *Mutat. Res.* 1995, 316, 103–122.7. Droege, W. *Physiol. Rev.* 2002, 82, 47–95. Schreck, R.; Baeuerle, P. A. *Trends Cell Biol.* 1991, 1, 39–42.
7. Finkel, T. *Curr. Opin. Cell Biol.* 1998, 10, 248–53.
8. deMagalhaes, J. P.; Church, G. M. *Exp. Gerontol.* 2006, 41, 1–10.
9. 8.17.Cheeseman K.H. and Slater T.F. (1993) Free radicals in medicine. Churchill Livingstone 9. Pub. British Med. Bull., 49: 479-724.
10. 10.SulekhaMandal, SatishYadav, SunitaYadav, Rajesh Kumar Nema. *Antioxidants: A Review* Journal of Chemical and Pharmaceutical Research, 2009, 1 (1):102-104.
11. 11.V S Sangeetha , Vanith A, Devi P, BhakyajothiV"Green synthesis of Zinc oxide nano particle using flower extract of phyla nodiflora" Scholar National School of leadership vol-9
12. 12.Dormandy TL. Free-radical reaction in biological systems Annals of the Royal College of Surgeons of England (1980) vol 62,
13. 13.Yadav R and Agarwala M: Phytochemical analysis of some medicinal plants. *Journal of Phytology* 2011; 3: 10-14.
14. 14.R Elayaperumal , G Vanaja, A Vanith,VSSangeetha "Green synthesis of Glycyrrhizagla silver nano particle and conformation of through Microscopy and Spectrophotometric techniques. "Eurasian journal of Analytical chemistry ,2017-Feb ,1680-168
15. 15.Xavier J and Reddy J: A study on antioxidant and antibacterial activities of the fruit and seed extracts of two different cultivars of *Momordicacharantia* *J Pharmacogn Phytochem* 2017; 6: 1182-87.
16. Kartning T. Clinical Application of *Centella asiatica* (L.) Urb. in Craker L.E. and Simon J.E (eds.), *Herbs Spices and Medicinal Plants*. Vol. II. Oryx Press, Phoenix, AZ. 1988:145.
17. Satheeja Santhi.S, Jose.A, and Solomon.J, R.D (2010), Isolation and Characterization of antagonistic actinomycetes from Mangrove sediments, *International Journal of Current Research* , 3: 020-023.
18. Khan, M.; Choi, J.; Lee, M.; Kim, E.; Nam, T. Anti-inflammatory activities of methanol extracts from various seaweed species. *J. Environ. Biol.* 2008, 29, 465–469.
20. Zuercher, A.W.; Fritsché, R.; Corthésy, B.; Mercenier, A. Food products, and allergy development, prevention, and treatment. *Curr. Opin. Biotechnol.* 2006, 17, 198–203.

Phytochemical Analysis And Antimicrobial Activity Of *Cardiospermum Halicacabum* And *Coccinica Indica*

G.Vanaja¹ , Chinnasamy¹ , M.Srinivasan¹ , V. Bhakyajothi¹ , V.S.Sangeetha^{1,2}Dr Bindu Alex

¹Dhanalakshmi Srinivasan College Of Arts And Science For Women (Autonomous), Perambalur -621212

²Mar IvaniosCollege(Autonomous) ,Thiruvananthapuram,Kerala

Abstract: Many medicinal plants are distributed throughout the world out of which only some plants are known and most of them remain unidentified. The natural product chemists in the world try to explore them so that they can utilize them for the welfare of human being including disease. The research work is still in progress. As a part of them, the plants selected for our work were *Cardiospermumhalicacabum* and *Coccinicaindica*, commonly known as “mudakathan” and “kovai” respectively in Tamil. The first plant (mudakathan) is applied to rheumatism and stiffness of the limbs. The second plant (kovai) having a remarkable effect in reducing the amount of sugar in the urine of the patient suffering from diabetes mellitus. The dried leaves of the plants were analyzed for the presence of pharmacologically active ingredients using GC-MS The chromatograms were found to contain coumarin,propylgallate,tropane& methyl heptenol(for first plant) piperidine, hexenal and gallic acid (for second plant). Then the methanolic extract of the leaves of *Cardiospermum halicacabum* and *Coccinicaindica* were tested for its pharmacological activities

Keywords: *Cardiospermumhalicacabum*, *Coccinicaindica*, methanol, streptococcus and *Escherichia coli*

INTRODUCTION

Many plants synthesize substances that are useful to the maintenance of health in humans and other animals. These include aromatic substances, most of which are phenols or their oxygen-substituted derivatives such as tannins. Many are secondary metabolites, of which at least 12,000 have been isolated, a number estimated to be less than 10% of the total. In many cases, substances such as alkaloids serve as plant defense mechanisms against predation by microorganisms, insects and herbivores. Many of the herbs and spices used by humans to season food yield useful medicinal compounds. Natural compounds extracted from plants, particularly higher plants, have been suggested as alternative sources for antibiotics. The chemical features of these constituents differ considerably among different species. This approach is alluring, in part, because they constitute a potential source of bioactive compounds that have been professed by the general public as comparatively safe and often act at multiple and novel target sites, thereby reducing the potential for resistance. The screening and testing of extracts against a variety of pharmacological targets in order to benefit from the immense natural chemical diversity is a concern in many laboratories worldwide¹ The increased popularity of herbal treatments, the safety and effectiveness of alternative medicines have not been scientifically collaborated and remain largely unknown. A number of herbs are thought to be likely to cause adverse effects. Adulteration, inappropriate formulation, or lack of understanding of plant action and drug interactions have led to adverse reactions that are sometimes life threatening or lethal. Traditionally used medicinal plants produce a variety of compounds of known therapeutic properties. The substances that can either inhibit the growth of pathogens or kill them and have no or least toxicity to host cells are considered for developing new antimicrobial drugs. In recent years, antimicrobial properties of medicinal plants are being increasingly reported from different parts of the world. It is expected that plant extracts showing target sites other than those used by antibiotics will be active against drug-resistant microbial pathogens. However, very little information is available on such activity of medicinal plants. Medicinal plants of India Traditional medicines are used by about 60 per cent of the world's population. These are not only used for primary health care not just in rural areas in developing countries, but also in developed countries as well where modern medicines are predominantly used. While the traditional medicines are derived from medicinal plants, minerals, and organic matter, the herbal drugs are prepared from medicinal plants only. Use of plants as a source of medicine has been inherited and is an important component of the health care system in India. In the Indian systems of medicine, most practitioners formulate and dispense their own recipes; hence this requires proper documentation and research. In western world also, the use of herbal medicines is steadily growing with approximately 40 percent of the population reporting use of herbs to treat medical illnesses within the past year. Public, academic and government interest in traditional medicines is growing exponentially due to the increased incidence of the adverse drug reactions and economic burden of the modern system of medicine There are about 45,000 plant species in India, with concentrated hotspots in the region of Eastern Himalayas, Western Ghats and Andaman & Nicobar Island. The officially documented plants with medicinal potential are 3000 but traditional practitioners use more than 6000. India is the largest producer of medicinal herbs and is appropriately called the botanical garden of the world. There are currently about 250 000 registered medical practitioners of the Ayurvedic system (total for all traditional systems: approximately 291 000), as compared to about 700,000 of the modern medicine system. In rural India, 70 percent of the population is dependent on the traditional system of medicine, the Ayurveda. Secondary metabolism refers to compounds present in specialized cells that are not necessary for the cells survival but are thought to be required for the plants survival in the environment. These compounds are believed to aid plant fitness by preventing insect herbivory and pathogen attack as well as aiding reproduction through providing pollinator attraction as either floral scent or colouration. This requirement for secondary metabolites to have highly diverse biological activities has led plants to accumulate a vast catalogue of compounds. The catalogue in vascular plants is at least several hundred thousand secondary metabolites. Most of the secondary metabolite structural diversity is generated by differentially modifying common backbone

structures, with the derived compounds having potentially divergent biological activities. Differential modification of common backbone structures can alter the biological activity of a number of plant hormones and secondary metabolites including auxins, glucosinolates, gibberellins and phenylpropanoid derivatives. This modification of common backbone structures or precursors produces approximately 12 000 known alkaloid structures. One explanation for this modular diversity is that selection favours plants with newly derived defences when insects or other pests have evolved the ability to overcome existing defences. New defensive compounds can be synthesized by structurally modifying a toxic compound to evade the pest's counter-defence while maintaining the compound's toxic activity. The reiteration of this process over millennia may explain the vast range of plant secondary metabolic chemistry. In addition to aiding plant survival, this chemical diversity has led to the development of numerous medical treatments and assisted in significant nutritional advancements. The biological impact of small molecular changes is significant enough that the pharmaceutical industry is creating combinatorial chemistry technologies to generate the same structural diversity *in vitro*. Despite the biological and medical importance of structural variation, little is known about how plants generate this variation, why it has arisen and whether it impacts plant biology.

MATERIALS AND METHODS

Plant

Cardiospermum halicacabum and *Coccinia indica* herbs collected in March 2009 from Painganadu near Mannargudi, Tamil, India

Uses in traditional medicine

First Plant

The plant has been used in traditional medicine for the treatment of diaphoretic, diuretic, aperients, fever, emetic, bleeding piles, amenorrhoea, gonorrhoea, erysipelas and scorpion-sting. The plant belongs to the family Sapindaceae. The leaf has been used for rheumatism, lumbago, sore-eyes, snake-bite, cuts, injuries, dysenteries, diarrhoeas, headache, stiffness of the limbs and reducing swelling²⁻⁴.

Second plant

This plant belongs to the family Cucurbitaceae. These leaves are used to kapha, pitta, itching, biliousness, jaundice, fever, gonorrhoea, diabetes, reduce blood sugar, snake-bite, ear ache and ulcer.⁵⁻⁸

Chemical constituents

Coccinia indica weight contains as an enzyme with amylolytic properties a hormone and traces of an alkaloid and OMBUIN-3-ARABINOFRANOSE (triterpenoids)⁹⁻¹¹

Tested Material

Methanolic extract of two plant leaves.

Microorganism

- i. *Streptococcus*
- ii. *Escherichia coli*

Experimental Methods

Gc-Ms Study

These leaves were collected from Painganadu near Mannargudi, Tamil Nadu and then dried under shade. The dried leaves were then pulverized well in a Udy cyclone mill and 10 g of the powdered leaves were then soaked in 100% 45 ml of methanol. The supernatant was collected after 24 hours and stored at -20°C. The residue was re-extracted twice with 50% and 25% methanol using the same procedure. The collected supernatant was kept at -20°C till they solidified. The solidified samples were subjected to GC-MS¹⁹. Before analyzing the extract using, the temperature of oven, flow rate of the gas used and the energy of the electron gun was programmed initially. The temperature of the oven was 230°C. The gas used as carrier as well as an eluent was helium. The flow rate of helium was set to 1.4 ml/min. The electron gun of mass detector liberated electrons having energy of about 70 eV. The column employed here for the separation of components was Elite 1 (100% dimethylpolysiloxane). About 100 mg/ml of the methanolic extract was injected into the GC-MS using a micro syringe. Scanning was done for 45 minutes. A chromatogram was obtained with retention time in the abscissa, abundance of the peak in the ordinate (the time elapsed between injection and elution is called the "RETENTION TIME"). The retention time can help to differentiate between some compounds. Also from the mass spectral data, the compounds present in the extract were identified¹²⁻¹⁵.

Antimicrobial Activity

Disc diffusion method was adopted to study the anti-bacterial activity of plant extracts. Before starting inoculation all the

required instruments such as media containing culture tubes, sprit lamp, sterile water etc , were transferred to the laminar air flow chamber and the platform surface of the chamber was swapped with 70% alcohol¹⁸⁻¹⁹. After swapping , the uv light become “off” and on” the ordinary light. Before inoculation , hands were rinsed with 70% alcohol. Sterile What man No.1. Paper of discs were used. Discs were stored at 5°C prior to use. Tests were performed by the disc diffusion method. Extract impregnated discs were placed on culture inoculation agar plate and incubated either at 37 °C for 24 hours. Anti-bacterial activities were then measured indicated by the clear zones of inhibition¹⁶⁻¹⁸. Antibacterial screening of diffusion percentage of methanol plant extract of *Cardiospermumhalicacabum* and *Cocciniaindica* in terms of average zone of inhibition for streptococcus and *Escherichia coli*.

RESULTS AND DISCUSSION

The beneficial medical effect of plant materials typically result from the combination of the secondary products in the plants *Cardiospermumhalicacabum* and *Cocciniaindica*. The medicinal action of plants are unique to particular species or groups is consistent with this concept as the combination of secondary products in a particular plant are after taxonomically distinct. GC-MS study reveals that the components present the plants *Cardiospermumhalicacabum* and *Cocciniaindica* have possessed significant antimicrobial activity¹⁹

Table: I Phtocomponents Identified In the Methonolic Extract Of Plant *Cardiospermumhalicacabum* (Gc-Ms Study)

S.No	Name Of The Compound	Molecular Formula	Molecular Weight	Compound Nature	Activity
1	Coumarin	C ₉ H ₆ O ₂	146.14	Coumarin compounds	Anti-fungal, anti-plasmodial,anti-cancer,anti-microbial, anti-arrhythmic
2	Propyl gallate	C ₃ H ₉ Ga	130.82	Gallium	Anti-fungal, Anti-oxidant Anti-microbial
3	Tropane	C ₈ H ₁₅ N	125.211	Bicyclic compounds	Anti-protozol, Anti-cancer, Anti- viral drug design
4	Methyl heptenone	C ₈ H ₁₈ O	130.22	Alcohol compounds	Anti – oxidant, Anti- microbial ,Anti-fungi

Table: II Phtocomponents Identified In The Methonolic Extract Of Plant *Cocciniaindica* (GC-MS STUDY)

S.No	Name Of The Compound	Molecular Formula	Molecular Weight	Compound Nature	Activity
1	Piperidine	C ₅ H ₁₁ N	85.14	Alkaloids compounds	Cytotoxicity ,DNA Modifying
2	Propyl gallate	C ₆ H ₁₀ O	98.14	Ketone compounds	Anti-oxidant ,Anti-microbial ,Anti-fungal
3	Tropane	C H ₃ Ga	100.75	Acid	Anti- oxidant, Anti-hypertensive, Anti- microbial

Table: III Antimicrobial Activity Of *Cardiospermumhalicacabum*

S.NO	SAMPLE	DIAMETER OF ZONE OF INHIBITION(mm)	
		Streptococcus	Escherichia coli
1	<i>Cardiospermumhalicacabum</i>	10	15
2	Standard	21	26
3	Control	NI	NI

Table: IV Antimicrobial Activity Of *Cocciniaindica*

S.No	Sample	Diameter Of Zone Of Inhibition(Mm)	
		Streptococcus	Escherichia coli
1	<i>Cocciniaindica</i>	11	9
2	Standard	26	21
3	Control	NI	NI

Standard : Nutrient agar medium.

NI : No inhibitory effect .

Solvent : Methanol.

CONCLUSION

The phytochemical analysis of the methanolic extract of *Cardiospermum halicacabum* and *Coccinia indica spectabilis* is carried out by GC-MS Techniques. Methanolic extracts of *Cardiospermum halicacabum* and *Coccinia indica spectabilis* suppressed antimicrobial activity responses against bacteria which may be due to the presence of coumarin, propyl gallate, tropane methyl heptenol present in *Cardiospermum halicacabum* and piperidine, hexenal, gallic acid is present in *Coccinia indica*²⁰.

CONFLICT OF INTEREST

Conflict of interest declared none.

REFERENCES:

1. Emmanuelle Lautié¹, Olivier Russo², Pierre Ducrot³ and Jean A. Boutin^{2*} Unraveling Plant Natural Chemical Diversity for Drug Discovery Purposes Front. Pharmacol., 07 April 2020.
2. Krithikar K.R and Basu B.D, Indian medicinal plants, periodical Expert book agency, New Delhi, 1990, **Vol. I**, 621P.
3. Delitheos .A.K., Papadimitriou.C.A., Yannitsaros.A.G., Investigation for antiphase activity in plant extracts, Fitoterapia, 1992, **63/5**, 446P.
4. Duke.J.A. and Ayensu,E.S.,medicinal plants of china reference publication Inc.,1985.
5. Krithikar K.R and Basu B.D, Indian medicinal plants, periodical Expert book agency, New Delhi, 1990, **Vol. I**, 1151-1153P.
6. Borthakur.S.K., Nath.K., Gogoi.P, Herbal remedies of the Nepalese of Assam,Fitoterapia, 1996, **67/3**, 234P.
7. Chopra.R.N., Nayar.S.L., Chopra.I.C., The Glossary of Indian Medicinal plants,CSIR, New Delhi, 1987, 198P.
8. Mukherjee.K, Glosch.N.C., Indian Journal of Experimental Biology, 1987, **27**, 347P.
9. Kundu.S., Roy.A.B., Journal of Indian Chemical Society, 1987, **64**, 76P.
10. Bhakw.D.S., Shrivastava.S.N., Sharma.N.V., Journal of the Science Industrial Research, 1962, **21**, 237P.
11. L. M. Sandratskii and P. Bruno, Phys. Rev. B 73 (2006) 045203.
12. Y. H. Zheng and J. B. Xia, Phys. Rev. B 72 (2005) 195204.
13. J. Kudrnovsk' u, V. Drchal, I. Turek, L. Bergqvist, O. Eriksson, G. Bouzerar, Sandratskii and P. Bruno, Phys. Condens. Matter, 16 (2004) S5571.
14. S. A. Chambers, T. Droubay, C. M. Wang, A. S. Lea, R. F. C. Farrow, L. Folks, V. Deline, and S. Anders, Appl. Phys. Lett., 82 (2003) 1257.
15. Y. Zou , Z. Qua, J. Fang, and Y. Zhang, J. Mag. Mag. Mat., 321(2009) 3352.
16. J. Iqbal, B. Wang, X. Liu, D. Yu, B. He, and R. Yu, New J. Phys., 11 (2009) 063009.
17. S. Ghoshal and P. S. Anil Kumar, J. Mag. Mag. Mat., 320 (2008) L93.
18. K. Ueda Tabata, H. Tabata, and T. Kawai, Appl. Phys. Lett., 79, 988 (2001).
19. C. Song, F. Zeng, K. W. Geng, X. B. Wang, Y. X. Shen, and F. Pan, J. Mag. Mag. Mat., 309 (2007) 25.
20. Oskay M, same A, Azeri C (2004). Antibacterial activity of some actinomycetes isolated from farming soils of Turkey. Afr. J. Biotechol 3: 441-6.
21. Satheeja Santhi.S, Jose.A, and Solomon.J, R.D (2010), Isolation and Characterization of antagonistic actinomycetes from Mangrove sediments, International Journal of Current Research , 3: 020-023.

Phytoremediation of Dairy Sludge and Its Plants Growth Promotion Efficiency

Nitha V Ravi*, Gajalakshmi P, Raja A and Amika A

PG and Research Department of Microbiology, DhanalakshmiSrinivasan College of Arts and Science For Women (Autonomous), Perambalur-621 212, Tamil Nadu, India,
Phone: +9190489 56511 Email: nitha.chuti2911@gmail.com

Abstract: The application of sewage sludge causes an improvement of soil parameters as well as increase in cation exchange capacity, The source of heavy metals in soil is an intense mining extraction, industrial activities, transport, power engineering, and agriculture. , it was discovered that many plants through their roots, stems and leaves metabolism, morphology and mechanisms can reduce the concentration of heavy metals. Phytoremediation, which is an emerging technology for cleaning up contaminated sites, is cost effective and has aesthetic advantages and long term applicability. The technology involves efficient use of plant species to remove, detoxify or immobilize contaminants in a growth matrix (soil, water or sediments) through natural processes. For this study we have selected *Sorghastrumnutans* for phytoremediation of dairy sludge.

Key Words- Phytoremediation,sewage sludge,Power engineering,Heavy metals

INTRODUCTION

Dairy sludge Milk is transformed into yogurt, soft and cottage cheese, cream ,condensed milk, icecream,lactose which is the main technique in diary industry. About 2.5 times higher the milk that is processed , wastewater is produced. Whey is the main pollutant in milk waste water. fat 0.4–0.5%, 1 to 3% salt,lactose, Proteins and lactic acid are the main constituents of whey¹. The pollutants that come depend on a number of factors such as wastewater reuse, management of waste products, the instruments that are used in various industries². People consume more dairy products as a result the number of dairy factories increase and thereby the pollution from these industries. Heavy metal contamination When the heavy metal reach unpolluted areas and when they come in contact with the slurry of sewage, it can effect the environment³In phytoremediation reduction of heavy metals in situ by plants will be a useful technique for detoxification of metal^{4,5}. In shoot and root tissue, nontoxic Cr(III) accumulate when *Eichhorniacrassipes*(water hyacinth) is supplied with Cr(VI) which can be seen using X-ray spectroscopy. To produce solutions for industrial purposes, studies are required on the process of how plant extract can act as corrosion inhibitors⁶. For Cancer cell lines dichloromethane (DCM) extracts and hexane from foliage and stem are useful. Fusarium inhibited by the hexane extract that is present in the leaves during the initial stages but declines after later stages⁷. From corrosion metal substances are protected by using natural extracts⁸. Not knowing the fertilizers of nitrogen or phosphorous replacement rate, sludge which is processing diary is being changed to grassland⁹.A fast growing aquatic or semi aquatic plant- *Nasturtium officinale* is used as a food ingredient as well as the leaves are used for the treatment of various infections and are also rich in various Vitamins¹⁰. The concentration of the biomass and the amount of pollutants in the plant biomass are the factors that depend for the removal of heavy metals by plants¹¹.When the waste gets mixed with plants, it becomes a problem for growth of plants¹².In phytoremediation reduction of heavy metals in situ by plants will be a useful technique for detoxification of metal¹³.The pollutants that come depend on a number of factors such as wastewater reuse, management of waste products, the instruments that are used in various industries¹⁴.People consume more dairy products as a result the number of dairy factories increase and thereby the pollution from these industries. These pollutions can lead to air pollution, water pollution, soil pollution¹⁵.

MATERIALS AND METHOD

Sample collection

The matured *Sorghastrumnutans* plants were collected and planted in polythene bag. Dairy sludge collected from AR dairy industry dindugal.

Seed germination test

In a sterile pot 2 parts of sludge and 1 part of soil are mixed and irrigated with water. The Seeds of *Vignaradiata* were soaked and tested for germination. Triplicates of setup was evaluated

Experimental Design

The study consisted of three different management variables—soil amendments (sludge and grass 1:1 and 1:2; control without sludge) were prepared. Within each of these, soil was planted (12 okra seeds)

100 g of fine sterile sand and 100g of sludge waste was used as base and subjected to phytoremediation. Different treatment groups were prepared as follows

Treatment 1: soil base + *Sorghastrumnutans*(1:1)

Treatment 2: soil base + *Sorghastrumnutans*(1:2)

Treatment 3: base alone

Treatment 3: soil alone

Moisture contents (MC) Moisture content (wet basis) was measured by drying at 105°C for approximately 2h at

constant weight(2g).

$$\text{Percentage of moisture} = \frac{\text{I wt-F t}}{\text{Iwt}} \times 100$$

Determination of pH

2 g of composted soil at the end of 15th day was taken and 50 ml water was mixed and kept under a magnetic stirrer for 15 min. the soil filtrate was taken and pH was determined^{10, 11}

Bio stimulant property

Based on pot culture seed germination pot culture was used. Two days Germinated seeds used in this study. Agricultural land soil mixed with compost at 5:1 ratio. T1-T4 and control group were prepared and then the seeds were sown in to pots containing sand, compost and watered. Pots were irrigated as needed. After 15 days of sowing Vigor index was recorded.¹³

$$\text{Vigor index} = (\text{mean root length} + \text{mean shoot length}) \times \% \text{ germination}$$

In vitro assay of chromium (VI) reduction

Reduction of Cr (VI) among sludge enriched pots followed by phytoremediation was performed at 20th day. 5g sample mixed with 50 ml sterile distilled water and stirred well at 200 rpm for 30min. soilfreefiltrate was taken and assayed for presence of chromiumusingdiphenylcarbazide method.1ml of extract 2ml of DPZ reagent mixed and incubated for 10 min at RT and changes of color recorded at450 nm against standard potassium dichromate¹⁵.

RESULTS AND DISCUSSION

Modified groundnut hull can absorb , chromium(VI) ¹⁶For the production of nanoiron suspension, a mixture of PG juice and RW along with GT extracts are effective which helps in the reduction of Cr(VI)¹⁷. Most heavy metal causes serious hazards to humans. Some are carcinogenic in nature.These heavy metals effect our environment as they get mixed with water particles and thereby come in contact with our water sources¹⁸. For the production of nanoiron suspension, a mixture of PG juice and RW along with GT extracts are effective which helps in the reduction of Cr(VI)^{19,20}. Lower concentration of dairy effluent showed promoting effect on seed germination on seedling growth, dry matter production. Maximum germination promoting effect was 90% recorded at 50 % concentration on day 4. Sludge at 25% gave 80% germination whereas 100% the rate of germination of *V.radiata* was 60% attained on 6th day. In control 100% germination was noted on 5th day. Results of present investigation by Prasannakumar et al(2007) support previous work of black gram and green gram with effect of dairy sludge. The promotion of seedling growth by lower concentration of effluent might be due to the presence of plant nutrient in the effluent and inhibition at high concentration due to heavy metal load(table 1). Germination percentage and seedling growth inhibited at 100% concentration due to phosphorylase and the increased activity of beta-amylase osmotic pressure caused due to high dose The moisture content of pot among *Sorghastrumnutans* were 36%, 39.5%, 11.5% and control have 30%(table 2). Morphological traits of the OKRA plants depending on the treatments are presented in Table 3-6. The overall growth of plant was stimulated by the treatment 1:2 and the vigor index was 1,489.95 and the VI was 1,190.96 on 1:1 treatment. Sludge alone have given VI 888. Plant height and root significantly increased by *Sorghastrumnutans* at 1:2 ratio and the mean of root and shoot were 4.8/11.755cm. The height of plants was increased by 34.5% when cultivated on 15% growth of control compared with *Sorghastrumnutans* showed decreased germination but the amended substrates enhance the growth of seed of okra plant. Root length was not significantly affected by the treatments *Sorghastrumnutans* but affected by sludge alone (plate 2-3).^{21,22} Another Important study effective data of this treatment is reduction of Chromium VI removal .pot treated with *Sorghastrumnutans* was observed complete reduction was recorded from 180 ppm to 30 ppm on 1:2 ratio and 45 ppm at 1:1 ratio phytoremediation. Control pots showed reduction of chromium as 120 ppm. *Sorghastrumnutans* showed reduction of chromium (plate 4) reveals the ability of phytochemicals are significant to remove Chromium .

Table 1.Seed germination

Treatment	No.Of Seed Germinate	% Germination	Duration Days
SOIL+SLUDGE (25%)	8	80%	4
SOIL+SLUDGE(50%)	9	90%	4
SLUDGE ALONE(100%)	6	60%	6
(CONTROL)	10	100%	5



Plate 1. Processing of dairy sample for phytoremediation

Table 2 Ph Moister Content Of Composting Samples

S.No:	Treatment	Moister Content	Ph
1	Treatment 1	36%	8.4
2	Treatment 2	39.5%	7.6
3	Treatment 3	11.5%	8.4
4	Control	30%	6.8

Table 3. Length Of Root And Shoot On Control

S.No	Stem	Root	No.Of.Leaf
1	9.5	1	3
2	11.5	2	4
3	12.6	2.5	3
4	11.5	2	3
5	11	3	4
6	10.6	3	4
7	11.6	3.3	4
8	11.5	3	4
9	12.4	3	3
10	12	4.7	4
TOTAL	114.1	27.5	36

Table 4 length of Root and Shoot On Treatment-1

S.No	Stem	Root	No.Of Leaf
1	10	1	3
2	9.8	3	4
3	10.5	3	4
4	13	1.5	4
5	13	3	4
6	12	2.5	4
7	12	2.5	4
8	11	11.3	4
9	—	—	—
10	—	—	—
TOTAL	91.3	27.8	31

Table 5.Length of Root and Shoot on Treatment-2

S.No	Stem	Root	No.Of Leaf
1	9.3	3.5	3
2	12.5	2.5	3
3	11	2.7	3
4	11.5	2.5	3
5	11.5	3	3
6	13	5	3
7	13	6	4
8	12	9	4
9	12	9	3
10	—	—	—
TOTEL	105	43.2	29

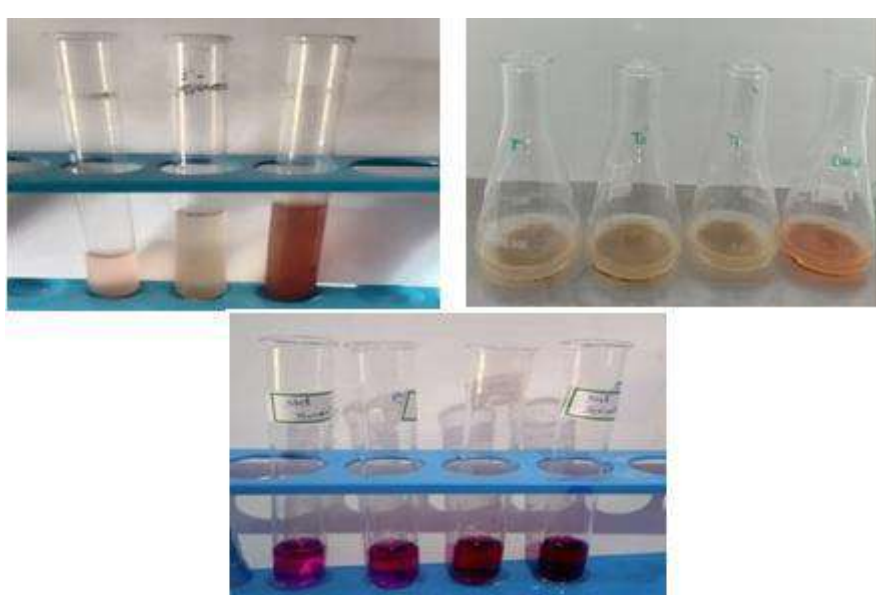
Table 6. Length On Root And Shoot On Treatment-3

S.No	Stem	Root	No.Of Leaf
1	10	3.2	4
2	10.5	3.7	3
3	12	3	4
4	10	4	4
5	12	3	3
6	10.5	3.5	4

7	10	3.5	4
8	11.5	3.5	3
9	13	4	3
10	12.5	4.7	3
TOTAL	112	36.1	35

Table 6.vigor index of tested plant seedling

Treatment	Mean Of Root	Mean Of Shoot Length	% Germination	Vigor Index
C(SOIL)	2.75	11.41	100%	1,416
T1(1:1)	3.475	11.412	80%	1,190.96
T2(1:2)	4.8	11.755	90%	1,489.95
T3(SLUDGE)	3.61	11.2	60%	888

**Plate 2. Treatment of dairy sludge with grass****Plate 3. Plant growth effect on lady finger under treated sludge****Plate 4. Detection of chromium**

SUMMARY AND CONCLUSION

During pot trials, treated sludge dairy sludge with *Sorghastrum nutans* showed significant results on seed germination of okra and

untreated appeared to be inhibited by the presence of chromium in sludge. Laboratory experiments confirmed this effect and showed that germination was not permanently inhibited instead merely delayed. The lag period of germination was dose-dependent, increasing in proportion of sludge added. *Sorghastrumnutans* exerts stimulatory effects growth, while the investigated physiological parameters were not affected at any point. When sludge is freshly incorporated with soil, intense microbial activity is to be expected leading to reduced oxygen tensions and conditions which favor the formation of volatile inhibitors were involved in the delayed seed germination and growth effect. A similar effect was induced by heavy metals removal in sludge, considering that *Sorghastrumnutans* to be a phytoremediant. Further testing need to be conducted to optimize the *Sorghastrumnutans* and dairy sludge application in order to improve crop fertilization and chromium removal.

CONFLICT OF INTEREST

Conflict of interest declared none.

REFERENCE

1. Gannoun H, Khelifi E, Bouallgui H, Touhami Y, Hamdi M (2008) Ecological clarification of cheese whey prior to anaerobic digestion in upflow anaerobic filter. *Bioresour Technol.* (14);6105-11.
2. Britz JT, van Schalwyk C, Hung YT. Treatment of dairy processing wastewaters. In: Wang LK, Hung YT, Lo HH, Yapijakis C, editors. *Waste treatment in the food processing industry*. Boca Raton 1–25.
3. Gaur A. and A. Adholeya,2004 “Prospects of arbuscularmycorrhizal fungi in phytoremediation of heavy metal contaminated soils,” *Current Science*, (86); 528–534.
4. Henry J. R. (2000): In An Overview of Phytoremediation of Lead and Mercury. –NNEMS Report. Washington,3-9.
5. Mel Lytle C., Farrel W. Lytle, Nancy Yang, Jin-Hong Qian, Drew Hansen, Adel Zayed, and Norman Terry(1998)Reduction of Cr(VI) to Cr(III) by Wetland Plants: Potential for In Situ Heavy Metal Detoxification 3087–3093
6. Alan Miralrio, and Araceli Espinoza Vázquez,(2020) Plant Extracts as Green Corrosion Inhibitors for Different Metal Surfaces and Corrosive Media: A Review(8);94
7. HernándezM.M,HerasoC,VillarrealM.L,largas-Arispurol.V,E.ArandaEthnoformacology Biological activities of crude plant extracts from *Vitextrifolia* L. (Verbenaceae) 37-44
8. Alan Miralrio, and Araceli Espinoza Vázquez,(2020) Plant Extracts as Green Corrosion Inhibitors for Different Metal Surfaces and Corrosive Media: A Review(8);942
9. Ashekuzzaman SM, Patrick Forrestal, Karl RichardsG, Karen Daly, Owen Fenton,(2021)Grassland Phosphorus and Nitrogen Fertiliser Replacement value of Dairy Processing Dewatered Sludge,Sustainable Production and Consumption, (25); 363-373,
10. Sachin Chaudhary,HazarHisham,DohaMohamed.A review on phytochemical and pharmacological potential of watercress plant. *Asian Journal of Pharmaceutical and Clinical Research*.2018;11(12):102
11. Mahmoud Seleiman,ArjaSantanen,SeijaJaakkola,PäiviEkhholm.Biomass yield and quality of bioenergy crops grown with synthetic and organic fertilizers. *Biomass and Bioenergy*.2013;07.021
12. Henry J. R. (2000): In An Overview of Phytoremediation of Lead and Mercury. –NNEMS Report. Washington,3-9.
13. Mel Lytle C., Farrel W. Lytle, Nancy Yang, Jin-Hong Qian, Drew Hansen, Adel Zayed, and Norman Terry(1998)Reduction of Cr(VI) to Cr(III) by Wetland Plants: Potential for In Situ Heavy Metal Detoxification 3087–3093
14. Britz JT, van Schalwyk C, Hung YT. Treatment of dairy processing wastewaters. In: Wang LK, Hung YT, Lo HH, Yapijakis C, editors. *Waste treatment in the food processing industry*. Boca Raton 1–25.
15. Talha Ahmad, Rana Muhammad Aadil, Haassan Ahmed, UbaidurRahman, BrunaSoares CV, Simone Souza LQ, Tatiana Pimentel C, Hugo Scudino, Jonas Guimarães T, Erick EsmerinoA, MônicaFreitas
16. Samson O.OwaludeAdedibuC.Tella (2016) Removal of hexavalent chromium from aqueous solutions by adsorption on modified groundnut hull 377-388.
17. MystriotiC.Sparis D. Papasiopi N. Xenidis A. Dermatas D. Chrysochoou M.(2014) Assessment of Polyphenol Coated Nano Zero ValentIronfor Hexavalent Chromium Removal from Contaminated Waters. *Bull Environ Contam Toxicol* 10.1007.
18. Yi Y, Tang C, Yi T, Yang Z, Zhang S.(2017) Health risk assessment of heavy metals in fish and accumulation patterns in food web in the upper Yangtze River, China. *Eco.Env.Saf.*, (145); 295–30
19. Tilman D, Balzer C, Hill J. &Befort B L, Global food demand and the sustainable intensification of agriculture.(108); 20260–20264.
20. MystriotiC.Sparis D. Papasiopi N. Xenidis A. Dermatas D. Chrysochoou M.(2014) Assessment of Polyphenol Coated Nano Zero ValentIronfor Hexavalent Chromium Removal from Contaminated Waters. *Bull Environ Contam Toxicol* 10.1007.
21. Akbar M, Yabuno Y. 1974. Breeding for saline-resistant varieties of rice. II. Comparative performance of some rice varieties to salinity during early developing stages. *Jap. J. Breed.* 25:176-181.
22. R.K. Sarkar ,Koushik Chakraborty, K. Chattopadhyay, Soham Ray & A.M. Ismail(2019), Chapter 13 - Responses of Rice to Individual and Combined Stresses of Flooding and Salinity, *Advances in Rice Research for Abiotic Stress Tolerance*

Abiotic Stress Tolerance Screening In Traditional Rice Varieties Of Tamilnadu

Haseena M, Senthil Manikkam J, Sangavai C, Kaleeswari Sudha M, Valarmathi M, Afrin Banu B

Dhanalakshmi Srinivasan College Of Arts And Science For Women (Autonomous), Perambalur-621212.

Abstract: Rice is one of the major cereals of India. Rice is India's main crop and millions of Indians find comfort in it every day. With a presence of high carbohydrate content, it provides instant energy and is an essential exhausted by the majority of the population in India. Abiotic stress is one of the most important challenges facing Agriculture. *Oryza sativa* (Rice) is a crop that is grown significantly in areas with high crop stresses, has high heat and drought tolerance, and is considered a model crop for tolerance studies. The present study was to find out the drought, salinity, submergence tolerance of Rice varieties in Tamil Nadu. The twenty rice varieties are collected from various regions of Tamil Nadu. As plants in the Rice seedlings stage exhibit high sensitivity to Abiotic stresses. We use hydroponic solutions for the assay of salt tolerance of Rice. For drought, the plants are grown in soil and subjected to waterlogging. Assessing the performance of seedlings using IRRI, SES Score 2002.

Keywords: *Oryza sativa*, Drought, Salinity, Submergence tolerance.

INTRODUCTION:

Since the dawn of civilization, rice has served humans as a life-giving cereal in the humid regions of Asia and to a lesser extent, in West Africa. Introduction to rice into Europe and America has led to its increased use in human diets. There are 42 rice-producing countries throughout the world but China and India are the major rice-producing countries throughout the world but China and India are the major rice-producing centers. Rice is grown in a wide range of agro-climatic conditions ranging from mountainous (Jammu) lands to low land delta areas (Sundarbans), but about 90% of the crop is grown and consumed in Asia. According to one estimate, around 28 percent of the world's land is too dry to support vegetation¹. Rice is the essential source of food for more than half of the world's population. In today's climatic change scenario's most rice varieties are severely injured by abiotic stresses, with strong social and economic impact². This describes the experimental conditions established at the Genomics of the plant to three different abiotic stresses-high salinity, drought, and submergence³. Drought is a major Abiotic stress factor that controls rice production worldwide. A total of 20 high yielding rice varieties were collected from various regions of Tamil Nadu in India to evaluate the osmotic stress responses in drought tolerant rice varieties. Submergence affects low-lying areas of crops. Submergence is defined based on duration, depth, and frequency. Flooding causes submersion and damage to rice crops. Flash flood submergence and stagnant floods are treacherously affecting rice production in South and Southeast Asia. Different categories of flash floods cause rice production losses of up to 100%⁴. Salinity stress causes various physiological and biological processes, depending on the severity and period of the stress, and finally suppresses crop production⁵. During the initial stage of salinity stress, it decreases the water absorption capacity of root systems, and water loss from leaves is expedited due to osmotic stress of high salt aggregation in soil and plants, and therefore salinity stress is also considered as hyperosmotic stress⁶.

MATERIALS AND METHODS

The present study was undertaken to identify the traditional rice varieties tolerant/resistant to major Abiotic Stresses viz, drought, salinity, and submergence. All the traditional rice varieties used in this study were collected from the different regions of Tamil Nadu. The Rice varieties are Karunguruvai, Aruvatham kuruvai, Kalli mudaiyan, Kichall Samba, Navara, Poongar, Poomuthigar, Salem channa, Basmath, Thuya malli, Sivan samba, Chithrakar, ADT45, Sivappu Kavuni, Karuppu kavuni, Thanga samba, Seeraga samba, Chinnar, Mapillai Samba, Kullakar, and Sembuli Samba.

Responses against salinity during germination:

About twenty one rice varieties are collected from the different places of Tamil Nadu. Fifteen seeds of each rice variety are placed in a petri dish containing 10ml of 100mM NaCl concentration. Germination % was calculated by counting the number of seeds germinated on the fifth day and expressed in percentage⁷.

Response against salinity during vegetative stage:

Responses to salinity stress exhibited by seedlings selected were assessed using the modified standard evaluation Scoring (SES) System of IRRI⁸. A 21 rice varieties were germinated in Petri dishes and transferred to hydroponic conditions (Thermocole sheets floating on trays containing Yoshida solution) and allowed for establishment. Salinity stress was imposed (15 days at 100mM NaCl Stress) under hydroponic conditions. Leaf rolling and drying symptoms of seedling of different genotypes were recorded.

Evaluation of seed germination against dehydration

All the 21 seed varieties were evaluated for their responses against dehydration induced by -0.5 MPa PEG treatment was dissolved in 200 ml of water to achieve -0.5 MPa water potential. Seedlings were subjected to dehydration stress stimulated by -0.5 MPa Polyethylene glycol (PEG 4000). After 15 days plants were scored for their responses against osmotic stress using the Standard Evaluation system¹⁹. The germination percentage of the Seedlings was also observed.

Screening For Submergence Tolerance At Seedling Stage:

About twenty rice varieties have collected the seeds. Flooding was imposed on the seedlings. After two weeks observations on seedling survival were recorded. The recovery ability of BILS and parents were assessed after 15 days of de-Submergence using the Standard evaluation score¹⁹.

RESULT

Evaluation of rice accession against dehydration stress

In this study, we collected 21 rice varieties from the various places of Tamil Nadu. All the 21 rice accessions were evaluated for their tolerance against dehydration stress during the germination stage and the effect of -0.5 PEG on seed germination was measured to determine the tolerance of rice genotypes to water deficit conditions. We checked the yielding capacities of rice in drought and the water control¹⁹. The Effect of dehydration stress on the seed germination of rice varieties was analyzed. The 50% of seed germination was reduced in drought conditions by comparing normal growing plants (Table. I). We measured the root and shoot of all 21 rice varieties against drought stress conditions. The root and shoot length were decreased in the drought conditions¹⁰. The germination of seeds under drought stress was found to be affected significantly with -0.5 MPa PEG in all the rice accessions and severe reduction in root and shoot length were recorded and presented in Table. I.

Table:1. Effect of dehydration stress on the seed germination of rice accessions.

S. No.	Rice Varieties	Germination Percentage (- 0.5 MPa)	
		Control(cm)	Stress(cm)
1.	Aravatham Kuruvai	60	40
2.	Salem Channa	46.6	26.6
3.	Thuyamalli	66.6	53.3
4.	Poomuthigar	46.6	33.3
5.	ADT 45	26.6	20
6.	Seeraga Samba	40	40
7.	Kalli Mudaiyan	60	33.3
8.	Sembuli Samba	33.3	26.6
9.	Poongar	73.3	40
10.	Mapillai Samba	86.6	46.6
11.	Kullakar	40	26.6
12.	Chithrakar	13.3	6.6
13.	Basmathi	80	33.3
14.	Navara	73.3	26.6
15.	Karunguruvai	40	33.3
16.	Chinnar	73.3	40
17.	Sivan Samba	40	13.3
18.	Thanga Samba	26.6	20
19.	Karuppu Kavuni	86.6	40
20.	Kichallai Samba	80	46.6
21.	Sivappu Kavuni	46.6	33.3

Table:2. Root and shoot length of rice accessions against drought stress

S.No	Rice Varieties	ROOT LENGTH		SHOOT LENGTH	
		Control (cm)	Stress (cm)	Control(cm)	Stress(cm)
1.	Aravatham kuruvai	14	6	10	10
2.	Salem Channa	12	4	19	12
3.	Thuyamalli	7	4	12	13
4.	Poomuthigar	13	6	12	16
5.	ADT45	16	11	13	12
6.	Seeraga Samba	16	7	10	7
7.	Kalli mudaiyan	13	5	9	13
8.	Sembuli Samba	13	6	21	13
9.	Poongar	17	6	25	10
10.	Mapillai Samba	4	6	10	10
11.	Kullakar	11	6	6	10

12.	Chithrakar	14	7	12	14
13.	Basmathi	14	4	12	14
14.	Navara	14	9	12	11
15.	Karunguruvai	11	9	19	14
16.	Chinnar	4	4	11	15
17.	Sivan samba	5	5	14	12
18.	Thanga samba	17	12	12	11
19.	Karuppu kavuni	10	4	16	14
20.	Kichalli Samba	10	4	18	10
21.	Sivappu kavuni	9	5	14	10

Evaluation of Salinity tolerance at Seedling stage

A total 21 accessions of traditional rice varieties were imposed with salinity stress (15 days at 100 mM NaCl stress) under hydroponics condition. The salinity stress NaCl were induced to the seed germination. The evaluate the stress in rice varieties under salinity stress the NaCl were induced in a 100mM concentration and the seed were kept for germination. After 10-15 days from the germination of seed we compare the growth of the seed in water content and salinity stress. Saline soils are usually under waterlogged condition: other crops could not grow except rice. Salt tolerance is generally a sustained growth of the plant in the soil environment impregnated with Nails worth or other salt combinations¹¹. Karunguruvai, Aruvatham kuruvi, Kalli mudaiyan, Kichalli Samba, Navara, Poomuthigar, Salem channa, Basmath, Thuya malli, Sivan samba, ADT45, Sivappu Kavuni, Karuppu kavuni, Thanga samba, Seeraga samba, Chinnar, Mapillai Samba, Kullakar and Sembuli Samba rice varieties of growth were completely ceased most of the leaves were dried; some plants died (Table. 4). Poongar and Chithrakar rice varieties of Growth were nearly normal but there was some reduction in tillering and some leaves were discolored (alkali)/whitish and rolled (salt). Two accessions viz., Chitrakar and Poongar were moderately tolerant with the SES score 3, while the other accessions were susceptible and exhibited an average SES score of 7.

Evaluation of rice accessions against submergence

In our study demonstrated that the rice is a semi aquatic cereals. Submergence stress severely reduced the germination growth of the seed in the flooded. we checked that the seed varieties whether able to tolerate during the submergence¹². For that we take 21 rice varieties from the various places of tamilnadu. The seed are fully submerged in a water. The water level is nearly 75% and allow to grow the seed in the submergence stress. The growth rate in submergence conditions rice varieties and their survived rates are Salem channa(80%), Poomuthigar(80%), Mapillai samba(70%), Basmathi(30%), Navara(20%), Karunguruvai(70%), Chinnar(80%), Thanga Samba(50%), Sembuli samba(30%), Karuppu kavuni(90%), Kichalli samba(90%), Sivappu kavuni(90%), Kalli mudaiyan(90%). There is no survival rate in Thuyamalli, Aruvatham kuruvi, ADT45, Seeraga Samba, Poongar, Kullakar, Chithrakar, Sivan samba rice varieties (IRRI 2002). Seed germination and SES core ratio were reduced in Submergence conditions of Rice.

Table:3. Seed germination percentage and SES score in Submergence conditions

S. No.	Rice accessions	Seed germination percentage	Seed germination under complete submergence	SES Score
1	Seeraga samba	66.6 %	No germination	0
3	Sembuli Samba	73.3%	Poor germination	3
4	Poongar	46.6%	Poor germination	0
5	Mapillai Samba	66.6%	Moderately tolerant	5
6	Chitrakar	0	No germination	0
7	Kullakar	6.6	No germination	0
8	Navara	73.3	Poor germination	4
9	Basmati	53.3%	Poor germination	3
10	Karuppu Kavuni	60	Tolerant	8
11	Sivan Samba	13.3%	No germination	0
12	Sivappu Kavuni	66.6	Tolerant	8
13	Thanga samba	26.6%	Moderately tolerant	4
14	Thuyamalli	53.3%	Poor germination	0
15	Karunguruvai	33.3%	Moderately tolerant	6
16	Chinnar	53.3%	Tolerant	8
17	Aruvatham Kuruvi	66.6%	Moderately tolerant	5
18	Karunguruvai	60	Moderately tolerant	5
19	Salem sanna	33.3%	Tolerant	8
20	Kichili samba	60	Tolerant	8
21	Poomuthigan	53.3%	Tolerant	7

CONCLUSION

India is fortunate with great rice germplasm diversity, and these are still preserved for many reasons. Plants are non mobile

organisms and therefore need to adapt to environmental stresses mostly by modulating their growth and development in addition to physiological and biochemical changes. The plant life style of continuous development also requires proper maintenance of many important functions in the stress environment¹³. Plants may acclimate to the limited stress conditions by integrating stress information with developmental programs. Salinity tolerance involves a complex of responses at cellular, molecular, metabolic, physiological, and whole-plant levels. It elucidated that among various salinity responses, mechanisms or strategies controlling ion uptake, transport and balance, osmotic regulation, hormone metabolism, antioxidant metabolism, and stress signalling play critical roles in plant adaptation to salinity stress¹⁴. Drought stress causes to growth reduction, which is affected in plant height, biomass and other growth functions in which deep rooting is a target trait in rice improvement programs under drought stress¹⁵. The intercellular and intracellular molecular interaction are the further characterization involved in salinity stress response of rice. We analysed wide genetic distance among the genotypes deliberated. Highly significant associations among the traits studied were revealed simple correlation analysis. The combination of morphological findings and molecular evaluation revealed better salt-tolerance in a few genetic variants¹⁶. Further biochemical and molecular works are needed to confirm the tolerance or susceptibility of *Oryza sativ*¹⁷. Salinity, osmotic stress, temperature extremes, and plants use their genetic mechanism and different adaptive and biological approaches for survival and high production also analysed¹⁸. Genetic engineering is an efficient approach. The salinity-tolerant plants development has been proved by Genetic engineering¹⁹⁻²⁰.

CONFLICT OF INTEREST

Conflict of interest declared none.

REFERENCE

1. Kramer., P. J and J. S. Boyer. (1995). Water relations of plants and soils(Book). Academic Press.,San Diego
2. Gupta, A. Rico-Medina, A.I. Caño-Delgado(2020), The physiology of plant responses to drought, Science, 368 (2020), pp. 266-269
3. Jyotirmay Kalita, Bhaben Tanti, (2019),Screening of Some Traditional Rice Cultivars of Assam, India, for Their Response to Arsenic-Induced Abiotic Stress, Original research paper in physiology
4. R.A. Fischer(1980), Influence of water stress on crop yield in semi arid regions, N. C Turner, P.C Kramer (Eds.), Adaptation of Plants to Water and High Temperature Stress., Willey and Son, New York (1980), pp. 323-340.
5. Sajid Hussain,Sheng-miano YU,James Allen Bohr, Effects of salt stress on rice growth,development characteristics, and the regulatory ways(2017) pp.2357-2374.
6. Bhaskar Gupta and Bingru Huang (2014), Mechanism of Salinity Tolerance in Plants: Physiological, Biochemical, and Molecular Characterization, Article ID 701596
7. Bradford, K. J. (1986). Manipulation of seed water relations via osmotic priming to improve germination under stress conditions. HortScience 21, 1105-1112.
8. Chaudhary, R. C. (1996). Standard evaluation system for rice. Manila: International Rice Research Institute
9. Rima kumari,Sharma V.K seed culture of rice cultivars under salt stress(2015)pp191-202.
10. M. Farooq, N. Kobayashi, A. Wahid, O. Ito, S.M.A. Basra, Strategies for producing more rice with less water , Adv Agron, 101 (2009), pp. 351-388
11. S. Khatun, T.J. Flowers, Effects of salinity on seed set in rice, Plant Cell Environ, 18 (1) (1995), pp. 61-67
12. Akbar M, Yabuno Y. 1974. Breeding for saline-resistant varieties of rice. II. Comparative performance of some rice varieties to salinity during early developing stages. Jap. J. Breed. 25:176-181.
13. R.K. Sarkar ,Koushik Chakraborty, K. Chattopadhyay, Soham Ray & A.M. Ismail(2019), Chapter 13 - Responses of Rice to Individual and Combined Stresses of Flooding and Salinity, Advances in Rice Research for Abiotic Stress Tolerance
14. V.R.P. Gowda, A. Henry, A. Yamauchi, H.E. Shashidhar, R. Serraj, Root biology and genetics improvement for drought avoidance in rice, Field Crops Res, 122 (1) (2011), pp. 1-13
15. M. Ismail, E.S. Ella, G.V. Vergara, D.J. Mackill, Mechanisms associated with tolerance to flooding during germination and early seedling growth in rice (*Oryza sativa L.*), Ann Bot,103 (2) ,(2009), pp. 197-209
16. Vignesh Mohanavel, Anbu selvam Yesudhas,Anket Sharma,Anandan Ramasamy,Prakash Muthu ArjunaSamy, Murugan Subramanian, Ramakrishnan Muthusamy(2021), Haplotype and diversity analysis of indigenous rice for salinity tolerance in early-stage seedling using simple sequence repeat markers, Biotechnology Reports 31.
17. Glenn B. Gregorio, Dharmawansa Senadhira, and Rhulyx D. Mendoza, Screening rice for salinity tolerance, IRRI Discussion Paper Series No. 22.
18. Fahad, S., Hussain, S., Bano, A., Saud, S., Hassan, S., Shan, D., et al., 2014a. Potential role of phytohormones and plant growth-promoting rhizobacteria in abiotic stresses: consequences for changing environment. Environ. Sci. Pollut. Res. Available from: [11356-014-3754-2](https://doi.org/10.1007/s10653-014-3754-2). Standard Evaluation system.(IRRI,2002
19. Elumalai Kannan(2017), Spatial and Temporal Patterns of Rice Production and Productivity, The Future Rice Strategy for India.

Evaluation of the Antioxidant Property of 4, 6-Diphenylpyrimidine-2-Thione

Suju C. Joseph* and Ratheesh S. Nair

PG & Research Department of Chemistry, Mar Ivanios College (Autonomous), Thiruvananthapuram-695015, Kerala, India

Abstract: Nitrogen-containing heterocyclic compounds dihydropyrimidinone and its sulphur analog, diphenylpyrimidine-2-thione, have been reported to possess many pharmacological properties such as anticancer, anti-HIV, antibacterial, antimalarial, antihypertensive, sedative, hypnotics, anticonvulsant, antithyroid, and antibiotics. In the present study, the antioxidant property of 4, 6-diphenylpyrimidine-2-thione was evaluated by Halliwell's method using Fenton's reagent and deoxyribose. 4, 6-diphenylpyrimidine-2-thione was found to scavenge the hydroxyl radicals generated by Fenton's reagent preventing the degradation of deoxyribose into malondialdehyde as indicated by the Thiobarbituric acid test, illustrating the antioxidant property of 4, 6-diphenylpyrimidine-2-thione.

Keywords: 4, 6-diphenylpyrimidine-2-thione, Halliwell's method, antioxidant property, Nitrogen-containing, degradation of deoxyribose

INTRODUCTION

A large number of pyrimidines are known for their varied biological properties. Brugnatelli was the first scientist to isolate alloxan, a pyrimidine derivative in 1818, and later this compound was found to possess anti-antineoplastic properties. Nucleosides of pyrimidine bases have been used extensively as antiviral and anticancer agents. Recently, fluoropyrimidines¹ and fluorouracil-based combination therapy is used in the treatment of gastrointestinal cancer and solid tumors. Fluoropyrimidinones are found to be metabolites of dihydropyrimidinones that are subtype-selective antagonists of the 1a-adrenergic receptor antagonists. The pyrimidine entities are one of the most prominent structures found in nucleic acid chemistry. Pyrimidinones play a vital role in many biological processes since their ring system is present in several vitamins, coenzymes, and nucleic acids. Several pyrimidine derivatives have wide varieties of usages and its nucleus is also present in vitamin B2 and folic acid. As pyrimidine is a basic nucleus in DNA and RNA it is associated with diverse biological activities. Pyrimidine derivatives are an important class of heterocyclic chemistry and are associated with various biological, pharmaceutical, and therapeutical activities like anticancer, anti-inflammatory, anti-HIV, etc. It is evident from the literature that pyrimidinones played an essential role in several biological processes² and have considerable chemical and pharmacological importance. One of the methods for the synthesis of such compounds is from α, β unsaturated carbonyls by the cyclization with urea and thiourea. Synthesis of sulphur, oxygen-containing heterocyclics has been explored for their therapeutic activity. Chalcones have been proved to be an important intermediate for the synthesis of many heterocyclic compounds. Chalcone and its derivative possess some interesting biological properties such as antibacterial, antifungal, insecticidal, anti-inflammatory, analgesic, anticanceretic Chalcones possess conjugated double bonds and completely delocalized³ pi electrons system on both benzene rings. Molecule possessing such a system has relatively low redox potential and have a great probability of undergoing electron transfer reaction. Chalcones exist as either E or Z isomers. E isomers are the most stable form and consequently, the majority of the chalcones are isolated as E isomers. The highly polarised pyrimidinones can add a carbon nucleophile at either C-4 or C-6 to form the corresponding 3,4 or 3,6-dihydro derivatives. Dihydropyrimidinones have always remained in the forefront due to their therapeutic and pharmacological properties were patented for the protection of wool moths. Dihydropyrimidinones derivatives were synthesized by the modification of the substituents in virtually⁴ all the six positions of the pyrimidines nucleus which provided interesting activity against HIV, Sendai virus, and Rubella virus. Besides these, substituted pyrimidines derivatives have been used as antihypertensive agents. Anticancer agents, antimicrobial, antifungal agents, anti-inflammatory agents. Calcium channel blockers, neuropeptides, γ -antagonists, and some pyrimidinones carrying an arylidne moiety have potential as antitumor agents. Some of these analogs also showed, besides broad-spectrum, antitumor activity, a distinctive pattern of selectivity towards individual cell lines, such that of leukemia based on the observation it is worthwhile to prepare newer compounds for their antimicrobial anti-inflammatory and anticancer activities. Because of the varied biological pharmacological application is synthesized⁵ some new pyrimidine derivatives from chalcones and evaluated for antioxidant, anti-inflammatory, anticancer activity. Nitrogen heterocycles are of special interest as they constitute an important class of natural and non-natural products, many of which exhibit useful biological activities. They are mostly used as calcium channel blockers, alpha- antagonists,⁶ and neuropeptide-antagonists. Alkaloids containing the dihydro pyrimidine structure have been isolated from various marine sources which have been shown some interesting biological properties. Most important among these alkaloids was batzelladine, which was found to be potent HIV GP-120-CD4 inhibitors. Because of these efficient applications of the above compound, our interest in the synthesis of Dihydropyrimidinone and their thio analog is increasing tremendously. These compounds have been screened for their antifungal activity against *A. niger* and *C. Albicans*^{7,8}. The objectives of the present study are: (1) to develop an oxidation system using deoxyribose assay and (2) to arrive at an IC₅₀ value of 4,6-diphenylpyrimidine-2-thione.

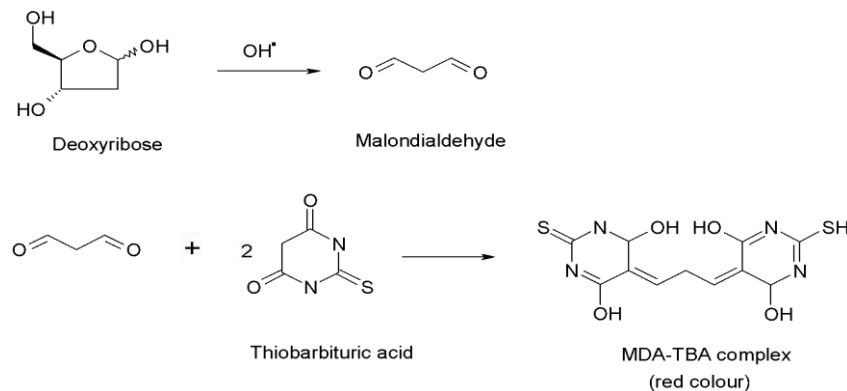
MATERIALS AND METHODS

Deoxyribose assay method as described by Halliwell has been followed to determine the antioxidant property of 4, 6-diphenylpyrimidin--2-one. This method uses the hydroxyl radicals generated from Fenton's reagent to degrade 2-deoxy-D-ribose

resulting in the formation of malondialdehyde (MDA), which could be identified by a red color formed on treatment with thiobarbituric acid (TBA). The red color is due to the formation of the MDA-TBA⁹ complex. Fenton's reagent is prepared by the addition of ferrous sulphate to hydrogen peroxide in equimolar proportion. Ferrous Iron (II) is oxidized by hydrogen peroxide to ferric iron (III), a hydroxyl radical, and a hydroxyl anion¹⁰. The hydroxyl free radical generated by Fenton's reagent is a powerful, non-selective oxidant. Oxidation of an organic compound by Fenton's reagent is rapid and exothermic (heat-producing) and results in the reduction of contaminants to primarily carbon dioxide and oxygen.



The hydroxyl free radical then reacts with deoxyribose degrading it to form malondialdehyde. The extent of the degradation depends on the available hydroxyl free radicals. The malondialdehyde is identified by the red complex formed on reaction with thiobarbituric acid that absorbs strongly at 532 nm (Scheme 1). The decomposed products of deoxyribose are 2-thiobarbituric acid-reactive substances (TBARS). If an antioxidant is present in the system, it scavenges the hydroxyl radicals generated and protects the deoxyribose from degradation producing a lesser amount of TBARS; accordingly, the intensity of red color produced will be less.



Scheme 1

4, 6-Diphenylpyrimidin-2-one has a conjugated system and is expected to be easily oxidized. The capability of 4, 6-Diphenylpyrimidin-2-one to scavenge hydroxyl radicals¹¹ has been studied by preparing various concentrations of them in ethanol and measuring the intensity of the red color formed in each case by UV absorbance at 530 nm.

Experimental Section: Determination Of The Antioxidant Property Of 4, 6-Diphenylpyrimidine-2-Thione

Deoxyribose Assay

The assay was performed as described by Halliwell. All solutions were freshly prepared. Into a solution of 2-deoxyribose (1 mL, 0.00037 M) was added buffer phosphate (1 mL) (pH 7.4), H_2O_2 (1 mL, 0.004 M), 1 mL of various concentrations of 4, 6-diphenylpyrimidine-2-thione (0.0140 M, 0.0280 M, 0.0559 M) and ferrous sulphate (1 mL, 0.004 M). After an incubation period of 30 min at 310 K, the extent of deoxyribose^{11,12} degradation was measured by the TBA reaction. 3 mL of TBA (prepared by dissolving 100 mg in 10 mL ethanol) was added to the reaction mixture and heated for 15 min at 353 K. After the mixture was cooled, the absorbance at λ 532 nm is noted against a blank (the same solution but without sample).

RESULTS AND DISCUSSION

The activity test as a hydroxyl radical scavenger was conducted *in vitro* by using the Halliwell method. The reaction was started by adding ferrous sulphate and H_2O_2 to produce a radical that will react with deoxyribose¹³. The reaction was stopped by adding a TBA reagent that would give a red color if the malondialdehyde was formed as the result of the reaction between the radical and deoxyribose. The absorbance of the red color was measured by using a UV spectrophotometer at the optimum wave number. The percentage (%) activity as an antioxidant was calculated as the percentage of the absorbance decrease of the product of the synthesis that could prevent the degradation of the 2-deoxyribose compared to the blank. When the sample of the synthesis works well as the hydroxyl radical scavenger, then it will decrease the deoxyribose degradation so that the malondialdehyde-TBA complex will only give the low intensity of red color. Thus, the more intense the red color, the less active the sample is. The graph showing the absorbance sample at different concentrations¹⁴⁻¹⁶ against wavelength is then obtained as shown in figure 1. The percentage inhibition (I %) was calculated by the formula for the concentrations of the sample.

$$I \% = \frac{A_{\text{blank}} - A_{\text{sample}}}{A_{\text{sample}}} \times 100 \%$$

The IC_{50} value represented the concentration of the compounds that caused 50% inhibition. 50 % inhibition was determined to

be 0.028 M for 4, 6-diphenylpyrimidine-2-thione¹⁷⁻²⁰.

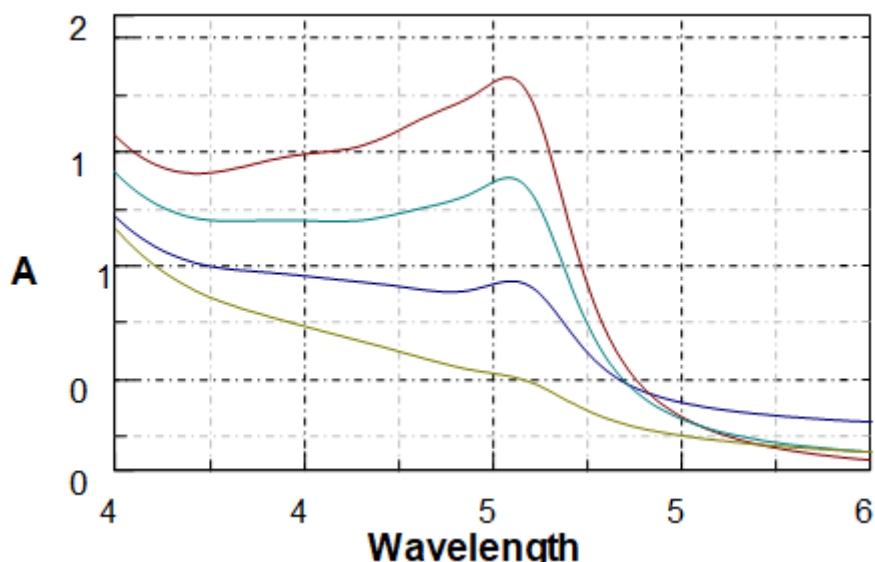


Figure 1

Colour code	Concentration	Absorbance	I %
Blank (without sample)		1.77	
0.014		1.38	22.13
0.0280		0.87	50.08
0.0559		0.50	71.74

CONCLUSION

4, 6-diphenylpyrimidine-2-thione was found to be an effective active hydroxyl radical scavenger as determined by Halliwell's method. 50 % inhibition was determined to be 0.028 M for 4, 6-diphenylpyrimidine-2-thione.

ACKNOWLEDGEMENT

UGC, New Delhi is gratefully acknowledged for the financial support.

CONFLICT OF INTEREST

Conflict of interest declared none.

REFERENCES

- Greene, T. W.; Wuts, P. G. *Protective Groups in Organic Synthesis*; third edn., Wiley: New York, 1999, pp. 47–53.
- Barton, D. H. R.; Beaton, J. M. A synthesis of aldosterone acetate. *J. Am. Chem. Soc.* 1961, 83, 4083–4089.
- Hosseinzadeh, R.; Tajbakhsh, M.; Niaki, M. Y. 2,6-Dicarboxypyridinium chlorochromate: A mild, efficient, and selective reagent for oxidative deprotection of oximes to carbonyl compounds. *Tetrahedron Lett.* 2002, 43, 9413–9415.
- Salehi, P.; Khodaei, M. M.; Goodarzi, M. A mild and selective deoxygenation method using γ -picolinium chlorochromate (γ -pcc). *Synth. Commun.* 2002, 32, 1253–1263.
- Khazaei, A.; Vaghei, R.G. Facile regeneration of carbonyl compounds from oximes using poly[4-vinyl-N,N-dichlorobenzenesulfonamide]. *Tetrahedron Lett.* 2002, 43, 3073–3074.
- Barton, D. H. R.; Lester, D. J.; Ley, S. V. Oxidation of ketone and aldehyde hydrazones, oximes, and semicarbazones and of hydroxylamines and hydrazo-compounds using benzeneseleninic anhydride. *J. Chem. Soc. Perkin Trans.* 1980, 11, 1212–1217.
- Shim, S. B.; Kim, K.; Kim, Y. H. Direct conversion of oximes and hydrazones into their ketones with dinitrogen tetroxide. *Tetrahedron Lett.* 1987, 28, 645–648.
- Bose, D. S.; Narraiah, A. V. **A facile method for the conversion of oximes and tosylhydrazones to carbonyl compounds with dess-martin periodinane.** *Synth. Commun.* 1999, 29, 937–941.
- Nattier, B. A.; Eash, K. J.; Mohan, R. S. Deprotection of ketoximes using bismuth(III) nitrate pentahydrate. *Synthesis* 2001, 1010–1012.

10. Bandgar, B. P.; Shaikh, S. I.; Iyer, S. Oxidative deoximation with sodium perborate. *Synth. Commun.* 1996, 26, 1163–1168.
11. Olah, G. A.; Aravanaghi, M.; Parakash, G. K. S. Synthetic methods and reactions; Reductive cleavage of oximes with vanadium(II) chloride. *Synthesis*. 1980, 79, 220–221.
12. Hill, C. L. Introduction: Polyoxometalates multicomponent molecular vehicle to probe fundamental issues and practical problems. *Chem. Res.* 1998, 98, 1–2.
13. Keggin, J. F. Structure of the molecule of i2-phosphotungstic. *Nature* 1933, 131, 908–909.
14. Misono, M. Heterogeneous catalysis by heteropoly compounds of molybdenum and tungsten. *Catal. Rev. Sci. Eng.* 1987, 29, 269–321.
15. Kozhevnikov, I. V. Heteropoly acids and related compounds as catalysts for fine chemical synthesis. *Catal. Rev. Sci. Eng.* 1995, 37, 311–352.
16. Hersberg, E. B. Regeneration of steroid ketones from their semicarbazones with pyruvic acid. *J. Org. Chem.* 1948, 13, 542 – 546.
17. Shiraishi, Y.; Hirai, T. Selective organic transformations on titanium oxide-based photocatalysts. *J. Photochem. Photobiol. C* 2008, 9, 157–170.
18. Selvam, K.; Swaminathan, M. A green chemical synthesis of 2-alkylbenzimidazoles from 1,2-phenylenediamine and propylene glycol or alcohols mediated by Ag-TiO₂/clay composite photocatalyst. *Chem. Lett.* 2007, 36, 1060–1061.
19. Pal, B.; Torimoto, T.; Okazaki, K.; Ohtani, B. **Photocatalytic syntheses of azoxybenzene** by visible light irradiation of silica-coated cadmium sulfide nanocomposites. *Chem. Commun.* 2007, 5, 483–485.
20. Pal, B.; Ikeda, S.; Kominami, H.; Kera, Y.; Ohtani, B. Photocatalytic redox-combined synthesis of L-pipecolinic acid from L-lysine by suspended titania particles: Effect of noble metal loading on the selectivity and optical purity of the product. *J. Catal.* 2003, 217, 152–159.

Science Of Street Art: Techniques And Methods Of Life Science In Art In Public Spaces.

Arunima S*,

*Research Scholar, Dept. Of English Mar Ivanios College (Autonomous), Kerala, Trivandrum.
Corresponding Author: Arunima S Email: Arunima009@Gmail.Com

Abstract: Life science is a branch of science that studies the life processes of living organisms. As it deals with the life processes of organisms its connectivity with street art could be beneficial in all walks of life. Art and science are no two entities to be kept aloof. Human Societies can be benefited from the comingling of these two disciplines along with Life Sciences. These disciplines effectively interact with each other and influence each other mutually information of new principals. Close analysis of works of art in public spaces can prove the impact of life sciences in street art. Moreover, the theoretical basis of various concepts from different branches of science could be found in street art practice. This paper is an exploration of different concepts of life science associated with Street Art. Street Art includes any work of art installed in the streets or public spaces. The connection between public art and science is a topic that arouses curiosity in the academic milieu. The paper is an attempt to look at the role of life science involved in the processes of production and reception of works of art in public spaces.

Keywords: Street Art, public space, behavior setting, stigmergy, stimulus-response.

INTRODUCTION

Street art refers to any work of art created in a public space. It includes graffiti mural stencil, wheat pastings, wall paintings, posters ¹, etc. Origins of street art could be traced back to the cave paintings or the paintings that appeared on the walls of tribal settlements in ancient times. The art form gained wide currency during the 1960s. Street art has a significant role in urban placemaking ² as it changes not only the geographical street space but also the socio-political landscape of the locality. Street art has the capability of stimulating feelings and emotions in the onlookers through the representation of reality and hence forming public opinion. Studying the science of street art could be done concerning ³ various theories explaining different mechanisms (biological, psychological) operating in various organisms. As Life Science as a discipline comprises various branches of science that revolves around the scientific study of life in general i.e life of organisms, insects, plants, animals, and human beings, connecting life science and street can open up a new intellectual space that could help out humanity in divergent ways.

Street Art in the Light of Science

The methods, concepts, and techniques of science make their presence directly or indirectly in Street Art. In one sense, works of art in public spaces have some scientific base. Even though the artist doesn't have any knowledge of science, the work and the impact of the work of art on the onlookers could be explained and understood in the light of scientific knowledge. Even if the artist is not purposefully mixing science with works of art, patterns, methods, and concepts in science creep through. A work of art may not be the result of scientific research, but it is a product of human creativity. Even the physical and psychological environments of the artist form the catalyst in the creative process could be explained in the light of science.

Gaps and Bridging

Art and science are two inseparable entities as C.P Snow argues ⁸. There should always be an effort to bridge the gap between these two disciplines as both streams can benefit each other. Unfortunately, all over the ages, only a few attempts are made to bridge the gap between the two disciplines. Taking up the public art domain for delineating the presence of principles of science in artworks will serve the purpose well. Street art belongs to the category of visual media, and it directly catches the attention of the onlooker with its visual effect. Creating structures, shapes through myriads of colors forms ⁹⁻¹² the primary task of the artist. Even in this primary task of the art science of mixing different colors of paint gets involved. The process of combining colors to make secondary and tertiary colors help the artist in creating more and more vibrant colors. Even uneducated and illiterate painters used to practice this method which is purely based on science. The creativity of an artist is stirred by several factors including his experiences, life situations, living environment, political situation of the place in which he lives. Any work of art is one way or the other connected with the living environment i.e. socio-political situation of the locality. It could be proved that even in this process of creativity or imagination the processes or patterns of science is at work. Theories of biological sciences such as stigmergy, behavior pattern, emergence, and stimulus-response can be used in studying works of art in public spaces. Concepts from science, particularly from biology are used in connection with street art.

Connecting the disciplines

In the process of connecting science and street art, some questions regarding street art are to be addressed. The evolution of street art and its growing popularity have to be understood clearly. The increasing number of street art signals its social relevance. Social issues, political environment, or even personal issues may push an artist to create a work of art. At times, there may be a large number of artists dealing ¹³⁻¹⁶ with the same theme for their works. They may be taking up one social issue for painting different pictures in one single area. Artists could be inspired by a common emotion/collective emotion for putting up their works of art. Art in any form communicates or shares some message to the audience, sometimes it may try to educate the

audience, create awareness, persuade or it can even turn into a call for an uprise.

Theory of Stigmergy

The making of street art by the artists and its communicative function in society can be read through the lens of theories and concepts from biology. The theory of stigmergy was first introduced by the great biologist Pierre Paul Grasse in the 1950s to refer to the pattern of indirect coordination found in insects. It refers to a mechanism of coordination between the actions of social insects. According to Pierre Paul Grasse¹⁷⁻²⁰, the environment stimulates action and this individual action may help stimulate another response from other insects of the ant community. In the light of this theory, one could easily figure out the fact that the artist community also works in the same pattern as stigmergy explains the coordination mechanism found in insects. Creativity is stirred by the living environment of the artist, the socio-political environment of the artist function as the primary agent in the making of a work of art, being influenced by the environment or the agent the individual artist reacts to it by creating his piece of art. Once the work of art is visible to the audience, the artwork acts as another agent in invoking responses from the onlookers. To an extent the artist's attempt to elicit similar emotions (that once worked within his mind, or his /her emotion or response to some issue that resulted in the creation of that particular work of art) from the onlooker becomes successful. The theory of stigmergy that speaks of indirect coordination, the presence of common trace elements, agents of action could be connected well with the production and reception processes of street art. The behavior of the artist could be studied in connection with and behavior. The way an individual of the ant community starts responding to an environmental factor and its impact on all the members of the community could be linked with the individual artist's reaction to specific external factors and the pattern in which the creative action initiates the generating similar actions in other individuals.

Stimulus-response mechanism

The stimulus-response mechanism is the one on which the works of art in public spaces function. Street art, in simple terms, could be described as the artist's response to some stimulus. The work of art in turn evokes different human emotions. Art is the product of creativity which involves human emotions and feelings. Psychologist Daniel Berlyne's theories could also be connected concerning the study. Berlyne's theory focuses on the properties of art and the effect of arousal systems. Psychological reading can offer a lot to the study of street art. The science of emotion can offer a better study of stimulus-response action pattern working of street art. The interaction of various elements plays a significant role in the creation of artworks. Human interaction with the world or the living environment is the basis of any work of art. According to theories of behavior, Interaction with the living world forms human behavior. Activities or human actions form human behavior. Barker's theories on human behavior study patterns of behavior. He considers the individual as a functioning organism filled with strange feelings, emotion, and cognition likely to come out with significant performances. He tried connecting social systems and natural environment that the social system is part of Artist could be identified with Barker's individual having various emotions stored at his heart and the significant performance outcomes or actions point to the work of art installed in the public space. The specific behavior pattern of the artist results in the creation of art and pattern further influencing the societal structure points towards the behavior setting of the total community. The impact of art on society and the impact of environment and society on art could be brought into light in connection with these theories.

CONCLUSION

The functioning of the street art realm can be studied concerning science. Many of the existing theories of science have to be utilized in explaining the art form. More theories are to be explored for a better understanding of art in the public space. Application of theories of Life Science to Street Art provides a better understanding of the art forms, throws light on how the artistic processes of creative work are in line with methods and patterns of science, also provides a deeper insight into the realm of the psychological impact of street art that could do a lot in connection with medical sciences, as much studies are taking place globally in theorizing and making use of the visual impact of street art in treating stress in human beings. Combining performative actions with processes of the functioning of the brain becomes more beneficial in devising new neuro treatment methods.

CONFLICT OF INTEREST

Conflict of interest declared none.

REFERENCE

1. Barker, R. *Ecological Psychology*.Stanford University Press, 1968
2. Berlyne, D.E. *Aesthetics, and Psychobiology*.Appleton,1971.
3. Berlyne, D .E . *Conflict, Arousal, and Curiosity*. New York, McGraw Hill,1960.
4. Bolles, R.C *Theory of Motivation* New York.Harper and Row, 1967.
5. Campos, Cristian. *Street Art*.Loft,2015.
6. Deutsche, Rosalyn. *Evictions, Art and Spatial Politics*.Cambridge.MIT Press,1996.
7. Hull, C. *L.A Behavior System*. New Haven, Yale University Press.1952.
8. Snow, C.P . *Two Cultures*.Cambridge University Press, 1959.
9. Waclawek, Anna. *Graffiti and Street Art*. Thames and Hudson, 2011.
10. Young, Alison. *Street Art World*. Reaktion Books, 2016.
11. C. Moureu and C. Dufraisse, *Chem. Ind.*, 47, 819, 1928.
12. D. Lowry, G. Egloff, J. C. Morrel, and G. C. Dryer, *Ind. Eng. Chem.*, 25, 804, 1933.
13. J. L. Bolland and P. tenHave, *Discuss. Farad.Soc.*, 2, 252, 1947.

14. H. S. Olcott and H. A. Mattill, *J. Am. Chem. Soc.*, 58, 1627 and 2208, 1936.
15. K. C. Bailey, *The Retardation of Chemical Reactions*, Edward Arnold Co., London, 1937, pp. 111, 179.
17. G. Scott, *Atmospheric Oxidation and Antioxidants*, Elsevier, London, 1965, pp. 1 and
18. M. W. Ranney, *Antioxidants Recent Developments*, Noyes Data Corp., Park Ridge, New Jersey, 1979.
20. F. Shahidi and P. K. J. P. D. Wanasundara, *Crit. Rev. Food Sci. Nutr.*, 32, 67, 1992.
21. E. N. Frankel, *Lipid Oxidation*, The Oily Press, West Ferry, Dundee, 115, 129, 1998
22. D. G. Bradley and D. B. Min, *Crit. Rev. Food Sci. Nutr.*, 31, 211, 1992.

Larvicidal Activity Against Mosquito Of Bis-(4-Benzylidene-3-Methyl-1H-Pyrazol-5(4H)-One)-Copper (II) & Bis-(1,3-Cyclohexanedione)-Copper (II) Complexes : A Comparative Study

V.S Sangeetha*, R.Elayaperumal ,G.Vanaja, A .Vanitha

Dhanalakshmi Srinivasan College of Arts and Science for Women Autonomous Perambalur Tamilnadu-621212

*Corresponding Author Mail id :sangeethavasanth23@gmail.com

Abstract: Copper exhibits considerable biochemical action either as an essential trace metal or as a constituent of various exogenously administered compounds in humans. In its former role it is bound to ceruloplasmin, albumin, and other proteins, while in its latter it is bound to ligands of various types forming complexes that interact with biomolecules, mainly proteins and nucleic acids. The multifaceted role of copper in biological systems is demonstrated by several studies. In particular the involvement of copper in human diseases has been described from a medicinal-chemical and a biochemical view focusing on the molecular physiology of Cu transport. Current interest in Cu complexes is stemming from their potential use as antimicrobial, antiviral, anti-inflammatory, antitumor agents, enzyme inhibitors, or chemical nucleases. Markedly, the biochemical action of Cu complexes with non-steroidal anti-inflammatory drugs (NSAIDs) has been studied. Numerous Cu (II) complexes of NSAIDs showing enhanced anti-inflammatory and antiulcerogenic activity, as well as reduced gastrointestinal toxicity compared to the complexed drug, have been prepared and structurally characterized.

Keywords: Copper, antimicrobial, antiviral, anti-inflammatory, Larvicidal Activity

INTRODUCTION

Several authors have brought to attention the antiviral and antibacterial activity of Cu (II) complexes. For instance, it was shown that the infectivity of influenza virus is reduced after exposure on copper surfaces. The mechanism of this process is only partly understood, but it has been speculated the degradation of the viral nucleic acid takes place after the intervention of copper ions¹. In addition, the study and development of Cu complexes could be helpful in the design and production of antiviral and antibacterial materials, able to deactivate HIV or H1N1 viruses and antibiotic resistant bacteria, respectively. Medicinal inorganic chemistry offers additional opportunities for the design of therapeutic agents not accessible to organic compounds². The wide range of coordination numbers and geometries, available redox states, thermodynamic and kinetic characteristics, and intrinsic properties of the cationic metal ion and ligand itself offer the medicinal chemist a large variety of reactivities to be exploited. The widespread success of cisplatin in the clinical treatment of various types of neoplasias has placed coordination chemistry of metal-based drugs in the frontline in the fight against cancer³⁻⁴. Copper-based complexes have been investigated on the assumption that endogenous metals may be less toxic for normal cells with respect to cancer cells. However, copper can also be toxic due to its redox activity and affinity for binding sites that should be occupied by other metals. The copper concentration in the human body is tightly regulated at the levels of cells, organs, and body, since copper free ions are potentially harmful⁵⁻⁶. Once absorbed in the small intestine and stomach (adult human dietary recommendation is estimated at between 1.5 and 3.0 mg Cu/d), distribution of copper is regulated by the liver into the bloodstream through ceruloplasmin and albumin. Then, sophisticated mechanisms control the transport of copper across the cell membrane mainly via the copper transporter protein (CTR1) during import and the Cu ATP7A/B transporters during export⁷⁻⁸.

MATERIALS AND METHODS

Chemicals and reagents

All chemicals were purchased from Merck, Sigma-Aldrich, and used without further purification. Solvent was dried and distilled prior to use. Merck pre-coated silica gel plates with a fluorescent indicator were used for analytical TLC. Flash column chromatography was performed using silica gel (Merck). Ethyl acetate, hexane was used as an eluting solvent for TLC and column chromatography⁹. Melting points were recorded in open capillary tubes and were uncorrected. The UV-Visible spectra (KBr) were recorded on a Shimadzu UV - 1280 (200-800 nm) spectrometer. The FT-IR spectra (KBr) were recorded on a Shimadzu 8201pc (4000-400 cm⁻¹) spectrometer.

Method of preparation

Preparation of Bis-(4-benzylidene-3-methyl-1H-pyrazol-5(4H)-one)-Copper (II) complex (I).

The compounds 4-benzylidene-3-methyl-1H-pyrazol-5(4H)-one (0.01mol, 1.86g) in 5ml ethanol is refluxed over a water bath in a magnetic stirrer with CuCl₂.2H₂O (0.005mol, 0.85g) in 5ml ethanol for three hours at 60°C. The reaction mixture was washed with excess ice-cold water¹⁰. Brown coloured precipitate was formed. It is filtered and dried. The product was confirmed by TLC. The product was recrystallized in ethanol to get pure product.

Bis-(4-benzylidene-3-methyl-1H-pyrazol-5(4H)-one)-copper (II) chloride (I)

Brown solid; mw: 358.71; mp: 246°C; UV $\lambda_{\text{MeOH}}^{\text{max}}$ nm (abs): 236 (1.24), 274 (1.41); IR (cm⁻¹): 3317.02 (NH), 2982.07 (CH),

1709.53 (C=O), 1499.48 (C-N); Elemental analysis: Calculated. For $C_{10}H_{16}Cl_2CuN_4O_2$: C, 33.48; H, 4.50; N, 15.62; %. Found: C, 33.50; H, 4.49; N, 15.61; %.

Preparation of Bis-(1,3-cyclohexanedione)-Copper (II) complex (2).

The compounds 1,3-cyclohexanedione (0.01 mol, 1.12) in 5ml ethanol is refluxed over a water bath in a magnetic stirrer with $CuCl_2 \cdot 2H_2O$ (0.005mol, 0.85g) in 5ml ethanol for three hours at $60^\circ C$ ¹²⁻¹³. Then 30ml of 10% NaOH solution was added. Green coloured precipitate was formed. It is filtered and dried. The product was confirmed by TLC. The product was recrystallized in ethanol to get pure product.

Bis-(1,3-cyclohexanedione)-copper (II) (2)

Black solid; mw: 287.80; mp: $>360^\circ C$; UV λ_{MeOH}^{MeOH} nm (abs): 291 (4.00), 391 (2.60), 395 (2.42) and 664 (1.05); IR (cm^{-1}): 2102.55 (CH), 1639.52 (C=O), 1188.22 (C-O); Elemental analysis: Calculated. For $C_{12}H_{16}CuO_4$: C, 50.08; H, 5.60; %. Found: C, 50.07; H, 5.61; %.

RESULTS AND DISCUSSION

UV-VIS profile of complex 1 was studied at a wavelength range of 200 to 800 nm. Two major bands were noticed at 236 and 274 nm with absorbance values of 1.24 and 1.41 respectively. FT-IR spectrum of complex 1 was performed to identify the functional groups present in the complex based on the peak values in the region of infrared radiation¹⁴. The major bands were observed at $V^{KBr} cm^{-1}$: 3317.02, 2982.07, 1709.53, 1499.48, 745.22 and 670.80. The peak at $3317.02 cm^{-1}$ indicates the absorption arising from Cu-NH stretching. The peak at $2982.07 cm^{-1}$ indicates the absorption arising from C-H stretching. The peak at $1709.53 cm^{-1}$ corresponds to the presence of Cu-CO stretching frequency. The peak at $1499.48 cm^{-1}$ corresponds to the presence of C-N stretching frequency. The peak at $745.22 cm^{-1}$ indicates the bending vibration of aliphatic C-H bonds¹⁵⁻¹⁶. The peak at $670.80 cm^{-1}$ corresponds to the disubstituted moiety in the aliphatic compound. In addition, some weak absorption bands were also recorded in the spectra¹⁷⁻¹⁸. UV-VIS profile of complex 2 was studied at a wavelength range of 200 to 800 nm. Four major bands were noticed at 291, 391, 395 and 664 nm with absorbance values of 4.00, 2.60, 2.42 and 1.05 respectively¹⁹⁻²⁰. FT-IR spectrum of complex 2 was performed to identify the functional groups present in the complex based on the peak values in the region of infrared radiation. The major bands were observed at $V^{KBr} cm^{-1}$: 2102.55, 1639.52, 1188.22, 745.22 and 670.80. The peak at $2102.55 cm^{-1}$ indicates the absorption arising from C-H stretching²¹. The peak at $1639.52 cm^{-1}$ corresponds to the presence of Cu-CO stretching frequency. The peak at $1188.22 cm^{-1}$ corresponds to the presence of C-O stretching frequency²¹⁻²². The peak at $745.22 cm^{-1}$ indicates the bending vibration of aliphatic C-H bonds. The peak at $670.80 cm^{-1}$ corresponds to the disubstituted moiety in the aliphatic compound. In addition, some weak absorption bands were also recorded in the spectra²³. The fluorescence micrograph was obtained by the excitation of the sample with blue light between 450 and 490 nm.

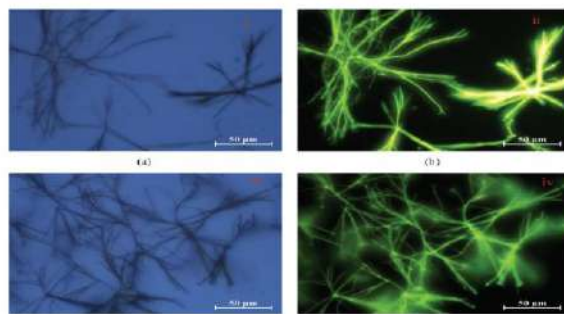


Fig: 1. Optical and fluorescence micrographs of complex-1 (a and b) and complex-2 (c and d) with DNA microwires, respectively.

Larvicidal activity

Complex 1 was more active against the *Culex quinquefasciatus* LD_{50} value of 45.28 $\mu g/ml$ than complexes 3 with the LD_{50} value of 84.73 $\mu g/ml$. Among the complexes 1 - 2 the complex 2 was less active against *Culex quinquefasciatus* with the LD_{50} values of 84.73 $\mu g/ml$ respectively. The synthesized complex 1 was highly active and to the positive control *Permethrin* with the LD_{50} value of 60.03 $\mu g/ml$. The values are summarized in Table I

Table I. Larvicidal activity of synthesized complexes (1 - 2)

Comp.No.	Mortality (%)Room temp Concentration($\mu g /mL$) ^a				LD_{50} ($\mu g /mL$)
	100	50	25	10	
1	80± 1.44	60± 1.30	40± 1.43	20± 1.29	45.28
2	60± 1.64	30± 0.54	10± 0.34	0± 0.00	84.73
Positive control	-	-	-	-	60.03
Negative control	0.0 ± 0.0	0.0 ± 0.0	0.0 ± 0.0	0.0 ± 0.0	0.0± 0.0

Positive control: Permethrin **Negative control:** DMSO ^aValue were the means of three replicates \pm SD.

Antifeedant activity (Ichthyotoxicity activity)

Complex I showed high toxicity compared with other complexes 2. Toxicity was measured as death percentage at 24hr. Complex I produced 60% mortality in 24hr at 100 μ g/ml²⁴. The values are summarized in Table 2. Among the synthesized complexes I - 2 the complex I was highly active with the LD₅₀ value of 71.89 μ g/ml.

Table 2. Antifeedant activity of synthesized complexes (1 - 2)

Comp.No.	Mortality (%)Room temp Concentration(μ g /mL) ^a				LD ₅₀ (μ g /mL)
	100	50	25	10	
1	66 \pm 2.12	41 \pm 1.34	22 \pm 1.73	10 \pm 1.47	71.89
2	33 \pm 1.22	0 \pm 0.00	-	-	>100
Negative control	0.0 \pm 0.0	0.0 \pm 0.0	0.0 \pm 0.0	0.0 \pm 0.0	0.0 \pm 0.0

Negative control: DMSO ^aValue were the means of three replicates \pm SD.

CONCLUSION

From the present study, it can be concluded that the potency of the copper (II) complexes shows significant activity in larvicidal and less toxic in antifeedant bioassays. The 3-methyl-1H-pyrazol-5(4H)-one derived complex I shows significant activity against mosquito larvae compared with positive control and shows less toxic in antifeedant activity. Therefore, these compounds might be a potential source for developing ecologically significant bioactive compounds, including biodegradable pesticides, and biopharmaceuticals.

CONFLICT OF INTEREST

Conflict of interest declared none.

REFERENCES

1. A. Chakraborty, P. Kumar, K. Ghosh, and P. Roy, Evaluation of a Schiff base copper complex compound as potent anticancer molecule with multiple targets of action, *European Journal of Pharmacology*, vol. 647, no. 13, pp. 112, 2010.
2. R. H. Holm, P. Kennepohl, and E. I. Solomon, Structural and functional aspects of metal sites in biology, *Chemical Reviews*, vol. 96, no. 7, pp. 22392314, 1996.
3. M. A. Ali, C. M. Haroon, M. Nazimuddin, S. M. M.-U. Majumder, M. T. H. Tarafder, and M. A. Khair, Synthesis, characterization and biological activities of somenewnickel(II), copper(II), zinc(II) and cadmium(II) complexes of quadridentate SNNS ligands, *Transition Metal Chemistry*, vol. 17, no. 2, pp. 133136, 1992.
4. D. T. Minkel, C.H. Chanstier, and D. H. Petering, Reactions of 3-Ethoxy-2-oxobutyraldehyde Bis(N4-dimethylthiosemicarbazonato)- Zinc(II) with tumor cells and mitochondria, *Molecular Pharmacology*, vol. 12, no. 6, pp. 10361044, 1976.
5. V. Rajendiran, R. Karthik, M. Palaniandavar et al., Mixed lig and copper (II)-phenolate complexes: effect of coligand on enhanced DNA and protein binding, DNA cleavage, and anticancer activity, *Inorganic Chemistry*, vol. 46, no. 20, pp. 8208 8221, 2007.
6. A. E. Liberta and D. X. West, Antifungal and antitumor activity of heterocyclic thiosemicarbazones and their metal complexes: current status, *Biometals*, vol. 5, no. 2, pp. 121126, 1992.
7. Y. Harinath, D. H. K. Reddy, B. N. Kumar, C. Apparao, and K. Seshaiah, Synthesis, spectral characterization and antioxidant activity studies of a bidentate Schiff base, 5-methyl thiophene-2-carboxaldehyde-carbohydrazone and its Cd(II), Cu(II), Ni(II) and Zn(II) complexes, *Spectrochimica Acta Part A: Molecular and Biomolecular Spectroscopy*, vol. 101, pp. 264272, 2013.
8. J. Sheikh, H. Juneja, V. Ingle, P. Ali, and T. B. Hadda, Synthesis and in vitro biology of Co(II), Ni(II), Cu(II) and Zinc(II) complexes of functionalized beta-diketone bearing energy buried potential antibacterial and antiviral O,O pharmacophore sites, *Journal of Saudi Chemical Society*, vol. 17, no. 3, pp. 269276, 2013.
9. C. Marzano, M. Pellei, F. Tisato, and C. Santini, Copper complexes as anticancer agents, *Anti-Cancer Agents in Medicinal Chemistry*, vol. 10, no. 2, pp. 191196, 2013.
10. S. M. Saadeh, Synthesis, characterization and biological properties of Co(II), Ni(II), Cu(II) and Zn(II) complexes with an SNO functionalized ligand, *Arabian Journal of Chemistry*, vol. 6, no. 2, pp. 191196, 2013.
11. J. Garcí'a-Tojal, A. Garcí'a-Orad, A. A. D'íaz et al., "Biological activity of complexes derived from pyridine-2-carbaldehyde thiosemicarbazone: structure of [Co(C7H7N4S)2][NCS]," *Journal of Inorganic Biochemistry*, vol. 84, no. 3-4, pp. 271–278, 2001.
12. P. R. Reddy and A. Shilpa, "2-hydroxynaphthalene-1-carbaldehyde- and 2-aminomethyl)pyridine-based Schiff base CuII complexes for DNA binding and cleavage," *Chemistry & Biodiversity*, vol. 9, no. 10, pp. 2262–2281, 2012.
13. N. Shahabadi, M.M. Khodaei, S. Kashanian, and F. Kheirdoosh, Interaction of a copper (II) complex containing an artificial sweetener (aspartame) with calf thymus DNA, *Spectrochimica Acta Part A: Molecular and Biomolecular Spectroscopy*, vol. 120, pp. 16, 2014.

14. A. J. Steckl, DNAa new material for photonics *Nature Photonics*, vol. 1, pp. 35, 2007.
15. S. Bandyopadhyay, M. Tarek, and M. L. Klein, Molecular dynamics study of a lipid-DNA complex, *The Journal of Physical Chemistry B*, vol. 103, no. 46, pp. 1007510080, 1999.
16. M. Hazra, T. Dolai, A. Pandey, S. K. Dey, and A. Patra, Fluorescent copper (II) complexes: the electron transfermechanism, interaction with bovine serum albumin (BSA) and antibacterial activity, *Journal of Saudi Chemical Society*, 2014.
17. A. D. Becke, Density-functional thermochemistry. III. The role of exact exchange," *The Journal of Chemical Physics*, vol. 98, article 5648, 1993.
18. C. Lee, W. Yang, and R. G. Parr, "Development of the Colle-Salvetti correlation-energy formula into a functional of the electron density, *Physical Review B*, vol. 37, no. 2, pp. 785789, 1998.
19. S. Roy, T. K. Mondal, P. Mitra, E. L. Torres, and C. Sinha, Synthesis, structure, spectroscopic properties, electrochemistry, and DFT correlative studies of N-[(2-pyridyl)methylidene]-6-coumarin complexes of Cu(I) and Ag(I), *Polyhedron*, vol. 30, no. 6, pp. 913922, 2011.
20. J.A. Pople, M. J. Frisch, G.W. Trucks et al., *Gaussian 09, Revision B.01*, Gaussian, Wallingford, UK, 2009.
21. M. E. Reichman, S. A. Rice, C. A. Tgomas, and P. Doty, A further examination of the molecular weight and Size of desoxypentose nucleic acid, *Journal of the American Chemical Society*, vol. 76, no. 11, pp. 30473053, 1954.
22. D. Lahiri, T. Bhowmick, B. Pathak et al., Anaerobic photocleavage of DNA in red light by dicopper(II) complexes of 3,3-dithiodipropionic acid, *Inorganic Chemistry*, vol. 48, no. 1, pp. 339349, 2009.
23. Singh and P. Singh, Synthesis, spectroscopic characterization, and in vitro antimicrobial studies of pyridine-2-carboxylic acid N-(4-chloro-benzoyl)-hydrazide and its Co(II), Ni(II), and Cu(II) complexes, *Bioinorganic Chemistry and Applications*, vol. 2012, Article ID 104549, 7 pages, 2012.

Green Synthesis And Characterization Of Copper Nanoparticles Derived From Murraya Koenigii Leaves Extract

Dr .K.Sowmiya, Dr. R. Purushothaman, Dr. Shalini, Chinnadurai

Dhanalakshmi Srinivasan College of Arts and Science for Women(Autonomous) Perambalur - 621212.

Abstract: In recent years the green and eco-friendly method of synthesis for metal nanoparticles is an emerging field in nanotechnology and nanoscience. The importance of nanoparticles in society and industries is due to the remarkable change in the physical and chemical properties of the materials in the nano dimension. The Copper nanoparticles (CuNPs) are mostly found in their applications in the field of medical, electronic devices, biosensors, reagents in various reactions, lubricants, anti-biotic, anti-fungal, anti-microbial agents, and many more. The present study involves the green and eco-friendly synthesis of CuNPs using the leaves extracts of the plant MurrayaKoenigii (Curry leaves) and 1 mM Copper Sulphate ($\text{CuSO}_4 \cdot 5\text{H}_2\text{O}$) solution. For this synthesis, the different bio-components present in the leaves extract works as a reducing agent. The synthesized CuNPs were characterized by UV-visible spectroscopy, Scanning Electron Microscopy (SEM and FTIR). The CuNPs formed were confirmed by the characteristics surface plasmon resonance (SPR) peak found at 340nm in UV-visible spectra. The morphological study from SEM images, it is confirmed that unsymmetrical spherical size Copper nanoparticles settled on leaves extract residue. FTIR spectrum clearly illustrates the green synthesis of copper nanoparticles mediated by the leaves extract. The method is fast and easy. As it does not involve the use of harmful and costly chemicals, it is more economical.

Keywords: Copper nanoparticles (CuNPs), Plant extract, Characterization, UV-Vis. Spectra, SEM, FTIR.

INTRODUCTION

Nanoscience and Nanotechnology are modern and very useful fast-growing branches of science and technology which deals with fabrication, characterization, and applications of various nano (which is the billionth part of meter i.e. 10^{-9} m.) metallic and non-metallic nanostructured materials of different compositions, sizes, and shapes¹ that are playing an ever-increasing role in day to day life, as more and more products based on nanostructured materials are introduced in the market. The properties of nanomaterials are found to be very distinct and more superior to the macroscale properties of the same substance. This leads to the increasing importance of research interest in these materials. Copper nanoparticles (CuNPs) are mostly found in their applications in the field of medical, electronic devices, biosensors, reagents in various reactions, lubricants, and biotechnology². Among various types of nanoparticles available, copper nanoparticles (CuNPs) are the most commonly employed as they are simple to produce by reducing copper ions in the aqueous solution of copper sulphate. Further, copper has also been used as an anti-biotic, anti-fungal, anti-microbial agent in the treatment of wounds³. Various attempts have been made for the synthesis of CuNPs by the methods of laser ablation, gamma irradiation, electron irradiation, thermal decomposition of metal compounds, chemical reduction, photochemical methods, microwave processing, and biological methods⁴. The major drawback of these methods is the use of toxic and expensive chemicals⁵. Nowadays, therefore it is the need of the hour to investigate a new route of synthesis which should be green and eco-friendly. Therefore bio-synthesis of CuNPs by employing different medicinal plant leaves extracts is found to be a simple, easy, low cost, and eco-friendly green technique for the production of CuNPs in bulk⁶. The main mechanism considered in such synthesis of nanoparticles is the role of phytochemicals present in the extract which acts as the reducing agents to reduce the aqueous metal ions. The phytochemicals that mainly cause the reduction of metal ions are flavonoids, terpenoids, carboxylic acids, quinones, aldehydes, ketones, and amides⁷. Different plants are being currently investigated for their role in the synthesis of nanoparticles. The literature review showed that many researchers have synthesized metal nanoparticles from the leaves extracts of the plants like *Buteamonosperma*⁸⁻¹⁰, *Piper longum*, *Nerium oleander*¹¹⁻¹², *Ocimum sanctum*, *Tealeaf*¹³, *Glycine Max*¹⁴⁻¹⁶, *Aloe vera* plant¹⁷⁻¹⁹, etc. In the present study, the synthesis of CuNPs from the leaves extracts of the plant MurrayaKoenigii²⁰ was selected due to its potential medicinal value.

MATERIALS AND METHODS

Chemicals: Copper Sulphate ($\text{CuSO}_4 \cdot 5\text{H}_2\text{O}$), Double Distilled water.

Glassware: All glasswares (Conical flasks, Measuring cylinders, Beakers, Petri plates, and Test tubes, etc.) of borosil were used.

The plant used: The present work involves the synthesis of copper nanoparticles (CuNPs) by a green method using the leaves extract of the plant MurrayaKoenigii (Curry leaves).^{3,4}

Preparation of the plant extract: The Plant leaf extract was prepared by using 25g of fresh leaves, collected from the local area. Fresh leaves were washed extensively with water followed by a final wash twice/thrice with distilled water to remove all the dust and unwanted visible particles. The leaves were cut into small pieces and then shade-dried for 2-3 days (figure 1). The shade-dried small leaves pieces were then put in 100 mL of distilled water and boiled on a water bath for 15 minutes. After boiling, the solution was cooled and filtered using Whatman filter paper no. 1 to remove particulate matter and to get the clear

solution which was then stored at 4°C until further use within one week (Gardea-Torresdey, 2003). During every process, cleanliness and hygiene were maintained for good results⁶⁻⁸.



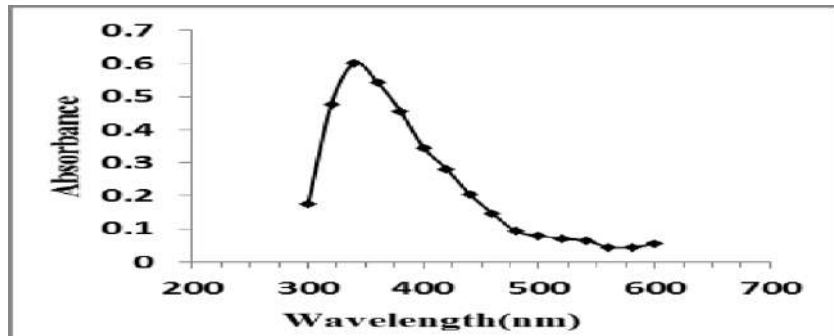
Figure.1.The shade-dried Curry leaves

Characterization of Copper nanoparticles:

Characterization of Synthesized Cu-nanoparticles can be carried out by UV- Vis spectroscopy. Metal nanoparticles have free electrons, which are responsible for a characteristics surface plasmon resonance (SPR) absorption band in UV- Vis spectra. This peak in the UV-Vis spectrum is because of the strong interaction between the free electrons present on the surface of metal nanoparticles and the light of specific wavelengths. The color of Metal nanoparticles depends upon their shape and size. The reduction of Cu⁺⁺ was confirmed from the UV-Vis spectrum of the solution from region 300-600nm using an Equiptronics microprocessor-based Single-beam spectrophotometer (EQ-825A). The FT-IR Characterization is used to find the entities with their functional group associated with the synthesized Nanoparticles. High-resolution Scanning electron microscope (SEM) analysis is employed to study the shape, size & surface morphologies of the nanoparticle.

RESULTS AND DISCUSSIONS

UV-Vis Spectra: Synthesized Copper nanoparticles (CuNPs) were characterized by UV-Vis spectroscopy. The UV-Visible spectrum of the CuNPs solution recorded after 24 hours is shown in Figure.3. The sharp and high peak is appearing in the spectrum at 340 nm, suggesting the stability and size of the Copper nanoparticles (Gopinath, 2014; Ajitha, 2014). High absorbance indicates a high conversion of Cu⁺⁺ to Cu as nanoparticles leading to a higher concentration of CuNPs (Mathur, 2014). ISSN: 0974-2115 www.jchps.com Journal of Chemical and Pharmaceutical Sciences



FT-IR spectra: FTIR gives information about entities with their functional group associated with the synthesized Nanoparticles. FTIR spectrum as shown in Figure 4 clearly illustrates the eco-friendly green synthesis of Copper nanoparticles mediated by the leaves extract. In the spectra, the broad peak at 3273.40 cm⁻¹ corresponds to N-H or O-H stretching in amino acids, alcohols, and phenols. The peak at 2926.81cm⁻¹ corresponds to C-H stretching in alkanes and aldehydes¹⁴⁻¹⁶, The weak peak at 2104.74 cm⁻¹ corresponds to C≡C stretching in alkynes, The peak at 1587.34 cm⁻¹ corresponds to C=C stretching, The peak at 1393.29 cm⁻¹ corresponds to CH₂ & CH₃ deformation, The peak at 1043.06 cm⁻¹ corresponds to C-O stretching, The weak peaks in between 850-550 cm⁻¹ are associated to C-Cl stretching in halo compounds. Thus the nanoparticles formed seemed to be associated with metabolites and proteins like terpenoids having functional groups as ketons, aldehydes, alcohols, phenols, and carboxylic acids. As the phenolic group has the more tendency to bind metal indicates that the phenols might be acting as the capping agent for the metal nanoparticles and thus prevent agglomeration, thereby stabilizing the medium. This suggests that the bio-entities could probably play the dual role of fabrication and stabilization of Cu nanoparticles in the aqueous solution .

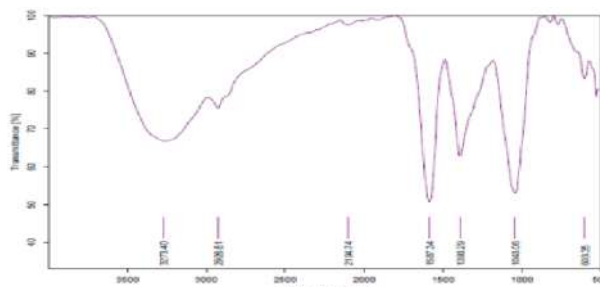


Figure.4. FTIR spectra of CuNPs using Curry leaves extract

SEM:

After the evaporation of the water solvent, the surface morphology of the nanoparticles was obtained by Scanning Electron Microscopy (SEM) analysis. Figure.5, shows the SEM image of Copper nanoparticles. From the image, one can notice the existence of unsymmetrical spherical tiny copper nanoparticles settled on extract residue as the sample was prepared by the method of evaporation. However, we couldn't investigate the exact surface texture of the observed nanoparticles.¹⁸

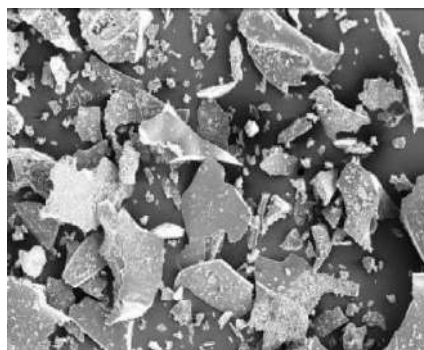


Figure.5. SEM Image of CuNPs using Curry leaves extract

CONCLUSION

It is strongly desired in the field of Nanoscience and Nanotechnology to develop the reliable, easy, low cost, safe, non-toxic, and eco-friendly process for the synthesis of metal nanoparticles. Eco-friendly green synthesis of Copper nanoparticles by using plant leaves extract has all these aspects thus acts as an eco-friendly path of synthesis which can be adopted for the bulk production of CuNPs. The UV peak at 340nm indicates the synthesis of CuNPs. The SEM studies helped study the surface texture of CuNPs. FTIR studies confirmed the green synthesis of the CuNPs by the action of various phytochemicals with their different functional groups in the extract solution. It can be concluded that CuNPs synthesized in the present work are found very stable because of the capping and stabilizing materials present in the leaves extract.

CONFLICT OF INTEREST

Conflict of interest declared none.

REFERENCES

1. Ajitha B, Reddy Y.A.K, Reddy P.S, Biosynthesis of silver nanoparticles using *Plectranthusamboinicus* leaf extract and its antimicrobial activity. *Spectrochimica Acta Part A, Molecular and Biomolecular Spectroscopy*, 128, 2014, 257-262.
2. Chandran S. P, Chaudhary M, Pasricha R, Ahmad A, Sastry M. Synthesis of gold nano triangles and silver nanoparticles using *Aloe vera* plant extract, *Biotechnology progress*, 22 (2), 2006, 577-583.
3. Chatterjee A.K, Chakraborty R, Basu T, Mechanism of antibacterial activity of copper nanoparticles, *Nanotechnology*, 25 (13), 2014, 135101.
4. Chaturvedi V, Verma P, Fabrication of silver nanoparticles from leaf extract of *Buteamonosperma*(Flame of Forest) and their inhibitory effect on bloom-forming cyanobacteria, *Bioresources and Bioprocessing*, 2 (18), 2015.
5. Din M.I, Rehan R, Synthesis, Characterization and Applications of Copper Nanoparticles, *Analytical Letters*, 49, 2016, 50-62.
6. Gardea-Torresdey J.L, Gomez E, Peralta-Videa J.R, Parsons J.G, Troiani H, Jose-Yacaman M, Alfalfa sprouts: a natural source for the synthesis of silver nanoparticles. *Langmuir*, 19 (4), 2003, 1357-1361.
7. Gopinath M, Subbaiyal R, MasilamaniSelvam M, Suresh D, Synthesis of Copper Nanoparticles from *Nerium oleander* Leaf aqueous extract and its Antibacterial Activity, *Int.J. Curr. Microbiol. App. Sci.*, 3 (9), 2014, 814-818.
8. Jacob S.J, Finub J.S, Narayanan A, Synthesis of silver nanoparticles using *Piper longum*leaf extracts and its cytotoxic activity against Hep-2 cell line. *Colloids and Surfaces B: Bio interfaces*, 91, 2012, 212-214.

9. Kulkarni V, Kulkarni P, Synthesis of copper nanoparticles with aegle marmelos leaf extract, Nanoscience and nano technology an Indian journal, 8 (10), 2014, 401-404.
10. Kulkarni V.D, Kulkarni P.S, Green Synthesis of Copper Nanoparticles Using *Ocimum sanctum* Leaf Extract, International Journal of Chemical Studies, 1 (3), 2013, 1-4.
11. Lengke F.M, Fleet E.M, Southam G. Biosynthesis of silver nanoparticles by filamentous cyanobacteria a from a silver (I) nitrate complex, Langmuir, 23, 2007, 2694–2699.
12. Mathur A, Kushwaha A, Dalakoti V, Dalakoti G, Singh D.S, Green synthesis of silver nanoparticles using medicinal plant and its characterization, Der Pharmacia Letter, 5, 2014, 118-122.
13. Murugan K, Senthilkumar B, Senbagam D, Al-Sohaibani S, Biosynthesis of silver nanoparticles using *Acacia leucophloea* extract and their antibacterial activity. Int J Nanomedicine, 9, 2014, 2431-2438.
14. Prabhu S, Poulose E, Silver nanoparticles: mechanism of antimicrobial action, synthesis, medical applications, and toxicity effects, International Nano Letters, 2 (32), 2012.
15. Sadowski Z, Biosynthesis and Application of Silver and Gold Nanoparticles, Silver Nanoparticles, David Pozo Perez (Ed.), In Tech, 2010.
16. Saranyaadevi K, Subha V, Ernest Ravindran R.S, Renganathan S, Synthesis and Characterization of Copper Nanoparticle using *Cappariszeylanica* leaf Extract, Int. J. Chem. Tech. Research, 6 (10), 2014, 4533-4541.
17. Vaseeharan B, Ramasamy P, Chen J.C, Antibacterial activity of silver nanoparticles (AgNPs) synthesized by tea leaf extracts against pathogenic *Vibrio harveyi* and its protective efficacy on juvenile *Feneropenaeusindicus*, Letters in applied microbiology, 50 (4), 2010, 352-356.
18. Vivekanandhan S, Misra M, Mohanty A.K, Biological Synthesis of Silver Nanoparticles using Glycine Max (Soybean) Leaf Extract: An Investigation on different Soybean Varieties, Journal of Nanoscience and Nanotechnology, 9 (12), 2009, 6828-6833.
19. D. G. Shchukin, J. H. Schattka, M. Antonietti, R. A. Caruso, J. Phys. Chem. B., 2003, 107(4), 952-957.
20. R. Veerasamy, TZ. Xin, S. Gunasagaran, TFW. Xiang, EFC. Yang, N. Jeyakumar, Journal of Saudi Chemical Society, 2011, 15(2), 113-120.
21. I. N. Michiraa, D.N. Katithib, P. Gutoc, G. N. Kamaud, P. Bakere, E. Iwuohaf, International Journal of Sciences: Basic and Applied Research, 2014, 13(2), 63-76.
22. Azizova, O. A. 2002. Role of free radical processes in the development of atherosclerosis. *Biologicheskie Membrany*, 19: 451–471.

Detection Of Antioxidant Potential Of Azima Tetracantha Lam.

Dr.Surya.C, S.Sathish, Nirmala Devi. P, Punitha

Department of Biochemistry, Dhanalakshmis Srinivasan College of Arts and Science for Women (Autonomous), Perambalur

Abstract: *Azimatetracantha.Lam* (Salvadoraceae) is widely used in folklore herbal medicine practices in the villages of southern Kerala. The plant is claimed to have anti-inflammatory, antiperiodic, analgesic, and wound healing properties. The present study evaluated the antioxidant and anti-inflammatory activity of *azimatetracantha* leaves. Qualitative analysis of *Azima* revealed the presence of flavonoids, alkaloids, glycosides, phenolic compounds, tannins, and terpenoids. Methanolic extract showed greater antioxidant activity than chloroform extract. The extract showed both the radical scavenging activity and reducing capability to fight against free radicals. The results from antioxidant and antiinflammation of *A. tetracantha* Lam leaves showed significant medicinal properties.

Key Words: *azimatetracantha, alkaloids ,antiperoidic , antioxidant, Extract.*

INTRODUCTION

Nature has been a source of medicinal agents for thousands of years and impressive medicinal drugs have been prepared from natural sources¹. Herbal medicines are currently in demand and their popularity is increasing day by day. Throughout the ages, humans have relied on nature for their basic needs, for the production of food, shelter, clothing, transportation, fertilizers, flavors, and fragrances². Medicinal plants have formed the basis of sophisticated traditional medicinal systems that have been in existence for thousands of years and continue to provide mankind with new remedies. The various indigenous systems such as Siddha, Ayurvedha, and Unani are used in several plant species to treat different ailments. The use of herbal medicine is increasingly popular due to the toxicity and side effects of allopathic medicines. World Health Organization (WHO) estimated that 80 % of the population of developing countries relies on traditional medicines, mostly plant drugs, for their primary health care needs³. The primary benefits of plant-derived medicines are relatively safer than synthetic alternatives, offering profound therapeutic benefits and more affordable treatment. Although herbs had been priced for their medicinal, flavoring, and aromatic qualities for centuries, the synthetic products of the modern age surpassed their importance for a while⁴. Natural products and their derivatives represent more than 50 % of all the drugs in clinical use in the world today. Medicinal plants play an important role in the development of potent therapeutic agents. Plant-derived substances collectively called phytonutrients or phytochemicals are increasingly known for their antioxidant activities⁵. Naturally occurring plant metabolites are divided into two groups(primary and secondary metabolites). Primary metabolites are involved directly in the growth and metabolism of plants and secondary metabolites are considered as an end product of primary metabolites and in general, it is not involved in any metabolism. It comprises common sugars, amino acids, proteins, and chlorophyll⁶⁻⁷. Antioxidant Substances that can neutralize reactive molecules and reduce oxidative damage. Result of metabolic processes and environmental sources. Vitamin C, vitamin E, beta-carotene, Vitamin A, Selenium, iron, zinc, copper, and manganese. Free radicals are electrically charged molecules i.e., they have an unpaired electron which causes them to seek out and capture electrons from other substances to neutralize themselves⁸. Reactive oxygen species is a term that encompasses all highly reactive and oxygen-containing molecules, including free radicals. Reactive oxygen species such as superoxide radicals, hydrogen peroxide, hydroxyl free radical, singlet oxygen, nitric oxide can directly lead to DNA mutation, alteration of gene expression, modification of cell signal transduction, cell apoptosis, lipid peroxidation, and protein degradation by reacting with membrane lipid, nucleic acids, proteins and enzymes⁹. Anti-inflammatory of a substance or treatment that reduces inflammation. Anti-inflammatory drugs make up about half of analgesics remedying pain by reducing inflammation as opposed to opioids which affect the central nervous system.¹⁰. *Azima* is a dioecious shrub, erect or scrambling, glabrous, much-branched, smelling rancid when it rubbed. Leaves are simple, opposite, and present in the entire plant. Flowers are small, unisexual, or sometimes partially bisexual. Pedicels are absent or very short. The calyx is campanulate. It has 4 free, oblong, or lanceolate petals. Flowers are bisexual. Berries are globose or ovoid with 2 or 3 seeded¹¹⁻¹². It has a thin membranous endocarp. Seeds are compressed globous with a thick and leathery testa. The Genus *Azima* further organized into finer groups including, *A.angustifolia*, *A. diacantha*, *A. nova*, *A. pubescens*, *A. sarmentosa*, *A. scandens*, *A. spinosissima*, and *A. tetracantha*. It leaves its oval to circular arranged oppositely and nearby¹³⁻¹⁴. Each pair are right angle to the others. It is light green, leathery, and hairy. Apex has a short tip and entire margin tapering at both ends with short petioles.

MATERIALS AND METHODS

Potassium dichromate was dissolved in warm water, cooled, and sulfuric acid was added slowly and up to 1 liter. It was mixed thoroughly and used for cleaning glassware. Then the glassware was rinsed thrice in tap water, finally rinsed in distilled water, and dried in a hot air oven. These glasswares were used in further experiments.

Collection and preparation of plant material

Fresh leaves of *Azimatetracantha* were collected from Red Hills, Thiruvalluvar Taluk, Chennai, Tamil Nadu, India. The plant specimen was authenticated by Prof. S. Jayaram, Plant Anatomy Research Centre, Tambaram, Chennai. Fresh leaves of *A.tetracantha* were washed in running tap water followed by double distilled water then shade dried for two weeks. Dried leaves

were grounded as a coarse powder using an electrical blender.

Preparation of extract

100 g of powdered leaves were used for successive soxhlet extraction with 500 ml hexane, dichloromethane, ethyl acetate, ethanol at the respective temperature. The extract was then concentrated using a rotary evaporator under reduced pressure at 40 °C. Organic solvents were selected based on their polarity.

Screening of bioactive constituents

Detection of Alkaloids

Solvent-free extract, 50 mg is stirred with a few ml of concentrated hydrochloric acid and filtered. The filtrate is tested carefully with various alkaloid reagents.

Detection of Flavonoids

50 mg of extract was dissolved in 5 ml of distilled water and used for further studies.

Detection of Carbohydrates

The extract (100 mg) is dissolved in 5 ml of water and filtered. The filtrate is subjected to the following tests.

Benedict's test

To 0.5 ml of filtrate, 0.5 ml of Benedict's reagent is added. The mixture is heated in a boiling water bath for 2 minutes. A characteristic colored precipitate indicates the presence of sugar.

Benedict's test

Sodium citrate (173 g) and sodium carbonate (100 g) are dissolved in 800 ml of distilled water and boiled to make it clear. Copper sulphate (17.3 g) dissolved in 100 ml of distilled water is added to it, made up to 1 liter.

Detection of Saponins

a.

b. Honeycomb test

50 mg of the extract is dissolved in 5 ml of distilled water and a few drops of 5 % sodium bicarbonate solution were added to it. The mixture was shaken vigorously and kept for 3 minutes. The formation of honeycomb-like froth shows the presence of saponins.

b. Foam test the extract (50 mg) is diluted with distilled water and made up to 20 ml. The suspension in a graduated cylinder was shaken for 15 minutes. A 2 cm layer of foam indicates the presence of saponins.

Detection of Phenolic compound and Tannins

a) Ferric Chloride Test

The extract (50 mg) is dissolved in 5 ml of distilled water. To this, a few drops of neutral 5 % ferric chloride solution are added. The dark green color indicates the presence of phenolic compounds.

b) Lead acetate Test

The extract (50 mg) is dissolved in distilled water, to this; 3 ml of 10 % lead acetate solution is added. A bulky white precipitate indicates the presence of phenolic compounds.

C. Alkaline reagent test

An aqueous solution of the extract is treated with 10 % sodium hydroxide solution.

Evaluation of antioxidant and radical scavenging activity by *in vitro* techniques **Antioxidant activities**

The antioxidant potential was evaluated by the following methods

1. Total antioxidant activity by phosphomolybdenum method
2. Reducing potential assay

I. Total antioxidant activity by phosphomolybdenum method

The total antioxidant activity of all the extracts was evaluated by the phosphomolybdenum assay method .436 mg of 28 mM sodium phosphate and 465 mg of 4 M ammonium molybdate were dissolved in 100 ml of sulfuric acid.0.3 ml of different concentrations of extracts were mixed with 3 ml of reagent (0.6 M sulfuric acid, 28 mM sodium phosphate, and 4 mM ammonium molybdate) and incubated in a water bath at 95 °C for 90 minutes. A blank solution was prepared with 3 ml of reagent solution and 1 ml of methanol and it was incubated under the same condition as the sample treated. The absorbance of the reaction mixture was measured at 695 nm. The antioxidant capacity of the sample was expressed as ascorbic acid equivalents (mg/g of extract).

In-vitro radical scavenging activities**I. DPPH radical scavenging activity**

The DPPH radical scavenging activity of all the extracts was assessed spectrophotometrically by the method of Blois (1958).

Percentage inhibition = [(Absorbance of control – Absorbance of the sample)/Absorbance of control] × 100

Superoxide radical scavenging activity

The influence of extracts on the generation of superoxide was assessed spectrophotometrically by the method of (Nishikimiet al., (1972).

Percentage inhibition = [(Absorbance of control – Absorbance of the sample)/Absorbance of control] × 100

RESULTS

Natural antioxidants present in the plants are closely related to their medicinal and pharmaceutical properties. Thus antioxidant capacity is a widely used parameter for assessing the bioavailability of foodstuffs such as medicinal plants.

Yield percentage

Table I: Yield % of successive extracts from the leaves of *A.tetraacantha*

Extracts	Yield %
Hexane	4
Dichloromethane	3.2
Ethyl acetate	2
Ethanol	16

Solvent extraction is the most commonly used method in sample preparations from plants. The total yield value of all the extracts of leaves of *A. tetraacantha* was given in the table. I. The yield percentage of all the extracts was found to be in the order of ethanol > hexane > dichloromethane > ethyl acetate. Ethanolic extract was found to possess high recovery than the other extracts.

Screening of bioactive constituents

Phytoconstituents	Assays	Hxn	Dcm	Ea	Etoh
Alkaloids	Wagers	+	++	+++	++
Flavonoids	Shinoda Lead acetate	+	+	+++	++
Phenolics and tannins	Lead acetate Ferric chloride Sodium hydroxide	+	-	+	+
Steroids and sterols	Salkowski	+	+	+	+
Carbohydrates	Fehlings Benedicts	-	+	+++	+

HXN – Hexane; DCM – Dichloromethane; EA – Ethyl acetate; EtOH – Ethanol

Antioxidant assays

There are several methods for the determination of antioxidant activities. The chemical complexities of the extracts often a mixture of dozens of compounds with different functional polarities and chemical behavior, could lead to scattered results depending on the test employed. Therefore approaches with different assays for evaluating the antioxidant potential of extracts would be more informative and even necessary. In this study, mainly 6 methods such as DPPH radical, superoxide radical, nitric oxide radical, metal chelating, reducing power, and total antioxidant activities were used.

I. Total antioxidant assay by phosphomolybdenum method

Antioxidant activity of leaves of *A.tetraacantha* was expressed as the number of ascorbic acid equivalents. The phosphomolybdenum method was based on the reduction of Mo (VI) to Mo (V) by the antioxidant compound in the crude extracts and the formation of the green phosphate/Mo (V) complex with maximum absorption at 695 nm.

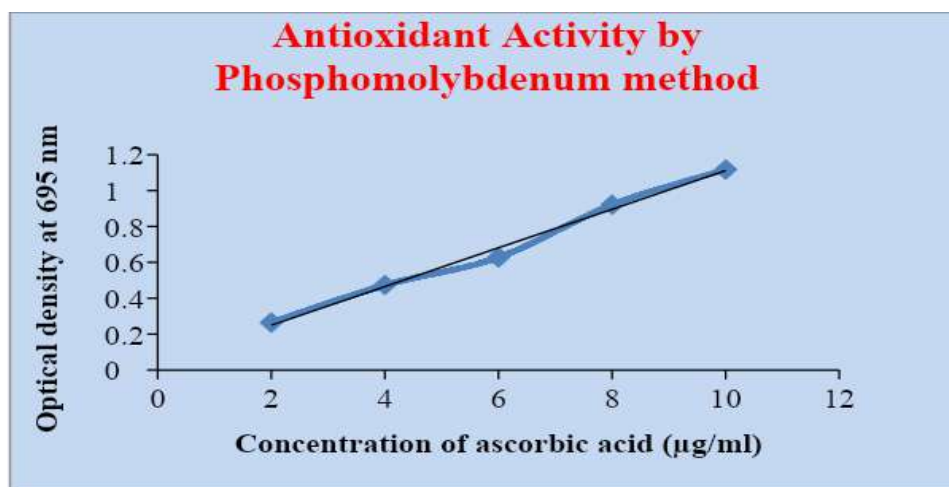


Table I: Total antioxidant activity by phosphomolybdenum method for extracts from leaves of *Azimateetracantha*.

Ethyl acetate extract exhibited high antioxidant capacity than all the other extracts. The antioxidant capacity of the extracts decreases in the order of ethyl acetate > dichloromethane > ethanol > hexane (Table 4). The standard calibration curve of ascorbic acid was shown in (figure 7).

Radical scavenging assays

a. DPPH radical scavenging activity

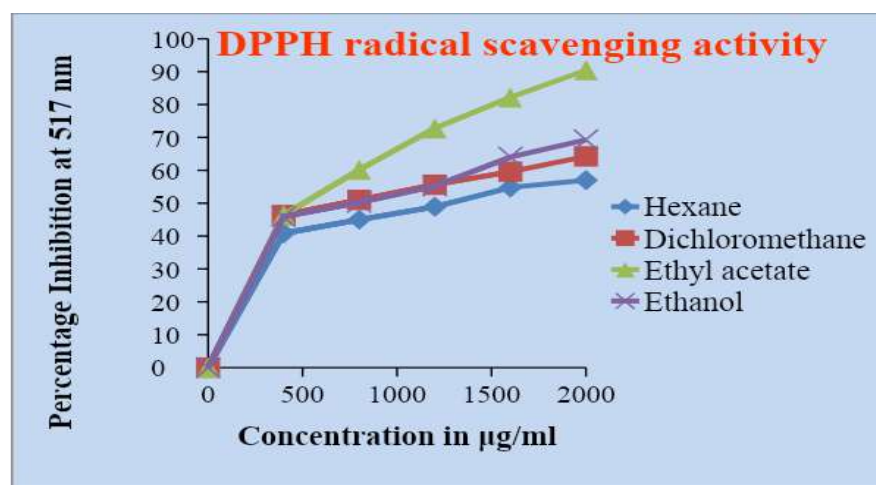


Figure 1: DPPH radical scavenging activities of extracts from leaves of *Azimateetracantha*.

Radical scavenging was determined in the concentration of (400 - 2000 μg/ml) the extracts and shown in figure 7. For each extract, IC_{50} value was calculated as the concentration that causes a 50 % reduction in DPPH free radical (Table 5). Hence ethyl acetate extract exhibited potent IC_{50} with a maximum inhibition at 2mg/ml concentration.

b. Superoxide radical scavenging activity

Superoxide radical is one of the major reactive oxygen species known to be deleterious, highly contributing towards tissue damage and various diseases. This radical is known to be produced *in vivo* and generates hydrogen peroxide.

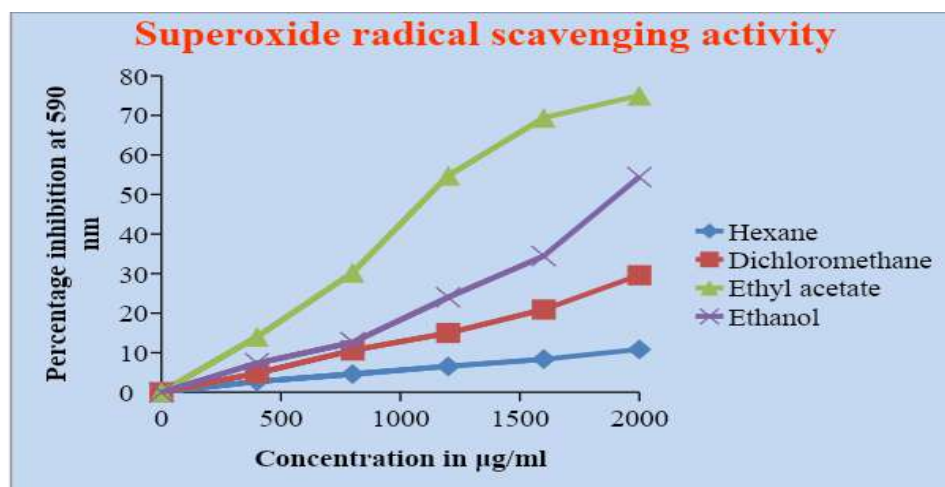


Figure 2: Superoxide radical scavenging activities of extracts from leaves of *Azimatetrapetala*.

DISCUSSION

In the present study, leaves of *Azimatetrapetala* were used for the evaluation of yield percentage, screening of phytoconstituents, quantification of total phenolics and flavonoids, *in vitro* antioxidant, radical scavenging, and *in vitro* anti-inflammatory activities. Successive Soxhlet extraction was carried out using 4 different solvents¹⁵⁻¹⁶. Solvents were chosen based on their polarity. Soxhlet extraction is a classical technique for the solvent extraction of obtaining bioactive compounds. Even though, some of the heat-sensitive compounds may decompose in the Soxhlet extraction. However thermostable compounds cannot be dehydrolyzed due to the stability of the compounds¹⁷. Leaves of *Azimatetrapetala* were revealed to contain saponins, which are known to produce an inhibitory effect on inflammation. The spectrophotometric method for the development of antioxidant capacity by the phosphomolybdenum method¹⁸. It is based on the reduction of Mo (VI) and Mo (V) by the sample and subsequent formation of a green phosphate/Mo (V). From the results, the antioxidant capacity of the extracts was able to inhibit the Mo (V) complex¹⁹. DPPH is a stable free radical and accepts an electron or hydrogen radical to become a stable diamagnetic molecule and reported that phenolics and flavonoids reduce the DPPH radical by their hydrogen donating abilities. The result obtained in this investigation revealed that DPPH radical scavenging activities of leaves of *A. tetracantha* might be attributed to the hydrogen donating ability.

SUMMARY AND CONCLUSION

The present study elucidated the antioxidant and anti-inflammatory properties of leaves of *Azimatetrapetala*. Among four extracts, ethyl acetate extract possesses good antioxidant, radical scavenging, and anti-inflammatory activities which might help prevent the progression of various oxidative stress-related disorders. Therefore, it can be concluded that the leaves of *Azimatetrapetala* have a potential natural antioxidant and radical scavenger, and this can act as an effective ingredient in food industries²⁰. Hence further research is in need to isolate and analyze the bioactive constituents which are responsible for antioxidant activities.

CONFLICT OF INTEREST

Conflict of interest declared none.

REFERENCES

1. Agarwal, A. 2005. Critical issues in quality control of herbal products. *Pharma Times*, 37: 9-11.
2. Aiyegeoro, O. A., and Okoh, A. 2009. Preliminary phytochemical screening and *In vitro* antioxidant activities of the aqueous extract of *Helichrysum longifolium* DC. *BMC Complementary and Alternative Medicine*, 10: 21
3. Aoki, T., Akash, T., Ayabe, S. Flavonoids of leguminous plants: Structure, biological activity, and biosynthesis. *Journal of Plant Research*. 113; 475-488.
4. Arunkumar, S., Muthuselvam, K. 2009. Analysis of phytochemical constituents and antimicrobial activities of *Aloe vera* L. against clinical pathogens. *World J. Agril. Sc.*, (5)572-576.
5. Ashok Kumar, D., Mazumder, U. K., Gupta, M., Senthil Kumar, G. P., Selvan, V. T. Evaluation of antioxidant and free radical scavenging activities of *Oxystelma esculentum* in various *in vitro* Models. *J Comp Integ Med* 2008, 5 (1): 9.
6. Awah, F. M., Uzoegwu, P. N., Oyugi, J. O., Rutherford, J., Ifeonu, P., Yao, X. J., Fowke, K. R., Eze, M., O. 2010. Free radical scavenging activity and immunomodulatory effect of *Stachytarpheta angustifolia* leaf extract. *Food Chemistry*, 119: 1409–1416.
7. AzimaLamarck, Encycl. I: 343. 1783. Fl. China 11: 497. 2008.
8. Azizova, O. A. 2002. Role of free radical processes in the development of atherosclerosis. *Biologicheskie Membrany*, 19: 451–471.
9. Bahramikia, S., Ardestani, A., Yazdanparast, R., 2009. Protective effects of four Iranian medicinal plants against free radical-mediated protein oxidation. *Food Chem.* 115, 37–42.

10. Balakrishnan, M. 2010. Studies on Pharmacognostic specifications of *Azimatetrapetala* Lam. 35-42.
11. Basnal, S., Malwal, M., Sarin, R. 2010. Anti-Bacterial efficacy of some plants used in folkloric medicines in the arid zone. *Journal of Pharmacy Research*, (11); 2640-2642.
12. Beck, J. G., Mathieu, D., Loudet, C., Buchoux, S., JDufourc, E. J. 2007. Plant sterols in "rafts": a better way to regulate membrane thermal shocks. *FASEB J.* 21(8): 1714-23.
13. Begum, M., Dhanalakshmi, A., Muthukumaran, P. 2013. *In vivo* evaluation of the antidiarrhoeal activity of the leaves of *Azimatetrapetala* Linn. *International Journal of Nutrition and Metabolism*.5 (8): 140-144.
14. Begum, T. N., Muhammad Ilyas, M. H., Burkanudeen, A., Kalavathy, S., VijayaAnand, A., Sampathkumar, P., Jaswanth, K. 2009. Hypoglycemic and antihyperlipidemic activity of ethanolic leaf extract of *Azimatetrapetala* Lam. on alloxan-induced diabetic rats. *J. Cell Tissue Res.* 9 (1): 1681-1685.
15. Bennett, R. N., Rosa, E. A., Perkins, L., Kroon, P.A. 2004. Profiling glucosinolates, flavonoids, alkaloids, and other secondary metabolites in tissues of *Azimatetrapetala* L (Salvadoraceae). *J. Agric. Food Chem.* 5 (19); 5856-5862
16. Virginia, H., Sarah, L. E., Rachel, J. S., Nathaniel, T., Joseph, S., Adam, E., Cecilia, G., 2003. Mitochondrial nitric-oxide synthase: role in pathophysiology. *UBMB Life* 55(10 -11), 599-603
17. Williams, L. A. D., Connar, A. O., Latore, L., Dennis, O., Ringer, S., Whittaker, J. A. 2008. The *in vitro* anti-denaturation effects induced by natural products and non-steroidal compounds in heat treated (Immunogenic) bovine serum albumin is proposed as a screening assay for the detection of anti-inflammatory compounds, without the use of animals, in the early stages of the drug discovery process. *West Indian Med J.* 7: 32
18. Yu L. 2001. Free radical scavenging properties of conjugated linoleic acids. *J Agric Food Chem*, 49: 3452-3456.
19. Zhao, M., Yang, B., Wang, J., Li, B., Jiang, Y. 2006. Identification of the major flavonoids from pericarp tissues of lychee fruit in relation to their antioxidant activities. *Food Chem*, 98: 539-544.
20. Zheng, W., Wang, S. Y. 2001. Antioxidant activity and phenolic compounds in selected herbs. *International Journal of Agricultural and Food Chemistry*, 49: 5165-5170.

Anticancer Activity of Polyherbal Formulation against Human Blood Cancer Cells

Sujithra.M ,Nirmala Devi,Sathish.S ,Oviya.M

Dhanalakshmisrinivasan College of Arts and Science for Women (Autonomous), Perambalur.

Abstract: The *Ficusreligiosa*, *Allium sativum*, *Sennaauriculata*, *Andrographispaniculata*, *Momordicacharantia* and *Eugenia jambolana*, are well-known plants available throughout India and they are commonly used for the treatment of various diseases. The polyherbal formulation was formulated using the hydroalcoholic extracts of the *Ficusreligiosa*, *Allium sativum*, *Sennaauriculata*, *Andrographispaniculata*, *Momordicacharantia*, *Eugenia jambolanaby* the Soxhlet extraction method. The phytochemical characterization was carried out for the polyherbal formulation. Further, the anticancer activity of polyherbal formulation was studied using MOLT-4 cells and their mechanism of action was analyzed by ETBr/AO staining method. The ETBr/AO staining results further confirmed the polyherbal formulation. Taken together, these results showed that the polyherbal formulation has anti-cancer potential and can be used for the treatment of blood cancer.

Keyword: Anti-cancer, Polyherbal formulation, phytochemical, MOLT-4 cells, *Ficusreligiosa*, *Allium sativum*.

INTRODUCTION

The total research and development (R&D) spending for drug discovery worldwide has increased at least 15-fold from 1975¹. There are four broad categories of blood cancers: leukaemia, myeloma, Hodgkin lymphoma and non-Hodgkin lymphoma. Together, these account for around 9 % of all cancers and are currently the fourth most common in both males and females in the world¹⁻³. Increasing age has been historically implicated in higher mortality after high-dose allogeneic hematopoietic cell transplantation (HCT) for patients with hematologic malignancies⁴. These transplants are preceded by intense, cytotoxic conditioning regimens that are aimed at reducing tumor burden. The risk of organ toxicities has limited the use of high-dose regimens to younger patients in good medical condition. Therefore, age cut-offs of 55–60 years have been in place for decades for high-dose HCT. This excluded the vast majority of patients from allogeneic HCT given that median ages of patients at diagnosis of most hematologic malignancies range from 65–70 years⁵⁻⁶. *Morindacitrifolia L.* (noni) is an example of a plant used as a functional food and has been widely studied due to its apparent beneficial effects on human health⁷. It has been investigated as an alternative in anticancer, antibacterial, and antimicrobial therapies, and in the treatment of esophageal reflux and ulcers in animals. One of the explanations for the medicinal action of noni fruits is that xeronine could modulate the conformation and stability of specific proteins⁸. Heinicke described beneficial effects of noni fruits, such as in menstrual cramps, hypertension, burns, depression, atherosclerosis, digestion, relief for pain, and many others. *Lantana camara Linn.* (family: Verbenaceae), an ornamental shrub, has spread as an intractable weed in many parts of the world⁹⁻¹⁰. The genus Lantana contains many species that are native to the Americas and Africa, and has become naturalized as a noxious weed in tropical, subtropical, and warm temperate countries. *Lantana camara* has been found in nearly 50 countries and is the principal weed in 12 countries. It is a serious weed spreading over Australia, Asia, Africa, South America, and North America¹¹⁻¹². Strategies for the control of lantana have been reviewed in a recent monograph by Day and coworkers. The present study was to prepare a polyherbal formulation and phytochemical characterization for the treatment of human blood cancer and their mechanism of action by ETBr/AO staining method.

MATERIALS AND METHODS

Chemicals and reagents

DMEM medium, Fetal Bovine Serum (FBS) and antibiotic solution were from Gibco (USA), DMSO (Dimethyl sulfoxide) and MTT (3-4,5 dimethylthiazol-2yl-2,5-diphenyl tetrazolium bromide) (5 mg/ml) were from Sigma, (USA), IX PBS was from Himedia, (India). 96 well tissue culture plates and wash beakers were from Tarson (India). DMEM medium, Penicillin/Streptomycin antibiotic solution, Trypsin-EDTA was purchased from Gibco (USA), ETBr and Acridine orange was purchased from Sigma Aldrich (USA).

Preparation of polyherbal formulation

The fresh leaves were collected and cleaned with distilled water and shade dried for 1 week. The dried leaves were grounded in a mixer grinder. The polyherbal formulation was made from different ratios of herbal powders listed in table I.

S.No	Name of the medicinal Plants	Weight
1	<i>Ficuspumila</i>	5 gm
2	<i>Andrographispaniculata</i>	10 gm
3	<i>Morindacitrifolia</i>	7 gm
4	<i>Lantana camara</i>	3 gm
5	<i>Colocasia</i>	5 gm
6	<i>Cymbopogoncitratus</i>	10 gm

7	Piper nigrum	10 gm
Ratio of polyherbal formulation		

Phytochemical Extraction (soxhlet apparatus)

The plant powdered sample (10 g) is used for extraction by Soxhlet apparatus at a boiling temperature. The crude powders were defatted with 1 litre of petroleum ether (60°- 80°C) using soxhlet apparatus. After defatting, the extraction was carried out using 1000 mL of 100% ethyl alcohol (75.0°C) for 4 h. After extraction, the samples were evaporated to remain with important ingredients.

Detection of Glycosides

To 0.5ml of extract, 0.5ml of Benedict reagent is added and boiled for 2 min. Colour changes and ppt is formed. It indicates the presence of carbohydrates.

To prepare Hydrosalyte

To 50mg of extract, 2ml of conc. HCL is added and kept in the water bath for 1 hour and then filtration methods. The filtrate is hydrated.

Born- Trageru's Test

Take 2ml of hydrolysate, add 3ml of chloroform, shake vigorously, then the chloroform layer gets separated. To form 10% ammonia solution of pink colour indicates the presence of glycosides.

Saponification test

To 1 or 2ml of normal sodium hydroxide, 2ml of extract is added and boiled for 2 minutes. Formation of soap or fat indicates the positive test for saponification.

Detection of Proteins by BradFورد Method:

To 500 and 1 of extract, add 5ml of bradford reagent, Take OD at 575nm.

Detection of Phenol by Biuret Test

To 2ml of extract, 1 drop of 2% CuSO_4 solution. Add 1 ml of 95% ethanol, then add 2 to 3 sodium hydroxide pellets. Formation of pink colour indicates the test is positive.

MTT Assay

The FALMPCC sample was tested for *in vitro* cytotoxicity, using MOLT 4 cells by 3-(4,5-dimethylthiazol-2-yl)-2,5-diphenyltetrazolium bromide (MTT) assay. Briefly, the cultured A549 cells were harvested by trypsinization, pooled in a 15 ml tube. Then, the cells were plated at a density of 1×10^5 cells/ml cells/well (200 μL) into 96-well tissue culture plate in DMEM medium containing 10 % FBS and 1% antibiotic solution for 24-48 hour at 37°C. The wells were washed with sterile PBS and treated with various concentrations of the MOLT 4 sample in a serum free DMEM medium. Each sample was replicated three times and the cells were incubated at 37°C in a humidified 5% CO_2 incubator for 24 h. After the incubation period, MTT (20 μL of 5 mg/ml) was added into each well and the cells incubated for another 2-4 h until purple precipitates were clearly visible under an inverted microscope

ETBr /AO staining

Briefly, 5×10^5 cells/ml of MOLT 4 cells were plated to a 24 well tissue culture plate and incubated for 24 hr in a DMEM growth medium. After incubation, the plate was washed with PBS and treated with 3.46 $\mu\text{M}/\text{ml}$ of compound 8 sample in a serum free DMEM medium. The plate was incubated at 37 °C at 5% CO_2 incubator for 24 hours. After incubation, 50 μl of 1 mg/ml acridine orange and ethidium bromide were added to the wells and mixed gently. Finally, the plate was centrifuged at 800 rpm for 2 minutes and evaluated immediately within an hour and examined at least 100 cells by fluorescence microscope using a fluorescent filter.

RESULTS

Polyherbal formulation

The polyherbal formulation was made from seven different types of medicinal plants. Soxhlet extraction was done with various ratios of plant extracts such as, *Ficus pumila*(5gm), *Andrographis paniculata*(10gm), *Lantana camara*(3gm), *Morinda citrifolia* (7gm), *Cymbopogon citratus*(10gm), *Colocasia* (5gm) and *Piper nigrum* (10 gm). After evaporation, totally 4 gm of polyherbal formulation was obtained.

Phytochemical analysis

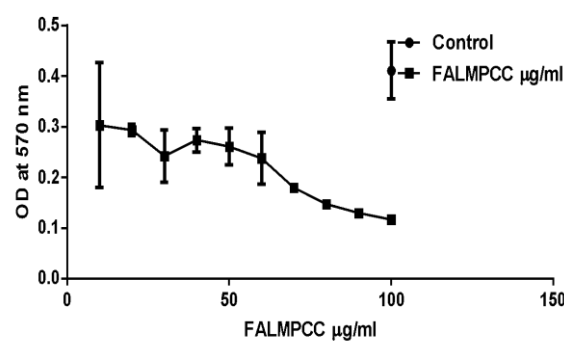
The extracts of poly herbal formulation were used for the qualitative phytochemical characterization for the identification of the various classes of active chemical constituents, using standard prescribed methods shows in the following table.

S.No	Name of the test sample	Phytochemical analysis	Result
I		Resin	+++

2	FALMPCC	Carboxylic acid	+++
3		Steroids	++
4		Flavonoids	+++
5		Carbohydrates	++
6		Protein	+
7		Biuret	-
8		Saponin	+
9		Glycoside	+

Anticancer activity of polyherbal formulation

The anticancer activity of polyherbal formulation was carried out against MOLT- 4 at different concentrations to determine the IC₅₀ (50% growth inhibition) by MTT assay. Results of different concentrations of polyherbal formulation were shown in Fig. The formation of formazan crystals decreases when the concentration of polyherbal formulation increases in MOLT- 4 cells. MTT assay of polyherbal formulation showed significant effect on MOLT- 4 cell line in a concentration range between 100 µg/ml to 10 µg/ml compared with control. Similarly, polyherbal formulation inhibited cancer cell growth more than 50%. This polyherbal formulation exerts high cytotoxicity in 100 µg/ml concentration against MOLT- 4 cell line. The IC₅₀ values of polyherbal formulation on MOLT- 4 cell line were 61.91 µg/ml. Taken together, these results showed that the polyherbal formulations are toxic to MOLT- 4 cells and effective in inhibition of cancer cell proliferation.



Graph I OD Value at 570 nm
Control Mean OD value: 0.411

Cell Viability (%)

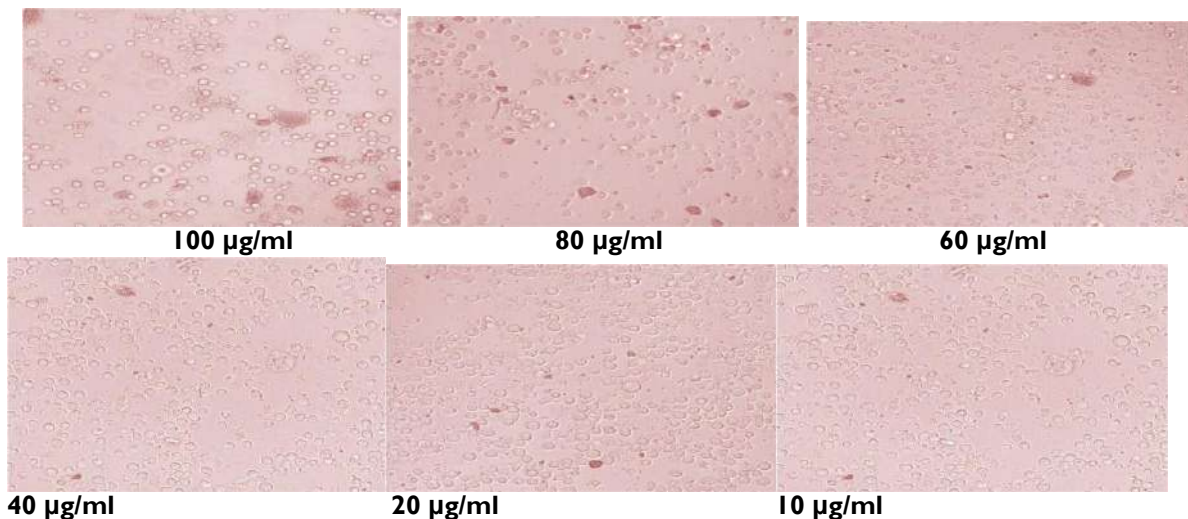
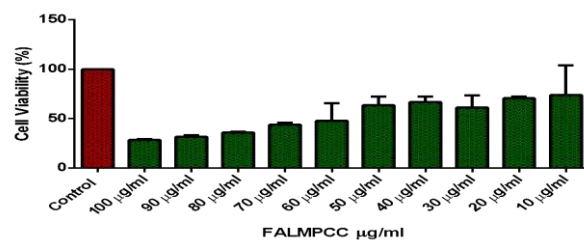
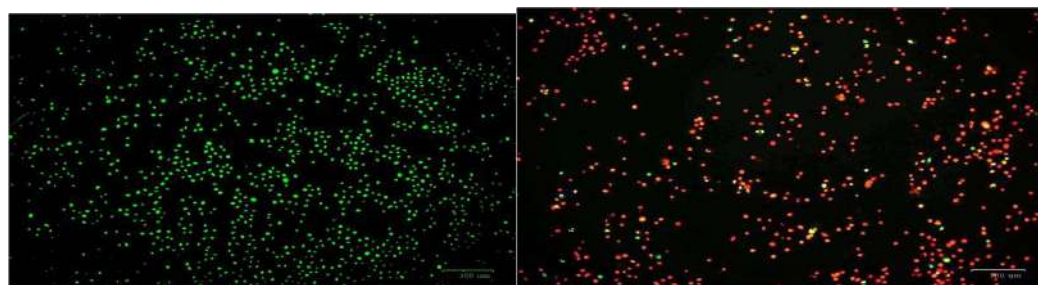


Figure I. Images of control cells andpolyherbal formulation treated cells

I.I. ETBr/AO staining result

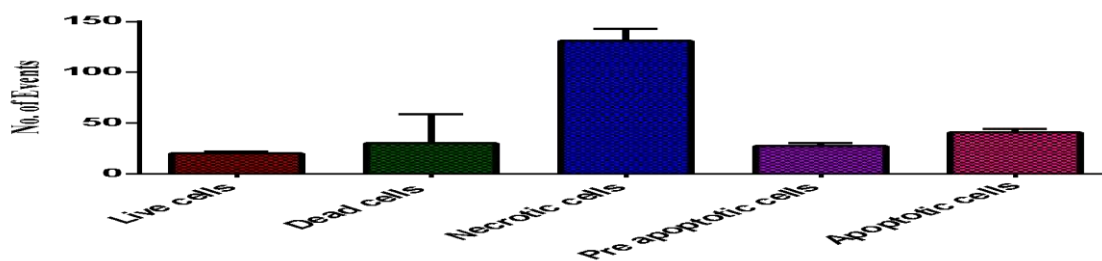
The polyherbal formulation treated MOLT- 4 cells were subjected to AO/EB staining. AO will enter the nucleus and stain live cells as green color fluorescence and EB will penetrate the nucleus of dead cells due to loss of membrane integrity and stain as red colour fluorescence. In the present study, the MOLT- 4 cells were treated with 61.91 μ g/ml of polyherbal formulation and the cells were examined using fluorescent microscopy. Normal viable cells appeared as green fluorescence with highly organized nuclei. Early apoptotic cells (9.47 %) appeared as a crescent-shaped or granular yellow-green with AO nuclear staining. Late apoptotic cells (14.21%) appeared as a concentrated and asymmetrically localized orange nuclear ETBr staining. Necrotic cells (45.96%), Live cells (7.07%) and Dead cells (26.31%) showed uneven, orange-red fluorescence at their periphery without chromatin fragmentation. The IC₅₀ values of plant extracts 61.91 μ g/ml treated cells showed typical apoptotic and necrotic morphological features such as condensed nuclei, membrane blebbing and formation of apoptotic bodies, which were clearly observed under the fluorescence microscope.



Control
Apoptotic and necrotic indexes of 61.91 μ g/ml of herbal formulation treated cells

Figure 2. ETBr/Ao staining showing the apoptotic and necrotic indexes of Herbal formulation in MOLT- 4 cells

Table 4. Apoptotic and necrotic indexes of polyherbal formulation treated cells



DISCUSSION

The polyherbal formulation was used against cancer in Indian traditional systems of medicines like Ayurvedic, Siddha and Unani¹²⁻¹³. The formulated herbal drugs have become a boon for mankind since ancient times and still are, used worldwide for the treatments of various human ailments¹⁴⁻¹⁵. There 7 different types of medicinal herbs such as *Lantana camara*, *Colocasia*, *Cymbopogon citratus*, *Ficus pumila*, *Andrographis paniculata*, *Morinda citrifolia*, *Piper nigrum* was found to be rich in anticancer activity against blood cancer cells¹⁶⁻¹⁷.

CONCLUSION

Our polyherbal formulation FALMPCC showed significant anti-cancer activity against the blood cancer cells lines in invitro condition¹⁸⁻¹⁹. In order to evaluate the anticancer properties, further research will be continued by following this polyherbal formulation in *in vivo* studies using mice, rat, rabbit etc.²⁰

CONFLICT OF INTEREST

Conflict of interest declared none.

REFERENCE

1. Ding L, Ley TJ, Larson DE, et al. Clonal evolution in relapsed acute myeloid leukaemia revealed by whole-genome sequencing. *Nature*. 2012; 481:506-10.
2. Fadul N, Elsayem A, Palmer JL, et al.: Predictors of access to palliative care services among patients who died at a Comprehensive Cancer Center. *J Palliat Med* 10:1146-1152,2007
3. Pui CH, Campana D, Pei D, et al. Treating childhood acute lymphoblastic leukemia without cranial irradiation. *N Engl J Med*. 2009;360(26):2730-2741.
4. Wu D, Sherwood A, Fromm JR, et al. High-throughput sequencing detects minimal residual disease in acute T lymphoblastic leukemia. *SciTransl Med*. 2012;4(134):134ra63
5. Canellos GP, Rosenberg SA, Friedberg JW, Lister TA, Devita VT. Treatment of Hodgkin lymphoma: a 50-year perspective. *J Clin Oncol*. 2014;32(3):163-168

6. Oki Y, Neelapu SS, Fanale M, et al. Detection of classical Hodgkin lymphoma specific sequence in peripheral blood using a next-generation sequencing approach. *Br J Haematol.* 2015;169(5):689-693
7. Vandenberghe P, Wlodarska I, Tousseyn T, et al. Non-invasive detection of genomic imbalances in Hodgkin/Reed-Sternberg cells in early and advanced stage Hodgkin's lymphoma by sequencing of circulating cell-free DNA: a technical proof-of-principle study. *Lancet Haematol.* 2015;2(2):e55-e65.
8. Kristinsson SY, Anderson WF, Landgren O. Improved long-term survival in multiple myeloma up to the age of 80 years. *Leukemia.* 2014; 28(6):1346-1348.
9. Fonseca R, Bergsagel PL, Drach J, et al.; International Myeloma Working Group. International Myeloma Working Group molecular classification of multiple myeloma: spotlight review. *Leukemia.* 2009; 23(12):2210-2221.
10. Vieaud J., Gao J., Stchakovsky M., Naciri A.E., Ariga K., Oda R., Pouget E., Battie Y. Gold Nanoparticle Chains: Synthesis, Characterization, and Modeling Using Spectroscopic Ellipsometry. *J. Phys. Chem.* 2018
11. Khan S., Alam F., Azam A., Khan A.U. Gold nanoparticles enhance methylene blue-induced photodynamic therapy: A novel therapeutic approach to inhibit *Candida albicans* biofilm. *Internat. J. Nanomed.* 2012;7:3245
12. O'Neal D.P., Hirsch L.R., Halas N.J., Payne J.D., West J.L. Photo-thermal tumor ablation in mice using near infrared-absorbing nanoparticles. *Cancer Lett.* 2004;209:171-176.
13. Singh, H.; Du, J.; Singh, P.; Mavlonov, G.T.; Yi, T.H. Development of superparamagnetic iron oxidenanoparticles via direct conjugation with ginsenosides and its in-vitro study. *J. Photochem. Photobiol. B Biol.* 2018, 185, 100–110.
14. Singh P., Ahn S., Kang J.P., Veronika S., Huo Y., Singh H., Chokkaligam M., El-AgamyFarh M., Aceituno V.C., Kim Y.J., et al. In vitro anti-inflammatory activity of spherical silver nanoparticles and monodisperse hexagonal gold nanoparticles by fruit extract of *Prunus sibirica*: A green synthetic approach. *Artif. Cells Nanomed. Biotechnol.* 2017;1–11.
15. Jain K.K. Applications of nanobiotechnology in clinical diagnostics. *Clin. Chem.* 2007;53:2002–2009.
16. Aggarwal P., Hall J.B., McLeland C.B., Dobrovolskaia M.A., McNeil S.E. Nanoparticle interaction with plasma proteins as it relates to particle biodistribution, biocompatibility and therapeutic efficacy. *Adv. Drug Deliv. Rev.* 2009;61:428–437.
17. Kennedy LC, Bickford LR, Lewinski NA, Coughlin AJ, Hu Y, Day ES, et al. A New Era for Cancer Treatment: Gold-Nanoparticle-Mediated Thermal Therapies. *Small.* 7(2), 169–183 (2011).
18. Lu W, Xiong C, Zhang G, Huang Q, Zhang R, Zhang JZ, et al. Targeted Photothermal Ablation of Murine Melanomas with Melanocyte-Stimulating Hormone Analog-Conjugated Hollow Gold Nanospheres. *Clin. Cancer Res.* 15(3), 876–886 (2010).
19. Qaddare S.H., Salimi A. Amplified fluorescent sensing of DNA using luminescent carbon dots and AuNPs/GO as a sensing platform: A novel coupling of FRET and DNA hybridization for homogeneous HIV-1 gene detection at femtomolar level. *Biosens. Bioelectron.* 2017;89:773–780.
20. Rasheed P.A., Sandhyarani N. Electrochemical DNA sensors based on the use of gold nanoparticles: A review on recent developments. *Microchim. Acta.* 2017;184:981–1000.

Biosynthesis and Characterization of Gold Nanoparticles from *Aralia elata* Plant Extract

Sujithra.M ,Sathya.R, NirmalaDevi.P, Nivetha.S

Dhanalakshmisrinivasan College of Arts and Science for Women (Autonomous), Perambalur

Abstract: Gold nanoparticles (AuNPs) are a promising class of nanomaterials with many varieties of applications. The aim of the present study was to green synthesis of gold nanoparticles (AuNPs) from *Aralia elata* leaf extract and their biological activity. The gold nanoparticles synthesized using the aqueous extract of *Aralia elata*. Synthesized A-AuNPs was further characterized using SEM, UV and XRD. The biological activity such as antioxidant, anti-inflammatory, antidiabetic, antibacterial and antifungal activity was analysed for A-AuNPs. The SEM analysis results showed that the gold nanoparticles were nano in size and spherical in shape. The XRD analysis also confirmed the presence of gold nanoparticles. The antioxidant activity by DPPH assay revealed the antioxidant potential of A-AuNPs. The A-AuNPs showed anti-inflammatory, antidiabetic activity. A-AuNPs exhibited potential antibacterial activity against *Streptococcus pyogenes*, *Streptococcus oralis* and *Streptococcus faecalis*. The maximum zone of inhibition was found at 1000 µg/ml. Similarly, A-AuNPs showed antifungal activity against *Aspergillusniger* and *Candida albicans*.

Keywords: Nanoparticles, *Aralia elata*, Antioxidant, *Streptococcus pyogenes*, Antidiabetic ,DPPH.

INTRODUCTION

Nano-biotechnology is an interdisciplinary research field involving biology, medicine and molecular engineering¹⁻². Its aim is the production of biocompatible and environmentally safe nanoparticles for medical applications using green synthesis methodologies²⁻³. In the production of biocompatible nanoparticles, the use of plants or microorganisms is increasingly being used, and nanoparticles from such “green synthesis” have been applied for drug and gene delivery and various medical treatments including antimicrobial, anticancer, anti-inflammatory, antiaging, antioxidant and anti-biofilm inhibition³⁻⁴. Gold nanoparticles (AuNPs) are very popular for their biocompatible nature and were recently applied for the identification of chemical and biological molecules, photoimaging and photothermal therapy against cancer cells for control and treatment of many infectious diseases, such as inflammation and skin whitening⁴⁻⁵. This increasing need for biocompatible nanoparticles requires new nanotechnology solutions for green synthesis of these metallic nanoparticles with biocompatible surfaces⁵⁻⁶. Recently, metallic nanoparticles have received much attention because of their distinctive optical, magnetic, and catalytic properties⁷. The size, shape, monodispersity, and morphology of the particles are essential to tune these properties. Various synthesis methods have been developed to formulate such nanoparticles, including chemical, physical, and biological methods⁷⁻⁸. Gold nanoparticles (AuNPs) are a promising class of nanomaterials with many varieties of applications, which includes cancer hyperthermia treatment, surface-enhanced Raman spectroscopy (SERS), and infrared radiation absorbing optics⁹. Consequently, a variety of synthetic procedures for the formation of various shapes and sizes of AuNPs have been reported. Several isotropic shapes including rods, wires, plates, and teardrop structures can be obtained by wet chemical synthesis routes¹⁰⁻¹¹.

MATERIALS AND METHODS

Biosynthesis of AuNPs from *Aralia elata* aqueous extract

Aralia elata (10g) was taken with 100 ml of double distilled water and then boiled 60°C for 30 minutes. Then the extract was filtered through the muslin cloth followed by the filtered paper. The filtered extract of *Aralia elata* was used for the synthesis of AuNPs. To synthesize AuNPs from, different ratio of 0.1N gold chloride and *Aralia elata* extract were taken (5:5, 6:4, 7:3, 6:4, 8:2, 9:1). The mixture was incubated at room temperature for 24 hr. The best ratio was taken for bulk synthesis of gold nanoparticles. For the synthesis of gold nanoparticles (GNPs) from 70 ml of 0.1 N gold chloride solution and 30 ml plant extract were mixed in the 50 ml tubes. After 24 hours the centrifuged at 3000 RPM for 10 minutes. The supernatant was then discarded, and the pellets were dissolved in 1ml of ethanol and dried.

Characterization of AuNPs

The green synthesized gold nanoparticles along with gold chloride solution were analysed using UV- Vis spectrophotometry and their size and shape was analysed through the SEM analysis.

UV- Vis spectrophotometry analysis

The biosynthesis of AuNPs nanoparticles were monitored periodically by UV-vis spectroscopy. The samples used for analysis were diluted with 2 mL deionized water and subsequently measured by the UV-vis spectrum at regular different time intervals (Raut Rajesh et al). A UV-vis spectrograph of silver nanoparticles was recorded as a function of time by using a quartz cuvette with water as reference. The UV-vis spectrometric readings were recorded at a scanning speed of 200 to 1100 nm.

SEM analysis of biosynthesized AuNPs

The biosynthesized gold nanoparticles were characterized using high resolution SEM analysis. The samples were prepared by simple drop coating of the suspension of gold solutions onto an electric clean glass and allowing the solvent (water) to evaporate. The samples were left to dry completely at room temperature.

Analysis of β -Galactosidase Activity

For the inhibition of β -galactosidase activity, a total of 0.5 mL of the different concentration of A-AuNPs sample was pre-incubated with β -galactosidase in Na-acetate buffer at room temperature for 20 min. Then 0.5 mL of substrate mixture (8.3 mM o-nitrophenyl b-D-galactopyranoside, 1 mM MgCl₂, and 0.1 M b-mercaptoethanol in 0.1 M Na-phosphate buffer, pH 7.0) was added to the sample mixture. After the incubation at 30°C for 20 min, the reaction was terminated with 0.5 mL of 0.5 M Na₂CO₃ buffer. Release of o-nitrophenol was recorded at 420 nm using a microplate reader (Thermo scientific, USA). Each measurement was performed with three independent biological replicates using 96 well plate. Inhibition of enzyme activity was determined by using the following formula.

$$\text{Percentage of inhibition (\%)} = \frac{\text{Absorbance of control} - \text{Absorbance of test sample} \times 100}{\text{Absorbance of control}}$$

RESULTS AND DISCUSSION

Biosynthesis and characterization of AuNPs using *Aralia elata*

The present study, we synthesized A-AgNPs from the aqueous extract of *Aralia elata*. The reduction of AuNPs was observed maximum at the ratio of 5:5¹². The gold nanoparticles reduction was taken place immediately after the addition of 1mM HAuCl₄ solution to the *Aralia elata* extract. The formation of gold nanoparticles was further confirmed by UV- Vis and SEM analysis. The UV-Vis spectrophotometric analysis confirmed the presence of gold nanoparticles by the representation of peaks at 400- 450 nm. The shape of the biosynthesized A-AuNPs was found to be round in shape¹³⁻¹⁴.



Figure 4. Biosynthesized A-AuNPs gold nanoparticles

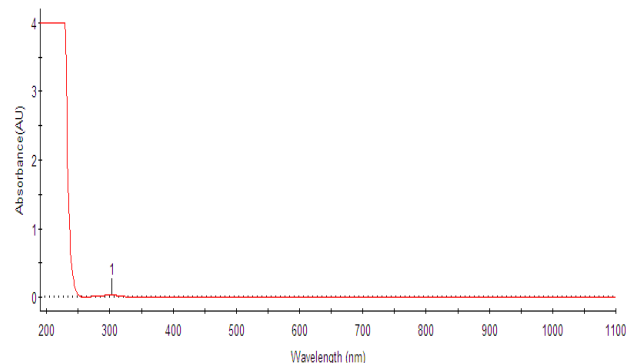
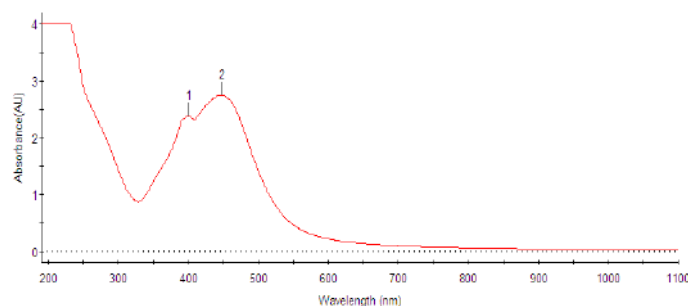
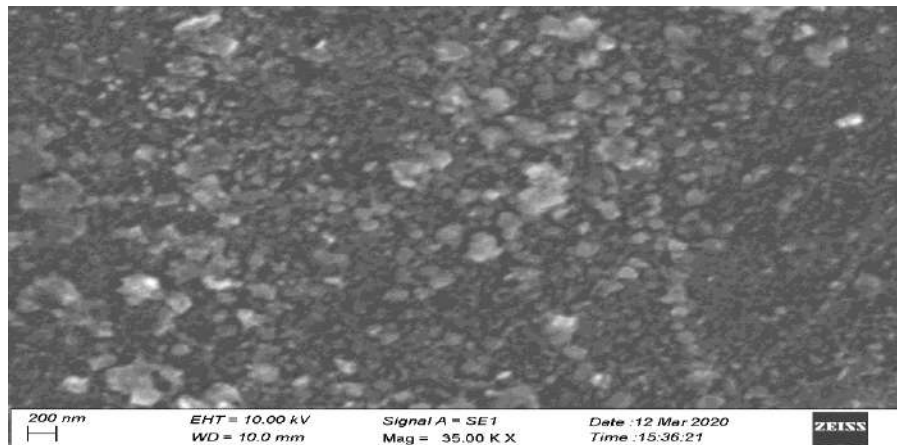
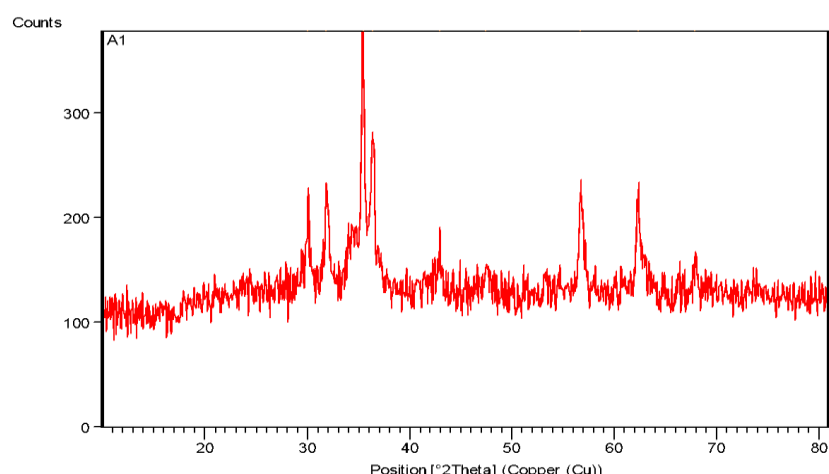


Figure 5. UV spectrophotometer analysis of blank



Name	No.	Peak (nm)	Peak (AU)	No.	Valley (nm)	Valley (AU)
7:3	1	401.25	2.3813			
	2	448.30	2.7506			

Figure 6. UV spectrophotometer analysis A-AUNPS**Figure 7. SEM analysis of A-AuNps****Figure 8. XRD analysis of A-AuNps**

CONCLUSION

In this work we successfully synthesized gold nanoparticles from *Aralia elata* leaf extract. The synthesized A-AuNPs were thoroughly characterized by UV-Vis, SEM, and XRD¹⁶⁻¹⁷. The current work demonstrates promising results on the antioxidant, anti-inflammatory, antidiabetic and antimicrobial activities of A-AuNps¹⁷⁻¹⁸. The synthesized A-AuNps¹⁹ were found to be the most promising approach and could be used for the treatment of various biomedical applications²⁰⁻²².

CONFLICT OF INTEREST

Conflict of interest declared none.

REFERENCES

- El-Sayed, M. Some interesting properties of metals confined in time and nanometer space of different shapes. *Acc. Chem. Res.* 2001, 34, 257–264.
- Shankar, S.; Rai, A.; Ahmad, A.; Sastry, M. Rapid synthesis of Au, Ag, and bimetallic Au core—Ag shell nanoparticles using Neem (*Azadirachtaindica*) leaf broth. *J. Colloid Interface Sci.* 2004, 275, 496–502.
- Shakibaie M, Khorramizadeh MR, Faramarzi MA, Sabzevari O, Shahverdi AR. Biosynthesis and recovery of selenium nanoparticles and the effects on matrix metalloproteinase-2 expression. *BiotechnolApplBiochem.* 2010;56(1):7–15.
- Hecker JFC. Der schwarzenodimvierzehntenjahrhundert: Nach den quellen, fürärzte und gebildetenichtärzte [The black death and the dancing mania]. Berlin: Herbig; 1832. German
- Joshi BP, Duan X, Kwon RS, Piraka C, Elmunzer BJ, Lu S et al (2016) Multimodal endoscope can quantify wide-field fluorescence detection of Barrett's neoplasia. *Endoscopy.* 48(2):A1–a13.
- Tipirneni KE, Rosenthal EL, Moore LS, Haskins AD, Udayakumar N, Jani AH et al (2017) Fluorescence imaging for cancer screening and surveillance. *Mol Imaging Biol* 19(5):645–655.
- Pham-Huy LA, He H, Pham-Huy C. Free radicals, antioxidants in disease and health. *Int J Biomed Sci* 2008;4(2):89–96.

8. Sinclair AJ, Barnett AH, Lunec J. Free radicals and antioxidant systems in health and disease. *Br J Hosp Med* 1990;43(5):334-44.
9. IDF. IDF Diabetes Atlas, 7th ed.; IDF: Brussels, Belgium, 2015
10. Sena, C.M.; Pereira, A.M.; Seica, R. Endothelial dysfunction—A major mediator of diabetic vascular disease. *Biochimica et Biophysica Acta* 2013, 1832, 2216–2231.
11. Zhao P., Li N., Astruc D. State of the art in gold nanoparticle synthesis. *Coord. Chem. Rev.* 2013;257:638–665.
12. Vieaud J., Gao J., Stchakovsky M., Naciri A.E., Ariga K., Oda R., Pouget E., Battie Y. Gold Nanoparticle Chains: Synthesis, Characterization, and Modeling Using Spectroscopic Ellipsometry. *J. Phys. Chem.* 2018
13. Khan S., Alam F., Azam A., Khan A.U. Gold nanoparticles enhance methylene blue-induced photodynamic therapy: A novel therapeutic approach to inhibit *Candida albicans* biofilm. *Internat. J. Nanomed.* 2012;7:3245
14. O’Neal D.P., Hirsch L.R., Halas N.J., Payne J.D., West J.L. Photo-thermal tumor ablation in mice using near infrared-absorbing nanoparticles. *Cancer Lett.* 2004;209:171–176.
15. Singh, H.; Du, J.; Singh, P.; Mavlonov, G.T.; Yi, T.H. Development of superparamagnetic iron oxidenanoparticles via direct conjugation with ginsenosides and its in-vitro study. *J. Photochem. Photobiol. B Biol.* 2018, 185, 100–110.
16. Singh P., Ahn S., Kang J.P., Veronika S., Huo Y., Singh H., Chokkaligam M., El-AgamyFarh M., Aceituno V.C., Kim Y.J., et al. In vitro anti-inflammatory activity of spherical silver nanoparticles and monodisperse hexagonal gold nanoparticles by fruit extract of *Prunus serrulata*: A green synthetic approach. *Artif. Cells Nanomed. Biotechnol.* 2017;1–11.
17. Jain K.K. Applications of nanobiotechnology in clinical diagnostics. *Clin. Chem.* 2007;53:2002–2009.
18. Aggarwal P., Hall J.B., McLeland C.B., Dobrovolskaia M.A., McNeil S.E. Nanoparticle interaction with plasma proteins as it relates to particle biodistribution, biocompatibility and therapeutic efficacy. *Adv. Drug Deliv. Rev.* 2009;61:428–437.
19. Kennedy LC, Bickford LR, Lewinski NA, Coughlin AJ, Hu Y, Day ES, et al. A New Era for Cancer Treatment: Gold-Nanoparticle-Mediated Thermal Therapies. *Small.* 7(2), 169–183 (2011).
20. Lu W, Xiong C, Zhang G, Huang Q, Zhang R, Zhang JZ, et al. Targeted Photothermal Ablation of Murine Melanomas with Melanocyte-Stimulating Hormone Analog-Conjugated Hollow Gold Nanospheres. *Clin. Cancer Res.* 15(3), 876–886 (2010).
21. Qaddare S.H., Salimi A. Amplified fluorescent sensing of DNA using luminescent carbon dots and AuNPs/GO as a sensing platform: A novel coupling of FRET and DNA hybridization for homogeneous HIV-1 gene detection at femtomolar level. *Biosens. Bioelectron.* 2017;89:773–780.
22. Rasheed P.A., Sandhyarani N. Electrochemical DNA sensors based on the use of gold nanoparticles: A review on recent developments. *Microchim. Acta.* 2017;184:981–1000.

A Review on Modern Nanotechnology and Fibers Using Distillation Process.

Ramasamy Shanmugapriya* Dr Gurumoorthi, Dr. P.Visvamithran G Vanaja ,Bhakiyajothi

DhanalakshmiSrinivasan College of Arts &Science for Women (Autonomous) Perambalur, Tamil nadu-621212

Abstract: The significance of the nanofiber networks increases quickly because of their profoundly permeable construction, limited pore size, and dissemination; explicit surface region and similarity with inorganics. Electrospinning has been presented as one of the most effective strategy for the creation of polymeric nanofibers because of its capacity to manufacture nanostructures with remarkable properties like a high surface region and porosity. The cycle and the working boundaries influence the nanofiber manufacture and the utilization of nanofibers in different fields, like sensors, tissue designing, injury dressing, defensive garments, filtration, desalination, and refining. In this survey, a complete report is introduced on the boundaries of electrospinning framework including applications. More accentuation is given to the use of nanofibers in film refining (MD). The examination advancements and the current circumstance of the nanofiber networks in MD are likewise talked about.

Key words; nanofibers, electrospinning, filtration, desalination, and refining etc

INTRODUCTION

The designed materials have acquired enormous interest during the last a very long time because of progress in innovation and expansion in requests¹. A large number of the applications commonly require precisely solid, consumption opposition, lightweight, dependable, recyclable, simple to measure, simple to deal with, regenerative, and low value materials². Polymeric materials can satisfy the overall requests for upper qualified applications^{3,4}. At present, polymers are utilized wherever in our day to day existence. Alongside inorganic materials, polymers are effectively utilized in nanotechnology. Nanotechnology implies the science and innovation happens in nanometer dimensions. The greatest significance of nanotechnology is their angle proportion which is connected with the huge surface region to volume proportions and their quantum impacts. It isn't easy to bring polymer science into nanotechnology⁵. One of the promising spaces of nanofiber is that fundamentally polymeric materials are utilized. During the cycle, the polymeric arrangement/liquefy is expelled, drawn or parted into exceptionally fine strands utilizing outer compound or actual techniques like an electrical field, drawing power, parting into more modest pieces. There have been different strategies in the writing for the arrangement of nanofibers. A portion of these strategies are drawing,¹ electrospinning,²⁻⁵ dissolve blowing,⁶ format synthesis,^{7,8} self-assembly,^{9,10} stage separation¹¹ island in the sea,¹² power spinning,^{13,14} and bubble electrospinning.¹⁵ Among all, electrospinning is the most regularly and for the most part utilized strategy for production of nano-filaments. Electrospinning is so far the most utilized technique for modern creation. The greater part of the examination articles which identified with nanofiber are supportive of produced by electro-spinning methods.

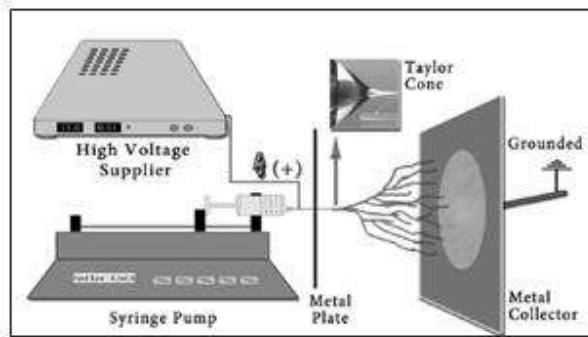
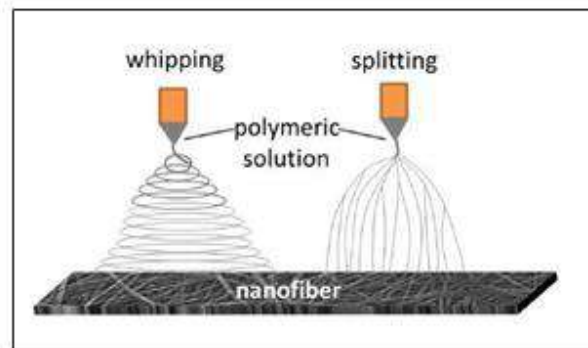


Figure 1.The whipping and splitting behavior of system ² Figure 2. Diagram of needle electrospinningsystem ¹³



Electrospinning

Electrospinning essentially requires a polymeric arrangement/soften and an electrical field. In the majority of the electrospinning arrangement plans, there is a taking care of unit which ships the polymeric arrangement/liquefy into the electrical field. There is a high-voltage provider associated with the feed arrangement. On the contrary side of the feed arrangement, there is a metallic authority which can be oppositely charged or grounded. The electrical field is created between the feed arrangement and the contrary side authority. In the event that the produced electrical field beats the surface pressure of the polymeric solution, Taylor's cone¹⁶ is noticed; then, at that point, the arrangement begins to push toward to authority and under the power and instability starts, the whipping or parting of the polymeric arrangement will be noticed. During the whipping, the drawing proceeds until the polymeric arrangement contacts the authority. Whipping unsteadiness causes bowing and stretching of the jet¹⁷. On the other hand, in case there is parting, the polymeric arrangement parts into numerous fibers. The solvent begins to vanish during whipping or parting. The instrument of the bowing flimsiness was clarified by Yarin et al.¹⁸ They work out the state of the envelope cone which encompasses the bowing circles of the stream during the whipping of polymeric arrangement. The picture of whipping and parting is displayed in Figure 1. Electrospinning strategies can be assembled into two as needle and

needleless electrospinning. As a rule, single spout or needle framework is utilized in the electrospinning framework for research objectives. In single needle electrospinning framework, the polymeric arrangement is put away inside a needle which is connected to a high-voltage provider. A needle siphon is utilized for the taking care of the answer for needle tip as displayed in Figure There are different boundaries in needle framework which plays a successful part in the morphology and usefulness of nanofibers. These boundaries can be sorted into two gatherings as framework and interaction boundaries. The framework boundaries incorporate the properties of a polymeric arrangement like focus, consistency, conductivity, surface tension, permittivity, and the sub-atomic load of the polymer. Then again, measure boundaries are identified with gadget arrangement and climate like applied voltage, the distance between anodes (tip to authority), the fed pace of arrangement, the breadth of the needle tip, and encompassing conditions. Every boundary influences the surface morphology of the nanofibers. Deitzelet al.¹⁹ showed that deformity free polyethylene oxide (PEO)/water nanofibers were delivered at 5.5 kV. At the point when the voltage expanded to 9 kV, dab structures occurred. The outcome showed that the applied voltage significantly affected the state of the drop and globules free construction²⁰. They likewise tracked down that the PEO arrangement fixation significantly affects the last size and dissemination of particles. PEO at a sub-atomic weight 400,000 g/mol, concentrations in the scope of 4–10 wt% delivered filaments. At the point when the fixation diminished, the filaments had a sporadic shape; drops with strands were seen during electrospinning. For arrangements with a centralization of 15 wt% or more, the consistency of the PEO arrangements became hard to turn because of power through the needle of the device, and the drop toward the finish of the hairlike extended into a thick breadth around 0.5mm. Resultant filaments have a normal, barrel shaped morphology and on normal have a bigger and more uniform distance across. Much of the time, an expansion in the focus and the applied voltage brings about an expanded fiber breadth. Comparable outcomes were found in another works^{20–22} Matabola and Moutloali²³ utilized sodium chloride (NaCl) salt as an added substance to polyvinylidene fluoride (PVDF)/dimethylacetamide answer for work on surface morphology of the nanofibers. Expansion in NaCl content respects expansion in fiber width. In the past work, the lithium chloride (LiCl) and tetraethylene ammonium brother mide (TEAB) salts were into PEO/water arrangement in different ratios.^{24,25} Adding salt builds the conductivity while diminishing the spinnability and usefulness of the nanofibers. It was disclosed that adding salt to PEO builds the conductivity of the arrangement which shows a conduct as a conductor²⁶. Therefore, the arrangement loses the quality of a cracked model which prompts the deficiency of capacity to make Taylor cones.a similar conduct was seen with adding a different centralization of sodium hydroxide²⁷ (NaOH) salt into polyvinyl liquor (PVA)/water solution. despite what might be expected, it was discovered that adding TEAB and LiCl salts into polyurethane (PUR)/dimethylformamide expanded

Table 1 Electropunnnanofibers and their application using needle electrospinning systems

Nanofiber	Application
PLA, HA, FHA bioceramics, poly(vinylidene fluoride-trifluoroethylene), poly(hydroxybutyrate-co-hydroxyvalerate), PA6/lecithin, and PCL	Biomedical application
Poly(D,L-lactide-co-glycolide), starch/PCL, PLA	Tissue engineering scaffolds
PVA-Ag, vitamin E-loaded SF, and PVA-Au	Cosmetics
PANI/CPI and PVA/PAA	High-performance energy storage devices
MnO and hexagonal boron nitride/PAN	Lithium-ion batteries
Graphite	X-ray radiography
PSU amide/PUR	High-performance apparels
Polyimide	Self-cleaning materials
Fluorescent polymers PAA-poly(pyrene methanol)	Optical chemical sensors
PVDF, Ag/TiO ₂ nanofiber, PAN, PSU, and chitosan/PEO	Water purification
PUR, chitosan/PEO, PVA, PA6, and PA66	Air filtration
PVA/indium acetate	CO gas sensor

Table 2. Electropunnnanofibers and application using needle-free electrospinning system.

Nanofiber	Application
CS, PVA, cellulose acetate, and PUR/copper oxide	Air filtration
CS/PCL, collagen, gelatin, PCL, and poly(L-lactide-co-glycolide)	Tissue engineering
Cellulose, PA6, PVDF, PAN, PVDF/PAN, PVDF, PUR, and polypropylene	Membrane for water purification
Gelatin, silk, PCL, CS-PEO, PA6, and dextran	Biomedical applications
PVA and PA6	Acoustics
PVA, polyvinyl butyral, PUR, and PAN	High-performance
CS, PVA, cellulose acetate, and PUR/copper oxide	Air filtration
CS/PCL, collagen, gelatin, PCL, and poly(L-lactide-co-glycolide)	Tissue engineering

The quantity of planes which results in higher productivity^{25,29–31} Casper et al.³² arranged polystyrene (PS)/tetrahydrofuran nanofibers in various atomic load of PS (31,600, 171,000, 190,000, and 560,000 g/mol) at different mugginess. The resultant filaments showed that both dampness and the sub-atomic weight influence the outer layer of

electrospun PS. Bigger fiber distance across and less uniform pore-formed nanofibers were created by increasing the atomic weight. Additionally, expanding moistness causes an expansion in the measurement, shape, and dispersion of the pores. Smooth nanofibers were delivered at moistness under 25%, while pore structures were seen at 30% relative dampness. In another work, different sub-atomic weight polyamide 66 nanofibers were electrospun. Resultant filaments showed that expanding the sub-atomic weight causes an increment in fiber width. It was recommended that a basic low sub-atomic weight was vital for electrospinning.³³ The sub-atomic weight doesn't just affect fiber width yet in addition on the mechanical strength of the fiber. An increment in sub-atomic weight expands the elasticity and modulus of the nanofiber mat.³⁴ Utilizing a needle and sans needle electrospinning framework, different polymeric arrangements were utilized to deliver nanofibers in different applications. A few instances of them are displayed in Tables 1 and 2. Single needle electrospinning framework isn't sufficient to ful-ill the usefulness. Different electrospinning frameworks have as of now been intended to work on the usefulness of the nanofibers. These strategies incorporate air pocket electrospin-ning,^{96,97} two-layer liquid electrospinning,⁹⁸ multi-stream electrospinning,⁹⁹ conelike wire curl electrospinning,¹⁰⁰ edge plate electrospinning,¹⁰¹ pivoting roller electrospin-ning,^{102,103} wire electrospinning,^{104,105} etc. Contrasted with needle electro-turning framework, sans needle electrospinning framework has benefits. For example, the stopping up of needles is a problem and there must be a legitimate distance between needles. In any case, the electrical fields around the needle influence one another and stop the turning. Both roller and wire electrospinning framework are at present utilized in modern scale under the trademark Nanospider with an alternate age. The original of Nanospider is a pivoting roller electrospinning licensed by Jirsaket al.¹⁰² as displayed in Figure 3. In the guideline of the roller electrospinning framework, there is a turning roller drenched in a polymer arrangement tank which is associated with a high-voltage provider. The polymer solu-tion is taken care of to the outer layer of the roller by means of turn. Turning begins at the outer layer of the roller. The turning is done in a shut chamber to keep up with encompassing conditions and keep it settled during the cycle. Both the framework and the favorable to cess boundaries assume a major part in the end result. The cycle boundaries of the roller electrospinning framework are very unique contrasted with needle electrospinning because of an alternate arrangement. In writing by Yalcinkaya et al.,¹⁰⁶⁻¹⁰⁸ the boundaries of the sans needle electrospinning framework are delegated "reliant and free boundaries" as displayed in Table 3. Then again, the boundaries for the wire electrospinning framework are as yet not explored. The functioning rule of the wire electrospinning is different roller electrospinning. The polymeric arrangement is set into a shut tank which is the taking care of the unit. In the arrangement tank, there is a wire giving turning region. The wire is associated with a high-voltage sup-plier. The arrangement tank is moving to and fro and the arrangement is benefiting from the wire. The second wire cathode is put on the vertical that by and large has the contrary charge to the descending wire anode or is grounded. A transport supporting material is put before the vertical elec-trode to gather the nanofibers.¹⁰⁴ Figure 4 shows the schematic graph of wire electrospinning framework. The benefits of the wire framework contrasted with the roller are that the arrangement is in a shut tank and the outer layer of the wire cathode is smaller which expands the electri-cal field power around the wire.

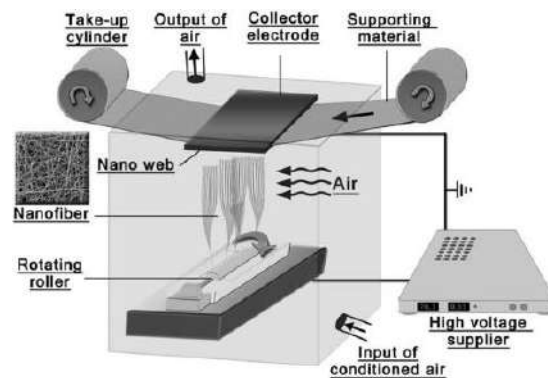


Figure 3. Diagram of roller electrospinning system (ref 17).

Different polymeric solutions are feasible to electrospun in modern scale. The principle benefits of nanofibers are their particular surface region, high perspective proportion, outrageous permeable design, and little pore size²⁵. Nanofibers have shown extraordinary qualities and colossal application potential. One of the effective application spaces of nanofiber is water refinement. Nanofiber films in the layer refining (MD) application are examined in the following segment²⁶.

Table 3. Dependent and independent parameters of needleless electrospinning system

Independent parameters	Dependent parameters
Polymer solution properties (concentration, viscosity, composition, surface tension, conductivity, and molecular weight)	Number of cones and the density of jets Lifetime of jets
Applied voltage	
Distance between electrodes	Total average Current and current/jet
The velocity of rotating roller	The thickness of polymer solution layer on the surface of the roller

The velocity of take-up fabric	Spinning area
The velocity of take-up fabric	Spinning area
Geometry of electrode	The distance between neighboring jets
Geometry of collector	Jet length in the stable zone
Ambient conditions (temperature and relative humidity)Fiber diameter and distribution	

The guideline is that fume transport across the hydro-phobic microporous layer driven by the fume pressure angle across the film because of a temperature slope. The unstable dissolvable vanishes through the layer by means of dissemination and additionally convection. The fume is moved to the compartment with low fume pressure where they are con-densed in the cool fluid/fume stage (Figure 5). MD innovation is appropriate for some application regions like wastewater remediation, ocean water distilla-tion, and division of unpredictable fluids. Despite the fact that the dismissal of MD films is 100%, this innovation has not discovered a spot in the modern stage. The explanation is because of low motion and penetrability of the films, potential pores wetting and water misfortune, energy utilization, and apparatus cost. Other than drawbacks, there are a few benefits of MD, like full dismissal, lower pressure-driven partition measure because of low prerequisite for mechanical properties and low working temperature. There are a few designs of MD unit announced in the writing by Khayet and Matsuura¹¹⁰ and Wang and Chung,¹¹¹ for example, direct contact layer refining (DCMD), air hole film refining, clearing gas membrane distillation (SGMD), and vacuum membrane- distillation (VMD). The membrane is the most important part of the MD process

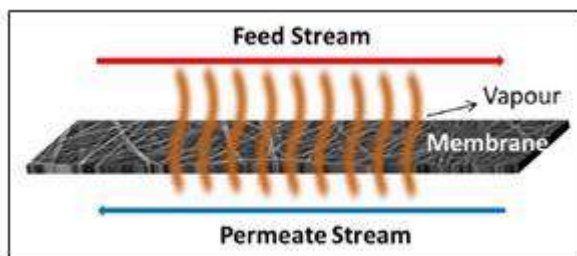


Figure. 4 schematic graph of wire electrospinning framework (ref 19)

In DCMD, a membrane is placed between permeate and a hotter feed solution. It has to have a temperature between feed and permeate. The membrane is in con- tact both the feed and the permeated side. A magnetic stirrer or circulating pumps are used to circulate feed and permeate solution to the membrane surfaces. As a result of heat difference on both sides of the membrane, vapor pressure is generated. The vapor of the feed solution is passing through the membrane pores via diffusion or convection. In air gap membrane distillation (AGMD), there is a gap between permeate and membrane. The membrane is in direct contact with the feed solution. The vapor of feed solu- tion is passing through the membranes to air gap and con- dense on the condensing plate. The filtered liquid is collected between feed and permeate solution. In SGMD, instead of a cold feed solution, a cold inert gas sweeps in the permeate side of the membrane²⁸. The volatile liquid molecules are passing through to membrane pores toward the cold gas side and condensation takes place out of the MD module. In VMD, there is no cooling system. Using a vacuum pump, a lower vacuum pressure is applied to permeate side. The feed side has higher saturation pressure which results in separation of the volatile molecules from the feed solution. As in the SGMD, the condensation takes place out of the MD module

CONCLUSION

In this review, the properties, the spinning parameters, and the software vicinity of the electrospunnanofibers had been dis-cussed. Electrospinning approach is a captivating technique to put together membranes in micro or nanopore size. One can put together porous shape the usage of a range of polymeric electro- spun nanofiber layers. Electrospunnanofiber layers havehigher porosity with uniform pore size appropriation com-pared to ordinary layers. The profoundly permeable construction respects the increment the penetrability of the mem-branes while high surface region permits layers to be functionalized easily. It was tracked down that noteworthy supportofgress has been made in the creations of electrospun layers for water treatment. MD is one of the most encouraging application fields for the electrospunnanofiber layers. The permeable construction, hydrophobicity, and the presentation of the film are pivotal for additional devel-opments in MD. This audit uncovers that conceivable applica-tion of nanofiber layers in MD.

CONFLICT OF INTEREST

Conflict of interest declared none.

REFERENCES

1. Ondarçuhu T and Joachim C. Drawing a single nanofibre over hundreds of microns. *EurophysLett* 1998; 42(2): 215–220.
2. Norton C. Method of and apparatus for producing fibrous or filamentary material, <https://www.google.com/patents/US2048651> (1933, accessed 3 January 2018).

3. Formhals A. Process and apparatus for preparing artificial threads, <https://www.google.com/patents/US1975504> (1930, accessed 6 September 2017).
4. Formhals A. Method and apparatus for spinning, <http://www.google.com/patents/US2349950> (1938, accessed 3 January 2018).
5. Dalton PD, Grafahrend D, Klinkhammer K, et al. Electrospinning of polymer melts: phenomenological observations. *Polymer* (Guildf) 2007; 48: 6823–6833.
6. Hassan MA, Yeom BY, Wilkie A, et al. Fabrication of nanofibermeltblown membranes and their filtration properties. *J Membr Sci* 2013; 427: 336–344.
7. Wang Y, Zheng M, Lu H, et al. Template synthesis of carbon nanofibers containing linear mesocage arrays. *Nanoscale Res Lett* 2010; 5(6): 913–916.
8. Zelenski CM and Dorhout PK. Template synthesis of near- monodisperse¹ microscalenanofibers and nanotubules of MoS₂. *J Am Chem Soc* 1998; 120(4): 734–742.
9. Rolandi M and Rolandi R. Self-assembled chitin nanofibers and applications. *Adv Colloid Interface Sci* 2014; 207: 216–222.
10. Liao HS, Lin J, Liu Y, et al. Self-assembly mechanisms of nanofibers from peptide amphiphiles in solution and on substrate surfaces. *Nanoscale* 2016; 8(31): 14814–14820.
11. Katsogiannis KAG, Vladislavljević GT and Georgiadou, Porous electrospun polycaprolactone fibers: Effect of process parameters, *Polym. Phys.* 2016, 54, 1878–1888.
12. S. Porous electrospun polycaprolactone (PCL) fibres by phase separation. *EurPolym J* 2015; 69: 284–295.
13. Zhang Z, Tu W, Peijs T, et al. Fabrication and properties of poly(tetrafluoroethylene) nanofibres via sea-island spinning. *Polymer* (Guildf) 2017; 109: 321–331.
14. Hammami MA, Krifa M and Harzallah O. Centrifugal force spinning of PA6 nanofibers—processability and morphology of solution-spun fibers. *J Text Inst* 2014; 105(6): 637–647.
15. Sarkar K, Gomez C, Zambrano S, et al. Electrospinning to forcespinning™. *Mater Today* 2010; 13(11): 12–14.
16. Yu L, Shao Z, Xu L, et al. High throughput preparation of aligned nanofibers using an improved bubble-electrospinning. *Polymers (Basel)* 2017; 9(12): 658.
17. Taylor G. Disintegration of water drops in an electric field. *Proc R Soc A Math Phys Eng Sci* 1964; 280: 383–397.
18. Shin YM, Hohman MM, Brenner MP, et al. Electrospinning: a whipping fluid jet generates submicron polymer fibers. *Appl Phys Lett* 2001; 78: 1149–1151.
19. Yarin AL, Koombhongse S and Reneker DH. Bending instability in electrospinning of nanofibers. *J Appl Phys* 2001; 89(5): 3018–3026.
20. Deitzel J., Kleinmeyer J, Harris D, et al. The effect of processing variables on the morphology of electrospun nanofibers and textiles. *Polymer* (Guildf) 2001; 42(1): 261–272.
21. Zong X, Kim K, Fang D, et al. Structure and process relationship of electrospun bioabsorbable nanofiber membranes. *Polymer* (Guildf) 2002; 43: 4403–4412.
22. Meechaisue C, Dubin R, Supaphol P, et al. Electrospun mat of tyrosine-derived polycarbonate fibers for potential use as tissue scaffolding material. *J Biomater Sci Polym Ed* 2006; 17(9): 1039–1056.
23. L.I. Portela, S. Ramos, A.T. Teixeira
24. Nafion. Available online: <https://www.fuelcellstore.com/membranes/nafion/> (accessed on 3 February 2020).
25. <https://www.fuelcellstore.com/membranes/nafion/>
26. J.N. Tiwari, R.N. Tiwari, K.S. Kim, Zero-dimensional, one-dimensional, two-dimensional and three-dimensional nanostructured Mater for advanced electrochemical energy devices, *Progress in Materials Science*, 57 (2012), 724-803
27. A. Lobo-Guerrero, X-ray analysis and Rietveld refinement of polyvinyl alcohol, *Materials Letters*, 10.1016/j.matlet.2020.127434, (127434),

2-Iminopyrazole Having Remarkable Activity in Bacterial Strains *E. coli* and *B. Subtilis*

M.Deepa, Chinnasamy, M.Srinivasan R.Shanmugapriya, V.Swetha

Dhanalakshmi Srinivasan College Of Arts And Science For Women (Autonomous), Perambalur Tamilnadu-621212

Abstract: The synthesis of pyrazole analogue 3-methyl-5-(2-phenylhydrazono)-4,5-dihydro-1H-pyrazole (2) via Schiff base reaction by using grindstone chemistry technique. In this method, inexpensive and easily available $\text{CuCl}_2 \cdot 2\text{H}_2\text{O}$ was used as a catalyst and this gives excellent yields. Synthesized pyrazole derivatives were confirmed by, ^1H NMR, and ^{13}C NMR spectral analysis. All the synthesized compounds were screened for in vitro antibacterial activity. Ciprofloxacin and were used as a standard for the comparison of antibacterial activity. The synthesis of the title compound (2) was illustrated in scheme 1. The synthesized compounds were characterized by FT-IR, ^1H NMR, and ^{13}C NMR. Compound 2 was synthesized by the condensation method. In this method, inexpensive and easily available $\text{CuCl}_2 \cdot 2\text{H}_2\text{O}$ was used as a catalyst and this gives excellent yields.

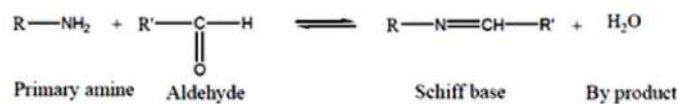
Keywords: ^1H NMR, and ^{13}C NMR spectral analysis, *E. COLI*, *B. SUBTILIS*, Pyrazole

INTRODUCTION

Metabolism studied using hepatic microsomes suggest that this procedure would be a useful in vitro method for the appropriate animal model for testing oral absorption.¹ Selecting In vitro anti-inflammatory activity of the synthesized compounds was investigated against inhibition of Albumin Denaturation and Membrane Stabilization test methods. Majority of the compounds showed good activity when compared with the standard drugs.² Numerous pyrazole derivatives have been found to possess a broad spectrum of biological activities, which stimulated the research activity in this field. Pyrazoles and its derivatives represent one of the most active classes of compounds, which possess wide range of biological activities like anti-bacterial, anti-convulsant, analgesic, anti-microbial, anti-inflammatory, ant diabetic, sedative anti-rheumatic, anticancer, and anti-tubercular activities.³ Attributed to its several potential applications, there is a rise in the significance of designing novel pyrazoles, disclosing innovative routes for synthesizing pyrazoles, examining different potencies of pyrazoles, and seeking for potential applications of pyrazoles.⁴ While the presence of solvents in drugs is not usually considered an environmental impact, they may be considered a form of pollution for the purposes of this review as they affect us directly as does other pollution⁵. A series of substituted chalcones and their corresponding pyrazoles were synthesized and evaluated for in vitro cytotoxic activity against a panel of human cancer cell lines.⁶ Under transition-metal-free conditions, calcium carbide was used as the acetylide source to react with a wide range of *N*-tosylhydrazones derived from aldehydes or ketones, affording various substituted pyrazoles in good yields with high regioselectivities.⁷ The heterocyclic compounds have been extensively studied not only for their intrinsic interest, but also because many natural products, many drugs and medicines, and many dyestuffs belong to this group.⁸

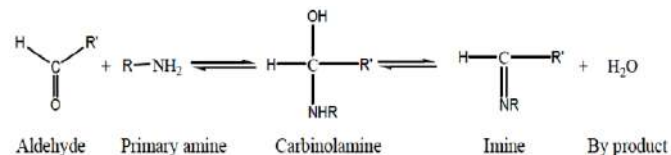
SCHIFF BASE

Schiff bases are condensation products of primary amines with carbonyl compounds and they were first reported by Hugo Schiff in 1864. The common structural feature of these compounds is the azomethine group with a general formula $\text{RN}=\text{CH}-\text{R}'$, where R and R' are alkyl, aryl, cycloalkyl, or heterocyclic groups which may be variously substituted. These compounds are also known as imines or azomethines.



Scheme 1. Process of condensation of aldehyde and primary amine

Schiff bases of aliphatic aldehydes are relatively unstable and readily polymerizable, while those of aromatic aldehydes have effective conjugation and stability. The formation of Schiff bases from aldehydes or ketones is a reversible reaction and generally takes place under acid or base catalysis or upon heating.



Scheme 2. Process of formation of Schiff base with carbinolamine intermediate

The mechanism of Schiff base formation is nucleophilic addition to the carbonyl group. In the first part of the mechanism (Scheme 2), the amine reacts with the aldehyde or ketone to give an unstable addition compound called carbinolamine. Typically the dehydration of the carbinolamine is the rate-determining step of Schiff base formation and that is why the reaction is catalyzed by acids. If the amine is protonated and becomes non-nucleophilic, equilibrium is pushed to the left and carbinolamine formation cannot occur. Therefore, syntheses of many Schiff bases are best carried out at mildly acidic pH. The dehydration of carbinolamine is also catalyzed by a base. This reaction is similar to the E_2 elimination of alkyl halides except that it proceeds in two steps through an anionic intermediate. i.e., addition followed by elimination. Owing to the relative easiness of preparation, synthetic flexibility, and the unique property of the C=N group, the azomethine group facilitates the formation of five or six-membered rings with the metal ion. Several studies showed that the presence of a lone pair of electrons in the sp^2 hybridized orbital of a nitrogen atom in the azomethine group is of considerable chemical and biological importance. The electron-donating groups, such as azomethines, can trap metal ions with large radii and high coordination numbers. In such a case, two or more metal atoms are located in one cavity, i.e., close to each other and contributing to unusual magnetic properties and catalytic activity. The versatility of Schiff base ligands and biological, analytical, and industrial applications of their complexes make further investigations in this area highly desirable. One-pot condensations of ketones, aldehydes and hydrazine monohydrochloride readily formed pyrazoline intermediates under mild conditions. In situ oxidation employing bromine afforded a wide variety of pyrazoles in very good yields.⁹ methods of synthesis and transformation of styrylpyrazoles; thus, highlighting the interest and huge potential for application of this kind of compound.¹⁰ First synthetic method for the synthesis of pyrazole was explored by Knorr in 1883 which employed the reactions of 1,3-dicarbonyl compounds with arylhydrazines to afford pyrazoles derivatives¹¹. An efficient protocol for the one pot regioselective synthesis of 4-bromopyrazole derivatives from 1,3-diketones, arylhydrazines and N-bromosaccharin, in the presence of silica gel supported sulfuric acid as heterogeneous catalyst, under solvent free conditions,¹² An efficient protocol for the one pot regioselective synthesis of 4-bromopyrazole derivatives from 1,3-diketones, arylhydrazines and N-bromosaccharin, in the presence of silica gel supported sulfuric acid as heterogeneous catalyst, under solvent free conditions, is reported.¹³ An environmentally benign **multicomponent** strategy for the synthesis of fused **pyrazole** derivatives has been developed¹⁴ There are several applications of pyrazole core based organic molecules in various areas including pharmacy and agro-chemical industries. There is an increase in the interest of synthesizing, analyzing different properties, and seeking possible applications of pyrazole derivatives¹⁵ Diazo compounds derived from aldehydes were reacted with terminal alkynes to furnish regioselectively 3,5-disubstituted pyrazoles.¹⁶ Subsequent quenching with strong acids such as TFA is essential to achieve good yields.¹⁷ The screening for the in vitro antimicrobial activity against eleven bacterial and three fungal/yeast strains exhibited complete inactivity of these aldehydes, but Bu imines of ortho and meta derivs. showed moderate activity compared to those of the used stds¹⁸

MATERIAL AND METHODS

General materials and characterization techniques:

All materials were purchased from Nice and Loba chemicals. The IR spectra (KBr) was recorded in KBr on a Shimadzu 8201pc (4000-400 cm^{-1}). The ^1H NMR and ^{13}C NMR spectra were recorded on a JEOL-300 MHz.

A general method for the synthesis of 2-iminopyrazole (2) via Schiff base reaction.

The reactants 3-methyl-1H-pyrazol-5(4H)-one (1) (0.01mol, 0.98g), Phenylhydrazine (0.01 mol, 1mL), $\text{CuCl}_2\cdot 2\text{H}_2\text{O}$ (0.005mol, 0.85g) and few drops of con. HCl was mixed in a pestle and mortar. The reaction was monitored by TLC. After the completion of the reaction specified by TLC, the reaction mixture was cored into ice-cold water. The white-colored precipitate was formed it is filtered and dried. The product was recrystallized in ethanol to get pure product.

3-methyl-5-(2-phenylhydrazono)-4,5-dihydro-1H-pyrazole (2)

White solid; mw: 188.23; m.p. 198°C; IR (cm^{-1}): 3321.09 (NH), 3118.48 (Ph-CHstr), 2920.27 (Ar-H), 2852.23 (CH_2), 1597.19 (C=N); $^1\text{H-NMR}$ (400 MHz, CDCl_3): δ = 9.23 (1H, s, NH), 8.20 (1H, s, NH), 7.35, 7.20, 6.80 (5H, m, Phenyl ring), 1.94 (3H, s, CH_3), 1.36 (2H, s, - CH_2); $^{13}\text{C-NMR}$ (100 MHz, CDCl_3): δ = 159.50 (1C, C=N), 157.0 (1C, C=N), 148.0, 129.50, 122.40, 113.90 (6C, Phenyl), 40.0 (1C, - CH_2), 12.10 (1C, CH_3). Elemental analysis: Calcd. for $\text{C}_{10}\text{H}_{12}\text{N}_4$: Elemental Analysis: C, 63.81; H, 6.43; N, 29.77 %; Found: C, 63.80; H, 6.45; N, 29.75 %.

Biological screening

In vitro activities of the title compounds, 1 and 2 were tested in Nutrient broth (NB) for bacteria by the two-fold serial dilution method. Seeded broth (broth containing microbial spores) was prepared in NB from 24 hold bacterial cultures on nutrient agar (Hi-media) at $37 \pm 1^\circ\text{C}$. The bacterial suspension was adjusted with sterile saline to a concentration of $1 \times 10^4 - 10^5$ CFU. The synthesized compounds and standard drugs were prepared by two-fold serial dilutions to obtain the required concentrations of 100, 50, 25, 12.5, 6.25, and 3.13 mg/mL. The tubes were incubated in BOD incubators at $37 \pm 1^\circ\text{C}$ for bacteria. Antimicrobial screening was carried out for the synthesized compounds along with a series of N(2)-pyridyl tetrahydroindazoles.¹⁹

RESULTS AND DISCUSSION

The synthesis of the title compound (2) was illustrated in scheme 1. The synthesized compounds were characterized by FT-IR, ^1H NMR, and ^{13}C NMR. Compound 2 was synthesized by the condensation method. The optimization of catalyst was shown in Table. 1. The formation of the title compound was confirmed by recording the IR, ^1H NMR, ^{13}C NMR spectra, and elemental analyses.¹⁹ The IR spectra of compound 2 showed absorption bands at 3321.09, 2920.27 and 1597.19 cm^{-1} confirms the presence of NH, Phenyl, and C=N groups, respectively. The ^1H NMR spectra of compound 2 showed a sharp singlet at 9.23 for

NH proton and a singlet at δ 1.40 for $-\text{CH}_2-$ proton. The ^{13}C NMR spectra of compound 2 showed characteristic peaks at δ 159.50 and 12.10 ppm corresponding to C=N and $-\text{CH}_3$ carbons, respectively. The catalytic hydrogenation of 4-silylmethylisoxazole derivative 34 produced β -enaminoketones, which afforded Michaeli substrates, and they are reactive toward malononitrile as nucleophiles to produce 3-cyano-2-pyridones 36 in 56% yield²⁰

Table 1: Optimization of catalyst

S. No.	Catalysts	Yield (%)		
		0.5 equivalent	1 equivalen t	2 equival ent
1	TiCl ₂	-	-	-
2	FeCl ₂	-	-	34
3	ZnCl ₂	20	32	40
4	ZrOCl ₂	-	-	18
5	SnCl ₂	10	30	48
6	CuCl ₂ .2H ₂ O	48	78	-



Scheme 1: Synthetic route of proposed compound (2)

Table 2. Antibacterial activity of title compounds (1 and 2)

Comp.No.	MIC $\mu\text{g/mL}$	
	<i>E. coli</i>	<i>B. subtilis</i>
1	29.91 \pm 2.15	35.41 \pm 2.41
2	24.16 \pm 1.43	33.16 \pm 1.95
Positive control	25.00 \pm 0.95	50.00 \pm 1.75
Negative control	0.0 \pm 0.0	0.0 \pm 0.0

Positive control: Ciprofloxacin **Negative control: DMSO** ^aValue were the means of three replicates \pm SD.

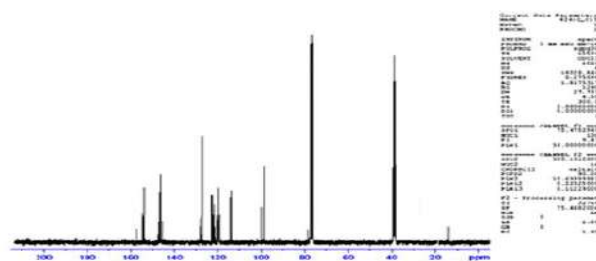


Figure 1: ^1H NMR spectrum of compound 2.

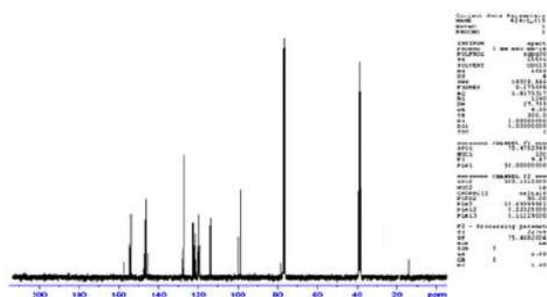


Figure 2: ^{13}C NMR spectrum of compound 2.

CONCLUSION

The synthesis of pyrazole analogue 3-methyl-5-(2-phenylhydrazone)-4,5-dihydro-1H-pyrazole (2) via Schiff base reaction by using grindstone chemistry technique. In this method, inexpensive and easily available $\text{CuCl}_2 \cdot 2\text{H}_2\text{O}$ was used as a catalyst and this gives excellent yields. Synthesized pyrazole derivatives were confirmed by ^1H NMR and ^{13}C NMR spectral analysis.

CONFLICT OF INTEREST

Conflict of interest declared none.

REFERENCES

1. Schallner, O.; Heinz, K. H.; Karl, K. J. *Ger. Offen DE*, 1997, 19615259; *Chem. Abstr.* 1997, 127, 346387.
2. Elkholy, Y. M.; Erian, A. W.; Elassar, A. A. *Pig. Resin Technol.* 1993, 25, 4.
3. Krygowski, T. M.; Anulewicz, R.; Cyrafiski, M. K.; Puchala, A.; Rasata, D. *Tetrahedron*, 1998, 54, 12295.
4. Behr, L. C.; Fusco, R.; Jarboe, C. H., *The Chemistry of Heterocyclic Chemistry: Pyrazoles, Pyrazolines, Pyrazolidines, Indazoles, and Condensed Rings*; Wiley & Sons: London, 1967.
5. Dale, D. J.; Dunn, P. J.; Golightly, C.; Hughes, M. L.; Levett, P. C.; Pearce, A. K.; Searle, P. M.; Ward, G.; Wood, A. S. *Org. Process Res. Dev.* 2000, 4,
6. Bhat, B. A.; Puri, S. C.; Qurishi, M. A.; Dhar, K. L.; Qazi, G. N. *Synthetic Commun.* 2005, 35, 1135.
7. Guzman-Perez, A.; Wester, R. T.; Allen, M. C.; Brown, J. A.; Buchholz, R.; Cook, E. R.; Day, W. W.; Hamanaka, E. S.; Kennedy, S. P.; Knight, D. R.; Kowalczyk, P. J.; Marala, R. B.; Mularski, C. J.; Novomisle, W. A.; Ruggeri, R. B.; Tracey, W. R.; Hill, R. J. *Bioorg. Med. Chem. Lett.* 2001, 11, 803.
8. Gupton, J. T.; Clough, S. C.; Miller, R. B.; Norwood, B. K.; Hickenboth, C. R.; Chertudi, I. B.; Cutro, S. R.; Petrich, S. A.; Hicks, F. A.; Wilkinson, D. R.; Sikorski, J. A. *Tetrahedron* 2002, 58, 5467.
9. Deng, X.; Mani, N. S. *Org. Lett.* 2008, 10, 1307. (b) Fong, T. M.; Heymsfield, S. B. *Int. J. Obesity* 2009, 33, 947.
10. Pinto, D. C. G. A.; Silva, A. M. S.; Levai, A.; Cavaleiro, J. A. S.; Patonay, T.; Elguero, J. *Eur. J. Org. Chem.* 2000, 2593.
11. Bishop, B. C.; Brands, K. M.; Gibb, A. D.; Kennedy, D. *Synthesis* 2004, 43.
12. Wang, X.; Tan, J.; Grozinger, K. *Tetrahedron Lett.* 2000, 41, 4713.
13. Wang, X.; Tan, J.; Grozinger, K. *Tetrahedron Lett.* 2000, 41, 4713.
14. Liu, H. L.; Jiang, H. F.; Zhang, M.; Yao, W. J.; Zhu, Q. H.; Tang, Z.; *Tetrahedron Lett.* 2008, 49, 3805
15. Wang, Z. X.; Qin, H. L. *Green Chem.* 2004, 6, 90.
16. Aggarwal, V. K.; De Vicente, J.; Bonnert, R. V. *J. Org. Chem.* 2003, 68, 5381.
17. Deng, X.; Mani, N. S. *Org. Lett.* 2006, 8, 3505.
18. Zora, M.; Gormen, M. *J. Organomet. Chem.* 2007, 692, 5026.
19. Katritzky, A. R.; Wang, M.; Zhang, S.; Voronkov, M. V. *J. Org. Chem.* 2001, 66, 6787.
20. Alberola, A.; Gonzalez-Ortega, A.; Sadaba, M. L.; Sanudo, M. C. *J. Chem. Soc. Perkin Trans. I* 1998, 4061. (b) Calvo, L. A.; Gonzalez-Nogal, A. M.; Gonzalez-Ortega, A.; Carmen Sanudo, M. *Tetrahedron Lett.* 2001, 42, 8981. z, J. M. *Angew.*

Helation Stabilised Complex Based On Stablishing Tri Aza Macro Cyclic Ligands

RamasamyShanmugaPriya, Dr.T.Adinaveen,Dr.A.Priya , G Vanaja

DhanalakshmiSrinivasan College of Arts &Science for Women (Autonomous) Perambalur, Tamil nadu-621212

Abstract: A few novel chelators dependent on 1-hydroxy-2(1H)- pyridinone organizing bunches improving a triazamacrocyclic spine framework were orchestrated as potential amazing Fe^{3+} chelators equipped for contending with bacterial siderophores. Specifically, a novel chloromethyl subsidiary of 1-hydroxy-2(1H)-pyridinone. A misusing a novel defensive gathering for this group of planning bunches was created. These are the primary instances of hexadentatechelators dependent on 1-hydroxy-2(1H)-pyridinone to appear to have a biostatic movement against a scope of pathogenic microscopic organisms. Their adequacy as biostatic specialists was evaluated, uncovering that minor varieties in the design of the chelator can influence viability significantly. The insignificant inhibitory groupings of our best tried novel chelators approach or are practically identical to those for 1,4,7-tris(3-hydroxy-6-methyl-2-pyridylmethyl)- 1,4,7-triazacyclononane, the best Fe^{3+} chelator known to date. The impending impact these chelators have on microbial development proposes that they could have an expected application as a co-dynamic close by antimicrobials in the battle against contaminations.

Key words; 1,4,7-triazacyclononane, chelators, Fe^{3+} chelator, helation, cyclic ligands

INTRODUCTION

Bacterial protection from once compelling anti-toxins has arisen as a significant wellbeing danger of the 21st century^{1,2} here is accordingly a pressing need to grow new systems to battle the spread of multidrug safe contaminations. One of the potential alternatives as of now being contemplated is the utilization of biostatic specialists (for example inhibitors of bacterial development) that could work synergistically with existing anti-toxins and lift their viability^{3,4,5,6,7} Metal chelators can be utilized with that impact as their biostatic action upon microorganisms has for quite some time been known. Their method of activity is believed to be the inconvenience of metal starvation on the microorganisms^{8,9,10} To rival solid siderophores, the correct decision of planning bunches is urgent. While considering just the thermodynamic rivalry between bacterial siderophores and an additional chelator, one should essentially consider the particular pFe^{3+} values (characterized as $-\log[\text{Fe}^{3+}]_{\text{free}}$, typically determined at pH 7.4,¹¹ with $[\text{Chelator}]_{\text{total}} = 10 \mu\text{M}$ and $[\text{Fe}^{3+}]_{\text{total}} = 1 \mu\text{M}$ and referred to thus in these states) of the two chelators to appraise which is destined to be powerful in complexing the metal. No doubt three isomers of the hydroxypyridinone (HOPO) family (Fig. 1) have the correct blend of pK_a and $\log\beta(\text{Fe}^{3+})$ to give high pFe^{3+} values and in this manner thermodynamically contend with siderophores (that are ordinarily founded on planning gatherings, for example, α -hydroxycarboxylic acids, hydroxamic acids and catechols)¹²

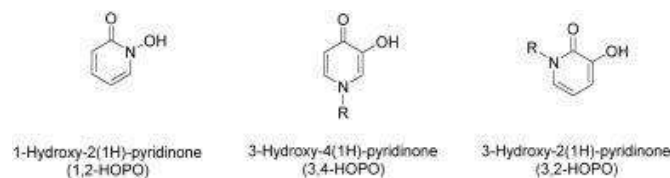


Fig. 1. Three relevant isomers of the HOPO family.

These hydroxypyridinones likewise offer alluring extra possibilities. Numerous microorganisms can utilize siderophores expounded by those of another species¹² to be powerful biostatic specialists, manufactured chelators should not experience the ill effects of this "siderophore robbery" and really advance bacterial development. Since not many HOPO are found in nature and just one has been portrayed as a siderophore ligand (1-hydroxy-5-methoxy-6-methyl-2(1H)-pyridinone likewise called cepabactin), the probability of the metallatedchelators being perceived by bacterial receptors and utilized as a wellspring of Fe^{3+} is required to be little. Also, tainted human hosts are known to utilize different Fe^{3+} retaining methodologies to restrict bacterial development. One of these depends on the action of siderocalin, a protein that basically goes about as a snare for some siderophores. A remedial chelator should not cooperate with siderocalin and restrains its defensive activity¹³. It is realized that some 1-hydroxy-2(1H)- pyridinone (1,2-HOPO) based chelators don't tie unequivocally to siderocalin, recommending that this class of planning gatherings would supplement as opposed to overpower this protection technique¹⁴. Individuals from the 3-hydroxy-4(1H)-pyridinone (3,4-HOPO) sub-family have been broadly concentrated in chelation treatments¹⁵. A critical number of reports have likewise portrayed development restraint of a scope of pathogenic microorganisms by bidentate or hexadentatechelators dependent on 3,4-HOPO. To accomplish high pFe^{3+} , hexadentatechelators are wanted to bidentate ones, particularly since their method of activity as biostatic specialists is relied upon to be extracellular and hence don't experience the ill effects of size limitation to enter the organisms¹⁶. An extremely modest number of mixes having a place with the 1,2-HOPO sub-family were depicted as antimicrobial specialists yet these are for the most part bidentatechelators. No hexadentate individual from that 1,2-HOPO sub-family has been portrayed as antimicrobial specialist. This nonattendance of reports is amazing looking at that as a couple hexadentatechelators dependent on 1,2-HOPO were depicted (for complexation of non-organically important metals) whose primary highlights and chelation

properties make them alluring contender for this reason (for instance exacerbates 1 and 2, Fig. 2)¹⁷ Albeit marginally more vulnerable planning bunches than their 3-hydroxy-2(1H)- pyridinone (3.2-HOPO) and 3,4-HOPO isomers, 1,2-HOPO organizing bunches have another favorable position that make them more alluring than their isomers¹⁸. Their lower pKa esteems (commonly 6 versus 8.5–10 relying upon replacement make them charged atoms at physiological pH and consequently less inclined to infiltrate cells of the host. This could have helpful security benefits in treating foundational contaminations.

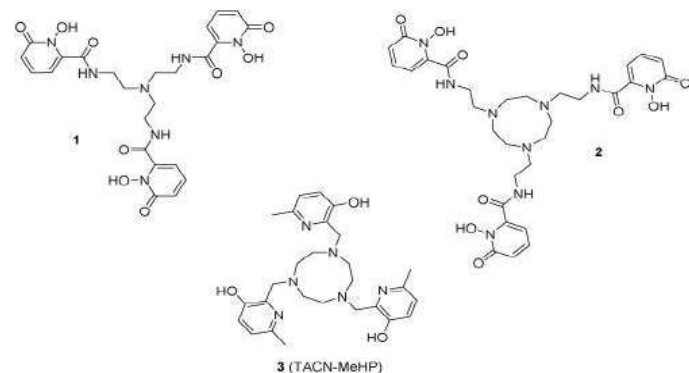


Fig. 2. Examples of known hexadentatechelators based on 1,2-HOPO (1, 3) and 1,4,7-tris(3-hydroxy-6-methyl-2-pyridylmethyl)-1,4,7-triazacyclononane (TACN-MeHP) ¹⁸.

Albeit not founded on HOPO, compound 3 has the most elevated known estimation of pFe3 + (see beneath) and is subsequently expected to have the option to contend well with siderophores for ferric cations at low focus and along these lines show high biostatic viability. Regardless of its high pFe3 + esteem, to the most amazing aspect our insight this compound has never been depicted as a biostatic specialist. It was along these lines thought to be important to blend, screen and utilize compound 3 as a benchmark¹⁹. Our premium in growing ground-breaking Fe3 +-upgraded chelators as biostatic specialists incited us to explore a scope of hexadentatechelators dependent on 1,2-HOPO and a triazamacrocyclic spine platform to attempt to distinguish novel microbiostaticchelators. Not many polyazamacrocycles bearing HOPO planning bunches have been depicted Macrocycles offer the possibility to adjust the metal chelating properties by differing the cycle's size and flexibility. Our point was to join key underlying components of siderophores, HOPO and 1,4,7-tris(3-hydroxy-6-methyl-2-pyridylmethyl)- 1,4,7-triazacyclononane (TACN-MeHP, 3) into a novel arrangement of chelators. Specifically by relationship with enterobactin (Fig. 3, compound, it is theorized that the impact of the macrocyclic spine framework could be helpful to the adequacy of metal authoritative and according to the base inhibitory focus (MIC) of the chelator. Besides, no past amalgamation of hexadentatechelators where 1,2-HOPO moieties where connected to the sub-atomic platform by means of a methylene connect were ever detailed, the emphasis having been on a carbonyl linker. The effect of that linker on metal chelation viability can be emotional and along these lines merits top to bottom examination. Detailed in this is the amalgamation of novel triazamacrocyclicchelators bearing 1,2-HOPO moieties, connected through methylene or carbonyl gatherings and the investigation of their biostatic impact on a scope of microorganisms, incorporating an examination with that of known mixes 1–3.

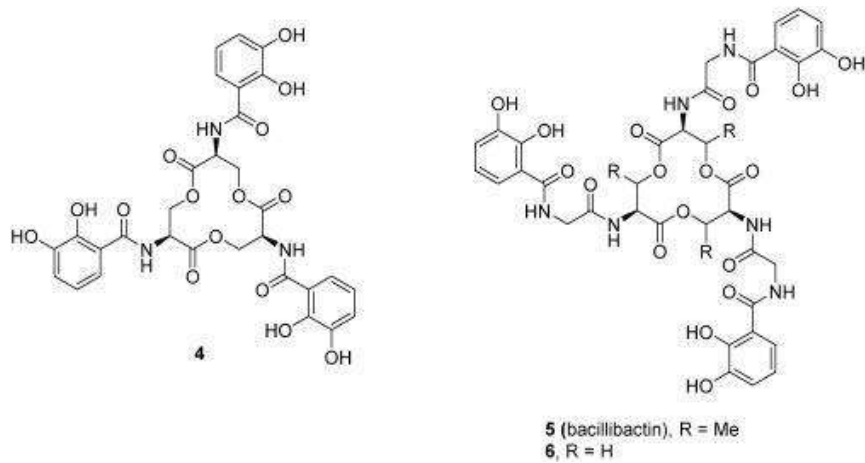


Fig. 3. Structure of siderophores enterobactin (4), bacillibactin (5) and synthetic analogue 6. Experimental Arrangement of stock arrangements

China was flushed with a deionised fluid arrangement of EDTA (0.1 M) at that point washed together with deionised water (18 m^W) before ligands were broken up in deionised water to the ideal focus (5 mM; 5 mL). The stock arrangement was then gone through a layer channel (0.22 μM) into a sterile bijoux tube (7 mL) and put away at 4 °C until required²⁰.

4.2. Bacterial strains

All strains were bought from DSMZ. *E. coli* DSM-18,039, *K. pneumoniae* DSM-30,104, *P. aeruginosa* DSM-19,880 and *S. aureus*

DSM-1104 were refined onto cerebrum heart imbuement (BHI) agar and brooded at 37 °C for 24 h. Comparative techniques were directed for strains of *A. baumannii* DSM-30,007 and *C. albicans* DSM-1386 brooded at 30 °C and *B. subtilis* brooded at 25 °C, just for 48 h. The refined plates were then put away at 4 °C until required.

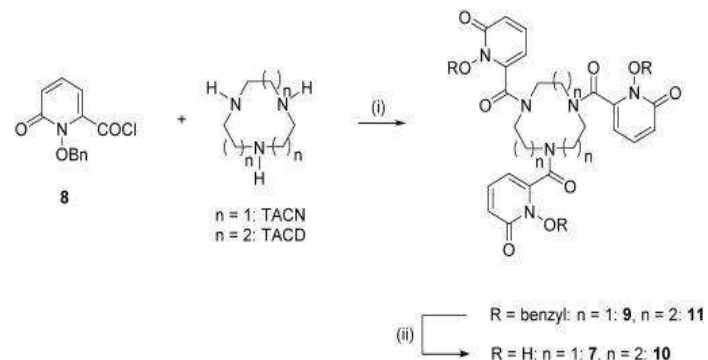
Antimicrobial test

The test depended on a comparative writing methodology Stock arrangements of ligands (5000 μ M) were added to the primary wells of a 96 well plate (200 μ L) and sterile BHI stock (100 μ L) was added to the leftover wells in the line. Ligand arrangement from the primary well (100 μ L) was added to the following great in the column and blended. The method was then rehashed along the column from the weakened arrangements and disposed of after the penultimate well. Inoculum (105 CFU/mL; 100 μ L) was then added to all wells and the plate brooded without unsettling at 37 °C. Readings were taken after for 24 and 48 h, contingent on the microorganism, and the MIC decided based on visual turbidity of the well. Measures were acted in three-fold

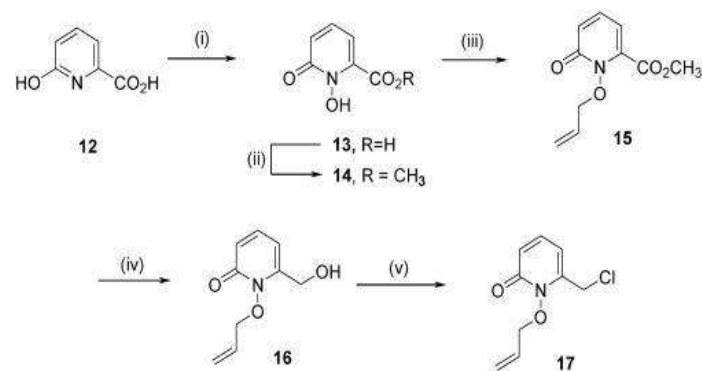
RESULTS AND DISCUSSION

Natural union

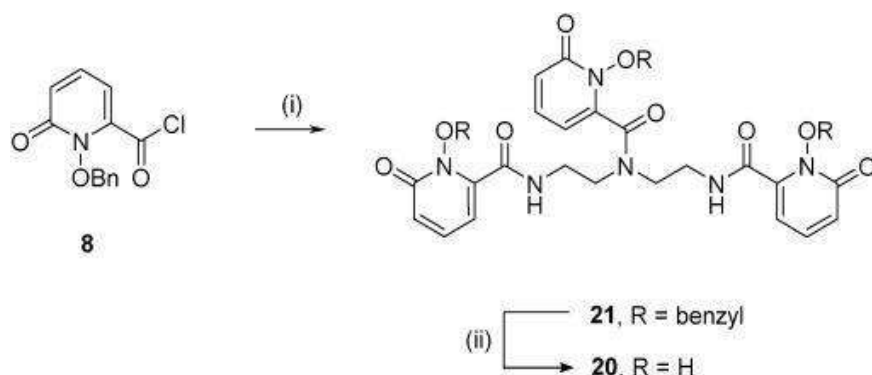
Our chelator configuration has zeroed in on thermodynamics ($p\text{Fe}^{3+}$) as opposed to active contemplations. Quite possibly the most amazing bacterial siderophores is enterobactin (4), whose platform is made out of a triserinemacrocycle (Fig. 3), and has been widely contemplated inferable from its exceptionally ground-breaking Fe^{3+} chelation ($\log\beta_{110} = 49$ and $p\text{Fe}^{3+} = 34.3$, where β_{110} is characterized as the balance steady for the response $\text{L} + \text{M} + \text{h H}^+ \rightleftharpoons \text{LIMmHh}$ [25]). The starting point of its proficient restricting has been explained and demonstrated to be affected by the pre-association of the planning gatherings, itself to a great extent impacted by the cyclic construction of its framework and intra-sub-atomic hydrogen holding. Curiously, bacillibactin (5), a siderophore simple of enterobactin with glycine spacers connected to a tris-threonine macrocyclic framework likewise shows enormous $\log\beta_{110}$ and $p\text{Fe}^{3+}$ values (47.6, 33.1 individually). Nonetheless, engineered simple 6, likewise made out of a glycine spacer yet of a tris-serine platform has less fortunate $\log\beta_{110}$ and $p\text{Fe}^{3+}$ values (44.1 and 29.6 separately). No doubt the idea of the spacer and the idea of the platform profoundly affect $p\text{Fe}^{3+}$ that we estimate as impacting development hindrance²¹.



Scheme 1. Reagents and conditions: $n = 1$: (i) TACN, NEt_3 , THF , 60°C ; 25% (ii) HCl : AcOH ; 97%; $n = 2$: (i) TACD, NEt_3 , DMF , 60°C ; 49% (ii) HCl : AcOH ; 71%.



Scheme 3. Reagents and conditions: (i) TACN, K_2CO_3 , CH_3CN , reflux; 93% (ii) BCl_3 , CH_2Cl_2 ; 87%.



Scheme 4. Reagents and conditions: (i) diethylenetriamine, NEt₃, THF, 60 °C; 91% (ii) HCl: AcOH; 70%.

The initial phase in the arrangement of 7 was performed dependent on a current technique by responding to known acyl chloride 8 with TACN in THF [60]. Secured chelator 9 was acquired in low yield (25%). Expulsion of the benzyl bunches from 9 utilizing a combination of concentrated hydrochloric and icy acidic corrosive yielded 7 in fantastic yield (97%). A simple of that compound with the bigger triazamacrocyclic (for example 1,5,9-triazacyclododecane, TACD) was likewise blended to consider correlation of the impact of the ring size upon bacterial development hindrance (Scheme 1). Response of acyl chloride 8 with TACD in DMF considered the disconnection of the bigger center ensured atom 11 in 49% yield. A comparable corrosive deprotection gave 10 in great yield (71%). Oxidation to the costly 1,2-HOPO-6-carboxylate 12 was performed utilizing industrially accessible peroxyacetic corrosive, an adjustment to the current strategy of Xu et al. [60], bringing about a somewhat expanded yield (77%) without the utilization of likewise costly trifluoroacetic corrosive. Treatment of the free corrosive 13 with thionyl chloride in methanol, following the strategy for Burgada et al. gave the methyl ester 14 in magnificent yield (96%). Ensuring assurance of the N-hydroxyl gathering, utilizing allyl bromide and potassium carbonate, yielded the novel methyl ester 15 (94%). Decrease of the ester 15 to the methyl liquor 16 was refined by moderate expansion of methanol to sodium borohydride in THF, astoundingly without decrease of the allylbunch. Eminently, a large portion of these means offered satisfactory to superb yields. Workup of the response combinations were not difficult to perform and the items either required no refinement at all or were not difficult to sanitize. In spite of the fact that chelators 1–3 were recently depicted in the writing they have not been assessed as biostatic specialists subsequently their blend was likewise embraced to evaluate their antimicrobial properties

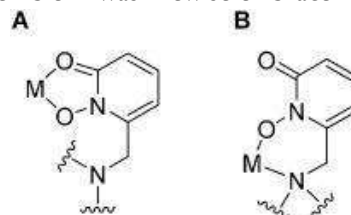


Fig. 4. Possible coordination modes for compound 19 with trivalent metal M (e.g. Fe³⁺, Ga³⁺).

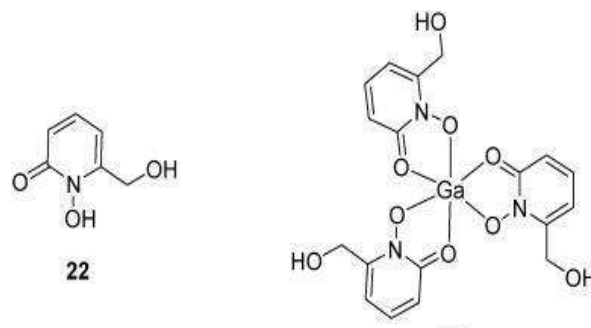


Fig. 5. 6-hydroxymethyl-1-hydroxy-2(1H)-pyridinone ²²and its expected 3:1 complex with Ga(III) ²³

To additional investigation the specific coordination method of ligand 19, specifically by NMR, Ga³⁺ was utilized as a proxy for Fe³⁺. No top to bottom investigation by MS or NMR of 1,2-HOPO based edifices of Ga(III) exist in the writing. For instance, just a single subsidiary of 1,2-HOPO complex (in light of the 1-oxo-2-hydroxy-isoquinoline-3-carboxylic corrosive) of Ga(III) has been described by NMR in CDCl₃. Basically, no investigation of the chelation by NMR or MS was acted in water, a dissolvable more pertinent to our development media and where protonation responses can dramatically affect the species framed ²⁴. To attempt to set up spectroscopic highlights that would permit us to recognize a N3O₃ from an O₆ coordination mode, we had to initially explore by MS and NMR the complexation of Ga(III) on a model framework. Compound 22 that we depicted for another kind of utilization has been chosen as a particularly model of ligand 19. It was judged that compound 22 in the presence of Ga(III) would form a 3:1 complex via the six oxygen atoms of three 1,2-HOPO bidentate ligands (Fig. 5). Therefore, compound 23 would be a good model of the coordination environment around Ga(III) if ligand 19 coordinated Ga(III) in a O₆ mode (Fig. 4A) and by extension, would give us some information on the way Fe³⁺ is chelated by 19. Proton and carbon NMR were first performed on solutions of 22 and 19 in D₂O. To these solutions, a stoichiometric amount of Ga(acac)₃ (acac = acetylacetone) was then added and the solutions incubated at room temperature for 24 h. The ¹H and ¹³C

NMR of the resulting complexes were then recorded. Also, these solutions, after dilution with methanol (non-deuterated), were analysed by MS. Starting with MS, 22 + Ga(acac)₃ (3:1 molar ratio) gave major peaks that match (*m/z* values and isotopic distribution) the formula [(22 – 3H)Ga + Na]⁺ at *m/z* 511.93 (expected 512.02), 512.93 (expected 513.02), 513.93 (expected 514.02), 515.00 (expected 515.02) and 516.00 (expected 516.02) (Fig. S1), confirming the displacement of the three acac ligands and strongly suggesting the formation of the 3:1 complex 23 as expected. In NMR, we expected that coordination of the HOPO moiety to Ga(III) would bring about particular changes to the substance movements of key protons and additionally carbon molecules of the ligand and it was foreseen that these could be normal for the two coordination modes. The ¹H and ¹³C NMR spectra are given in Figs. S3 and S4 separately. The ¹H of ligand 22 in D₂O in the nonattendance or presence of 1/3 molar likeness Ga(acac)₃ showed that upon complexation, the three signs of the 1.2-HOPO bunch are moved downfield by close to 0.3 ppm. The ¹H NMR of 19 + Ga(acac)₃ additionally indicated a downfield move of the substance moves however by a bigger estimation of 0.6 ppm. These distinctions could propose an alternate coordination mode. The presence of just one bunch of somewhat expanded signals for the 1.2-HOPO moiety on account of 19 + Ga(acac)₃ demonstrates that they are altogether to a great extent same and thus all comparatively planning, as proposed by the mass range. The signs for the TACN platform are significantly more affected by the presence of the metal. Rather than all around characterized singlet in the ligand, different expansive signs are seen somewhere in the range of 3.1 and 4.1 ppm. Appearance of wide signals for In(III) edifices of NOKA has been seen at raised temperature (in opposition to the Ga(III)NOKA complex where the signs stayed also characterized multiplets even at 85 °C). This has been credited to fast trade between the Δ and Λ isomers. The wide signals in our complex recommend that this quick trade exist even at room temperature ²⁵. In the ¹³C range of 22 with and without Ga(acac)₃, the sign appointed to the carbon particle of the carbonyl is additionally moved, upfield this time by 3.3 ppm. Curiously, the most affected signs relate to the three C-single bond H gatherings. The ¹³C NMR of 19 + Ga(acac)₃ is definitely not the same as that of the parent ligand and that of the similar complex 23. Once more, zeroing in on the signs for the TACN's methylene gathering, a few signs are currently seen, affirming the misshaped idea of the framework. The signs related with the carbon molecules in the 1.2-HOPO bunches are likewise definitely moved upon complexation. For instance, one sign was found at 195.4 ppm relating to a quaternary carbon particle that didn't show up in the range of the free ligand. The contrasts between the ¹H and ¹³C NMR of 19 and 22 with and without Ga(III) recommend that the two ligands give an alternate coordination mode. Since 22 is relied upon to give an O₆ coordination climate, we probably recommend that a N₃O₃ coordination mode exists for ligand 19 + Ga(III) and thusly likewise to 19 + Fe(III) however further work will be important to reach a firmer inference.

CONCLUSION

We report the union of a scope of hexadentatechelators dependent on triazamacrocycles, including the principal report of the utilization of a methylene as a linker between a 1.2-HOPO organizing gathering and the atomic framework. The ligands have an obvious biostatic impact upon the development of a scope of microorganisms. It is proposed that metal chelation is the fundamental method of activity of these chelators yet that a straightforward thermodynamic rivalry between the chelator and bacterial siderophore for Fe³⁺ is too basic an image. Further work is in progress to comprehend the method of activity of these chelators in detail and to orchestrate a more extensive scope of hexadentatechelators dependent on 1.2-HOPO to evaluate their viability as biostatic specialists. These mixes will likewise shape the reason for the investigation of the impact of the linker between the 1.2-HOPO moiety and the atomic spine on the thermodynamic adequacy of Fe³⁺ chelation through estimations of pKa and β110 values.

CONFLICT OF INTEREST

Conflict of interest declared none.

REFERENCE

1. Z.L. Wang, J. Song, Piezoelectric nanogenerators based on zinc oxide nanowire arrays, *Science* 312 (2006) 242–246.
2. D.C. Look, Recent advances in ZnO materials and devices, *Mater. Sci. Eng. B* 80 (2001) 383–387.
3. M. Kitano, M. Shiojiri, Benard convection in ZnO/resin lacquer coating – a new approach to electrostatic dissipative coating, *Powder Technol.* 93 (1997) 267–273.
4. I.O. Sosa, C. Noguez, R.G. Barrera, Optical properties of metal nanoparticles with arbitrary shapes, *J. Phys. Chem. B* 107 (2003) 6269–6275.
5. C.N. Proudfoot, *Handbook of Photographic Science and Engineering*, second ed., IS & T, 1997.
6. N. Kakuka, N. Goto, H. Ohkita, T. Mizushima, Silver bromide as a photocatalyst for hydrogen generation from CH₃OH/H₂O solution, *J. Phys. Chem. B* 103 (1999) 5917–5919.
7. Y. Zang, R. Farnood, J. Currie, Photocatalytic activities of AgBr/Y-zeolite in water under visible light irradiation, *Chem. Eng. Sci.* 64 (2009) 2881 – 2886.
8. O.E. Kartal, M. Erol, H. Oguz, **Photocatalytic destruction of phenol by TiO₂ powders**, *Chem. Eng. Technol.* 24 (2001) 645–649.
9. C. Galindo, P. Jacques, A. Kalt, Photooxidation of the phenylazonaphthol AO 20 on TiO₂: kinetic and mechanistic investigations, *Chemosphere* 45 (2001) 997–1005.
10. C. Chen, T.C. Chou, Kinetics of photodecolorization of methyl orange using titanium dioxide as catalyst, *Ind. Eng. Chem. Res.* 32 (1993) 1520–1527.
11. L. Wenhua, L. Hong, C. Suo'an, Z. Jianqing, C. Chunyan, Kinetics of photocatalytic degradation of aniline in water over TiO₂ supported on porous nickel, *J. Photochem. Photobiol. A* 131 (2000) 125–132.

12. Hassan MA, Yeom BY, Wilkie A, et al. Fabrication of nanofibermeltblown membranes and their filtration properties. *J MembSci* 2013; 427: 336–344.
13. Wang Y, Zheng M, Lu H, et al. Template synthesis of carbon nanofibers containing linear mesocage arrays. *Nanoscale Res Lett* 2010; 5(6): 913–916.
14. Zelenski CM and Dorhout PK. Template synthesis of near- monodisperse¹ microscalenanofibers and nanotubules of MoS₂. *J Am ChemSoc* 1998; 120(4): 734–742.
15. Rolandi M and Rolandi R. Self-assembled chitin nanofibers and applications. *Adv Colloid Interface Sci* 2014; 207: 216–222.
16. Liao HS, Lin J, Liu Y, et al. Self-assembly mechanisms of nanofibers from peptide amphiphiles in solution and on substrate surfaces. *Nanoscale* 2016; 8(31): 14814– 14820.
17. Katsogiannis KAG, Vladislavljević GT and Georgiadou, Porous electrospun polycaprolactone fibers: Effect of process parameters, *Polym. Phys.* 2016, 54, 1878–1888.
18. S. Porous electrospunpolycaprolactone (PCL) fibres by phase separation. *EurPolym J* 2015; 69: 284–295.
19. Zhang Z, Tu W, Peijs T, et al. Fabrication and properties of poly(tetrafluoroethylene) nanofibres via sea-island spinning. *Polymer (Guildf)* 2017; 109: 321–331.
20. Hammami MA, Krifa M and Harzallah O. Centrifugal force spinning of PA6 nanofibers—processability and morphology of solution-spun fibers. *J Text Inst* 2014; 105(6): 637–647.
21. Sarkar K, Gomez C, Zambrano S, et al. Electrospinning to forcespinning™. *Mater Today* 2010; 13(11): 12–14.
22. Yu L, Shao Z, Xu L, et al. High throughput preparation of aligned nanofibers using an improved bubble-electrospinning. *Polymers (Basel)* 2017; 9(12): 658.
23. Taylor G. Disintegration of water drops in an electric field. *Proc R Soc A Math PhysEngSci* 1964; 280: 383–397.
24. Shin YM, Hohman MM, Brenner MP, et al. Electrospinning: a whipping fluid jet generates submicron polymer fibers. *ApplPhysLett* 2001; 78: 1149–1151.
25. Yarin AL, Koombhongse S and Reneker DH. Bending instability in electrospinning of nanofibers. *J ApplPhys* 2001; 89(5): 3018–3026.

Solanum Torvum Unripe Fruit Extract Mediated Photosynthesized Nickel Oxide Nanoparticles

M.Deepa¹,V.Vijayakumar, S.Sathyakumar, G.vanaja

DhanalakshmiSrinivasan College Of Arts And Science For Women (Autonomous), Perambalur Tamilnadu-621212

Abstract: The nickel oxide nanoparticle has been synthesized by using unripe fruit extract of *Solanumtorvum*. The synthesized NiO nanoparticle have been characterized by various techniques and effectively utilized for *in vitro* antifungal activity. In recent years the fabrication of NPs using plants/fruits has fascinated researchers because of its simple, cost-effective, fast, and environmentally friendly protocol. The reduction of Ni²⁺ ions to NiO NPs by unripe fruit of *Solanumtorvum* extract was visually monitored by a color change in the mixture. The gradual color change in solution color from pale green to dark brown color was observed and this indicates that the phenolic compounds and phytochemicals present in unripe fruit extract act as a good reducing agent for the synthesis of NiO NPs. The synthesized NiO shown good *in vitro* antifungal activity.

Keyword: The reduction ,UV-Visible spectroscopy, FT-IR, SEM, *Solanumtorvum*, nickel oxide nanoparticles

INTRODUCTION

The field of Nanotechnology has blossomed over the last twenty years and the need for nanotechnology will only increase as miniaturization becomes more important in areas such as computing, sensors, and medical applications. Advances in this field largely depend on the ability to manufacture nanoparticles of various nanomaterials, based on their shapes and sizes as well as their efficiency to assemble them into diverse architectures. Results Preliminary phytochemical investigation revealed the presence of Saponins, glycosides, tannins, alkaloids, volatile oils and flavonoids.^{1,2} Nanotechnology provides the ability to engineer the properties of materials by controlling their size, and this has driven research toward a multitude of potential uses for Nanomaterial. The NiO nanoparticles showed inhibitory activity in both strains of bacteria with best selectivity against gram-positive bacteria². Synthesis and study of their size and properties of fundamental importance in the advancement of recent research, it is found that the optical, electronic, magnetic, and catalytic properties of metal nanoparticles also depend on their size, shape, and chemical surroundings. Magnetic nanostructures have been widely studied due to their potential applicability into several research fields such as data storage, sensing and biomedical applications. Focusing on the biomedical aspect, some new approaches deserve to be mentioned: cell manipulation and separation, contrast-enhancing agents for magnetic resonance imaging, and magnetomechanically induced cell death.³ Cytotoxicity suppression and cellular uptake enhancement of surface modified magnetic nanoparticles,⁴ Synthesis and characterization of magnetite nanoparticles via the chemical co-precipitation method was required.⁵ The science of nanometer-scale objects however was not discussed until much later. Interestingly, it would be, in principle, possible for a physicist to synthesize any chemical substance that the chemist writes down. Give the orders and the physicist synthesizes them. How? Put the atoms down where the chemist says, and so you make the substance. The problems of chemistry and biology can be greatly helped if our ability to see what we are doing and to do things on an atomic level, is ultimately developed—a development which I think cannot be avoided" Synthesis of nickel nanoparticles in water-in-oil microemulsions was absorbed, Hydrothermal synthesis and characterization of nanocrystalline Fe₂O₃ particles was prepared in this manner^{6,7} However, the world had to wait a long time to put down atoms at the requisite place. This talk would be credited as the genesis of the modern field of nanotechnology, the science of manipulating molecular- and atomic-level structures to engineer microscopic devices. The pure metals in nanoparticle form are useful in the field of diagnostics, antimicrobial agents, drug delivery, textiles (clothing), electronics, bio-sensing, food industry, paints, cosmetics, medical devices, and treatment of several acute and chronic diseases malaria, hepatitis, cancer, and AIDS. The properties of nanoparticles such as size, shape, composition, crystalline nature, and structure determine their applications. The nanoparticles (NPs) are metal atom clusters of ranging sizes (1-100 nm), highly promising due to their wide range of applications in commercial products. The metal nanoparticles are synthesized by various methods such as physical, chemical, and biological approaches. The organic synthesis of nanoparticles involves algae, actinomycetes, bacteria, fungi, and plants. Significance of Nickel Nanoparticles Electrospray of ionic precursor solutions to synthesize iron oxide nanoparticles: modified scaling law⁸ Nickel NPs find potential applications in various fields including electronics, magnetism, energy technology and biomedicines. Due to their high reactivity, operational simplicity, Laser ablation in liquids: applications in the synthesis of nanocrystals has noted in this progress.⁹ and eco-friendly properties they are used to catalyze various organic reactions Biosynthesis of gold nanoparticles of Ixoracoccinea flower extract & their antimicrobial activities¹⁰, Green and controlled synthesis of gold and platinum nanomaterials using vitamin B2: density-assisted self-assembly of nanospheres, wires, and rods are used production¹¹ Chemical synthesis of magnetic nanoparticles¹² Oxidation kinetics of nickel particles: comparison between free particles and particles in an oxide matrix are discussed about this progress.¹³ Bio-synthesis of NiO and Ni nanoparticles and their characterization is applied.¹⁴ including the chemoselective oxidative coupling of thiols¹⁵, reduction of aldehydes and ketones .nickel nanoparticles as efficient and recyclable catalysts for hydrogenation of olefins¹⁶ synthesis of stilbenes from alcohol through Wittig-type olefination¹⁷, and α -alkylation of methyl ketone¹⁸. They also catalyze certain inorganic reactions like the decomposition of ammonia¹⁹. One of their recent applications is their role in the fabrication of carbon nanotubes (CNTs)²⁰. Tannic acid assisted one-step synthesis route for stable colloidal dispersion of nickel nanostructures²¹. Synthesis of metallic nanoparticles using plant extracts,²² Plant-mediated synthesis of size-controllable Ni nanoparticles with alfalfa extract²³. Annonasquamosa leaf extract as an efficient reducing agent in the synthesis of

chromium and nickelization and antimicrobial study of nickel nanoparticles synthesized from *Dioscorea* (Elephant Yam) by green route,²⁴ they also find environmental applications in the field of adsorption of hazardous dye and inorganic pollutants and thus play a vital role in the cleanliness of the environment ²⁵. Due to their good antibacterial and anti-inflammatory activities, they are used in the field of biomedicine, Biochemical synthesis of nickel & cobalt oxide nano-particles by using biomass waste ²⁶. They also show cytotoxicity against cancerous cells as is evident from the distortion of the morphology of these cells after their treatment with Ni NPs. The biocompatibility of Ni NPs capped with biomolecules such as glucose is highly increased and these are used as biosensors and heat non mediators for cancer hyperthermia. Strategies for Nanoparticles Synthesis Principally there are 2 approaches used to synthesize NPs including the top-down approach and the bottom-up approach. The mechanism for Biosynthesis of Metal and Metal Oxide Nanoparticles The secondary metabolites of plants and microbial/fungal enzymes are responsible for the reduction of metal ions into metal atoms. The metal salts like nitrates, chlorides, oxides, and sulphates have high reduction potential due to the attachment of metal with the chloride, oxide, and sulphide parts and their tendency to donate electrons. As a result of both these factors electronic density on the conjugative salts of metal increases. So metals in their ionic form can easily get detached from their anionic part and get reduced into stable form by using plant/microbial/fungal extract. The secondary metabolites of the plant including alkaloids, flavonoids, polyphenols, and terpenoids act as a chelator to metal ions and reduce them into zero-valent states. Mostly the -OH group of polyphenols and flavonoids develop coordination with metal ions, while in the case of microbial mediated synthesis the reductase enzyme of bacterial or fungal cell wall donates electrons for reduction of metal ions. In the case of metal oxide NPs the end product is air-dried or calcined in air to get final metal oxide NPs. As the growth phase duration increases, aggregation of NPs occurs and nano hexahedrons, nanotubes, nanoprisms, and different kinds of irregularly shaped NPs are formed. Mallikarjuna and coworkers reported that the hydroxyl and carbonyl groups of amino acid residues or proteins can strongly adhere to metal NPs as a capping agent and prevent them from aggregation.

Biosynthesis of Nickel Nanoparticles

Very little literature is available on the biological synthesis of Ni and NiO NPs as compared to chemical synthesis. The physical and chemical methods of NPs fabrication are accompanied by some disadvantages like high cost, complexity (involving multiple steps), use of harmful organic chemicals, and environmental pollution. So there is a great need to develop alternative eco-friendly and low-cost fabrication methods for NPs. Nature has devised numerous processes for the fabrication of micro-and nanoscaled inorganic materials using naturally occurring biomolecules or microorganisms and plant extract as a reducing agent. Green synthesis of NPs is a type of bottom-up technique where the main reaction takes place is reduction/oxidation. There are 3 basic requirements for the biosynthesis of NPs including (i) choice of proper solvent, (ii) choice of an eco-friendly reducing agent, and (iii) choice of nontoxic stabilizing agent for NPs. Thus by choosing proper solvent, surfactant, and reductant biosynthesis produce NPs with controlled morphology without producing any toxic environmental pollutants. In the plant-mediated synthesis of Ni NPs commonly extract of different parts of plants is used as a reducing agent, while in some other cases rather than using the extract either the whole plant is grown on a metal substrate or an entire part of the plant is soaked in the metal solution. Here, *in situ* reductions of metal ions occurs and their morphology can also be controlled as porous parts of plants also act as biotemplate]. Some naturally occurring biomolecules such as glucose, sucrose, or plant secretions may also work as good reducing agents and stabilizing agents and thus are used to fabricate Ni NPs²⁰. In recent years the fabrication of NPs using plants has fascinated researchers because of its simple, cost-effective, fast, and environmentally friendly protocol. Biosynthesis is a single-step technique for the synthesis of NPs which provides stable NPs of different morphologies. The rate of production is rapid compared to the microorganisms-based biosynthesis of NPs. Infra-red spectroscopy showed that secondary metabolites including terpenoids, flavones, pyrones, aldehydes, amides, and carboxylic acids derived from plant extracts are responsible for the reduction of metal salts into their respective NPs. Only a few research articles are reported so far on the synthesis of Ni NPs using plants. Different parts of plants such as leaves and roots are used for synthesizing Ni NPs.

Chemicals

All materials were purchased from Nice and Loba chemicals. Solvents used throughout the reactions were of high purity and used without further purifications. Collection of plant materials. The unripe fruit of *Solanumtorvum* was collected from the local places of the perambalur area. Fresh unripe fruit was used for the synthesis of nickel oxide nanoparticles.

Preparation of plant extract

The nickel chloride and *Solanumtorvum* unripe fruit extract were used as the starting materials. The *Solanumtorvum* unripe fruit extract solution was prepared using unripe fruits that had been rinsed with deionized water and finely cut into small pieces. The unripe fruits are grained, boiled with 100 mL distilled water for about 10 mins, filtered, and stored. The resulting extract was used as a *Solanumtorvum* extract solution.

Synthesis of Nickel oxide nanoparticles

In the preparation of Nickel Oxide nanoparticles, compounds $\text{NiCl}_2 \cdot 2\text{H}_2\text{O}$ (1 g) was first dissolved in 10 ml of deionized water and mixed with 10 ml of flower extract solution under vigorous stirring at room temperature for 3hr²¹. Then 1mL of 10% NaOH was added as a reducing agent. The mixture was maintained at 100 ° for 12 hrs in the oven. The obtained powder was calcined at 350 ° for 4 hrs.

Characterization studies

Nickel oxide nanoparticles synthesized by this green method were characterized by, UV-Visible spectrophotometer (Shimadzu) and Fourier-transform infrared (FTIR- Shimadzu) spectrum in the range 4000-400 cm^{-1} , SEM (Scanning Electron Microscope), EDX (Energy Dispersive Diagram)²², XRD (X-ray Diffraction Spectrophotometer) and also the synthesized nickel oxide

nanoparticles were tested for in vitro antifungal activity against four different fungal strains. The minimal inhibitory concentration (MIC) was determined by the broth microdilution method according to the Clinical and Laboratory Standards Institute (CLSI) (The National Committee for Clinical Laboratory Standards). In vitro antifungal activity of the final compounds I- Ia was evaluated against standard strains; *Aspergillus Niger*, *Microsporum audouinii*, *Cryptococcus neoformans*, and *Candida albicans*. The antibacterial and antifungal assays were performed in Mueller–Hinton broth and Sabouraud dextrose broth, respectively. All the synthesized compounds were weighed (10 mg), dissolved in DMSO (250 μ L), and diluted with water (750 μ L) to prepare the stock solutions of 10 mg/mL. The serial dilution from 2048 to 1 μ g/mL was made in a 96-well plate. Fifty μ L of a bacterial suspension, obtained from a 24 h culture (\sim 106 cfu/mL) was added to each well with a final DMSO concentration of 1:16. The plates were incubated at 35 °C for 24 h. We tested ceftazidime as antimicrobial agents for quality control of the method. Each experiment was carried out in duplicate.

RESULT AND DISCUSSION

Optical Characterization

The reduction of Ni^{2+} ions to NiO NPs by unripe fruit of *Solanumtorvum* extract was visually monitored by a color change in the mixture. The gradual color change in solution color from pale green to dark brown color was observed and this indicates that the phenolic compounds and phytochemicals present in unripe fruit extract act as a good reducing agent for the synthesis of NiONPs²³⁻²⁴. Phytochemicals in plant parts play a significant role in the reduction of metal ions to metal NPs. Surface plasmon resonance (SPR) excitation in UV-vis analysis was used to characterize the metallic nature of the nanoparticles in colloidal dispersion. Figure 1 represented the UV-vis spectra of green synthesized NiO NPs using unripe fruit extract. A progressive strong broadening of SPR was observed in the visible region from 320 to 430 nm representing the formation of NiO NPs²³⁻²⁵. In this study, the maximum absorption peak that appeared at 329 nm indicates the formation of NiO NPs.

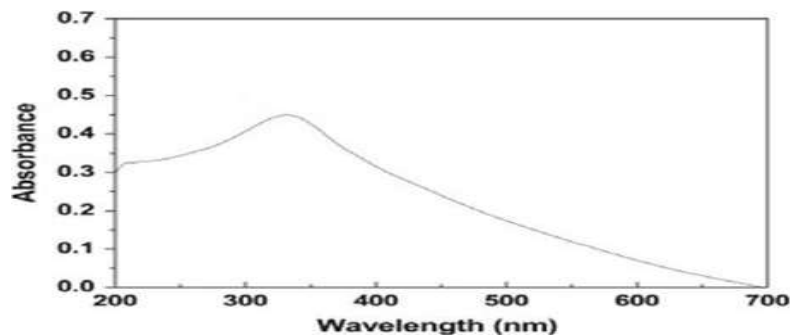


Figure 1.UV-Visible spectra of synthesized nickel oxide nanoparticles.

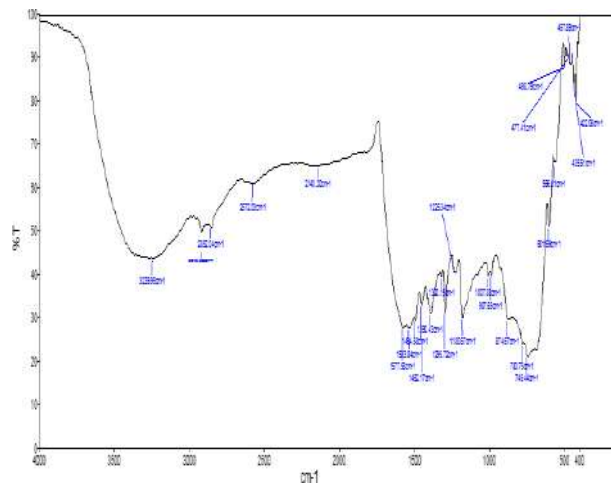


Figure 2. FT-IR analysis of NiO nanoparticle synthesized using unripe fruit extract of *Solanumtorvum*. represented FTIR spectrum recorded in the range of 400-4000 cm^{-1}

Compds	MIC ($\mu\text{g/mL}$)			
	<i>Aspergillus Niger</i>	<i>Candida albicans</i>	<i>Microsporum audouinii</i>	<i>Cryptococcus Neoformans</i>
I	45	25	64	16
2	56	01	02	26
ClotrimaLe	01	02	04	05

Broadband at 3239.95 cm^{-1} corresponds to the N-H group which may be appeared due to the presence of alkaloids. The peaks 2919.48 cm^{-1} and 2852.48 cm^{-1} represent the presence of the C-H functional group of alkanes. The bands 1583.84 cm^{-1} were attributed to (C=S) functional groups²⁵⁻²⁷. FTIR analysis confirmed the presence of functional groups for NiO and NiO NPs surface bioactive capping agents. The peaks (1452.17 cm^{-1}) showed the presence of imine moiety (C=N) which are the characteristic of proteins/enzymes present in the unripe fruit extract. The peak at 422.08 cm^{-1} confirms the presence of Ni-O vibrations.

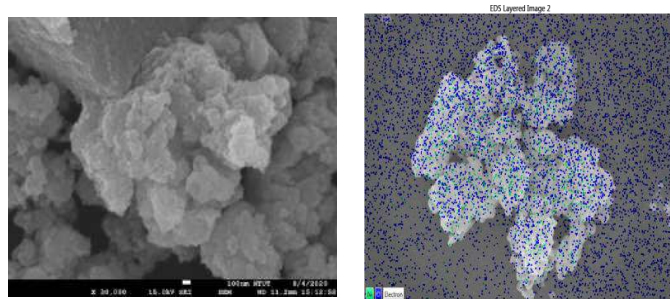


Figure3 SEM and Mapping studies NiO nanoparticle

The investigation Scanning Electron Microscopy (SEM) was performed to govern the size and morphology of the synthesized NiO NPs. SEM image shown in Figure 3 confirmed that the obtained NiO NPs were spherical shaped²⁷⁻²⁸. The synthesized NiO NPs were dispersed as distinct particles and monodispersity in nature. SEM mapping studies also conforms the synthesized nanoparticle was NiO. The green dots correspond to Nickel atoms and the blue dots represent Oxygen atoms. Figure 3 represents the SEM mapping studies of NiONps²⁹⁻³⁰.

CONCLUSION

In conclusion, the nickel oxide nanoparticle was synthesized using fresh unripe fruit extract of *Solanumtorvum*. The synthesized nanoparticles were characterized and confirmed using UV, FT- IR, and SEM analysis, the results showed that NiONps were synthesized properly. The in vitro antifungal activity depicts the effective antifungal activity of NiONps. This concludes that further studies on NiONps help for drug development.

CONFLICT OF INTEREST

Conflict of interest declared none.

REFERENCES

1. [Kannan Marikani](#) "antibacterial and antioxidant studies" *The Journal of Pharmacy* 20125:2418-2421 April 2012
2. [Dr.Kannan Marikani](#)" Phytochemical, antibacterial and antioxidant studies on medicinal plant Solanum torvum "*The Journal of Pharmacy* 20125:2418-2421 April 2012
3. J. M. DeSimone, "Practical approaches to green solvents," *Science*, vol. 297, no. 5582, pp. 799–803, 2002
4. H. Rui, R. Xing, Z. Xu, Y. Hou, S. Goo, and S. Sun, "Synthesis, functionalization, and biomedical applications of multifunctional magnetic nanoparticles," *Advanced Materials*, vol. 22, no. 25, pp. 2729–2742, 2010.
5. A. K. Gupta and M. Gupta, "Cytotoxicity suppression and cellular uptake enhancement of surface modified magnetic nanoparticles," *Biomaterials*, vol. 26, no. 13, pp. 1565–1573, 2005.
6. K. Petcharoen and A. Sirivat, "Synthesis and characterization of magnetite nanoparticles via the chemical co-precipitation method," *Materials Science and Engineering B: Solid-State Materials*
7. for Advanced Technology, vol. 177, no. 5, pp. 421–427, 2012.F. Jia, L. Zhang, X. Shang, and Y. Yang, "Non-aqueous sol-gel approach towards the controllable synthesis of nickel nanospheres, nanowires, and nanoflowers," *Advanced Materials*, vol. 20, no. 5, pp. 1050–1054, 2008.
8. D.-H. Chen and S.-H. Wu, "Synthesis of nickel nanoparticles in water-in-oil microemulsions," *Chemistry of Materials*, vol. 12, no. 5, pp. 1354–1360, 2000.
9. D. Chen and R. Xu, "Hydrothermal synthesis and characterization of nanocrystallineγ-Fe₂O₃ particles," *Journal of Solid State Chemistry*, vol. 137, no. 2, pp. 185–190, 1998.
10. S. Basak, D.-R. Chen, and P. Biswas, "Electrospray of ionic precursor solutions to synthesize iron oxide nanoparticles: modified scaling law," *Chemical Engineering Science*, vol. 62, no. 4, pp. 1263–1268, 2007.
11. G. W. Yang, "Laser ablation in liquids: applications in the synthesis of nanocrystals," *Progress in Materials Science*, vol. 52, no. 4, pp. 648–698, 2007.
12. B. Nagaraj, N. B. Krishnamurthy, P. Liny, T. K. Divya, and R. Dinesh, "Biosynthesis of gold nanoparticles of *Ixoracoccinea* flower extract & their antimicrobial activities," *International Journal of Pharma and Bio Sciences*, vol. 2,

no. 4, pp. 557–565, 2011.M. Kowshik, S. Ashtaputre, S. Kharrazi, et al., "Extracellular synthesis of silver nanoparticles by a silver-tolerant yeast strain MKY3," *Nanotechnology*, vol. 14, no. 1, pp. 95–100, 2003.

13. M. N. Nadagouda and R. S. Varma, "Green and controlled synthesis of gold and platinum nanomaterials using vitamin B2: density-assisted self-assembly of nanospheres, wires, and rods," *Green Chemistry*, vol. 8, no. 6, pp. 516–518, 2006.

14. T. Hyeon, "Chemical synthesis of magnetic nanoparticles," *Chemical Communications*, vol. 9, no. 8, pp. 927–934, 2003.

15. R. Karmhag, T. Tesfamichael, E. W'ackelgård, G. A. Niklasson, and M. Nygren, "Oxidation kinetics of nickel particles: comparison between free particles and particles in an oxide matrix," *Solar Energy*, vol. 68, no. 4, pp. 329–333, 2000.

16. A. A. Mariam, M. Kashif, S. Arokiyaraj, et al., "Bio-synthesis of NiO and Ni nanoparticles and their characterization," *Digest Journal of Nanomaterials and Biostructures*, vol. 9, no. 3, pp. 1007–1019, 2014.

17. A. Saxena, A. Kumar, and S. Mozumdar, "Ni-nanoparticles: an efficient green catalyst for chemo-selective oxidative coupling of thiols," *Journal of Molecular Catalysis A: Chemical*, vol. 269, no. 1-2, pp. 35–40, 2007.F. Alonso, P. Riente, and M. Yus, "Hydrogen-transfer reduction of carbonyl compounds promoted by nickel nanoparticles," *Tetrahedron*, vol. 64, no. 8, pp. 1847–1852, 2008.

18. A. Dhakshinamoorthy and K. Pitchumani, "Clay entrapped nickel nanoparticles as efficient and recyclable catalysts for hydrogenation of olefins," *Tetrahedron Letters*, vol. 49, no. 11, pp. 1818–1823, 2008.

19. F. Alonso, P. Riente, and M. Yus, "Wittig-type olefination of alcohols promoted by nickel nanoparticles: synthesis of polymethoxylated and polyhydroxylatedstilbenes," *European Journal of Organic Chemistry*, vol. 2009, no. 34, pp. 6034–6042, 2009.

20. F. Alonso, P. Riente, and M. Yus, "Alcohols for the α -alkylation of methyl ketones and indirect aza-Wittig reaction promoted by nickel nanoparticles," *European Journal of Organic Chemistry*, vol. 2008, no. 29, pp. 4908–4914, 2008.

21. X.-K. Li, W.-J. Ji, J. Zhao, S.-J. Wang, and C.-T. Au, "Ammonia decomposition over Ru and Ni catalysts supported on fumed SiO₂, MCM-41, and SBA-15," *Journal of Catalysis*, vol. 236, no. 2, pp. 181–189, 2005.

22. Y. Li, B. Zhang, X. Xie, J. Liu, Y. Xu, and W. Shen, "Novel Ni catalysts for methane decomposition to hydrogen and carbon nanofibers," *Journal of Catalysis*, vol. 238, no. 2, pp. 412–424, 2006.

23. A. Dutta and S. K. Dolui, "Tannic acid assisted one-step synthesis route for stable colloidal dispersion of nickel nanostructures," *Applied Surface Science*, vol. 257, no. 15, pp. 6889–6896, 2011.

24. A. K. Mittal, Y. Chisti, and U. C. Banerjee, "Synthesis of metallic nanoparticles using plant extracts," *Biotechnology Advances*, vol. 31, no. 2, pp. 346–356, 2013.

25. H. Chen, J. Wang, D. Huang, et al., "Plant-mediated synthesis of size- controllable Ni nanoparticles with alfalfa extract," *Materials Letters*, vol. 122, pp. 166–169, 2014.

26. S. A. Mamuru, A. S. Bello, and S. B. Hamman, "Annonasquamosa leaf extract as an efficient reducing agent in the synthesis of chromium and nickelization and antimicrobial study of nickel nanoparticles synthesized from *Dioscorea* (Elephant Yam) by green route," *International Journal of Science and Research*, vol. 4, no. 11, pp. 216–219, 2015.

27. F. T. Thema, E. Manikandan, A. Gurib-Fakim, and M. Maaza, "Single-phase BunseniteNiO nanoparticles green synthesis by *Agathosmabetulinanatural* extract," *Journal of Alloys and compounds*, vol. 657, pp. 655–661, 2016.

28. M. Ullah, A. Naz, T. Mahmood, M. Siddiq, and A. Bano, "Biochemical synthesis of nickel & cobalt oxide nanoparticles by using biomass waste," *International Journal of Enhanced Research in Science Technology & Engineering*, vol. 3, pp. 415–422, 2014.

Molecular Cloning Of Amylase Encoding Gene From *Bacillus Subtilis*

Dr.Surya.C, Dr.Sathyia.R, Nirmaladevi.P, Soniya.A

Dhanalakshmi Srinivasan College of Arts and Science for Women (Autonomous), Perambalur.

Abstract: The study aimed to amplify the amylase coding gene from *B. Subtilis* & Clone the gene in *E.Coli*. The amylase-producing microorganisms were isolated using starch agar media. Isolation of genomic DNA from the Characterized strain. Then the 5'-CCTACAACATTGTGC-3' and TAATCTCGAGTACGTATTTAAAAGTCACGTAC3' primers were used to amplify the DNA using the following cycle in PCR Method, The amplification reaction of 40 cycles was generated & bands with sizes ranging from 675 bps & up to 9742 bps. DNA fragment of 2000bps carrying the amylase gene was obtained & it was cloned in PUC 18 plasmid. *E.Coli* was used as a host to clone the gene. As a result, from the soil sample, the present study deals with the cloning and expression of amylase gene from *Bacillus subtilis* to *E.coli* was expressed to produce more amount of the industrial important amylase enzyme.

Keywords: *B.sutillis*, *E.Coli*, PCR, Genomic DNA, Amylase.

INTRODUCTION

Microorganisms have become increasingly important as a producer of industrial enzymes¹. Due to their biochemical diversity and the ease with which enzyme concentrations may be increased by environmental and genetic manipulation, attempts are now being made to replace enzymes, which traditionally have been isolated from complex eukaryotes²⁻³. Starch degrading amylolytic enzymes are most important in the biotechnology industries with huge applications in food, fermentation, textile, and paper⁴⁻⁵. Amylases can be obtained from several sources such as plants, animals, and microbes. These enzymes work either from the non-reducing end of the chain acting as exo-enzymes producing low molecular weight products (i.e., β -amylase, glucoamylase, and α -glucosidase) or in the interior of the chain and in a random fashion acting as endo enzymes and producing linear and branched saccharides with various lengths (i.e., α - amylase⁶). Amylases are important enzymes, particularly in the process involving starch hydrolysis⁷⁻⁸. Though they originate from different sources (plants, animals, and microorganisms), in industry, they are mainly produced from microbes, due to their higher yield and thermostability⁹⁻¹⁰. *Bacillus* spp. is considered to be the most important source of α -amylase and has been used for its production¹¹. *Bacillus* strains produce the enzyme in the exponential phase, whereas some others in the mid stationary phase. Though the pattern of growth and the enzyme profiles of *Bacillus* spp. have similarities, the optimized conditions¹²⁻¹³. Although purification of many amylases and cloning of their genes have been reported, amylases from *Pseudoalteromonasspecies* have not been purified to date, except for *Pseudoalteromonas haloplanktis*, a psychrophilic bacterium isolated from Antarctica (In this, study, we have isolated a marine bacterium producing extracellular α -amylase from seawater and have identified this strain as a member of *Pseudoalteromonas* species. Here, we report the cloning and expression of this α -amylase gene in *Escherichia coli* and characterization of the purified recombinant α -amylase.¹⁴⁻¹⁵ Cloning of genes has been done extensively for the molecular study of proteins, their hyperproduction, and protein engineering. Cloning of α -amylases has been done for studying their sequence, characteristics, hyperproduction, and expression and for enzyme engineering. α -Amylase genes from different fungal and bacterial sources have been cloned in appropriate host organisms using suitable vectors.¹⁶⁻¹⁷

MATERIALS AND METHOD

Collection Of Sample

The samples were collected from different locations. Soil received from the waste of the sago industry to isolate the amylase-producing microorganisms.

Isolation Of Microorganism From Sample

1g of soil sample was weighed and suspended in 10ml of sterile water and then diluted using the serial dilution method. A diluted sample was spread on the Starch agar plate containing 2% Soluble Starch, 0.3% Beef extract, 0.5% Peptone, and 1.5% Agar. Incubation was kept at 37 °C for 48 hrs.

Morphological Identification

Gram staining was preferred to know whether the isolated colony was Gram-positive or Gram-negative. Morphology was observed under a light microscope.

Gram Staining

A Clean glass slide was taken and a bacterial smear was made and heat-fixed. The Smear was then flooded with the crystal violet stain and kept for 1 minute and washed with the tap water by holding the slide parallel to the direction of the running water. The Slide was then flooded with Gram's iodine to fix the primary stain and kept for 1 minute and washed with tap water. The smear was flooded with alcohol, the decolorizing agent for 30 seconds, and washed with tap water and Counter Stain

safranin was added, the slide was left undisturbed for 1 minute. This was then washed in tap water and allowed to air dry. The Stained smear was taken then viewed under an oil immersion microscope.

Biochemical Test Indole Production From Tryptophan

Prepare tryptone broth and inoculate it with bacterial culture. Incubate the culture at 37°C for 48 hours. Add 0.5ml of the Kovac's reagent after the bacteria growth. After 2 minutes a red color band appears at the junction of medium and reagent as in the case of *E.Coli* on the other hand, indole is diffused above the medium, and the paper strip turned pink if the strip is already impregnated with oxalic acid.

Methyl Red (Mr) Test

Methyl redVoges Pruskauer broth is prepared and sterilized at 121°C for 15 mins. The tubes are inoculated with test cultures and incubated at 37 °C for 48 hrs. After incubation, 5-6 drops of methyl red indicator are added and thoroughly mixed. This methyl red is an acid-base indicator. It is used only below pH 4.2.

Isolation Of Genomic Dna

About 2 ml of sample was taken and centrifuged at 10,000 rpm for 10 minutes. To this 1 ml of lysis buffer was added and incubated at room temperature for 5 min. The Eppendorf tubes were centrifuged at 10,000 rpm for 10 mins to lyse the cells. About 750 μ l of supernatant was collected and add phenol: chloroform: Isoamyl alcohol in the ratio of 500: 480: 20 μ l and incubated in ice for 5 mins. The Eppendorf tubes were centrifuged at 10, 000 rpm for 10 mins. The aqueous layer was collected in a separate Eppendorf tube and an equal volume of ice-cold ethanol was added and then incubate in ice for 5 mins. The supernatant was discarded and the pellet (DNA) was dissolved in 50 μ l TE buffer.

Polymerase Chain Reaction

The solutions were gently vortexed and briefly centrifuged after thawing. All the contents were added in a thin-walled PCR tube.

S. No	Reagent Mixture	Quantity for 15 μ l reaction
1.	Template DNA	4 μ l
2.	Tag DNA polymerase	1.5 μ l
3.	dNTPs mix	1.5 μ l
4.	Forward primer	3 μ l
5.	Reverse primer	3 μ l
6.	10x Assay buffer	1 μ l
7.	Nuclease free water	1 μ l

The total volume was made up to 25 μ l using sterile nuclease-free water. The sample was vortexed and centrifuged to collect all drops from the walls of the tube. The sample was placed in a thermocycler and started the PCR. The steps were repeated for 40 cycles and the final extension lasted for 4 mins. The amplified expected PCR product was checked by 1.5%. Agar uses gel electrophoresis with a 1kb ladder.

Determination Of Molecular Weight Of Amplified Fragments

The image of the gel was transferred to appropriate software in defined formation.

The molecular weight differentiation between the simplified bands was analyzed using non – linear dynamics software.

The dendograms were constructed by the UPGMA method according to the dice co-efficient method.

RESULTS

Collection Of Samples

The samples were collected from urban areas receiving sago factory waste.

Isolation Of Amylolytic Bacteria

The collected samples were serially diluted for the reduction of bacterial cells and the least dilution of 0.1ml was pipette out and spread over the starch enrichment agar media. Fine growth was observed and a few colonies were produced zones. This confirms that the zones forming isolates were amylase-producing microorganisms. Figure-2.



Figure.1 – Screening of amylase producing microorganism

Identification Of Bacteria

The selected colonies from the enrichment media were identified by morphological and biochemical characterization by standard procedure. The results of biochemical characteristics were given (Table: I and Figure:3) and the bacteria was identified as *Bacillus subtilis*.

Morphological and biochemical characterization of microorganism

Tests	Organism I
Gram Staining	+ ve Rod
Indole test	-
MR test	+

Isolation Of Genomic Dna

Genomic DNA was isolated by the buffer lysis method. The presence of DNA was confirmed by Agarose gel electrophoresis. Orange-colored bands were observed under a UV transilluminator and confirms the presence of DNA.

Amplification Of Dna

Amplification were performed in 15 reaction mixture consisting of forward and reverse primer 5'-AAGAATTCTGGCACCTACAACATTGTGC-3' and 5'TAATCTGAGTACGTATTAAAAGTCACGTAC-3'). The amplified products were resolved by electrophoresis in 1% agarose gel. The gel was visualized under a UV transilluminator and the banding patterns were photographed over the UV transilluminator and shown in (Figure-4). The amplification reaction of 40 cycles was generated and bands with sizes ranging from 675bps and up to 9742 bps. The PCR product was purified by modified electroelution²⁰

Production And Purification Of Recombinant Amylase

The recombinant strain was inoculated in a production broth and incubated at 37°C for 24 hrs. The amount of enzyme produced was determined by quantitative estimation. The media was centrifuged and the enzyme present in the supernatant was collected in a fresh tube. It was, further purified by the ammonium sulfate salt precipitation method and it was characterized by SDS-PAGE (Figure-6).

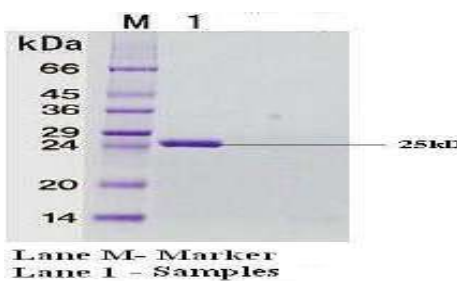


Figure. 6 – SDS – PAGE for characterization of amylase enzyme

Although nucleotide sequences of the amylase gene from *Pseudomonas haloplanktis*(AA0762321), *Pseudomonas Atlantica* T6c(YP_662421), and *Pseudomonas Tunicata* D2(ZP_01134110) were deposited in the GenBank database except for amylase from *Pseudomonas haloplanktis*(Feller G and Gerday C,2003). It is known that because of the complex gene regulatory and secretion mechanisms, overproduction of extracellular enzymes as active enzymes in heterologous hosts like *Escherichia coli* is difficult (Baneyx F, 1999).

DISCUSSION

The starch degrading microorganisms were isolated from the soil sample collected from the areas receiving sago factory waste¹⁸.

The organism was identified by morphological and biochemical characterization. The pure culture of isolation was made in nutrient agar and the genomic DNA was isolated from the starch degrader¹⁹. The isolated genetic material was confirmed by agarose gel electrophoresis. The specific gene code for the enzyme was amplified using specific primers and their amplifications were confirmed by the agarose gel electrophoresis. The 2000bps molecular weight fragment was eluted from the gel and the fragment was inserted into the toPUC18 plasmid²⁰. The plasmid was ligated with amylase enzyme and the recombinant plasmid was transformed to Escherichia Coli strains expression of the cloned gene was screened using starch enrichment agar diffusion method by degradation of turbid starch emulsion. The recombinant protein was characterized with SDSPAGE.

CONCLUSION

The microbial amylase enzyme has received much attention because of its potential use in a variety of biotechnological applications. So, in conclusion, the present study deals with the cloning and expression of the amylase gene from *Bacillus subtilis* to *Escherichia coli* was successfully expressed to produce more amount of industrially important enzymes.

CONFLICT OF INTEREST

Conflict of interest declared none.

REFERENCES

1. Abe J, Bergman FW, Obeta K, Hizukuri S (1988). Production of the raw starch degrading amylase of *Aspergillus* sp K-27. *Appl. Microbiol.Biotechnol.* 27: 447-450.
2. Adebiyi CAB, Akinyanju JA (1998). Thermophilic amylase producers from the soil. *Nigerian J. Sci. Technol.* 11 (1) 30-38.
3. Aiba S, Kitai K, Imanaka T (1983). Cloning and Expression of Thermostable α -Amylase Gene from *Bacillus stearothermophilus* in *Bacillus stearothermophilus* and *Bacillus subtilis*. *Appl. Environ. Microbiol.* 46: 1059-1065.
4. Akpan I, Bankole MO, Adesemowo AM., (1999a). A rapid plate culture method for screening of amylase-producing microorganisms. *Biotechnol. Tech.* 13: 411-413.
5. Antelmann, H., Darmon, E., Noone, D., Veening, J.W., Westers, H., Bron, S., Kuipers, O.P., Devine, K.M., Hecker, M., van Dijken, J.M., 2003. The extracellular proteome of *Bacillus subtilis* under secretion stress conditions. *Mol. Microbiol.* 49, 143-156.
6. Anthony OE, Yusuf C, Murray M (1996). Culture of *Saccharomyces cerevisiae* on hydrolyzed waste cassava starch for the production of baking quality yeast. *Enzyme Microbial Technol.* 18(7): 519 – 525.
7. Antranikian, G., 1990. Physiology and enzymology of thermophilic anaerobic bacteria degrading starch. *FEMS Microbial.Rev.* 75:201-218.
8. Asgher, M., M.J. Asad, S.U. Rahman, R.L. Legge, 2007. A thermostable α -amylase from a moderately thermophilic *Bacillus subtilis* strain for starch processing. *J. Food Eng.*, 79: 950-955.
9. B.H. Lee: Other Microorganism Based Products. In: *Fundamentals of Food Biotechnology*, Wiley-VCH Inc., New York, USA (1996) pp. 291-352.
10. B.K. Gogoi, R.L. Bezbarua, K.R. Pillai, J.N. Baruah, Production, purification and characterization of an α -amylase produced by *Saccharomyces cerevisiae*, *J. Appl. Bacteriol.* 63 (1987) 373-379.
11. B.K. Lonsane, N.P. Ghildyal, S. Budiatman, S.V. Ramakrishna, Engineering aspects of solid-state fermentation, *Enzyme Microb. Technol.* 7 (1985) 258-265.
12. B.S. Chadha, S. Singh, G. Vohra, H.S. Saini, Shake culture studies for the production of amylases by *Thermomyces lanuginosus*, *Acta Microbiol. Immunol. Hung.* 44 (1997) 181-185.
13. B.W. Matthews, H. Nicholson, W.J. Bechtel, Enhanced protein thermostability from site-directed mutations that decrease the entropy of unfolding, *Proc. Natl. Acad. Sci. The USA*, 84 (1987) 6663-6667.
14. Baum J.S. and W. John-Hill. 1995. Polysaccharides. In: Introduction to Organic and biological chemistry. MacMillan Publishing Company. New York.
15. Beck, E. and Ziegler, P. (1989) Biosynthesis and degradation of starch in higher plants In *Ann.Rev.Plant Phys. and Mol.Biol.* 40, 95-117.
16. Beers,E.P.,Duke,S.H. and Henson,C.A.(1990) Partial characterization and subcellular location of three α -glucosidase isoforms in pea (*Pisum sativum* L.) Seedlings. *Plant Physiol.*94,738-744.
17. Belisario,M.A.,Buonocore,V.,Cantarella,M.,Scardi,V. and Silano,V.(1981)Qual. Plant. Plant Foods Hum.Nutr.31, 21-30.
18. Ben A M,Khemakhem B,Robert X,Haser R and Bejar S (2006)*Biochem J* 394,51-56.
19. Bessler, J. Schmitt, K. Maurer, D.R. Schmid, Directed evolution of a bacterial amylase: Toward enhanced pH-performance and higher specific activity, *Protein Sci.* 12(2003) 2141-2149.
20. Bhabla T C and Chtanta D K (2000) in *Food Processing Biotechnological Applications* (Marwiche S .S and Horra J K, Ed), pp 123-132, Assisted Publishers, New York.
21. Bibb, M. J., Chater, K. F. & Hopwood, D. A. (1983). Developments in *Streptomyces* cloning. In *Experimental Manipulation of Gene Expression*. pp. 54-80. Edited by M. Inouye. London: Academic Press.
22. Bilinski CA, Stewart GG (1990). Yeasts protease and Brewing. In: *Yeast Biotechnology and Biocatalyst* ed. Verachtert, H and Mot, New York: Marcel Dekker.R. pp 147 – 162.

Effect of Bacterial Feed on Protein Profile of *Bombyx Mori*

Sangavai C, Dr.P.Viswanathan, Haseena M, KaleeswariSudha M.

DhanalakshmiSrinivasan College of Arts and Science for Women (Autonomous), Perambalur-621212.

Abstract: Naturally-colored silk has natural luster, a soft texture, and avoids the use of chemical dyeing. It has become one of the most important aspects of sericulture development and offers considerable market and developmental potential. Mulberry leaves are the main food source for silkworms, which means that they are also the main source of the pigments that determine cocoon color. The study examined the role of carotenoid-like binding protein (CBP) in hemelymph pigmentation on *B.mori*. *Bombyxmori* (*B. mori*) larvae to induced to feed the pigment coated leave and effect of feed compared with untreated control. Initially pigment producing *Serratiamarcescens* was isolated from rhizosphere soil and characterized. Optimum pigment production was noted on lactose and starch. No variation or influence of nitrogen sources found. The results showed that there were generally pigmented silk gland and was found in the blood of silkworm tested. The method used to detect visible pigments reported here could be used to breed new colors of cocoons and to develop and utilize the pigments found in mulberry. The results suggest that the extracted pigment that selectively absorbed by heme lymph proteins and influence the protein profile. further studies on silk gland is much needed for dying of silk with natural pigment.

Keywords: Mulberry leaves, silkworms, cocoons, Hemelymph proteins

INTRODUCTION

Textiles and their end products constitute the world's second largest industry, only ranking below food products. Textile production involves several wet processes that include scouring, bleaching, dyeing, and finishing of textile fibers. Because the largest use of textiles is in the retail apparel market, most textile fibers (both natural and synthetic) undergo a dyeing process to obtain colored fabric. Dyeing is the application of color, mostly with aqueous solutions of synthetic organic dyes, to fiber, yarn, or fabric. Despite a century of process improvements, dyeing remains one of the most polluting chemical processes because it produces large volumes of toxic wastewater as a byproduct. Hence, new "green" dyeing methods have to be developed to solve this enormous problem. Among natural fabrics, silk has been used as a textile fabric for thousands of years. Silk is a fine, smooth, lustrous fiber produced by a variety of insects, moths, and worms. Silk fiber consists of two proteins: sericin and fibroin. Sericin forms the outer protective coat, while fibroin is the main structural protein. Sericin is hydrophilic in nature and can be easily removed by boiling the silk in alkaline solution. This process is called degumming. The fibroin protein gives the silk its characteristic luster and feel. The fibroin molecule is amphiphilic in nature; it consists of alternating hydrophilic and hydrophobic domains. Silk used in textile applications is produced in variety of qualities, which include raw silk or undegummed silk (sericin and fibroin) and either partially or fully degummed silk (only fibroin). Treating mulberry leaves with specific dyes with known concentration and feeding silkworm larvae has been reported for obtaining naturally colored silk¹. Color is one of the qualitative parameter for silk filament. Giving the color to silk after reeling the cocoons is exclusively mechanical. It is creating environmental troublesome situations. Artificial silk coloring is affecting the natural and original quality of water. Toxic materials are released in the natural water bodies through the process of coloring the silk filament. Moreover, use of water in large quantity for the purpose to give color to silk is not affordable for existing environmental situations. The literature on technology of coloring the silk and recommended some eco-friendly alternatives. Artificial coloring the silk, unique parameter is labeling the sericulture industry as most polluting industry. It requires establishing environmentally protected silk coloring technology. Silk is a fine continuous protein fiber produced by spiders or insect larvae. Spiders spin threads of silk to make cocoons for their eggs and webs to catch prey, and such silks have been admired for their extraordinary mechanical properties since ancient times. A key factor that makes silk fabrics popular in China and throughout the world is their lustrousness, which is due to their special mesoscopic structure and reflective properties. Silk fabrics hold color well, and the Chinese characters (deep red), (red), and (green), which incorporate the character (silk), refer to the colors of silk.

MATERIALS AND METHOD

Isolation of Strain

Microorganism from onion root surface adhered soil (rhizoplane) was collected and serially diluted. 10^7 was plated on modified nutrient agar plate and medium composition was comprised off the following: Yeast extract 3.0 g; peptone NaCl 5 g; 10.0 g; Glucose 4.0 g; Agar 20.0 g; Distilled water 1.0 L; pH 7.2–7.4. After incubation colony morphology were recorded and screened for inulinase production

Biochemical Identification of Clinical Isolates

Isolated colonies were subjected to microscopy (Gram's staining) and biochemical test such as Indole Test, Methyl Red Test, VogusProskauer Test, Citrate Utilization Test, Catalasetest, Oxidase test for further identification of the pathogens.

Effect of substrate on pigment production

Five g of substrate barley was taken in 50 mL flask and mixed with a known quantity of distilled water to adjust the moisture at 56% (pH 6.5). The flak were enriched with 10 ML OF 1% of peptone, yeast extract, NB, ammonium sulphate then autoclaved at 121°C for 15 min, cooled, inoculated with 1 mL of culture of bacterium and incubated at 37°C for 48h. pigment were extracted

from 1 g of sample with 25 ml methanol and centrifuge at 10,000 rpm. OD values were recorded and yield was calculated $OD \times (dilution\ factor) \times (total\ volume\ of\ pigment) / Weight\ of\ substrate$.

Purification and characterization of pigment

Extracted pigment purified with silica column with methanol solvent and detected by TLC using acetone and methanol as mobile phase. The nature of pigment such as presence of protein backbone and amino acid were detected by ninhydrin test.

Feed efficiency

Two group of 3rd instar *B. mori* with known average weight (9.2 g) was fed with mulberry leaves freshly. feed 3 times approximately 0.8g per day. Test leaves coated with pigment 1 mL per day and Control treated with fresh leaf at same quantity. Treatment carried out for 14 days and end of 14th day hemlymph was collected and total protein was measured. The characteristics of protein changes was analysed by SDS PAGE and compared with control and marker.

RESULTS AND DISCUSSION

Isolation of pigment producing bacteria

Bacterial colonies on Agar plates showed 28×10^7 CFU (colony forming unit)/g of soil. Mostly (26 colonies) of the colonies were formed after 24 h and two were developed after 48 h. based on colony morphology (table 1) colonies were designated as onion Root soil bacteria 1-5 (OS1-5). The organism selected under study was Pinkish orange pigmented bacterium which is gram negative, rod, KOH positive, catalyst positive, oxidase negative identified as *Serratiamarcescens*. The pigment from isolate grown on selected 4carbon and two nitrogen was extracted by solvent extraction. The coloured crude supernatant was collected (plate 2) and the process was repeated until the pellet turned white and purified with column. The yield of pigment on extracellularly was given in table 2. Lactose in combination with peptone (80U) and yeast (78U) gave maximum pigment yield followed by starch (60 and 58 U). Other carbon sources found to be ineffective. The data indicates carbon plays critical role on pigment production. The crude pigment extract reveals presence of protein and amino acid (plate 3). TLC analysis of pure pigments reveals presence of one fraction found to be aminoacid Histidine based on its *Rf* value 0.12 (plate 3b). Peptone was used as nitrogen source when used with glycerol and gave the highest production of prodigiosin which was similarly observed with ² other inorganic nitrogen sources didn't support prodigiosin production and that was in accordance with ³ where sodium nitrate, ammonium sulfate, and potassium nitrate medium didn't support production of prodigiosin.

Table 1. Biochemical characteristic of bacterial isolate

TEST	RESULT
Grams stain	- rod
Oxidase	Negative
Catalase	Positive
Ninhydrin test	Positive
CuSo ₄ test	Positive



Plate 1. Isolation Of pigment Producing Bacteria

Table 2 Fermentation and pigment quantification

S.No	Sample	Units Of Yield
1.	Glucose +peptone	12
2.	Glucose +yeast	08
3.	Lactose +peptone	80
4.	Lactose +yeast extract	78
5.	Sucrose +peptone	18
6.	Sucrose +yeast extract	22
7.	Starch +peptone	60
8.	Starch + yeast extract	58



Plate 2 Effect of Carbon and Nitrogen on Pigment Production



Plate 3. Detection of amino acid and protein on pigment



Effect of pigment on *B. mori*

Treatment of *B. Mori* with 10 number of 3rd instar larvae was taken for feed efficiency test(plate 4). The feed efficiency of encapsulated feed tested for 15 days by feeding 0.8g of feed 3 time per day. Control fed with fresh leaves at same condition. Weight of *B. Mori* taken at the end of experiment and found to gained 5% greater than control. The test have average mean weight 16.8 increased from 9.2g. Similarly control gained 12.8 g . The protein profile of hemelymph of control and test wasstudied and it was found entrapment of pigment on heme lymph (plate 5) where as control its clear. The concentration of protein on treated is 6.4mg/mL and 3.4mg/mL in control(fig 1). The protein profile shows variation in bands on test have7 bands comparative with molecular weight of 20, 15,12,10,8,5,2 Da. In control only5different bands were observed with known molecular weight of 20, 15, 12, 10, 8 (plate 6)

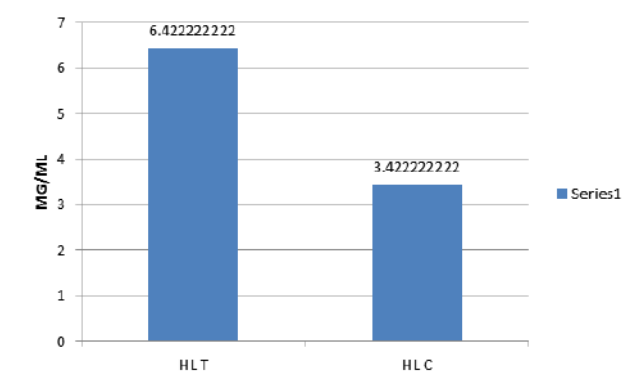


Figure 1. Concentration Of Total Protein



Plate 4. Pigmented feed mulberry leaf and feed on *B.mori*



Plate 5.Haemolymph of control and test

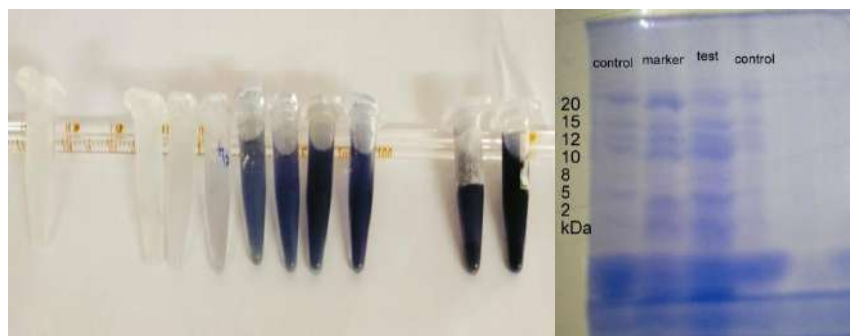


Plate 6.Total protein and SDS PAGE

Silver nanoparticles (Ag-NPs) are known as a noble metal, and owing to their exclusive properties, their use is widespread in consumer products and they are mostly incorporated into food packaging and food contact products⁴. Silkworms, *Bombyxmori*, are a promising model animal in health safety and environmental pollution⁵. *Bombyxbatryticatus* is a well-known animal in traditional Chinese medicine⁶. Silkworm pupae is the main by-product of the sericulture industry with an interesting nutritional profile, especially in terms of proteins⁷. Silkworm *Bombyxmori*, pigment mutants with diverse body colors have been maintained throughout domestication for about 5000 years⁸. The thermoprotective mechanisms of insects remain largely unknown⁹. There exists an increasing need to produce useful proteins in recombinant technologies¹⁰. *Bombyxmori* nuclear polyhedrosis virus (BmNPV) is the most damaging virus for the production of silkworm cocoons¹¹. The storage proteins are haemolymph-specific proteins in insects, mainly synthesized in the fat body, released into the haemolymph, and then selectively reabsorbed by the fat body before pupation¹². The d-3-phosphoglycerate dehydrogenase (PHGDH) is a key enzyme involved in the synthesis of L-serine¹³. The L-Deoxyojirimycin (DNJ) is the most abundant poly-hydroxylated alkaloid in the latex of mulberry leaves and it protects mulberry from insect predation¹⁴. The silkworm infection model has the potential to replace conventional animal models for evaluation of the efficacy and toxicity of investigational antifungal agents¹⁵. The organophosphate pesticides are widely applied worldwide for agricultural purposes, and their exposures often result in adverse effects on *Bombyxmori*¹⁶. The silkworms are economically important insects because of the value of their silk¹⁷. The olfaction plays an essential role in feeding and information exchange in insects¹⁸. The insect midgut secretes a semi-permeable, acellular peritrophic membrane (PM) that maintains intestinal structure, promotes digestion, and protects the midgut from food particles and pathogenic microorganisms¹⁹. The juvenile hormone (JH) plays important roles in the control of many biological processes in insects, such as development, reproduction, and polyphenism²⁰. On this study used the larval tissues and colored cocoons of silkworms, *Bombyxmori* L. (Lepidoptera: Bombycidae), that were fed leaves of cultivated mulberry, Husang 32, as experimental material²¹. An entomopathogenic bacterial strain SCQ1 was isolated from silkworm (*Bombyxmori*) and identified as *Serratiamarcescens* via 16S rRNA gene analysis²².

CONFLICT OF INTEREST

Conflict of interest declared none.

Conflict of interest declared none.

REFERENCE

1. Nisal A, Trivedy K, Mohammad H, Panneri S, Sen Gupta S, Lele A, Manchala R, Kumar N S, Gadgil M, Khandelwal H, et al,(2014). Uptake of Azo Dyes into Silk Glands for Production of Colored Silk Cocoons Using a Green Feeding Approach *ACS Sustainable ChemEng* 2, 312–317.
2. Gulani C, Bhattacharya S, Das A,(2012). Assessment of process parameters influencing the enhanced production of prodigiosin from *Serratiamarcescens* and evaluation of its antimicrobial, antioxidant and dyeing potentials. *Malays J Microbiol.* 8(2):116–122
3. Sumathi C, MohanaPriya D, Swarnalatha S, Dinesh M G, Sekaran G,(2014), Production of prodigiosin using tannery fleshing and evaluating its pharmacological effects *Sci World J* 8
4. Abdelli N, Peng L , Liang C , Yan P, Yanhua Y, Keping C(2018). Silver effects on silkworm, *Bombyxmori*.*toxicologicalscience*43(12):697-709.
5. NouaraA ,Lü P , Chen K (2018).*SilkworBombyxmori* as an alternative model organism in *toxicological* research 25(35):35048-35054.
6. Dongxu X , Guanwang S , Qingrong L , Yang X , Qiong Y , Qingyou X(2019) . Quality Formation Mechanism of Stiff Silkworm, *Bombyxbatryticatus* Using UPLC-Q-TOF-MS-BasedMetabolomicsMolecular.24(20):3780.
7. Cristina L , Francesco G , Simona C , Marzia G , Micol P , Marcello M , Emilio M , Benedetto S , Alessio S , Silvia C , Maria G , Laura C (2019).Investigation of the protein profile of silkworm (*Bombyxmori*) pupae reared on a well-calibrated artificial diet compared to mulberry leaf *diet**Peer J* 7:6723.
8. Hongyi N , Chun L , Tingcai C , Qiongyan L , Yuqian W , Mengting Z , Yinxia Z ,(2014). *Qingyou Xia* ITranscriptome analysis of integument differentially expressed genes in the pigment mutant (quail) during molting of silkworm, *Bombyxmori**PLoS One* 9(4)
9. Hongyi N , Tingcai C , Xiaofeng H , Mengting Z , Yinxia Z , Fangyin D , Kazuei M , Qingyou X , Chun L (2015).Functional Loss of Bmsei Causes Thermosensitive Epilepsy in Contractile Mutant Silkworm, *Bombyxmori**Sci* 5:12308
10. Masahiro T ,Yakugaku Z (2018). [Development of Large Scale Silkworm-rearing Technologies for the GMP Production of Biologics]*138*(7):875-884.
11. Yuan Z , Dinggue , Qiaoling Z , Guozheng Z , Yeshun Z , Zhiyong Q, Dongxu S , Cheng L(2019).Label-free proteomic analysis of silkworm midgut infected by *Bombyxmori* nuclear polyhedrosis virus*Proteomics* 200:40-50.
12. Ruilin L , Congwu H , Tao G , Dingding L , Kun G , Xijie G , Chengxiang H(2020). Expressional analysis of the silkworm storage protein and identification of its interacting proteins*InsectMolBiol* 29(1):66-76
13. Kohji Y,Shinya M, Shigeki FD-3-phosphoglycerate dehydrogenase from the silkworm *Bombyxmori*(2021). Identification, functional characterization, and expression*ArchInsect Biochem Physiol.* 106(1):21751
14. Hongxia C , Yueqin L , Wenbing W , Opeyemi J O, Gang P , Zhen O (2018).Proteomic-Based Approach to the Proteins Involved in 1-Deoxynojirimycin Accumulation in Silkworm *Bombyxmori* (Lepidoptera: Bombycidae) *J insert science* 18(2):42.
15. Masaki I , Yasuhiko M, Ikuiko N , Kazuhisa S(2017). Silkworm fungal infection model for identification of virulence genes in pathogenic fungus and screening of novel antifungal drugs*DrugDiscovTher* 11(1):1-5.
16. Fanchi L , Mengxue L , Tingting M , Hui W , Jian C , Zhengting L , Jianwei Q , Yilong F, Zhiya G , Bing L (2020).Effects of phoxim exposure on gut microbial composition in the silkworm, *Bombyxmori**Ecotoxicol Environ Saf.* 189:110011.
17. Hongling L , Ying L , Guanwang S , Jianjian G , Yang R , Jinxin W , Yujing Z , Kairong L , Wei L , Linbang J , Qingyou X (2019).silkworm *Bombyxmori**Insect BiochemMol Biol.* 107:10-18.
18. ShanghongX ,Wenjun Z (2020).Construction and analysis of the protein-protein interaction network for the olfactory system of the silkworm *Bombyxmori**Arch Insect Biochem Physiol*105(3):21737.
19. Xu X Z, Zhang Y, Yang S, Huang K, Li L, He X, (2018). Genome editing reveals the function of Yorkie during the embryonic and early larval development in silkworm, *Bombyxmori**Insect MolBiol*27(6):675-685.
20. Yuri H , Kouhei T , Takaaki D , Tetsuro S , Toru T (2020).A mitochondrial phosphatase PTPMT1 is essential for the early development of silkworm, *Bombyxmori**BiochemBiophys ResCommun*530(4):713-718.
21. Lin Zhu and Yu-Qing Zhang (2014)Identification and Analysis of the Pigment Composition and Sources in the Colored Cocoon of the Silkworm, *Bombyx mori* , by HPLC-DAD.*Journal of Insect Science* 14(31):31
22. Wei Z (2010). Apoptosis of human lung adenocarcinoma A549 cells induced by prodigiosin analogue obtained from an entomopathogenic bacterium *Serratiamarcescens**ApplMicrobiolBiotechnol* 88(6):1269-75

Green Synthesis of Silver Nanoparticles from *Sanseviaeria* Extract

Dr .Surya .C¹ , Sathish.S¹ DrJijimon K Thomas², Nirmaladevi.P¹ ,Dr.Sathya.R¹, Bharathi¹

¹Dhanalakshmi Srinivasan College of Arts and Science for Women (Autonomous), Perambalur.

²Mar IvaniosCollege ,Thiruvananthapuram,Kerala

Abstract: Recent advances in nanoscience and nanotechnology radically changed the way we diagnose, treat, and prevent various diseases in all aspects of human life. Silver nanoparticles (AgNPs) are one of the most vital and fascinating nanomaterials among several metallic nanoparticles that are involved in biomedical applications. AgNPs play an important role in nanoscience and nanotechnology, particularly in nanomedicine. Although several noble metals have been used for various purposes, AgNPs have been focused on potential applications in cancer diagnosis and therapy. The current study concerned with the synthesis of silver nanoparticles from leaf extract of *Sansevieriatrifasciata*. Thus it is important to characterize different types of medicinal plants for their antioxidant and antimicrobial potential.

Keyword: Nanoparticle, *Sansevieriatrifasciata*, AgNP, Cancer, Nanotechnology, Diagnosis.

INTRODUCTION

Nanotechnology is mainly concerned with the synthesis of nanoparticles of variable sizes, nanoparticles¹. The methods are quite expensive and potentially dangerous to the environment. The use of biological organisms such as microorganisms, plant extract, or plant biomass could be an alternative to chemical and physical methods for the production of nanoparticles in an eco-friendly manner² . Silver nanoparticles (AgNPs) have been proven to possess immense importance and have been extensively studied. AgNPs find use in several applications such as electrical conducting, catalytic, sensing, optical, and antimicrobial properties³⁻⁴. In the last some years, there has been an upsurge in studying AgNPs on account of their inherent antimicrobial efficacy. They are also being seen as future-generation therapeutic agents against several drug-resistant microbes. Physicochemical methods for synthesizing AgNPs thus, pose problems due to the use of toxic solvents, high energy consumption, and generation of by-products⁵⁻⁶. Accordingly, there is an urgent need to develop environment-friendly procedures for synthesizing AgNPs⁷. Plant extracts have shown large prospects in AgNPs synthesis . Leaf extract is a good antioxidant and the compound obtained from has been identified as a flavonol compound and named 'Kaempferol' . *Sansevieriatrifasciata* is categorized under the family Fabaceae, a pantropical ornamental shrub, 2-3m high, widely distributed in tropical countries, stretching from Tropical America to India, Fiji, Indonesia, Malaysia, and Africa⁸⁻⁹. *Sansevieriatrifasciata*Linn (Fabaceae) is an ornamental shrub, which grows well in forest areas of West Africa. It is locally used in Nigeria in the treatment of several infections which include ringworm, parasitic skin diseases¹⁰. Many of the plant materials used in traditional medicine are readily available in rural areas at relatively cheaper than modern medicine. Thus it is important to characterize different types of medicinal plants for their antioxidant and antimicrobial potential¹¹⁻¹³ .

Air-Purifying Plant: *Sansevieriatrifasciata* is in NASA's list of air-purifying plants, improving indoor

MATERIALS AND METHODS

Collection Of Plant Material And Preparation Of Extracts

Matured leaves of *Sansevieriatrifasciata* were collected from the local field of AalavanthanNallur, Kuzhumani road, Trichy, India. The leaves were shade dried, ground into a coarse powder. The powder was first defatted with Acetone and then extracted with ethanol which is further evaporated to dryness to obtain the alcoholic extract. The aqueous extract was obtained by maceration for 24 hrs

Aqueous Extraction

100g of coarse powder of leaves of *Sansevieriatrifasciata* was taken and dissolved in 300ml of sterile distilled water. It is allowed to stand for 3 days with intermittent shaking. Then the extracts were filtered through a three-layered muslin cloth and condensed into solid form at 40° C using a hot air oven. The extracts were weighed to find out the extracted value and stored in a sterile container for further use.

Alcohol Extraction

100g of coarse powder of leaves of *Sansevieriatrifasciata* was taken and dissolved in 300ml of alcohol. It is allowed to stand for 3 days at 37°C under occasional shaking. Then the extracts were filtered through a three-layered muslin cloth and condensed into solid form at 40° C using a hot air oven. The extracts were weighed to find out the extracted value and stored in a sterile container for further use.

Phytochemical Test

Alkaloids

To 2 ml of extract was measured in a test tube to which picric acid solution was added. An orange coloration indicated the presence of alkaloids.

Anthraquinone

To 1 ml of methanolic extract, 2 ml of 5% KOH was added. Then the solution was filtered. A color change was observed. The pink color shows the presence of anthraquinones.

Coumarin

To 1 ml of extract, 1 ml of concentrated sulphuric acid was added and was allowed to stand for some time to develop color. The development of red color shows the presence of quinine.

Flavonoids

To 5 ml of methanolic extract, 1 ml of 10% NaOH solution was added. From the side of the beaker, 2 drops of concentrated HCl were added. Yellow color turning colorless is an indication of the presence of flavonoids.

Glycosides

To 25ml of dilute sulphuric acid was added to 5ml extract in a test tube and boiled for 15 minutes, cooled and neutralized with 10% NaOH, then 5ml of Fehling solution added. Glycosides are indicated by a brick-red precipitate.

Phenol

To 1 ml of extract and a few drops of alcohol and ferric chloride solution was added and allowed for a few minutes. The development of yellow color shows the presence of phenol.

Saponins

Saponins were detected using the froth test. 1g of the sample was weighed into a conical flask in which 10ml of sterile distilled water was added and boiled for 5 minutes. The mixture was filtered and 2.5 ml of the filtrate was added to 10ml of sterile distilled water in a test tube. The test tube was stoppered and shaken vigorously for about 30 seconds. It was then allowed to stand for half an hour. Honeycomb froth indicated the presence of saponins.

Steroids

The powder was dissolved in two ml of chloroform in a dry test tube. 10 drops of acetic anhydride and two drops of concentrated sulphuric acid were added. The solution becomes red, then blue, and finely bluish indicated the presence of steroids.

Tannins

To a portion of the extract diluted with water, 3-4 drops of 10% ferric chloride solution are added. The blue color is observed for Gallic tannins and the green color indicates catecholic tannins.

Terpenoids

Four milligrams of extract were treated with 0.5 ml of acetic anhydride and 0.5 ml of chloroform. Then a concentrated solution of sulphuric acid was added slowly and a redviolet color was observed for terpenoid.

Preparation Of Silver Nit-Rate Solution

Commercially purchased silver nitrate (molecular weight-169.87) was used to prepare 1mM concentrations. appropriate amount of silver nitrate was weighed and dissolved in distilled water.

Preparation Of Silver Nanoparticles

To 750 ml of each millimolar concentration of silver nitrate, 7.5 ml of the flower extract homogenate was added, respectively into a clean conical flask. The conical flasks were then exposed to the sunlight (while being continuously shaken) for the synthesis of the nanoparticles to begin. The colors of the mixture turn from green to brown when exposed to sunlight and once it turns colorless the particles were settled at the bottom of the flasks. The particles were then centrifuged (highspeed centrifuge) and the supernatant was removed. To the particles now settled at the bottom of the centrifuge tubes, about 1ml acetone was added for the removal of the moisture content from the nanoparticles. The nanoparticle suspension was transferred to a watch glass, air dried, collected, weighed, and stored in a sterile container.

Uv-Vis Spectra Analysis

The bioreduction of Ag^+ ions in solutions was monitored by measuring the UV-VIS spectrum of the reaction medium. The UV-VIS spectral analysis of the sample was done by using U-3200 Hitachi spectrophotometer at room temperature operated at a resolution of 1 nm between 200 and 800 nm ranges.

RESULTS

Table-I: Preliminary Phytochemical Screening Of *Sansevieria Trifasciat*

S.No	Test	Aqueous	Ethanol
------	------	---------	---------

1	Alkaloids	+	+
2	Anthraquinone	-	-
3	Coumarin	+	+
4	Flavonoids	-	+
5	Glycosides	-	+
6	Phenols	+	+
7	Saponin	+	+
8	Steroids	-	+
9	Tannins	+	+
10	Terpenoids	-	-

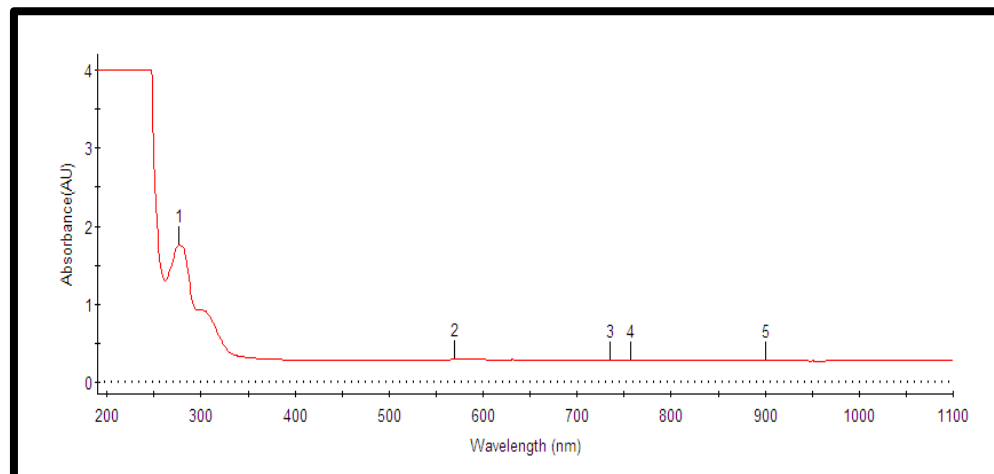
Table 3: Indication Of Color Change In The Synthesis Of Silver Nanoparticle (Snps)

S.No	Plant leaf extract+AgNo3	Color change		pH change		Color intensity	Time	Result
		Before	After	Before	After			
I	<i>Sansevieriatrifasciata</i>	Light yellow	Brown	4.0	4.60	+++	20 min	Positive

Note: +++: Dark brown

Confirmation And Characterization Of Phyto Silver Nanoparticles (Snps) Synthesis:**Visual Observation:**

In the present study, SNPs were synthesized by using leaf extract of *Sansevieriatrifasciata* rapidly within 20 min of incubation period and yellowish-brown color was developed by addition of Silver Nitrate. The time duration of change in color and thickness of the color varies from plant to plant. The time is taken for the reaction mixture to change color and the pH was changed from 4.0 to 4.60.

Fig 2: Uv-Vis Analysis Of Sansevieria Trifasciata**Table: 2uv-Vis Analysis Of Sansevieria Trifasciata**

S.NO	WaveLength	Absorbance
1	276.15	1.7600
2	570.20	0.2963
3	735.40	0.2896
4	756.55	0.2901
5	901.15	0.2892

UV- VIS SPECTROSCOPY

The reduction of silver metal ions to silver nanoparticles was preliminarily analyzed using UV-Vis Spectrophotometer between 300-700nm (Table 2 and fig 1). This analysis showed an absorbance peak at 420 nm which was specific for Ag nanoparticles. UV-visible spectroscopy is an important technique to determine the formation and stability of metal.Nanoparticle in aqueous solution. The reaction mixture changes the color by adding various concentrations of -metal ions. These color changes arise because of the excitation of surface plasmon vibrations in the silver Nanoparticle. It shows yellowish to dark brown. The dark

brown color of silver colloid is accepted to surface plasmon resonance (SPR) arising due to the group of free conduction electrons induced by an interacting electromagnetic field. The photosynthesis of silver nanoparticles was confirmed firstly by visual observation: the yellowish color of petal extracts turned to brown after the addition of AgNO_3 10.3 M solution due to excitation of surface plasmon vibrations indicating the formation of silver nanostructures

DISCUSSION

A large number of medicinal plants and their purified constituents have shown beneficial therapeutic potentials¹⁴⁻¹⁵. To promote the use of medicinal plants as potential sources of antimicrobial compounds, it is important to thoroughly investigate their composition and activity and thus validate their use¹⁶. In the present investigation, preliminary phytochemical analysis was carried out in the extracts of *Sansevieriatrifasciata*. The extracts showed the presence of alkaloids, reducing sugar, coumarin, tannin, and phenolic compounds¹⁷⁻¹⁸. Common human pathogens such as *Streptococcus pneumonia*, *Proteus* and *Enterobacter* which are the causative agents of the respiratory tract and urinary tract infections were selected and assayed for their susceptibility for green Silver Nano Particle (SNPs) synthesized from *Sansevieriatrifasciata* leaves extract. The formation of SNPs was identified in different techniques¹⁹.

CONCLUSION

In conclusion, this green chemistry approach toward the synthesis of AgNPs or SNPs possesses several advantages viz, the easy process by which this may be scaled up, economic viability, etc. Applications of such eco-friendly nanoparticles in bactericidal, wound healing, other medical and electronic applications makes this method potentially stimulating for the large-scale synthesis of nanomaterials²⁰. The present study included the bio-reduction of silver ions through medicinal plants extracts and testing for their antimicrobial activity¹⁹.

CONFLICT OF INTEREST

Conflict of interest declared none.

REFERENCES

1. Abha v, Prakash J, Arvind A. synthesis of plant-mediated silver nanoparticles using plant Extract of asper. International Journal of Nanotechnology and Application. (2013); 3(4): 11-18.
2. Akujobi C, Anyanwu BN, Onyeze C and Ibekwe VI. Antibacterial activities and preliminary phytochemical screening of four medicinal plants. J. Appl. Sci. 2004; 7 (3): 4328 – 4338.
3. Alalor, C. A., Igwilo, C. I. and Jeroh, E. (2012). Evaluation of the antibacterial properties of aqueous and methanol extracts of *Cassia alata*. J. Pharm. and Allied Hea-lth Sci. 2(2): 40-46.
4. Alche, LE. An antiviral principle present in a purified fraction from *Melia azedarach* Linn. Leaf aqueous extract restrains herpes simplex virus type I propagation. Phytother. Res. 2002;16(4): 348-52.
5. Amao, S. Y., Ajani, R.S. and Oladapo, O. (2010). *Cassia alata* alters Liver Structure in Rat. Afr. J. Biomed. Res. 13:231 – 233.
6. Ankamwar B, Damle C, Ahmad A and Sastry M. Biosynthesis of gold and silver nanoparticles using *Emblica Officinalis* fruit extract, their phase transfer and transmetallation in an organic solution. J. Nanosci. Nanotech. 2005; 5 (10): 1665–1671.
7. Ankanna S and N. savithramma. Biological synthesis of silver nanoparticles by using the stem of *Shorea tumbuggiaroxb*.and its antimicrobial efficacy. Asian Journal of Pharmaceutical and Clinical Research. 2012; 40(1): 120-129.
8. Arora, D.S.; Kaur, J(1999)., ll Antimicrobial activity of spices., ll, Int. J. Antimicrob. Agents 123, 257-62.
9. Asra P, Aashis SR, and Srinath R. Biosynthesis and characterization of silver nanoparticles from *Cassia auriculata* leaf extract and in vitro evaluation of the antimicrobial activity. J. Appl. Biol. Pharm. Tech.2012; 3:222–228.
10. Bar H, Bhui, DK, Sahoo GP, Sarkar P, Pyne S, Misra A. Green synthesis of silver nanoparticles using seed extract of *Jatropha curcas* . Colloids Surf. B Biointerfaces. 2009; 348 (1–3):212–216.
11. Begum NA, Mondal S, Basu S, Laskar RA, Mandal D. Biogenic synthesis of Au and Ag nanoparticles using aqueous solutions of black tea leaf extracts. Colloids Surf. B Biointerfaces .2009, 71 (1):113–118.
12. Biswas A, Aktas OC, Schumann U, Saeed U, Zaporjtchenko V and Faupel F. (2004).Tunable multiple plasmon resonance wavelengths response from multicomponent polymer-metalnanocomposite systems. Applied Physical Letter, 2004; 84: 2655-2657.
13. Biswas K, Chattopadhyay I, Banerjee RK and Bandyopadhyay U. Biological activities and medicinal properties of neem (*Azadirachta indica*). CurrSci, 2002; 82(11): 1336 – 1345.
14. Charleston DS. Impact of botanical pesticides derived from *Melia azedarach* and *Azadirachta indica* plants on the emission of volatiles that attracts Parasitoids of the diamondback moth to cabbage plants. J. Chem. Ecol. 2006; 32(2): 325-49.
15. Cox PA. In: The ethnobotanical approach to drug discovery: strengths and limitations. In, ethnobotany and the search for the new drugs.1994; pp. 25-36. John Wiley & Sons. England.
16. Dalziel, J.M. (1956). The Useful Plants of West Tropical Africa. Crown .Agents, London, p: 612.
17. Daniels, R. and Knie, U. (2007). Galenics of dermal products vehicles, properties, and drug .
18. Shi J., Chan C., Pang Y., Ye W., Tian F., Lyu J., Zhang Y., Yang M. A fluorescence resonance energy transfer (FRET) biosensor based on graphene quantum dots (GQDs) and gold nanoparticles (AuNPs) for the detection of *mecA* gene sequence of *Staphylococcus aureus*. Biosens.Bioelectron. 2015;67:595–600.
19. J. Phys. Chem. 103, 4212–4217 (1999). 18.Baetsen-Young A.M., Vasher M., Matta L.L., Colgan P., Alocilja E.C., Day B. Direct colorimetric detection of unamplified pathogen DNA by dextrin-capped gold nanoparticles. Biosens.Bioelectron.

2018;101:29–36.

- 19. Morris CJ. Carrageenan-induced paw edema in the rat and mouse. *Inflammation Protocols* Springer. 2003;225:115–121.
- 20. Euliss, L. E., DuPont, J. A., Gratton, S. & DeSimone, J. Imparting size, shape, and composition control of materials for nanomedicine. *Chem. Soc. Rev.* 35, 1095–1104 (2006).
- 21. Link, S. & El-Sayed, M. A. Size and temperature dependence of the plasmon absorption of colloidal gold nanoparticles

Synthesis and Characterization of Cobalt Oxide Nanoparticles and Evaluation of It's Antibacterial Activity

G.Vanaja , Dr.T.Adinaveen, Dr.A.Priya, R Shanmugapriya

DhanalakshmiSrinivasan College of arts and science for women (Autonomous),Perambalur-621212

Abstract: synthesize cobalt oxide nanoparticles by using fresh leaf extract of *Chenopodium Album*. Characterize the synthesized cobalt oxide nanoparticle. Evaluate the in vitro antibacterial activity using synthesized nanoparticle. Literature survey of synthesis of cobalt oxide nanoparticle using plant extracts. Selection of plant *Chenopodium Album*. Preparation of fresh leaf extract. Synthesis of cobalt oxide nanoparticles can be done using fresh leaf extract of selected plants. Characterization was determined using UV-Visible spectroscopy, FT- IR, SEM, EDX and XRD analysis.

INTRODUCTION

Nanomaterials

The exact definition of nano-materials remained unavailable in the literature until Schmidt provided a clear-cut definition of nanoscale materials as described below. According to Finke, it is very difficult to classify a material either as a bulk or as a nanostructured material without precise data of composition, size and phase purity. Now, it is possible to classify any material into discrete single metal complexes; metal clusters including nanoclusters $< 100 \text{ \AA}$; traditional colloids $> 100 \text{ \AA}$; and bulk metal¹⁻³.

Transition metal oxides

Transition metal elements are significantly different from the other metal elements in the periodic table due to the fact that their valence electrons may be present in more than one shell. Therefore, most of them exhibit variable oxidation states. As the number of transition metal elements is large, they are subdivided into three main groups: the main transition elements (d-block elements), the lanthanide elements and the actinide elements. Only those elements that have partially filled d shells can be included into the main transition elements .Sc, Ti, V, Cr, Mn, Fe, Co, Ni and Cu typically form the first or 3d transition series. Except, Cu and Zn, all the elements have partially filled 3d shells either in ground state of the free atom or in one or more of their important ions (except Sc). Cu has a completely filled 3d shell in ground state, however a partially filled 3d shell can be obtained in excited states. Zn, on the other hand, has a complete octet (3d104s2) and no ionization of the 3d shell can be observed under any circumstance and thus its behavior is different from transition metals⁴⁻⁵.

Nanotechnology

Nanotechnology is a profoundly and popularly used term these days to label a wide variety of research activities around the world. It is the discovery of properties of materials at nanoscale. Generally, NPs are particles having the size range of 100 nm and are clusters of atoms. Nanotechnology is expected to play a vital role in various disciplines and is becoming the most innovative scientific field. Nanotechnology mainly concerns the synthesis of NPs of variable sizes, shapes, chemical compositions and the potential use for human benefits. Nanotechnology is an exciting and powerful discipline of science and is considered the most important technological advancement in recent years, due to its new and profitable applications. Industries such as food, agriculture, electronics, medicine, automotive, information and communication technologies, energy, textile, construction, etc. have been investing and reorganizing their future in the light of nanotechnological developments⁶.

Importance of being Nano

NPs are in great demand by the scientific community due to their fascinating properties and for their many technological applications. This interest halts from the radical property, varies with the particle size and reduces from macro/micro scale to the nanoscale. An increase in the surface area per unit mass is an effect of reduced dimensions of nanocrystals which alters the physical and chemical properties of a material. The large fractions of surface atoms and surface energy may influence thermal stability and catalytic properties of nanomaterials. Owing to high surface area to volume ratio, they have exhibited lower melting point as well as high mechanical strength due to crystal defects compared to their bulk materials.

EXPERIMENTAL METHODS

Chemicals

All materials were purchased from Nice and Loba chemicals. Solvents that were used during the reactions were of high purity and used without further purification.

Collection of plant materials

The plant material *Chenopodium album* was collected from the local places of Trichirappalli area. Freshly collected whole plants were cast-off for AgONp synthesis.

Preparation of plant extract

The extract solution was equipped by using leaves from the *Chenopodium album* plant. The leaves of fresh plant that had been rinsed with deionized water and finely cut into small pieces. Then the plant material was boiled with 100 mL of distilled water at

100°C, sifted by using whatman No. 1 filter paper then kept at 4°C for additional experimentation³.

Synthesis of Cobalt oxide nanoparticles

In the preparation of Silver oxide nanoparticles, samples $\text{CoCl}_2 \cdot 6\text{H}_2\text{O}$ (0.1g) was first dissolved in enough quantity of deionized water and mixed with 10mL of *Chenopodium album* plant extract solution under vigorous stirring with magnetic stirrer at 1000 rpm at room temperature for 3hr. Then 1ml of 10% NaOH solution was added to the reaction mixture to adjust the pH of the reaction mixture. The precipitated solid was filtered and dried. The crude product was maintained at 150°C for 12 hrs in the oven. The obtained powder was calcined at 500 °C for 3 hrs and then crushed into fine powder by using pestle mortar⁹⁻¹⁰

Characterization studies

Silver oxide nanoparticles synthesized by using green chemistry technique were confirmed with the help of UV-Visible spectrophotometer (Shimadzu) and FT- IR spectrophotometer (Shimadzu) spectrum in the range 4000-400 cm^{-1} , Powder XRD, SEM and EDX examination¹¹.

Antibacterial activity

Antibacterial behavior of the aqueous leaf extract of *Chenopodium album* (1) Co_3O_4 NPs (2) was checked against two gram negative bacteria (*Escherichia coli*, *Pseudomonas aeruginosa* along with two gram positive bacteria *Staphylococcus aureus* and *Bacillus cereus*) that were preserved on the agar slants of the nutrient¹⁴. The antimicrobial behavior was performed as defined by Institute of Clinical and Laboratory Standards. Bacterial immunity to Co_3O_4 NPs was tested using an assay to disperse the disks. Triplicates of the Co_3O_4 NPs were used in sterile deionized water dilutions of (200, 100, 50, 25, and 12.5). Initially, the isolates were incubated at 40°C for 15min, and then overnight at 37°C. Good test outcomes were graded when an inhibition zone was found across the well after the incubation time then a digital vernier caliper was used to calculate the inhibition zone diameter.¹¹⁻¹³

Minimum inhibitory concentration (MIC) determination

The bacterial isolates, which were used to prepare 0.5 McFarland, were incubated at 37°C overnight. A minimum of 10ml tube nutrient broth medium was equipped and each sample was injected aseptically by 1ml of the particular bacterial suspension (about 108 CFU / mL). Five dilutions of aqueous leaf extract of *Chenopodium album* (1) Co_3O_4 NPs (2) (200, 100, 50, 25 and 12.5) were prepared in sterile deionized water and a negative control (without Co_3O_4 NPs) was used. Assessments for each isolate were performed in triplicates. The inoculated sets were overnight incubated to 37°C. The apparent turbidity in each tube was examined during the incubation time. Of the measured strain the lowest concentration without turbidity is defined as the MIC¹⁷. Tubes showed no turbidity on nutrient agar plates cultivated and incubated overnight at 37°C.

RESULTS AND DISCUSSION

The *Chenopodium album* plant was collected around Tiruchirappalli and was identified using the *Flora of presidency of Madras* and the fresh plant extract plays a key role in zincoxide nanoparticle synthesis¹⁴⁻¹⁵. Optical Characterization The reduction of Co^{2+} ions to Co^0 NPs by aqueous leaf extract of *Chenopodium album* was visually observed by color variation in the reaction mixture. The gradual color change in solution from pink to brown. This indicates that the metal chlorides were reduced to form its respective nanoparticles. UV-Visible analysis of Co_3O_4 NPs The UV-visible absorption peak arises from 320-380 nm denoting the development of Co_3O_4 NPs. In our work, two absorption bands in the wavelength ranges of 200-350 and 380-600 nm. As has been reported in the literature, these bands can be assigned to the $\text{O}^- \rightarrow \text{Co}^+$ and $\text{O}^- \rightarrow \text{Co}^+$ charge transfer processes, respectively¹⁶⁻¹⁸.

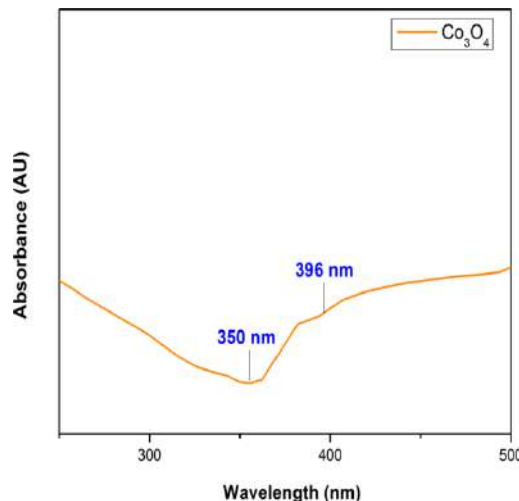


Figure 1 UV - Visible spectra of Co_3O_4 nanoparticle. FT-IR Analysis of Co_3O_4 Nps

The FT-IR spectrum noted in the range from 400-4000 cm^{-1} . A wide peak at 3465.93 cm^{-1} agrees to the NH group which may be appeared as a result of the manifestation of amine moiety. The bands at 2800 - 3000 cm^{-1} signify the existence of the C-

H functional group of alkanes. The peaks at 1644.01 cm^{-1} showed the incidence of C=O from the PVP moiety. The band at 584.80 cm^{-1} approves the existence of octahedral Co-O vibrations and 509.59 cm^{-1} approves the existence of tetrahedral Co-O vibrations. FT-IR analysis confirmed the presence of functional groups in the capping agent and also the formation of Co_3O_4 NPs. FT-IR spectra of synthesized Co_3O_4 NPs was represented in Figure 2.

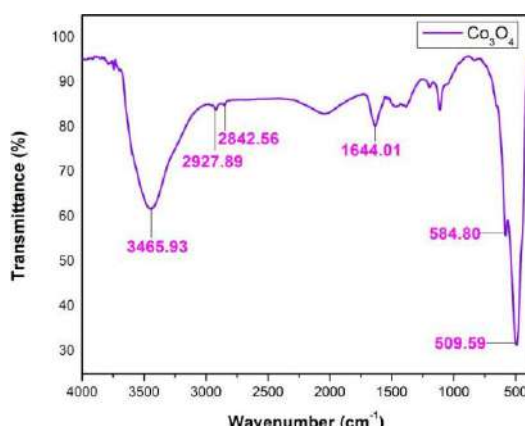


Figure 2. FT-IR spectra of Co_3O_4 nanoparticle.

SEM and Mapping studies Co_3O_4 nanoparticle

The investigation Scanning Electron Microscopy (SEM) was performed to govern the size and morphology of the synthesized Co_3O_4 NPs. The SEM image shown in Figure 3 confirmed that the obtained Co_3O_4 NPs were spherically shaped. The synthesized Co_3O_4 NPs were dispersed as distinct particles and monodispersity in nature. SEM mapping studies also confirm the synthesized nanoparticle was Co_3O_4 . The rose dots correspond to Cobalt atoms and green dots represent Oxygen atoms. Figure 4 represents the SEM mapping studies of Co_3O_4 NPs¹⁹.

EDX Analysis of Co_3O_4 nanoparticle

The synthesized Co_3O_4 NPs elemental composition was confirmed by EDX examination. The manifestation of zinc and oxygen peaks in the EDX spectra confirmed that the synthesized material was Co_3O_4 NPs (Figure 5). The weight percentage of Cobalt and Oxygen atoms were 35.80 and 64.20 respectively. The further peaks extant in the spectra may be as a result of the existence of bioorganics or impurities in the solution. The elemental composition of Co_3O_4 nanoparticle was represented in Table I.

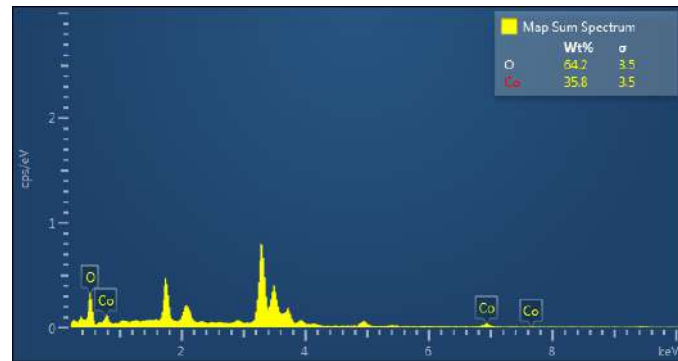


Figure 5. EDX spectra of Co_3O_4 nanoparticles.

Table I. Elemental composition of Co_3O_4 nanoparticle

Element	Atomic Number	Weight %	Weight %Error
O	8	44.94	3.50
Co	27	55.06	3.50
Total	-	100.00	-

XRD Analysis

The XRD pattern of synthesized Co_3O_4 NPs was represented in Figure 6. The diffraction peaks at $2\theta = 31.2^\circ, 37.6^\circ, 38.7^\circ, 44.8^\circ, 55.6^\circ, 59.8^\circ$, and 66.3° were respectively indexed to (220), (311), (222), (400), (422), (511) and (440) planes of pure face centered cubic spinel phase structure of Co_3O_4 NPs. The obtained diffraction peaks were matched with standard Co_3O_4 NPs. All the diffraction peaks are in decent agreement with the standard pattern for pure Co_3O_4 nanoparticles (JCPDS No. 00-042-1467). There some impurity peaks observed. The intense peaks indicates extremely crystalline nature of the formed nanoparticles. From the observed main diffracted peak, the average crystalline size can be calculated using the Scherer equation,

$$(hkl) = \frac{1}{\beta \cos \theta}$$

Where, $D_{(hkl)}$ is the average crystallite size, k is shape constant (0.89), λ is the wavelength of the incident x-ray (CuK α source, $\lambda = 0.15405$ nm), β is the full width half maximum (FWHM), θ is the incident angle of x-ray. The average crystallite size of the synthesized Co_3O_4 nanoparticles was 22.70 nm.

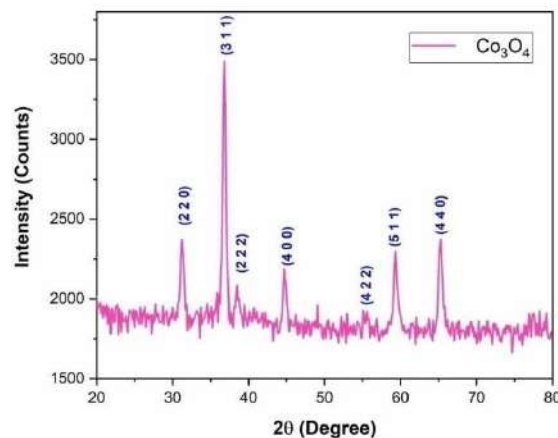


Figure 6.XRD spectra of Co_3O_4 nanoparticles.

In vitro antibacterial activity

The assessment of in vitro antibacterial activity against two Gram-negative bacteria specifically, *E. coli*, *P. aeruginosa* and two Gram-positive bacteria explicitly, *S. aureus*, *B. cereus* utilizing standard drug ciprofloxacin. Minimum inhibitory concentration (MIC) values were evaluated via standard agar method. MIC values of the aqueous leaf extract of *Chenopodium album* (1) and synthesized Co_3O_4 nanoparticle (2) were presented in Table 3. The synthesized Co_3O_4 nanoparticle shows remarkable antibacterial activity than aqueous leaf extract of *Chenopodium album* (1). Co_3O_4 nanoparticle 2 shows higher antibacterial activity with the MIC value of 23.60 $\mu\text{g}/\text{mL}$ than control ciprofloxacin with the MIC value of 25.00 $\mu\text{g}/\text{mL}$ in *E. coli*. Co_3O_4 nanoparticle 2 shows higher antibacterial activity with the MIC value of 26.56 $\mu\text{g}/\text{mL}$ than control ciprofloxacin with the MIC value of 50.00 $\mu\text{g}/\text{mL}$ in *B. cereus*. Co_3O_4 nanoparticle 2 displayed moderate activity in bacterial cultures *P. aeruginosa* and *S. aureus* with the MIC value of 34 and 28 $\mu\text{g}/\text{mL}$ than standard ciprofloxacin. Interestingly, the synthesized Co_3O_4 nanoparticle (2) shows remarkable antibacterial activity than control Ciprofloxacin in both pathogens *E. coli* and *B. cereus* respectively.

Table 2. Antibacterial activity of aqueous leaf extract of *Chenopodium album* (1) and synthesized Co_3O_4 nanoparticle (2)

Comp.No.	MIC $\mu\text{g}/\text{mL}$			
	<i>E. coli</i>	<i>P. aeruginosa</i>	<i>S. aureus</i>	<i>B. cereus</i>
1	32.10 \pm 0.24	40 \pm 1.23	32 \pm 0.62	52.23 \pm 1.24
2	23.60 \pm 1.25	34 \pm 0.21	28 \pm 1.12	26.56 \pm 0.56
Ciprofloxacin	25.00 \pm 0.95	30 \pm 0.0	20 \pm 0.0	50.00 \pm 1.75

^a Value were the means of three replicates \pm SD.

CONCLUSION

In conclusion, the Cobalt oxide nanoparticle was synthesized using fresh leaf extract of *Chenopodium album*. The synthesized nanoparticle was characterized and confirmed using UV, FT-IR, XRD and SEM analysis, the results showed that Co_3O_4 Nps were synthesized properly. The in vitro antibacterial activity depicts the effective antibacterial activity of Co_3O_4 Nps. This conclude that the further studies on Co_3O_4 Nps helps for the drug development ²⁰.

CONFLICT OF INTEREST

Conflict of interest declared none.

REFERENCE

1. <http://www.its.caltech.edu/feynman/plenty.html>, APS Annual Meeting, 1959.
2. Hapgood, Fred (November 1986). "Nanotechnology" / "Tinytech". *Omni*: 56.
3. Drexler, Eric (15 December 2009). "The promise that launched the field of nanotechnology". Metamodern: The Trajectory of Technology. Retrieved 13 May 2011.
4. Freestone, I. Meeks, N. Sax, M. Higgitt, C. (2007) *Gold Bull.* 40, 270.

5. Walter, P. Welcomme, E. Hallegot, P. Zaluzec, N. J. Deeb, C. Castaing, J. Veyssiere, P. Breniaux, R. Leveque, J.-L. Tsoucaris, G. (2006) *Nano Lett.* 6, 2215.
6. Binnig, G. Rohrer, H. Gerber, Ch. Weibel, E. (1982) *Phys. Rev. Lett.* 49, 57.
7. Binnig, G. Quate, C. F. Gerber, Ch. (1986) *Phys. Rev. Lett.* 56, 930.
8. Binnig, G.; Quate, C. F. Gerber, Ch. (1986) *Phys. Rev. Lett.* 56, 930.
9. Schmid, G. (1990) *Endeavour* 14, 172.
10. Antonelli, D.M. Ying, J. Y. (1996) *Chem. Mater.* 8, 874.
11. Corma, A. Atienzar, P. Garcia, H. Chane-Ching, J. Y. (2004) *Nat. Mater.* 3, 394.
12. Deshpande, S. Pinna, N. Smarsly, B. Antonietti, M. Niederberger, M. (2005) *Small* 1, 313 Ba, J. Polleux, J. Antonietti, M. Niederberger, m. (2005) *Adv. Mater.* 17, 2509.
13. Cotton, F. A. Wilkinson, G. *Advanced Inorganic Chemistry*; Wiley- Interscience: New York 1988.
14. V S Sangeetha , Vanith A, Devi P, BhakajothiV"Green synthesis of Zinc oxide nanao particle using flower extract of phyla nodiflora" Schoolar National School of leadership vol-9
15. S. Deka, R. Paricha, and P. A. Joy, *Chem. Mater.*, 16 (2004) 1168.
16. O. D. Jayakumar, I. K. Gopalakrishnan, C. Sudakar, R. M. Kadam, and S. K. Kulshreshtha, *J. Alloys Compnd.*, 438 (2007) 258
17. R Elayaperumal , G Vanaja, A Vanith,VSSangeetha "Green synthesis of Glycrrhizagla silver nano particle and conformation of through Microscopy and Spectrophotometric techniques. "Eurasian journal of Analytical chemistry ,2017-Feb ,1680-168.
18. C. N. R. Rao and F. L. Deepak, *J. Mater. Chem.*, 15 (2005) 573.
19. R. Podila, W. Queen, A. Nath, J. T. Arantes, A. L. Schoenhalz, A. Fazzio, G. Dalpian, J. He, S.
20. J. Hwu, M. J. Skove, and A. M. Rao, *Nano Lett.*, 10 (2010) 1383.
21. C.W. Bunn, *Proc. Phys. Soc., London*, 47 (1935) 835.
22. A. Gosh, N. Kumari, S. Tiwari and A. Bhattacharjee, *Indian J. Phys.*, 87(11) i.(2013)1099-1104.

Investigation and Characterization of Copper Oxide Nanoparticle Using Fresh Leaves of *Chenopodium Album*

V.Bhakyajothi¹, SenthilKumaran¹, V.S.Sangeetha¹, M.Deepa¹

¹. Dhanalakshmi Srinivasan college arts and science for women (Autonomous), perambalur

Abstract: Functional groups present in the CuO NPs crystal were identified in the FT-IR spectral investigation. UV-Visible spectroscopy of CuO NPs. predicts cut-off wavelength was 278 nm. Synthesize copper oxide nanoparticles by using a fresh leaf of *Chenopodium album*. characterization and synthesized copper oxide nanoparticles. Synthesis of the copper-oxide nanoparticle can be done using fresh leaf extract of the selected plant.

Keywords: *Chenopodium album*, copper oxide nanoparticles, ZnO NPs, XRD, SEM, and EDX

INTRODUCTION

Nanomaterials are products of at least one size (1–100 nm) in the spectrum of the nanometer scale or whose basic unit is beyond this spectrum in the threedimensional space¹⁻⁵. In particular, NPs have demonstrated antibacterial broad-spectrum properties against both Gram-positive and Gram-negative bacteria. For eg, ZnO NPs have been found to inhibit *Staphylococcus aureus*, and Ag NPs have antimicrobial activity based on concentration against *Escherichia coli* and *Pseudomonas aeruginosa*^{9,10}. Nevertheless, the precise antibacterial functions of NPs have not been thoroughly described, and opposing symptoms sometimes arise in the same forms of NPs. NPs' antimicrobial action mechanism is defined as genetically adhering to one of three models: oxidative stress induction, metal ion release, or non-oxidative mechanisms¹¹⁻¹³. Simultaneously, all three forms of processes may occur. Several experiments have indicated that Ag NPs cause neutralization of the bacterial membrane's surface electric charge and change its penetrability, eventually contributing to bacterial death¹⁴. In addition, reactive oxygen species (ROS) generation inhibits antioxidant protection mechanisms and induces mechanical harm to the cell membrane. The main processes influencing the antibacterial effects of NPs are, according to existing research, 1) degradation of the bacterial cell membrane; 2) production of ROS; 3) penetration of the bacterial cell membrane; and 4) activation of intracellular antibacterial effects, including interactions with DNA and protein.

Bacterial resistance to NPs

Significant in combating drug resistance is the search for new, effective bactericidal materials and NPs have been established as a promising approach to solving this problem⁹. In certain situations, however, NPs may also facilitate the evolution of bacterial resistance¹⁹. We address the positive and negative aspects of the interactions between NPs and drug-resistant bacteria in this portion.

The effects of NPs on microbial resistance

As a new line of defense against microbial resistance and MDR, increasing numbers of NP variants and NP-based materials have been utilized. Various types of NPs have different mechanisms to counter microbial resistance. The section "Antibacterial Mechanisms of NPs" presents various antibacterial mechanisms of NPs according to the metabolic process involved. One of the agreed associations between nanomaterials and antibacterial activity is as follows: "Nanomaterials are highly promising as antibacterial complements to antibiotics and are gaining considerable interest as they could fill the gaps where antibiotics frequently struggle."¹⁶ "However, nanomaterials as a strong carrier will supplement and endorse conventional antibiotics' This section focuses on the distinct features and complementary advantages of using NPs/nanotechnologies as antibacterial agents compared to traditional antibiotics, which can be summarized as follows: 1) overcoming existing antibiotic resistance mechanisms listed in the section 'Antibacterial activity of NPs' including disruption of bacterial membranes and hindrance of Supervising the current processes of antibiotic resistance, 2) combatting microbes using multiple mechanisms simultaneously¹⁷, and 3) acting as good carriers of antibiotics.

MATERIAL AND METHODS

Chemicals

All materials were purchased from Nice and Loba chemicals. Solvents that were used during the reactions were of high purity and were used without further purification.

Collection of plant materials

The plant material *Chenopodium album* was collected from the local places of the Ariyalur area. The freshly collected whole plant was used for the synthesis of copper oxide nanoparticles.

Preparation of plant extract

The extract solution was equipped by using leaves of the *Chenopodium album* plant. The leaves of the fresh plant had been rinsed with deionized water and finely cut into small pieces. Then the plant material was boiled with 100 mL of distilled water at 100°C, filtered by using Whatman No. 1 filter paper, and stored at 4°C for further experimentation.

Synthesis of Copper oxide nanoparticles

In the preparation of Copper Oxide nanoparticles, samples $\text{Cu}(\text{NO}_3)_2 \cdot 3\text{H}_2\text{O}$ (0.1g) was first dissolved in enough quantity of deionized water and mixed with 10mL of *Chenopodium album* plant extract solution under vigorous stirring with a magnetic stirrer at 1000 rpm at room temperature for 3hr. Then 1ml of 10% NaOH solution was added to the reaction mixture to adjust the pH of the reaction mixture. The precipitated solid was filtered and dried. The crude product was maintained at 150°C for 12 hrs in the oven. The obtained powder was calcined at 500 °C for 3 hrs and then crushed into fine powder by using pestle mortar.¹⁴⁻¹⁸

Characterization studies

Copper oxide nanoparticles synthesized by using green chemistry technique were confirmed with the help of UV-Visible spectrophotometer (Shimadzu) and FTIR spectrophotometer (Shimadzu) spectrum in the range 4000-400 cm^{-1} , Powder XRD, SEM, and EDX examination.

Antibacterial activity

Antibacterial behavior of the aqueous leaf extract of *Chenopodium album* (I)

CuO NPs (2) were checked against two gram-negative bacteria (*Escherichia coli*, *Pseudomonas aeruginosa* along with two gram-positive bacteria *Staphylococcus aureus* and *Bacillus cereus*) that were preserved on the agar slants of the nutrient. The antimicrobial behavior was performed as defined by the Institute of Clinical and Laboratory Standards. Bacterial immunity to CuO NPs was tested using an assay to disperse the disks. Triplicates of the CuO NPs were used in sterile deionized water dilutions of (200, 100, 50, 25, and 12.5). Initially, the isolates were incubated at 4°C for 15min, and then overnight at 37°C. Good test outcomes were graded when an inhibition zone was found across the well after the incubation time then a digital vernier caliper was used to calculate the inhibition zone diameter.

Minimum inhibitory concentration (MIC) determination

The bacterial isolates, which were used to prepare 0.5 McFarland, were incubated at 37°C overnight. A minimum of 10ml tube nutrient broth medium was prepared and each sample was inoculated aseptically with 1ml of the respective bacterial suspension (approximately 108 CFU / mL). Five dilutions of aqueous leaf extract of *Chenopodium album* (I) CuO NPs (2) (200, 100, 50, 25, and 12.5) were prepared in sterile deionized water and negative control (without CuO NPs) was used. Tests for each isolate were performed in triplicates. The inoculated sets were overnight incubated to 37°C. The apparent turbidity in each tube was examined during the incubation time. Of the measured strain, the lowest concentration without turbidity is defined as the MIC. Tubes showed no turbidity on nutrient agar plates cultivated and incubated overnight at 37°C.

RESULTS AND DISCUSSION

The *Chenopodium album* plant was collected around Ariyalur and was identified using the *Flora of the presidency of Madras* and the fresh plant extract plays a key role in copper oxide nanoparticle synthesis.

Optical Characterization

The reduction of Cu^{2+} ions to Cu^0 NPs by aqueous leaf extract of *Chenopodium album* was visually observed by color variation in the reaction mixture. The gradual color change in solution from light green to sky blue. This indicates that the metal nitrates were reduced to form their respective nanoparticles.¹⁹⁻²⁰

UV-Visible Spectroscopy

The UV-visible absorption peak arising from 300-380 nm denotes the development of CuO NPs. In this study, the extreme absorption peak seemed at 365 nm directs the individual SPR band for CuO NPs with lesser particle size. Figure I displays UV-vis spectra of CuO NPs synthesized by greener protocol.

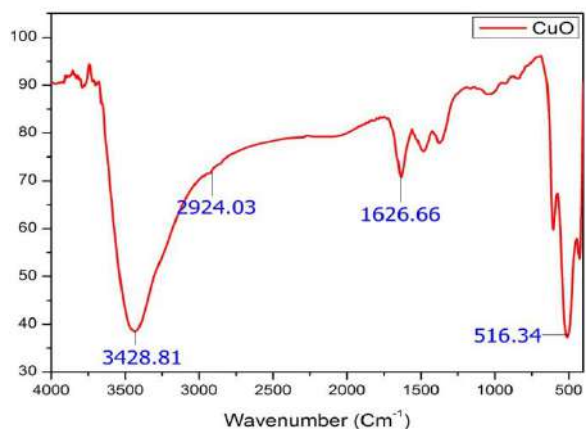


Fig 2. FT-IR spectra of CuO nanoparticles.

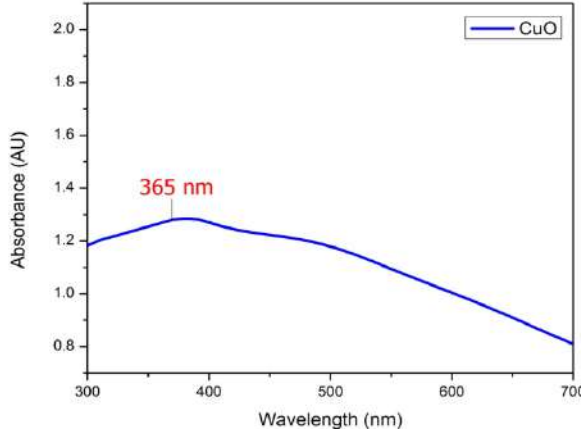


Fig. I UV – Visible spectra of CuO nanoparticle.

FT-IR Analysis of metal oxide nanoparticles synthesized by using aqueous leaf extract of *Chenopodium album*.

The FT-IR spectrum noted in the ranges from 400-4000 cm^{-1} . A wide peak at 3428.71 cm^{-1} agrees to the O-H group which may be appeared as a result of the manifestation of Hydroxyl moiety 131. The bands at 2800 - 3000 cm^{-1} signify the existence of the C-H functional group of alkanes 130 [56]. The peaks (1626.66 cm^{-1}) showed the incidence of carbonyl moiety (C=O) which confirms the leaf extract has enzymes or proteins 129. The band at 516.34 cm^{-1} approves the existence of Cu-O vibrations 131. FT-IR analysis confirmed the presence of functional groups in the capping agent and also the formation of CuO NPs. FT-IR spectra of green synthesized CuO NPs were represented in Figure 2.

SEM and Mapping studies CuO nanoparticle

Scanning Electron Microscopy (SEM) investigation was performed to govern the size and morphology of the green synthesized CuO NPs by *Chenopodium album* (aqueous leaf extract). SEM image shown in Figure 3 confirmed that the obtained CuO NPs were flake-like morphology. The green synthesized CuO NPs were dispersed as distinct particles and monodispersity in nature. Phytochemicals in *Chenopodium album* aqueous leaf extract turn as a capping agent which prevents the aggregation of particles causes monodispersity of CuO NPs. SEM mapping studies also conforms the synthesized nanoparticle was CuO. The blue dots correspond to the Copper atom and rose dots represent the Oxygen atom. Figure 4 represents the SEM mapping studies of Cu nanoparticles.

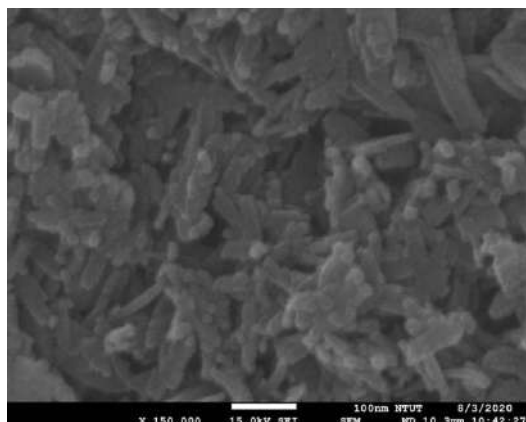


Fig 3. SEM image of CuO nanoparticle.

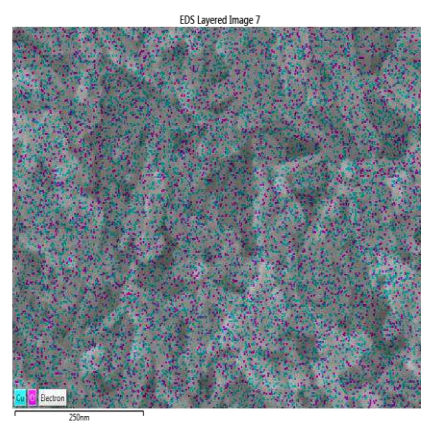


Fig 4. SEM image mapping of CuO nanoparticle

CONCLUSION

In conclusion, the copper oxide nanoparticle was synthesized using fresh leaf extract of *Chenopodium album*. The synthesized nanoparticle was characterized and confirmed using FE-SEM, EDX, and SEM mapping analysis, the results showed that CuO NPs were synthesized properly. The *in-vitro* antibacterial assay depicts the effective antibacterial activity of CuO NPs. This concludes that further studies on CuO NPs help for drug development.

CONFLICT OF INTEREST

Conflict of interest declared none.

REFERENCES

1. Hsueh PR. New Delhi Metallo- β -lactamase-I (NDM-1): an emerging threat among Enterobacteriaceae. *J Formos Med Assoc.* 2010;109(10):685–687.
2. Poole K. Mechanisms of bacterial biocide and antibiotic resistance. *J Appl Microbiol.* 2002;92(suppl):55–64.
3. Jayaraman R. Antibiotic resistance: an overview of mechanisms and a paradigm shift. *Curr Sci India.* 2009;96(11):1475–1484.
4. Knetsch MLW, Koole LH. New strategies in the development of antimicrobial coatings: the example of increasing usage of silver and silver nanoparticles. *Polymers Basel.* 2011;3:340–366.
5. Romero D, Aguilar C, Losick R, Kolter R. Amyloid fibers provide structural integrity to *Bacillus subtilis* biofilms. *Proc Natl Acad Sci U S A.* 2010;107(5):2230–2234.
6. Huh AJ, Kwon YJ. “Nanoantibiotics”: a new paradigm for treating infectious diseases using nanomaterials in the antibiotics resistant era. *J Control Release.* 2011;156(2):128–145.
7. Hajipour MJ, Fromm KM, Ashkarran AA, et al. Antibacterial properties of nanoparticles. *Trends Biotechnol.* 2012;30(10):499–511.
8. Reyes VC, Opot SO, Mahendra S. Planktonic and biofilm-grown nitrogen-cycling bacteria exhibit different susceptibilities to copper nanoparticles. *Environ Toxicol Chem.* 2015;34(4):887–897.
9. Edmundson M, Thanh NT, Song B. Nanoparticles based stem cell tracking in regenerative medicine. *Theranostics.* 2013;3(8):573–582.
10. Ramalingam B, Parandhaman T, Das SK. Antibacterial effects of biosynthesized silver nanoparticles on surface ultrastructure and nanomechanical properties of gram-negative bacteria viz. *Escherichia coli* and *Pseudomonas aeruginosa*. *ACS Appl Mater Interfaces.* 2016;8(7):4963–4976.

11. Gurunathan S, Han JW, Dayem AA, Eppakayala V, Kim JH. Oxidative stress-mediated antibacterial activity of graphene oxide and reduced graphene oxide in *Pseudomonas aeruginosa*. *Int J Nanomedicine*. 2012;7:5901–5914.
12. Nagy A, Harrison A, Sabbani S, Munson RS Jr, Dutta PK, Waldman WJ. Silver nanoparticles embedded in zeolite membranes: release of silver ions and mechanism of antibacterial action. *Int J Nanomedicine*. 2011;6:1833–1852.
13. Leung YH, Ng AM, Xu X, et al. Mechanisms of antibacterial activity of MgO: non-ROS mediated toxicity of MgO nanoparticles towards *Escherichia coli*. *Small*. 2014;10(6):1171–1183.
14. Jung WK, Koo HC, Kim KW, Shin S, Kim SH, Park YH. Antibacterial activity and mechanism of action of the silver ion in *Staphylococcus aureus* and *Escherichia coli*. *Appl Environ Microbiol*. 2008;74(7):2171–2178.
15. Abbara A, Chitty S, Roe JK, Ghani R, Collin S, Ritchie A. (2017). Drug-induced liver injury from antituberculous treatment: a retrospective study from a large TB center in the UK. *BMC Infectious Diseases*; 17: 231- 240.
16. Tostmann A, Boeree MJ, Aarnoutse RE, de Lange WC, van der Ven AJ, Dekhuijzen R (2008). Anti-tuberculosis drug-induced hepatotoxicity: a concise up-to-date review. *J Gastroenterol Hepatol*; 23:192–202
17. India TB report, 2019. Revised National TB Control Programme Annual Report, Central TB Division, Min. of Health Govt. of India; I – 244.
18. Ramaswamy S, Musser JM. Molecular genetic basis of antimicrobial agent resistance in *Mycobacterium tuberculosis*: 1998 update. *Tuber Lung Dis*. 1998;79(1):3-29
19. Devarbhavi H. Antituberculous drug-induced liver injury: current perspective. *Trop Gastroenterol*. 2011 Jul-Sep;32(3):167-74
20. Keshavjee S, Gelmanova I. Y, Shin S. S, Mishustin Y S, Andreev P. G, Atwood S, Furin J. J, Miller A. (2012). Hepatotoxicity during treatment for multidrug-resistant Tuberculosis: occurrence, management, and outcome. *Int j tube lung dis* 16(5): 596–603.

Dpph Scavenging Techniques, Soxhlet Extraction Studies On *Centella Asiatica*

S.Suguna, S.SenthilKumaran, V.S.Sangeetha, V.Bhakkiyajothi

DhanalakshmiSrinivasan College Of Arts And Science For Womens (Autonomous) Perambalur.621212

Abstract: In vitro antioxidant activity of *Centellaasiatica* (Leaf.) and the impact of extraction solvent polarity on the antioxidant potential were investigated in the present study. 100% ethanol, 50% ethanol and water were chosen as extraction solvent due to arithmetic progression of their polarity. Total polyphenol, flavonoid, β -carotene, tannin and vitamin C content of these three extracts were determined while their antioxidant potentials were assayed by total reducing power assay and 2, 2-diphenyl-1-picrylhydrazyl (DPPH)-scavenging activity. 50% ethanol extract of *C. asiatica* contained a significantly higher amount of polyphenol, flavonoid while moderate amount of carotene and tannin but the lowest amount of vitamin C compared to 100% ethanol and water extract. All the phytochemicals showed solvent polarity specific extraction patterns. Total reducing power and DPPH-radical scavenging activity of 50% ethanol extract also were significantly higher when compared to those of the 100% ethanol and water extracts. Significant variations of antioxidant potentials of *C.*

Keywords: DPPH, Scavenging Technique *Centellaasiatica*; extraction;

INTRODUCTION

Centella Asiatic (synonym: *Hydrocotyleasiatica* L.), belonging to the family of Mackinlayaceae is native to most of the countries of Asia. Being herbaceous, it contains stems which are long, filiform and prostrate with long internodes containing roots, 1-5 leaves per node which are 50-350cm in radius, reniformed, deeply cordate, long petioles and oval or orbicular in shape, 3-6 small flowers which are purple to white-green in color and are arranged in umbels arising from the axils of the leaves ¹. It grows well in both tropical and subtropical countries. It is a popular herb that is either consumed fresh, or processed into tea or juice. The plant has been claimed to exert various physiological effects and is traditionally used for various ailments including wound healing, bronchitis, asthma, diabetes, kidney troubles, urethritis, liver complaints, allergy, cancer, diuretic, and hypertension and to improve mental ability ². In ulcer, depression and venomous insufficiency *Centella Asiatic* is a potent drug ³⁻⁴. The plant is also found to improve the general behavior and mental ability of retarded children ⁵. The anti-diabetic property of *C. asiatica* has been known to the ancient people of Bangladesh for centuries that are following Ayurvedic system of medicine. Although the plant is being long used in our country, a very few chemical and pharmacological studies on the extract of this plant have been done in Bangladesh till now. The search for the phytochemical bioactive compounds from medicinal plant is always an alternative means of finding new drugs. Phytochemical screening of *C. asiatica* will lead to the rationalization of the use of this plant in various diseases as mentioned and will also lead to the discovery of specific causative compounds which have effective treatment roles against specific diseases ⁶. Alzheimer's disease (AD) is a progressive neurodegenerative disorder which has the characteristic features of memory impairment, cognitive dysfunction, behavior disturbances and deficits in activities of daily living ⁷. Although the etiology of the disease is still not very clearly known there are two major hypotheses which inadequately explain the molecular mechanism of AD, namely: the cholinergic hypothesis and the amyloid cascade hypothesis ⁸. The cognitive dysfunction in AD is supposed to be a result of degeneration of cholinergic neurons in the basal forebrain and associated loss of cholinergic neurotransmission in cerebral cortex and some other areas ⁹. The enzyme acetylcholinesterase (AChE) and butyrylcholinesterase (BChE) play an important role in the cholinergic deficit through enhanced degradation of the neurotransmitter acetylcholine (ACh). So, in most cases to improve neurotransmission and to alleviate cholinergic deficit, the focus is mainly on acetylcholinesterase (AChE) and butyrylcholinesterase (BChE) ¹⁰. According to the amyloid cascade hypothesis, AD is associated with the accumulation of β -amyloid (A β) fibrils and senile plaque in the brain parenchyma. Several studies have reported that increased oxidative stress has a potential role in the inflammatory processes that eventually lead to the lipid peroxidation and formation of A β ¹¹. Many studies have shown that increased level of free radicals and reactive oxygen species induced the degeneration of neurons ^{12,13,14}. Antioxidants can scavenge free radicals and ROS and can also attenuate inflammation pathways. Hence, antioxidants may be useful in the protection from neurodegeneration in AD. Although in some previous study ¹⁵. The effect of *C. asiatica* extract on the A β levels in the hippocampus of the AD animal model was observed; no study has yet been done on its cholinesterase (ChEs) inhibitory effect. Diabetes mellitus is a metabolic disease characterized by high blood glucose levels due to absolute or relative deficiency of circulatory insulin levels ¹⁶. It has an adverse effect on carbohydrate, lipid and protein metabolism resulting in chronic hyperglycemia and abnormality of lipid profile. These lead to a series of secondary complications including polyuria, polyphagia, ketosis, retinopathy as well as cardiovascular disorder ¹⁷. The disease is a major degenerative ailment in the world today, affecting at least 15 million people ¹⁹. Currently available therapy for diabetes includes insulin and various oral hypoglycemic agents such as sulfonylureas, metformin, glucosidase inhibitors, troglitazone, etc. But these are reported to produce serious adverse side effects such as liver problems, lactic acidosis and diarrhea. In addition they are not suitable for use during pregnancy. Moreover increased oxidative stress and generation of excessive free radicals in diabetic patients are thought to be the etiology of chronic diabetic complications. Increased reactive oxygen species and oxidative stress are observed in type-1 and type-2 diabetes mellitus in some studies. Besides, in diabetes glucose autoxidation, polyol pathway and non-enzymatic glycation of proteins lead to irregular formation of free radical ²⁰. This increased free radical generation along with a decreased antioxidant defense system may damage enzymes, cellular organelles, lipid peroxidation and further diabetic abnormalities. So, if any medicinal plant can work as a potential antioxidant together with having anti-diabetic property then it could prevent or reduce diabetic complication more effectively.

MATERIALS AND METHODS

Collection and Identification of plant materials

Fresh leaves of *C. asiatica* were collected from Savar, Dhaka, Bangladesh in July, 2011 and the plant samples were identified and authenticated by Bangladesh National Herbarium with accession number DACB 33537. 2.2 Preparation of plant extract leaves were washed with distilled water without squeezing to remove debris and dust particles, dried at room temperature and pulverized into a coarse material of about 1 mm in diameter. Pulverized powdered leaves (1.2 kg)² of the plant were macerated with 6.0 and 5.0 L of ethanol, respectively at room temperature for 15 days with occasional shaking. The ethanolic extracts of leaves were collected, filtered by cotton plug followed by whatman filter paper (no. 1) and evaporated to dryness (45°C) under reduced pressure by a rotary evaporator. The obtained crude extract was stored in a refrigerator at 4°C until time of use. The percentage yield of the extract was calculated using the formula below:

$$\% \text{ yield} = (\text{weight of the extract} / \text{weight of plant material}) \times 100$$

Photochemical Screening For preliminary phytochemical analysis the freshly prepared crude ethanolic extracts of leaves were tested for the presence or absence of phytoconstituents such as reducing sugar, tannins, flavonoids, saponins, gums, steroids and alkaloids by using standard phytochemical procedures .

Evaluation of antioxidant activity⁴⁻⁵

DPPH radical scavenging activity

The free radical scavenging activities of the ethanolic extracts of leaves of the plant on the stable radical 1, 1-diphenyl-2-picrylhydrazyl (DPPH) were estimated by the method of Brand-Williams

Inhibitions were calculated by using the following equation:

$$\% \text{ inhibition} = [1 - (\text{ABSsample} / \text{ABScontrol})] \times 100 \text{ ---- 1)}$$

Where ABScontrol is the absorbance of the control reaction (containing all reagents except the test material) and ABSsample is the absorbance of the sample material. Then percent inhibitions were plotted against respective concentrations. IC50 values were calculated as the concentration of each sample required to give 50% DPPH radical scavenging activity from the graph. Tert-butyl-1- hydroxytoluene (BHT) and Ascorbic acid were used as positive control¹⁵. The experiment was performed thrice and the result was expressed as Mean±Standard Error of Mean (SEM) in every case.

Superoxide radical scavenging activity :

The super oxide radical scavenging activity was assayed by the nitro blue tetrazolium reduction method which is based on the capacity of the sample to inhibit blue formazan formation by scavenging the superoxide radicals generated in -sodium carbonate-EDTA-NBT system. 1 mL of 50 mM sodium carbonate, 0.4 mL of 24 µM nitrobluetetrazolium and 0.2 mL of 0.1 mM EDTA were taken in a test tube¹⁵⁻¹⁶. Then 100 µL of plant extract (conc. ranging from 1000 µg/mL to 7.513 µg/mL) was added to the test tube. Reaction was initiated by adding 0.4 mL of 1 mM hydroxylamine hydrochloride. The reaction mixture was incubated for 5 min at ambient temperature and then the absorbance at 562 nm was measured against an appropriate blank to determine the quantity of formazan generated¹⁸. The percentage inhibition of superoxide anion generation (I %) was calculated by formula (1). The experiment was performed and the result was expressed as mean±SEM in every case.

Anti-diabetic study :

Alloxan monohydrate solution of 10 mg/ml was prepared in ice-cold citrate buffer (0.1M); pH of the ice was kept at 4.5 and was administered to the rats within 5 mins at a dose of 50 mg/kg bodyweight intraperitoneally¹². The fasting blood sugar levels of each of the rats were checked every day with an autoanalyzer (Glucometer, Bioland G-423 S) glucose kit. After 8 days, animals with fasting blood sugar levels of 250 mg/dl and above were considered to be diabetic and were used for the study and assigned into five groups of five rats each. Group I served as the negative control and received tween 80 solutions (solvent used to dissolve the extract) (10 ml/kg), group II-IV received the *C. asiatica* extract at the dose of 250, 500 and 1000 mg/kg respectively while group V served as the positive control and received the standard reference drug glibenclamide (2 mg/kg) all by gastric gavage. The blood glucose levels of the rats were measured at 0, 1, 2 and 3 h after administration of drug and extracts. Blood samples were collected by tail snipping the blood glucose measured with an autoanalyzer (Glucometer, Bioland G-423 S) glucose kit. At the end of the experiment percentage¹⁵.Results were presented as mean±Standard Error of Mean (SEM) and the statistical analysis was done using one way reduction of the glucose levels of the rats at the 3rd hour was calculated using the formula below:

$$\% \text{ reduction in glucose level} = \{(\text{V}0 - \text{V}t) / \text{V}0\} \times 100$$

Where V0= value at zero hour and Vt= value at subsequent hours.

Maceration

Maceration is a technique in which plant materials are soaked in a solvent at a specific temperature and time .The extract from this method is concentrated using a rotary evaporator to obtain the final solvent-free crude extract. This process softens the plant cells and eventually releases the bioactive compounds from the cells. The solvent used for maceration is based on the study objectives. Maceration is a simple extraction method and has broad applicability. However, it has a long extraction time, high temperature, high mass transfer resistance, low extraction efficiency, and requires a large volume of solvent ¹⁷.

In the case of *C. asiatica*, organic solvents like ethanol, methanol, or a mixture of alcohol and water are typically used. Aqueous extracts obtained by this technique usually show antioxidant and cytotoxic activity. Maceration has also been used in cosmetics manufacturing, in which propylene glycol and water are used as solvents, and the leaves and stalks of *C. asiatica* are extracted for a few days. In a study by Monton et al. using maceration, the highest amounts of madecassoside, asiaticoside, madecassic acid, and asiatic acid (0.855%, 0.174%, 0.053%, and 0.025%, respectively) were extracted at optimal conditions of 60 °C and 120 min extraction time. In a study using cold maceration, Pittella et al. obtained phenolic and flavonoid constituents from *C. asiatica*. Maceration of *C. asiatica* is also able to extract various types of compounds such as triterpenoids, flavonoids, phenolics, saponins, alkaloids, tannins, and carotenoids, primarily based on the solvents used and period of extraction.²⁰

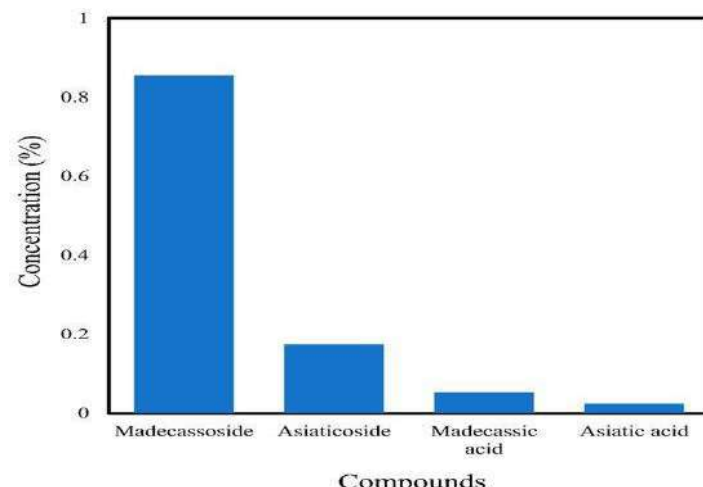


Figure 2. Triterpenoids found in *Centella asiatica* extract using the maceration method of Monton et al.⁶

Distillation

Distillation is the separation of components at a particular boiling point and condensation. There are two types of distillation used in extraction: steam distillation that is performed by passing dry steam through the plant material, and water distillation in which elevated pressure is used with plants whose essential oil is difficult to extract at a higher temperature. Steam distillation using distilled water and vinegar has been used to extract dry and fresh leaves of *C. asiatica*. Steam distillation is an efficient technique for obtaining the best quality of oil, and by employing fresh leaves over dry leaves in extraction, many constituents can be detected. The essential oil of *C. asiatica* obtained from steam distillation yielded more sesquiterpenoid hydrocarbons; 43 constituents were identified, representing 98.60% of the composition of the oil. On the other hand, water distillation is an excellent method for extracting caryophyllene and monoterpenoid hydrocarbons from *C. asiatica*; 54 constituents were identified, representing 98.29% of the total composition. However, water distillation utilizes a tremendous amount of water besides consuming a lot of energy and time. A study by Orhanetal.successfully extracted 47 components representing 88.9% of the essential oil. The dominant compound was α -copaene (22.0%), followed by alloaromadendrene (7.6%), β -caryophyllene (7.1%), α -humulene (6.7%), and β -cubebene (5.9%). Paudel et al.discovered that distillation of 85 g of dry *C. asiatica* leaves for 4 h extracted a 0.05% yield of essential oil composed of 33 compounds. The essential oil was rich in sesquiterpene hydrocarbons (74.1%) and oxygenated sesquiterpenoids (13.0%), the most abundant compounds being β -farnesene (26.5%), α -humulene (20.9%), β -caryophyllene (13.3%), and falcarinol (8.8%) (Figure 3).

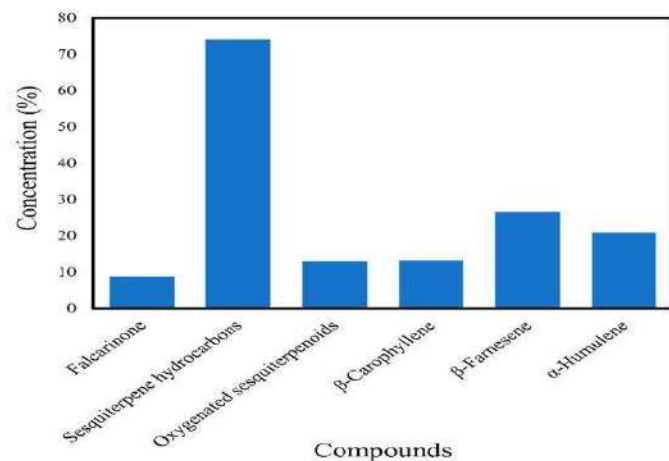


Figure 3. Compounds obtained from *Centella asiatica* using the distillation method of Paudel et al. 2.3. Soxhlet Extraction

Soxhlet extraction has also been used to obtain the crude extract of *C. asiatica*, which will be later screened for its antimicrobial activity. Several organic solvents such as hexane, chloroform, methanol, petroleum ether, acetone and water have been used in

the extraction for this purpose. Byakodi et al. discovered that the methanolic extract of *C. asiatica* from the Soxhlet method contained phenols, tannins, flavonoids, terpenoids, saponin, and alkaloids. Another study by ThamaraiSelvi et al. found that 500 g of powdered *C. asiatica* subjected to Soxhlet extraction for 8 h using an ethanol to solid ratio of 1:4 resulted in extracts containing saponins, terpenoids, alkaloids, and phenols but no steroids, flavonoids, tannins, proteins, carbohydrates, or glycosides. In a preliminary phytochemical screening of the *C. asiatica* extract, Jayaprakash and Nagarajan discovered the existence of alkaloids, saponins, flavonoids, phenols, steroids, tannins, glycosides, triterpenoids, and terpenoids. The extract also contained 1–8% saponins, 0.1% volatile oils, triterpenic acids (e.g., terminolic acid, brahmic acid, centellic acid, madasiatic acid), and glycosides (e.g., madasiaticoside, brahminoside, centelloside). Rahman et al. used 100% ethanol, 50% ethanol, and water as solvents for Soxhlet extraction to obtain total polyphenols, flavonoids, β -carotene, tannins, and vitamin C from *C. asiatica*. The study showed that the 50% ethanol extract of *C. asiatica* contained a significantly higher amount of polyphenols and flavonoids while 100% ethanol extracted the highest amount of β -carotene and tannins. On the other hand, the water extract of *C. asiatica* contained more vitamin C than the 50 and 100% ethanol extracts

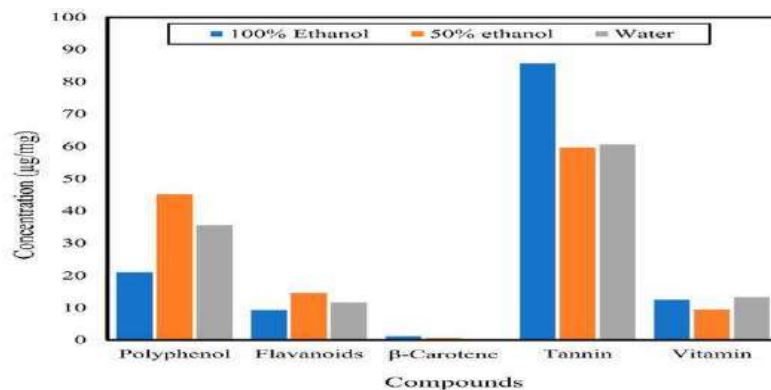


Figure:4

DISCUSSION

Several methods have been used to extract compounds from *C. asiatica*. The efficiency of extraction is based on the extraction method, extraction solvent, and extraction time. The desired compounds extracted also influence the choice of extraction method aside from cost and availability. Among the applications, the antimicrobial action of *C. asiatica* has been widely studied, mostly in extracts obtained conventionally¹³. To date, very few microbial species have been tested using *C. asiatica* extracts obtained by modern extraction techniques. Thus, more studies are necessary for these extracts to determine their effect on microorganisms. The modern extraction techniques also seem to be more promising for obtaining antimicrobial compounds in terms of cost, time, and better efficacy toward certain microbes compared to conventional techniques¹⁵. In particular, solventless extraction hinders the possible retention of the chemical solvent in the extract.

CONCLUSION

Therefore, the extracts obtained from these modern techniques are worthy as antimicrobial agents. Both in vitro and in vivo studies have shown that *C. asiatica* possesses antimicrobial activity, although there have been few in vivo studies due to their complexity. Nevertheless, the extracts have the potential to be used in the medicinal, cosmeceutical, and food sectors.

CONFLICT OF INTEREST

Conflict of interest declared none.

REFERENCES

- Ullah, M. O., Sultana, S., Haque, A., & Tasmin, S. Antimicrobial, cytotoxic and antioxidant activity of *Centellaasiatica*. *J. Sci. Res.*, 2009; 30(2): 260-264.
- Oyedele, O. A., Afolayan, A. J. Chemical composition and antibacterial activity of the essential oil of *Centellaasiatica* growing in South Africa. *Biol.*, 2005; 43(3): 249-52.
- Gershenzon, J., Dudareva, N. The function of terpene natural products in the natural world. *Nat Chem Biol.*, 2007; 3(7): 408-414.
- Arumugam, T., Ayyanar, M., Pillai, Y.J.K., Sekar, T. Phytochemical screening and antibacterial activity of leaf and callus extracts of *Centellaasiatica*. *Bangladesh J. Pharmacol.*, 2011; 6(1): 55-60.
- Pitinandhipat, N., Yasurin, P. Antibacterial Activity of *Chrysanthemum indicum*, *Centellaasiatica* and *Andrographispaniculata* on *Bacillus cereus* and *Listeria monocytogenes* under Osmotic Stress. *AU J. T.*, 2012; 15(4): 239-245.
- Utami, C.V., Pitinandhipat, N., Yasurin, P. Antibacterial Activity of *Chrysanthemum indicum*, *Centellaasiatica* and *Andrographispaniculata* on *Bacillus cereus* and *Listeria monocytogenes* under Low pH Stress. *KMITL Sci. Tech. J.*, 2012; 12(1): 49-54.

7. Mamtha, B., Kavitha, K., Srinivasan, K.K., Shivananda, P.G. An in vitro study of the effect of *Centellaasiatica* [Indian pennywort] on enteric pathogens. *Indian J. Pharmacol.*, 2004; 36(1): 41-44.
8. Lee, T.K., Vairappan, C.S. Antioxidant, antibacterial and cytotoxic activities of essential oils and ethanol extracts of selected South East Asian herbs. *Med. Plants. Res.*, 2011; 5(21): 5284-5290.
9. Samy, P.R., Ignacimuthu, S. Antibacterial activity of some folklore medicinal plants used by tribals in Western Ghats of India. *Ethnopharmacol.*, 2000; 69(1): 63-71.
10. Dash, B.K., Faruquee, H.M., Biswas, S.K., Alam, M.K., Sisir, S.M., Prodhan, U.K. Antibacterial and antifungal activities of several extracts of *Centellaasiatica* against some human pathogenic microbes. *Life. Sci. Med. Res.* 2011; (2011): 1-4.
11. Jagtap, N.S., Khadabadi, S.S., Ghorpade, D.S., Banarase, N.B., Naphade, S. Antimicrobial and antifungal activity of *Centellaasiatica* (L.) Urban, *Umbelliferae*, *Reseach. J. Pharm. and Tech.*, 2009; 2 (2):328-330.
12. Pittella, F., Dutra, R.C., Junior, D.D., Lopes, M.T., Barbosa, N.R. Antioxidant and cytotoxic activities of *Centellaasiatica* (L) Urb. *J. Mol. Sci.*, 2009; 10(9): 3713-3721.
13. Kormin, S. The effect of heat processing on triterpene glycosides and antioxidant activity of herbal pegaga (*Centellaasiatica* urban) drink [dissertation]. UniversitiTeknologi Malaysia; 2005.
14. Aiyeoro, O. A., and Okoh, A. 2009. Preliminary phytochemical screening and *In vitro* antioxidant activities of the aqueous extract of *Helichrysumlongifolium*DC. *BMC Complementary and Alternative Medicine*, 10: 21
15. Aoki, T., Akash, T., Ayabe, S. Flavonoids of leguminous plants: Structure, biological activity, and biosynthesis. *Journal of Plant Research*. 113; 475-488.
16. Arunkumar, S., Muthuselvam, K. 2009. Analysis of phytochemical constituents and antimicrobial activities of *Aloe vera* L. against clinical pathogens. *World J. Agril. Sc.*, (5)572-576.
17. Ashok Kumar, D., Mazumder, U. K., Gupta, M., Senthil Kumar, G. P, Selvan, V. T. Evaluation of antioxidant and free radical scavenging activities of *Oxystelmaesculentum* in various *in vitro* Models. *J Comp Integ Med* 2008, 5 (1): 9.
18. Awah, F. M., Uzoegwu, P. N., Oyugi, J. O., Rutherford, J., Ifeonu, P., Yao, X. J., Fowke, K. R., Eze, M., O. 2010. Free radical scavenging activity and immunomodulatory effect of *Stachytarphetaangustifolia* leaf extract. *Food Chemistry*, 119: 1409–1416.
19. AzimaLamarck, Encycl. I: 343. 1783. Fl. China 11: 497. 2008.
20. Azizova, O. A. 2002. Role of free radical processes in the development of atherosclerosis. *Biologicheskie Membrany*, 19: 451-4.

Assessment of Liver Profile in Multi Drugs Resistant (MDR) Tuberculosis Patients on Treatment

Pradhumna Katara*, Juhi Aggarwal*, Hunny Tyagi*, Sojit Tomo*, Jyoti Batra*

*Santosh Deemed to be University, Ghaziabad, Uttar Pradesh -201009. Corresponding Author: Dr. sojito@sojito@gmail.com

Abstract: *M. tuberculosis* mainly infects the lungs, which is known as pulmonary tuberculosis, but it can infect other organs also such as the gastrointestinal tract, central nervous system, lymph nodes, bones, joints, urinary tract, and other sites, which is known as extrapulmonary tuberculosis. Drug-resistant *M. tuberculosis* isolates are a serious threat to TB control because only a few effective drugs are available for the treatment of this disease. Directly observed treatment short course (DOTS) is the main pillar employed for the control of tuberculosis under the National Tuberculosis Elimination Programme (NTEP) in India. Treatment of tuberculosis either drug-sensitive or drug-resistant involves drugs that are potentially hepatotoxic and may lead to drug-induced liver injury (DILI). Research has noticed the inevitability and cyclicity of pandemics during the last two centuries and highlighted it through smallpox, Tuberculosis, Plague, Influenza, HIV/AIDS, Ebola, and COVID-19.¹⁸

Keywords: *M. tuberculosis*, Tuberculosis, Plague, Influenza, HIV/AIDS, Ebola, and COVID-19

INTRODUCTION

Tuberculosis (TB) is a major public health problem in the Indian subcontinent. TB is spread from person to person through droplet infection in the air. Although the most commonly affected organ is the lungs (pulmonary TB), other organs such as the brain, spine, bones may also get affected by TB bacilli (extra-pulmonary TB)¹. *Mycobacterium tuberculosis* is a non-motile, non-spore-forming; obligate aerobe, acid-fast bacillus. As it multiplies more slowly than the majority of bacteria, *Mycobacterium tuberculosis* has a slower evolution. Mycolic acids present in the cell wall of *Mycobacterium tuberculosis* make the cell wall extremely hydrophobic and enhance resistance to desiccation, disinfectants, and drugs. These unique features of the *Mycobacterial* cell wall structure provide the basis for special laboratory considerations when performing direct stains from specimens, growing organisms in culture, and determining species identification by molecular methods². As *M. tuberculosis* is a strictly aerobic bacterium it, therefore, multiplies better in pulmonary tissue (in particular at the apex, where oxygen concentration is higher) than in the deeper organs. India has the highest burden of tuberculosis accounting for one-fifth of global TB incidence with 1.9 million new cases occurring every year and 0.87 million being smear-positive infections³. Tuberculosis is an important health problem requiring early diagnosis for timely initiation of therapy and control of disease transmission⁴. Drug-resistant TB has emerged now as a major public health threat. Worldwide in 2019, close to half a million people developed Rifampicin-resistant TB (RR-TB), of which 78% had multidrug-resistant TB (MDR-TB)^{5,6}. The three countries with the largest share of the global burden were India (27%), China (14%), and the Russian Federation (9%). Globally in 2019, 3.4% of new TB cases and 17.7% of previously treated cases had MDR/RR-TB. The highest proportions (>50% in previously treated cases) were in countries of the former Soviet Union. Despite the availability of effective anti-tubercular chemotherapy for more than fifty years and major advances in the biology and epidemiology of *Mycobacterium tuberculosis*, pulmonary and extrapulmonary tuberculosis remains the leading cause of mortality and morbidity both in adults and children due to its disease progression and also because of unwanted toxic side effects of drugs leading to the involvement of the liver, kidney and other parts of the body⁷. Treatment for TB can cause reactions such as skin rash, visual and gastrointestinal disturbance, and neurological disorders. However, the most common side effect is hepatotoxicity which can range from a transient rise in transaminases to acute liver failure or even death when therapy is not interrupted⁸. Treatment of multidrug resistance (MDR) tuberculosis is expensive and riddled with increased adverse effects. Hepatotoxicity can prolong the duration of illness and diminish treatment effectiveness by contributing to non-adherence and treatment failure. This can lead to relapse and even the emergence of drug resistance⁹. Limited studies have been done on hepatotoxicity involving MDR-TB patients in India. The present study aimed to screen subjects with multidrug resistance (MDR) tuberculosis and analyze their liver function to evaluate the prevalence of hepatotoxicity in Indian patients with MDR tuberculosis.

MATERIAL AND METHODS

The study was carried out at the chest clinic and Department of Biochemistry, Santosh Deemed to be University in collaboration with the Intermediate Reference Laboratory New Delhi Tuberculosis Centre (NDTBC) New Delhi from September 2019 to August 2020. Pulmonary Tuberculosis (TB) positive patients aged between 18 and 65 years and on ATT treatment were recruited for the study. Pediatric / Old age patients, patients with extrapulmonary TB, HIV / AIDS Patients, HBV/HCV positive patients, transplant recipients, and patients with any previous history of liver disorder were excluded from the study. A total of 50 Drug-resistant TB patients were enrolled in the study following inclusion criteria and were followed up at 3rd and 06th months. Details of patients in the form of demographic information, clinical history, weight, etc. were recorded on a pre-defined proforma. The recruited subjects were instructed to provide a sputum sample (3-5ml) as per National Tuberculosis Elimination program (NTEP) guidelines. 5 ml of whole blood was collected in Plain and EDTA Vials for further hematological and biochemical examinations. Investigations including Sputum microscopy by Fluorescent Microscopy (FM), Gene-expert, Line Probe Assay First Line (FL) and Second Line (SL), and Biochemical Test such as Hemoglobin and Liver Function Tests (Serum Bilirubin, SGOT, SGPT & Alkaline Phosphatase (ALP)) were performed at baseline and follow-up visits.

RESULTS

Demographic information of the patients

The average age of the study patients was 29.7 years (range: 18 – 58 years). The majority of the patients were in the age group of 18 – 27 years (56%) followed by 28 – 37 years of age (20%). Among entire patients; 68% were the males (N = 34) and remaining were the females 32% (N = 16). In the study, the majority (76%) of the enrolled patients were married (N = 38). Further, among the study population, the majority of the patients were MDR (60%; N = 30) and the remaining were Rifampicin resistant and Isoniazid sensitive (40%; N = 20).

Baseline laboratory parameters:

The baseline parameters for the recruited study subjects are given in Table 1. At baseline, we observed nearly all (except two) participants to have normal serum levels. Serum SGOT of 07 participants was elevated at baseline. 13 participants had elevated serum SGPT at baseline. However, the baseline serum ALP of all participants was elevated.

Table 1: Baseline parameters for the recruited study subjects

Parameters	Total participants (N = 50) Average (Range)	Male (N = 34) Average (Range)	Female (N = 16) Average (Range)
Weight (Kg)	46.4 (19 - 70)	49.7 (28 – 70)	39.4 (19 – 50)
Hemoglobin (g/dl)	11.45 (8.2 - 15)	12.0 (9.5 – 15)	10.2 (8.2 – 11.8)
S.Bilirubin (mg/dl)	0.83 (0.3 – 8.2)	0.7 (0.3 – 2)	7.2 (0.45 – 8.2)
SGOT (unit/L)	35.8 (7 – 29.6)	32.4 (7 – 110)	42.9 (8 – 29.6)
SGPT (unit/L)	33.8 (12 – 109)	31.8 (12 – 105)	38 (15 – 109)
ALP (IU/L)	110.5 (65 – 319)	102 (65 – 145)	129 (73 – 319)

Follow-up of laboratory parameters at 3 months:

The laboratory parameters at the 3rd-month follow-up for the recruited study subjects are given in Table 2.

Table 2: Laboratory parameters at 3rd-month follow-up for the recruited study subjects

Parameters	Total participants (N = 50) Average (Range)	Male (N = 34) Average (Range)	Female (N = 16) Average (Range)
Weight (Kg)	47.5 (30 – 74)	50.3 (30 – 74)	41.5 (30 – 50)
Hemoglobin (g/dl)	11.6 (8.2 – 14.2)	12.1 (9.8 – 14.2)	10.6 (8.2 – 12.8)
S.Bilirubin (mg/dl)	0.7 (0.4 – 1.7)	0.7 (0.4 – 1.7)	0.7 (0.4 – 1.4)
SGOT (unit/L)	42.8 (12 – 190)	50.6 (15 – 190)	26.4 (12 – 62)
SGPT (unit/L)	38.6 (14 – 146)	42.8 (18 – 146)	29.8 (14 – 81)
ALP (IU/L)	122 (60 – 989)	135 (68 – 989)	95 (60 – 182)

During follow-up after 3 months, all the participants showed an increase in body weight ranging from 30 to 70 Kg. Hemoglobin was comparable to the baseline values. Serum SGOT of the study population was slightly elevated as compared to the baseline. Serum SGPT is found to be slightly elevated at the third month of follow-up as compared to baseline. However, serum ALP was slightly elevated when compared to baseline. 04 male patients had significantly higher serum ALP levels ranging from 175 – 989 IU/L. At 3 months follow up, we observed 10% of the study population to be having Grade 3 and 2 % of the study population to be having Grade 4 Hepatotoxicity as per the WHO definition. The number of participants having each grade has been mentioned in Table 3.

Table 3: WHO Adverse Drug-induced hepatotoxicity classification at 3rd-month follow-up

WHO definition of Value	Number of participants
-------------------------	------------------------

hepatotoxicity		
Grade 1	<2.5 times ULN (ALP 51–125 U/L)	44
Grade 2 (mild)	2.5–5 times ULN (ALP 126–250 U/L)	05
Grade 3 (moderate)	5–10 times ULN (ALP 251–500 U/L)	00
Grade 4 (severe)	>10 times ULN (ALP > 500 U/L)	01

Follow-up of laboratory parameters at 6 months

The laboratory parameters at the 6th-month follow-up for the recruited study subjects are given in Table 4. The bodyweight of all the participants during the 06th month of follow-up revealed continuous improvement ranging from 34 - 72 Kg. Hemoglobin also markedly improved when compared with the baseline and 03rd follow-up. Serum Bilirubin was comparable with the baseline and the 3rd monthly follow-up values. There was marked improvement in the serum SGOT level of most of the study population in the 06th month of follow-up. The serum SGPT level of the majority of the study participants was within the normal range. Noticeable improvement was seen in the serum ALP levels at the 06th month of follow-up.

Table 4: Laboratory parameters at 6th-month follow-up for the recruited study subjects

Parameters	Total participants (N = 50) Average (Range)	Male (N = 34) Average (Range)	Female (N = 16) Average (Range)
Weight (Kg)	48.9 (34 – 72)	51.7 (34 – 72)	43 (37 – 51.4)
Haemoglobin (g/dl)	11.8 (8.9-15.2)	12.3 (8.9-15.2)	10.8 (9.5-12.4)
S.Bilirubin (mg/dl)	0.8 (0.4 – 1.3)	0.8 (0.1 – 1.3)	0.8 (0.4 – 1.2)
SGOT (unit/L)	42.6 (18 – 91)	45.7 (20 – 91)	36.2 (18 – 88)
SGPT (unit/L)	47.6 (15 – 126)	51.5 (16 – 126)	39.2 (15 – 96)
ALP (IU/L)	119 (51 – 263)	120 (56 – 255)	115 (51 – 263)

At 6 months follow up, we observed 28% of the study population to be having Grade 2 and 4% of the study population to be having Grade 3 and none having Grade 4 Hepatotoxicity as per the WHO definition. The number of participants having each grade has been mentioned in Table 5.

Table 5: WHO Adverse Drug-induced hepatotoxicity classification at 6th-month follow-up

WHO definition of hepatotoxicity	Value	Number of participants
Grade 1	<2.5 times ULN (ALP 51–125 U/L)	34
Grade 2 (mild)	2.5–5 times ULN (ALP 126–250 U/L)	14
Grade 3 (moderate)	5–10 times ULN (ALP 251–500 U/L)	02
Grade 4 (severe)	>10 times ULN (ALP > 500 U/L)	00

DISCUSSION

Tuberculosis is one of the leading infectious causes of death among adults globally, accounting for an estimated 1.7 million deaths each year. MDR-TB has been observed to have increased morbidity and mortality. The treatment of MDR-TB is drug intensive and involves multiple second-line anti-tuberculosis agents given over 18–24 months ¹⁰ One of the main concerns about MDR-TB regimens is their potential to cause adverse effects. The development of hepatotoxicity including hepatitis (hepatocellular necrosis), cholestasis (impairment of bile flow), and zonal necrosis—is one of the most commonly reported adverse effects associated with first- and second-line anti-tuberculosis treatment ¹¹ Drug-induced liver injury (DILI) secondary to antituberculous treatment (ATT) is reported in 2–28% of patients ¹². The prevalence of DILI is much higher in developing countries owing to several factors such as acute or chronic liver disease, alcoholism, malnutrition, indiscriminate drug use, advanced TB, and other coexisting chronic illness. ATT drugs may cause hepatotoxicity ranging from a transient asymptomatic rise in liver enzymes to acute liver failure. The reported mortality from DILI after the development of jaundice varies from 4% to 12%. It is to be noted that the frequency of DILI in different countries varies widely from 2% to 39% ¹³ In our study, the majority of the study population were in the age group of 18 – 47 years which is considered to be an economically productive age group for any of the country. This is in line with many of the studies which have also found a similar type of observation ¹⁴. Rifampicin (RIF) was introduced in 1972 as an antituberculosis drug and has excellent sterilizing activity. It is a bactericidal drug that kills growing,

metabolically active bacilli, as well as bacilli in the stationary phase, during which metabolism is reduced. Rifampicin inhibits the gene transcription of mycobacteria by blocking the DNA-dependent RNA polymerase, which prevents the bacillus from synthesizing messenger RNA and protein, causing cell death ¹⁵. On the other hand, Isoniazid (INH) is one of the most effective and specific antituberculosis drugs and it is introduced in 1952. It has a bactericidal effect on rapidly growing bacilli and has a limited effect on slow-growing and intermittently growing bacilli. Isoniazid is a prodrug and is activated by the *M. tuberculosis* catalase-peroxidase enzyme *KatG*. The activation of isoniazid produces oxygen-derived free radicals (superoxide, hydrogen peroxide, and peroxy nitrite) and organic free radicals that inhibit the formation of mycolic acids of the bacterial cell wall, causing DNA damage and, subsequently, the death of the bacillus. INH is only active against growing tubercle bacilli and is not active against non-replicating bacilli or under anaerobic conditions. Mutations in several genes, including *KatG*, *alpC*, and *inhA*, have all been associated with isoniazid resistance. When TB bacteria are resistant to at least isoniazid and rifampin, the two most potent TB drugs, the disease is termed as Multidrug-Resistant tuberculosis. These MDR cases are difficult to treat with an extensive duration of treatment, more side effects, and a high financial burden to the patient and its family. In this study 60% of the study population is MDR and 40% are Rifampicin resistant and Isoniazid sensitive. Our study demonstrates a slight non-significant elevation in liver enzymatic profile till the third month of follow-up. In our study, none of the known liver markers mentioned were significantly associated with DILI. This is interesting as many of these markers are independently and significantly associated with DILI in different studies. The development of DILI during TB treatment is the most common reason leading to interruption of therapy. However, in a UK based study, the drug-induced liver injury (DILI) expert working group categorically stated that it may not be appropriate to say that anti-TB drugs are a causative agent for granulomatous hepatitis with raised ALP, but instead of that, a rising ALP on treatment may indicate a paradoxical reaction rather than true DILI ¹². The incidence of DILI from TB treatment was reported from Taiwan at 12% (111/926) within a median of 38 days from the initiation of treatment and China at 10.4% (267/2457) within the first 2 months of treatment ¹⁶. Independent risk factors for DILI in these studies came out to be overweight/ obesity status, high alcohol intake, and HBV co-infection. The use of alcohol and co-infection with HIV or viral hepatitis is often considered to be a major predisposing risk factor for the development of hepatitis among patients on anti-tuberculosis treatment ¹⁷. However, we in our study, have not included alcoholic, HIV reactive, or HBV/HCV positive patients. The limited sample size and short follow-up duration are the limitations of our study.

CONCLUSION

The therapeutic approach in DILI is quite demanding. According to the present recommendations, anti-TB drugs should be suspended until the normalization of liver function ¹⁸⁻¹⁹. The American Thoracic Society recommends the initiation of a new treatment regimen provided that liver enzymes are below twice the upper limit of normal ²⁰. Reintroduction of hepatotoxic ATT drugs must be balanced carefully with their benefit by thorough supervision and close monitoring of baseline laboratory testing ²⁰⁻²¹. Our study demonstrates that at 6 months, 28% of the study population had Grade 2 and 4% of the study population had Grade 3 Hepatotoxicity as per the WHO definition. Further, long-term studies are necessary to understand the hepatic adverse effects of these drugs and their role in the quality of life in MDR tuberculosis patients.

CONFLICT OF INTEREST

Conflict of interest declared none.

REFERENCES

1. Ravilione M, Sulis G. Tuberculosis 2015: Burden, Challenges, and Strategy for Control and Elimination. *Infect Dis Rep* 2016;8:6570.
2. Cruz A, Starke J. 2014. Tuberculosis, p 1335–1380. In Cherry J, HarrisonG, Kaplan S, Steinbach W, Hotez P (ed), Feigin and Cherry's textbook of pediatric infectious diseases. Elsevier Saunders,Philadelphia,PA.
3. Colon DL, Bustero F, and Ravilione MC. Drugs resistant tuberculosis: a review of worldwide situation and the WHO/IUATLD global surveillance project. *Clin Infect Dis* 24 1997:S121-30.
4. Central TB Division, Indian medical association, and WHO-INDIA Training module for Medical Practitioners. RNTCP Guideline Dec 2010.
5. Comas I, GagneuxS. The past and future of tuberculosis research. *PLoS Pathog* 2009; 5(10): e1000600
6. Cruz A, Starke J. 2014. Tuberculosis, p 1335–1380. In Cherry J, HarrisonG, Kaplan S, Steinbach W, Hotez P (ed), FeiginCherry's textbook of pediatric infectious diseases. Elsevier Saunders,Philadelphia,PA.
7. Kallmann F &Reisner D 1942. Twin studies the significance of genetic factors in tuberculosis. *Am Rev Tuberc*, 47: 549-547.
8. Baddeley A, Dean A, Monica-Dias H, Falzon D, Floyd K, Garcia I. Global Tuberculosis Report 2013. World Health Organization. 2013; 306.
9. R.P. Cusack, L. Chawke, D.J. O'Brien, B. O'Connor and T.M. O'Connor Predictors of hepatotoxicity among patients treated with antituberculous medication 24 September 2016.
10. Chaudhuri AD. Recent changes in guidelines on programmatic management of drug-resistant tuberculosis in India 2019: a paradigm shift in tuberculosis control The Journal of Association of Chest Physicians. 2020:8 (2); 53 – 63.
11. Durand F, Jebrak G, Pessaire D, Fournier M, Bernau J (2016). Hepatotoxicity of antitubercular treatments: rationale for monitoring liver status. *Drug Safety*; 16: 394–405.
12. Abbara A, Chitty S, Roe JK, Ghani R, Collin S, Ritchie A. (2017). Drug-induced liver injury from antituberculous treatment: a retrospective study from a large TB center in the UK. *BMC Infectious Diseases*; 17: 231- 240.

13. Tostmann A, Boeree MJ, Aarnoutse RE, de Lange WC, van der Ven AJ, Dekhuijzen R (2008). Anti-tuberculosis drug-induced hepatotoxicity: a concise up-to-date review. *J Gastroenterol Hepatol.*; 23:192–202
14. India TB report, 2019. Revised National TB Control Programme Annual Report, Central TB Division, Min. of Health Govt. of India; I – 244.
15. Ramaswamy S, Musser JM. Molecular genetic basis of antimicrobial agent resistance in *Mycobacterium tuberculosis*: 1998 update. *Tuber Lung Dis.* 1998;79(1):3-29
16. Devarbhavi H. Antituberculous drug-induced liver injury: current perspective. *Trop Gastroenterol.* 2011 Jul-Sep;32(3):167-74
17. Keshavjee S, Gelmanova I. Y, Shin S. S, Mishustin Y S, Andreev P. G, Atwood S, Furin J. J, Miller A. (2012). Hepatotoxicity during treatment for multidrug-resistant Tuberculosis: occurrence, management, and outcome. *Int j tube lung dis* 16(5): 596–603.
18. Singh, U. N. (2021) "After The Deluge: An Action Notebook for a Responsible Sociolinguist", IARS' International Research Journal. Vic. Australia, 11(1), pp. 44–50. DOI: 10.51611/iars.irj.v1i1.2021.155.
19. Saha A, Shanthi F X M, Winston A B, Das S, Kumar A, Michael JS, Balamugesh T. Prevalence of Hepatotoxicity From Antituberculosis Therapy: A Five-Year Experience From South India. *J Prim Care Community Health.* 2016 Jul;7(3):171-4
20. Saukkonen JJ, Cohn DL, Jasmer RM, Schenker S, Jereb JA, Nolan CM, Peloquin CA, Gordin FM, Nunes D, Strader DB, Bernardo J, Venkataraman R, Sterling TR; ATS (American Thoracic Society) Hepatotoxicity of Antituberculosis Therapy Subcommittee. An official ATS statement: hepatotoxicity of antituberculosis therapy. *Am J RespirCrit Care Med.* 2006 Oct 15;174(8):935-52
21. JyotiBatra, V.K. Arora, Oxidative Stress and Tuberculosis; *Indian J Tuberc.* 2014 61 183-185

A Review On Green Synthesis Of Cu And CuO Nanomaterials And Its Applications Comparing Some Medicinal Plants Evaluating Using Sem & Edx Analysis

S.Suguna*, S.Sathyakumar, V.Vijayakumar, M.Deepa

Dhanalakshmi Srinivasan College of Arts and Science for Womens (autonomous) perambalur.621212

Abstract: Green routes of synthesis are simple, safe, nontoxic and eco-friendly methods to synthesize nanoparticles of various metals and their oxides by the application of bioactive compounds of plants, algae, fungi, yeast, etc. Green engineered copper and copper oxide nanoparticles (Cu and CuO NPs) synthesis has been reported to be more economical and best alternative method among available methods. Cu and CuO NPs have been applied as dietary additives, lubricant supplements, chemical sensors, coating materials in addition to a large number of biotechnological and pharmaceuticals applications. The present review aims to bring awareness about various aspects of biogenic synthesis of Cu and its oxide NPs for multifunctional applications and discusses their characterization techniques and applications in antimicrobial activity of chenopodium album and evaluating its spectral studies by using SEM & EDX analysis.

Keywords: Antimicrobial activity; Catalysis; Cu and CuO NPs; Green synthesis; Multifunctional.

INTRODUCTION

The research on synthesis and characterization of metallic nanomaterials is an emerging field of nanotechnology due to applications of nanoparticles for scientific, technological, pharmacological and biomedical sectors. Various physical and chemical routes have been employed to synthesize nanoparticles. The chemical method of synthesizing nanoparticles is an extremely costly affair with additional environmental and biological risk. But biogenic synthesis which involves plants for the production of nanoparticles, is a cheap, less costly and environment-friendly method. Metallic nanoparticles are multifunctional in nature and hence finds huge number of applications in various sectors for environmental, biomedical and antimicrobial, solar power generation and catalytic causes.¹ Application of plant extracts to synthesize copper and its oxide nanoparticles is a green chemistry methodology which establishes strong relationship between natural plant material and nanosynthesis.² It has been reported in the earlier works^{3,4} that copper, gold and silver nanoparticles exhibited excellent antimicrobial activity against various disease -causing pathogens. In recent years, copper nanoparticles (Cu NPs) have gained significance due to their multifunctional uses in industries and medicine. However, other nanoparticles, such as platinum, gold, iron oxide, silicon oxides and nickel have not shown bactericidal effects in studies with *Escherichia coli*.⁵ The antibacterial study on *E. coli* and *Bacillus subtilis* using Cu and Ag NPs, revealed the fact that Cu exhibited superiority over Ag.⁶ Cu NPs have wide applications as heat transfer systems⁷ antimicrobial materials,⁸ sensors,⁹ and catalysts.¹⁰ In addition, copper and its compound have been applied as antifungal, antiviral, and molluscicidal agents. The synthesis of Cu NPs by using extracts of various plants found all over the globe have been reported by many researchers in the past.^{11,12} It is essential to develop clean, reliable, biocompatible, cheap, and nontoxic green methods of nanoparticle's synthesis. Many plants parts or whole plants have been used for the green synthesis of Cu NPs¹³ due to the presence of large number of bioactive compounds in plants. The extracts of plants *Nerium oleander*,¹⁴ *Punica granatum*,¹⁵ *Aegle marmelos* & *Ocimum sanctum*,^{16,17} *Zingiber officinale*¹⁸ have been efficiently applied for this purpose. The present review concentrates on biogenic synthetic processes for Cu NPs using extracts of diverse range of plant species including medicinal plants found across the globe and their applications in electronic, magnetic, optoelectronic, biomedical, pharmaceutical, cosmetic, energy and catalysis.

Green Synthesis of Cu and CuO NPs

Plants consists of a large number of biologically active compounds and hence, most of the plants havea proven record for their anthelmintic, antitumor, antimutagenic, antibacterial and fungicidal properties. The synthesis of metallic NPs involves simple mixing of metal solution with extract of plant. Nanoparticles are produced in the medium due to reduction of metal ions. The reaction to give metallic NPs is as shown in Figure 1. Many earlier investigations revealed that Cu NPs can be synthesised by the application of most common precursor copper salts namely, cupric acetate (monohydrate) $((CH_3COO)_2Cu \cdot H_2O)$,¹⁹ Copper chloride di-hydrate ($CuCl_2 \cdot 2H_2O$)²⁰ and Copper sulfate pentahydrate ($CuSO_4 \cdot 5H_2O$). Various factors such as concentration, pH, temperature, influence the nature and properties of synthetic Cu NPs as well as CuO NPs.

Characterization of Cu and CuO NPs

The Characterization of biogenically synthesized Cu and CuO nanoparticles has been carried out by using analytical tools namely, UV-Visible spectroscopy, XRD, EDS, DLS, SEM, TEM, FTIR, HRTEM, particle analyzer, Surface Plasmon resonance etc. The UV-Vis absorption spectroscopy was applied to detect color change in Cu nanoparticle prepared by using *Ziziphus spinchristi* leaves which is possibly due to the surface plasmon vibrations. The surface plasmon vibration bands for Cu-NPs synthesised by many plant extracts was found to be between 191 nm and 721 nm as given in Table I.

SEM and Mapping studies CuO nanoparticle

Scanning Electron Microscopy (SEM) investigation was performed to govern the size and morphology of the green synthesized CuO NPs by *Chenopodium album* (aqueous leaf extract). SEM image shown in Figure 3 confirmed that the obtained CuO NPs were flake like morphology. The green synthesized CuO NPs were dispersed as distinct particles and monodispersity in nature. Phytochemicals in *Chenopodium album* aqueous leaf extract turn as a capping agent which prevents the aggregation of particles causes monodispersity of CuO NPs. SEM mapping studies also conforms the synthesized nanoparticle was CuO. The blue dots corresponds to Copper atom and rose dots represents Oxygen atom. Figure 4 represents the SEM mapping studies of CuO nanoparticle.

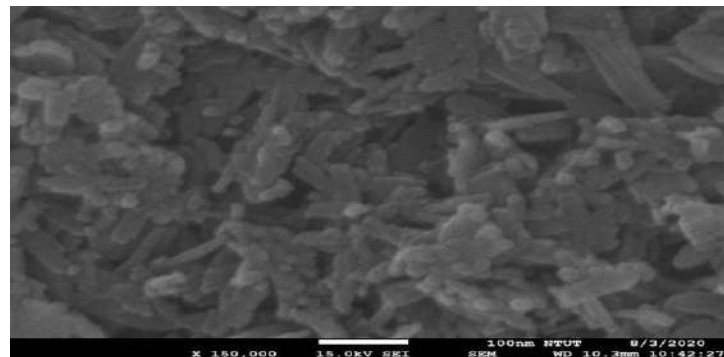


Fig 3. SEM image of CuO nanoparticle.

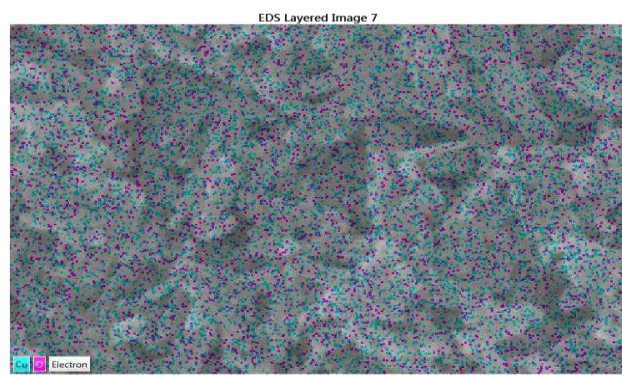


Fig 4. SEM image mapping of CuO nanoparticle.

EDX Analysis of CuO nanoparticle

The elemental composition of the synthesized CuO NPs was confirmed by EDX analysis. The manifestation of copper and oxygen peaks in the EDX spectra confirmed that the synthesized material was CuO NPs (Figure 5). The weight percentage of Copper and Oxygen atoms were 71.10 and 28.90 respectively. The further peaks extant in the spectra may be as a result of the existence of bio organics or impurities in the solution. The elemental composition of CuO nanoparticles was represented in Table 2.

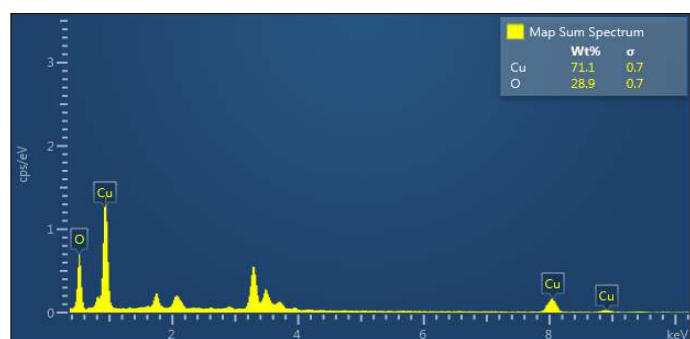


Fig 5. EDX spectra of CuO nanoparticles.

Table 2. Elemental composition of CuO nanoparticle

Element	Atomic Number	Weight %	σ
O	8	28.90	0.7
Cu	30	71.10	0.7
Total	-	100	-

XRD Analysis

The XRD pattern of aqueous leaf extract of *Chenopodium album* derived CuO NPs was represented in Figure 6. The diffraction peaks at $2\theta = 32.4^\circ, 35.5^\circ, 38.7^\circ, 46.1^\circ, 48.8^\circ, 53.6^\circ, 58.4^\circ, 61.6^\circ, 66.2^\circ, 68.0^\circ, 72.4^\circ$ and 75.2° were respectively indexed to (110), (111), (111), (112), (202), (020), (202), (113), (310), (220), (311) and (310) planes of monoclinic structure of CuO NPs. The obtained diffraction peaks were matched with standard CuO NPs. All the diffraction peaks are in good agreement with the standard pattern for pure monoclinic phase of copper oxide nanoparticles (JCPDS No. 80-0076). There no impurity peaks observed. The intense peaks indicate the highly crystalline nature of the formed nanoparticles. From the observed main diffracted peak, the average crystalline size can be calculated using the Scherer equation,

$$(hkl) = \beta \cos \theta$$

Where, $D_{(hkl)}$ is the average crystalline size, k is shape constant (0.89), λ is the wavelength of the incident x-ray (CuK α source, $\lambda = 0.15405$ nm), β is the full width half maximum (FWHM), θ is the incident angle of x-ray. The average crystallite size of the synthesized CuO nanoparticles was 12.45 nm. XRD patterns obtained for the Cu NPs synthesized using citron juice and *Aloe vera* extract showed intense peak confirming crystalline copper and crystalline CuO NPs respectively. The analysis of FT IR spectra provides information about functional groups of biomolecules present in plant extracts. IR peaks were observed at 3,333 cm^{-1} for the hydroxyl group (H-bonded OH stretch); 2,917 cm^{-1} for methylene C-H asym. / sym. stretch; 1,615 cm^{-1} for aromatic ring stretch. The peaks at about 3400, 1650, 1595, 1400 and 1100 cm^{-1} corresponds to -OH, C=O, C=C, C-OH and C-H vibrations. The common IR bands for cellulose were usually found at 3304 cm^{-1} , 2891 cm^{-1} , 1664 cm^{-1} , 1011 cm^{-1} corresponds to vibrations of -OH, CH₂, H₂O, and C-OH groups. Peaks at 610, 499 and 415 cm^{-1} confirmed Cu-O bond vibrations that support the presence of monoclinic phases of CuO synthesised by *Aloe barbadensis Miller* extract. The IR band recorded at about 800 cm^{-1} corresponds to C-H out of plane bending vibrations due to adsorbed phenolic compound on to the CuO NPs. Electron microscopy is used for morphological characterization and internal composition of biogenic copper and silver nanoparticles. EDS will reveal the elemental composition of the particles. Homogeneous and spherical morphology of biogenic Cu NPs were revealed by FESEM images. The average particle size varied from 20 nm to 500 nm. TEM micrographs also revealed spherical nature for NPs with least tendency towards agglomeration. DLS studies reveal size distribution of Cu NPs. The average particle size of NPs synthesised by using *Azadirachta indica* leaves was found to be around 50 nm. The spherical morphology and narrow diameter distributions of Cu NPs were also confirmed by TEM images. Biomolecules present in *Aloe vera* extract believed to act as stabilizing and capping agent for copper caused a raise in the size of NP up to 30 nm but without change in shape. FESEM images of CuO NPs too confirmed their spherical nature (20 nm to 300 nm). CuO NPs synthesised by Oak fruit extract exhibited average diameter of 34 nm. CuO NPs were found to exhibit agglomeration tendency thus enhancing average particle size to as high as 300 nm. HRTEM studies involving in-depth analysis of CuO NPs synthesised by using fruit extract of *Syzygium alternifolium* recorded particle size of 2 nm. CuO NPs synthesised by *ferulago angulata* (schlecht) extract revealed shell-like sheet structure. CuO NPs with relatively good monodispersed and virtually spherical structures were obtained with size range of 15 to 25 nm without agglomeration. TEM analysis of CuO NPs synthesized using *B. tomentosa* leaf extract also showed spherical morphology (size of 22 to 40 nm).

Applications of Cu and CuO NPs

Cu and CuO nanoparticles are multifunctional in nature and hence finds significant role in applications that include antimicrobial activities, catalytic degradation, anticancer activity, photocatalytic degradation, antiviral activity, Biofilm formation, nitrates removal, upshot against human pathogens, photoluminescent activities, organic dye degradation catalysis, etc., Cu NPs demonstrated good antimicrobial influence on *Bacillus* spp. and prominent fungicidal influence on *Penicillium* spp. microorganisms.¹⁹ Cu NPs exhibited greater inhibition on *Escherichia coli* in comparison with *Klebsiella pneumoniae*, *Pseudomonas aeruginosa*, *Propionibacterium acnes* and *Salmonella typhi*. *Fusarium culmorum* was found to establish more sensitive plant pathogenic fungi. Cu NPs were also used for antioxidant and cytotoxic activities. Cu NPs green engineered by *Ginkgo biloba* L. leaf extract found catalytic application for Huisgen [3 + 2] reaction. Cu- NPs synthesized with *Z. spina-christi* fruits extract proved to be excellent nanoadsorbent for Crystal Violet removal from aqueous solution. Catalytic degradation of basic violet 3 dye in water was successful with CuO NPs obtained by using extract of Oak fruit hull. The extract of *Rheum palmatum* L was also used to synthesize CuO nanoparticles which proved to be efficient catalyst for degradation of 4-nitrophenol, methylene blue rhodamine B and Congo red. Effective catalytic application The role of CuO as catalyst can be attributed to high surface to volume ratio associate with large number of active sites. On the same line these particles were found to be photocatalyst for Congo red degradation and nanocatalyst for arylation recation. CuO NPs synthesised by aqueous extracts of *Anthemis nobilis* flowers, *Thymus vulgaris* L. leaves and *Euphorbia esula* L were reported to be catalytically active for the synthesis of propargylamines via aldehyde-amine-alkyne (A³) coupling reaction, and Ullmann- coupling reaction respectively. CuO particles synthesized by *Saraca indica* Leaves exhibited photoluminescence properties. *Aloe vera* leaf extract mediated biogenic CuO NPs exhibited the capability to serve as antimicrobial agents against fish bacterial pathogens. Cu nanoparticles and nano biocomposites synthesised using plants animal sources found to have potential electronic device applications. Cu NPs synthesized by using peel extract of *Punica*

*granatu*⁸ have demonstrated significant antibacterial inhibition against pathogens. In general, a large number of plant extracts have been applied towards the green synthesis of Cu and CuO nanoparticles for applications such as catalytic, antimicrobial activity (urinary tract), photocatalytic, antioxidant and organic dye degradation.

CONCLUSION

Green synthesis of metallic and metallic oxide particles has gained great significance in the recent past due to its simplicity, cost effectiveness and environment friendly nature. It has been considered as an alternative method to all existing methods. UV-Visible spectroscopy, XRD, SEM, and Surface Plasmon Resonance are the most applied analytical tools for the characterization of copper and its oxide nanoparticles. Cu and CuO NPs were found to exhibit spherical morphology with size range of 2 – 500 nm depending on concentration of extracts as well as on preparative conditions. Cu and CuO nanoparticles proved to be multifunctional in nature with significant applications with great future implications in the fields of catalysis, photocatalysis, organic dye degradation, cosmetics, biomedicine and pharmaceuticals.

CONFLICT OF INTEREST

Conflict of interest declared none.

REFERENCE

1. Chandran S. P, Chaudhary M, Pasricha R, Ahmad A, Sastry M. Synthesis of Gold Nanotriangles and Silver Nanoparticles Using Aloe Vera Plant Extract. *Biotechnol. Prog.* 2006;22:577–583.
2. Akhtar M. S, Panwar J, Pilani S, Yun Y. Biogenic synthesis of metallic nanoparticles by plant extracts. *ACS Sustain. Chem. Eng.* 2013;591–602.
3. Mubarakali D, Thajuddin N, Jeganathan K, Gunasekaran M. Plant extract mediated synthesis of silver and gold nanoparticles and its antibacterial activity against clinically isolated pathogens. *Colloids Surfaces B: Biointerfaces.* 2011;85:360–365
4. Ravindra S, Mohan Y. M, Reddy N. N, Raju K. M. Fabrication of antibacterial cotton fibres loaded with silver nanoparticles via “Green Approach”. *Colloids Surfaces A: Physicochem. Eng. Asp.* 2010;367:31–40.
5. Williams D. N, Ehrman S. H, Holoman T. R. P. Evaluation of the microbial growth response to inorganic nanoparticles. *J. Nanobiotechnology.* 2006;4:1–8.
6. Yoon K., Byeon J. H, Park J, Hwang J. Susceptibility constants of Escherichia coli and Bacillus subtilis to silver and copper nanoparticles. *Sci. of the Total Environ.* 2007;373:572–575.
7. Eastman J. A, Choi S. U. S, Li S, Yu W, Thompson L. J. Anomalously increased effective thermal conductivities of ethylene glycol-based nanofluids containing copper nanoparticles. *Appl. Phys. Lett.* 2012;718:4–7.
8. Guduru R. K, Murty K. L, Youssef K. M, Scattergood R. O, Koch C. C. Mechanical behavior of nanocrystalline copper. *Mater. Sci. Eng.* 2007;463:14–21.
9. Xu, Q, Zhao Y, Xu J. Z, Zhu J. Preparation of functionalized copper nanoparticles and fabrication of a glucose sensor. *Sensors Actuators B.* 2006;114:379–386.
10. Rodriguez J. A, Liu P, Hrbek J, Evans J, Pørez M. Water Gas Shift Reaction on Cu and Au Nanoparticles Supported on CeO₂(111) and ZnO(0001): Intrinsic Activity and Importance of Support Interactions. *Heterog. Catal.* 2007;2:1329–1332.
11. Kumar A, Chisti Y, Chand U. Synthesis of metallic nanoparticles using plant extracts. *Biotechnol. Adv.* 2013;31:346–356.
12. Borkow G, Gabbay J. Copper, An Ancient Remedy Returning to Fight Microbial, Fungal and Viral Infections. *Curr. Chem. Biol.* 2009;3:272–278.
13. Mondal A. K, Parui S. M, Samanta S, Mallick S. Synthesis of Ecofriendly Silver Nanoparticle from Plant Latex used as an Important Taxonomic Tool for Phylogenetic Inter-relationship. *Adv. Biores.* 2011;2:122–133.
14. R Elayaperumal, G Vanaja, A Vanith, VS Sangeetha “Green synthesis of Glycyrrhizagla silver nano particle and conformation of through Microscopy and Spectrophotometric techniques. “Eurasian journal of Analytical chemistry ,2017-Feb ,1680-1686
15. Gopinath M, Subbaiya R, Selvam M. M, Suresh D. Synthesis of Copper Nanoparticles from *Nerium oleander* Leaf aqueous extract and its Antibacterial Activity. *Orig. Res. Artic.* 2014;3:814–818.
16. V S Sangeetha, Vanith A, Devi P, Bhakyajothi V”Green synthesis of Zinc oxide nano particle using flower extract of *phylla nodiflora*” Scholar National School of leadership vol-9
17. Kaur P, Thakur R, Chaudhury A. Biogenesis of copper nanoparticles using peel extract of *Punica granatum* and their antimicrobial activity against opportunistic pathogens. *Green Chem. Lett. Rev.* 2016;9:33–38.
18. Science N., Technology N, Paper F. Synthesis of copper nanoparticles with *aegle marmelos* leaf extract. *NNano Sci. Nano Technol. An Indian J.* 2014;8:401–404.
19. C.W. Bunn, Proc. Phys. Soc., London, 47 (1935) 835.
20. A. Gosh, N. Kumari, S. Tiwari and A. Bhattacharjee, Indian J. Phys., 87(11) i.(2013)1099– 1104.

Screening of Enzyme Inhibitors Compound from Squid Ink

Sangavai C, Dr.P.Viswanathan, HaseenaM,KaleeswariSudha M, Dhanalakshmi G

DhanalakshmiSrinivasan College of Arts and Science for Women (Autonomous),Perambalur-621212.

Abstract: This study aims to analyze the presence of active compounds in squid ink extract powder can be used as Pharmacological active compounds against Alzheimer's and Diabetic disease. The method used in this research is explorative and *in vitro* experimental method. Squid ink was collected from cuttle fish and processed. The results showed that the squid ink extract contained aminoacid and carboxylic acid from the FTIR test results. Limited enzyme inhibition by squid inhibitors was detected at low concentration and significant at 100µL indicate the presence of several enzyme inhibitors in squid extract. It showed both tested enzyme inhibition and found to be superior than standard drugs amantidine and acarbose.

Keyword: Squid ink, Cuttle fish, Amantaidine, Acarbose, inhibitors

INTRODUCTION

The squid world comprises around 304 species that belongs to the order Teathed, in cephalopods. Anatomically it have eight arms and longer tentacles that helps them to swim. Some of them can even "fly" out of the water for short distance. The identified squids are classified into two categories ¹; either myopsida or oegopsida and it can be found in several sizes. The majority of these species are not more than 60 cm (24 ft) in length. The giant squid has a maximum size of 13 m (43 ft) and a colossal squid can weigh up to 1,000 pounds and grow to a length of 35 feet which is the largest species in the squid world. It tends to stay in cold, deep water. Another type of squid is known as vampire squid that have a capability to jump out of water. It is black in color and has long arms that can move like a black cape. These squid are normally around the size of 1 foot and have small suckers on the arms. In American countries, squid as food is often marketed using the Italian word calamari². Table I describes different types of squid discovered in the world including its species name, family, common name and catch tones. The goal of this review is to describe the squid ink including different types of squid currently available, chemical constituents of squid ink ³ and its pharmacological activities along with the traditional / homeopathic effects affecting human body.

Types Scientists believe that there are four different types of squid

- 1) Squidussquida: is the main ingredient in calamari.
- 2) Squidusblooperus is found in the seas of the Mushroom Kingdom.
- 3) Squidusflyidae is similar to Squidusblooperus in structure, but its habitat is the skies of the Mushroom Kingdom instead of the seas.
- 4) Jellyfishussquida: It is a type of jellyfish that many scientists believe may actually be a squid

Table a :Types of squids discovered in world

Species	Family	Common Name
Loligo gahi Or Doryteuthisgahi	Loliginidae	Patagonian Squid
Loligopealei	Loliginidae	Longfin Inshore Squid
Common squid	Loliginidae	-
Ommastrephusbartramii	Ommatrophidae	Neon Flying Squid
Ilex argentinus	Ommatrophidae	Argentine Shortfin Squid
Dosidicusgigas	Ommatrophidae	Humboldt Squid
Todarodes	Ommatrophidae	Japanese Flying Squid
Nototodarussloanii	Ommatrophidae	Wellington Flying Squid
Squid nei	Various	-

Table b: Types of squids discovered in world

Species	Family	Common Name	Catch Tones
<i>Loligo gahi Or Doryteuthis gahi</i>	Loliginidae	Patagonian Squid	24,976
<i>Loligo pealei</i>	Loliginidae	Longfin Inshore Squid	16,684
Common squid	Loliginidae		22,5958
<i>Ommastrephus bartramii</i>	Ommatrophidae	Neon Flying Squid	22,483
<i>Ilex argentinus</i>	Ommatrophidae	Argentine Shortfin Squid	511,087
<i>Dosidicus gigas</i>	Ommatrophidae	Humboldt Squid	406,356
<i>Todarodes</i>	Ommatrophidae	Japanese Flying Squid	504,438
<i>Nototodaros sloanii</i>	Ommatrophidae	Wellington Flying Squid	62,234
<i>Squid nei</i>	Various		414,990
Total			2,189,206

Types of squid ink

Squidussquida: It is the main ingredient in calamari. 2) Squidusblooperus: It is found in the seas of the Mushroom Kingdom. 3) Squidusflyidae: It is similar to Squidusblooperus in structure, but its habitat is the skies of the Mushroom Kingdom instead of the seas. 4) Jellyfishussquida: It is a type of jellyfish that many scientists believe may actually be a squid. The ink produced from cephalopod species is a dark cloudy liquid ⁴ which is released as a defense that helps to escape from predator. Each species in this family can produce slightly different colored inks and it is popular in many names such as squid ink, cuttlefish ink, tintacalamar, nero di seppia, black squid ink, cephalopod ink and octopus ink. Commonly octopuses produce black ink while squid ink is blue-black in colour and cuttlefish ink is like a shade of brown. Squid ink is most popular in Italy and Spain, due to its unique appearance. It contains a large number of important nutrients particularly antioxidants and is low in fat and calories. The striking blue – black color of squid ink is due to the presence of large amounts of melanin. The melanin pigment is produced in mature cells of the ink gland which is present in the bottom of the ink sac. Additionally, it also contains large quantities of proteins, lipids, minerals, taurin and dopamine ²⁻⁴. The food chemistry studies using ink of the neon flying squid, boreal clubhook and boreo pacific gonate squid reveals that they are also rich in taurin and hydroxypyroline ⁵. The tyrosinase in the ink is converted to toxic quinines that act as detergent for predator..

MATERIALS AND METHODS

Squid (Loligo sp.) Ink Extraction

The making of squid ink extract powder starts with taking ink from squid. The squid used came from trichy fish market in a ice cold condition. 1 kg of fish is used to collect ink from a sack. Taking ink begins with cutting the part of the mantle (the lower part of the squid body) vertically or longitudinally. The tool used to take squid ink bag is tweezers ⁵. Taking is done carefully to avoid tearing the ink bag. Then, the squid ink bag is placed in the container. The squid ink bag is cut using scissors and squeezed to take the black ink. Drop of squid is added to ninhydrin for detection of amino group.

Amylase inhibition

Briefly, 0.2ml of 5mg/mL concentration of extracted microbial metabolite made upto 0.2 ml with distilled water, and 400 μ L of starch solution were mixed. The reaction started by the addition of 200 μ L of the enzyme solution (pancreatic extract) and the tubes were incubated at 25°C for 5 min at room temperature.. 200 μ L of DNS color reagent (50.68 g sodium potassium tartrate dissolved in 70 mL of 2 M NaOH with 0.026 mM of 3,5-dinitrosalicylic acid) ⁷ and placed in a water bath maintained at 85–90°C for 15 min. The mixture in each tube was diluted with 900 mL of distilled water and the absorbance was measured at 540 nm. For each concentration of the extract used, blank incubation was prepared by replacing the enzyme solution with distilled water (200 μ L) at the start of the reaction, to correct for the absorbance generated by the plant extract. Control incubations, representing 100% enzyme activity,

$$\text{Inhibition (\%)} = 100 - \% \text{ reaction (at min)},$$

where % reaction = mean glucose in sample \times 100/mean glucose in control.

AchE inhibition (Eldee et al.,2005)

To determine the Acetylcholineesterase inhibition were modified and applied. Electronic multichannel pipette (Eppendorf, USA) was used to transfer exact 10 μ L of enzyme solution to 0.5M Phosphate buffer pH 7 further mixed with 25, 50 and 100 μ L of tested compounds in solution diluted to final volume0.2 ml . This was followed by adding 20 μ L of acetylthiocholine iodide (0.4 mM) and DTNB (Sigma-Aldrich, USA) (0.3 mM) to enzyme solution to observe the reaction. Yellowish or colorless solution was

observed during reaction for 30 minutes at room temperature. Changes in absorbance were recorded at 412 nm. Enzyme concentrations used were within the linear range of their toxicity activity. Amantadine used as standard drug. Tube without test/standard used as control.

Abs of control(C) –Test / C x100

Fourier Transform Infrared (FTIR)

Fourier Transform Infrared (FTIR) analysis was performed on pellet⁶ samples made from KBr (99.99%) mixed with squid ink extract powder. Samples of squid ink extract powder for FTIR test of about 4 mg. This amount is mixed with about 1400 mg KBr. To ensure that the resulting pellets allow an accurate spectrum, the mixture is mixed using mortar and pestle.

RESULT AND DISCUSSION

The squid ink bag from cuttle fish (fig 3) is cut using scissors and squeezed into a test tube diluted with ethanol (fig 4). Presence of amino group confirmed by ninhydrin test. Squid (Loligo sp.) ink extract identified the contents of its active compound using FTIR in transmission mode (400-4000 cm⁻¹). The results obtained can be seen in Figure 1. Based on the above results, it can be seen that the squid (Loligo sp.) ink extract contains compounds in absorbance of 3436 cm⁻¹ at peak 1; 2074 cm⁻¹ at peak 2; 1634 cm⁻¹ at peak 3; 1273 cm⁻¹ at peak 4; The absorbance at: 1. 3500-3370 cm⁻¹ is a bond of N-H group^{3,16} 2. 3100-2800 cm⁻¹ is a bond of C-H group^{3,17}. Beside amine group, squid ink extract powder contains carboxylic group. This is indicated by the absorption that height and width is 1634 cm⁻¹ which is part of the C=O double bond that belongs to the carboxylic group, one of the derivatives from carboxylic acid is oleic acid¹⁴. Oleic acid content in squid ink raw extract could kill the bacteria and fungi¹⁵

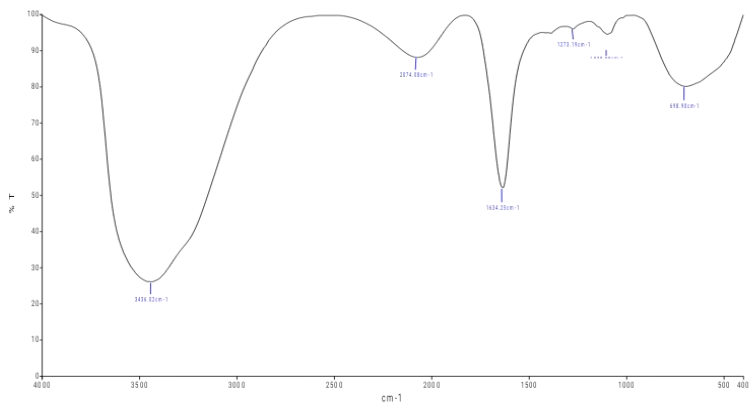
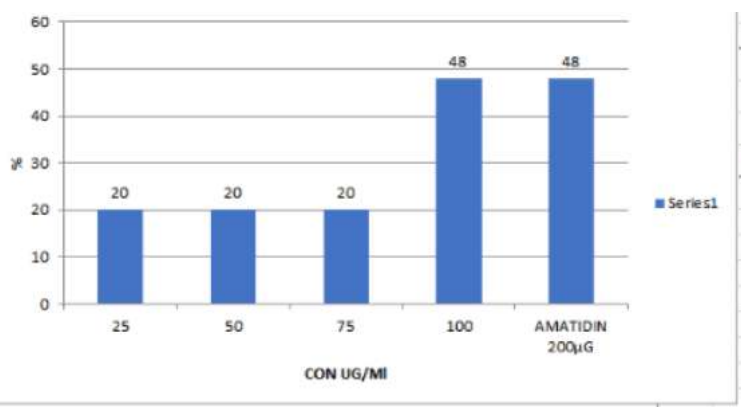
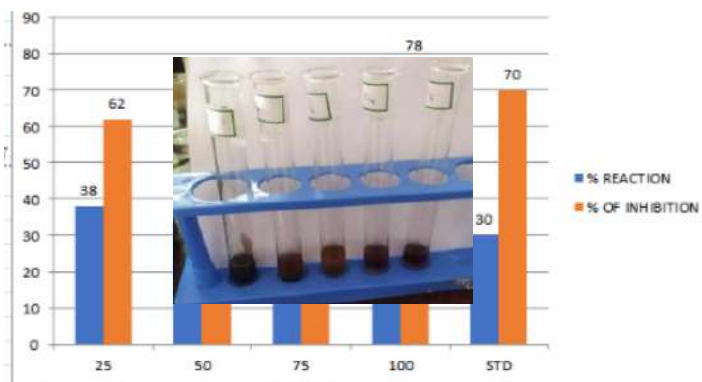
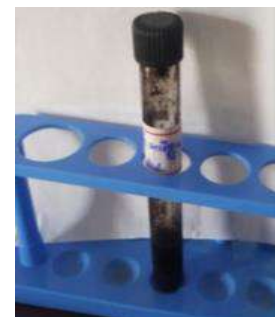
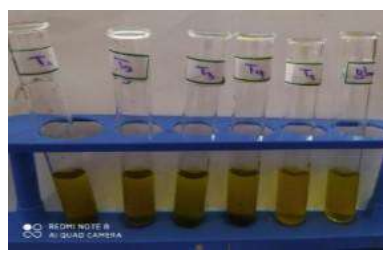


Fig 1. FTIR analysis

Enzyme inhibition

Cholinesterases (ChEs) are serine hydrolases that catalyze the hydrolysis of choline esters and are classified according to their substrate specificities. acetylcholineacetylhydrolase or acetylcholinesterase from brain extract activity was retained in control and inhibited on test (plate 3). The percentage of inhibition was calculated and represented on figure 1. Among 4 different concentrations maximum 48% inhibition was noted at 100µL squid ink whereas 20% recorded between 20-75µL. The acetylcholinesterase inhibition of squid ink is concentration dependent. This result is found to be similar to the result of the standard. Acetylcholinesterase (AChE) is essential for hydrolysis of the neurotransmitter acetylcholine (ACh), and, therefore, for termination of impulse transmission at cholinergic synapses. Irreversible inhibition of AChE can result in accumulation of ACh at cholinergic synapses and, ultimately, to death. Antidiabetic activity extracted SQUID INK with ethyl acetate (plate 4) and its inhibition of quantitative alpha amylase and AchE inhibitory⁶. Activity at amylase inhibition among 4 concentration inhibitions was found best at 100 µg (Fig 2). Chick pancreas used as amylase source and found released sugar from starch estimated as 0.3 mg/ml by DNS method. Enzymes treated with sample and standard showed decreased levels of sugar. The concentration of sugar estimated from standard and given in figure 2b. From the amount of sugars the enzyme inhibition was calculated and given in figure 2. The data reveals squid ink has 78 % inhibition of amylase activity which is greater than standard acarbose inhibition (70%). The minimum activity was 62% at 25 µl and reached maximum 70-78 between 75-100µL of squid ink

**Fig 1. AchE inhibition activity****Fig 1. Pancreatic amylase inhibition activity****Fig 3. squid ink collected from cuttle fish****Fig 4. AchE inhibitor study****Fig 5. Amylase inhibition**

The plant leaves were extracted with various solvents like n-butanol, methanol and aqueous. Among the different plant tested, all the three solvents, the methanolic extracts of *Lawsonia inermis* showed maximum activity against *Pythium debaryanum* ⁷⁻⁸. The study was conducted to explore the effects of squid ink on growth performance, immune functions and antioxidant ability of broiler chickens during a period of six weeks. The protective effects of squid ink in chemotherapy, BALB/c mice were used as animal models of injuries induced by cyclophosphamide, a well known chemotherapeutic drug ⁸⁻⁹. In recent years many bioactive compounds have been extracted from various marine animals like tunicates, sponges, soft corals, cephalopods, sea slugs, etc. ⁹⁻¹⁰ In the subclass Coleidea (virtually all the cephalopods belong here) the shell is either considerably external or internal or has been completely lost. Oxidation injury to skin is one of the main reasons for skin aging. The aim of the present study was to explore the protective effect of squid ink post damage. The proteomics analysis of crude squid ink isolated from *Sepia esculenta*

for their antibacterial, antifungal, antibiofilm and cytotoxic properties¹²⁻¹³ A new type of wound healing agent was developed using two marine biomaterials (squid ink polysaccharide and chitosan) as carriers and calcium chloride as an initiator for coagulation .Melanin is a dark naturally occurring pigment produced in nature and in many organisms. Although several reports have demonstrated applications for melanins in various therapeutic treatments, to date, no research has examined the anti-allergic effect of melanin¹⁴⁻¹⁶ .One of the most distinctive and defining features of coleoid cephalopods-squid, cuttlefish and octopus-is their inking behavior¹⁷ . Acetylcholine is essential to neural function. Its synthesis is catalyzed by choline acetyltransferase, the enzyme responsible for the acetylation of choline by acetyl coenzyme¹⁸⁻²⁰.

CONFLICT OF INTEREST

Conflict of interest declared none.

REFERENCE

1. Caldwell, P.E., Walkiewicz, M., Stern, M. (2005). Ras activity in the Drosophila prothoracic gland regulates body size and developmental rate via ecdysone release. *Curr. Biol.* 15(20): 1785--1795.
2. Palumbo M. E., Geballe T. R., and Tielens A. G. G. M. (1997) Solid Carbonyl Sulfide (OCS) in Dense Molecular Clouds, *The Astrophysical Journal*, Volume 479, 479 839.
3. Silvia A. CentenoSilvia A. CentenoJacob ShamirJacob Shamir (2008) Surface enhanced Raman scattering (SERS) and FTIR characterization of the *sepia* melanin pigment used in works of art, *Journal of Molecular Structure* 873(1-3):149-159
4. Ambikapathy V., Gomathi S., and Panneerselvam A (2014). Effect of antifungal activity of some medicinal plants against *Pythiumdebaryanum* *PelagiaResearchLibraryAsian JournalofPlantScienceandResearch* 131-134.
5. Jie-Ping Zhong, Guang Wang, Jiang-Hua Shang, Jiang-Qiu Pan, Kun Li, Yan Huang, and Hua-Zhong Liu (2009), Protective Effects of Squid Ink Extract Towards Hemopoietic Injuries Induced by Cyclophosphamide, *Mar Drugs.* Mar; 7(1): 9-18.
6. Haefner, B. (2003). Drug from deep sea. *Drug Discov. Today* 8:536-544.
7. Colwell, R.R. (2002). *Biotechnol. Adv.* 20: 215-228
8. Andriantsitohaina R., Duluc L., Garcia-Rodriguez J. C., Gil-Del Valle L., Guevara-Garcia M., Simard G., et al. (2012). Systems biology of antioxidants. *Clin. Sci. (Lond.)* 123, 173–192. 10.1042/CS20110643
9. Babior B. M. (1999). NADPH oxidase: an update. *Blood* 93 (5), 1464–1476. 10.1053/beh.1999.0025
10. Bedard K., Krause K. H. (2007). The NOX family of ROS-generating NADPH oxidases: physiology and pathophysiology. *Physiol. Rev.* 87, 245–313. 10.1152/physrev.00044.2005
11. Carmichael J., Degraff W. G., Gazdar A. F., Minna J. D., Mitchell J. B. (1987). Evaluation of a tetrazolium-based semiautomated colorimetric assay: assessment of radiosensitivity. *Cancer Res.* 47 (4), 943–946.
12. Zhong J.P., Wang G., Shang J.H., Pan J.Q., Li K., Huang Y., Liu H.Z. (2009) Protective effects of squid ink extract towards hemopoietic injuries induced by cyclophosphamide. *Mar. Drugs.*.. Darwin C. On the formation of mould. *Proc. Geol. Soc. Lond.* 1838;2:574–576.
13. Vate N.K., Benjakul S., Agustini T.W. Application of melanin-free ink as a new antioxidative gel enhancer in sardine surimi gel. *J. Sci. Food Agric.* 2015;95:2201–2207.
14. Agrawal P.B., Pandit A.B. Isolation of α -glucosidase from *Saccharomyces cerevisiae*: Cell disruption and adsorption. *Biochem. Eng. J.* 2003.
15. Bayir H. Reactive oxygen species. *Crit Care Med.* 2005;33:S498–501.
16. Darwin C. John Murray; London, UK: 1859. On the origin of species by means of natural selection, or the preservation of favoured races in the struggle for life. Darwin C. John Murray; London, UK: 1881. The formation of vegetable mould through the action of worms, with some observations on their habits.
17. Bohlen P. J., Scheu S., Hale C. M., McLean S. M., Groffman P. M., Parkinson D. Non-native invasive earthworms as agents of change in northern temperate forests. *Frontiers in Ecology and the Environment.* 2004;2:427–435.
18. Brussaard L, Aanen DK, Briones MJI, Decaëns T, Deyn GBD, Fayle TM, et al. Biogeography and Phylogenetic Community Structure of Soil Invertebrate Ecosystem Engineers: Global to Local Patterns, Implications for Ecosystem Functioning and Services and Global Environmental Change Impacts In: *Soil Ecology and Ecosystem Services*.
19. Wall DH, Bardgett RD, Behan-Pelletier V, Henrrick J, Jones H, Ritz K, et al. editors. Oxford: University Press; 2013. pp. 201–232.
20. Venables BJ, Fitzpatrick LC, and Goven AJ 1992 Earthworms as indicators of ecotoxicity. In: *Ecotoxicology of Earthworms*, ed Greig-Smith PW, Becker H, Edwards PJ, Heimbach F. Intercept, Ltd, Andover, Hants, UK, 197–206.
21. Jones, Lawton &Shachak (1994) Jones CG, Lawton JH, Shachak M. Organisms as ecosystem engineers. *Oikos.* 1994;69:373–386.
22. Turbé et al. (2010) Turbé A, De Toni A, Benito P, Lavelle P, Lavelle P, Ruiz N, Van der Putten WH, Labouze E, Mudgal S. Soil biodiversity: functions, threats and tools for policy

Antioxidant and Antidiabetic Potential Of Areca Nut Extract

Haseena M, Dr.P.Viswanathan, Sangavai C, &Kaleeswari Sudha M

Dhanalakshmi Srinivasan College Of Arts And Science For Women (Autonomous), Perambalur-621212

Abstract: Diabetes involved acute disease that requires continuous medical care with complex risk reduction strategies as diabetes weak almost all organs of the body. The most important thing in controlling the risk of diabetes is to control the level of sugar in the blood and not to cause hypoglycemia. Areca catechu fruit (Areca nut) is one of the most traditional components used in betel chewing. There is premise that the antidiabetic effect of chewing betel is sourced from areca nut. This present study aims to determine the anti-hyperglycemic effect and antioxidant activity of ethanol extract of areca nut (Areca catechu) seed. The objectives are to extract and detect the phytochemicals and estimate the total polyphenol content in areca nut, to find out the antioxidant property of DPPH, determine the anti-inflammatory activity, and evaluate anti-diabetic potential by *in vitro* method(amylase inhibition- glycosylation method in Areca nut.

Keywords: Areca nut, Diabetes, Phytochemicals, Anti-inflammatory.

INTRODUCTION

Areca nut is the seed of *Areca catechu*, It is otherwise called betel nut. It grows in the tropical Pacific, East Africa, and Asia. It belongs to the family of Arecaceae. The Areca nut causes a wide range of effects on the human body. It is related to central obesity and type II diabetes. It is one of the most widely consumed drugs in the world after nicotine, ethanol, and caffeine, and is consumed by about 10% of the world's population. Many reports that chewing gum begins at an early age and is ingested freely by children¹. Areca nut extract is used to treat diabetes. It contains alkaloids such as arecoline. It immediately crosses the blood-brain barrier. It increased the capacity to work and creates a warm sensation throughout the body². As of 2019, 463 million people worldwide have diabetes (8.8% of adults), and type 2 diabetes accounts for 90% of cases(WHO, 2014). Areca nut extract possesses an α - glucosidase inhibitory activity and is useful for preventing the formation of high glucose levels in the blood. It involves the hypoglycaemic effect at lower dose (0.05-0.25 mg/kg) body weight in the diabetic animal. The water, ethanolic, acetic acid, calcium hydroxide extract of the areca nut possess a capillary shrinking/contraction effect. It is administered and effective by both routes subcutaneous (SC) and intravenous (IV) and it is useful in the treatment of cardiac depression³.

Antioxidants Agents:

Due to the presence of some bioactive compounds such as phenolic compounds, flavonoids in methanolic extract of the plant showed significant effect against oxidation. Areca nut is also used for several natural anti-oxidative agents production³. Ethanol extract of Areca nut showed powerful anti-oxidant, free radicals scavenging, and anti-hyaluronidase activity. The anti-oxidant effect of the extract was low Butylated hydroxydoline, but related to Tocopherol and greater than ascorbic⁴.

Anti-inflammatory agents:

Areca nut has main constituents like polyphenols, fat polysaccharides, fiber, and protein. These results confirm that extract of Areca nut can lower the inflammatory on skin. The skin whitening effect of wild oil extract has been shown to inhibit the activity of fungal tyrosinase and the synthesis of melanin in the B16 melanoma cell. Electron spin resonance (ESR) technique is used to evaluate the 1, 1 diphenyl 2-picryl (DPPH) free radical scavenging activity 10 and strong scavenging activity against superoxide anion radical (O_2^-) of Areca cut extract⁴.

Antidiabetic agents:

Research Based on the results from Areca catechu leaves are famed to be effective as anti-diabetic^{5,6}. In a study of glucose tolerance testing in Swiss albino mice, the methanolic extract of areca nut leaves at 100,200 and 400 mg/kg BW significantly reduced serum glucose levels compared to the control group receiving only glucose⁷. while for areca nut, there are two different opinions. Examined the α -glycosidase *in-vitro* inhibitory activity and hypoglycemic effect by oral administration of Areca nut ethanol extract in mice⁸. Areca nut extract pretended *in-vitro* inhibitory activity of intestinal α -glucosidase enzymes maltase, IC50 values of maltase, and sucrase. 12 μ g / ml and 30 g / ml, were found to be sucrase activity in areca nut extract respectively.

MATERIALS AND METHOD

Preparations of the Areca nut extract

Areca nut was collected from the local market nearby our college, Perambalur, Tamilnadu, India. The Areca nuts were rinsed with distilled water thoroughly washed. The Areca nuts extract was prepared by taking 20 g of thoroughly washed and finely cut Areca nuts in a 250 ml Erlenmeyer flask with 100 ml of sterile distilled water and then boiled the mixture for 10 min.⁸ The solution was then removed from the t source and left at room temperature. Following this step, the extract was then filtered through a Whatman filter paper No.1. The extract was kept in the refrigerator at 4°C for further experiments⁹.

Phytochemical analysis of Areca nut:

Phytochemical components of the aqueous extracts of areca nut were screened by using standard methods. The components such as carbohydrates, Tannins, Saponins, Flavonoids, Keller-Kiliani Test, Salkowski's Test, Glycosides, Steroids, Terpenoids &

Phenol were analyzed by standard protocols.⁹

Determination of Total Phenolic Content (TPC)

Determination of Total Polyphenols (TP) for the optimization and standardization of the spectrophotometric method using the Folin-Ciocalteau reagent, three parameters were analyzed: The total phenolic content (TPC) of the different plant extracts was determined using Folin- Ciocalteu reagent, with slight modification¹⁰. In brief, 1 mL of crude extract (1 mg/mL) was mixed with 1 mL of Folin-Ciocalteu reagent followed by the addition of 5 mL of distilled water in a volumetric flask. After 5 min, 1 mL of sodium carbonate (10%) was added and shaken vigorously¹¹. Then, the final mixture was incubated in the dark condition at room temperature for 60 min, and the absorbance was measured against the blank at 725 nm using a UV-VIS spectrophotometer. The total phenolic content of plant samples is calculated from the calibration curve of stable gallic acid (10–250 mg / L) and expressed as the equivalent of gallic acid (GAE) per gram of dry extract weight.

Antioxidant assay

1,1-Diphenyl-2-picrylhydrazyl (DPPH) Test 1 mg of the f extract was dissolved in 1 ml ethanol. The standards used in this test were ascorbic acid uses at the same concentration. For the DPPH reagent (light-sensitive), the concentration used was 2.5 mg/ml. The DMSO solution was added to each 96-well plate followed by the addition of leaf extract on first row wells. Once suspended, the mixture of leaf extract was diluted from the first row to the second row and the dilution process was continued until the last row. The DPPH reagent was added to each well plate. It was wrapped in aluminum foil and incubated on the shaker at room temperature for 20 minutes. The absorbance was recorded at 517 nm¹².

alpha-amylase inhibition assay

Briefly, 0.2 ml of the plant extract at 25,50,75 and 100 μ g/ml concentrations (diluted in a phosphate buffer) was added to 25 μ l of enzyme porcine pancreatic solution into a test tube. After 10 min of incubation at 37°C, the reaction was initiated by adding 20 μ l of 1% starch solution and further incubated for 30 min at 37°C¹³. The reaction was then stopped by adding 10 μ l 1M of HCl to each well followed by 75 μ l of iodine reagent. A phosphate buffer (pH 6.9) is used to blank instead of the extract and positive control (acarbose, 64 μ g/ml) prepared. No enzyme control and no starch control were included for each test sample. The absorbance was measured at 580 nm and the percentage inhibitory activity was calculated by using the following equation: $I = \frac{A_{sample} - A_{blank}}{A_{control} - A_{blank}} \times 100$

in vitro glycation of albumin

BSA was glycated using BSA (1 mL, 10 mg/mL) was incubated along with aqueous plant extracts (1 mL) and fructose (1 mL, 250 mM) in potassium phosphate buffer saline (PBS), (2 mL, 200 mM, pH 7.4) containing 0.02% sodium azide, in the dark at 37 °C for 4 days in sealed tubes under sterile conditions (0.22 μ filter), hereafter referred to as glycated sample¹. Negative control (1 mL BSA +3 mL PBS) and positive control (1 mL BSA +1 mL fructose +2 mL PBS) were maintained under similar condition. After incubation, unbound fructose was removed by dialysis against PBS, and dialysate was used for further analysis. All additions and analyses were performed in triplicates¹⁴.

Determination of amyloid β -aggregation by congo red

Aggregation in the glycated sample was measured using amyloid-specific Congo red dye according to the method described previously (Congo red (100 μ M), which was prepared in PBS (pH 7.4) containing ethanol (10%, v/v). Glycated sample (500 μ L), was incubated with Congo red solution (100 μ L) and absorbance was measured after incubation for 20 min, at 530 nm.

RESULT AND DISCUSSION

Phytochemical Analysis

The collected and powdered Arachea nut (plate 1a) was extracted with ethanol and ethyl acetate at 5%. qualitative analysis both extract given in table 1. The data reveals a sample extracted with ethyl acetate that presence of Carbohydrate, Amino acid, Protein, Terpenoids, Flavonoids, Quinones and negative on alkaloid and phenols in contrast positive on ethanolic extract (plate 2). Ethanolic extract gave 8 positive results and 4 were negative. Whereas Ethyl acetate showed 6 positive and 6 were negative. In the present study, suspected polyphenols were profiled is quantified by and total phenolic using the Folin-Ciocalteu method (plate 3, and the concentration from gallic acid standard was given in figure 1 and estimated as 5.85 mg/ml. The higher content of total phenol from betel nut seed as 70% ethanol extraction¹⁵. This study also evaluates the antioxidant activity and the total phenolic compound of ethanolic extract of seeds. The antioxidant activity was determined using the 1, 1 -diphenyl-2-picrylhydrazyl (DPPH) radical scavenging assay The results from this study showed that the antioxidant activities of ethanolic extracts of the seeds as determined by the 1, 1 -Diphenyl-2- picrylhydrazyl (DPPH) presented higher percentage inhibition at 100 μ g gave 90%. at minimum concentration of 25 μ g/ml, the percentage of inhibition was 8 3 and was found to be increased by increasing concentration(table 3). Antioxidant activity and the effect of different parts of areca catechu extracts were reported¹⁶⁻¹⁹ and showed 70% by methanolic extraction

Antidiabetic activity

Plant extracts were tested for alpha-amylase inhibitory activity at 25-100 but inhibition was found at 100 μ g. chick pancreas used as amylase source and found released sugar from starch estimated as 0.3 mg/ml by DNS method. Enzyme treated with sample and standard showed a decreased level of sugar. The concentration of sugar is estimated from standard and given in figure 2 a-b. From the number of sugars, the enzyme inhibition was calculated and given in Figure 2c. the data reveals 40% inhibition at 100 μ g and 365 by standard were recorded. It would be expected that amylase inhibitors should possess a sugar-like structure e.g. acarbose. However, alpha-amylase inhibitory activity has been demonstrated for other non-sugar naturally occurring products such as

hibiscus acid and flavonoids including luteolin^{17,18-20}. Products, by checking browning intensity, determination of aggregation index, and Congo red assays. Our findings demonstrated that ginger extract (100 µg/mL) significantly reduced the browning, compared to control

Table 1. Qualitative Phytochemical Analysis

	Concentration	Percentage
Ascorbic acid	100	95
T1	25	83
T2	50	85
T3	75	87
T4	100	90

Table 2. Antioxidant Assay DPPH

SAMPLE	Ethyl Acetate	ETHANOL
Carbohydrate	Positive	Positive
Saponin	Negative	Negative
Flavonoids	Positive	Positive
Quinones	Positive	Negative
Alkaloids	Negative	Positive
Terpenoids	Positive	Positive
Phlobatannis	Negative	Negative
Tannin	Negative	Positive
Reducing sugar	Negative	Negative
Phenol	Negative	Positive
Amino acid	Positive	Positive
Protein	Positive	Positive

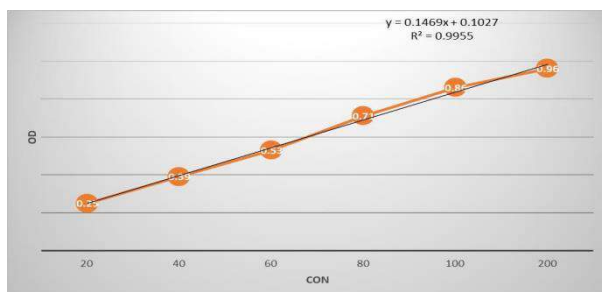
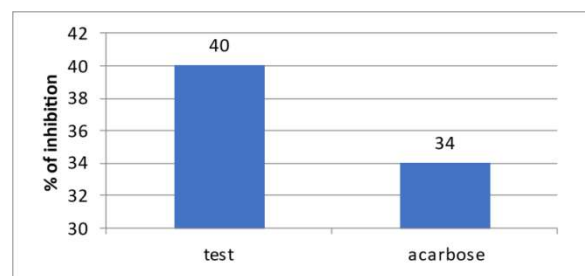


Fig 2 a)standard sugar



2b) amount of sugar release

CONCLUSION

Polyphenols are functional compounds in plants, which include many bioactivities beneficial for humans. This study was to establish a highly efficient method for extracting polyphenol compounds from areca seeds and further to identify polyphenols and antioxidant properties of the seed extract. By comparison with ascorbic acid (Vc), the antioxidant activities of the ethanol extracts were evaluated by inhibition of the DPPH (1,1-diphenyl-2-picrylhydrazyl) radical- scavenging activity found good antioxidant property. Screened plants exhibited significant (40%) alpha-amylase inhibitory activity comparatively higher than standard at tested concentration 100µg/mL. These findings support the hypoglycemic activity of these species and give insight into the rich antioxidant potential and promising mechanism of their hypoglycemic activity by amylase inhibition and antiglycosylation will develop new insights on Areca nut.

CONFLICT OF INTEREST

Conflict of interest declared none.

REFERENCE

1. Apurva Garg, Pankaj Chaturvedi, and Prakash C. Gupta(2014),A review of the systemic adverse effects of areca nut or betel nut, Indian J Med Paediatr Oncol. 35(1): 3–9.
2. Stephen Cox,Mafaz Ullah, Hans Zoellner(2016), Chapter 78 - Oral and Systemic Health Effects of Compulsive Areca Nut Use, Neuropathology of Drug Addictions and Substance Misuse,Volume 3:Pages 785-793
3. Shashank Tiwari and Shreya Talreja(2020),A Pharmacological And Medicinal Study Of Areca Palm And Nuts: AnOverview, Research Journal of Pharmaceutical, Biological and Chemical Sciences, RJPBCS 11(5) Page No. 100

4. M. Senthil Amudhan, V Hazeena Begum and K. B. Hebbar(2012), A REVIEW ON PHYTOCHEMICAL AND PHARMACOLOGICAL POTENTIAL OF ARECA CATECHU L. SEED, IJPSR, Vol. 3(11): 4151-4157.
5. Mondal Suvankar, Bhattacharya Sanjib, Moulisha Biswas Antidiabetic activity of Areca catechu leaf extracts against streptozotocin induced diabetic rats.2012.Adv Pharm Educ Res. 2
6. M Y Musdja, A Nurdin and A Musir (2020),Antidiabetic effect and glucose tolerance of areca nut (Areca catechu) seed ethanol extract on alloxan-induced diabetic male rats, IOP Conf. Series: Earth and Environmental Science 462 (2020) 012036
7. S. Keshava Bhat, D. Ashwin and S. Mythri(2017), Antidiabetic potential of Areca catechu L.and certain Areca nut formulations available for treating Diabetes, Indian journal of Arecanut, Spices and Medicinal plants, Vol-19(1).
8. Senthil Amudhan M, Hazeena Begum V (2008). Research Article Alpha – glucosidase inhibitory and hypoglycemic activities of Areca catechu extract; 4(15): 223-227.
9. Ranjithkumar Rajamani, Selvam Kuppusamy, Shanmugavadiu. M and D. Rajmohan(2016), Preliminary Phytochemical screening of Aqueous extract of Betel ut and Betel leaves, International Journal of Biosciences and Nanoscieces: Vol-3, Issue 1 (2016), 14-18.
10. V. L. Singleton and J. A. Rossi, "Colorimetry of total phenolics with phosphomolybdic-phosphotungstic acid reagents," American Journal of Enology and Viticulture, vol. 16, no. 3, pp. 144–158, 1965.
11. Elizabeth Fitriana Sari, Grace Puspita Prayogo, Yit Tao Loo, Pangzhen Zhang, Michael John McCullough & Nicola Cirillo(2020), Distinct phenolic , alkaloid and antioxidant profile in betel quids from four regions of Indonesia, Scientific Reports, 10:16254
12. Rahim, Nurhidayah Ab, Zakaria, Noorzafiza, Dzulkarnain, Syarifah Masyitah Habib, Azahar, Nazar Mohd Zabadi Mohd, Abdulla, Mahmood Ameen (2017), Antioxidant activity of alstonia Angustifolia ethanolic leaf extract, AIP Conference Proceedings [Author(s) THE 2ND INTERNATIONAL CONFERENCE ON APPLIED SCIENCE AND TECHNOLOGY 2017 (ICAST'17)-
13. Idowu Jonas Sagbo,1 Maryna van de Venter,2 Trevor Koekemoer,2 and Graeme Bradley(2018), In Vitro Antidiabetic Activity and Mechanism of Action of Brachylaena elliptica (Thunb.) DC, Volume 2018 |Article ID 4170372.
14. Rashmi S. Tupe, Nisha G. Kemse, Amrita A. Khaire, and Shamim A. Shaikh(2016), Attenuation of glycation-induced multiple protein modifications by Indian antidiabetic plant extracts, Pharm Biol. 2017; 55(1): 68–75.
15. Michael Zahn, Thao Trinh, Mijeong Lee Jeong, Desheng Wang, Padmapriya Abeysinghe, Qi Jia, Wenwen Ma. A reversed-phase high-performance liquid chromatographic method for the determination of aloesin, aloeresin a and anthraquinone in Aloe ferox.2008 phytochemical analysis 19(2).
16. Hamsar M.N., S. Ismail, M.N. Mordi, S. Ramanathan, S.M. Mansor, 2011, Antioxidant activity and the effect of different parts of Areca catechu extracts on Glutathione-S- Transferase activity in vitro,Free Radicals and Antioxidants, 1:28-33.
17. Hansawasdi C, Kawabata J, Kasai T. Alpha amylase inhibitors from Roselle (*Hibiscus sabdariffa* Linn.) tea. Biosc. Biotech. Biochem. 2000; 64: 1041 -1 043.
18. Keshava Bhat S, Mythri S, Ashwin D(2017). Antimicrobial properties of areca nut, areca catechu,L; Int. J. Ayurveda Pharm.8(3).
19. Musdja MY., Nurdin A, and Musir A(2020). Antidiabetic effect and tolerance of areca nut (areca catechu) seed ethanol on alloxan induced diabetic male rats.
20. S. W. Odeyemi, A comparative study of the in vitro antidiabetic properties, cytotoxicity and mechanism of action of *Albuca bracteata* and *Albuca setosa* bulb extracts Doctoral dissertation [Doctoral, thesis], University of Fort Hare, 2015.

Biosynthesis of Silver Nanoparticles from *Artocarpus Hirsutus* Leaf Extracts

Dr .K.Sowmiya, Dr. R. Purushothaman, R. Ramya, Chinnadurai

Dhanalakshmi Srinivasan College of Arts and Science for Women(Autonomous) Perambalur - 621212.

Abstract: Green synthesis of silver nanoparticles was achieved by reducing the bioavailability of silver nitrate using *Artocarpus Hirsutus* leaf aqueous extract. The formation of AH-AgNPs was confirmed by UV-Vis spectroscopy. The synthesized silver nanoparticles were monitored by recording the surface plasmon resonance peak observed at 425nm. Functional groups of biomarkers in the extracts and their interaction with AgNPs were identified by FTIR analysis. XRD analysis confirmed the nature and presence of silver. The developed method for the synthesis of silver nanoparticles using *Artocarpus Hirsutus* leaf extract is an eco-friendly and convenient method. In the future, integrated AH -AgNPs may be used in the biomedicine, biosensor, and nanotechnology fields.

Keywords: *Artocarpus Hirsutus*, Silver nanoparticles, XRD, UV, FTIR.

INTRODUCTION

In recent years, numerous approaches using chemicals or electrochemistry have been investigated for the preparation of silver nanoparticles (AgNPs). However, most of the techniques have difficulties during the refining phase as the used chemicals or the byproducts created are hazardous and require more energy to manufacture ^{1,2}. Numerous materials are used in the preparation of nanoparticles such as metal oxide ceramics, metals, silicate, and non-oxide ceramics. Currently, the most widely used methods for the production of nanoparticles are reduction of chemical or light chemistry and electrochemistry ³. Controlling the size shape of nanoparticles and achieving monodispersity are common challenges faced by researchers ⁴. The characterization of synthesized silver nanoparticles was performed using SEM, FTIR, DLS, and XRD imaging.

MATERIAL and METHODS

Plant Material Source

Plant material leaves of *Artocarpus Hirsutus* (figure 1) were collected from Trichy, Tamilnadu.



Fig.1 *Artocarpus Hirsutus*

Preparation of plant extract

Fresh leaves of *Artocarpus Hirsutus* were gathered from Trichy, India. Silver nitrate was obtained from Sigma-Aldrich. *Artocarpus Hirsutus* leaves were washed with tap water to remove dirt, then washed with double distilled water and dried in the dark to remove moisture completely. 10 g of dried leaves grained in Mortor is added to 100 ml of double-distilled water and boiled for 5 minutes at 60 ° C. After cooling, the plant extract was filtered done Whatman's Number 1 filter paper and the liquid was stored at 4 ° C for the synthesis of silver nanoparticles (AgNPs)

Biosynthesis of AgNPs

Bioenergetics of AgNPs, 10 mL of liquid extract was added to 100 mL of 5 mL of fluid AgNO₃⁵ solution. The mixture was boiled for 10 min at 95 ° C. The reaction of silver nanoparticles was observed by a change in the color of the mixture during the temperature treatment. A control group was also developed without leaf extract. The solution of AgNPs was purified by repeated centrifugation at 10000 rpm for 20 min 4 °C. The resulting hole was suspended in distilled double distilled water and

dried using Archive. The reduction of silver nanoparticles was observed by the change in color Reaction compound during temperature treatment ⁶⁻¹⁰



Fig.2 Colour changed from brown to pale yellow

Characterization

UV-Vis Spectra Analysis

The absorption spectrum of AgNPs and Plant Extract aqueous solutions were stored with a UV-Vis Spectrophotometer ¹¹⁻¹⁶ (Perkin Elmer) in the range of 0–900nm at room temperature. Analysis Quartz was carried out with quartz. The reaction mixture was monitored spectroscopically from 0 to 150 min every 30 min. There was distilled water used as a blank solution.

FTIR Analysis

The presence of plant elements on the surface of AgNPs was determined by Fourier to transform infrared spectroscopy (FT-IR). Potassium bromide atoms were prepared for Plant Extract and AgNP. This analysis helps determine which bonds are responsible for the synthesis and stability of silver nanoparticles. The biogeochemistry of NPs was demonstrated by a comparative study of FTIR (Perkin Elmer 400 FTIR) spectroscopy in the range of 4000-500cm⁻¹.

PXRD Analysis

X-ray diffraction (XRD) analysis was performed to study the crystal structure AgNPs. The XRD method was recorded using an embryo X-ray diffractometer.

RESULT AND DISCUSSION

UV-vis spectrum Analysis

The use of a UV-vis spectrophotometer induces localized surface plasmon vibrations in the metal, causing an electric field to resonate at a certain wavelength, causing a strong beam dispersion at that wavelength. Assessment of spectrophotometric measurements at this level; Color or color calibration estimation is performed at different wavelengths. Surface plasmon resonance was induced by reducing the Ag + ion in the AgNP complex by extracting the horse chestnut leaf and, consequently, quantifying the UV-Vis spectrophotometer. AgNP formation is expected in the wavelength range of 386 nm, according to UV-Vis measurements. The synthesis of AgNPs in liquid solution was observed by measuring the absorption spectra in the wavelength range of 300–1100 nm (Figure 3). The solution of silver nitrate became dark brown with the juice of the leaves. In the UV-vis spectrum; The single, strong, and wide surface plasmon resonance peak was observed at 464 nm, which confirmed the synthesis of AgNPs ¹⁷⁻¹⁹

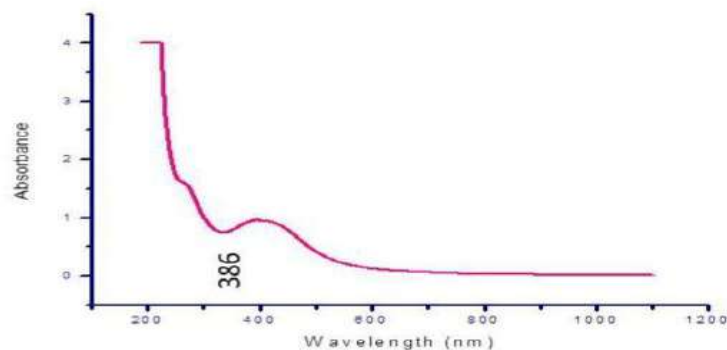


Fig.3 UV-Vis spectrum of AgNPsUsing *Artocarpus Hirsutus* Leaf leaf extract

FTIR Analysis

The FTIR spectrum confirmed the interaction between silver nanoparticles and capping agents. FTIR spectra of 3381, 2925, 2865 cm⁻¹ (phenolic OH) and 1598 cm⁻¹ (aromatic N-H stretches) in speciosa leaf extracts (Figure S3 (a))., 1384 cm⁻¹ (-OH Stretch), 1072 cm⁻¹ (Aromatic C-H Stretch), 914 cm⁻¹ (Protein Binding due to Carbonyl Stretching in Proteins), 830 cm⁻¹ (Aromatic ring Stretch), 667 cm⁻¹ (C-C bond or set group II of the aromatic ring), 607 cm⁻¹ (aromatic secondary amine CN stretching. which indicates the reduction of the corresponding functional groups (figure. 4). The results obtained show that the

polyphenols in Cassia anceolata leaf extracts are extended in the C-C and CNresonance.

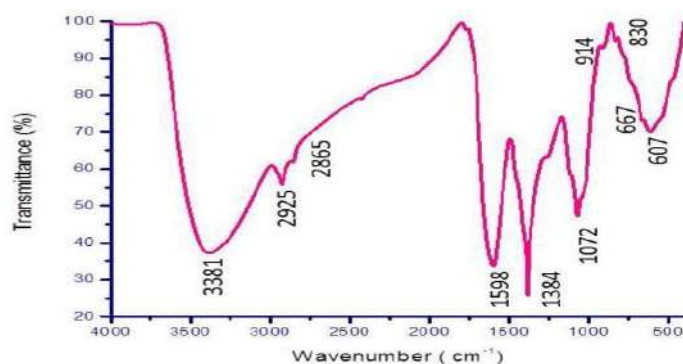


Fig 4 FT-IR spectrum of AgNPs Using ArtocarpusHirsutus leaf extract

PXRD Analysis

The crystallinity of silver nanoparticles was confirmed by analysis of XRD shape as shown in Figure 3. Five different difference peaks in the values of 38.03° , 44.29° , 64.49° , 77.49° and 81.51° which can be indexed to the (1 1 1), (2 0 0), (2 2 0), (3 1 1) and (2 2 2) reflective planes of the face-centered cube structure (figure. 5). The intensity of 100% was observed 2θ value with 38.03° . These peaks are caused by existing organic compounds that are responsible for the extraction and reduction of silver ions and the stabilization of the resulting nanoparticles²¹.

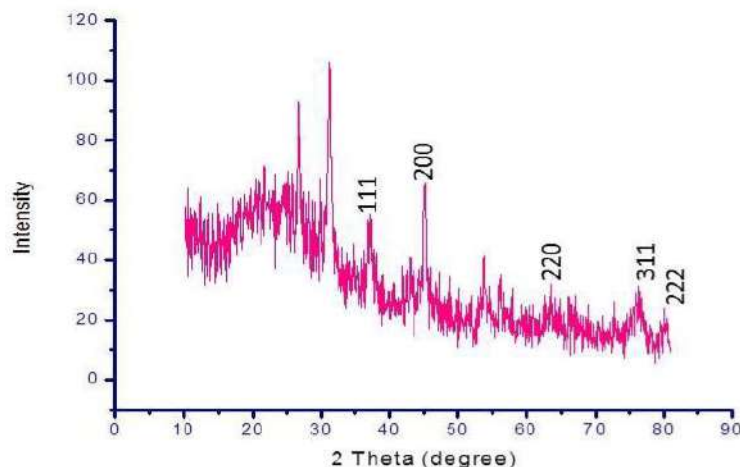


Fig.5 PXRD pattern of AgNPs synthesized using the supernatant of ArtocarpusHirsutus leaf

CONCLUSIONS

The biocompatible synthesis of silver nanoparticles (AgNO_3) was achieved by applying a simple and novel green chemistry procedure involving the use of Cassia anceolata leaf extract as a reducing and capping agent. The biosynthesis of silver nanoparticles was carried out via hydroxide precipitation at room temperature followed by calcination at 450°C . The successful formation of silver nanoparticles was confirmed by UV, FTIR, XRD analyses. XRD results confirm the average crystallite size observed from the intense plane of (1 1 1) was measured as 38.03 nm.

CONFLICT OF INTEREST

Conflict of interest declared none.

REFERENCE

1. Kim JS, Kuk E, Yu KN, Kim JH, Park SJ, Lee HJ, et al. Antimicrobial effects of silver nanoparticles. *Nanomedicine* 2007;3:95–101.
2. Mukunthan KS, Elumalai EK, Patel TN, RamachandraMurty FV. *Catharanthusroseus*: a natural source for the synthesis of silver nanoparticles, Asian Pacific. *J Trop Biomed* 2011;1:270–4.
3. Sharma VK, Yngard RA, Lin Y. Silver nanoparticles: green synthesis and their antimicrobial activities. *Adv Colloid Interface Sci* 2009;145:83–96.
4. Saifuddin N, Wong CW, NurYasumira AA. Rapid biosynthesis of silver nanoparticles using culture supernatant of bacteria with microwave irradiation. *E-J Chem* 2009;6:61–70.
5. Satishkumar G, Titelman L, Landau MV. The mechanism for the formation of tin oxide nanoparticles and nanowires inside the mesopores of SBA-15. *J Solid State Chem* 2009;182:2822–8.

7. Kalishwaralal K, Deepak V, Pandian SRK, Kottaisamy M, Kartikeyan B, Gurunathan S. Biosynthesis of silver and gold nanoparticles using *Brevibacteriumcasei*. *Colloids Surf, B* 2010;77:257–62.
8. Vigneshwaran N, Ashtaputre NM, Varadarajan PV, Nachane RP, Paralikar KM, Balasubramanyan RH. Biological synthesis of silver nanoparticles using the fungus *Aspergillusflavus*. *Mater Lett* 2007;61:1413–8.
9. Gajbhiye M, Kesharwani J, Ingle A, Gade A, Rai M. Fungus-mediated synthesis of silver nanoparticles and their activity against pathogenic fungi in combination with fluconazole. *Nanomed Nanotech Biol Med* 2009;5:382–6.
10. Krishnaraj C, Jagan EG, Rajasekar S, Selvakumar P, Kalaichelvan PT, Mohan N. Synthesis of silver nanoparticles using *Acalyphaindica* leaf extracts and its antibacterial activity against waterborne pathogens. *Colloids Surf, B* 2010;76:50–6.
11. Sathishkumar M, Sneha K, Won SW, Cho CW, Kim S, Yun YS. Cinnamon *zeylanicum* bark extract and powder mediated green synthesis of nano-crystalline silver particles and its bactericidal activity. *Colloids Surf, B* 2009;73:332–8.
12. Parashar V, Parashar R, Sharma B, Pandey AC. *Parthenium* leaf extract mediated synthesis of silver nanoparticles: a novel approach towards weed utilization. *Digest J NanomatBiostruct* 2009;4:45–50.
13. Jain D, Kumar Daima H, Kachhwaha S, Kothari SL. Synthesis of plant-mediated silver nanoparticles using papaya fruit extract and evaluation of their antimicrobial activities. *Digest J NanomatBiostruct* 2009;4:557–63.
14. Song JY, Jang HK, Kim BS. Biological synthesis of gold nanoparticles using *Magnolia kobus* and *Diopyros kaki* leaf extracts. *Process Biochem* 2009;44:1133–8.
15. Narayanan KB, Sakthivel N. Green synthesis of biogenic metal nanoparticles by terrestrial and aquatic phototrophic and heterotrophic eukaryotes and biocompatible agents. *Adv Colloid Interface Sci* 2011;169:59–79.
16. Ramirez IM, Bashir S, Luo Z, Liu JL. Green synthesis and characterization of polymer-stabilized silver nanoparticles. *Colloids Surf, B* 2009;73:185–91.
17. Biswas K, Chattopadhyay I, Banerjee RK and Bandyopadhyay U. Biological activities and medicinal properties of neem (*Azadirachta indica*). *Curr Sci*, 2002; 82(11): 1336 – 1345.
18. Charleston DS. Impact of botanical pesticides derived from *Melia azedarach* and *Azadirachta indica* plants on the emission of volatiles that attracts Parasitoids of the diamondback moth to cabbage plants. *J. Chem. Ecol.* 2006; 32(2): 325–49.
19. Cox PA. In: The ethnobotanical approach to drug discovery: strengths and limitations. In, ethnobotany and the search for the new drugs.1994; pp. 25-36, John Wiley & Sons. England.
20. Dalziel, J.M. (1956). The Useful Plants of West Tropical Africa. Crown .Agents, London, p: 612.
21. Daniels, R. and Knie, U. (2007). Galenics of dermal products vehicles, properties, and drug .
22. Shi J., Chan C., Pang Y., Ye W., Tian F., Lyu J., Zhang Y., Yang M. A fluorescence resonance energy transfer (FRET) biosensor based on graphene quantum dots (GQDs) and gold nanoparticles (AuNPs) for the detection of *mecA* gene sequence of *Staphylococcus aureus*. *Biosens. Bioelectron.* 2015;67:595–600.
23. Baetsen-Young A.M., Vasher M., Matta L.L., Colgan P., Alocilja E.C., Day B. Direct colorimetric detection of unamplified pathogen DNA by dextrin-capped gold nanoparticles. *Biosens. Bioelectron.* 2018;101:29–36.

Catalyst Free Synthesis of Bis-(N Aminoethylethanolamine)-Copper (II) Complex and Its Medicinal Activity Studies

V.S.Sangeetha*, Dr.P.Viswamithran, Dr.Gurumoorthy ,Bhakya jothi V

DhanalakshmiSrinivasan College of Arts and Science for Women Autonomous Perambalur Tamilnadu-621212

*Corresponding Author Mail id :sangeethavasanth23@gmail.com

Abstract: In this work, the copper complexes was synthesised in the conventional method. It was an eco-friendly method with less amount of solvent was preferred. In this method the catalyst free synthesis of copper complexes are more preferable. The reaction was carried out in the room temperature . The complexes has been synthesised and the formation of the complexes were confirmed by Its melting point ,the characterisation studies like UV-Visible as well as FT-IR ,Antimicrobial studies based on the ant feeding and larvicidal activity against mosquito. In scope of this work, the pharmacological activity of the newly synthesised copper complex has a positive affects in the biological activity. Present work has focused on the larvicidal activity. But it can be analysis for the anti-inflammatory, anti-cancer, antiallergic activity and so on.

Key words: Eco friendly, Larvicidal, Anti feeding, Ligand, CU(II) Complex

INTRODUCTION

Copper exhibits considerable biochemical action either as an essential trace metal or as a constituent of various exogenously administered compounds in humans. In its former role it is bound to ceruloplasmin, albumin, and other proteins, while in its latter it is bound to ligands of various types forming complexes that interact with biomolecules, mainly proteins and nucleic acids ¹⁻⁴. The multifaceted role of copper in biological systems is demonstrated by several studies. In particular the involvement of copper in human diseases has been described from a medicinal-chemical and a biochemical view focusing on the molecular physiology of Cu transport ⁵⁻⁷. Much of the current research effort is cited on copper homeostasis and its relation to iron metabolism as well as the role of copper in biological processes related to human physiology and pathology. While a lot of the functions that have been proposed to account for the homeostasis of inorganic noncomplexed copper in humans have been described, only a limited number of review studies have focused on the multiple biochemical events which could be directly implicated in the use of copper complexes in medicine.⁸⁻¹¹ To be considered as Molecular Biology International a functional index of Cu status, the chosen marker must (a) respond sensitively, specifically, and predictably to changes in the concentration and/or supply of readily available (and potentially toxic) copper, (b) be accessible for measurement and measurable, and (c) impact directly on health. It is estimated that less than 5% of the total copper concentration circulates independently of binding proteins such as ceruloplasmin.¹²⁻¹⁴ The concentration of protein-free copper is very low relative to the total serum copper concentration, and therefore a clinically significant change in the free copper concentration may not be detected through measuring total copper concentrations in serum alone. Because copper is most toxic in the unbound form, measurement of unbound copper in circulation would theoretically be the most direct laboratory test for detecting potentially toxic copper overload. For these reasons, a single index, such as total copper concentration in serum (determined by several standardized methods, including atomic absorption spectrometry (AAS), inductively coupled plasma emission spectroscopy (ICP), and colorimetric methods applied to autoanalyzers), is inadequate for assessing the total body copper nutriture of an individual and must be supported by collaborating evidence ¹⁵⁻¹⁷. Usually, immunoreactive or enzymatically measured ceruloplasmin (Cp) levels are used to evaluate the body storage of copper. Cp levels are a good reflector (or biomarker) to keep copper status in the right therapeutic window, avoiding clinical copper deficiency. The specific activity of copper-containing enzymes in blood cells, such as erythrocyte superoxide dismutase and platelet or leukocyte cytochrome c oxidase, may be a better indicator of metabolically active copper stores than the serum concentration of copper or ceruloplasmin, since the enzyme activities are sensitive to changes in copper stores but are not sensitive to factors not related to copper nutriture. Despite the fact that the ideal index of copper status in adult humans has not been established yet, certain novel potential biomarkers that could be analyzed to screen for copper deficiency are currently under evaluation. Copper chaperon for superoxide dismutase (CCS) has been proposed as a sensitive and accurate biomarker since it reflects both deficiency and excess states of Cu. CCS levels in blood erythrocytes and white cells are determined with specific antibodies and have been shown to vary inversely proportional to Cu status .

MATERIALS AND METHODS

All chemicals were purchased from Merck, Sigma-Aldrich, and used without further purification. Solvent was dried and distilled prior to use. Merck pre-coated silica gel plates with a fluorescent indicator were used for analytical TLC. Flash column chromatography was performed using silica gel (Merck). Ethyl acetate hexane was used as an eluting solvent for TLC and column chromatography ¹⁸. Melting points were recorded in open capillary tubes and were uncorrected. The UV-Visible spectra (KBr) were recorded on a Shimadzu UV - 1280 (200-800 nm) spectrometer. The FT-IR spectra (KBr) were recorded on a Shimadzu 8201pc (4000-400 cm⁻¹) spectrometer.¹⁹

Preparation of Bis-(N-aminoethylethanolamine)-Copper (II) Complex (I).

The compoundsN-aminoethylethanolamine (0.02mol, 2ml) in 5ml ethanol is stirred in a magnetic stirrer with CuCl₂.2H₂O

(0.01mol, 1.7g) in 5ml ethanol for one hour. Blue coloured precipitate was formed. The solvent ethanol was evaporated under vacuum. The product was confirmed by TLC. The product was recrystallized in ethanol to get pure product ²⁰⁻²².

Bis-(N-aminoethylethanolamine)-Copper (II) chloride(I).

Blue solid; mw: 398.86; mp 195°C; UV $\lambda_{\text{MeOH max}}^{\text{nm}}$ (abs): 225 (0.65), 253 (0.79), 591 (0.02); IR (cm⁻¹): 3759.70 (OH), 3410.74 (NH), 2922.91 (CH), 1474.46 (C-N) 1018.83 (C-O), 745.22 (CHbend) 670.80 (Disubstituted); Elemental analysis: Calculated. for: C₁₂H₃₂Cl₂CuN₄O₂: C, 36.14; H, 8.09; N, 14.05 %; Found: C, 36.12; H, 8.10; N, 14.06; %

RESULTS AND DISCUSSION

The complex I was prepared according to the synthesis sequences illustrated in scheme I. Complex I was synthesised by the condensation reaction using N-aminoethylethanolamine reacted with CuCl₂.2H₂O in ethanol medium (Scheme I). The compounds were confirmed by recording the UV and IR spectra ²⁵. UV-VIS profile of complex I was studied at a wavelength range of 200 to 800 nm ²⁶. Three major bands were noticed at 225, 253 and 591 nm with absorbance values of 0.65, 0.79 and 0.02 respectively. FT-IR spectrum of complex I was performed to identify the functional groups present in the complex based on the peak values in the region of infrared radiation. The major bands were observed at $\nu_{\text{KBr}}^{\text{cm}^{-1}}$: 3759.70, 3410.74, 2922.91, 1474.46, 1018.83, 745.22 and 670.80. The peak at 3759.70 cm⁻¹ indicates the absorption arising from Cu-OH stretching. The peak at 3410.74 cm⁻¹ indicates the absorption arising from Cu-NH stretching ²⁷⁻²⁹. The peak at 2922.91 cm⁻¹ indicates the absorption arising from C-H stretching. The peak at 1474.46 cm⁻¹ corresponds to the presence of C-N stretching frequency. The peak at 1018.83 cm⁻¹ confirms the stretched vibration of C-O bond in the alcohol moiety. The peak at 745.22 cm⁻¹ indicates the bending vibration of aliphatic C-H bonds ³⁰⁻³². The peak at 670.80 cm⁻¹ corresponds to the disubstituted moiety in the aliphatic compound. In addition, some weak absorption bands were also recorded in the spectra.

Larvicidal activity

Complex I was active against Culexquinquefasciatus LD₅₀ value of 69.83 $\mu\text{g/ml}$

Table 1.Larvicidal activity of synthesized complexes .

Comp.No.	Mortality (%)Room temp Concentration($\mu\text{g /mL}$) ^a				LD ₅₀ ($\mu\text{g /mL}$)
	100	50	25	10	
I	68 \pm 0.67	40 \pm 1.29	24 \pm 1.78	12 \pm 0.98	69.83
Positive control	-	-	-	-	60.03
Negative control	0.0 \pm 0.0	0.0 \pm 0.0	0.0 \pm 0.0	0.0 \pm 0.0	0.0 \pm 0.0

Positive control: Permethrin Negative control:DMSO, ^aValue were the means of three replicates \pm SD.

Antifeedant activity (Ichthyotoxicity activity)

Complex I showed high toxicity. Complex I produced 66% mortality in 24hr at 100 $\mu\text{g/ml}$ respectively. Toxicity was measured as the death percentage at 24hr. The values are summarized in Table 2. Complex I was highly active with the LD₅₀ value of 69.57 $\mu\text{g/ml}$.

Table 2.Antifeedantactivity of synthesized complexes .

Comp.No.	Mortality (%)Room temp Concentration($\mu\text{g /mL}$) ^a				LD ₅₀ ($\mu\text{g /mL}$)
	100	50	25	10	
I	66 \pm 1.45	42 \pm 0.78	28 \pm 1.18	12 \pm 0.06	69.57
Negative control	0.0 \pm 0.0	0.0 \pm 0.0	0.0 \pm 0.0	0.0 \pm 0.0	0.0 \pm 0.0

Negative control:DMSO ^aValue were the means of three replicates \pm SD

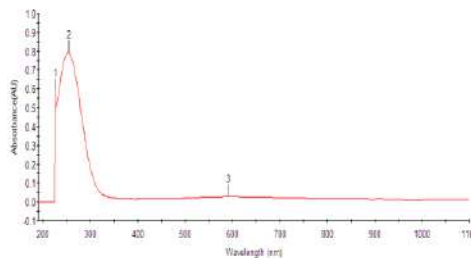


Fig 1. UV spectrum of complex I.

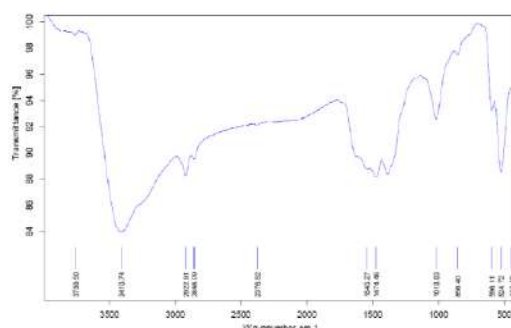


Fig.2.. IR spectrum of complex I

CONCLUSION

From the present study, it can be concluded that the potency of the copper (II) complexes shows significant activity in larvicidal and less toxic in antifeedant bioassays. The derived complex I shows significant activity against mosquito larvae compared with positive control and shows less toxic in antifeedant activity. Therefore, these compounds might be a potential source for developing ecologically significant bioactive compounds, including biodegradable pesticides, and biopharmaceuticals.

CONFLICT OF INTEREST

Conflict of interest declared none.

REFERENCES

- Chakraborty, P. Kumar, K. Ghosh, and P. Roy, Evaluation of a Schiff base copper complex compound as potent anticancer molecule with multiple targets of action, *European Journal of Pharmacology*, vol. 647, no. 13, pp. 112, 2010.
- R. H. Holm, P. Kennepohl, and E. I. Solomon, Structural and functional aspects of metal sites in biology, *Chemical Reviews*, vol. 96, no. 7, pp. 22392314, 1996.
- M. A. Ali, C. M. Haroon, M. Nazimuddin, S. M. M.-U. Majumder, M. T. H. Tarafder, and M. A. Khair, Synthesis, characterization and biological activities of somenewnickel(II), copper(II), zinc(II) and cadmium(II) complexes of quadridentate SNNS ligands, *TransitionMetal Chemistry*, vol. 17,no. 2, pp. 133136, 1992.
- D. T. Minkel, C.H. Chanstier, and D. H. Petering, Reactions of 3-Ethoxy-2-oxobutyraldehyde Bis(N4-dimethylthiosemicarbazonato)- Zinc(II) with tumor cells and mitochondria, *Molecular Pharmacology*, vol. 12, no. 6, pp. 10361044, 1976.
- V. Rajendiran, R. Karthik, M. Palaniandavar et al., Mixedlig and copper (II)-phenolate complexes: effect of coligand on enhanced DNA and protein binding, DNA cleavage, and anticancer activity, *Inorganic Chemistry*, vol. 46, no. 20, pp. 8208 8221, 2007.
- E. Liberta and D. X. West, Antifungal and antitumor activity of heterocyclic thiosemicarbazones and their metal complexes: current status, *Biometals*, vol. 5, no. 2, pp. 121126, 1992.
- 7.Y. Harinath, D. H. K. Reddy, B. N. Kumar, C. Apparao, and K. Seshaiah, Synthesis, spectral characterization and antioxidant activity studies of a bidentate Schiff base, 5-methyl thiophene-2-carboxaldehyde-carbohydrazone and its Cd(II), Cu(II), Ni(II) and Zn(II) complexes, *Spectrochimica Acta Part A: Molecular and Biomolecular Spectroscopy*, vol. 101, pp. 264272, 2013.
- J. Sheikh, H. Juneja, V. Ingle, P. Ali, and T. B. Hadda, Synthesis and in vitro biology of Co(II), Ni(II), Cu(II) and Zinc(II) complexes of functionalized beta-diketone bearing energy buried potential antibacterial and antiviral O,O pharmacophore sites, *Journal of Saudi Chemical Society*, vol. 17, no. 3, pp. 269276, 2013.
- C. Marzano, M. Pellei, F. Tisato, and C. Santini, Copper complexes as anticancer agents, *Anti-Cancer Agents in Medicinal Chemistry*, vol. 9, no. 2, pp. 185211, 2009.
- 10.S. M. Saadeh, Synthesis, characterization and biological properties of Co(II), Ni(II), Cu(II) and Zn(II) complexes with an SNO functionalized ligand, *Arabian Journal of Chemistry*, vol. 6, no. 2, pp. 191196, 2013.
- J. Garcí a-Tojal, A. Garcí a-Orad, A. A. Díaz et al., "Biological activity of complexes derived from pyridine-2-carbaldehyde thiosemicarbazone: structure of [Co(C7H7N4S)2][NCS]," *Journal of Inorganic Biochemistry*, vol. 84, no. 3-4, pp. 271–278, 2001.
- P. R. Reddy and A. Shilpa, "2-hydroxynaphthalene-1-carbaldehyde- and 2-aminomethyl)pyridine-based Schiff base CuII complexes for DNA binding and cleavage," *Chemistry & Biodiversity*, vol. 9, no. 10, pp. 2262–2281, 2012.
- N. Shahabadi, M.M. Khodaei, S. Kashanian, and F. Kheirdoosh, Interaction of a copper (II) complex containing an artificial sweetener (aspartame) with calf thymus DNA, *Spectrochimica Acta Part A: Molecular and Biomolecular Spectroscopy*, vol. 120, pp. 16, 2014.
- A. J. Steckl, DNA a new material for photonics *Nature Photonics*, vol. 1, pp. 35, 2007.
- S. Bandyopadhyay, M. Tarek, and M. L. Klein, Molecular dynamics study of a lipid-DNA complex, *The Journal of Physical Chemistry B*, vol. 103, no. 46, pp. 1007510080, 1999.

16. M. Hazra, T. Dolai, A. Pandey, S. K. Dey, and A. Patra, Fluorescent copper (II) complexes: the electron transfer mechanism, interaction with bovine serum albumin (BSA) and antibacterial activity, *Journal of Saudi Chemical Society*, 2014.
17. D. Becke, Density-functional thermochemistry. III. The role of exact exchange," *The Journal of Chemical Physics*, vol. 98, article 5648, 1993.
18. Lee, W. Yang, and R. G. Parr, "Development of the Colle-Salvetti correlation-energy formula into a functional of the electron density, *Physical Review B*, vol. 37, no. 2, pp. 785789, 1998.
19. S. Roy, T. K. Mondal, P. Mitra, E. L. Torres, and C. Sinha, Synthesis, structure, spectroscopic properties, electrochemistry, and DFT correlative studies of N-[(2-pyridyl)methylidene]-6-coumarin complexes of Cu(I) and Ag(I), *Polyhedron*, vol. 30, no. 6, pp. 913922, 2011.
20. J.A. Pople, M. J. Frisch, G.W. Trucks et al., *Gaussian 09, Revision B.01*, Gussian, Wallingford, UK, 2009.
21. M. E. Reichman, S. A. Rice, C. A. Tgomas, and P. Doty, A further examination of the molecular weight and Size of desoxypentose nucleic acid, *Journal of the American Chemical Society*, vol. 76, no. 11, pp. 30473053, 1954.
22. D. Lahiri, T. Bhowmick, B. Pathak et al., Anaerobic photocleavage of DNA in red light by dicopper(II) complexes of 3,3-dithiodipropionic acid, *Inorganic Chemistry*, vol. 48, no. 1, pp. 339349, 2009.
23. J. Singh and P. Singh, Synthesis, spectroscopic characterization, and in vitro antimicrobial studies of pyridine-2-carboxylic acid N-(4-chloro-benzoyl)-hydrazide and its Co(II), Ni(II), and Cu(II) complexes, *Bioinorganic Chemistry and Applications*, vol. 2012, Article ID 104549, 7 pages, 2012.
24. S. Dey, T. Mukherjee, S. Sarkar, H. S. Evans, and P. Chattopadhyay, 5-Nitro-1,10-phenanthroline bis(N,Npyridylmethylthio-K)- bis(perchlorato) copper(II):synthesis, structural characterization, and DNA-binding study," *Transition Metal Chemistry*, vol. 36, no. 6, pp. 631–636, 2011.
25. M. Valko, R. Boca, R. Klement et al., "Effect of hydrogenation on electronic and distant magnetic properties in copper (II) complexes with derivatives of tetrahydrosalen and salen. X-ray crystal structure of [CuBu₂Me(saltmen)] complex, *Polyhedron*, vol. 16, pp. 903908, 1997.
26. S. Dey, S. Sarkar, H. Paul, E. Zangrando, and P. Chattopadhyay, Copper (II) complex with tridentate N donor ligand: synthesis, crystal structure, reactivity and DNA binding study, *Polyhedron*, vol. 29, no. 6, pp. 15831587, 2010.
27. B. H. Chen, H. H. Yao, W. T. Huang, P. Chattopadhyay, J. M. Lo, and T. H. Lu, Syntheses and molecular structures of three Cu(II) complexes with tetridentate imine-phenols, *Solid State Sciences*, vol. 1, no. 2-3, pp. 119131, 1999.
28. B. P. Lever, *Inorganic Electronic Spectroscopy*, Elsevier, Amsterdam, The Netherlands, 2nd edition, 1984.
29. S. Sarkar, A. Patra, M. G. B. Drew, E. Zangrando, and P. Chattopadhyay, Copper (II) complexes of tetridentate N₂S₂ donor sets: synthesis, crystal structure characterization and reactivity, *Polyhedron*, vol. 28, no. 1, pp. 16, 2009.
30. W. Kemp, *Organic Spectroscopy*, Macmillan Press, New York, NY, USA, 1975.
31. R. A. Sheikh, S. Shreaz, G. S. Sharma, L. A. Khan, and A. A. Hashmi, Synthesis, characterization and antimicrobial screening of a novel organylborate ligand, potassium hydro(phthalyl)(salicylyl)borate and its Co(II), Ni(II), and Cu(II) complexes, *Journal of SaudiChemical Society*, vol. 16,no. 4, pp. 353361, 2012.
32. D. Kulkarni, S. A. Patil, and P. S. Badami, Electrochemical properties of some transition metal complexes: synthesis, characterization and in-vitro antimicrobial studies of Co(II), Ni(II), Cu(II), Mn(II) and Fe(III) complexes, *International Journal of Electrochemical Science*, vol. 4, pp. 717729, 2009.
33. S. Konar, A. Jana, K. Das et al., Synthesis, crystal structure, spectroscopic and photoluminescence studies of manganese(II), cobalt(II), cadmium(II), zinc(II) and copper(II)

Synthesis and Characterization of Nickel Complexes by Using Various Organic Ligands and It's Mosquito Larvicidal Activity Evaluation

G.Vanaja, Dr.A.Priya, Dr.Tadinaveen, J. Dhebiga

Dhanalakshmisrinivasan College of arts and science for women (Autonomous), Perambalur-621212

Abstract: In this work, the nickel complexes were synthesised in a convenient method like the conventional method. It was an eco-friendly method with less amount of solvent. In this method the catalyst free synthesis of nickel complexes is more preferable. The reaction was carried out in the room temperature for such ligands and reflux temperature for such types of ligands. This will be helpful to carryout in normal condition. The complexes have been synthesized and the formation of the complexes were confirmed by its melting point, the characterization studies like UV-Visible as well as FT-IR. Antimicrobial studies based on the ant feeding and larvicidal activity against mosquitoes

Keywords: FT-IR.,UV-Visible, Antimicrobial,Nickel oxide

INTRODUCTION

Nickel has a lot of compounds and complexes which present the oxidation states -I, 0, +I, +2, +3, +4. The compounds of Ni (0) are quite usual, with special relevance to the carbonyl Ni (CO)₄, and they are a very volatile colorless liquid used in material plating. The oxidation state +2 is the most common one, being known a great number of compounds, namely the hydroxide Ni (OH)₂, the oxide NiO, salts of all the inorganic acids and of a great number of organic acids. Among these we refer the sulfate, usually used in electroplating solutions, the acetate, used as catalyst and mordant in the textile industry, the formate, used in the production of catalysts, the isodecyl orthophosphate and the naphthenate, used as motor oil and lubricants additives, and many other, with several applications in the laboratory and in chemical industry.¹ Metal complexes of Schiff base derived from 2-thiophene carboxaldehyde and 2-aminobenzoic acid (HL) and Fe (III) or Co (II) or Ni (II) or UO₂ (II) showed a good antibacterial activity against *Escherichia coli*, *Pseudomonas aeruginosa* and *Staphylococcus pyogenes*. Fe (III), Cu (II), Zn (II) and UO₂ (II) complexes caused inhibition for *E. coli*. The importance of this lies in the fact that these complexes could be applied fairly in the treatment of some common diseases caused by *E. coli*. However, Fe (III), Co (II), Cu (II), Zn (II) and UO₂ (II) complexes were specialized in inhibiting Gram-positive bacterial strains (*Staphylococcus pyogenes* and *P. aeruginosa*). The importance of this unique property of the investigated Schiff base complexes lies in the fact that it could be applied safely in the treatment of infections caused by any of these particular strains².

MATERIALS AND METHODS

Chemicals and reagents

All chemicals were purchased from Merck, Sigma-Aldrich, and used without further purification. Solvent was dried and distilled prior to use. Merck pre-coated silica gel plates with a fluorescent indicator were used for analytical TLC. Flash column chromatography was performed using silica gel (Merck). Ethyl acetate – hexane was used as an eluting solvent for TLC and column chromatography. Melting points were recorded in open capillary tubes and were uncorrected. The UV-Visible spectra (KBr) were recorded on a Shimadzu UV - 1280 (200-800 nm) spectrometer. The FT-IR spectra (KBr) were recorded on a Shimadzu 8201pc (4000-400 cm⁻¹) spectrometer³⁻⁵

Method of preparation

Preparation of Bis-(N-aminoethylethanolamine)-Nickel (II) Complex (1).

The compounds N-aminoethylethanolamine (0.01mol, 1ml) in 5ml ethanol is stirred in a magnetic stirrer with NiCl₂.4H₂O (0.005mol, 1g) in 5ml ethanol for one hour at 60°C. Skyblue coloured precipitate was formed. The solvent ethanol evaporated under vacuum. The product was confirmed by TLC. The product was recrystallized in ethanol to get pure product.Bis-(N-aminoethylethanolamine)-Nickel (II) chloride (1).Skyblue solid; mw: 394.01; mp: >360°C; UV λ_{MeOH} nm (abs): 225 (0.21), 359 (0.02); IR (cm⁻¹): 3426.21 (OH), 3238.61 (NH), 2925.86 (CH), 1467.97 (C-N)1063.84 (C-O), 789.99 (CHbend), 630.03 (Disubstituted); Elemental analysis:Calculated.for: C₁₂H₃₂Cl₂NiN₄O₂; C, 36.14; H, 8.09; N, 14.22 %; Found: C, 36.12;H, 8.10; N, 14.23; %Preparation of Bis-(4-benzylidene-3-methyl-1H-pyrazol-5(4H)-one)-Nickel (II) complex (2).The compounds 4-benzylidene-3-methyl-1H-pyrazol-5(4H)-one (0.01mol, 0.98) in 5ml ethanol is refluxed over a water bath in a magnetic stirrer with NiCl₂.4H₂O (0.005mol, 1g) in 5ml ethanol for three hours at 60°C. Then 30ml of 10% NaOH solution was added. Pale green coloured precipitate was formed. It is filtered and dried. The product was confirmed by TLC. The product was recrystallized in ethanol to get pure product⁶⁻⁸. Bis-(4-benzylidene-3-methyl-1H-pyrazol-5(4H)-one)-nickel (II) (2) Pale green solid; mw: 353.86; mp: >360°C; UV λ_{MeOH} max nm (abs): 252 (1.42); IR (cm⁻¹): 3433.42 (NH), 2928.32 (CH), 1631.73 (C=O), 1458.31 (C-N) 820.93(CHbend), 626.65 (Disubstituted); Elemental analysis: Calculated. ForC₁₀H₁₆Cl₂NiN₄O₂; C, 33.94; H, 4.56; N, 15.83; %. Found: C, 33.96; H, 4.55; N,15.82; %.Preparation of Bis-(1,3-cyclohexanedione)-Nickel (II) complex (3). The compounds 1,3-cyclohexanedione (0.01mol, 1.12) in 5ml ethanol is refluxed over a water bath in a magnetic stirrer with NiCl₂.4H₂O (0.005mol, 1g) in 5ml ethanol for three hours at 60°C. Then 30ml of 10% NaOH solution was added. Green

coloured precipitate was formed. It is filtered and dried. The product was confirmed by TLC. The product was recrystallized in ethanol to get pure product.

Bis-(1,3-cyclohexanedione)-nickel (II) (3) Pale green solid; mw: 282.95; mp: >360°C; UV λ^{MeOH} nm (abs): 225 (3.95), 244 (0.79), 271 (0.85) and 276 (0.87); IR (cm^{-1}): 2940.85 (CH), 1639.52 (C=O), 1186.56 (C-O), 865.55 (CHbend), 610.95 (disubstitutedmoity); Elemental analysis: Calculated. For $\text{C}_{12}\text{H}_{16}\text{NiO}_4$: C, 50.94; H, 5.70; %. Found: C, 50.95; H, 5.69; %.

Larvicidal activity

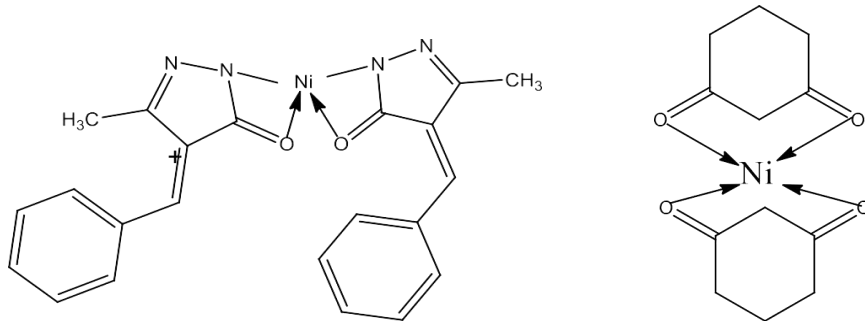
Larvicidal bioassay procedure from the previous literature (Song, G.P. et al.). Assessments were made on a dead/alive basis. Evaluations are based on a percentage scale of 0–100, which 0 equals no activity and 100 equals total kill. The bioassay was repeated three times, and the result of bioactivity was the average of these replicates. The values are compared with the positive control *Permethrin*. The LD₅₀values of some active title compounds were evaluated using probit analysis and the results were analysed using the SPSS v16 software⁹⁻¹¹.

Larvicidal Activity against Mosquito (*Culexquinquefasciatus*).

The larvicidal activity was evaluated at the preliminary test concentration of 100 $\mu\text{g mL}^{-1}$ against the fourth-instar *Culexquinquefasciatus* by the water immersion method 44 under conditions of (27 ± 2) °C, photoperiod of 10:14 (light:dark), and relative humidity 50–70%. All the test beakers containing twenty *Culexquinquefasciatus* were evaluated 8 days after treatment. The results were recorded by average percentage mortality.

Antifeedant activity

Fingerlings (1.5–2.0 cm) of marine acclimated *Oreochromismossambicus* were used for evaluating ichthyotoxic potential. Ten fingerlings were introduced in experimental and control glass bowls, each containing one L of seawater and the selected concentration of compound. Immediate reflex changes and mortality were observed continuously for the first 6 h, and then at 1-h intervals for the next 12 h. After 24 h of exposure, the number dead and live fish were counted.



Scheme 1. One-pot two component synthesis of Bis-(1,3-cyclohexanedione)-nickel(II) (3).

RESULTS AND DISCUSSION

The complex 1 was prepared according to the synthesis sequences illustrated in scheme 1. The complex 2 was prepared according to the synthesis sequences illustrated in scheme 2. The complex 3 was prepared according to the synthesis sequences illustrated in scheme 3. Complex 1 was synthesised by the condensation reaction using N-aminoethylethanolamine reacted with $\text{NiCl}_2 \cdot 4\text{H}_2\text{O}$ in ethanol medium. The complex 2 was synthesised by 3-methyl-1H-pyrazol-5(4H)-one reacted with $\text{NiCl}_2 \cdot 4\text{H}_2\text{O}$ by condensation method. The complex 3 was synthesised by 1,3-cyclohexanedione reacting with $\text{NiCl}_2 \cdot 4\text{H}_2\text{O}$ by condensation method (Scheme 1). The compounds were confirmed by recording the UV and IR spectra. UV-VIS profile of complex 1 was studied at a wavelength range of 200 to 800 nm. Three major bands were noticed at 225 and 359 nm with absorbance values of 0.21 and 0.02 respectively¹²⁻¹. FT-IR spectrum of complex 1 was performed to identify the functional groups present in the complex based on the peak values in the region of infrared radiation. The major bands were observed at V^{KBr} cm^{-1} : 3426.21, 3238.61, 2925.86, 1467.97, 1063.84, 789.99 and 630.03. The peak at 3426.21 cm^{-1} indicates the absorption arising from Ni-OH stretching. The peak at 3238.61 cm^{-1} indicates the absorption arising from Ni-NH stretching. The peak at 2925.86 cm^{-1} indicates the absorption arising from C-H stretching. The peak at 1467.97 cm^{-1} corresponds to the presence of C-N stretching frequency. The peak at 1063.84 cm^{-1} confirms the stretched vibration of C-O bond in the alcohol moiety. The peak at 789.99 cm^{-1} indicates the bending vibration of aliphatic C-H bonds. The peak at 630.03 cm^{-1} corresponds to the disubstituted moiety in the aliphatic compound. In addition, some weak absorption bands were also recorded in the spectra. UV-VIS profile of complex 2 was studied at a wavelength range of 200 to 800 nm. One major band was noticed at 252 nm with absorbance values of 1.42 respectively. FT-IR spectrum of complex 2 was performed to identify the functional groups present in the complex based on the peak values in the region of infrared radiation. The major bands were observed at V^{KBr} cm^{-1} : 3433.42, 2928.32, 1631.73, 1458.31, 820.93 and 626.65. The peak at 3433.42 cm^{-1} indicates the absorption arising from Ni-NH stretching. The peak at 2928.32 cm^{-1} indicates the absorption arising from C-H stretching. The peak at 1631.73 cm^{-1} corresponds to the presence of Ni-CO stretching frequency. The peak at 1458.31 cm^{-1} corresponds to the presence of C-N stretching frequency. The peak at 820.93 cm^{-1} indicates the bending vibration of aliphatic C-H bonds. The peak at 626.65 cm^{-1} corresponds to the disubstituted moiety in the aliphatic compound. In addition, some weak absorption bands were also recorded in the spectra. UV-VIS profile of complex 3 was studied at a wavelength range of 200 to 800 nm. Four major bands were noticed at 225, 244, 271 and 276 nm with absorbance values of 3.95, 0.79, 0.85 and 0.87 respectively. FT-IR spectrum of complex 3 was performed to identify the functional groups present in

complex based on the peak values in the region of infrared radiation. The major bands were observed at ν^{KBr} cm^{-1} : 2940.55, 1639.52, 1186.56, 865.55 and 610.95.80. The peak at 2940.55 cm^{-1} indicates the absorption arising from C-H stretching. The peak at 1639.52 cm^{-1} corresponds to the presence of Ni-CO stretching frequency. The peak at 1186.56 cm^{-1} corresponds to the presence of C-O stretching frequency. The peak at 865.55 cm^{-1} indicates the bending vibration of aliphatic C-H bonds. The peak at 610.95 cm^{-1} corresponds to the disubstituted moiety in the aliphatic compound. In addition, some weak absorption bands were also recorded in the spectra 15-16.

Larvicidal activity

Complex 2 was highly active against *Culexquinquefasciatus* LD_{50} value of 18.52 $\mu\text{g}/\text{ml}$ than complexes 1 and 3 with the LD_{50} value of 59.97 and 84.73 $\mu\text{g}/\text{ml}$. Among the complexes 1 - 3 the complex 3 was less active against *Culexquinquefasciatus* with the LD_{50} values of 84.73 $\mu\text{g}/\text{ml}$ respectively. The synthesized complex 2 was highly active and 1 was moderately active compared to the positive control *Permethrin* with the LD_{50} value of 60.03 $\mu\text{g}/\text{ml}$. The values are summarized in Table 1.

Table 1.Larvicidal activity of synthesized complexes (1 - 3)

Comp.No.	Mortality (%)Room temp Concentration($\mu\text{g}/\text{mL}$) ^a				LD50 ($\mu\text{g}/\text{mL}$)
	100	50	25	10	
1	80 \pm 1.78	42 \pm 0.67	20 \pm 1.87	0 \pm 0.00	59.97
2	100 \pm 0.00	80 \pm 1.42	68 \pm 1.54	34 \pm 1.23	18.52
3	60 \pm 1.64	30 \pm 0.54	10 \pm 0.34	0 \pm 0.00	84.73
Positive control	-	-	-	-	60.03
Negative control	0.0 \pm 0.0	0.0 \pm 0.0	0.0 \pm 0.0	0.0 \pm 0.0	0.0 \pm 0.0

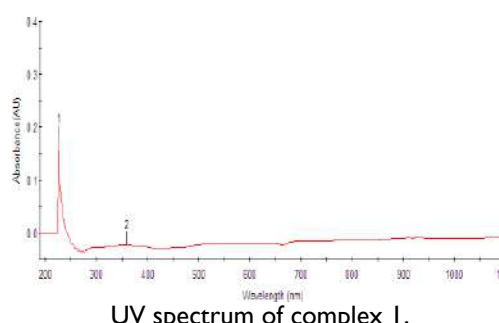
MSO^aValue were the means of three replicates \pm SD.

Antifeedant activity (Ichthyotoxicity activity) Complex 1 showed high toxicity compared with other complexes 1 and 2. Complex 1 produced 80% mortality in 24hr at 100 $\mu\text{g}/\text{ml}$ respectively. Toxicity was measured as the death percentage at 24hr. Complex 2 produced 43% mortality in 24hr at 100 $\mu\text{g}/\text{ml}$. The values are summarized in Table 2. Among the synthesized complexes 1 - 3 the complex 1 was highly active with the LD_{50} value of 46.08 $\mu\text{g}/\text{ml}$ ¹⁷⁻¹⁹.

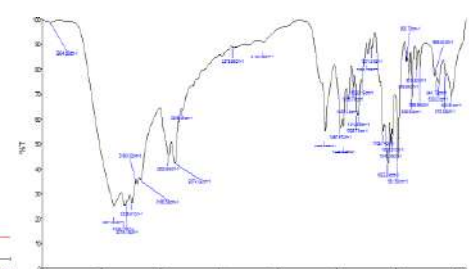
Table 2.Antifeedantactivity of synthesized complexes (1 - 3)

Comp.No.	Mortality (%)Room temp Concentration($\mu\text{g}/\text{mL}$) ^a				LD50 ($\mu\text{g}/\text{mL}$)
	100	50	25	10	
1	80 \pm 1.54	60 \pm 0.56	40 \pm 1.21	18 \pm 1.87	46.08
2	43 \pm 0.87	20 \pm 0.07	0 \pm 0.00	-	>100
3	60 \pm 2.12	44 \pm 1.47	20 \pm 0.67	0 \pm 0.00	75.96
Negative control	0.0 \pm 0.0	0.0 \pm 0.0	0.0 \pm 0.0	0.0 \pm 0.0	0.0 \pm 0.0

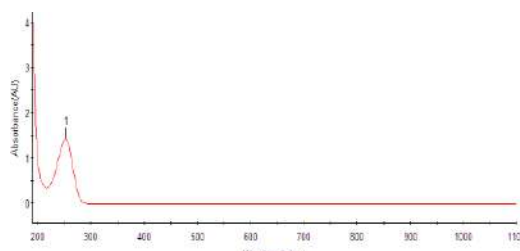
Negative control:DMSO^aValue were the means of three replicates \pm SD.



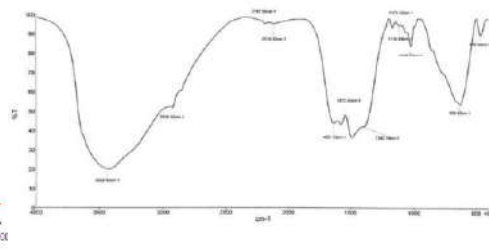
UV spectrum of complex 1.



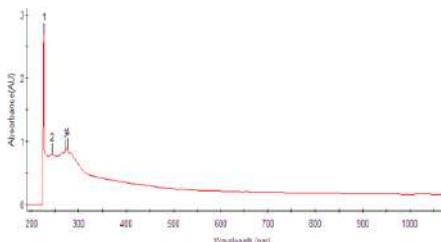
IR spectrum of complex 1.



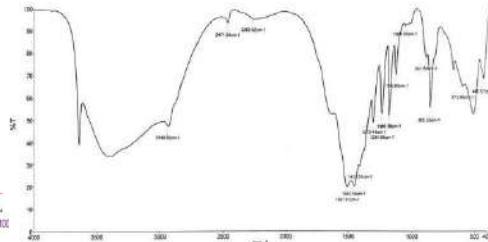
UV spectrum of complex 2



IR spectrum of complex 2



UV spectrum of complex 3



.IR spectrum of complex 3

CONCLUSION

From the present study, it can be concluded that the potency of the nickel(II) complexes shows significant activity in larvicidal and less toxic in antifeedant bioassays. The 3-methyl-1H-pyrazol-5(4H)-one derived complex 2 shows significant activity against mosquito larvae compared with positive control and shows less toxic in antifeedant activity. Therefore, these compounds might be a potential source for developing ecologically significant bioactive compounds, including biodegradable pesticides, and biopharmaceuticals²⁰

CONFLICT OF INTEREST

Conflict of interest declared none.

REFERENCE

1. A. Chakraborty, P. Kumar, K. Ghosh, and P. Roy, Evaluation of a Schiff base copper complex compound as potent anticancer molecule with multiple targets of action, *European Journal of Pharmacology*, vol. 647, no. 13, pp. 112, 2010.
2. R. H. Holm, P. Kennepohl, and E. I. Solomon, Structural and functional aspects of metal sites in biology, *Chemical Reviews*, vol. 96, no. 7, pp. 2239-2314, 1996.
3. M. A. Ali, C. M. Haroon, M. Nazimuddin, S. M. M.-U. Majumder, M. T. H. Tarafder, and M. A. Khair, Synthesis, characterization and biological activities of somenewnickel(II), copper(II), zinc(II) and cadmium(II) complexes of quadridentate SNNS ligands, *Transition Metal Chemistry*, vol. 17, no. 2, pp. 133-136, 1992.
4. D. T. Minkel, C. H. Chanstier, and D. H. Petering, Reactions of 3-Ethoxy-2-oxobutyraldehyde Bis(N4-dimethylthiosemicarbazonato)- Zinc(II) with tumor cells and mitochondria, *Molecular Pharmacology*, vol. 12, no. 6, pp. 1036-1044, 1976.
5. V. Rajendiran, R. Karthik, M. Palaniandavar et al., Mixed lig and copper (II)-phenolate complexes: effect of coligand on enhanced DNA and protein binding, DNA cleavage, and anticancer activity, *Inorganic Chemistry*, vol. 46, no. 20, pp. 8208-8221, 2007.
6. A. E. Liberta and D. X. West, Antifungal and antitumor activity of heterocyclic thiosemicarbazones and their metal complexes: current status, *Biometals*, vol. 5, no. 2, pp. 121-126, 1992.
7. Y. Harinath, D. H. K. Reddy, B. N. Kumar, C. Apparao, and K. Seshaiah, Synthesis, spectral characterization and antioxidant activity studies of a bidentate Schiff base, 5-methyl thiophene-2-carboxaldehyde-carbohydrazone and its Cd(II), Cu(II), Ni(II) and Zn(II) complexes, *Spectrochimica Acta Part A: Molecular and Biomolecular Spectroscopy*, vol. 101, pp. 264-272, 2013.
8. J. Sheikh, H. Juneja, V. Ingle, P. Ali, and T. B. Hadda, Synthesis and in vitro biology of Co(II), Ni(II), Cu(II) and Zinc(II) complexes of functionalized beta-diketone bearing energy buried potential antibacterial and antiviral O,O pharmacophore sites, *Journal of Saudi Chemical Society*, vol. 17, no. 3, pp. 269-276, 2013.
9. C. Marzano, M. Pellei, F. Tisato, and C. Santini, Copper complexes as anticancer agents, *Anti-Cancer Agents in Medicinal Chemistry*, vol. 9, no. 2, pp. 185-211, 2009.
10. S. M. Saadeh, Synthesis, characterization and biological properties of Co(II), Ni(II), Cu(II) and Zn(II) complexes with an SNO functionalized ligand, *Arabian Journal of Chemistry*, vol. 6, no. 2, pp. 191-196, 2013.
11. J. Garcí'a-Tojal, A. Garcí'a-Orad, A. A. D'iaz et al., "Biological activity of complexes derived from pyridine-2-carbaldehyde thiosemicarbazone: structure of [Co(C7H7N4S)2][NCS]," *Journal of Inorganic Biochemistry*, vol. 84, no. 3-4, pp. 271-278, 2001.
12. P. R. Reddy and A. Shilpa, "2-hydroxynaphthalene-1-carbaldehyde- and 2-aminomethyl)pyridine-based Schiff base CuII complexes for DNA binding and cleavage," *Chemistry & Biodiversity*, vol. 9, no. 10, pp. 2262-2281, 2012.
13. N. Shahabadi, M. M. Khodaei, S. Kashanian, and F. Kheirdoosh, Interaction of a copper (II) complex containing an artificial sweetener (aspartame) with calf thymus DNA, *Spectrochimica Acta Part A: Molecular and Biomolecular Spectroscopy*, vol. 120, pp. 16, 2014.
14. A. J. Steckl, DNAa new material for photonics *Nature Photonics*, vol. 1, pp. 35, 2007.
15. S. Bandyopadhyay, M. Tarek, and M. L. Klein, Molecular dynamics study of a lipid-DNA complex, *The Journal of Physical Chemistry B*, vol. 103, no. 46, pp. 10075-10080, 1999.
16. M. Hazra, T. Dolai, A. Pandey, S. K. Dey, and A. Patra, Fluorescent copper (II) complexes: the electron transfer mechanism, interaction with bovine serum albumin (BSA) and antibacterial activity, *Journal of Saudi Chemical Society*, vol. 21, S240-S247, 2017.

17. A. D. Becke, Density-functional thermochemistry. III. The role of exact exchange," *The Journal of Chemical Physics*, vol. 98, article 5648, 1993.
18. C. Lee, W. Yang, and R. G. Parr, "Development of the Colle-Salvetti correlation-energy formula into a functional of the electron density, *Physical Review B*, vol. 37, no. 2, pp. 785–789, 1998.
19. S. Roy, T. K. Mondal, P. Mitra, E. L. Torres, and C. Sinha, Synthesis, structure, spectroscopic properties, electrochemistry, and DFT correlative studies of N-[(2-pyridyl)methyliden]-6-coumarin complexes of Cu(I) and Ag(I), *Polyhedron*, vol. 30, no. 6, pp. 913–922, 2011
20. Romero D, Aguilar C, Losick R, Kolter R. Amyloid fibers provide structural integrity to *Bacillus subtilis* biofilms. *Proc Natl Acad Sci U S A*. 2010;107(5):2230– 2234.

Green Synthesis Nickel Oxide Nanoparticle Using Unripe Fruit Extract Of *Solanum Torvum* and Evaluating Its *In-Vitro* Antifungal Activity

V.Bhakyajothi¹, S.Suguna¹, Dr A Priya¹, A.Priyadharshini¹

¹Dhanalakshmi Srinivasan college arts and science for women (Autonomous), Perambalur, Tamilnadu 621212

Abstract: Biological method for the synthesis of nanomaterials has been suggested as an ecofriendly method. The synthesis of Nickel oxide nanoparticles (NiO NPs) is reported in this paper using *Solanum trilobatum* leaf extract as the fuel and nickel nitrate as the precursor through biological method. X-ray diffraction (XRD) study confirmed that the formed product has face centered cubic phase with high crystallinity and an average crystallite size of 23.21 nm. A cylindrical and rod like morphology was confirmed from morphological studies. The NiO formation with high purity phase was also confirmed by XRD study. The functional group of the NiO was confirmed with FT-IR study.

Keywords: *Solanum torvum*, NiO₂, UV-Visible spectroscopy, FT-IR, EDX, and XRD analysis

INTRODUCTION

Ni based nanoparticles have recently become a fundamental building block in nanotechnology due to their unique optical, electronic, catalytic, and chemical properties. The high surface-to-volume ratio, size and shape-dependent optical features, their size-dependent electrochemistry, high chemical stability, and facile surface chemistry have made them the model system of choice for exploring a wide range of phenomena including self-assembly, bio-labeling, catalysis, etc.¹⁻². One attractive feature of nonoble metal/transition metal nanoparticles is that their surfaces can be derivatized with thiols, phosphines, alkynes, and amines in both aqueous and organic solvents, allowing a range of chemistry to be utilized in particle modification³⁻⁷. Noble/transition metal nanoparticles are often modified by soaking the colloid in a solution of the ligand of interest, making modification straightforward. Another advantage is that gold nanoparticle size can be easily modified to suit the needs of the experiment. For example, larger gold nanoparticles (> 80 nm) scatter light very effectively, making them useful labels in optical microscopy. In contrast, smaller nanoparticles (~ 5 nm) can be used as a size-control template for biomimetic high-density lipoprotein structures. A fascinating and useful trait of gold nanoparticles is their electronic interactions causing a distance-dependent color change. This effect is observed in solutions when the particles come within less than one particle diameter of each other. Importantly, almost any surface modification that can be made to the gold nanoparticle that can cause particle cross-linking in the presence of a specific analyte, in principle, can result in a colorimetric sensor. Even today, the biological aspects of metallic gold nanoparticles (GNPs) are very useful to human health and cosmetic applications. Gold nanoparticles have widespread applications in targeted drug delivery, imaging, diagnosis, and therapeutics due to their extremely small size, high surface area, stability, non-cytotoxicity, and tunable optical, physical, and chemical properties. In some ways, it has revolutionized the field of medicine. Functionalized gold nanoparticles with various biomolecules such as DNA, amino acids, and carboxylic acids have been used in cancer therapy and offer outstanding drug delivery systems. Targeted drug delivery and programmed release of curative drugs to the specific site is achieved by using gold nanoparticles because they can tolerate high drug load and release it to the specific site through various administration routes and can act together with cancerous cells. Side effects of generic drugs have been reduced by conjugation with gold nanoparticles and they increase the quality of life of patients.

MATERIEL AND METHODS

All materials were purchased from Nice and Loba chemicals. Solvents used throughout the reactions were of high purity and used without further purifications. Collection of plant materials. The unripe fruit of *Solanum torvum* was collected from the local places of the perambalur area. Fresh unripe fruit was used for the synthesis of nickel oxide nanoparticle Preparation of plant extractThe nickel chloride and *Solanum torvum* unripe fruit extract were used as the starting materials. The *Solanum torvum* unripe fruit extract solution was prepared using unripe fruits that had been rinsed with deionized water and finely cut into small pieces. The unripe fruits are grained, boiled with 100 mL distilled water for about 10 mins, filtered, and stored. The resulting extract was used as a *Solanum torvum* extract solution.

Synthesis of Nickel oxide nanoparticles

In the preparation of Nickel Oxide nanoparticles, compounds NiCl₂.2H₂O (1 g) was first dissolved in 10 ml of deionized water and mixed with 10 ml of flower extract solution under vigorous stirring at room temperature for 3hr. Then 1mL of 10% NaOH was added. The mixture was maintained at 100 ° for 12 hrs in the oven. The obtained powder was calcined at 350 ° for 4 hrs.

Characterization studies

Nickel oxide nanoparticles synthesized by this green method were characterized by, UV-Visible spectrophotometer (Shimadzu) and Fourier-transform infrared (FTIR- Shimadzu) spectrum in the range 4000-400 cm⁻¹, SEM (Scanning Electron Microscope), EDX (Energy Dispersive Diagram), XRD (X-ray Diffraction Spectrophotometer) and also the synthesized nickel oxide nanoparticles were tested for in vitro antifungal activity against four different fungal strains.⁹⁻¹³

Biological screening Antifungal activity

The minimal inhibitory concentration (MIC) was determined by the broth microdilution method according to the Clinical and Laboratory Standards Institute (CLSI) (The National Committee for Clinical Laboratory Standards). *In vitro* antifungal activity of the final compounds I- Ia was evaluated against standard strains; *Aspergillus Niger*,

RESULT AND DISCUSSION

Optical Characterization

The reduction of Ni^{2+} ions to NiO NPs by unripe fruit of *Solanum torvum* extract was visually monitored by color change in the mixture. The gradual color change in solution color from pale green to dark brown color was observed and this indicates that the phenolic compounds and phytochemicals present in unripe fruit extract act as a good reducing agent for the synthesis of NiO NPs. Phytochemicals in plant parts play a significant role in the reduction of metal ions to metal NPs. Surface plasmon resonance (SPR) excitation in UV-vis analysis was used to characterize the metallic nature of the nanoparticles in colloidal dispersion. Figure 1 represented the UV-vis spectra of green synthesized NiO NPs using unripe fruit extract. A progressive strong broadening of SPR was observed in the visible region from 320 to 430 nm representing the formation of NiO NPs. In this study, the maximum absorption peak appeared at 329 nm indicates the formation of NiO NPs.¹⁴⁻¹⁸ The synthesized NiO NPs elemental composition was confirmed by EDX examination. The manifestation of zinc and oxygen peaks in the EDX spectra confirmed that the synthesized material was NiO NPs. The weight percentage of Nickel and Oxygen atoms were 55.06 and 44.94 respectively. The further peaks extant in the spectra may be as a result of the existence of bio organics or impurities in the solution. The elemental composition of NiO nanoparticles was represented in Table

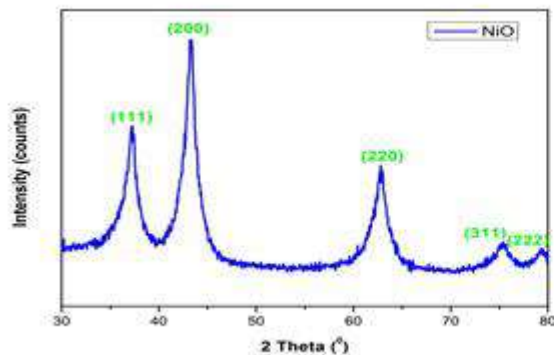


Fig:1 EDX Analysis of NiO nanoparticles

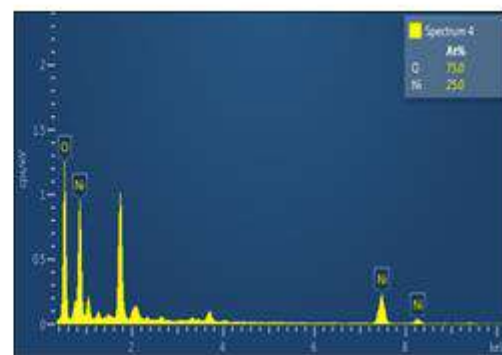


Fig:2 XRD of NiO

XRD Analysis

The XRD pattern of synthesized NiO NPs was represented in Figure . The diffraction peaks at $2\theta = 37.1^\circ, 43.2^\circ, 62.7^\circ, 75.3^\circ$, and $67.979.3^\circ$ were respectively indexed to (111), (200), (220), (311) and (222) planes of the pure cubic structure of NiO NPs (bunsenite, NaCl type structure). The obtained diffraction peaks were matched with standard NiO NPs. All the diffraction peaks are in decent agreement with the standard pattern for pure NiO nanoparticles (JCPDS No. 73-1519). There is some impurity peaks were observed. The intense peaks indicate the extremely crystalline nature of the formed nanoparticles. From the observed main diffracted peak, the average crystalline size can be calculated using the Scherer equation,¹⁹⁻²¹

Table I. Elemental composition of NiO nanoparticle

Element	Atomic Number	Weight %	Atom %	Weight % Error
O	8	44.94	75.00	1.13
Ni	28	55.06	25.00	1.13
Total	-	100.00	100.00	-

$$k\lambda \quad (hkl) = \beta \cos\theta$$

Where $D_{(hkl)}$ is the average crystalline size, k is shaped constant (0.89), λ is the wavelength of the incident x-ray (Cuk α source, $\lambda = 0.15405$ nm), β is the full width half maximum (FWHM), θ is the incident angle of x-ray. The average crystallite size of the synthesized NiO nanoparticles was 153.49 nm.

Antifungal activity

The synthesized nanoparticle 2 and *Solanum torvum* unripe fruit extract 1 were evaluated for antifungal activity against four

different fungal species. Compound 2 shows remarkable antifungal activity than compound 1. Compound 2 shows high antifungal activity in two fungal species namely *C. Albicans* and *M. audouinii*. Compound 1a with the MIC value of 01 $\mu\text{g/mL}$ was highly active than control clotrimale with the MIC value of 02 $\mu\text{g/mL}$ in *C. Albicans*. Compound 2 with the MIC value of 02 $\mu\text{g/mL}$ shows high antifungal activity than clotrimale with the MIC value of 04 $\mu\text{g/mL}$. The results were summarized in Table 2.

Table 2. Antifungal activity of *Solanum torvum* unripe fruit extract 1 and NiO nanoparticle 2

Compounds	MIC ($\mu\text{g/mL}$)			
	Aspergillus Niger	Candida albicans	Microspor audouinii	Cryptoco ccus Neoforma ns
1	45	25	64	16
2	56	01	02	26
Clotrimale	01	02	04	05

CONCLUSION

In conclusion, the nickel oxide nanoparticle was synthesized using fresh unripe fruit extract of *Solanum torvum*. The synthesized nanoparticles were characterized and confirmed using UV, FT- IR, XRD, and SEM analysis, the results showed that NiO NPs were synthesized properly. The *in vitro* antifungal activity depicts the effective antifungal activity of NiO NPs. This concludes that further studies on NiO NPs help for drug development.

CONFLICT OF INTEREST

Conflict of interest declared none.

REFERENCE

1. M.A.Albrecht, C.W. Evans, and C.L.Raston, "Green chemistry and the health implications of nanoparticles," *Green Chemistry*, vol. 8, no. 5, pp. 417–432, 2006.
2. J. M. DeSimone, "Practical approaches to green solvents," *Science*, vol. 297, no. 5582, pp. 799–803, 2002.
3. H. Rui, R. Xing, Z. Xu, Y. Hou, S. Goo, and S. Sun, "Synthesis, functionalization, and biomedical applications of multifunctional magnetic nanoparticles," *Advanced Materials*, vol. 22, no. 25, pp. 2729–2742, 2010.
4. I. Brigger, C. Dubernet, and P. Couvreur, "Nanoparticles in cancer therapy and diagnosis," *Advanced Drug Delivery Reviews*, vol. 54, no. 5, pp. 631–651, 2002.
5. A. K. Gupta and M. Gupta, "Cytotoxicity suppression and cellular uptake enhancement of surface modified magnetic nanoparticles," *Biomaterials*, vol. 26, no. 13, pp. 1565–1573, 2005.
6. K. Petcharoen and A. Sirivat, "Synthesis and characterization of magnetite nanoparticles via the chemical co-precipitation method," *Materials Science and Engineering B: Solid-State Materials for Advanced Technology*, vol. 177, no. 5, pp. 421–427, 2012.
7. F. Jia, L. Zhang, X. Shang, and Y. Yang, "Non-aqueous sol-gel approach towards the controllable synthesis of nickel nanospheres, nanowires, and nanoflowers," *Advanced Materials*, vol. 20, no. 5, pp. 1050–1054, 2008.
8. D.-H. Chen and S.-H. Wu, "Synthesis of nickel nanoparticles in water-in-oil microemulsions," *Chemistry of Materials*, vol. 12, no. 5, pp. 1354–1360, 2000.
9. D. Chen and R. Xu, "Hydrothermal synthesis and characterization of nanocrystalline γ -Fe₂O₃ particles," *Journal of Solid State Chemistry*, vol. 137, no. 2, pp. 185–190, 1998.
10. S. Basak, D.-R. Chen, and P. Biswas, "Electrospray of ionic precursor solutions to synthesize iron oxide nanoparticles: modified scaling law," *Chemical Engineering Science*, vol. 62, no. 4, pp. 1263–1268, 2007.
11. G. W. Yang, "Laser ablation in liquids: applications in the synthesis of nanocrystals," *Progress in Materials Science*, vol. 52, no. 4, pp. 648–698, 2007.
12. B. Nagaraj, N. B. Krishnamurthy, P. Liny, T. K. Divya, and R. Dinesh, "Biosynthesis of gold nanoparticles of *Ixora coccinea* flower extract & their antimicrobial activities," *International Journal of Pharma and Bio Sciences*, vol. 2, no. 4, pp. 557–565, 2011.
13. M. Kowshik, S. Ashtaputre, S. Kharrazi, et al., "Extracellular synthesis of silver nanoparticles by a silver-tolerant yeast strain MKY3," *Nanotechnology*, vol. 14, no. 1, pp. 95–100, 2003.
14. M. N. Nadagouda and R. S. Varma, "Green and controlled synthesis of gold and platinum nanomaterials using vitamin B2: density-assisted self-assembly of nanospheres, wires, and rods," *Green Chemistry*, vol. 8, no. 6, pp. 516–518, 2006.
15. Hsueh PR. New Delhi Metallo- β -lactamase-1 (NDM-1): an emerging threat among Enterobacteriaceae. *J Formos Med Assoc*. 2010;109(10):685–687.
16. Poole K. Mechanisms of bacterial biocide and antibiotic resistance. *J Appl Microbiol*. 2002;92(suppl):55–64.
17. Jayaraman R. Antibiotic resistance: an overview of mechanisms and a paradigm shift. *Curr Sci India*. 2009;96(11):1475–1484.
18. Knetsch MLW, Koole LH. New strategies in the development of antimicrobial coatings: the example of increasing usage of silver and silver nanoparticles. *Polymers Basel*. 2011;3:340–366.
19. Romero D, Aguilar C, Losick R, Kolter R. Amyloid fibers provide structural integrity to *Bacillus subtilis* biofilms. *Proc Natl Acad Sci U S A*. 2010;107(5):2230–2234.

21. Huh AJ, Kwon YJ. "Nanoantibiotics": a new paradigm for treating infectious diseases using nanomaterials in the antibiotics resistant era. *J Control Release*. 2011;156(2):128–145.
22. Hajipour MJ, Fromm KM, Ashkarran AA, et al. Antibacterial properties of nanoparticles. *Trends Biotechnol*. 2012;30(10):499–511.
23. Reyes VC, Opot SO, Mahendra S. Planktonic and biofilm-grown nitrogen-cycling bacteria exhibit different susceptibilities to copper nanoparticles. *Environ Toxicol Chem*. 2015;34(4):887–897.
24. Edmundson M, Thanh NT, Song B. Nanoparticles based stem cell tracking in regenerative medicine. *Theranostics*. 2013;3(8):573–582.